



Ng, Keng Tiong (2016) Studies Towards the Enhanced Detection and Identification of Pathogenic Bacteria. Doctoral thesis, The University of Sunderland.

Downloaded from: <http://sure.sunderland.ac.uk/id/eprint/16843/>

Usage guidelines

Please refer to the usage guidelines at <http://sure.sunderland.ac.uk/policies.html> or alternatively contact sure@sunderland.ac.uk.

STUDIES TOWARDS THE ENHANCED DETECTION AND IDENTIFICATION OF PATHOGENIC BACTERIA

KENG TIONG NG

A thesis submitted in partial fulfillment of the requirements of the University of
Sunderland for the degree of Doctor of Philosophy

This research programme was carried out in collaboration with the Freeman
Hospital (Newcastle-upon-Tyne) and bioMérieux (La Balme-les-Grottes, France)

October 2016

Acknowledgement

Firstly, I would like to express my sincere gratitude to my supervisory team, Prof. Roz Anderson, Dr. Mark Gray and Prof. John Perry for their patience, inspiration and outstanding knowledge to support me endlessly towards my PhD study and related research. I would not be able to learn and conduct this research without them. Special gratitude is given to Prof. Roz Anderson for her continuously support, regardless of any difficult circumstances. I would not be able to complete this huge project without you.

A special thanks goes to BioMérieux for their kind financial support throughout my PhD research, as well as provided me a good opportunity to join the research family led by Dr. Sylvain Orenge and Marie Cellier. I am grateful to get to know and work with other team members, Prof. Stephen Stanforth and *The Late* Prof. Arthur James, who deeply inspired me about chemistry related research work.

I also would like to express my deep appreciation to the University of Sunderland, which provide me a peaceful laboratory environment to work on my research. A special thanks to Dr. John Lough, Dr. Alexandre Bedernjak, Dr. Peter Dawson, Dr. Lisa Frost and Dr. Suresh Kottakota who provided me constructive support, encouragement and some helpful guidance.

A big thanks to the staff members of the university, Alan, Arun, Byron, Debs, John, Tom, Kevin and Norman for not only the technical support but also the good laughing session during the break time. Thanks to my colleagues and labmates who made every working day full of fun and joy: Alex, Clémence, Laszlo, Rachel, Stephen, Lisa and Suresh.

Last but not least, I would like to thank my beloved family members: my parents, siblings, brother-in-law and nephew for their spiritual and moral support throughout my life in the foreign country. A special personal thanks to my sweetheart MuhYuan for her continuous support even I am not around with her at all time. Without you, I would not be able to come up to this stage.

Abstract

The application of fluorogenic and chromogenic enzymatic substrates in culture media continues to offer huge potential for accessible bacterial detection and identification. However, their clinical use poses two major disadvantages: the presence of commensal and/or coliform bacteria camouflages the detection of bacteria of interest, and false results may arise due to secretion of a similar enzyme by a different species (or strain of) that acts upon the same enzymatic substrates. In the current work, selective antimicrobial agents or suicide substrates were developed and investigated in order to prevent the growth of these interfering bacteria, thus improving the integrity of the detection and diagnosis of common clinical infections. This project has been carried out under collaboration between University of Sunderland (UK), bioMérieux (France) and Freeman Hospital, Newcastle-upon-Tyne (UK).

The L-alanine analogues D/L-fosfalin and β -chloro-L-alanine were synthesised, both of which target alanine racemase, and different peptide derivatives based on these moieties were prepared using the well-established IBCF/NMM coupling approach with a series of protection/deprotection methods. Two dipeptide derivatives based on *para*-aminobenzoic acid (PABA) were also investigated. A series of synthetic derivatives were subjected to microbiology evaluation using 20 different clinical strains of clinical bacteria at the Freeman Hospital. The stability of β -Cl-L-Ala-D/L-Fos was investigated at pH 6.1 – 9.1; hydrolysis products were formed above pH 6.1.

The minimum inhibitory concentration (MIC) of L-Ala-L-Ala-D/L-Fos was double the concentration of L-Ala-L-Ala-L-Fos, showing that only the diastereoisomer with L-fosfalin exhibited significant inhibitory activity against the bacteria. The introduction of β -chloro-L-alanine into the phosphonopeptide derivatives enhanced the antibacterial activity; for example the growth of commensal bacterium, *Escherichia coli*, was inhibited at a low MIC (0.125 – 0.5 mg/L) by most X- β -Cl-L-Ala-D/L-Fos tripeptide analogues, except when X: sarcosine (MIC: 4 mg/L). However, no significant antibacterial activity was found in the PABA derivatives.

These di- and tri-peptide fosfalin-containing derivatives, especially with the inclusion of β -Cl-L-alanine, offer improved selectivity for the detection and identification of pathogenic bacteria in clinical samples by restricting the over-growth of commensal bacteria.

Symbols and abbreviations

$\bar{\nu}$	Wavenumber
δ	NMR chemical shift
% w/v	Weight over volume percentage
% v/v	Volume over volume percentage
2D NMR	2 Dimensional NMR
A or Å	Angstrom
AcOH	Acetic acid
α	Alpha
AF	Antagonist free
Ala	Alanine
approx.	Approximate
Ar	Aromatic ring
Arg	Arginine
Asn	Asparagine
Asp	Aspartic acid or aspartate
ATCC	American Type Culture Collection
ATP	Adenosine triphosphates
BCFIA	Bacterial concentration fluorescence immunoassay
β	Beta
Boc ₂ O	Di-tert-butyl dicarbonate
br	Broad
⁷⁹ Br	Bromine-79
⁸¹ Br	Bromine-81
°C	Degree celcius
¹³ C	Carbon-13
calcd	Calculated
Cbz	Benzyl carbamate
CDCl ₃	Deuterated chloroform
CD ₃ OD	Deuterated methanol
CHN	Carbon, hydrogen and nitrogen elemental analysis
Cit	Citrulline

Cont'd	Continued
³⁵ Cl	Chlorine-35
³⁷ Cl	Chlorine-37
cm	Centimetre
CTXM	Cefotaximas-Munich-β-lactamase
Cys	Cysteine
Cys ₂	Cystine
d	Doublet
dd	Doublet of doublets
ddd	Doublet of doublet of doublets
ddt	Doublet of doublet of triplets
DBU	1,8-Diazabicyclo[5.4.0]undec-7-ene
DCC	Dicyclohexylcarbodiimide
DCM	Dichloromethane
DCS	D-Cycloserine
D ₂ O	Deuterium oxide
Ddl	D-Alanyl-D-alanyl ligase
DEAD	Diethyl azodicarboxylate
DIEA	Diisopropylethylamine
DMAP	Dimethylaminopyridine
DMF	Dimethylformamide
DMSO	Dimethyl sulfoxide
DNA	Deoxyribonucleic acid
ε	Epsilon
EDCI	1-Ethyl-3-(3-dimethylaminopropyl)carbodiimide
ELISA	Enzyme-linked immunosorbent assay
ESI	Electrospray ionisation
equiv.	Equivalent
¹⁹ F	Fluorine-19
Fos	Fosfalin or 1-aminoethylphosphonic acid
g	Gram
Gln	Glutamine
Gly	Glycine

¹ H	Proton
HATU	2-(7-aza-1H-benzotriazole-1-yl)-1,1,3,3-tetramethyluronium hexafluorophosphate
HRMS	High Resolution Mass Spectrometry
hrs	Hours
His	Histidine
Hz	Hertz
IBCF	Isobutyl chloroformate
Ile	Isoleucine
IR	Infra-red
<i>J</i>	Coupling constant
K _i	Inhibitory constant
KPC	Carbapenem-Resistant- <i>Klebsiella pneumonia</i>
LAT	Cefoxitin-Hydrolysing-β-lactamase
LCS	L-Cycloserine
Leu	Leucine
lit.	Literature
logP	Partition coefficient
LPS	Lipopolysaccharide
Lys	Lysine
M	Mega (10 ⁶)
m	multiplet
<i>m/z</i>	Mass over charge of the ion
MALDI	Matrix-assisted laser desorption ionisation
Met	Methionine
MFS	Major facilitator superfamily
<i>m</i> -DAP	<i>Meso</i> -Diaminopimelate
m.p.	Melting point
μm	Micrometre
μg	Microgram
μL	Microlitre
mg	Miligram
mL	Millilitre

mmol	Milimole
MIC	Minimum inhibitory concentration
mins	Minutes
m-PCR	Multiplex polymerase chain reaction
MRSA	Methicillin-resistant <i>Staphylococcus aureus</i>
MS	Mass spectrometry
NAG or GlcNAc	<i>N</i> -Acetylglucosamine
NAM or MurNAc	<i>N</i> -Acetylmuramic
NaOD	Deuterated sodium hydroxide
NCTC	National Collection of Type Cultures
NDM	New Delhi Metallo- β -lactamase
NMM	<i>N</i> -Methylmorpholine
NMR	Nuclear magnetic resonance
NSI	Nano Spray Ionisation
Nva	Norvaline
OBzl	Benzyl ester protecting group
ODC	Ornithine decarboxylase
OMe	Methyl ester protecting group
OXA	Oxacillin-Hydrolysing- β -lactamase
^{31}P	Phosphorus-31
PABA	<i>Para</i> -Aminobenzoic acid
PBP	Penicillin binding protein
PCR	Polymerase chain reaction
Pd	Palladium
$\text{p}K_{\text{a}}$	Negative logarithm of acidic dissociation constant
Phe	Phenylalanine
PLP	Pyridoxal 5'-phosphate
PNA	Peptide nucleic acid
POT	Proton dependent oligopeptide transporter
ppm	Parts per million
PSA	Polar surface area
Pyroglu	Pyroglutamic acid
quat.	Quaternary

rt.	Room temperature
s	Singlet
Sar	Sarcosine
SDW	Sterile deionised water
Ser	Serine
sp.	Species (singular)
spp.	Species (plural)
t	Triplet
^t Boc	<i>Tert</i> -butoxycarbonyl
TCT	2,4,6-Trichloro[1,3,5]triazine
TEA or Et ₃ N	Triethylamine
TEM	Temoneira-β-lactamase
THF	Tetrahydrofuran
TMSBr	Bromotrimethylsilane
TPSA	Topological polar surface area
tRNA	Transfer ribonucleic acid
Trp	Tryptophan
Tyr	Tyrosine
UDP	Uridine diphosphate
Val	Valine

Bacterial abbreviations

Gram negative bacteria	Abbreviations
<i>Acinetobacter baumannii</i>	<i>A. baumannii</i>
<i>Actinobacillus actinomycetemcomitans</i>	<i>A. actinomycetemcomitans</i>
<i>Aeromonas hydrophila</i>	<i>A. hydrophila</i>
<i>Bacteroides intermedius</i>	<i>B. intermedius</i>
<i>Burkholderia cepacia</i>	<i>B. cepacia</i>
<i>Campylobacter coli</i>	<i>C. coli</i>
<i>Campylobacter jejuni</i>	<i>C. jejuni</i>
<i>Citrobacter freundii</i>	<i>C. freundii</i>
<i>Eikenella corrodens</i>	<i>E. corrodens</i>
<i>Enterobacter aerogenes</i>	<i>E. aerogenes</i>
<i>Enterobacter cloacae</i>	<i>E. cloacae</i>
<i>Escherichia coli</i>	<i>E. coli</i>
<i>Fusobacterium nucleatum</i>	<i>F. nucleatum</i>
<i>Haemophilus influenzae</i>	<i>H. influenzae</i>
<i>Klebsiella aerogenes</i>	<i>K. aerogenes</i>
<i>Klebsiella pneumoniae</i>	<i>K. pneumoniae</i>
<i>Legionella pneumophila</i>	<i>L. pneumophila</i>
<i>Porphyromonas gingivalis</i>	<i>P. gingivalis</i>
<i>Proteus mirabilis</i>	<i>P. mirabilis</i>
<i>Providencia rettgeri</i>	<i>P. rettgeri</i>
<i>Pseudomonas aeruginosa</i>	<i>P. aeruginosa</i>
<i>Pseudomonas fluorescens</i>	<i>P. fluorescens</i>
<i>Pseudomonas putida</i>	<i>P. putida</i>
<i>Salmonella typhimurium</i>	<i>S. typhimurium</i>
<i>Salmonella enterica</i>	<i>S. enterica</i>
<i>Salmonella enteritidis</i>	<i>S. enteritidis</i>
<i>Serratia marcescens</i>	<i>S. marcescens</i>
<i>Shigella flexneri</i>	<i>S. flexneri</i>
<i>Stenotrophomonas maltophilia</i>	<i>S. maltophilia</i>
<i>Vibrio cholera</i>	<i>V. cholera</i>
<i>Vibrio parahaemolyticus</i>	<i>V. parahaemolyticus</i>
<i>Yersinia enterocolitica</i>	<i>Y. enterocolitica</i>

Bacterial abbreviations (cont.d)

Gram positive bacteria	Abbreviations
<i>Bacillus stearothermophilus</i>	<i>B. stearothermophilus</i>
<i>Bacillus subtilis</i>	<i>B. subtilis</i>
<i>Clostridium difficile</i>	<i>C. difficile</i>
<i>Enterococcus faecalis</i>	<i>E. faecalis</i>
<i>Enterococcus faecium</i>	<i>E. faecium</i>
<i>Listeria monocytogenes</i>	<i>L. monocytogenes</i>
<i>Staphylococcus epidermidis</i>	<i>S. epidermidis</i>
<i>Staphylococcus aureus</i>	<i>S. aureus</i>
<i>Methicillin-resistant Staphylococcus aureus</i>	<i>S. aureus</i> (MRSA)
<i>Streptococcus agalactiae</i>	<i>S. agalactiae</i>
<i>Streptococcus pneumoniae</i>	<i>S. pneumoniae</i>
<i>Streptococcus pyogenes</i>	<i>S. pyogenes</i>

Contents

Acknowledgement.....	2
Abstract.....	3
Symbols and abbreviations.....	4
Bacterial abbreviations	9
Bacterial abbreviations (cont.d).....	10
Contents	11
CHAPTER 1	21
INTRODUCTION.....	21
1.1: Background	22
1.2: The Need for Bacterial Identification	26
1.2.1: Bacterial morphology.....	26
1.2.2: Bacterial cell structure	28
1.2.3: Gram staining.....	29
1.2.3.1: Gram-positive bacteria	31
1.2.3.2: Gram-negative bacteria	32
1.3: Bacterial detection and identification.....	33
1.3.1: Microscopic techniques.....	34
1.3.1.1: Light microscopy and electron microscopy.....	34
1.3.1.2: Flow cytometry	35
1.3.2: Immunological techniques	36
1.3.2.1: Enzyme-linked immunosorbent assay (ELISA).....	36
1.3.3: Genetic techniques	38
1.3.3.1: Polymerase chain reaction (PCR).....	38
1.3.3.2: Mass spectrometry (MS).....	39
1.3.4: Biochemical techniques	41
1.3.4.1: Chromogenic and fluorogenic substrates for bacterial detection	42
1.3.4.2: Selective growth media for bacterial detection.....	45
	11

1.3.4.3: Application of suicide substrates in chromogenic and fluorogenic media.....	48
1.4: Alanine racemase.....	50
1.4.1: Rationale for alanine racemase as a target for suicide substrate development...	50
1.4.2: Mechanism of alanine racemase	51
1.4.2.1: Internal aldimine formation	51
1.4.2.2: External aldimine formation.....	53
1.4.2.3: Roles of lysine and tyrosine residues within alanine racemase	55
1.4.3: Inhibitors of alanine racemase	56
1.4.3.1: Reversible inhibition with a slow rate of dissociation	56
1.4.3.2: Irreversible inhibition.....	59
1.4.4: Inhibitors of other enzymes	65
1.5: Development of di/tripeptide suicide substrates based on fosfalin and β -chloroalanine	67
1.5.1: Stages and challenges involved prior to the expression of inhibitory action of suicide substrates.....	67
1.5.2: Fosfalin	70
1.5.3: β -Chloroalanine	74
1.5.4: Rationale for synthesis of di/tripeptide suicide substrates based on fosfalin and β -chloroalanine.....	76
1.6: Aims and Objectives	78
CHAPTER 2	79
SYNTHESIS OF D/L-FOSFALIN AND SUICIDE SUBSTRATES BASED ON D/L-FOSFALIN.....	79
2.1: Synthesis of peptide derivatives containing D/L-fosfalin	80
2.2: Published methods for the synthesis of 1-aminoethylphosphonic acid (D/L-fosfalin)..	80
2.2.1: Synthesis of racemic 1-aminoethylphosphonic acid or D/L-fosfalin (13-DL)	84
2.3: Published methods for the protection of fosfalin as O,O-diethyl 1-aminophosphonate or D/L-fosfalin diethyl ester (84).....	87
2.3.1: Synthesis of diethyl (1-(2,2,2-trifluoroacetamido)ethyl)phosphonate or trifluoroacetyl-D/L-fosfalin diethyl ester (116)	88

2.3.2: Synthesis of <i>O,O</i> -diethyl 1-aminoethylphosphonate or <i>D/L</i> -fosfalin diethyl ester (84)	92
2.4: Published methods for the preparation of peptides containing the fosfalin moiety	92
2.4.1: Preparation of (1-((<i>S</i>)-5-oxopyrrolidine-2-carboxamido)ethyl) phosphonic acid or <i>L</i> -Pyroglu- <i>D/L</i> -fosfalin (141)	95
2.4.1.1: Synthesis of (<i>S</i>)-2-benzyl 1- <i>tert</i> -butyl-5-oxopyrrolidine-1,2-dicarboxylate or ^t Boc- <i>L</i> -Pyroglu-OBzl (143)	96
2.4.1.2: Synthesis of (<i>S</i>)-1-(<i>tert</i> -butoxycarbonyl)-5-oxopyrrolidine-2-carboxylic acid or ^t Boc- <i>L</i> -Pyroglu-OH (144)	98
2.4.1.3: Synthesis of (2 <i>S</i>)- <i>tert</i> -butyl 2-((1-(diethoxyphosphoryl)ethyl) carbamoyl)-5-oxopyrrolidine-1-carboxylate or ^t Boc- <i>L</i> -Pyroglu- <i>D/L</i> -Fos diethyl ester (145)	98
2.4.1.4: Synthesis of (1-((<i>S</i>)-5-oxopyrrolidine-2-carboxamido)ethyl) phosphonic acid or <i>L</i> -Pyroglu- <i>D/L</i> -fosfalin (141)	100
2.4.2: Preparation of phosphonotripeptide derivatives containing the <i>L</i> -Ala- <i>D/L</i> -fosfalin moiety	102
2.4.2.1: Synthesis of <i>N</i> -protected dipeptide derivatives (151a-c)	103
2.4.2.2: Synthesis of phosphonotripeptide derivatives (153a-c)	108
2.4.3: Preparation of phosphonotripeptide, <i>L</i> -Met- <i>L</i> -Ala- <i>D/L</i> -Fos (160)	121
2.4.3.1: Synthesis of <i>tert</i> -butyl ((2 <i>S</i>)-1-((1-(diethoxyphosphoryl)ethyl) amino)-1-oxopropan-2-yl)carbamate or ^t Boc- <i>L</i> -Ala- <i>D/L</i> -Fos diethyl ester (157)	122
2.4.3.2: Synthesis of (2 <i>S</i>)-1-((1-(diethoxyphosphoryl)ethyl)amino)-1-oxopropan-2-aminium chloride or <i>L</i> -Ala- <i>D/L</i> -Fos diethyl ester hydrochloride (158)	123
2.4.3.3: Synthesis of <i>tert</i> -butyl ((2 <i>S</i>)-1-(((2 <i>S</i>)-1-((1-(diethoxyphosphoryl) ethyl)amino)-1-oxopropan-2-yl)amino-4-(methylthio)-1-oxobutan-2-yl) carbamate or ^t Boc- <i>L</i> -Met- <i>L</i> -Ala- <i>D/L</i> -Fos diethyl ester (159)	124
2.4.3.4: Synthesis of (1-((<i>S</i>)-2-((<i>S</i>)-2-amino-4-(methylthio)butanamido)propanamido)ethyl)phosphonic acid or <i>L</i> -Met- <i>L</i> -Ala- <i>D/L</i> -Fos (160)	125
2.5: Conclusion	127
CHAPTER 3	128
SYNTHESIS OF SUICIDE SUBSTRATES BASED ON β -CHLORO- <i>L</i> -ALANINE AND STABILITY STUDY OF β -CHLORO- <i>L</i> -ALANYL- <i>D/L</i> -FOSFALIN ACROSS THE pH RANGE 6.1 - 9.1	128
3.1: Synthesis of peptides derivatives containing β -chloro- <i>L</i> -alanine- <i>D/L</i> -fosfalin	129
3.1.1: Published methods for the preparation of β -chloro- <i>L</i> -alanine derivatives	130

3.1.2: Synthesis of β -chloro-L-alanine derivatives.....	135
3.1.2.1: Synthesis of (<i>S</i>)-benzyl 2-((<i>tert</i> -butoxycarbonyl)amino)-3-hydroxypropanoate or ^t Boc-L-Ser-OBzl (178)	135
3.1.2.2: Synthesis of (<i>R</i>)-benzyl 2-((<i>tert</i> -butoxycarbonyl)amino)-3-chloropropanoate or ^t Boc- β -Cl-L-Ala-OBzl (179).....	136
3.1.2.3: Synthesis of (<i>R</i>)-2-((<i>tert</i> -butoxycarbonyl)amino)-3-chloropropanoic acid or ^t Boc- β -Cl-L-Ala-OH (181)	139
3.1.2.4: Synthesis of (<i>R</i>)-1-(benzyloxy)-3-chloro-1oxopropan-2-aminium chloride or β -Cl-L-Ala-OBzl hydrochloride (182)	139
3.2: Published methods for the preparation of peptides containing the β -chloro-L-alanine moiety.....	140
3.2.1: Preparation of phosphonodipeptide containing β -chloro-L-alanine and D/L-fosfalin	143
3.2.1.1: Synthesis of <i>tert</i> -butyl ((2 <i>R</i>)-3-chloro-1-((1-(diethoxyphosphoryl)ethyl)amino)-1-oxopropan-2-yl)carbamate or ^t Boc- β -chloro-L-Ala-D/L-Fos diethyl ester (195).....	144
3.2.1.2: Synthesis of (1-((<i>R</i>)-2-amino-3-chloropropanamido)ethyl) phosphonic acid or β -chloro-L-Ala-D/L-fos (196)	146
3.2.2: Stability study of β -chloro-L-Ala-D/L-Fos (196) under different pH conditions.....	148
3.2.2.1: NMR study of base-catalysed hydrolysis of β -chloro-L-Ala-D/L-Fos (196) ...	151
3.2.3: Attempted preparation of a phosphonodipeptide containing dehydroalanine and D/L-fosfalin	159
3.2.3.1: Synthesis of <i>tert</i> -butyl (3-((1-(diethoxyphosphoryl)ethyl)amino)-3-oxoprop-1-en-2-yl)carbamate or ^t Boc-dehydroala-D/L-Fos diethyl ester (206)	161
3.2.3.2: Attempted synthesis of 3-oxo-3-((1-phosphonoethyl)amino) prop-1-ene-2-aminium bromide or dehydroala-D/L-Fos hydrobromide (207)	162
3.2.4: Preparation of phosphonotriptides containing both β -chloro-L-alanine and D/L-fosfalin.....	167
3.2.4.1: Synthesis of <i>N</i> -protected dipeptide derivatives containing the β -chloro-L-alanine moiety (220b-c)	168
3.2.4.2: Synthesis of protected phosphonotriptides (221b-c) containing the β -chloro-L-Ala-D/L-fosfalin moiety	171
3.2.5: Preparation of phosphonotriptide, L-Met- β -chloro-L-Ala-D/L-Fos (225)	178

3.2.5.1: Synthesis of (2 <i>R</i>)-3-chloro-1-((1-(diethoxyphosphoryl)ethyl) amino)-1-oxopropan-2-aminium chloride or β-Cl-L-Ala-D/L-Fos diethyl ester hydrochloride (223)	179
3.2.5.2: Synthesis of <i>tert</i> -butyl ((2 <i>S</i>)-1-(((2 <i>R</i>)-3-chloro-1-((1-(diethoxyphosphoryl)ethyl)amino)-1-oxopropan-2-yl)amino)-4-(methylthio)-1-oxobutan-2-yl)carbamate or ^t Boc-L-Met-β-Cl-L-Ala-D/L-Fos diethyl phosphonate ester (224)	179
3.2.5.3: Synthesis of (1-((<i>R</i>)-2-((<i>S</i>)-2-ammonio-4-(methylthio)butanamido)-3-chloropropanamido)ethyl)phosphonic acid or L-Met-β-Cl-L-Ala-D/L-Fos (225)	181
3.3: Synthesis of dipeptide derivatives containing (PABA)	184
3.3.1: Synthesis of <i>C</i> -protected <i>para</i> -aminobenzoic acid, <i>tert</i> -butyl 4-aminobenzoate (229)	184
3.3.2: Published methods for the synthesis of amino acid-PABA derivatives	187
3.3.2.1: Synthesis of ^t Boc-L-Ala-PABA-O ^t butyl (232) and ^t Boc-β-chloro-L-Ala-PABA-O ^t butyl (233)	188
3.3.2.2: Synthesis of L-Ala-PABA (234) and β-chloro-L-Ala-PABA·TFA (235)	191
3.4: Conclusion	193
CHAPTER 4	194
MICROBIOLOGY TESTING	194
4.1: Introduction	195
4.2: Antibacterial activity of L-Ala-L-Ala-L-Fos (153a *) and L-Ala-L-Ala-D/L-Fos (153a)....	199
4.3: Antibacterial activity of L-Pyroglu-D/L-Fos (141), L-Nva-L-Ala-D/L-Fos (153b), Sar-L-Ala-D/L-Fos (153c) and L-Met-L-Ala-D/L-Fos (160)	202
4.4: Antibacterial activity of β-Cl-L-Ala-D/L-Fos (196), L-Nva-β-Cl-L-Ala-D/L-Fos (222b), Sar-β-Cl-L-Ala-D/L-Fos (222c) and L-Met-β-Cl-L-Ala-D/L-Fos (225)	208
4.5: Antibacterial activity of L-Ala-PABA (234) and β-Cl-L-Ala-PABA TFA salt (235)	213
4.6: Relationship between the physicochemical properties (logP and TPSA) and antibacterial activity of the tested compounds	217
4.7: Conclusion	220
CHAPTER 5	224
CONCLUSION AND FUTURE WORK	224
5.1: Conclusion	225
5.2: Future work	229

CHAPTER 6	231
EXPERIMENTAL.....	231
6.1: Chemistry.....	232
6.1.1: Reagents and instruments.....	232
6.1.2: Analytical instruments.....	232
6.1.3: Synthesis of D/L-fosfalin derivatives	233
6.1.3.1: 1-aminoethylphosphonic acid or D/L-fosfalin (13-DL).....	233
6.1.3.2: Diethyl (1-(2,2,2-trifluoroacetamido)ethyl)phosphonate or trifluoroacetyl-D/L-Fos diethyl ester (116).....	234
6.1.3.3: Diethyl 1-aminoethylphosphonate or D/L-Fos diethyl ester (84)	235
6.1.4: Synthesis of L-pyroglutamic acid derivatives	236
6.1.4.1: (S)-2-Benzyl 1- <i>tert</i> -butyl 5-oxopyrrolidine-1,2-dicarboxylate or ^t Boc-L-Pyroglu-OBzl (143)	236
6.1.4.2: (S)-1-(<i>Tert</i> -butoxycarbonyl)-5-oxopyrrolidine-2-carboxylic acid or ^t Boc-L-Pyroglu-OH (144)	237
6.1.5: General synthesis methods.....	238
6.1.5.1: Peptide coupling Method	238
6.1.5.2: Removal of benzyl ester protecting group under hydrogenation.....	238
6.1.5.3: Removal of <i>N-tert</i> -butoxycarbonyl protecting group under acidic conditions	239
6.1.5.4: Simultaneous removal of <i>tert</i> -butoxycarbonyl and diethyl phosphonate ester protecting groups from phosphonopeptides.....	239
6.1.6: Synthesis of L-Pyroglu-D/L-fosfalin (141)	240
6.1.6.1: (2S)- <i>Tert</i> -butyl 2-((1-(diethoxyphosphoryl)ethyl)carbamoyl)-5-oxopyrrolidine-1-carboxylate or ^t Boc-L-Pyroglu-D/L-Fos diethyl ester (145).....	240
6.1.6.2: (1-((S)-5-oxopyrrolidine-2-carboxamido)ethyl)phosphonic acid or L-Pyroglu-D/L-fosfalin (141)	241
6.1.7: Synthesis of phosphonotriptide derivatives containing L-Ala-D/L-Fos.....	242
6.1.7.1: (S)-Methyl 2-((S)-((<i>tert</i> -butoxycarbonyl)amino)propanamido) propanoate or ^t Boc-L-Ala-L-Ala-OMe (149a)	242
6.1.7.2: (S)-Benzyl 2-((S)-2-((<i>tert</i> -butoxycarbonyl)amino)pentanamido) propanoate or ^t Boc-L-Nva-L-Ala-OBzl (150b)	243

6.1.7.3: (S)-Benzyl 2-(2-((<i>tert</i> -butoxycarbonyl)(methyl)amino)acetamido) propanoate or ^t Boc-Sar-L-Ala-OBzl (150c)	244
6.1.7.4: (S)-Methyl 2-((S)-2-((<i>tert</i> -butoxycarbonyl)amino)propanamido) propanoic acid or ^t Boc-L-Ala-L-Ala-OH (151a)	245
6.1.7.5: (S)-2-((S)-2-((<i>Tert</i> -butoxycarbonyl)amino)pentanamido) propanoic acid or ^t Boc-L-Nva-L-Ala-OH (151b)	246
6.1.7.6: (S)-Benzyl 2-(2-((<i>tert</i> -butoxycarbonyl)(methyl)amino)acetamido) propanoic acid or ^t Boc-Sar-L-Ala-OH (151c)	247
6.1.7.7: <i>Tert</i> -butyl ((2S)-1-(((2S)-1-((1-(diethoxyphosphoryl)ethyl) amino)-1-oxopropan-2-yl)carbamate or ^t Boc-L-Ala-L-Ala-D/L-Fos diethyl ester (152a)	247
6.1.7.8: <i>Tert</i> -butyl ((2S)-1-(((2S)-1-((1-(diethoxyphosphoryl)ethyl) amino)-1-oxopropan-2-yl)amino)-1-oxopentan-2-yl)carbamate or ^t Boc-L-Nva-L-Ala-D/L-Fos diethyl ester (152b)	248
6.1.7.9: <i>Tert</i> -butyl (2-(((2S)-1-((1-(diethoxyphosphoryl)ethyl)amino)-1-oxopropan-2-yl)amino)-2-oxoethyl)(methyl)carbamate or ^t Boc-Sar-L-Ala-D/L-Fos (152c)	249
6.1.7.10: (1-((S)-2-((S)-2-Aminopropanamido)propanamido)ethyl) phosphonic acid or L-Ala-L-Ala-D/L-Fos (153a)	250
6.1.7.11: (1-((S)-2-((S)-2-Aminopentanamido)propanamido)ethyl) phosphonic acid or L-Nva-L-Ala-D/L-Fos (153b)	251
6.1.7.12: (1-((S)-2-(2-(Methylamino)acetamido)propanamido)ethyl) phosphonic acid or Sar-L-Ala-D/L-Fos (153c)	252
6.1.7.13: <i>Tert</i> -butyl ((2S)-1-((-1-(diethoxyphosphoryl)ethyl)amino)-1-oxopropan-2-yl)carbamate or ^t Boc-L-Ala-D/L-Fos diethyl ester (157)	253
6.1.7.14: (2S)-1-((1-(Diethoxyphosphoryl)ethyl)amino)-1-oxopropan-2-aminium chloride or L-Ala-D/L-Fos diethyl ester hydrochloride (158)	254
6.1.7.15: <i>Tert</i> -butyl ((2S)-1-(((2S)-1-((1-(diethoxyphosphoryl)ethyl) amino)-1-oxopropan-2-yl)amino)-4-(methylthio)-1-oxobutan-2-yl)carbamate or ^t Boc-L-Met-L-Ala-D/L-Fos diethyl ester (159)	255
6.1.7.16: (1-((S)-2-((S)-2-Amino-4-(methylthio)butanamido)propanamido)ethyl)phosphonic acid or L-Met-L-Ala-D/L-Fos (160)	256
6.1.8: Synthesis of β -chloro-L-alanine derivatives	257
6.1.8.1: (S)-Benzyl 2-((<i>tert</i> -butoxycarbonyl)amino)-3-hydroxy propanoate or ^t Boc-L-Ser-OBzl (178)	257
6.1.8.2: (<i>R</i>)-Benzyl 2-((<i>tert</i> -butoxycarbonyl)amino)-3-chloropropanoate or ^t Boc- β -Cl-L-Ala-OBzl (179)	258

6.1.8.3: (<i>R</i>)-2-((<i>Tert</i> -butoxycarbonyl)amino)-3-chloropropanoic acid or ^t Boc-β-Cl-L-Ala-OH (181)	259
6.1.8.4: (<i>R</i>)-1-(Benzyloxy)-3-chloro-1oxopropan-2-aminium chloride or β-Cl-L-Ala-OBzl hydrochloride (182)	259
6.1.9: Synthesis of β-chloro-L-Ala-D/L-fosfalin.....	260
6.1.9.1: <i>Tert</i> -butyl ((2 <i>R</i>)-3-chloro-1-((1-(diethoxyphosphoryl)ethyl) amino)-1-oxopropan-2-yl)carbamate or ^t Boc-β-chloro-L-Ala-D/L-Fos diethyl ester (195)	260
6.1.9.2: (1-((<i>R</i>)-2-Amino-3-chloropropanamido)ethyl)phosphonic acid, or β-chloro-L-Ala-D/L-Fos (196)	261
6.1.10: Synthesis of dehydroala-D/L-Fos hydrobromide.....	262
6.1.10.1: <i>Tert</i> -butyl (3-((1-(diethoxyphosphoryl)ethyl)amino)-3-oxoprop-1-en-2-yl)carbamate or ^t Boc-dehydroala-D/L-Fos diethyl ester (206).....	262
6.1.11: Synthesis of phosphonotripeptide derivatives containing the β-chloro-L-Ala-D/L-Fos moiety	263
6.1.11.1: (<i>R</i>)-Benzyl 2-((<i>S</i>)-2-((<i>tert</i> -butoxycarbonyl)amino)pentanamido)-3-chloropropanoate or ^t Boc-L-Nva-β-chloro-L-Ala-OBzl (219b)	263
6.1.11.2: (<i>R</i>)-Benzyl 2-(2-((<i>tert</i> -butoxycarbonyl)(methyl)amino) acetamido)-3-chloropropanoate or ^t Boc-Sar-β-chloro-L-Ala-OBzl (219c)	264
6.1.11.3: (<i>R</i>)-2-((<i>S</i>)-2-((<i>tert</i> -Butoxycarbonyl)amino)pentanamido)-3-chloropropanoic acid or ^t Boc-L-Nva-β-chloro-L-Ala-OH (220b)	265
6.1.11.4: (<i>R</i>)-2-(2-((<i>tert</i> -butoxycarbonyl)(methyl)amino)acetamido)-3-chloropropanoic acid or ^t Boc-Sar-β-chloro-L-Ala-OH (220c)	266
6.1.11.5: <i>Tert</i> -butyl ((2 <i>S</i>)-1-(((2 <i>R</i>)-3-chloro-1-((1-(diethoxyphosphoryl)-ethyl)amino)-1-oxopropan-2-yl)amino)-1-oxopentan-2-yl)carbamate or ^t Boc-L-Nva-β-chloro-L-Ala-D/L-Fos diethyl ester (221b)	267
6.1.11.6: <i>Tert</i> -butyl (2-(((2 <i>R</i>)-3-chloro-1-((1-(diethoxyphosphoryl)ethyl) amino)-1-oxopropan-2-yl)amino)-2-oxoethyl)(methyl)carbamate or ^t Boc-Sar-β-chloro-L-Ala-D/L-Fos diethyl ester (221c).....	268
6.1.11.7: (1-((<i>R</i>)-2-((<i>S</i>)-2-Ammoniopentanamido)-3-chloropropanamido)ethyl)phosphonic acid or L-Nva-β-chloro-L-Ala-D/L-Fos (222b)	269
6.1.11.8: 1-((<i>R</i>)-3-Chloro-2-(2-(methylammonio)acetamido)propanamido)ethyl)phosphonic acid or Sar-β-chloro-L-Ala-D/L-Fos (222c)	270
6.1.11.9: (2 <i>R</i>)-3-Chloro-1-((1-(diethoxyphosphoryl)ethyl)amino)-1-oxopropan-2-aminium chloride or β-Cl-L-Ala-D/L-Fos diethyl ester hydrochloride (223).....	271

6.1.11.10: <i>Tert</i> -butyl ((2 <i>S</i>)-1-(((2 <i>R</i>)-3-chloro-1-((1-(diethoxyphosphoryl) ethyl)amino)-1-oxopropan-2-yl)amino)-4-(methylthio)-1-oxobutan-2-yl) carbamate or ^t Boc-L-Met-β-CI-L-Ala-D/L-Fos diethyl ester (224)	272
6.1.11.11: (1-((<i>R</i>)-2-((<i>S</i>)-2-Ammonio-4-(methylthio)butanamido)-3-chloro propanamido)ethyl)phosphonic acid or L-Met-β-CI-L-Ala-D/L-Fos (225)	273
6.1.12: Synthesis of dipeptides containing <i>para</i> -aminobenzoic acid (PABA) derivatives	274
6.1.12.1: <i>Tert</i> -butyl 4-aminobenzoate or PABA-O ^t Butyl (229)	274
6.1.12.2: (<i>S</i>)- <i>Tert</i> -butyl 4-(2-((<i>tert</i> -butoxycarbonyl)amino)propanamido)-benzoate or ^t Boc-L-Ala-PABA-O ^t Butyl (232)	275
6.1.12.3: (<i>R</i>)- <i>Tert</i> -butyl 4-(2-((<i>tert</i> -butoxycarbonyl)amino)-3-chloro-propanamido)benzoate or ^t Boc-β-chloro-L-Ala-PABA-O ^t Butyl (233)	275
6.1.12.4: (<i>S</i>)-4-(2-Ammoniopropanamido)benzoic acid or L-Ala-PABA (234)	276
6.1.12.5: (<i>R</i>)-1-((4-Carboxyphenyl)amino)-3-chloro-1-oxopropan-2-aminium 2,2,2-trifluoroacetate or β-chloro-L-Ala-PABA·TFA (235)	277
6.2: LC-MS analysis	278
6.2.1: LC-MS conditions for diastereoisomeric phosphonopeptides analysis (153a , 153b , 153c , 160 , 196 , 222b , 222c and 225)	278
6.2.2: LC-MS conditions for diastereoisomeric ^t Boc-L-Ala-L-Ala-D/L-Fos diethyl ester (152a) and PABA based dipeptides analysis (234 and 235) analyses	278
6.3: Stability study	279
6.3.1: Reagents and instruments	279
6.3.2: Sample preparation	279
6.3.3: Sample analysis	279
6.4: Microbiological testing	280
6.4.1: Media constituents	280
6.4.2: Microbial strains	280
6.4.3: Preparation of antagonist-free (AF) medium	281
6.4.4: Preparation of media containing suicide substrates	282
6.4.5: Multipoint inoculation of agar	282
6.4.6: Determination of minimum inhibitory concentration (MIC)	283
CHAPTER 7	284

REFERENCES	284
7.1: Journals/Articles	285
7.2: Books.....	297
7.3: Theses.....	298
7.4: Patent	298
7.5: Webpages.....	298
CHAPTER 8	300
APPENDICES.....	300

CHAPTER 1

INTRODUCTION

1.1: Background

Bacteria are microscopic prokaryotic microorganisms that are unable to be seen by the naked eye. They exist everywhere where life is known and their presence can be classified into non-harmful and harmful bacteria. Commensal bacteria are generally non-harmful and co-exist with the host. These bacteria may, in some instances, provide benefits to the host. For instance, the commensal bacteria that are present in the human gastrointestinal tract improve the extraction and synthesis of nutrients and other metabolites from ingested food that are essential for humans (2013NI676). The intestinal flora prevents overgrowth of *C. difficile*, which is usually a minor presence in the human intestine, and may lead to colonic infection (2010EID674). However, commensal bacteria can be harmful if they are not present in an appropriate place. For instance, *S. aureus* is a usually benign commensal bacterium that is found on the human skin, but becomes infectious if it invades the bloodstream.

Pathogenic bacteria are harmful bacteria that cause severe diseases or illness to the hosts. They can be spread through the human population *via* a variety of routes, such as air, water, food, soil, medical equipment or through human physical contact. For instance, some cases of respiratory tract infections caused by *P. aeruginosa* were reported to be due to a non-sterile ultrasound gel used for trans-esophageal echocardiography, a technique that produces pictures of the heart (2012MMWR262). These contagious bacteria have become a huge challenge over recent decades in the medical and food industries, especially their ability to grow exponentially and to develop strains with resistance towards treatment and antibiotics.

For instance, the emergence of bacterial resistance towards carbapenems, a class of antibiotics formerly used for severe pathogenic infections that were unresponsive to other treatments (2012JACS18275), has been reported in the US, Greece and Israel (2009JAA105) (2009LID228). On average, approximately 23,000 people die each year due to antibiotic-resistant bacteria (2007JAMA1763). The first of the recent O'Neill reports estimate there will be 300 million additional deaths globally due to antibiotic-resistant bacteria by 2050 at an economic cost of

\$60-100 trillion USD (2014RAR1). The emergence of multi-drug resistant bacteria was also reported, where 20-30 % of extended-spectrum beta-lactamase (ESBL) strains are not susceptible to third-generation cephalosporins (2006AJM20). Apart from bacteria, the resistance of mycobacteria was also reported. For instance, multi-drug resistant *Mycobacterium tuberculosis* were found in the UK, Italy, Iran and India (2012CW48). This widespread resistance has drawn serious attention from the World Health Organization (WHO), especially over the most frequent multi-drug resistant bacteria, such as *E. faecium*, *S. aureus*, *K. pneumoniae*, *A. baumannii*, *P. aeruginosa* and *Enterobacter spp.*, which are simplified as a group of pathogens with the acronym ESKAPE (2011CC215).

Many investigations have been carried out in order to understand and reduce bacterial resistance. There are several common bacterial resistance mechanisms reported, represented in the diagram as follows, Figure 1.1 (1991NEJM601) (2011FIM1).

- i. Ineffective penetration of antibiotics across the bacterial cell, which restricts access to target binding sites
- ii. Presence of an active pump that eliminates antibiotics from the cell
- iii. Lack of affinity between antibiotics and target binding sites due to alteration to the binding sites
- iv. Presence of antibiotic hydrolysis enzymes, such as β -lactamases, macrolide esterases and epoxidases that are responsible for the hydrolysis of β -lactam antibiotics (2004CMLS2200), e.g. penicillins and cephalosporins; macrolide antibiotics (1999JIC61), e.g. erythromycin; and epoxide antibiotics (2003JACS15730), e.g. fosfomycin
- v. Presence of antibiotic modification enzymes, such as acyltransferases, phosphotransferases, thioltransferases, nucleotidyltransferases, ADP-ribosyltransferases and glycosyltransferases that are responsible for the group transfer and covalent modification of the structure of antibiotics for their impaired target binding (2005ADDR1451)
- vi. Over-production of target binding sites
- vii. Acquisition of alternative metabolic pathways

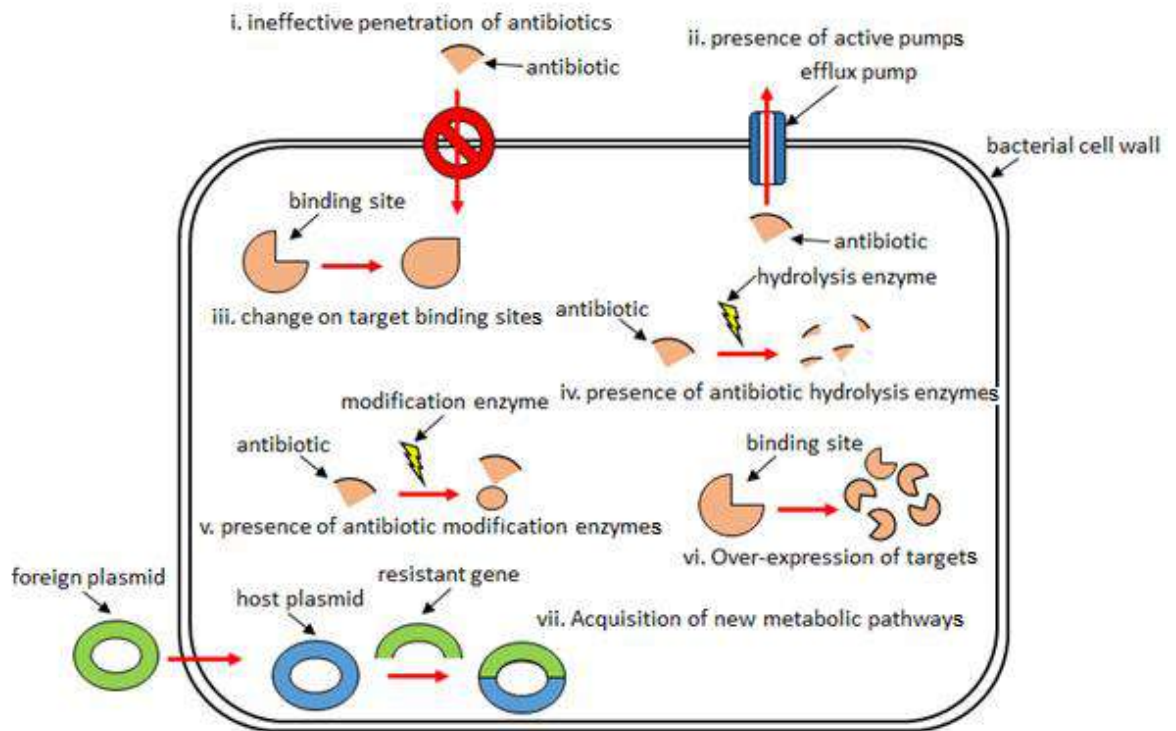


Figure 1.1: Summary of antibiotic resistance mechanisms

These resistance mechanisms (Figure 1.1) can be attained by resistant bacteria either through intrinsic or acquired routes. The intrinsic route refers to bacteria with natural resistance mechanisms that are thought to be present already when humans first started to exploit antibiotics. Examples of bacteria with intrinsic resistance towards antibiotics are summarised in Table 1.1. Acquired resistance, on the other hand, is gained by bacteria from gene mutation, genes transferred from other resistant bacteria, or a combination of these two mechanisms. Unlike intrinsic resistance, the acquired resistance traits are only found in some instances of each bacterial species. These acquired antibiotic resistance genes, found in different bacterial species with their respective resistant mechanisms were recently reviewed by van Hoek and co-workers (2011FIM1).

Table 1.1: Examples of reported intrinsic-resistant bacteria and their respective mechanisms (B-2007MI182) (B-2013MI3)

Species	Resistance against	Mechanism
Aerobic bacteria	Metronidazole	Unable to reduce antibiotic to its active form
Gram-positive bacteria	Aztreonam	Lack of affinity binding to penicillin binding proteins (PBPs) (2004IP359,1990SGO S19)
Gram-negative bacteria	Vancomycin	Ineffective penetration across the cell membrane
<i>Klebsiella spp.</i>	Ampicillin	Presence of β -lactamases
<i>S. maltophilia</i>	Imipenem	Presence of carbapenamases
<i>Lactobacillus</i> and <i>Leuconostoc</i>	Vancomycin	Lack of target binding site due to peptidoglycan precursor terminating in D-alanyl-D-lactate instead of D-alanyl-D-alanine (1994JB260)
<i>P. aeruginosa</i>	Sulfonamides, trimethoprim, tetracyclines and chloramphenicol	Ineffective penetration across the cell membrane
Enterococci, particularly <i>E. faecalis</i> and <i>E. faecium</i>	All cephalosporins	Lack of affinity binding to PBPs (2012V421)

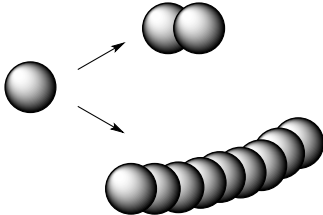
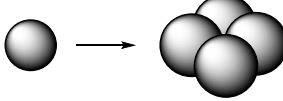
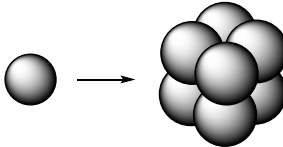
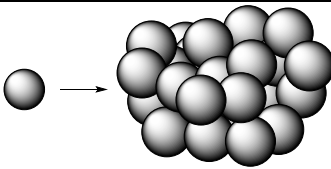




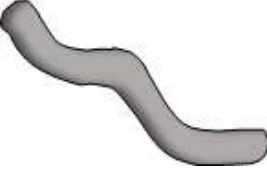

1.2: The Need for Bacterial Identification

Although this widespread resistance can be attained *via* intrinsic or acquired routes, other resistance-causing factors, such as inappropriate use of antibiotics in hospital, can be prevented with the aid of reliable diagnostic tools. A fast, accurate and reliable bacterial detection and identification tool is not only able to identify the disease-causing bacteria, but also to determine the suitable antibiotic or dosage needed in order to achieve the therapeutic effects, while reducing the creation of antibiotic resistant bacteria. A knowledge of bacterial morphology, cell structure and biosynthesis activities is essential in order to understand how the detection methods work and also to aid in choosing the appropriate methods for different detection needs.

1.2.1: Bacterial morphology

In a similar manner to other living organisms, bacterial species exist with a distinct morphology and therefore can be visually differentiated based on their different shape, size, and arrangement. Bacteria exist in three common shapes: spherical or ball shaped, known as cocci; rod or cylindrical shaped, known as bacilli; and a shape with two or more bacteria twisted along an axis, known as spiral. The size of spherical bacteria is 0.5-3.0 μm , while the size of the cylindrical bacteria is 0.15-2.0 μm in width and 0.5-20 μm in length (WS-1). Different arrangements of each shape are known and each is named differently (Table 1.2).

Table 1.2: Common arrangements of each different shape of bacteria

Shape	Arrangement*	Description
Cocci		Diplococci: cocci divide into pairs Streptococci: cocci divide into chain
		Tetrads: cocci divide into groups of four
		Sarcinae: cocci divide into groups of eight
		Staphylococci: cocci divide into clusters
Bacilli		Diplobacilli: bacilli divide into pairs
		Streptobacilli: bacilli divide into chains
		Coccobacilli: bacilli appear short and similar in shape to cocci
Spiral		Vibrio: spiral appear like curved rods
		Spirillum: spiral appear helical in shape with fairly rigid bodies
		Spirochetes: spiral appear helical in shape with flexible bodies

Diagrams were adapted from: <http://classes.midlandstech.edu/carterp/courses/bio225/chap04/lecture2.htm>
 (WS-2)

1.2.2: Bacterial cell structure

Bacteria are unicellular, indicating an organism that lives in as a single cell without the presence of a nucleus. Despite their structural simplicity, they contain many different organelles that play an important role for cell survival. The structure of the bacterial cell and the function of each component are shown in Figure 1.2 and Table 1.3, respectively.

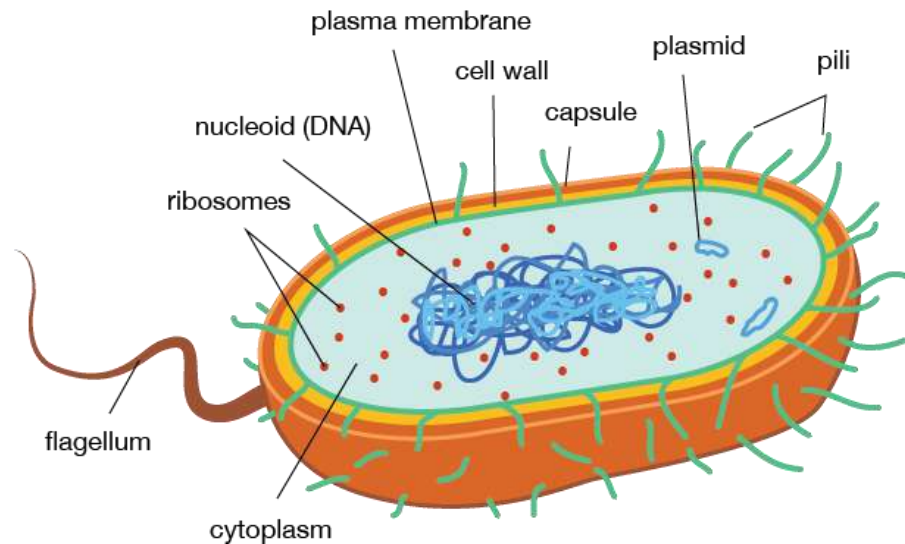


Figure 1.2: Simplified representation of a bacterial cell

Diagram was reproduced from <http://www.shmoop.com/biology-cells/prokaryotic-cells.html> with permission from the Shmoop Editorial Team (WS-3)

Table 1.3: Components and their function in bacterial cells

Component	Function
Nucleoid	Double-stranded DNA containing genetic information for the cell
Plasmid	Small circular double-stranded DNA containing genetic information that replicates independently and can be transferred from one cell to another
Ribosomes	Conduct protein synthesis by translating messages sent from DNA
Pili	Facilitate communication between cells by forming a channel (bacterial conjugation)
Flagellum	Facilitates bacterial movement (only found in some bacteria)
Cell wall	Provides rigidity to the cell and protects the cell from potentially harsh osmotic environments
Plasma membrane	Phospholipid bilayer serves as a permeability barrier for the transport of molecules into and out of the cell
Cytoplasm	Fluid-like substance inside the plasma membrane where organelles float within it
Capsule	Layer of protection that prevents phagocytosis by macrophages, dryness and hydrophobic toxic materials.

1.2.3: Gram staining

The bacterial cell wall is important for bacteria. It helps to maintain specific concentrations of specific ions within the cell and protect the cell from osmotic equilibrium. This is required for survival in the environment. In addition, the cell wall acts as a defence, limiting the passage of any foreign substances into the cell. The structural differences of the cell wall divide the bacteria into two groups, Gram-positive bacteria and Gram-negative bacteria, due to their different coloured appearance upon Gram staining. Gram-positive bacteria have higher peptidoglycan, less lipid and a thicker cell wall than Gram-negative bacteria; therefore, each group of bacteria retains colour differently upon Gram staining.

The Gram staining method was developed by Hans Christian Gram in 1884 for bacterial identification. The bacteria are first isolated from a sample and then stained with crystal violet (1) or methylene blue (2). Iodine is subsequently added to form a crystal violet-iodine complex to fix the colouration, known as dye fixation. At this stage, both Gram-positive and Gram-negative bacteria are stained purple. The dye is later decolourised using ethanol, which dissolves the lipid layer that binds with the complex (dye). Gram-negative bacteria contain more lipids; therefore, the purple dye is removed along with the lipid and solvent. Gram-positive bacteria are less affected, retain the dye, and thus remain purple. In order to enhance the visualisation of the colourless colonies, a counter dye (safranin, 3) is used, which results in pink staining of Gram-negative bacteria. The summary of this staining method is shown in Figure 1.3. Apart from the cell wall being important in rigidity, osmotic maintenance and self-defence, it also assists in basic bacterial identification due to different outer layer compositions. A brief discussion of Gram-positive and Gram-negative bacteria is presented in the following section.

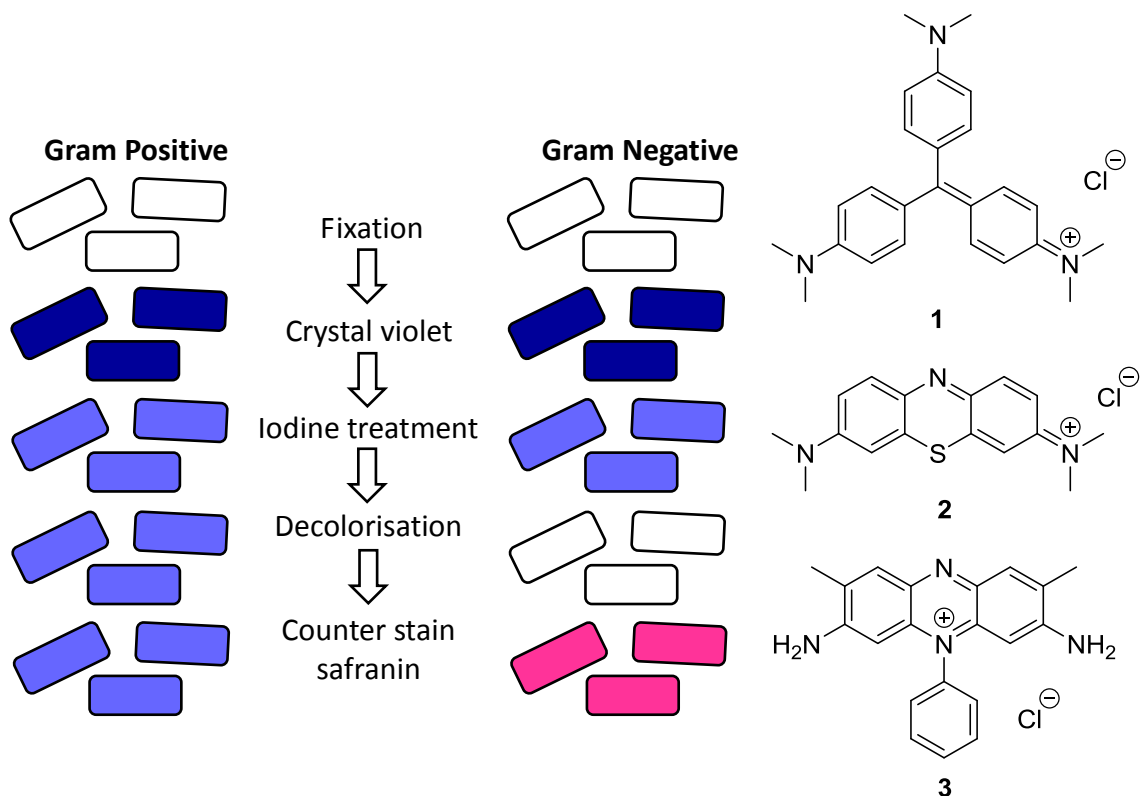


Figure 1.3: Summary of Gram staining method and different colour development in each step. Dye structures: crystal violet (1), methylene blue (2), safranin (3)

Diagram was adapted from <http://gmgmesjwk.pbworks.com/f/gram-stain.jpg> (WS-4)

1.2.3.1: Gram-positive bacteria

Gram-positive bacteria are surrounded by the plasma membrane with a thick cell wall containing peptidoglycan, lipoteichoic acid and teichoic acid. *N*-Acetylglucosamine (NAG) and *N*-acetylmuramic acid (NAM) are sugar residues that are linked together to form polymers. A tetrapeptide, containing L-Ala, D-Glu, L-Lys and D-Ala residues is linked to the sugar polymer *via* the NAM carboxylic acid residue (2006PNAS4404), forming a peptidoglycan subunit. Each subunit then cross-links to another with the aid of a pentaglycine bridge (five glycine residues), catalysed by peptidoglycan transpeptidase, forming the rigid cell wall structure. The Gram-positive bacterial cell wall and peptidoglycan structure are shown schematically in Figure 1.4.

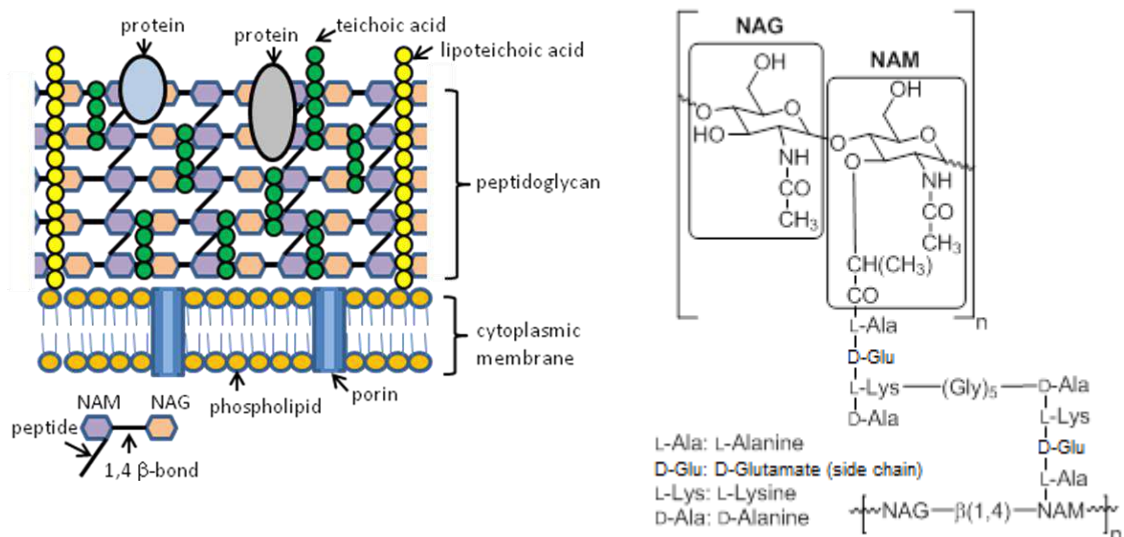


Figure 1.4: Representative diagram of Gram-positive bacterial cell wall (left) and peptidoglycan structure (right) (2010NRM890)

Diagram (left) was adapted from <http://www.studyblue.com/notes/note/n/bacteria-structure-and-function/deck/3870396> (WS-5)

Teichoic acids are covalently linked to the sugar backbone (NAM-NAG) and provide cell wall rigidity by preventing hydrolysis of the $\beta(1-4)$ bond between the NAM and NAG. A recent study showed that teichoic acids play important roles in cell shape determination, regulation of cell division and antibiotic resistance, thus their biosynthesis has become a target for new antimicrobial development (2013ARM1). Teichoic acids that are linked to lipids are known as lipoteichoic acids.

As a result of the relatively simple cell wall structure, Gram-positive bacteria possess a relatively permeable cell wall, depending on the complexity of the peptidoglycan layer and its cross-linking units. The relatively easy penetration across the cell wall and its distinct composition, including the teichoic acids only found on the Gram-positive bacteria, are beneficial in the design of both antimicrobial agents and bacterial detection strategies.

1.2.3.2: Gram-negative bacteria

The Gram-negative cell wall is much more complicated than the Gram-positive structure, as shown in Figure 1.5. Unlike the Gram-positive cell wall, teichoic acids are absent from the cell wall. Instead, lipid A, O-antigen polysaccharide side chains and porins are found. The lipid A is linked to the polysaccharide and O-antigen side chain. This combination is known as lipopolysaccharide (LPS), which is generally considered to be an endotoxin and potentially causes severe damage to the host cell or host immune system through systemic inflammation (2012AR2337). Although O-antigen polysaccharide side chain is only found in Gram-negative bacteria, it varies among some of these species. For instance, different strains of *Klebsiella* serotypes were reported to have different O-antigen polysaccharide side chain structure (1992JB4913).

This extra outer membrane not only differentiates the Gram-negative bacteria from the Gram-positive bacteria, but poses an extra barrier of defence from any foreign substances (e.g. antibiotics, hydrophilic molecules) crossing the cell. A thin layer of peptidoglycan is found sitting between the outer membrane and the cytoplasmic membrane. The thin peptidoglycan layer reflects a change of its structural characteristic, in which the L-Lys residue is replaced with *meso*-diaminopimelate (4) as compared to the Gram-positive peptidoglycan layer (Figure 1.5). A loss of the pentaglycine bridge is also observed. As a result of this more complicated cell wall, there are more considerations to be made for the design of antimicrobial agents for Gram-negative bacteria compared to Gram-positive bacteria.

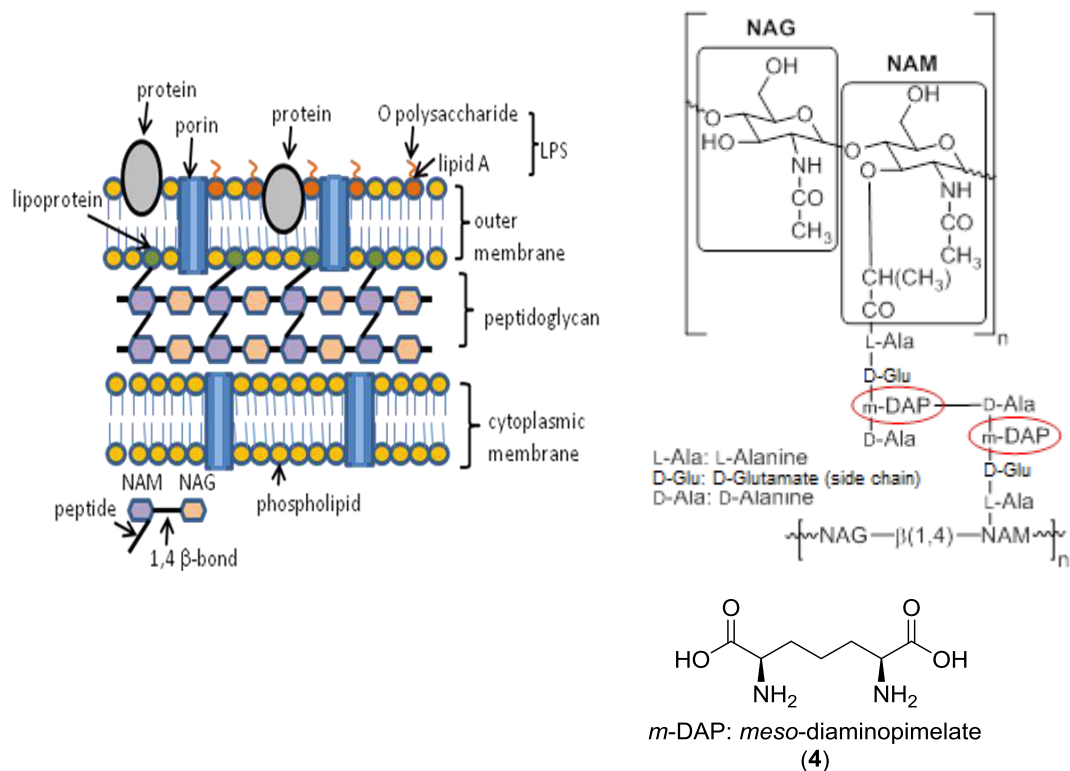


Figure 1.5: Representative diagram of Gram-negative bacterial cell wall (left) and peptidoglycan structure with the replacement of L-Lys residue with *m*-DAP (4) highlighted in red (right) (2007NRM264) (2005CMR521)

Diagram (left) was adapted from <http://www.studyblue.com/notes/note/n/bacteria-structure-and-function/deck/3870396> (WS-5)

1.3: Bacterial detection and identification

The periodic emergence of new drug resistant bacteria and the existence of pathogenic bacteria elevate the need for accurate and reliable bacterial detection and identification. The properties of bacterial cells, as discussed earlier, highlight the differences, such as morphology and cell structure, which serve as good targets for bacterial differentiation, detection and identification. Target specificity, selectivity, time and cost are important aspects in developing or designing bacterial detection methods. There are a number of rapid detection methods that have been developed since the Gram-staining era, in order to fulfil the above mentioned criteria. There are many current bacterial detection methods available, covering both conventional and sophisticated instrumental methods, such as microscopic, immunological, genetic and biochemical (B-2008MI31).

1.3.1: Microscopic techniques

1.3.1.1: Light microscopy and electron microscopy

There are two types of microscopic technique, light and electron microscopy commonly used for bacterial identification.

A light microscope is used to visualise cell and colony morphology, and to perform cell counting. Staining is often required in order to improve the resolution of the samples under the microscope. Basic dyes, such as crystal violet (1) and methylene blue (2) are often considered due to their high binding affinity with the surface of the cells and good visualisation upon staining (B-2006MI56). This simple staining, however, is unable to differentiate the type of bacteria within a class, whether Gram-positive, Gram-negative bacteria or both are present in a sample, due to all of the cells being stained with the same colour. Therefore, the Gram stain method is often used along with the light microscope. Based on the morphology and colour differences subsequently viewed under the microscope, the bacteria can be readily identified as Gram-positive or Gram-negative. An electron microscope, on the other hand, is able to provide cell detail at great depth; therefore, it is used to visualise internal structures of the cell, such as the sub-cellular components. The morphology and sub-cellular component details enable the identity of the bacteria to be determined.

The microscopic technique is time-consuming and costly, due to the lengthy preparation required when Gram staining, the lengthy processing time needed to view each sample slide individually and the requirement for trained personnel for verification. Even though the differentiation of Gram-positive and Gram-negative bacteria can be achieved upon Gram staining, the specific strain of each bacterial sample is unable to be identified.

1.3.1.2: Flow cytometry

Flow cytometry is an automated fluorescence microscopy technique. Unlike other microscopes, the sample used is not fixed or static when viewed under the microscope, but is injected into fluid which passes through the sensing region of the flow cell (Figure 1.6). In flow cytometry, sample pre-treatment steps are required, involving isolation of the cell, denaturation of DNA and labelling, prior to injection into the flow cytometer. The cells are usually labelled by immunofluorescent antibodies linked to fluorophore conjugates, while denatured DNA is labelled by peptide nucleic acid (PNA) probes conjugated to fluorophores. The antibodies recognize a target feature on the cell and bind specifically, depending on the cell antigens being targeted, while the PNA probes bind complementary to the denatured DNA. Each stained cell with its labelled DNA is then carried by the laminar flow of water to the sensing region, where the excitation light can be absorbed by the fluorophore conjugate. Different pulses of fluorescence are generated upon passing through the sensing region and the scattered light is collected by the detectors and later interpreted by a computer. The amount of light scattering generated is depending on the size of a cell, shape and structure, thus providing the detailed information about the cells, such as their cell mass and bacterial growth (B-1990MI105).

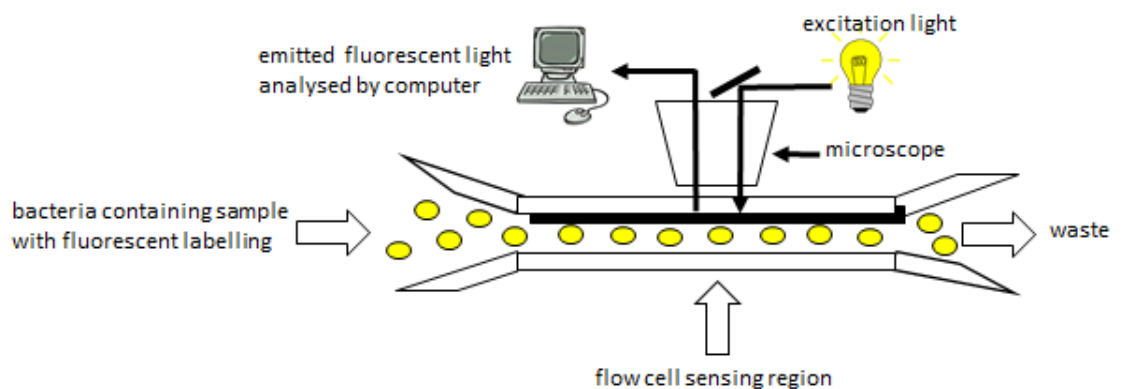


Figure 1.6: Schematic representation of basic flow cytometry using immunofluorescent
Diagram was adapted from B-1990MI105

The use of flow cytometry is rapid compared to other microscopic techniques; however, it is less frequently used in bacterial detection than for eukaryotic cell detection, due to the small size of bacteria and the presence of a low number of

DNA molecules, which complicates the staining (as sensitive detection is required). In addition, bacterial reproducibility under defined growth conditions is required in order to generate consistent data, as the bacterial characteristics vary depending on the growth conditions used (B-1993MI27).

1.3.2: Immunological techniques

1.3.2.1: Enzyme-linked immunosorbent assay (ELISA)

Enzyme-linked immunosorbent assays (ELISA) are immunological assays that use antibodies and an enzyme-mediated colour change to detect the presence of either an antigen or antibody in a sample. ELISA is useful in detecting antigens or antibodies present in small quantities or low concentrations in a sample, which is an added advantage in bacterial detection. This technique involves multiple washing steps and addition of different antibodies, as summarised in Figure 1.7.

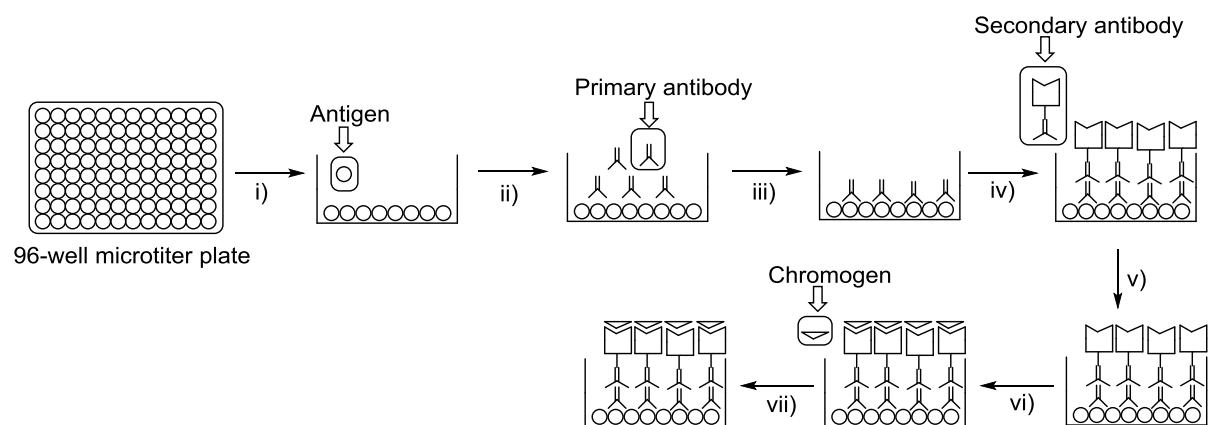


Figure 1.7: Representation of steps involved in enzyme-linked immunosorbent assay (ELISA) technique

Diagram was adapted from 2013JID1

Step: i) Sample containing antigens is added to the ELISA plate coated with antibody; ii) Primary antibody is added; iii) Unbound primary antibodies are washed off the plate; iv) Secondary antibody-conjugated with an enzyme is added; v) Excess secondary antibodies are washed off the plate; vi) Enzyme specific substrate (chromogen) is added; vii) Enzymatic reaction produces colour with intensity correlating to the level of antigen

Despite the low concentration needed for ELISA, a sample enrichment step (bacterial cell growth) is still required to generate a sufficient level of antigens produced by the targeted bacteria. The enriched sample containing antigen is added to the plate coated with specific and known antibody on the well surface. The unbound antibody on the well is blocked using bovine serum albumin, while the unbound antigen is washed off from the well. A specific primary antibody is added to bind to the antigen, while the non-antigen bound antibody is washed away. The secondary antibody, conjugated with an enzyme is added and the unbound secondary antibody is washed off. The enzyme reacts with a chromogenic substrate that is added, releasing the chromogen and causing colour production. The intensity of the colour change is measured spectrophotometrically to determine the bacterial antigen quantitatively or qualitatively.

The ELISA technique is useful to detect specific bacteria present in low concentrations. However, this specificity is only achieved through binding with the reciprocal antigen or antibody. Therefore, a known reciprocal antigen or antibody must be generated. False results will be generated due to the non-specific binding of antigen or antibody. Sample enrichment involving bacterial culture is required (for low concentrations of a given bacterial sample), which is time-consuming. Expensive instrumentation, software and reagents, as well as training are required for this technique.

There are other immunoassays also used in bacterial detection; for instance, bacterial concentration fluorescence immunoassays (BCFIA) were used to detect periodontopathic bacteria, *P. gingivalis*, *B. intermedius*, *A. actinomycetemcomitans*, *F. nucleatum* and *E. corrodens* (1991JCM1645; 1992JP1093). The principle of this method is similar to ELISA; however, with BCFIA, bacterial lipopolysaccharide is targeted by the specific antibodies and detection was fluorescence rather than colour.

1.3.3: Genetic techniques

1.3.3.1: Polymerase chain reaction (PCR)

Polymerase chain reaction (PCR) is a technique used to amplify a DNA fragment *via* enzymatic replication and it can be used for bacterial detection. Conventionally, the products of amplified DNA (amplicons) are separated on an agarose gel, then stained and the resulting fluorescent DNA bands are visualised. The DNA bands show the presence of the bacteria of interest after comparing with a specific DNA biomarker. This method, however, is time-consuming, due to the DNA separation step required, and only can be performed at the end of DNA amplification. Therefore, real-time PCR is often considered instead, as this technique allows the detection of amplicons while they are being formed.

In real-time PCR, a sample containing bacteria is initially cultured using non-selective enrichment broth. These bacteria are lysed to release their DNA, later mixed with DNA polymerase, nucleotides, specific primers and a non-specific fluorescent dye. The mixture is subjected to repeated heating and cooling in the automated PCR device. The DNA is denatured during heating, releasing two single-stranded DNA molecules. During cooling, the specific primers bind complementarily only to each target single-stranded DNA. Throughout the repeated heating and cooling cycles, multiple copies of the DNA (amplicons) are created to which the fluorescent dye is bound. Once the amplification is complete, the double-stranded DNAs are denatured at elevated temperature, resulting in the release of dye and thus a decrease in the fluorescent signal. The change of fluorescence signal is interpreted by the computer to determine the presence of specific bacteria in the sample. The use of this technique in *Salmonella* bacterial detection was published in 2005 (B-2008MI31).

Apart from real-time PCR, the use of rapid multiplex PCR (m-PCR) has also been reported for bacterial detection. According to Kong and his co-workers (2002WR2802), a sample containing six different types of bacteria, *S. flexneri*, *A. hydrophila*, *Y. enterocolitica*, *S. typhimurium*, *V. cholerae* and *V. parahaemolyticus* were detected simultaneously using m-PCR. This method is similar to the use of conventional PCR method as described above, but it uses more than one type of

primer and each primer is attached with a quencher and a specific fluorescent tag, to detect multiple bacterial species.

In general, the PCR methods are very sensitive and reliable. However, advanced knowledge of bacterial species present in the sample is essential, to decide specific primers to be used in the DNA amplification. Other drawbacks of using this technique are requirement of pure sample (DNA), instrumental cost and training (1996IJFM103).

1.3.3.2: Mass spectrometry (MS)

Mass spectrometry is an analytical tool that produces unique insight into the atomic and molecular composition of a sample; additional information can be achieved due to molecule fragmentation, which takes place within the MS. Components found in individual bacteria serve as good biomarkers to identify the bacteria, such as DNA, lipids and proteins. These components can be analysed by two types of MS, matrix-assisted laser desorption ionisation MS (MALDI MS) and electrospray ionisation MS (ESI MS). However, the use of ESI MS is less favourable, due to clogging of the electrospray needle during analysis of intact bacterial cells and the generation of complex MS spectra (2013IJMS67).

The first use of MALDI MS with the aid of PCR was introduced by Hurst in 1996, for detection of bacterial DNA (1996RCMS377). Using this technique, the Gram-negative bacteria *Legionella* were detected upon successfully identifying the presence of 108- and 168-base DNA biomarkers in negative ion mode, using 3-hydroxypicolinic acid as a matrix. The specific genes of *Methylosinus* and *Methylomicrobium* were also detected using a similar approach (1998AC2693). However, the detection of DNA using MALDI MS is limited due to the acidic matrices, which denature the double stranded DNA (1999AC2334), as well as causing fragmentation of the phosphate backbone during MALDI ionisation (2002JCB73). As a result, DNA is often transcribed to the RNA form prior to this analysis, as the RNA molecule is less fragmented (1994NAR3866) and more stable to MALDI ionisation (2013IJMS67). The use of this technique relies heavily

on the use of PCR, which poses some disadvantages as discussed previously (see 1.3.3.1).

The presence of abundant lipid and lipopolysaccharide in bacteria has led to further exploration using MALDI MS analysis. This technique was first performed by Heller in 1987 to measure laser desorption mass spectra of polar lipids in the presence of potassium chloride, when it was used to differentiate *E. coli* and *B. subtilis* based on their different lipid mass fingerprints (1987BBRC194). The different phospholipids are ionised differently in the MS, depending on the polar head of the molecule. The analysis of lipid, however, is less favourable, due to the ionisation of some phospholipids being hindered by strong suppression effects, especially in the positive ion mode. The suppression is caused by the presence of less volatile compounds that can influence the efficiency of droplet evaporation, which in turn affects the amount of charged ion that eventually reaches the detector (2003CC1041).

Aside from the analysis of DNA and lipid, identification of bacteria by their different protein compositions can also be performed by MALDI MS as well. For example, the protein profiling mass spectra generated from different bacterial cell lysates were established by Cain in 1994 for bacterial differentiation (1994RCMS1026). Recently, the use of intact bacterial cells has become common, providing sufficient information to specify the bacteria (2001MSR172). The signals detected from the intact cell were mostly originated from the ribosomal proteins (2001AC746). In this analysis, a high molecular mass region is monitored, instead of a specific molecular mass peak, matching the fingerprint groups of signals produced by the different strains of bacteria. Since the spectra obtained from different intact cells were reproducible under defined growth conditions, the establishment of a spectra database to facilitate bacterial identification was possible. Currently, there are three identification databases available: Bruker BioTyper, SARAMIS by AnagnosTec GmbH and Andromas by Andromas SAS (2013IJMS67).

The use of MALDI MS protein profiling for bacterial identification, however, is still challenging and low quality MS spectra were reported when dealing with Gram-positive bacteria (2011JCM2868). This is due to the nature of the thick

peptidoglycan cell wall, which disrupts the ionisation process and prevents a sufficient number of proteins from undergoing ionisation. As a result, additional steps or time-consuming sample pre-treatment is required, including disruption of cell wall and protein extraction prior to MALDI MS analysis. Although MALDI MS is reliable, accurate and its automation allows for possible routine analysis, a rapid analysis can only be achieved if these problems are overcome. In addition, MS instruments are very expensive pieces of equipment to acquire and maintain, and extensive training is required prior to handling.

1.3.4: Biochemical techniques

In general, the bacterial identification techniques discussed previously rely on specific staining or labelling of the essential components (cell wall, antigens, DNA, protein or lipid) on the target cell. However, these techniques are generally limited to non-routine use and they also pose other disadvantages, with the main reasons being cost and time. Biochemical tests, on the other hand, are able to overcome these problems by offering low-cost, well-designed kits that can be handled by non-specialised personnel.

The different biochemical characteristics of specific bacteria, such as the presence of certain characteristic enzymes, offer an alternative in bacterial identification. In other words, different bacteria can be differentiated by targeting the different enzymes present in the bacteria. For instance, catalase is an enzyme that induces the reduction reaction of hydrogen peroxide into water and oxygen. Differentiation between Streptococcaceae (catalase positive) and Micrococcaceae (catalase negative) can be achieved through the catalase test (1998CMR318). Visual indicators, such as chromogens, fluorogens, or precipitation are usually used, along with the specific enzyme substrate in the system to assist result visualisation. This has led to the further development of chromogenic and fluorogenic substrates used in the media to target specific bacteria of interest. The details of media based on chromogenic and fluorogenic substrates are discussed later (section 1.3.4.1).

Enzymatic assays can be classified according to the enzyme activities being targeted, such as esterases (2007JAM2046), L-alanyl aminopeptidase (2008BML832), and β -D-glucosidase (2009JMM139). Other classifications can be based on the different indicator response (colour, fluorescence, precipitation) or type of system used (e.g. agar plate, microarray).

1.3.4.1: Chromogenic and fluorogenic substrates for bacterial detection

Bacterial detection based on enzymatic activities has gained popularity in clinical applications due to its simplicity of use and low cost (depending on the complexity of substrate synthesis). By understanding the enzymatic activities and type of enzymes present in bacteria, specific chromogenic or fluorogenic substrates can be customised accordingly in the culture media. The use of chromogenic or fluorogenic substrates not only enhances the reliability of the result by targeting only specific enzymes present in the bacteria of interest, but also improves the visualisation of positive result (Figure 1.8).

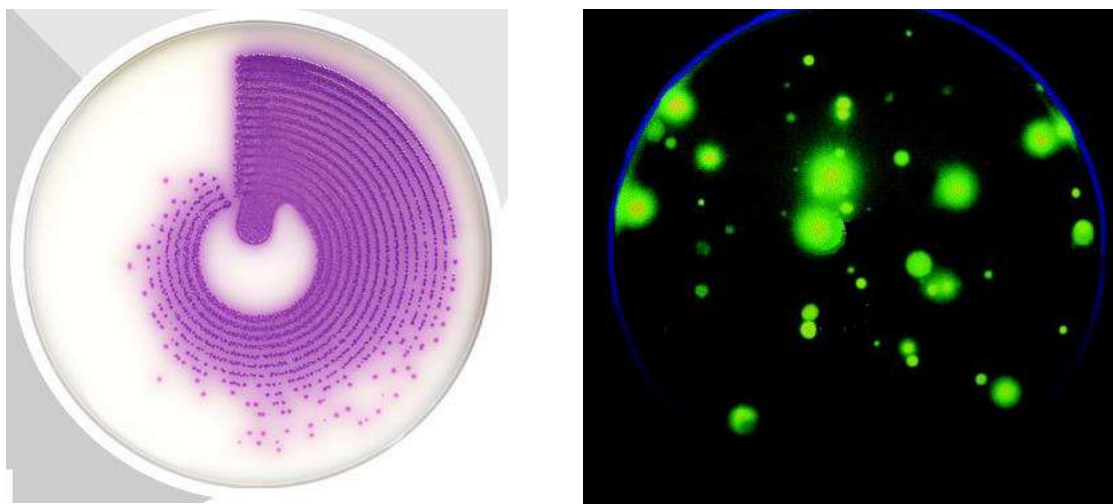


Figure 1.8: Example of chromogenic medium, chromID™ Salmonella Elite (left) shows the presence of *Salmonella* colonies in a faecal sample with a purple colour by targeting specific octylesterase activity (WS-6). A fluorescent response (right) shows the presence of bacterial colonies in a water sample with phosphatase activity on the fluorogenic medium (1999JMM25)

In this enzymatic substrate technique, a sample containing the bacteria of interest is cultured on a medium containing a chromogen or fluorogen that is attached to a specific substrate. The particular substrate used varies, depending on the specific enzymes secreted by the bacteria of interest that need to be targeted. More than one type of substrate can be incorporated into the medium for the detection of more than one type of bacteria simultaneously. The chromogenic or fluorogenic responses remain muted while the indicator is attached to the substrate. A change of colour or fluorescence is observed on the medium, if the bacteria of interest present in the sample causes the enzymatic reaction to occur. The specific enzyme secreted by the bacteria of interest catalyses reaction of the specific substrate and results in the release of a chromogen or fluorogen (2009JMM139), Figure 1.9.

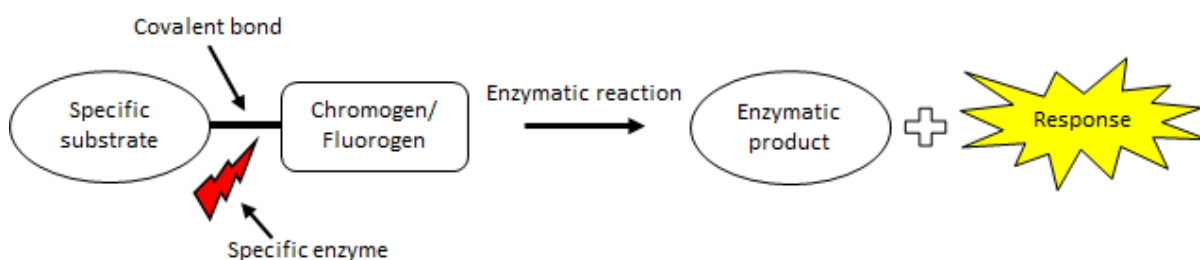
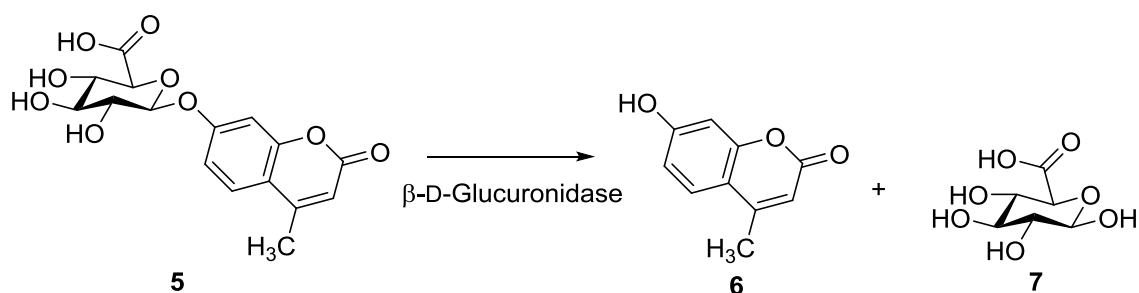


Figure 1.9: Enzymatic reaction initiated by the presence of bacteria of interest, in which a secreted enzyme (red) cleaves the covalent bond between the specific substrate and chromogen/fluorogen, resulting in colour or fluorescent response

For instance, 4-methylumbelliferyl- β -D-glucuronide (**5**), a fluorogenic substrate, was used to target β -D-glucuronidase activity present in *E. coli*. This substrate was broken down by the β -D-glucuronidase enzyme to β -D-glucuronic acid (**7**) and 4-methylumbelliferone (**6**), which displays a fluorescent blue colour under UV light (365 nm), signifying the presence of *E. coli* in clinical samples (Scheme 1.1) (1996IJFM45).



Scheme 1.1: Hydrolysis of fluorogenic substrate, 4-methylumbelliferyl-β-D-glucuronide (5) by the β-D-glucuronidase into 4-methylumbelliferone (6) and β-D-glucuronic acid (7).

The application of this technique in bacterial detection is beneficial in several aspects, such as cost, time and ease of use, compared to the instrumental techniques. More than one type of bacteria present in a sample can be detected simultaneously by using more than one chromogenic and/or fluorogenic substrate together in the same medium (2007JAM2046). For instance, *E. coli*, *Proteus spp.*, and *Enterococcus spp.* in a urine sample were detected simultaneously as different colours were observed on the chromogenic medium (Figure 1.10). This produces significant benefits for routine analysis in the microbiology laboratories, which may deal with hundreds of samples and types of bacteria daily from patients; in this case, a urinary tract infection is confirmed, allowing appropriate treatment to be commenced as early as possible.



Figure 1.9: Three different bacteria in a urine sample detected on bioMerieux chromID CPS media *E. coli* (pink to burgundy), *Proteus spp.* (light to dark brown) and *Enterococcus spp.* (turquoise) (WS-7)

Despite the demonstrable benefits associated with this technique, there is a serious practical limitation to its use when the medium involves polymicrobial cultures, as is usually the case in a clinical setting. Cautious selection of the specific substrate to be embedded in these media is important in order to prevent any false results, because a similar enzyme may be secreted by a different species or strain of bacteria, which can also act upon the enzymatic substrate. The presence of coliforms or interfering bacteria is another common problem encountered using these media, because they potentially camouflage the presence of bacteria of interest on the medium, especially when dealing with relatively low concentrations of the bacteria of interest.

1.3.4.2: Selective growth media for bacterial detection

The rapid growth and emergence of new microorganisms pressure the need for fast, reliable and user-friendly bacterial identification and detection methods, in order to evaluate the presence of microorganisms as a contaminant in foods and in clinical samples. Although the chromogenic and fluorogenic media offer alternative detection methods for the rapid identification of polymicrobial samples, their usage is still restricted, due to the problems discussed above. As a result, incorporation of specific and selective growth inhibitors, which target or inhibit the growth of the interfered microorganisms, into the growth media is favourable. For instance, selective inhibition of Gram-positive bacteria can be achieved in a MacConkey medium, which contains growth supplements and Gram-positive inhibitors, such as bile salts and crystal violet (1905JH333). This MacConkey medium can be further customised or improved for the growth selectivity of certain Gram-negative bacteria by varying the contents in the medium. For instance, replacement of lactose supplement with mannitol or glucose favours the growth of some Enterobacteriaceae (Gram-negative bacteria) in the modified MacConkey medium (1962JB381).

Apart from these inhibitors (bile salts and crystal violet), incorporation of antimicrobial agents into the growth medium is often used for similar applications (bacterial growth selectivity). For instance, the fastidious *Capnocytophaga* species, which were isolated orally, were grown selectively over the commensal bacteria in a VCAT medium containing different antimicrobial agents (Columbia agar, 10 % cooked horse blood, polyvitaminic supplements, 3.75 mg/L colistin, 1.5 mg/L trimethoprim, 1.0 mg/L vancomycin and 0.5 mg/L amphotericin B) (2013LAM303). The concentration of these antimicrobial agents is crucial in order to ensure the survival of the bacteria of interest.

The growth of bacteria can be inhibited differently depending on the types of important biochemical pathways; for example DNA synthesis, metabolic processes, protein synthesis and cell wall synthesis are targeted by different antimicrobial agents. There are many other selective growth media integrating antimicrobial agents reported for use in clinical diagnosis, Table 1.4.

Table 1.4: Example of selective growth media containing antimicrobial agents

Selectively grown bacteria	Growth Inhibited bacteria	Inhibitor(s)	Lit. reference
<i>C. difficile</i>	Commensal bacteria in faeces Enterobacteriaceae, faecal streptococci, bacteroides sp.	Cycloserine, cefoxitin Norfloxacin, moxalactam, cysteine salt	1979JCM214 1992JCP812
<i>C. jejuni</i> <i>C. coli</i>	Commensal bacteria in faeces	Polymyxin B, rifampicin, trimethoprim, actidione	1982JCP462
<i>L. pneumophila</i>		Polymyxin B, vancomycin, glycine	1982JCM697
MRSA	Methicillin and cefoxitin susceptible bacteria	Methicillin, cefoxitin	2005JCM5536
<i>Pseudomonas cepacia</i> *		Polymyxin B, bacitracin, lactose	1987JCM1730
<i>Salmonella spp.</i>	Commensal GI bacteria especially <i>E. coli</i> Gram-positive bacteria and Gram-negative bacilli <i>Proteus spp.</i> Commensal bacteria in intestine Gram-positive bacteria Some Enterobacteria and Gram-negative bacteria	Alafosfalin Brilliant green Novobiocin Potassium tellurite, tetrathionate Bile salts, sodium selenite Nalidixic acid	2002JCM3913 2012FC369
<i>Y. enterocolitica</i>	<i>P. aeruginosa, E. coli, K. pneumonia, P. mirabilis</i>	Cefsulodin, Irgasan, Novobiocin	1979CJM1298

* *Pseudomonas cepacia* is now known as *Burkholderia cepacia*

1.3.4.3: Application of suicide substrates in chromogenic and fluorogenic media

The feasibility of incorporation of antimicrobial agents into the growth media, which improves the growth selectivity of specific bacteria, is leading to further exploitation of other growth inhibitory agents or suicide substrates.

Suicide substrates refer to any foreign substrates that bind to or form a covalent bond in the active site of the targeted enzymes, or cause a conformational change of the enzyme and loss of the enzymatic activity on their natural substrate(s). For instance, penicillin (**8**), a suicide substrate, mimics the structure of the D-alanyl-D-alanine (**9**) terminus of the pentapeptide chain (Figure 1.11) and binds to the active site of PBP, preventing the process of forming cross-links in the peptidoglycan cell wall, catalysed by transpeptidase. Eventually this leads to cell death (1980JBC3977).

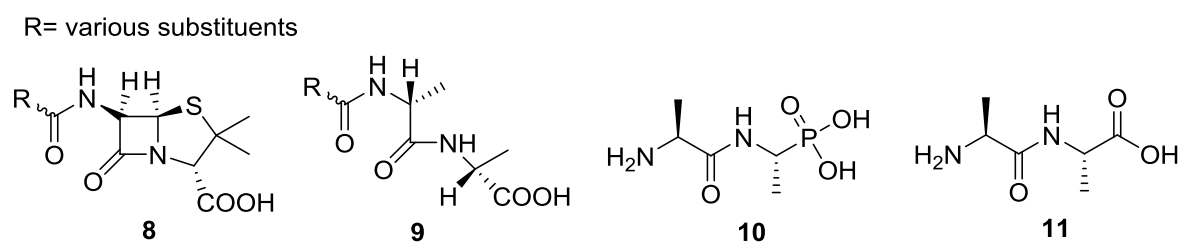
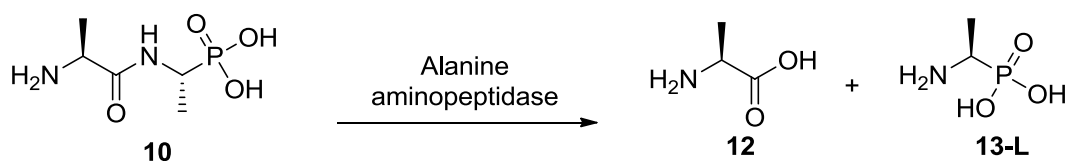


Figure 1.11: Structures of penicillin (**8**), D-alanyl-D-alanine (**9**), L-alanyl-L-fosfalin (**10**), and L-alanyl-L-alanine (**11**)

An appropriate selection of the suicidal substrates incorporated into the chromogenic and fluorogenic media is able to inhibit selectively the growth of commensal bacteria, while the growth of the bacteria of interest is unaffected. For instance, L-alanyl-L-fosfalin (**10**), a known suicide substrate (1980AAC897) allows the growth of *Salmonella* species at a crucial concentration, while preventing the growth of *E. coli*, commensal bacteria that are found in clinical faecal samples and often camouflage the presence of bacteria responsible for severe food-poisoning (2002JCM3913).

The antibacterial activity caused by L-alanyl-L-fosfalin (**10**) led to further investigation of its biochemical pathway inside bacterial cells. L-Alanyl-L-fosfalin (**10**) is a pseudo-dipeptide, in which it mimics the structure of the dipeptide L-alanyl-L-alanine (**11**) (Figure 1.11), and is transported by permeases into bacterial cells. The presence of abundant aminopeptidases inside the cells later cleaves and releases L-alanine (**12**) and L-fosfalin (L-1-aminoethylphosphonic acid), an L-alanine analogue (**13-L**) (Scheme 1.2). Once released inside the cell, L-fosfalin (**13-L**) binds to the bacterial enzyme alanine racemase and prevents cell wall formation (1998B10438).



Scheme 1.2: L-Alanyl-L-fosfalin (**10**) is subjected to alanine aminopeptidase enzymatic reaction to liberate L-alanine (**12**) and L-fosfalin (L-1-aminoethylphosphonic acid) (**13-L**)

There are other suicide substrates reported that target different enzymatic activities, present in either bacteria or humans. For instance, α -fluoromethyl histidine (**14**) targets histidine decarboxylase, α -fluoromethyl ornithine (**15**) and α, α -difluoromethyl ornithine (**16**) target ornithine decarboxylase (1982T871) (Figure 1.12). Depending on the enzymes present in the bacteria of interest, suicide substrates can be customised and synthesised to target them. For instance, α -fluoromethyl histidine (**14**) can be used as a treatment to target histidine decarboxylase found in histamine-producing bacteria, which are responsible for some cases of food poisoning upon ingesting fish containing these bacteria (2007AEM1467).

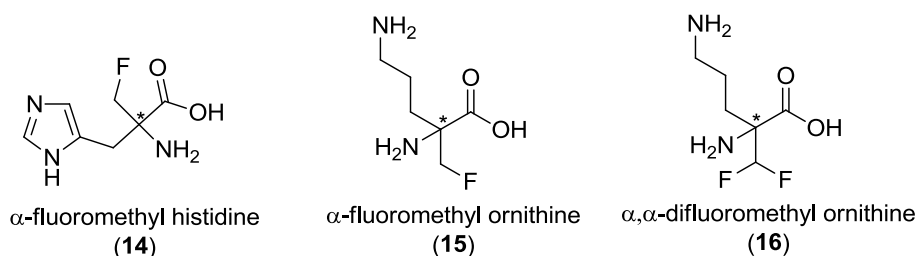


Figure 1.12: Structures of α -fluoromethyl histidine (**14**), α -fluoromethyl ornithine (**15**) and α, α -difluoromethyl ornithine (**16**) (1982T871)

* Stereochemistry of each inhibitor was not specified in the study (1982T871)

1.4: Alanine racemase

1.4.1: Rationale for alanine racemase as a target for suicide substrate development

In most bacteria, D-alanine serves as an important building block for the biosynthesis of the peptidoglycan cell wall. This amino acid is produced from the natural amino acid, L-alanine, by alanine racemases. The expression of these enzymes is different across species, as some bacteria contain only one alanine racemase, while others have more than one of these enzymes, encoded by *alr* and *dadX* genes (2002JB4321). Protein with about 85 % similarity is expressed by *dadX* and *dadB* genes (1994JB1500), with the result that *dadX* is sometimes known as *dadB*. The expression of *dadB* alanine racemase is induced by L-alanine and it functions in the isomerisation of L-alanine to D-alanine (1983JB1439). The resulting D-alanine is subsequently oxidised to pyruvate by D-alanine hydrogenase, an enzyme that is expressed by the *dadA* gene (1983JB1439). The *dadB* and *dadA* genes are co-regulated and play an important role in the catabolism of L-alanine, which serves as a source of carbon, energy and nitrogen (1983JB1439). The *alr* alanine racemase, on the other hand, is different, as it is not involved in catabolism, but in the constitutive synthesis of D-alanine to maintain bacterial cell growth (2002JB4321). Though both *dadX* and *alr* genes express alanine racemase, *alr* alanine racemase is of particular interest as an antibacterial target and its inhibition and inhibitors are well-documented (1998B10438, 1986B3261, 2008PS1066, 2009BBA1030, 2011PLoS20374).

Alanine racemase is a pyridoxal 5'-phosphate (PLP)-dependent enzyme. It catalyses the isomerisation between L-alanine and D-alanine, in the presence of the PLP cofactor, commonly known as vitamin B₆ (2011JACS15496). In the L to D direction, this enzyme acts as an important production source of D-alanine, a significant precursor required for the synthesis of the bacterial cell wall (1998B10438). Hence, bacterial growth will be halted upon the inhibition of alanine racemase. The mechanism for the racemisation of alanine by alanine racemase will be discussed in the following section.

Alanine racemase has become an interesting target for novel suicide substrate development, as this enzyme is present in the bacteria of interest. Although this enzyme is also found in some eukaryotic species, such as fungi, yeast and plants (2011CRV6919), the inhibition of this enzyme is still an interest, because it is present universally in all bacteria yet bacterial inhibition *via* this enzyme varies according to concentration. In other words, different bacteria have different inhibitory susceptibilities towards the suicide substrates used. For instance, a known suicide substrate, L-alanyl-L-fosfalin (**10**) that targets alanine racemase, resulted in selective inhibition of coliform bacteria, *E. coli*, but not *Salmonella* species at a crucial concentration (2002JCM3913). This finding is important as this provides a potential way to discriminate between bacteria that appear similar in other tests.

1.4.2: Mechanism of alanine racemase

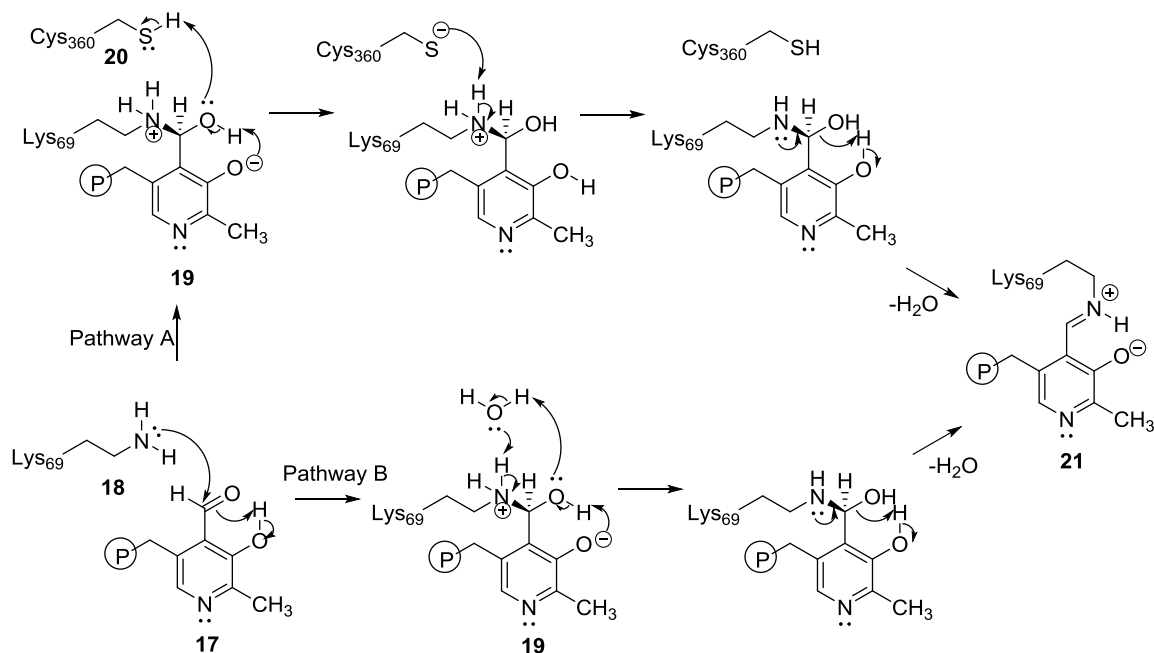
The enzymatic activity of alanine racemase is dependent upon the presence of its cofactor, pyridoxal 5'-phosphate (PLP, **17**). Many studies have been carried out to investigate its mechanism, which involves an internal aldimine formation stage and an external aldimine formation stage prior to liberation of the racemised substrate. The internal aldimine stage refers to the formation of a PLP-Lys complex (**21**, Scheme 1.3), while the replacement of Lys with an incoming L-amino acid (L-alanine), resulting in a PLP-L-alanine complex, is known as the external aldimine stage (Scheme 1.4). The detailed mechanism of both aldimine formation stages are discussed below.

1.4.2.1: Internal aldimine formation

Most of the studies performed so far have focussed on the enzymatic interaction during the external aldimine formation stage and only limited investigation has been carried out to study the enzymatic interaction involved in the initial stage (the internal aldimine formation). The mystery of this stage was revealed by Oliverira and co-workers, using the crystal structure model from the human ornithine decarboxylase (ODC) enzyme to study internal aldimine formation (2011JACS15496). Although the structure of the ODC enzyme may not be closely

related to alanine racemase, its mechanism of internal aldimine formation may be considered as a reference for alanine racemase, as the same cofactor, PLP (**17**), is involved in the reaction.

Oliverira and co-workers proposed that formation of the internal aldimine by either pathway begins with a Schiff's base reaction (Scheme 1.3), in which the ϵ -amino side chain of the Lys69 residue (**18**) acts as a nucleophile to attack the aldehyde group of PLP, resulting in the formation of a carbinolamine intermediate (**19**). This intermediate is later subjected to proton transfer *via* two different pathways, Pathway A or B, depending on which is most kinetically and thermodynamically favourable. In Pathway A, the three step reaction involves the participation of the neighbouring Cys360 residue (**20**), which acts as a proton donor/acceptor in close proximity to the intermediate, while a two step reaction involves the participation of a water molecule in Pathway B. Overall, the common intermediate (**19**) undergoes dehydration to form the PLP-Lys complex (**21**), known as an internal aldimine.



Scheme 1.3: Mechanism of internal aldimine **21** formation *via* two different pathways, Pathway A and Pathway B, as proposed by Oliverira and co-workers (2011JACS15496)

This proposed mechanism was based on the study of a human ornithine decarboxylase (ODC) enzyme, one of the PLP-dependent enzymes

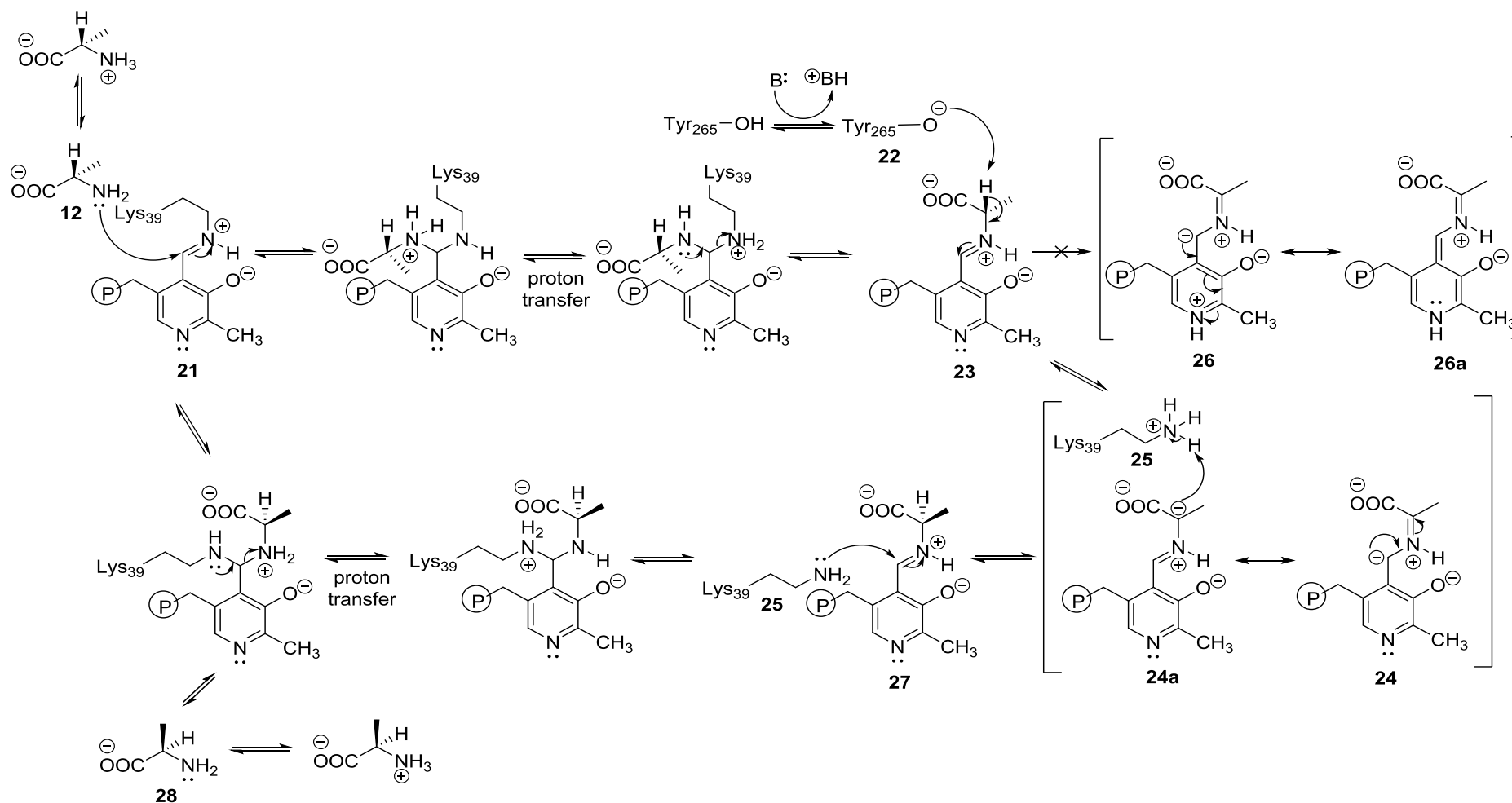
1.4.2.2: External aldimine formation

The external aldimine stage proceeds after the internal aldimine (**21**) has formed. In this stage (Scheme 1.4), the Tyr265 (**22**) and Lys39 (**25**) residues are proposed to be involved, acting as acid-base catalytic groups (2005ABB279), although Lys69 (**18**) was suggested as an alternative to Lys39 by Oliverira (2011JACS15496). The different position of the catalytic lysine residue arises because a different PLP-dependent enzyme was investigated; limited information on alanine racemase was available and ODC was used to study internal aldimine formation (2011JACS15496), while alanine racemase itself was used to study external aldimine formation (2002JBC19166, 2005ABB279).

As a result of alanine racemase catalysing the isomerisation of the L- and D-alanine, both alanine amino acids can act as an incoming substrate for the external aldimine formation. Here, the isomerisation from L-alanine to D-alanine direction is discussed (Scheme 1.4).

During formation of the external aldimine (**23**), an incoming substrate, L-alanine (**12**), replaces the lysine residue, while the Tyr265 residue (**22**) abstracts the α -proton of L-alanine to give a resonance stabilized carbanion (**24-24a**). Unlike other PLP-dependent enzymes, the PLP binding site of alanine racemase does not involve an acidic residue near to the pyridine ring of the PLP. In fact, the close proximity of this pyridine ring to Arg219 ensures the pyridine ring remains unprotonated or neutral (2005ABB279); hence, alternative intermediate **26-26a** is unlikely to be formed in alanine racemase.

Although some studies claimed that a protonated pyridinium ring of PLP lowers the acidity of the α -proton and facilitates its abstraction by Tyr265 (**22**), due to the extensive resonance stabilisation of the α -carbanion within the pyridinium ring (**26-26a**), the presence of an iminium group on the α -amino acid in the unprotonated pyridine ring (**23**) is sufficient to lower the pK_a of the α -proton, and thus the abstraction of the α -proton still can occur (B-2007MI285).



Scheme 1.4: Mechanism of alanine isomerisation, from L-alanine to D-alanine, via formation of L-alanine external aldimine (2002JBC19166) (1998B10438)

The lifetime of the PLP-carbanion complex (**24-24a**) is relatively short, due to the lack of pyridine nitrogen protonation and limited resonance stabilisation. This anion favours re-protonation of the carbanion of **24a** by Lys39 (**25**) to give the D-alanine-external aldimine complex (**27**). The D-alanine (**28**) is eliminated with the aid of Lys39 (**25**), while the internal aldimine (**21**) is regenerated, Scheme 1.4. Although the different PLP-dependent enzymes use lysine residues at a different position (Lys69 and Lys39) for the formation of the internal and external aldimines, the role of the lysine residue is significant in forming an internal aldimine upon reacting with the PLP (**17**).

1.4.2.3: Roles of lysine and tyrosine residues within alanine racemase

The lysine and tyrosine residues are important for the formation of internal and external aldimines. These residues play a significant role as acid-base catalytic groups for protonation and deprotonation of the α -proton of L-alanine bound in the active site. Although Tyr265 (**22**) is responsible for the α -proton abstraction (1998B10438), Lys39 (**25**) can also act as a base. Depending on the stereochemistry of the substrate binding to alanine racemase, the acid-base roles of these residues, Tyr265 and Lys39 can be inter-changed; for instance, Lys39 can act as the catalytic base for the abstraction of the α -proton of D-alanine (1997B1329, 2002JBC19166, 2005ABB279, B-2007MI285). A similar finding was also reported by Fenn, in which the α -proton of D-cycloserine and L-cycloserine was abstracted by Lys39 and Tyr265, respectively (Scheme 1.5) (2003B5775).

The acid-base action of these residues, Tyr265 and Lys39, was well defined *via* the X-ray crystallographic enzymatic study; however, most of the study performed was based on the interaction between L-fosfalin and the alanine racemase of *B. stearothermophilus* (1998B10438, B-2007MI285). As L-fosfalin is an analogue of L-alanine, a similar enzymatic interaction of L-alanine will be expected.

1.4.3: Inhibitors of alanine racemase

From the previous discussion, the PLP cofactor (**17**), and the Lys69 (**18**), Cys360 (**20**), Tyr265 (**22**), and Lys39 (**25**) residues play important roles within the active site of alanine racemase. Therefore, this enzymatic reaction can be disrupted by designing molecules to interfere with these residues' interactions. In other words, any analogues of alanine that can act as substrates of alanine racemase, and are able to form a covalent bond with the enzyme upon interacting with these important residues, are potential inhibitors of the function of alanine racemase.

Several types of suicide substrate that target PLP-dependent enzymes were reported by Walsh (1982T871) and classified into different groups of mechanism-based inactivators, depending on the functional groups involved in the inhibitory activities. Both reversible and irreversible inhibition pathways are well-documented. Reversible inhibitors bind strongly to the enzyme and their rates of dissociation are slow compared to normal enzymatic binding. This delay is sufficiently significant to cause cell death. Irreversible inhibitors bind and form a strong covalent bond to the active site or with the PLP cofactor and block the active site, preventing the normal enzymatic reaction.

1.4.3.1: Reversible inhibition with a slow rate of dissociation

L-Fosfalin or L-1-aminoethylphosphonic acid (**13-L**) is of interest due to its inhibitory action on alanine racemase, resulting in selectivity differences on bacterial growth (2002JCM3913). L-Fosfalin (**13-L**) is an example of a reversible inhibitor. It has a similar structure to L-alanine (**12**); therefore, it follows the initial steps of the racemisation mechanism, in a similar manner to the alanine substrate (Scheme 1.4). However, the binding of L-fosfalin (**13-L**) does not proceed to any racemisation as expected, instead its prolonged occupation of the active site blocks the access of L-alanine (**12**). The mechanism of action of L-fosfalin (**13-L**) was studied by Stampfer and co-workers (1998B10438). The detailed mechanism of action was explored *via* enzymatic study on the alanine racemase of *B. stearothermophilus* (Figure 1.13).

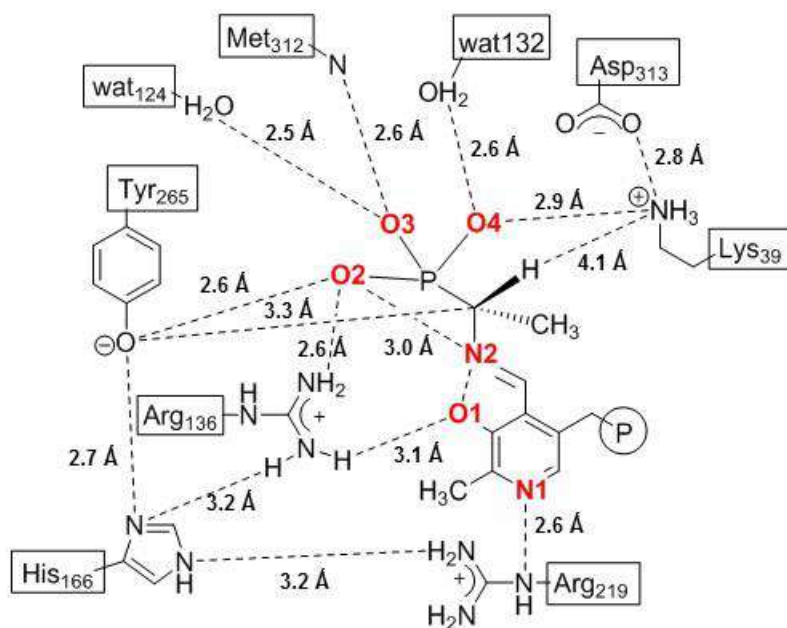


Figure 1.13: Hydrogen-bonding interactions between the L-fosfalin-PLP external aldimine and the important amino acid residues and water molecules in the active site of the alanine racemase of *B. stearothermophilus* (1998B10438) (B-2007MI285). Image was generated at 1.6 Å resolution

The L-fosfalin (**13-L**) binds and interacts differently at the active site due to the multiply ionised structure and the additional oxygen on the phosphonate group. According to Stamper and co-workers, many hydrogen-bonding interactions are involved between the phosphonate group of **13-L** and the active site residues (1998B10438). These hydrogen-bonding interactions and implications are as follows:

- Oxygen (**O4**) of the phosphonate group interacts with the amino side chain of Lys39 (2.9 Å) and a water molecule (wat132, 2.6 Å). These interactions result in the side chain of Lys39 pointing away from the cofactor and towards Asp313 (2.8 Å).
- Oxygen (**O3**) of the phosphonate group interacts with the amide of Met312 (2.6 Å) and a water molecule (wat124, 2.5 Å).
- Oxygen (**O2**) of the phosphonate group interacts with Tyr265 (2.6 Å), Arg136 (2.6 Å) and imine (**N2**) (3.0 Å).
- Additional hydrogen bonding was also reported at Arg136, where it interacts not only with the phosphonate oxygen (**O2**) (2.6 Å) but also with the phenolic oxygen of the cofactor (**O1**) (3.1 Å) and His166 (3.2 Å).

- The close proximity interaction between the pyridinium group (**N1**) and Arg219 (2.6 Å) results in this group (**N1**) remaining un-protonated at all times. This network is further reinforced by hydrogen bonding with His166 (3.2 Å).

These hydrogen-interactions and network formation not only displaces the important residue (Lys39), to prevent racemisation of L-fosfalin (**13-L**), but also reinforces the occupation of **13-L** in the active site, with a half-life of approximately 25 days (1986B3275), efficiently preventing the access of L-alanine.

Other reversible inhibitors, such as *O*-acetyl-L-serine (**29-L**) and *O*-carbamoyl-L-serine (**30-L**) (Figure 1.14) were also reported (1978B1313). The mechanism of action of these inhibitors is similar to that of L-fosfalin (**13-L**). The stereochemistry of these compounds (**29**, **30**) is important in order to retain their reversible inhibitory properties, because irreversible inhibitory activity was reported in the D-stereochemical forms, *O*-acetyl-D-serine (**29-D**) and *O*-carbamoyl-D-serine (**30-D**) (1978B1313). In short, reversible or irreversible inhibition by these compounds depends upon their stereochemistry.

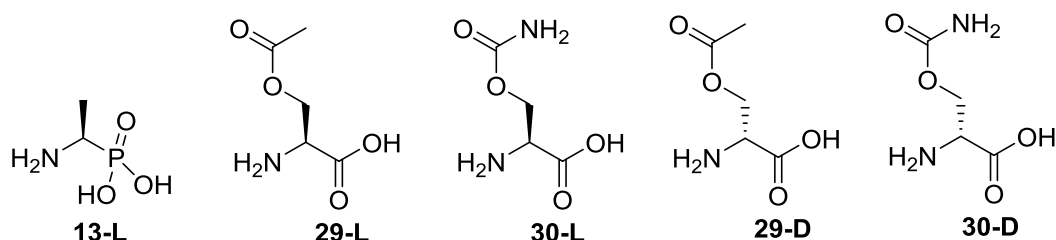


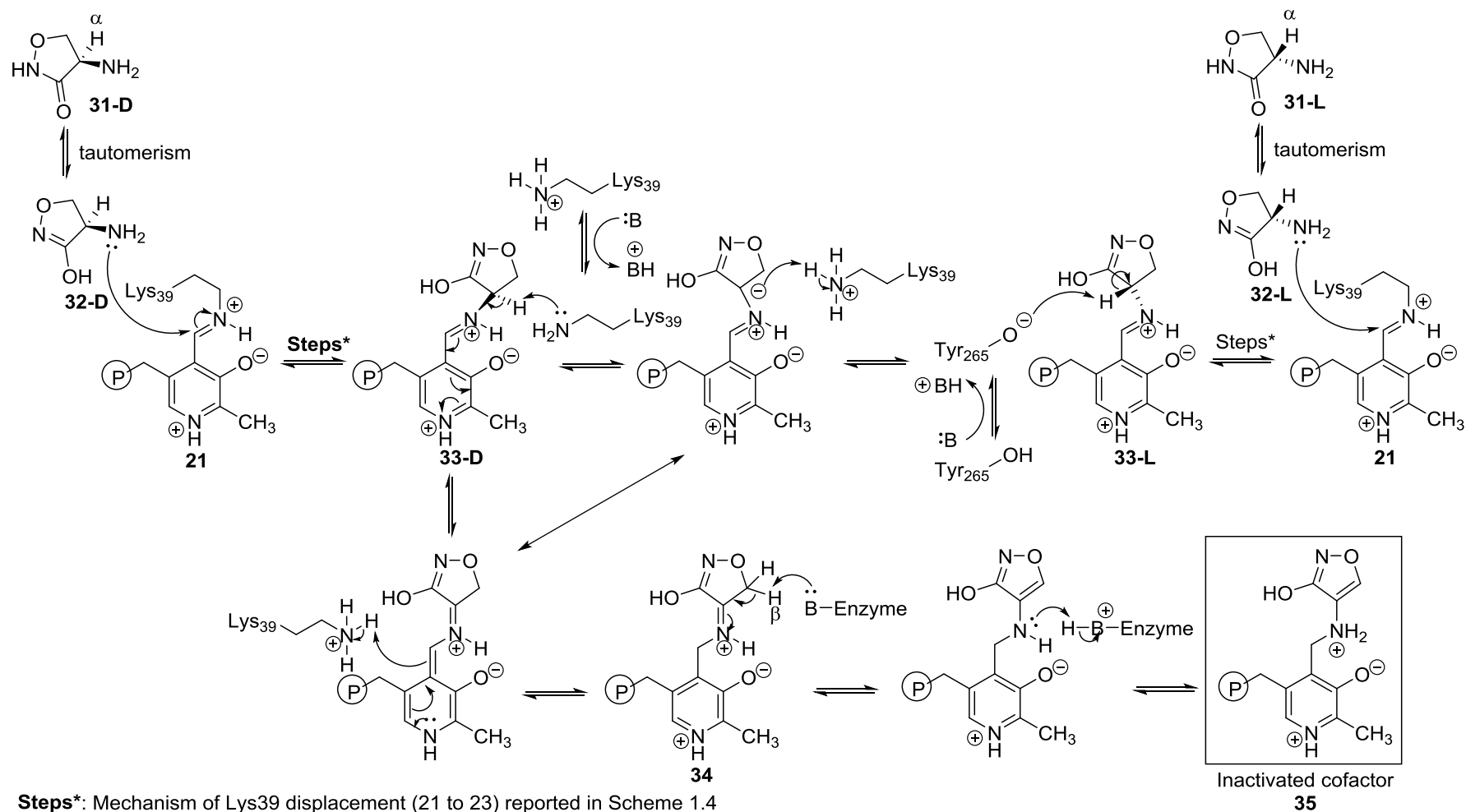
Figure 1.14: Examples of reversible inhibitors with L-stereochemistry (**13-L**, **29-L**, **30-L**) and irreversible inhibitors with D-stereochemistry (**29-D**, **30-D**) acting on alanine racemase

1.4.3.2: Irreversible inhibition

There are two types of irreversible alanine racemase inhibition reported, either covalent binding to the PLP cofactor or covalent binding to the active site. The binding of inhibitors to the PLP cofactor permanently modifies the PLP structure and prevents the normal internal aldimine formation with the enzyme, while the binding of inhibitors to the active site obstructs the incoming PLP cofactor from forming the internal aldimine for the subsequent enzymatic reaction.

Cycloserine (**31**) is an irreversible inhibitor and studies show that both D-cycloserine (DCS) (**31-D**) and L-cycloserine (LCS) (**31-L**) inactivate the alanine racemase of *B. stearothermophilus* (2003B5775). Although both DCS (**31-D**) and LCS (**31-L**) displayed good inhibition of the enzyme, the rate of inhibition by LCS (**31-L**) was slow, due to an additional isomerisation step to DCS (**31-D**) being required before reaction with the enzyme could take place.

According to Fenn (2003B5775), Scheme 1.5, the cycloserine first tautomerises to an iminic acid form (**32-D** and **32-L**), as the NMR and IR spectra showed that this form was present primarily in solution (2003B5775). The iminic form is important in order to promote the prototropic shift at the late stage of enzymatic reaction, by lowering the β -proton pK_a of ketimine (**34**) (1998JACS2268). Both of these tautomerised forms (**32-D**, **32-L**) can undergo a Schiff's base reaction with the internal aldimine (**21**), displacing the Lys39 moiety and forming the respective external aldimines (**33-D**, **33-L**), using a similar mechanism to that reported in Scheme 1.4 (**21** to **23**).



Scheme 1.5: Mechanism of inhibition of alanine racemase by D-cycloserine (DCS) (**31-D**) and L-cycloserine (LCS) (**31-L**), proposed by Fenn (2003B5775)

As a result of the different chirality of the tautomerised LCS-PLP complex (**33-L**) that is formed, an additional isomerisation step occurs, whereby abstraction of the α -proton by the Tyr265 and protonation by the Lys39 occurs to form the inverted DCS-PLP complex (**33-D**). The α -proton of this complex (**33-D**) is later removed and re-protonated by Lys39 at a different site, resulting in ketimine product (**34**) formation. This is followed by another proton transfer, converting **34** into a stable covalent adduct, 3-hydroxyisoxazole-PLP (**35**), with the aid of a protonated basic residue in the active site. The formation of stable adduct (**35**) reduces the availability of PLP for alanine racemisation, thereby no D-alanine is produced for used in cell wall formation, leading eventually to cell death. DCS is also reported to have inhibitory activity on another enzyme, D-Ala-D-Ala ligase (Ddl), which is responsible for the formation of the D-Ala-D-Ala dipeptide through coupling of two D-alanyl residues (1960JACS998, 2004JBC46153).

According to Fenn (2003B5775), Scheme 1.5, the carbanion formed upon α -proton abstraction was stabilised by electron delocalisation within the pyridinium ring of PLP. However, this proposed intermediate (**26-26a**) mechanism contrasts to the previously discussed mechanisms claimed by Stamper (1998B10438), Toney (2005ABB279) and Frey (B-2007MI285). The involvement of the pyridinium ring of PLP, as proposed by Fenn is less likely to occur because the pyridine nitrogen is close to the Arg219 residue in alanine racemase (1998B10438, 2002JBC19166, 2005ABB279, B-2007MI285). As a result of the pK_a of the arginine residue (~ 12.5) is higher than the pyridine (~ 5.3), the arginine residue will be protonated instead of the pyridine nitrogen.

Another mode of irreversible inhibition involves covalent binding between the active site residues, particularly Tyr265 and Lys39, and inhibitors. Several inhibitors have been reported to involve this mechanism, including 3-chlorovinylglycine (**36**) (1988AAC319), 3-fluorovinylglycine (**37**) (1988AAC319), β -chloroalanine (**38**) (1978B1313), β -fluoro-alanine (**39**) (1978B1313, 1981B7539), β,β -difluoroalanine (**40**) (1981B7539) and β,β,β -trifluoroalanine (**41**) (1981B7539) (Figure 1.15). These inhibitors work similarly, due to the presence of halogen at the β -position or 3-position of the inhibitors, although Thornberry and co-workers have proposed a different mechanism for 3-chlorovinylglycine (**36**) and 3-fluorovinylglycine (**37**) (1991JBC21657).

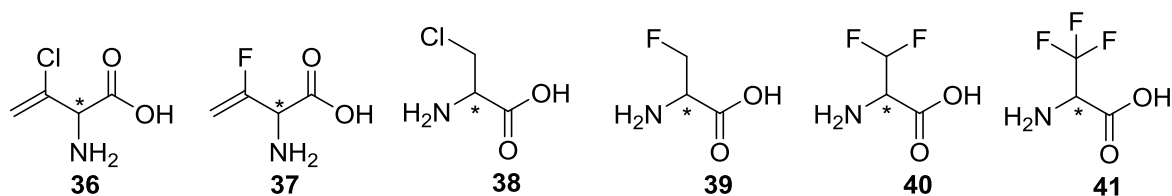
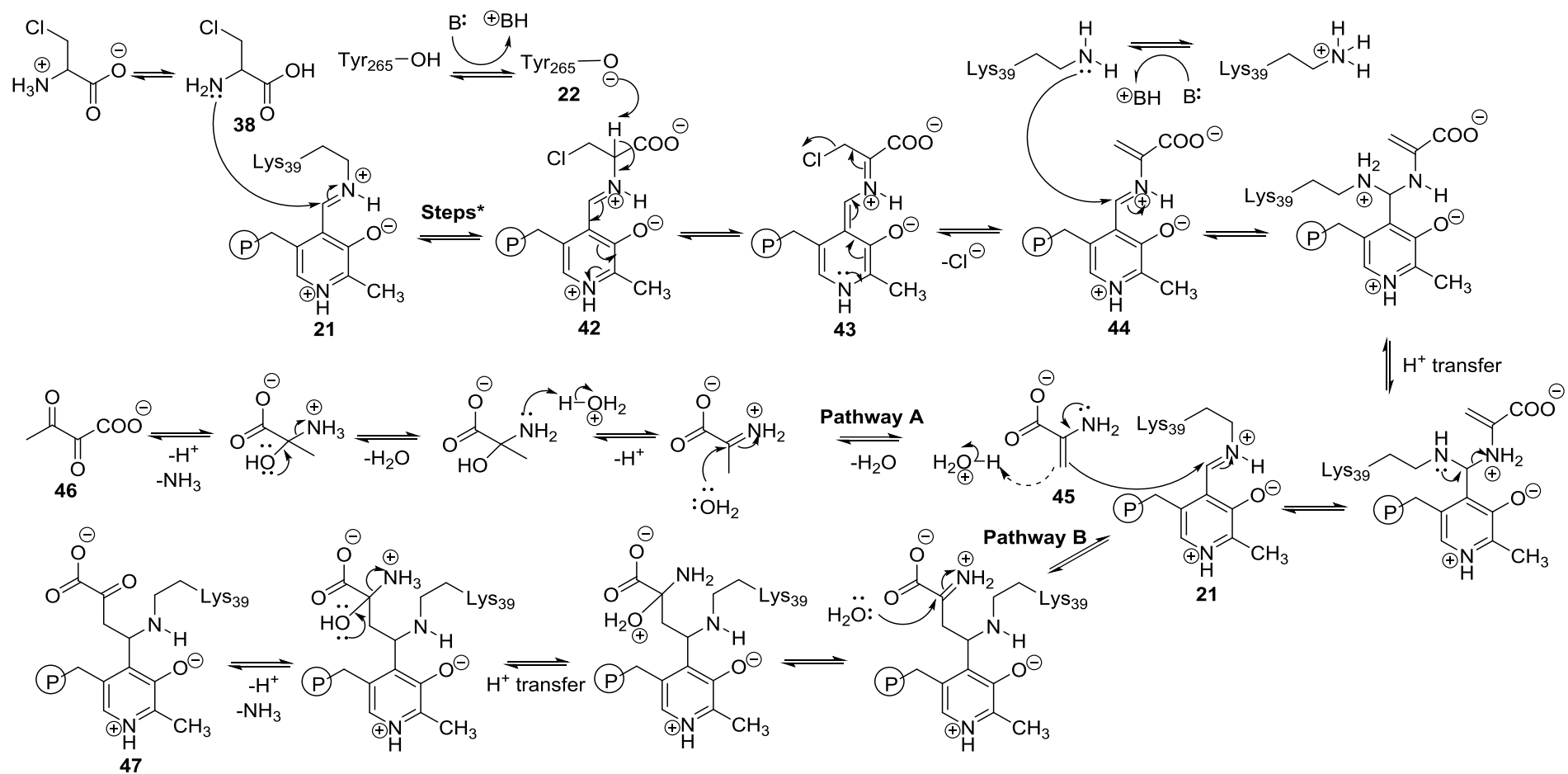


Figure 1.15: Examples of irreversible inhibitor that form a covalent bond with the active site of alanine racemase

* Stereochemistry of each inhibitor was reported in D- or L-form but not racemic

In general, the binding of these inhibitors to the PLP cofactor facilitates α,β -elimination, which releases a highly reactive species that contains a nucleophilic enamine functional group. This species alkylates key residues of the enzyme, preventing normal catalytic activity (1978B1313). As β -chloroalanine (**38**) is of interest due to its inhibitory effect and its mechanism of action is well-documented (1978B1313, 2000PAC373), the mechanism of action of **38** is detailed in Scheme 1.6.



Steps*: Mechanism of Lys39 displacement (21 to 23) reported in Scheme 1.4

Scheme 1.6: Mechanism of action of β -chloroalanine (**38**) on alanine racemase, proposed by Wang (1978B1313) and Adams (2000PAC373)

According to the mechanistic study of Wang (1978B1313), the incoming chlorinated alanine analogue, β -chloroalanine (**38**), binds to the internal aldimine (**21**), displacing Lys39 and forming the β -chloroalanine-PLP complex (**42**), using a similar mechanism to that reported in Scheme 1.4 (**21** to **23**). Abstraction of the α -proton of β -chloroalanine (**38**) by Tyr265 results in a negative charge that can delocalise within the external aldimine which is stabilised by the extended conjugated system (**42-43**). After this, the chlorine atom can be eliminated as chloride, forming an α,β -unsaturated external aldimine (**44**), instead of protonation of the α -carbon, as seen in the normal enzymatic reaction (1978B1313). The nitrogen lone pair of Lys39 later reacts with the external aldimine (**44**), releasing the α,β -unsaturated enamine species (**45**) and regenerating the internal aldimine (**21**). The released enamine (**45**) can react by two different pathways: in Pathway A, the enamine (**45**) decomposes into pyruvate (**46**) and ammonia by diffusing away from the alanine racemase (2000PAC373). In Pathway B, the enamine species (**45**) reacts with the internal aldimine (**21**), forming a permanent covalent bond and trapping the enzyme in the inactive form (**47**) (1978B1313).

Although the stereochemistry of β -chloroalanine (**38**), β -chloro-L-alanine (**38-L**) or β -chloro-D-alanine (**38-D**), was not defined in this mechanistic study, each enantiomer is assumed to undergo a similar mechanism as claimed by Wang (1978B1313). However, different levels of inhibition might be expected by these enantiomers, due to their different stereochemistry and interactions upon binding in the alanine racemase active site. A detailed kinetic study of these two enantiomers was performed by Henderson, which further supported this claim; β -chloro-D-alanine (**38-D**) inhibited alanine racemase at a very low concentration ($K_i = 0.005$ mM) compared to the enantiomeric β -chloro-L-alanine (**38-L**) ($K_i = 1.17$ mM) (1976BBRC793). The mechanism of inhibition by β -chloroalanine (**38**), involving the formation of quinonoid structure (**43**) as claimed by Wang (1978B1313) and Adams (2000PAC373), contradicts the alanine racemase mechanism as claimed by later studies (1998B10438, 2005ABB279, B-2007MI285), which recognise that protonation of the pyridine nitrogen of PLP is less likely to occur in alanine racemase.

As discussed previously, all of the amino acid analogues exhibit their inhibitory effect upon interacting with either the PLP cofactor or active residues of the alanine racemase. However, their effectiveness *in vivo* is very much dependent on their ability to penetrate across the bacterial cell wall to the target. Modifications of these analogues (e.g. by incorporating carrier moieties, such as amino acids or peptides, which are recognised by peptide transport proteins), while retaining their inhibitory pharmacophore (suicide substrate), may enhance their uptake across the cell *via* peptide transport proteins. Possible carrier moieties based on fosfalin and β -chloroalanine are discussed in the next section (section 1.5).

1.4.4: Inhibitors of other enzymes

Para-aminobenzoic acid (PABA) (**48**) (Figure 1.15) is an important intermediate in the biosynthesis of tetrahydrofolate (**49**) which is an essential cofactor required in the biosynthesis of purines and pyrimidines, formyl-methionine tRNA, and some other amino acids (2007AEM2673). Therefore, bacterial inhibitory effects can be achieved upon disrupting this biosynthetic pathway. A known competitive inhibitor of PABA, sulfanilamide (**50**), belonging to the sulfonamide class of antibacterial agents, is able to inhibit this biosynthesis, due to its structural similarity to PABA.

Although PABA is an important metabolic element in bacteria, surprisingly, it also shows some antibacterial activity at a high concentration without the presence of any sulfonamide. For instance, the growth of *E. coli* was disrupted by PABA at 150-1600 $\mu\text{g}/\text{mL}$ and was converted to bacteriostasis completely by the addition of L-aspartic acid (**51**) at 1.0 $\mu\text{g}/\text{mL}$ (1951JEM243). Other growth inhibition by PABA at a high concentration was also reported, with Rickettsiae (Gram negative bacteria) at 500-1000 $\mu\text{g}/\text{mL}$ (1952Sci710), *Saccharomyces cerevisiae* (yeast) at 25 $\mu\text{g}/\text{mL}$ (1959JBC904), *P. aeruginosa* at 1500 $\mu\text{g}/\text{mL}$ (1992IJP195) and *E. cloacae* at 1200 $\mu\text{g}/\text{mL}$ (1992IJP195). The inhibitory enhancement of PABA against *P. aeruginosa*, *E. cloacae*, *P. mirabilis* and *S. aureus* was also reported when PABA was used in combination with the antibiotics carbenicillin (**52**), dibromopropamide isethionate (**53**) or polymyxin B (**54**), Figure 1.15 (1992IJP107).

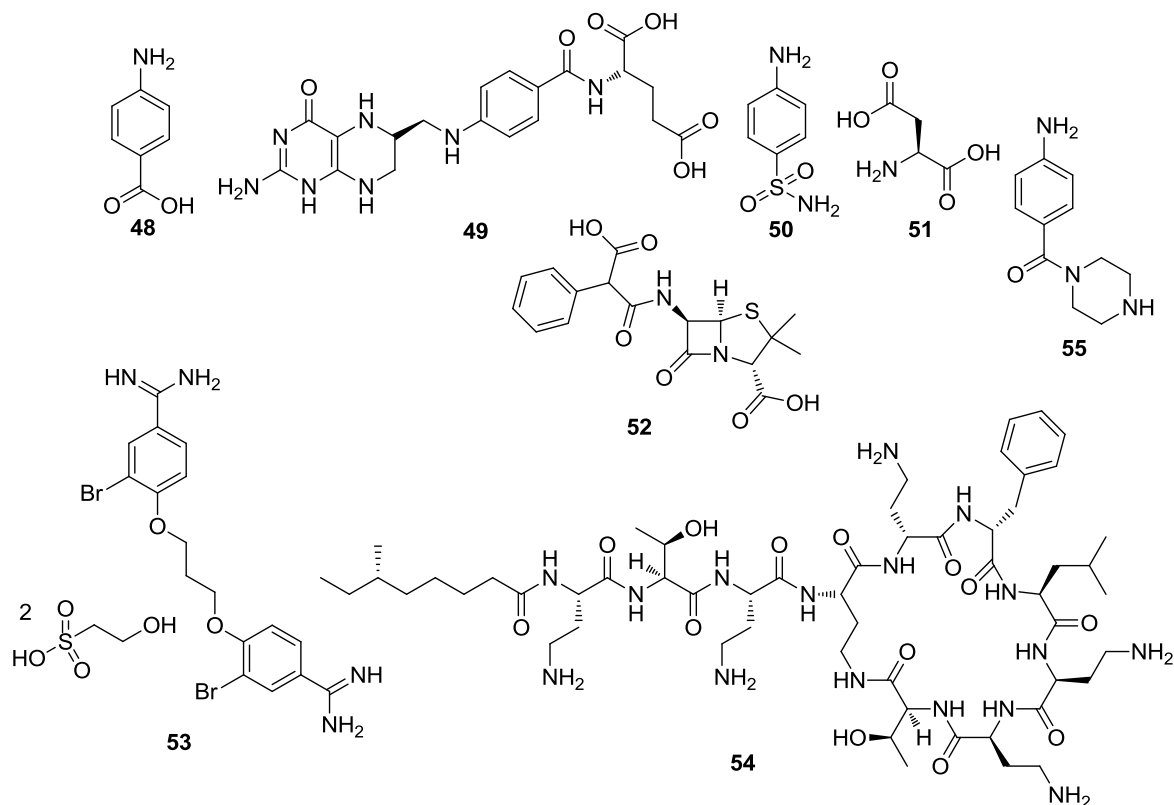


Figure 1.15: Structures of PABA (**48**), tetrahydrofolate (**49**), sulfanilamide (**50**), L-aspartic acid (**51**), carbenicillin (**52**), dibromopropamide isethionate (**53**), polymyxin B (**54**), 4-(piperazin-1-ylcarbonyl)aniline (**55**)

Although the inhibitory mechanism of PABA is still unclear, it was believed to have affected the peptidoglycan synthesis at a high concentration by blocking the dihydrofolate reductase enzyme, an enzyme involved in the tetrahydrofolate synthesis pathway (1995JAB209). All of these discoveries, consequently, inspire the development of new suicide substrates based on this molecule. For instance, Kulkarni and co-workers (2009AJRC300) have synthesised different amines based on PABA and, throughout the study, the antibacterial (zone of inhibition was observed at 100 $\mu\text{g}/\text{mL}$) and antifungal activities of 4-(piperazin-1-ylcarbonyl)aniline (**55**) were reported. This finding also leads to further investigations on other potential PABA based derivatives, such as, conjugation of another moiety to PABA that could potentially improve uptake into the cell or enhance the antibacterial activity.

1.5: Development of di/tripeptide suicide substrates based on fosfalin and β -chloroalanine

1.5.1: Stages and challenges involved prior to the expression of inhibitory action of suicide substrates

The inhibitory action and extensive mechanistic study of fosfalin and β -chloroalanine on alanine racemase, as previously discussed, led to further design and development of different novel compounds based on these inhibitors. Selective inhibition by these compounds can be achieved upon incorporation of these compounds into the detection kits (bacterial growth media). However, several conditions and factors have to be considered during the design of suicide substrates.

- Uptake of molecules across the bacterial cell

The suicide substrates are unable to exhibit any antibacterial activity without being transported into the cell and interacting with the target(s). Therefore, the uptake of drug-like molecules is essential and it can be achieved *via* either passive diffusion or active diffusion. The bacterial cell membrane is made of phospholipid bilayers and is lipophilic in nature; hence, lipophilic molecules can be transported easily across the cell wall *via* passive diffusion. Other molecules, on the other hand, require assistance as they cannot diffuse easily across the lipophilic membrane. In this case, porins and protein permeases play an important role to facilitate this transportation by active processes.

Porins are water-filled channels that are located in the outer (Gram negative bacteria) and cytoplasmic membranes (Gram negative and positive bacteria). These membrane proteins serve as a defence for bacteria, only allowing the passive influx of hydrophilic molecules. Non-specific and specific porins can be found at the outer membrane of Gram negative bacteria (2012CPPS843); for instance, in *E. coli*, the OmpC and OmpF porins mediate relatively non-specific and weakly cationic passive diffusion, while the PhoE porin only facilitates influx by anionic selective diffusion, known as phosphate transport (1985JB722). Although relatively specific, in the absence of peptide-specific porins, both OmpC and

OmpF porins mediate the permeation of a range of peptides across the outer membrane of *E. coli* (1985FML333). Another non-specific OprF porin (1991JBC770) and specific OprB (glucose), OprP (phosphate) and OprO (polyphosphate and tripolyphosphate) porins were noted in *P. aeruginosa* (1992JB471, 1992JB5196).

Protein permeases are transport proteins that are commonly found in the periplasm (Gram negative bacteria) and cytoplasmic membranes (Gram negative and positive bacteria). Unlike porins, permeases facilitate active diffusion in the presence of essential molecules, either protons or adenosine triphosphates (ATPs). Many permeases that facilitate the transportation of di- and tripeptides have been reported. Depending on the prerequisite molecules, permeases are categorised into two different families. For instance, the proton-dependent oligopeptide transporters (POTs) are classified under the PTR family, while the Dpp (dipeptide), Tpp (tripeptide) and Opp (oligopeptide) permeases are part of the ATP Binding Cassette (ABC) transporter family (2015BBA488). These permeases are from different families and are structurally and functionally distinct; they exhibit wide substrate promiscuity (2000PNAS12487, 2013NC1). In other words, they are not specific or restricted only to the uptake of specific peptides; instead they facilitate the uptake of a diverse range of peptides across the cell membrane. Although there is a lack of specific requirements for the uptake of peptides by these permeases, preferential transportation of di- and tripeptides with a positively charged amino terminus (1975JB1208) and large and/or hydrophobic side chains was reported (2012EMBO3411, 2013PNAS11343). Although porins and transport proteins are found in bacteria, the different morphology, with an outer membrane on the Gram negative bacteria, can result in a different level of molecule uptake between Gram positive and Gram negative bacteria.

Aside from the different morphology, variable and low uptake is seen in resistant bacteria. For instance, a lack of porin expression on resistant bacteria, such as *E. coli*, *E. cloacae*, *S. enterica*, *H. influenzae*, *K. pneumoniae* and *E. aerogenes*, was correlated with low inhibitory susceptibility, due to poor transportation of inhibitors into the bacteria (2005ADDR1486). The presence of efflux pumps can also affect the uptake of a molecule, as it can be removed prior to reaching to inhibitory

concentration in the bacterial cells. For example, the efflux mechanism in *S. pneumoniae* resulted in ineffective use of antibiotics, such as fluoroquinolones and macrolides, as these antibiotics are required to concentrate intracellularly in order to act on the cytoplasmic target(s) (2005ADDR1486).

- Release of inhibitor(s)

The uptake issues of antimicrobial molecules can be overcome by introducing the molecules in a prodrug manner. A prodrug is a masked form of an active drug, which is designed in a way that only can be activated by enzymatic or chemical reaction at the specific location(s) (2011PR750). In this case, lethal antibacterial residues can be incorporated with a natural residue(s), in order to facilitate transport across the bacterial cells. Depending on the type of moiety and chemical bond attached, specific enzymes or chemical reactions will be required for the release of the active inhibitor(s) within cells. The specificity requirements for the release of inhibitor(s) enable selective inhibition. For instance, L-fosfalin, a known inhibitor was released upon hydrolysis of L-alanyl-L-fosfalin by the specific alanine aminopeptidase present in Gram negative bacteria, Scheme 1.2 (1998B10438). However, extensive enzymatic study is required for the design of this prodrug in order to prevent false results, as similar enzymes can be encountered from different bacterial species.

- Expression of inhibitory action

Upon the successful uptake of drug molecules, and activation or release of active inhibitors within the target cells, the active inhibitor(s) exert inhibitory action by interacting with the target enzyme(s). However, different levels of inhibitory action were noted, even though the same target enzyme(s) was being targeted. For example, alafosfalin, targeting alanine racemase (1998B10438), inhibited the growth of non-*typhi Salmonella* strains and *E. coli* differently, at mean minimum inhibitory concentration (MIC) values of 10.2 mg/L and 0.7 mg/L, respectively (2002JCM3913). The factors that cause different levels of inhibition and selective inhibition on different bacterial species may be due to the reasons as discussed above. An interest of the current work is to find other alternatives to overcome the mentioned problems and, at the same time, to improve the selective inhibition. The attachment of different moieties to the inhibitor(s) for the enhancement of selective

inhibition will be investigated in the current work. Meanwhile, the literature evaluation of inhibitor(s) of interest and attachment of different carrier moieties will also be discussed in detail below.

1.5.2: Fosfalin

Atherton and co-workers found that L-fosfalin (**13-L**) displays better inhibition when compared to D-fosfalin (**13-D**) and D/L-fosfalin (**13-DL**) (Figure 1.16) (1979AAC677, 1979AAC696, 1970JOA567, 1986JMC29). Other studies also showed that L-fosfalin containing dipeptides or tripeptides display higher antibacterial activity compared to the single L-fosfalin pseudo-amino acid residue (**13-L**). The multiply ionised structure of fosfalin reduces its ability to penetrate the lipid bilayer cell membrane by itself, while the di/tripeptide inhibitors can be transported across the cell membrane with the aid of di/tripeptide transporter systems found on the cell membrane (1995AEM226).

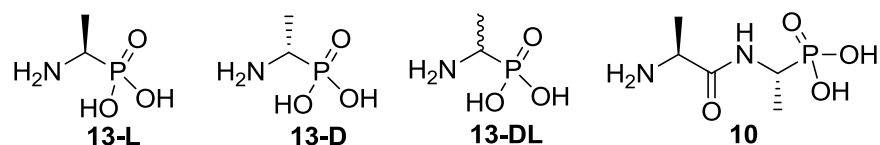


Figure 1.16: Structures of fosfalin stereoisomers (**13**) and alafosfalin (**10**)

The good inhibitory effects of alafosfalin, L-Ala-L-fosfalin (**10**), and its selective inhibition at low concentrations (2002JCM3913) led to exploitation of other derivatives based on L-fosfalin. A range of di/tripeptides based on L-fosfalin were studied and are summarised in Tables 1.5 and 1.6 (1980AAC897, 1979AAC677, 1986JMC29). Depending upon the carrier amino acid(s) coupled to L-fosfalin, different bacterial species can be inhibited at different concentrations. These inhibitory activities were measured by their MIC, usually quoted in $\mu\text{g/mL}$ or mg/L , which is the lowest concentration of an inhibitor to prevent the growth of visible microorganism after overnight incubation.

Table 1.5: Antibacterial activities of phosphonodipeptides, L-X-L-fosfalin (1980AAC897, 1979AAC677, 1986JMC29)

Species	Antibacterial activity MIC ($\mu\text{g/mL}$)														
	Nva	Met	Leu	Arg	Cit	Val	Phe	His	Trp	Cys ₂	Ala	Ser	Asn	Ile	Tyr
Gram negative bacteria															
<i>E. coli</i>	0.03	0.25	0.25	0.25	0.5	0.5	0.5	0.5	1	1	1	1	1	1	1
<i>K. aerogenes</i>	0.015	0.12	0.12	<0.12	0.12	0.25	1	1	0.25	0.5	0.5	0.5	0.5	1	1
<i>S. marcescens</i>	0.5	2	2	2	4	8	4	16	4	8	8	8	8	16	16
<i>S. typhimurium</i>	0.25	8	8	32	16	64	32	>128	16	64	64	32	64	128	>128
<i>H. influenzae</i>	4	16	32	128	64	64	32	128	128	128	64	16	128	32	128
<i>P. mirabilis</i>	16	32	32	128	64	>128	128	>128	>128	>128	>128	>128	>128	>128	>128
<i>P. aeruginosa</i>	32	NT	NT	NT	NT	NT	NT	NT	NT	NT	NT	NT	NT	NT	NT
Gram positive bacteria															
<i>E. faecalis</i>	1	1	2	16	4	8	2	4	64	4	2	16	32	4	4
<i>S. aureus</i>	8	1	8	16	8	8	4	8	16	64	32	64	8	128	8

Abv: Ala, Alanine; Arg, Arginine; Asn, Asparagine; Cit, Citrulline; Cys₂, Cystine; His, Histidine; Ile, Isoleucine; Leu, Leucine; Met, Methionine; Nva, Norvaline; Phe, Phenylalanine; Ser, Serine; Trp, Tryptophan; Tyr, Tyrosine; Val, Valine; NT, Not Tested

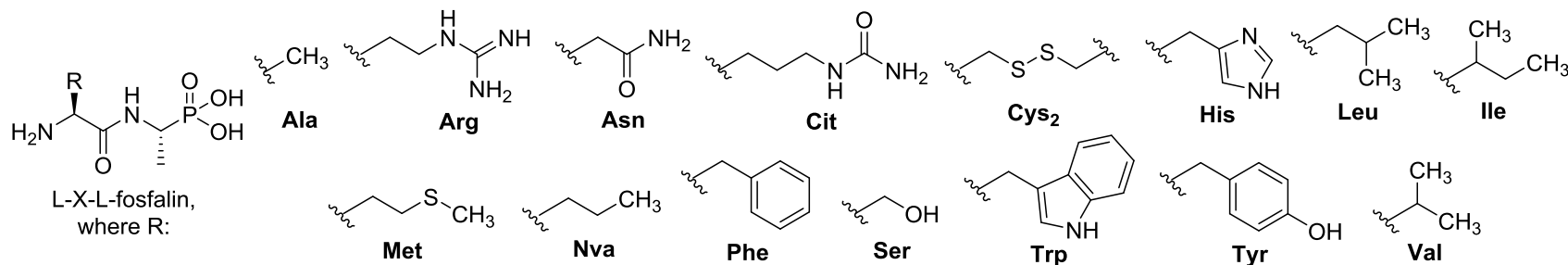


Table 1.5 shows that the incorporation of amino acids resulting in the dipeptides L-Met-L-fosfalin (**56**), L-Leu-L-fosfalin (**57**), L-Arg-L-fosfalin (**58**) and L-Nva-L-fosfalin (**59**) (Figure 1.17) achieves significant inhibitory effects, with MIC values below 0.25 $\mu\text{g/mL}$, and even as low as 0.03 $\mu\text{g/mL}$ on *E. coli*. These incorporated amino acids exhibited even lower MIC values when tested against *K. aerogenes*, while other species were inhibited at relatively higher MIC values. In short, these L-fosfalin based dipeptide derivatives, **56**, **57**, **58** and **59** showed a good inhibitory effect at a relatively low MIC compared to fosfalin derivatives with other amino acids. This could be due to the presence of the long hydrocarbon side chain on these amino acids (except Arg), resulting in elevation of their hydrophobicity, easier penetration across the bacterial cell membrane, as protein permeases prefer transportation of peptides with large and/or hydrophobic side chains (2012EMBO3411, 2013PNAS11343), and thus improved access to the inhibitory target. Although the side chain of arginine amino acid is not sufficiently hydrophobic due to its cationic guanidine properties, the uptake of L-Arg-L-fosfalin (**58**) could be facilitated by the specific or arginine permeases.

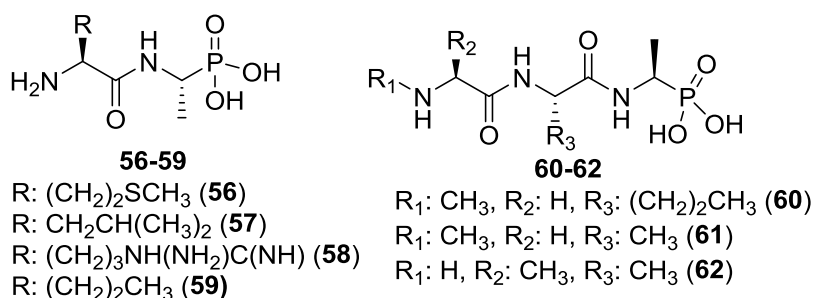


Figure 1.17: Structures of L-fosfalin based di/tripeptide derivatives (**56-62**)

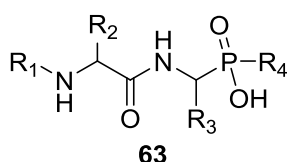
The phosphonotripeptide derivatives, where different dipeptides were conjugated with L-fosfalin were also reported and are summarised in Table 1.6. These results further support the previous claims that enhancement of the inhibitory activity is observed with the phosphonotripeptide derivatives with a long hydrocarbon side chain. For instance, a relatively low MIC was observed with Sar-L-Nva-L-fosfalin (**60**) compared to Sar-L-Ala-L-fosfalin (**61**). The side chain at the α -carbon also plays a significant role in affecting the inhibitory activity; a low MIC was observed with L-Ala-L-Ala-L-fosfalin (**62**) compared to Sar-L-Ala-L-fosfalin (**61**) (Figure 1.17).

Table 1.6: Antibacterial activity of phosphonotripeptides (1980AAC897)

Species	Antibacterial activity MIC ($\mu\text{g/mL}$)		
	60	61	62
Gram negative bacteria			
<i>E. coli</i>	0.5	1	0.5
<i>K. aerogenes</i>	0.5	4	0.12
<i>S. marcescenes</i>	64	>128	4
<i>S. typhimurium</i>	64	>128	32
<i>H. influenzae</i>	128	>128	<0.12
Gram positive bacteria			
<i>E. faecalis</i>	0.5	4	0.06
<i>S. aureus</i>	>128	>128	8

Abv: Ala, Alanine; Sar, Sarcosine; Nva, Norvaline

Based on the extensive antibacterial studies of these modified phosphonodipeptides and phosphonotripeptides, performed by Atherton and co-workers (1986JMC29), a detailed summary of structural requirements of phosphono-peptides to show *in vitro* antibacterial activity, using a simple structure (**63**) in Figure 1.18, is as follows:



- R₁ is L-amino acid or L-peptide but not simple acyl or alkyl groups.
- R₂ is natural or non-natural amino acid side chain or a chemically modified analogue.
- R₃ is CH₃ or H for good activity.
- R₄ is OH, CH₃ or H but not ester (OR).
- Free OH group on the phosphorus is essential
- L-Stereochemistry of phosphono-peptides is necessary for good activity.

Figure 1.18: Structure activity relationship of simple phosphopeptide analogues (1986JMC29)

All of this inhibitory evidence and the extensive studies on the phosphono-peptides, performed by Atherton and co-workers, provide good guidance for the current work in designing and synthesising fosfalin-based di/tripeptides for selective bacterial inhibition in the laboratory evaluation of clinical samples.

1.5.3: β -Chloroalanine

The antibacterial activity observed from fosfalin, an alanine analogue, led to the investigation and synthesis of other alanine analogues, such as β -haloalanine (e.g. β -chloroalanine) to target the bacterial enzyme alanine racemase. Many studies have been performed in the past by Cheung and co-workers (1983JMC1733, 1986 JMC2060) to evaluate the antibacterial activity of the synthesised β -chloroalanine and its dipeptide derivatives (Figure 1.19). According to their studies, both enantiomers, β -chloro-L-alanine (**38-L**), and β -chloro-D-alanine (**38-D**) showed antibacterial activity against the tested bacterial species, Table 1.7, which further support the similar claims made by Manning (1974PNAS417) and Henderson (1976BBRC793). For example, the antibacterial properties of β -chloro-L-alanine (**38-L**) extended to a limited number of Gram positive bacteria (*S. aureus*, *S. epidermidis*, *S. pyogenes*, *S. agalactiae*), while these bacteria were also inhibited by the enantiomer, β -chloro-D-alanine (**38-D**), but at higher MIC values compared to its L-isomer (1983JMC1733). Although the MIC values of the D-enantiomer (**38-D**) were high, a broad antibacterial spectrum, which extended to some Gram negative bacteria (*H. influenza*, *E. coli*, *S. flexneri*, *S. marcescens*, *E. aerogenes*), was observed.

The antibacterial activity of the β -chloro-L-alanine (**38-L**) was enhanced upon incorporation into L-alanyl dipeptides (**64**, **66**) and its inhibitory spectrum was extended to Gram negative bacteria by incorporation into dipeptide derivatives containing β -chloro-L-alanine, L-norvaline or L-methionine residues (**69-71**), Table 1.7. Although antibacterial activity and broad spectrum of β -chloro-D-alanine (**38-D**) were reported, its inhibitory activity was diminished upon forming the peptide derivatives (**65**, **67**, **68**); the intracellular peptidase activity may be restricted to cleavage of the peptide bond formed by L-amino acids (1975ARM485), although the peptides composed of D-amino acids can be transported across the bacterial cell wall (1977AAC638). As a result, the L-stereochemical form of β -chloroalanine serves as a good antimicrobial candidate.

Table 1.7: Antibacterial activity of β -chloroalanine dipeptides and the β -chloroalanine enantiomers (1983JMC1733)

Species	Antibacterial activities MIC ($\mu\text{g/mL}$)									
	Dipeptide derivatives								Amino acids	
	64	65	66	67	68	69	70	71	38-L	38-D
Gram negative bacteria										
<i>E. aerogenes</i>	>100	>100	>100	>100	>100	25	6.25	>100	>100	12.5
<i>E. cloacae</i>	>100	>100	>100	>100	>100	12.5	6.25	6.25	>100	>100
<i>E. coli</i>	>100	>100	>100	>100	>100	1.56	1.56	1.56	>100	6.25
<i>H. influenza</i>	>100	>100	>100	>100	>100	1.56	0.78	0.78	>100	6.25
<i>M. morgani</i>	>100	>100	>100	>100	>100	50	50	50	>100	>100
<i>P. mirabilis</i>	>100	>100	>100	>100	>100	50	100	12.5	>100	>100
<i>S. marcescenes</i>	>100	>100	>100	>100	>100	>100	50	>100	>100	25
<i>S. flexneri</i>	>100	>100	>100	>100	>100	12.5	>100	>100	>100	50
Gram positive bacteria										
<i>E. faecalis</i>	>100	>100	>100	>100	>100	3.12	0.39	0.39	>100	50
<i>S. aureus</i>	0.05	>100	0.0125	>100	>100	0.05	0.025	0.025	3.12	12.5
<i>S. epidermidis</i>	0.025	>100	0.0125	>100	>100	0.05	0.025	0.025	25	25
<i>S. pyrogenes</i>	>100	>100	>100	>100	>100	1.56	>100	>100	3.12	12.5
<i>S. agalactiae</i>	0.39	>100	0.20	>100	>100	0.39	0.20	0.20	3.12	12.5

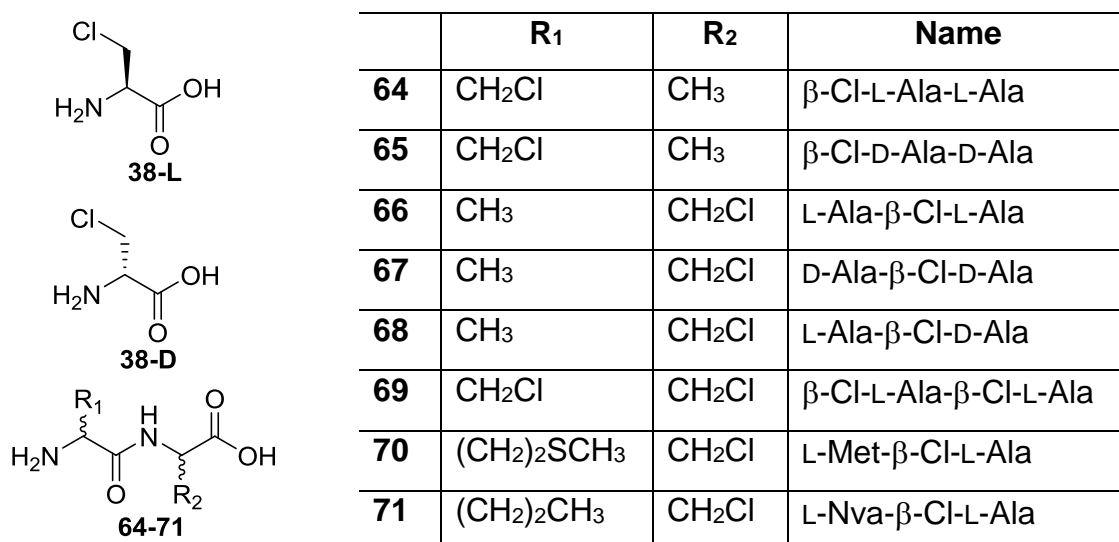


Figure 1.19: Structures of β -chloro-L-alanine (**38-L**), β -chloro-D-alanine (**38-D**) and dipeptides containing one or more β -chloroalanine residue(s) (**64-71**)

The inhibitory profile of both fosfalin and β -chloroalanine derivatives were well established a long time ago; however, their application in the enhancement of bacterial detection media has yet to be fully exploited. The synergistic effects of peptides consisting of both fosfalin and β -chloroalanine residues may offer a novel inhibitory effect or even extend the existing bacterial inhibitory spectrum, which is beneficial for a new era of bacterial detection applications. These potential synergistic effects will be investigated further as part of the current work.

1.5.4: Rationale for synthesis of di/tripeptide suicide substrates based on fosfalin and β -chloroalanine

The extensive studies performed by Atherton and Cheung as discussed previously not only provide a new lead of potential carrier moieties that can be used as suicide substrates, but also the design of the di/tripeptide phosphonopeptide derivatives. A good antibacterial activity with generally low MIC values (Table 1.5), typically with the use of L-norvaline and L-methionine as a carrier moiety for phosphonodipeptide derivatives, suggests the use of a long hydrocarbon side chain at the *N*-terminus of phosphonopeptide derivatives can enhance the antibacterial action. This favourable inhibitory action was also observed on the

dipeptide derivatives based on β -chloro-L-alanine (Table 1.7), which further support the use of long hydrocarbon side chain residues.

There are limited studies of phosphonotripeptide derivatives with different *N*-terminal residues attached. Therefore, investigation of phosphonotripeptides based on L-alanyl-fosfalin or β -chloro-L-alanyl-fosfalin will be performed as part of the current work. As a result of the good inhibitory action of phosphonopeptide derivatives with L-norvaline or L-methionine attached at the *N*-terminus (Table 1.5), these two residues will be used as a carrier moiety for the development of phosphonotripeptide derivatives. The use of L-alanine and sarcosine residues as a carrier moiety for tripeptide derivatives will be investigated as well, due to the inhibitory activities reported on some bacterial species (Table 1.6).

Although the study of phosphonotripeptide derivatives is the main interest of the current work, phosphonodipeptide derivatives will be investigated as well by incorporating L-pyroglutamic acid and β -chloro-L-alanine with the fosfalin in order to target different aminopeptidases present in the specific bacteria for selective inhibition activity. Using this approach, L-pyroglutamyl aminopeptidase expressing bacteria, *B. subtilis*, *E. cloacae*, *P. putida* and *P. fluorescens* (B-2011MI80), may be differentiated from L-alanyl aminopeptidase expressing bacteria.

The extended spectrum of antibacterial activities observed (Table 1.7) when a peptide derivative containing two inhibitors (**69**) was tested led to the idea of incorporating two suicide inhibitors into a single peptide derivative. A good comparison can be made between peptide derivatives containing one inhibitor (fosfalin) and two inhibitors (fosfalin and β -chloroalanine). This concept was also applied to other molecule, PABA. Although PABA does not target alanine racemase, its spectrum will also be investigated by conjugating with β -chloroalanine. The synthesis and evaluation of each compound will be discussed in detail in the following chapters.

1.6: Aims and Objectives

The aim of this work was to enhance the selectivity, sensitivity and resolution of chromogenic and fluorogenic media for bacterial detection and specific identification in clinical samples.

The known suicide inhibitors, D/L-fosfalin and β -chloro-L-alanine will be synthesised, prior to further coupling with other amino acid residues. A range of different di/tripeptide derivatives based on these inhibitors will be generated using the well-established peptide coupling approach, involving the use of common coupling reagents, isobutyl chloroformate and *N*-methyl morpholine. The synthesis of dehydroala-D/L-fosfalin will be attempted, due to the interesting antibacterial activity of β -chloro-L-Ala-L-fosfalin reported by Váradi (T-2013MI192), as well as the important role of dehydroalanine as an intermediate in alanine racemase inhibition (1978B1313, 2000PAC373). Derivatives of another potential inhibitor, not targeted at alanine racemase, *para*-aminobenzoic acid (PABA), will be synthesised for microbiological evaluation.

For a better understanding of the stability of the β -chloro-L-alanine moiety under the different pH conditions in the growth media, β -chloro-L-Ala-D/L-fosfalin will be used as a β -chloro-L-alanine based representative compound for evaluation. The pH range 6.1 – 9.1 will be studied over fixed time intervals using $^1\text{H-NMR}$ spectroscopy.

To investigate the feasibility and selectivity of these synthesised di- and tripeptide-based inhibitors for use in growth media containing chromogenic or fluorogenic substrates, microbiological evaluation will be carried out. Inhibitor performance against twenty different bacterial species, commonly found in clinical samples and covering both Gram-positive and Gram-negative strains, will be evaluated during the microbiology testing.

CHAPTER 2

SYNTHESIS OF D/L-FOSFALIN AND SUICIDE SUBSTRATES BASED ON D/L-FOSFALIN

2.1: Synthesis of peptide derivatives containing D/L-fosfalin

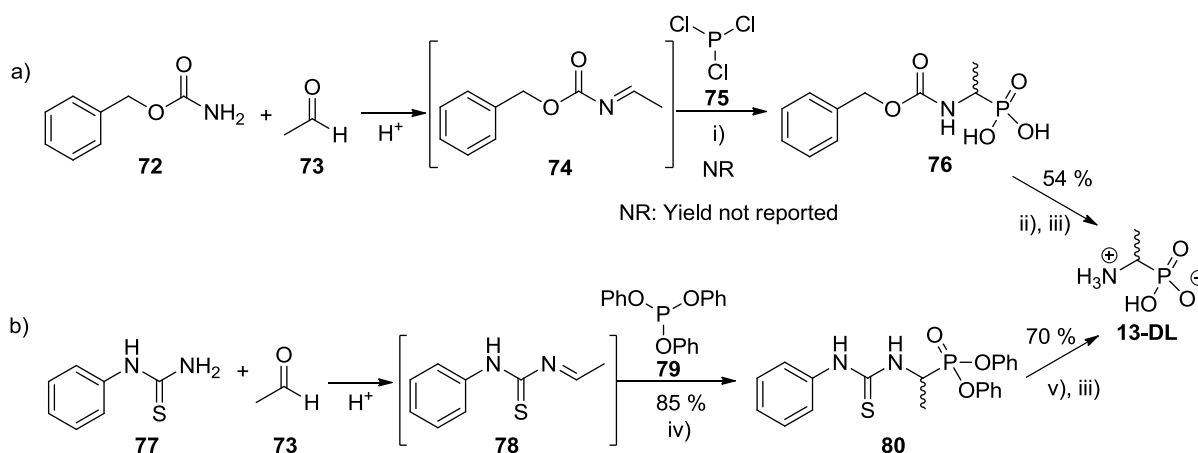
As outlined in Chapter 1, the inhibitory activity of L-fosfalin on alanine racemase and the antibacterial activity of its phosphonopeptide derivatives led to the current investigations. The extensive studies of many phosphonopeptide derivatives, performed by Atherton and co-workers (1979AAC677, 1986JMC29), provided a good starting point for the design and synthesis of new phosphonopeptide derivatives. Although studies showed that the most effective inhibitory action was observed from L-fosfalin derivatives (1986JMC29), one disadvantage to the use of this enantiomerically pure inhibitor is the cost of its production, which increases the cost of L-fosfalin containing culture plates. As a result, the inhibitory effect of di- and tripeptide derivatives of racemic fosfalin, D/L-fosfalin (**13-DL**), was investigated in this current work, due to its easy, rapid and economic synthesis. In the following section, the synthesis of D/L-fosfalin (**13-DL**) and a range of different peptide derivatives based D/L-fosfalin (**13-DL**) will be discussed.

2.2: Published methods for the synthesis of 1-aminoethylphosphonic acid (D/L-fosfalin)

Racemic and optically active fosfalin are both commercially available, but are very expensive, which presented a significant problem for this work, as a large quantity was required for the synthesis of a suitable range of peptide derivatives containing fosfalin. Review of the synthesis of fosfalin identified several methods for the synthesis of 1-aminoethylphosphonic acid (D/L-fosfalin), summarised as follows:

- Oleksyszyn reaction using phosphorus trichloride, acetaldehyde and benzyl carbamate, Scheme 2.1a (1978S479). In this reaction, the benzyl carbamate (**72**) reacted with acetaldehyde (**73**) *via* Schiff's base formation under acidic conditions, followed by attack of phosphorus trichloride (**75**) on the imine (**74**). The *N*-carboxylbenzyl group of **76** was later removed under acidic hydrolysis and treatment with propylene oxide formed racemic fosfalin (**13-DL**), with final yield of 54 %.
- Acidic hydrolysis of thioureidoalkanephosphonate, Scheme 2.1b (1978S469). Thioureidoalkanephosphonate (**80**) was synthesised *via* Schiff's base formation between *N*-phenylthiourea (**77**) and acetaldehyde (**73**), under

acidic conditions, followed by reaction between the resulting imine species (**78**) and triphenyl phosphite (**79**). Acidic hydrolysis removed both *N*-phenylthiourea and *O,O*-diphenyl ester protecting groups simultaneously from **80** and subsequent treatment with propylene oxide formed racemic fosfalin (**13-DL**), with an overall yield of 60 %.

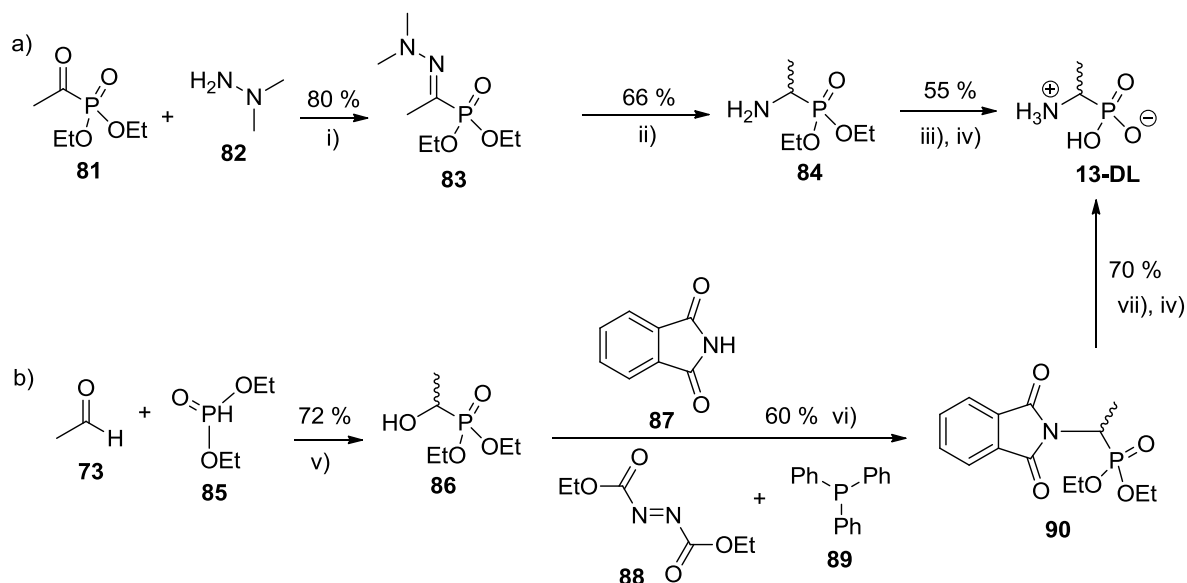


Scheme 2.1: a) Synthesis of racemic fosfalin (**13-DL**) via Oleksyszyn reaction (1978S479) and b) hydrolysis of thioureidoalkanephosphonate (**80**) (1978S469)

Reagents and conditions: i) AcOH, reflux 40mins; ii) HCl, reflux 30mins; iii) propylene oxide; iv) AcOH, 80°C 30mins then H₂O, r.t., 10hrs; v) AcOH/HCl (1:10), reflux 7hrs

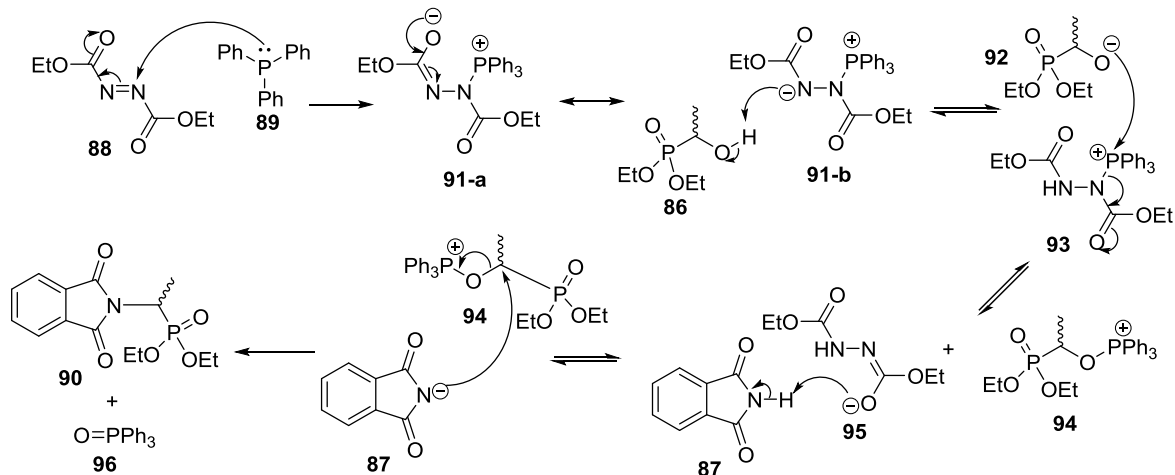
- Acidic hydrolysis of *O,O*-diethyl 1-aminoethylphosphonate, Scheme 2.2a (1980S1028). In this reaction, Schiff's base formation between *O,O*-diethyl 1-oxoethylphosphonate (**81**) and *N,N*-dimethylhydrazine (**82**) occurred under acidic conditions, to form the hydrazone intermediate (**83**). Intermediate (**83**) was subsequently reduced to *O,O*-diethyl 1-aminoethylphosphonate (**84**), using zinc and a mixture of acetic and trifluoroacetic acids. The *O,O*-diethyl ester groups were removed under acidic conditions and treatment with propylene oxide formed racemic fosfalin (**13-DL**), with an overall yield of 29 %.
- Hydrazinolysis and acidic hydrolysis of *O,O*-diethyl 1-phthalimidoethylphosphonate, Scheme 2.2b (1982S653). In this reaction, *O,O*-diethyl 1-hydroxyethylphosphonate (**86**) was synthesised, using acetaldehyde (**73**) and diethyl phosphite (**85**) under base-catalysed conditions, followed by a Mitsunobu reaction with phthalimide (**87**), in the presence of diethyl azodicarboxylate (**88**) and triphenylphosphine (**89**), resulting in formation of *O,O*-diethyl 1-phthalimidoethylphosphonate (**90**). The

detailed mechanism of compound **90** formation *via* the Mitsunobu reaction is described in Scheme 2.3. The *N*-phthalimide and the *O,O*-diethyl ester protecting groups of **90** were removed by *N,N*-dimethylhydrazine (**82**) and acid, respectively, to form the racemic fosfalin upon treatment with propylene oxide, with an overall yield of 30 %.



Scheme 2.2: Synthesis of racemic fosfalin *via* a) hydrolysis of *O,O*-diethyl 1-aminoethylphosphonate (**84**) (1980S1028) and b) *O,O*-diethyl 1-phthalimidoethylphosphonate (**90**) (1982S653)

Reagents and conditions: i) AcOH, r.t., 1hr; ii) Zn, CF₃COOH, AcOH, rt 2hrs; iii) AcOH/HCl (1:3), reflux 8hrs; iv) propylene oxide; v) TEA, 75°C 30mins; vi) THF, r.t., 48hrs; vii) *N,N*-dimethylhydrazine (**82**) in MeOH, r.t., 24hrs, then reflux 2hrs, HCl, reflux 6hrs



Scheme 2.3: Mechanism of the Mitsunobu reaction: formation of *O,O*-diethyl 1-phthalimidoethylphosphonate (**90**)

During the Mitsunobu reaction (Scheme 2.3), the complex (**91a-b**), formed upon reaction between triphenylphosphine (**89**) and diethyl azodicarboxylate (**88**), acts as a base to remove the hydroxyl proton from **86**. The resulting alkoxide ion (**92**) subsequently attacks the positively charged phosphorus of **93** forming phosphorus intermediate (**94**) and imidoyl anion (**95**), which removes the imide proton from **87** to result in a new anionic species (ionised **87**). Attack of the phosphorus derivative (**94**) by ionised **87**, liberates phosphine oxide (**96**) and racemic *O,O*-diethyl 1-phthalimidoethylphosphonate (**90**).

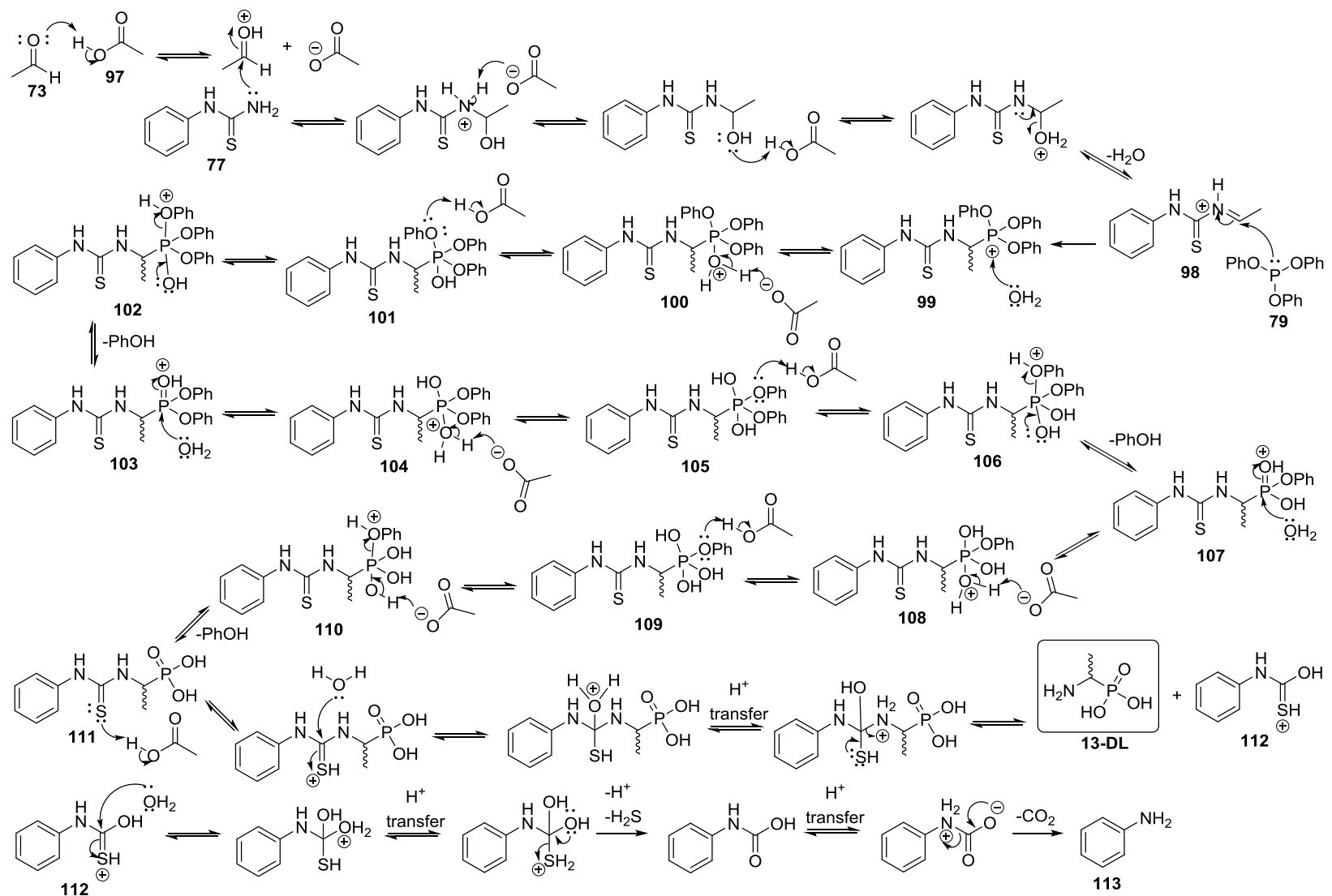
The Oleksyszyn method can be used in the synthesis of optically active fosfalin, *via* the selection of enantiomerically pure carbamate or urea derivatives, thus the (+)-product was synthesised from chiral (+)-carbamate or (+)-urea derivatives, while the (-)-product was prepared from chiral (-)-carbamate or (-)-urea derivatives (1989BCSJ3177). Some of the chiral carbamate and urea derivatives used in the reported synthesis are not available commercially or are costly; therefore, in-house synthesis was desirable. Although the synthetic methods of these chiral carbamate and urea derivatives are well established, their total synthesis would require more reaction steps and time. As a result, racemic fosfalin was chosen for the current work to allow rapid evaluation of selective inhibitors that could be synthesised later in chirally pure form if desired.

2.2.1: Synthesis of racemic 1-aminoethylphosphonic acid or D/L-fosfalin (13-DL)

The synthesis of D/L-fosfalin was achieved *via* thioureidoalkanephosphonate (**80**), Scheme 2.1b, due to the good overall yield obtained compared to other approaches. This method, however, was modified slightly: the thioureidoalkanephosphonate intermediate (**80**) was not isolated, but proceeded directly to the subsequent acidic hydrolysis. In other words, a one-pot reaction was performed using acetaldehyde (**73**), *N*-phenylthiourea (**77**) and triphenyl phosphite (**79**). The detailed mechanism is shown in Scheme 2.4.

In this reaction (Scheme 2.4), acetic acid (**97**) activated acetaldehyde (**73**) prior to the formation of Schiff's base (**98**) with *N*-phenylthiourea (**77**). The iminium species (**98**) was attacked by triphenyl phosphite (**79**) to form a phosphorus intermediate (**99**), which was subjected to attack by water and a series of proton transfers, *via* acid and base reactions (**100-110**), liberating three phenol molecules and *N*-phenylthiourea-D/L-fosfalin (**111**). Intermediate (**111**) proceeded to acidic hydrolysis, without isolation, to result in D/L-fosfalin (**13-DL**) and thioamide derivative (**112**), which was further degraded to other by-products, including aniline (**113**), carbon dioxide and hydrogen sulfide.

Evidence of the successful synthesis of D/L-fosfalin (**13-DL**) was obtained from the NMR spectra, melting point and mass spectrometry. In the $^1\text{H-NMR}$ spectrum (Figure 2.1), peaks corresponding to CH and CH_3 displayed additional coupling to the phosphorus: the double doublet of the methyl group at δ 1.40 ppm displayed a $^3J_{\text{H-P}}$ coupling constant of 14.7 Hz and a $^3J_{\text{H-H}}$ coupling constant of 7.2 Hz. A sextet signal (overlap of two quartets), corresponding to the CH proton was observed at δ 3.33 ppm, due to coupling to phosphorus and the CH_3 protons. Coupling to the phosphorus was also observed in the proton decoupled $^{13}\text{C-NMR}$ spectrum (Figure 2.2), in which the signals for CH at δ 44.7 ppm and CH_3 at δ 13.5 ppm were seen as doublets, with a typical $^1J_{\text{C-P}}$ coupling constant of 144.2 Hz to the CH carbon and a $^2J_{\text{C-P}}$ coupling constant of 2.6 Hz to the CH_3 carbon. Its purity was further confirmed by satisfactory CHN elemental analysis.



Scheme 2.4: Mechanism of D/L-fosfalin (**13-DL**) synthesis in a one-pot reaction, using acetaldehyde (**73**), N-phenylthiourea (**77**) and triphenyl phosphite (**79**)

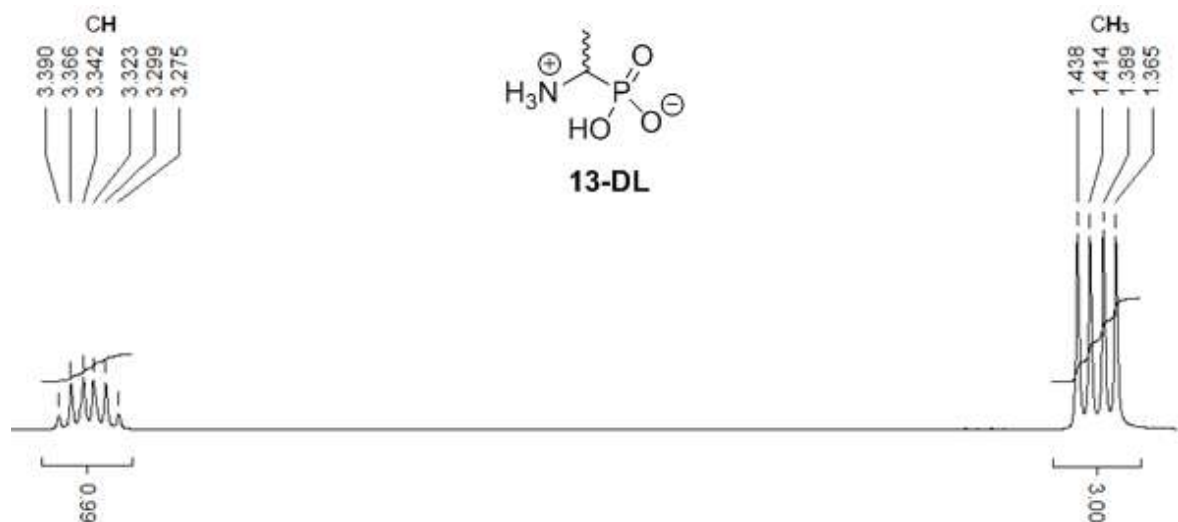


Figure 2.1: ¹H-NMR spectrum of fosfalin **13-DL** in D₂O at 300 MHz

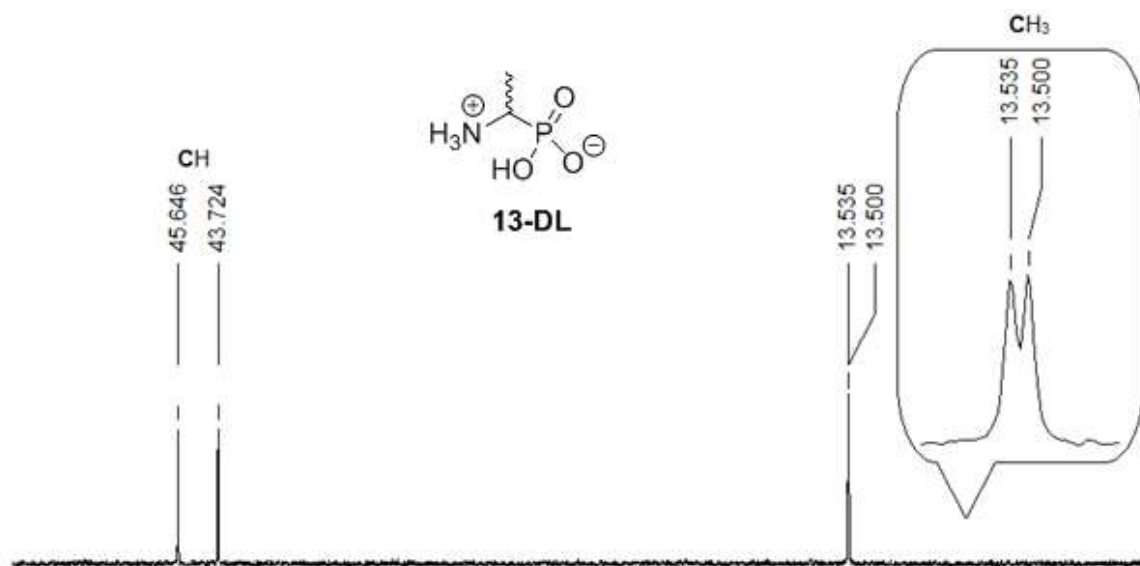
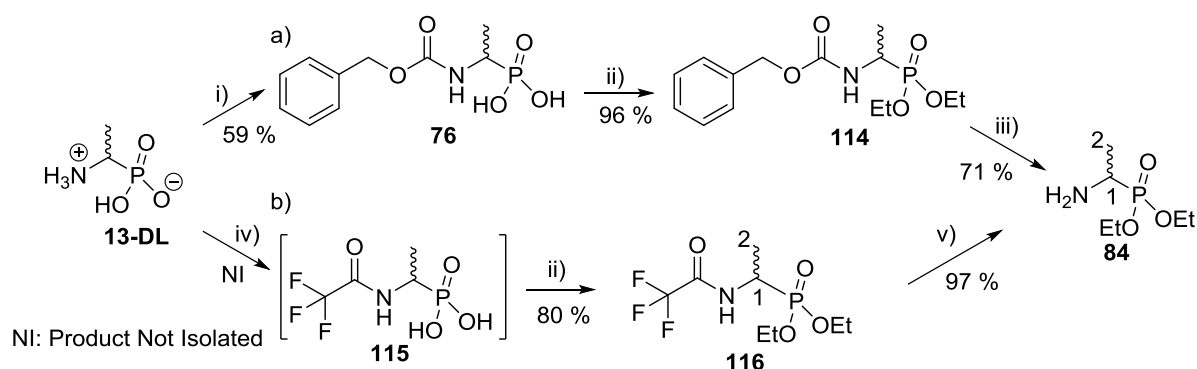


Figure 2.2: Proton decoupled ¹³C-NMR spectrum of fosfalin **13-DL** in D₂O at 75 MHz

2.3: Published methods for the protection of fosfalin as *O,O*-diethyl 1-aminophosphonate or *D/L*-fosfalin diethyl ester (**84**)

Prior to coupling with other amino acids of interest, the zwitterionic form of *D/L*-fosfalin (**13-DL**) required the introduction of protecting groups. Phosphonate ester protection was used due to easy access to many available methodologies. The chosen protected compound, *O,O*-diethyl 1-aminoethylphosphonate (**84**) can be obtained *via* *N*-Cbz protection (**76**) and phosphonate esterification (**114**), followed by the removal of the *N*-Cbz group, Scheme 2.5a (1975JMC106). Compound (**84**) can also be produced in one-pot reaction *via* *N*-trifluoroacetylation (**115**) and phosphonate esterification (**116**), followed by the removal of the *N*-trifluoroacetyl group, Scheme 2.5b (1995S509). Another synthetic route, discussed previously in Scheme 2.2 (1980S1028), can also be considered for this synthesis, using *O,O*-diethyl 1-oxoethylphosphonate (**81**), instead of *D/L*-fosfalin (**13-DL**), as a synthetic precursor.

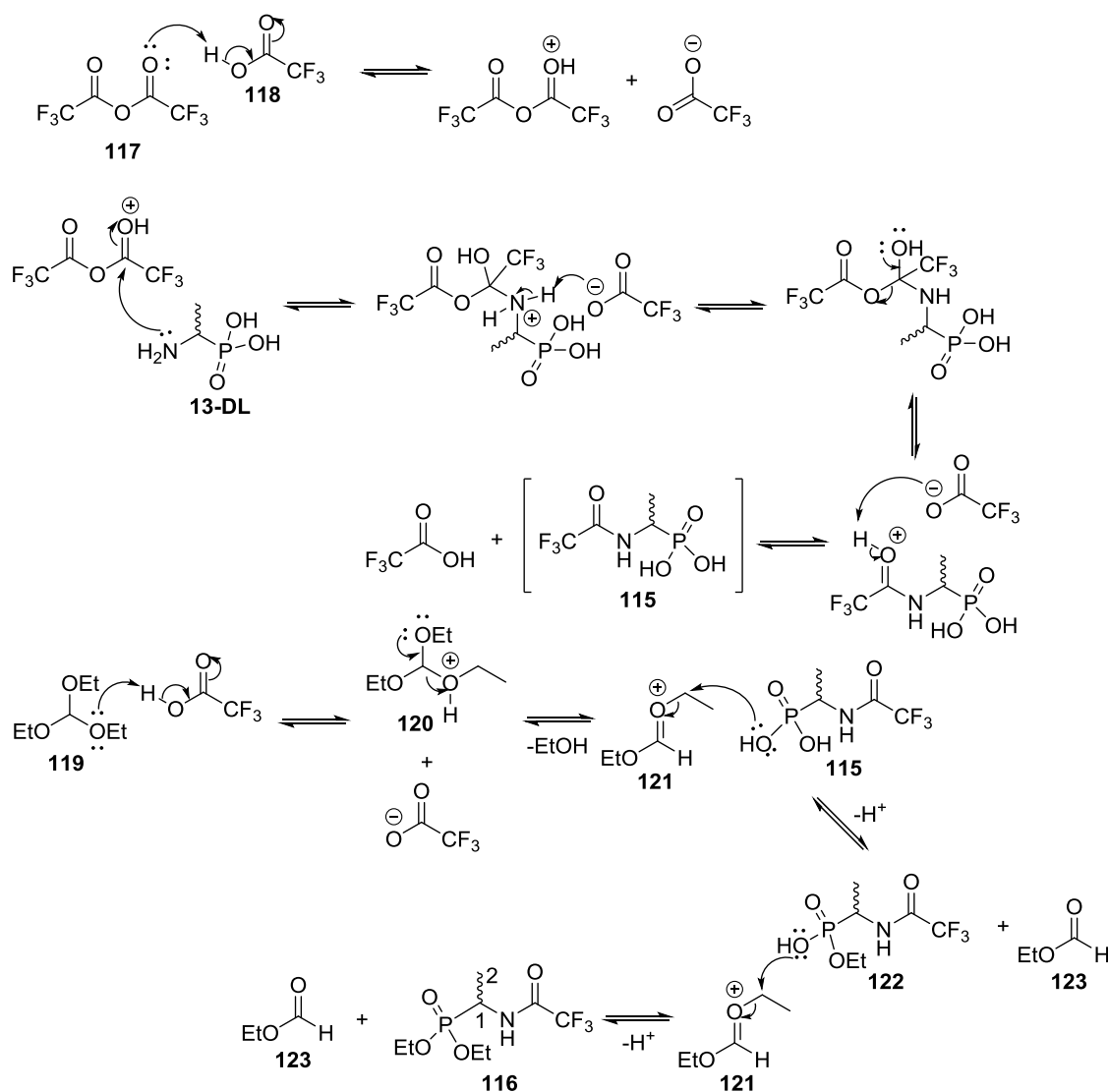


Scheme 2.5: Synthesis of *O,O*-diethyl 1-aminoethylphosphonate (**84**) (1975JMC106) (1995S509)

Reagents and conditions: i) pH9.5 by NaOH, benzyl chloroformate, Et₂O, 11.5hrs; ii) triethyl orthoformate, 135°C, 1hr; iii) H₂, 10% Pd/C, methanol, 24hrs; iv) CF₃COOH, (CF₃CO)₂O, reflux 1hr; v) NaBH₄, EtOH, reflux 4hrs

2.3.1: Synthesis of diethyl (1-(2,2,2-trifluoroacetamido)ethyl)phosphonate or trifluoroacetyl-D/L-fosfalin diethyl ester (116)

The synthetic route involving *N*-trifluoroacetylation and diethyl phosphonate esterification (Scheme 2.5a) was used to prepare trifluoroacetyl-D/L-fosfalin diethyl ester (116), as it is a two-step one-pot reaction without the need to isolate the intermediate (115) and with a good overall yield of 78 %. The mechanism of the selected one-pot reaction is shown in Scheme 2.6. In this reaction, acid-catalysed trifluoroacetylation produces intermediate (115), which subsequently undergoes acid-catalysed phosphonate esterification (119-122) to yield *N*- and *O*-protected fosfalin (116).



Scheme 2.6: Synthetic mechanism of trifluoroacetyl-D/L-fosfalin diethyl ester (116)

The successful synthesis of **116** was confirmed by NMR spectroscopy (Table 2.1), IR, melting point and mass spectrometry. Diastereotopic signals were observed for the phosphonate diethyl ester groups due to the presence of a chiral center at C-1. Therefore, each phosphonate ethyl ester group gave rise to an individual signal, as seen in the ^1H and ^{13}C -NMR spectra. In the ^1H -NMR spectrum (Figure 2.3), the individual peaks corresponding to the OCH_2CH_3 protons were unable to be resolved clearly due to the additional phosphorus coupling which complicated the splitting and resulted in overlapping multiplets at δ 4.06 ppm. A similar complicated signal was also observed at δ 4.39 ppm, corresponding to the CH-1 proton. The co-existence of proton and phosphorus coupling was clearly observed at δ 1.38 ppm, corresponding to the CH_3 -2 protons, which appeared as a doublet of doublets with $^3J_{\text{H-P}}$ coupling of 16.5 Hz and $^3J_{\text{H-H}}$ coupling of 7.2 Hz. Although the coupling constants reported in the literature (1995S509) were different, the chemical shifts were relatively comparable with the ^1H -NMR spectrum of **116** obtained in this synthesis.

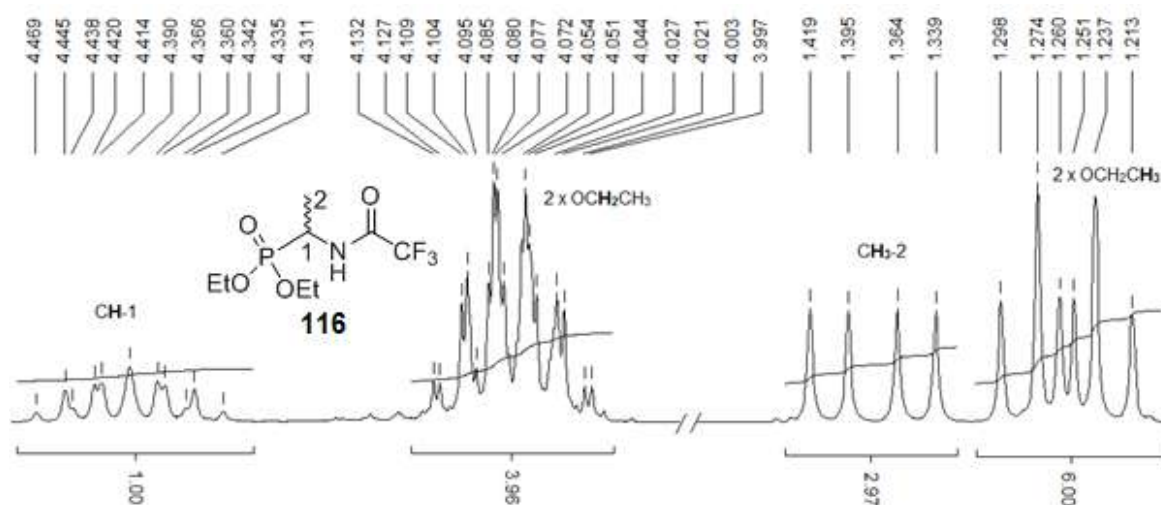


Figure 2.3: ^1H -NMR spectrum of compound **116** in CDCl_3 at 300 MHz, range between 1.20 ppm and 4.50 ppm

In the ^{13}C -NMR spectrum (Figure 2.4), the phosphorus coupling resulted in the splitting of peaks assigned to the carbon atoms in close proximity to the phosphorus atom. For instance, doublets observed at δ 16.2 ppm and δ 16.3 ppm, δ 62.8 ppm and δ 63.2 ppm were assigned to each diastereotopic OCH_2CH_3 methyl and methylene carbon, respectively, while the doublet at δ 41.8 was assigned to the CH-1 carbon. The values of each $J_{\text{C-P}}$ coupling constant are listed in Table 2.1. Apart from the phosphorus coupling, the fluorine-coupled signals were also observed as a quartet ($^1J_{\text{C-F}} = 285.8$ Hz) at δ 115.9 ppm, corresponding to the CF_3 carbon, and a quartet ($^2J_{\text{C-F}} = 5.8$ Hz) at δ 156.9 ppm, corresponding to the carbonyl carbon.

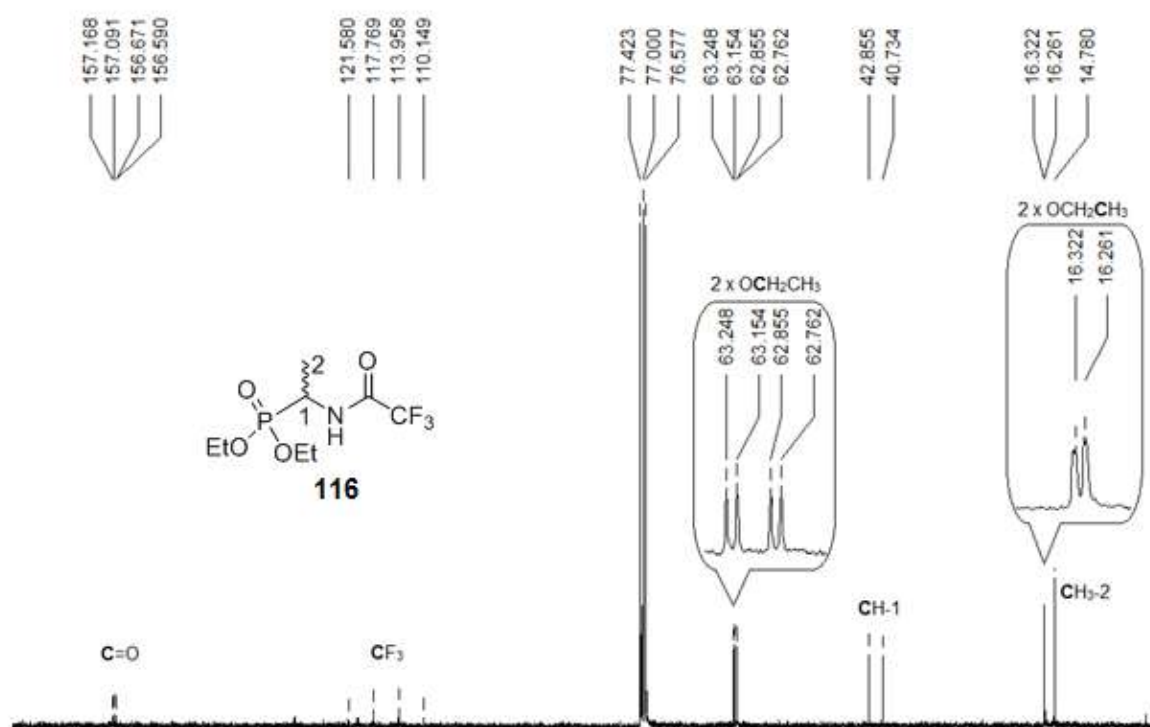


Figure 2.4: Proton-decoupled ^{13}C -NMR spectrum of compound **116** in CDCl_3 at 75 MHz, range between 0 ppm and 170 ppm

Table 2.1: Assignment of NMR signals and literature ¹H-NMR (1995S509) of trifluoroacetyl-D/L-fosfalin diethyl ester (**116**)

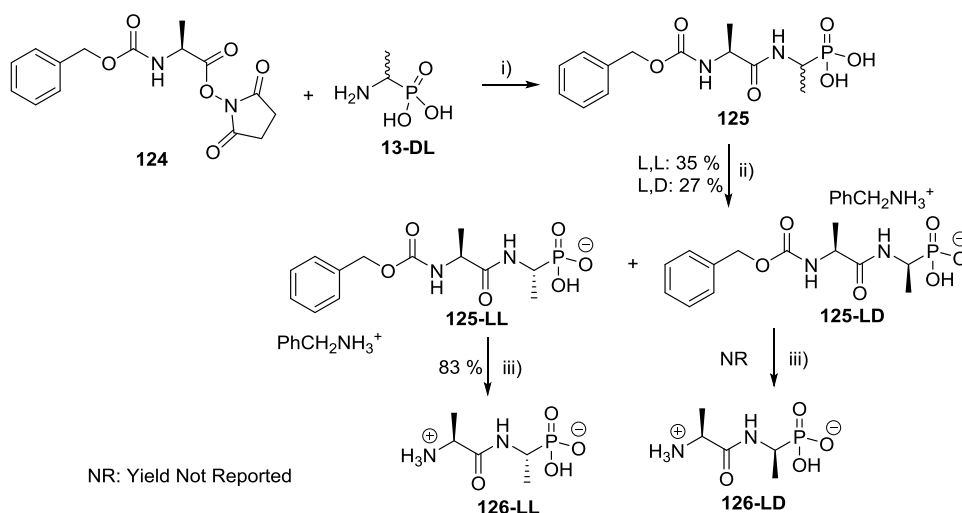
	δ_{H} (CDCl ₃), 300 MHz	δ_{C} (CDCl ₃), 75 MHz	δ_{H} (CDCl ₃), 200 MHz (1995S509)
OCH ₂ CH ₃	1.24 (3H, t, ³ J _{H-H} =7.2 Hz, CH ₃) 1.27 (3H, t, ³ J _{H-H} =7.2 Hz, CH ₃) 4.06 (4H, m, 2 x CH ₂)	16.2 (d, ³ J _{C-P} =2.3 Hz, CH ₃) 16.3 (d, ³ J _{C-P} =2.3 Hz, CH ₃) 62.8 (d, ² J _{C-P} =7.0 Hz, CH ₂) 63.2 (d, ² J _{C-P} =7.1 Hz, CH ₂)	1.30-1.65 (6H, m, 2 x CH ₃) 4.12 (4H, qq, J= 8.1, 1.1 Hz, 2 x CH ₂)
CH ₃ -2	1.38 (3H, dd, ³ J _{H-P} =16.5 Hz, ³ J _{H-H} =7.2 Hz)	14.8	1.29 (3H, dd, J=7.1, 0.5 Hz)
CH-1	4.39 (1H, m)	41.8 (d, ¹ J _{C-P} =159.1 Hz)	4.34-4.60 (1H, m)
NH	8.00 (1H, d, ³ J _{H-H} =6.0 Hz)	-	7.57-7.80 (1H, br)
CF ₃	-	115.9 (q, ¹ J _{C-F} =285.8 Hz)	-
C=O	-	156.9 (q, ² J _{C-F} =5.8 Hz)	-

2.3.2: Synthesis of *O,O*-diethyl 1-aminoethylphosphonate or *D/L*-fosfalin diethyl ester (**84**)

The *N*-protected phosphonate (**116**) was reduced with sodium borohydride to form *O,O*-diethyl 1-aminoethylphosphonate (**84**), with a free amino group for the subsequent peptide coupling. Evidence of the successful removal of the *N*-trifluoroacetyl group was provided by the disappearance of the strong absorbance peak at 1715 cm⁻¹ from the IR spectrum, corresponding to the carbonyl group of compound **116**. The reduction and removal of the trifluoroacetyl group were also supported by the ¹³C-NMR spectrum, in which the peaks at δ 115.9 ppm and δ 156.9 ppm, corresponding to the CF₃ and C=O carbons of compound **116**, respectively, had vanished.

2.4: Published methods for the preparation of peptides containing the fosfalin moiety

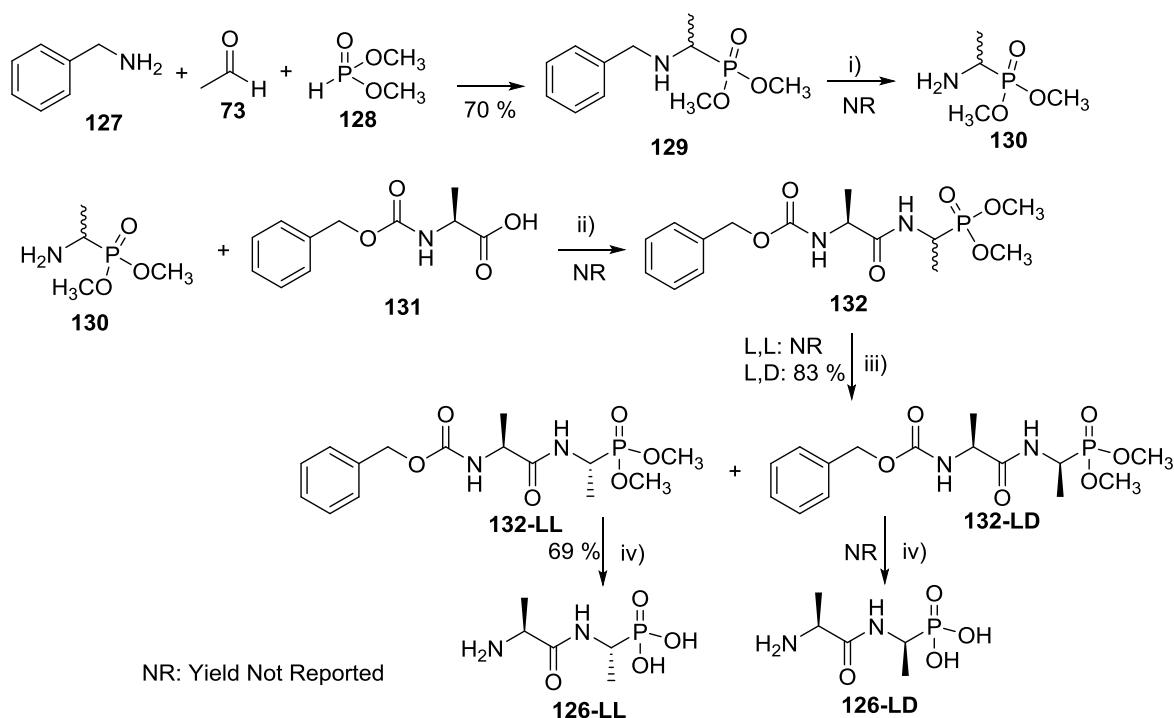
According to Atherton and co-workers, the phosphonodipeptide L-alanyl-*D/L*-fosfalin was synthesised by coupling *D/L*-fosfalin (**13-DL**) and *N*-Cbz-L-alanine-*N*-hydroxysuccinimide ester (**124**) (Scheme 2.7) (1986JMC29). The mixture of diastereoisomers formed (**125**), containing both L,L- and L,D- diastereoisomers, was separated as the benzylamine salts, affording optically pure **125-LL** and **125-LD**. The *N*-Cbz group was then removed under acidic conditions to afford optically pure L-alanyl-L-fosfalin (**126-LL**) and L-alanyl-D-fosfalin (**126-LD**). The overall yield of **126-LL** was 29 %, while the overall yield of **126-LD** was not reported.



Scheme 2.7: Synthetic route to optically pure L-Ala-L-Fos (**126-LL**) and L-Ala-D-Fos (**126-LD**) (1986JMC29).

Reagents and conditions: i) DMF, H₂O, Et₃N, 0 °C to r.t., 24hrs; ii) cation-exchange resin (RSO₃H), H₂O/EtOH, PhCH₂NH₂; iii) 48% HBr/AcOH, 2hrs then propylene oxide, r.t., 2hrs

The drawback of using this approach (Scheme 2.7) is not only the low overall yield of **126-LL** but also the involvement of water or aqueous dimethylformamide (DMF), due to the insolubility of D/L-fosfalin (**13-DL**) in common organic solvents. This was later overcome by the introduction of phosphonate ester groups to D/L-fosfalin (**13-DL**) to improve its organic solvent solubility prior to subsequent peptide coupling (Scheme 2.8).



Scheme 2.8: Synthesis of optically pure L-Ala-L-Fos (**126-LL**) and L-Ala-D-Fos (**126-LD**) via the phosphonate ester route (1986JMC29)

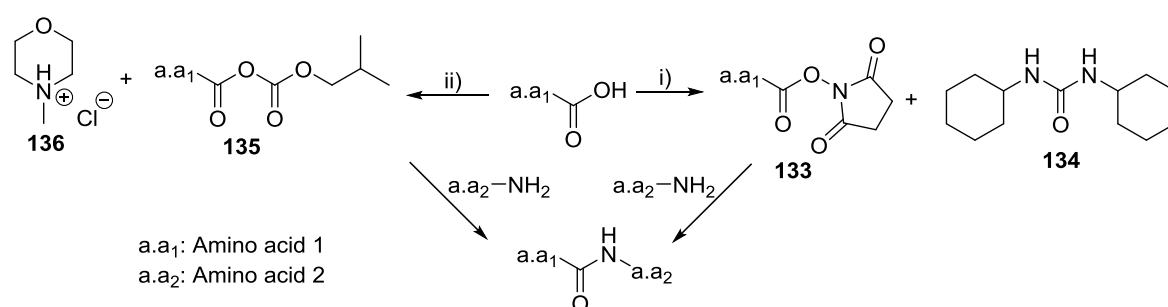
Reagents and conditions: i) H_2 , Pd/C, DCM; ii) Et_3N , DCM, DCC; iii) $EtOAc/Et_2O$; iv) HBr , $AcOH$, then propylene oxide

In this alternative synthesis, protected D/L-fosfalin dimethyl phosphonate ester (**129**) was synthesised from benzylamine (**127**), acetaldehyde (**73**) and dimethyl phosphite (**128**), followed by debenylation under hydrogenation to afford the D/L-fosfalin dimethyl phosphonate ester (**130**). Activation and coupling of *N*-Cbz-L-alanine (**131**) using dicyclohexylcarbodiimide (DCC) prior to reaction with D/L-fosfalin phosphonate dimethyl ester (**130**) resulted in a mixture of diastereoisomers (**132**). These L,L- and L,D- diastereoisomers were separated based on their different solubility properties in a mixed solvent (ethyl acetate and diethyl ether) to obtain optically pure **132-LL** and **132-LD** (1986JMC29). All of the

protecting groups, at the *N*-terminus and *O*-termini, were later removed simultaneously under acidic conditions to afford optically pure L-alanyl-L-fosfalin (**126-LL**) and L-alanyl-D-fosfalin (**126-LD**). This method (Scheme 2.8), however, involved several washing, recrystallizing and resolving steps to obtain the optically pure compound, affecting the overall yield.

Fortunately, the current work did not involve any separation or isolation of optically pure fosfalin, which is time-consuming. Direct peptide coupling involved the *O*-protected racemic fosfalin to avoid the issue of insolubility. Although two different *O*-protected racemic fosfalin derivatives, ethyl phosphonate ester (**84**) and methyl phosphonate ester (**130**), have been discussed, **84** was used due to its readily available synthetic methodology with a good reported yield.

In peptide coupling reactions (Scheme 2.9), DCC, triethylamine and *N*-hydroxysuccinimide esters are commonly used reagents in the production of activated esters (**133**). However, the dicyclohexylurea (**134**) by-product generated from this reaction is difficult to remove; several filtration steps are frequently required, which reduces the overall yield of the desired product. In the current work, alternative coupling reagents, isobutyl chloroformate (IBCF) and *N*-methylmorpholine (NMM), were used to produce an activated ester (**135**) from the carboxyl group of an amino acid. The *N*-methylmorpholine salt (**136**), generated as a by-product, can be readily removed by filtration due to its insolubility in the reaction solvent, dry dichloromethane and/or tetrahydrofuran.



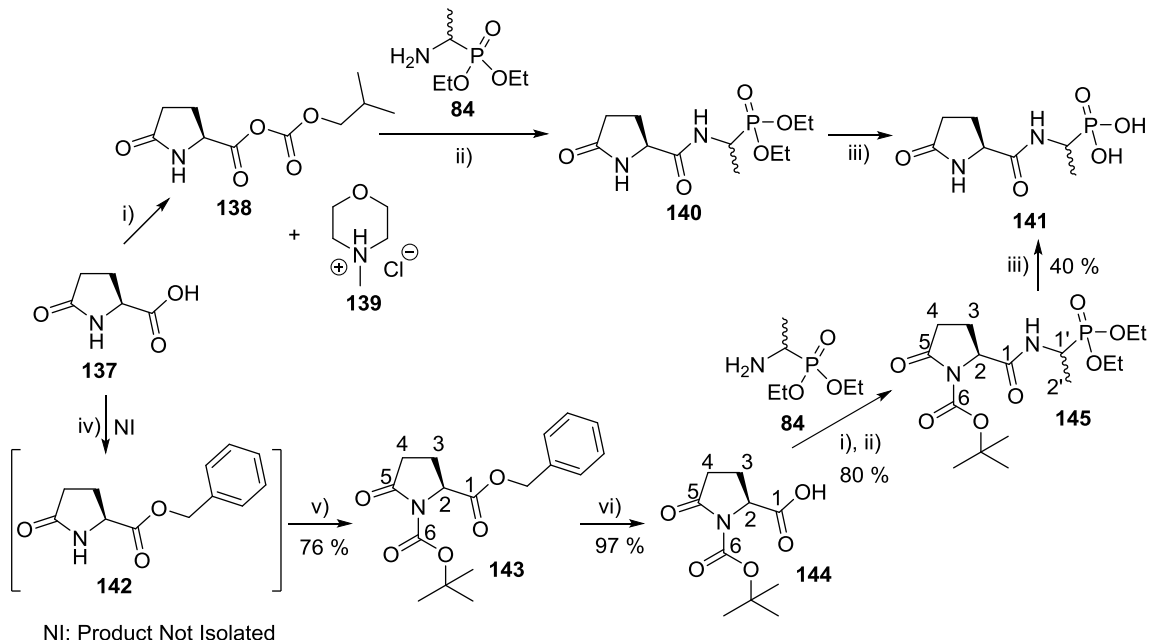
Scheme 2.9: Representation of a general coupling reaction showing two different sets of coupling reagents

Reagents and conditions: i) Et_3N , DCC, *N*-hydroxysuccinimide, 0 °C to r.t., DCM; ii) NMM, IBCF, -5 °C to r.t., dry THF and/or DCM

2.4.1: Preparation of (1-((S)-5-oxopyrrolidine-2-carboxamido)ethyl) phosphonic acid or L-Pyroglu-D/L-fosfalin (**141**)

Adopting the peptide coupling methodology discussed above, the dipeptide analogue, L-pyroglu-D/L-fosfalin (**141**) was anticipated to be obtained *via* the synthetic route shown in Scheme 2.10. In this method, L-pyroglutamic acid (**137**) was activated by isobutyl chloroformate (IBCF), in the presence of *N*-methylmorpholine (NMM), to generate the isobutyl mixed anhydride (**138**) and NMM hydrochloride salt (**139**). The activated ester (**138**) was then coupled with D/L-fos diethyl ester (**84**) to form L-pyroglu-D/L-fos diethyl ester (**140**), followed by acidic deprotection to generate the product of interest (**141**).

Using this method, however, the product of interest (**141**) was not generated as anticipated, due to the insolubility of L-pyroglutamic acid (**137**). In order to improve its solubility, a *tert*-butoxycarbonyl protecting group was introduced at the *N*-terminus of **137**, *via* two sequential reactions to yield intermediate (**144**) (Scheme 2.10), prior to coupling with D/L-fos diethyl ester (**84**). Concurrent acidic deprotection of the *N*-protected phosphonate ester **145** gave the desired L-pyroglutamyl-D/L-fosfalin (**141**).



Scheme 2.10: Synthesis of L-pyroglutamyl-D/L-fosfalin (**141**)

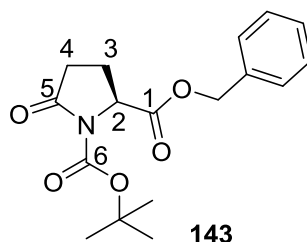
Reagents and conditions: i) IBCF, NMM, THF, -5 °C to r.t., 2hrs; ii) THF, -5 °C to r.t., 24hrs; iii) HBr, AcOH, 16-18hrs then propylene oxide; iv) THF, Et₃N, PhCH₂Br, reflux, 5days; v) Et₃N, DMAP, Boc₂O, 0 °C to r.t., 24hrs; vi) H₂, Pd/C, MeOH, 24hrs

2.4.1.1: Synthesis of (S)-2-benzyl 1-*tert*-butyl-5-oxopyrrolidine-1,2-dicarboxylate or ⁴Boc-L-Pyroglu-OBzl (**143**)

Two orthogonal protecting groups, benzyl ester and *tert*-butoxycarbonyl, were introduced at the C-terminus and N-terminus of L-pyroglutamic acid (**137**), respectively, as shown in Scheme 2.10. In this one-pot reaction, the benzyl ester of L-pyroglutamic acid (L-Pyroglu-OBzl) was generated as an intermediate (**142**), but was not isolated; subsequent addition of the *tert*-butoxycarbonyl group resulted in ⁴Boc-L-Pyroglu-OBzl (**143**). The successful synthesis of **143** was supported by its IR spectrum, in which three strong absorbance peaks, indicating the presence of three carboxyl functional groups, were observed at 1780, 1738 and 1702 cm⁻¹. The structure of **143** was confirmed by NMR spectroscopy (Table 2.2), which agreed with the literature ¹H-NMR results (2007BMC3474). The successful introduction of both protecting groups was confirmed by the presence of peaks corresponding to the *tert*-butyl and benzyl groups, as well as the extra peak at δ 148.3 ppm corresponding to the C=O-6 in the NMR spectrum.

The presence of a chiral center at C-2 results in diastereotopic signals, observed separately at δ 1.89-1.99 ppm, δ 2.16-2.30 ppm, and overlapping at δ 2.34-2.60 ppm, corresponding to each methylene proton at C-3 and C-4, respectively. The signals observed at these regions, however, were unresolved due to overlapping signals from geminal (²J_{H-H}) and vicinal (³J_{H-H}) couplings. These results contrasted to the distinct patterns, a doublet of doublet of triplets (ddt) and a doublet of doublet of doublets (ddd), reported in the literature (2007BMC3474). A resolved doublet of doublets, on the other hand, was observed for CH-2 at δ 4.57 ppm, resulting from coupling with each non-equivalent methylene proton at C-3, producing ³J_{H-H} coupling constants of 9.6 Hz and 2.8 Hz. A similar feature with two sets of doublets was observed at δ 5.11 ppm and δ 5.16 ppm due to geminal coupling between each inequivalent benzylic proton. Although most of the multiplets were unresolved, the assignment of these signals (Table 2.2), supported by the literature ¹H-NMR signals (2007BMC3474), confirmed the successful synthesis of ⁴Boc-L-Pyroglu-OBzl (**143**). The melting point (61-63 °C) corresponded to the literature value, which also supported its identity as the intended product.

Table 2.2: Assignment of NMR signals and literature ¹H-NMR signals (2007BMC3474) of 'Boc-L-Pyroglu-OBzl (**143**) at 300 MHz (¹H-NMR) and 75 MHz (¹³C-NMR). Frequency of the literature ¹H-NMR was not reported



	δ_H (CDCl ₃)	δ_C (CDCl ₃)	δ_H (CDCl ₃) (2007BMC3474)
C(CH ₃) ₃	1.39 (9H, s)	26.8 C(CH ₃) ₃ 82.6 C(CH ₃) ₃	1.41 (9H, s)
CH ₂ -3	1.89-1.99 (1H, m) 2.16-2.30 (1H, m)	20.6	2.05 (1H, ddt, $J=12.8, 10.3, 3.3$ Hz) 2.32 (1H, ddt, $J=12.8, 9.8, 9.4$ Hz)
CH ₂ -4	2.34-2.60 (2H, m)	30.1	2.47 (1H, ddd, $J=17.6, 9.4, 3.5$ Hz) 2.60 (1H, ddd, $J=17.5, 10.3, 9.8$ Hz)
CH-2	4.57 (1H, dd, $^3J_{H-H}=9.6, 2.8$ Hz)	58.2	4.62 (1H, dd, $J=9.4, 3.3$ Hz)
OCH ₂	5.11 (1H, d, $^2J_{H-H}=12.0$ Hz) 5.16 (1H, d, $^2J_{H-H}=12.2$ Hz)	66.4	5.18 (1H, d, $J=12.1$ Hz) 5.20 (1H, d, $J=12.1$ Hz)
C ₆ H ₅	7.28 (5H, m)	127.5, 127.6 (CH) 134.1 (C _{quat.})	7.54 (5H, m)
C=O-6	-	148.3	-
C=O-1	-	170.2	-
C=O-5	-	172.1	-

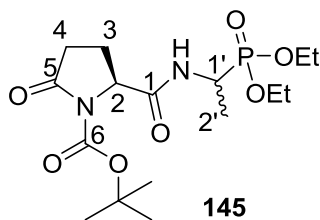
2.4.1.2: Synthesis of (S)-1-(*tert*-butoxycarbonyl)-5-oxopyrrolidine-2-carboxylic acid or ¹Boc-L-Pyroglu-OH (144)

Hydrogenolysis of the benzyl group of ¹Boc-L-Pyroglu-OBzl (**143**) gave rise to ¹Boc-L-Pyroglu-OH (**144**). The successful removal of this group was supported by the IR spectrum, where a broad absorbance peak and a strong absorbance peak were observed at 3134 cm⁻¹ and 1687 cm⁻¹, respectively, indicating the presence of the carboxylic acid OH and C=O functional groups. The disappearance of the benzyl ester group was also supported by NMR spectroscopy: there were no aromatic and benzylic peaks at δ 7.28 ppm and δ 5.11-5.16 ppm (¹H-NMR) and at δ 127.5-134.1 ppm and δ 66.4 ppm (¹³C-NMR), respectively. Meanwhile, a new broad peak at δ 9.20 ppm corresponding to the OH proton was observed in the ¹H-NMR spectrum. The identity of the intended product (**144**) was further confirmed by mass spectrometry and the melting point (76-79 °C) again corresponded to the reported value (2002AEJ2516).

2.4.1.3: Synthesis of (2S)-*tert*-butyl 2-((1-(diethoxyphosphoryl)ethyl) carbamoyl)-5-oxopyrrolidine-1-carboxylate or ¹Boc-L-Pyroglu-D/L-Fos diethyl ester (145)

¹Boc-L-Pyroglu-OH (**144**) and D/L-fosfalin diethyl ester (**84**) were coupled in the presence of IBCF and NMM, as shown in Scheme 2.10. The structure of the resulting diastereoisomeric compound, ¹Boc-L-pyroglutamyl-D/L-fosfalin diethyl ester (**145**) was confirmed by NMR spectroscopy. The assignments are summarised in Table 2.3.

Table 2.3: Assignment of NMR signals of diastereoisomers, ¹Boc-L-Pyroglu-L-Fos diethyl ester and ¹Boc-L-Pyroglu-D-Fos diethyl ester (**145-LL** and **145-LD**), at 300 MHz (¹H-NMR) and 75 MHz (¹³C-NMR)



	δ_{H} (CDCl ₃)	δ_{C} (CDCl ₃)
OCH ₂ CH ₃	1.19-1.37 (6H, m, 2 x CH ₃) 3.99-4.13 (4H, m, 2 x CH ₂)	15.4, 15.4, 15.5, 15.5 4 x (d, ³ J _{C-P} =2.3 Hz, CH ₃) 61.5, 61.6, 61.8, 61.9 4 x (d, ² J _{C-P} =6.8 Hz, CH ₂)
CH ₃ -2'	1.19-1.37 (3H, m)	14.5, 14.6
C(CH ₃) ₃	1.44 (9H, s)	26.9, 27.0 C(CH ₃) ₃ 82.5, 82.7 C(CH ₃) ₃
CH ₂ -3	1.95-2.07 (1H, m) 2.09-2.26 (1H, m)	21.3, 21.4
CH ₂ -4	2.32-2.43 (1H, m) 2.58-2.71 (1H, m)	30.5, 30.6
CH-2	4.36-4.53 (1H, m)	58.7, 59.0
CH-1'	4.36-4.53 (1H, m)	39.9 (d, ¹ J _{C-P} =156.0 Hz)
NH	6.89 (1H*, d, ³ J _{H-H} =9.0 Hz) 6.95 (1H*, d, ³ J _{H-H} =9.0 Hz)	-
C=O-6	-	148.9, 149.0
C=O-1	-	169.4, 169.5
C=O-5	-	172.5, 172.6

*Actual proton integration was 0.5

The NMR spectra of the phosphonate ester product (**145**) showed signals for both diastereoisomers, as well as phosphorus coupling. As a result, several overlapping signals, appearing as multiplets, were observed in the ¹H-NMR spectrum at δ 1.19-1.37 ppm and δ 3.99-4.13 ppm, corresponding to the respective methyl and methylene protons of the two OCH₂CH₃ groups. The methyl protons (CH₃-2') of

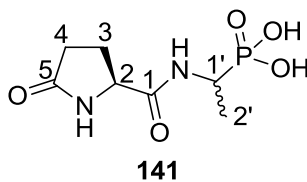
the fosfalin moiety were also assigned to δ 1.19-1.37 ppm, which further complicated this multiplet. A similar complication was also observed at δ 4.36-4.53 ppm, where the CH-1' and CH-2 proton signals coincided. Overlapping signals corresponding to the CH₂-3, CH₂-4 and NH protons of both diastereoisomers were also observed (Table 2.3).

In the ¹³C-NMR spectrum, the diastereotopic ethyl groups of the diastereoisomeric L,L-**145** and L,D-**145** resulted in four sets of signals being observed at δ 15.4-15.5 ppm and δ 61.5-61.9 ppm, corresponding to the methyl and methylene carbons of the OCH₂CH₃ groups, respectively. Each of these signals was also split by phosphorus coupling, displaying four sets of doublets with ³J_{C-P} and ²J_{C-P} coupling constants of 2.3 Hz and 6.8 Hz, respectively. Other phosphorus coupling was observed at 39.9 ppm, where a doublet displaying a ¹J_{C-P} coupling constant of 156.0 Hz was assigned to the CH-1' carbon of the fosfalin moiety. Several other sets of signals for the diastereoisomers were found and assigned accordingly (Table 2.3). The identity of diastereoisomeric compound (**145**) was further confirmed by mass spectrometry and its purity by CHN analysis.

2.4.1.4: Synthesis of (1-((S)-5-oxopyrrolidine-2-carboxamido)ethyl) phosphonic acid or L-Pyroglu-D/L-fosfalin (141)

Both sets of protecting groups, the *tert*-butoxycarbonyl at the *N*-terminus and the diethyl phosphonate ester groups at the *O*-termini, of compound **145** were removed simultaneously under acidic conditions. The successful removal of the diethyl phosphonate ester groups was supported by the IR spectrum, where a broad absorbance peak at 3255 cm⁻¹ was observed, indicating the presence of hydroxyl functional groups, and in both the ¹H- and ¹³C-NMR spectra, where the signals corresponding to OCH₂CH₃ of **145**, as shown in Table 2.3, had vanished. The signals indicating the *tert*-butyl and carbamate groups had also disappeared from the NMR spectra, supporting the successful removal of the *tert*-butoxycarbonyl group. The NMR signals corresponding to successful synthesis of final compound **141** are summarized in Table 2.4. The formation of product (**141**) was confirmed by high-resolution mass spectrometry.

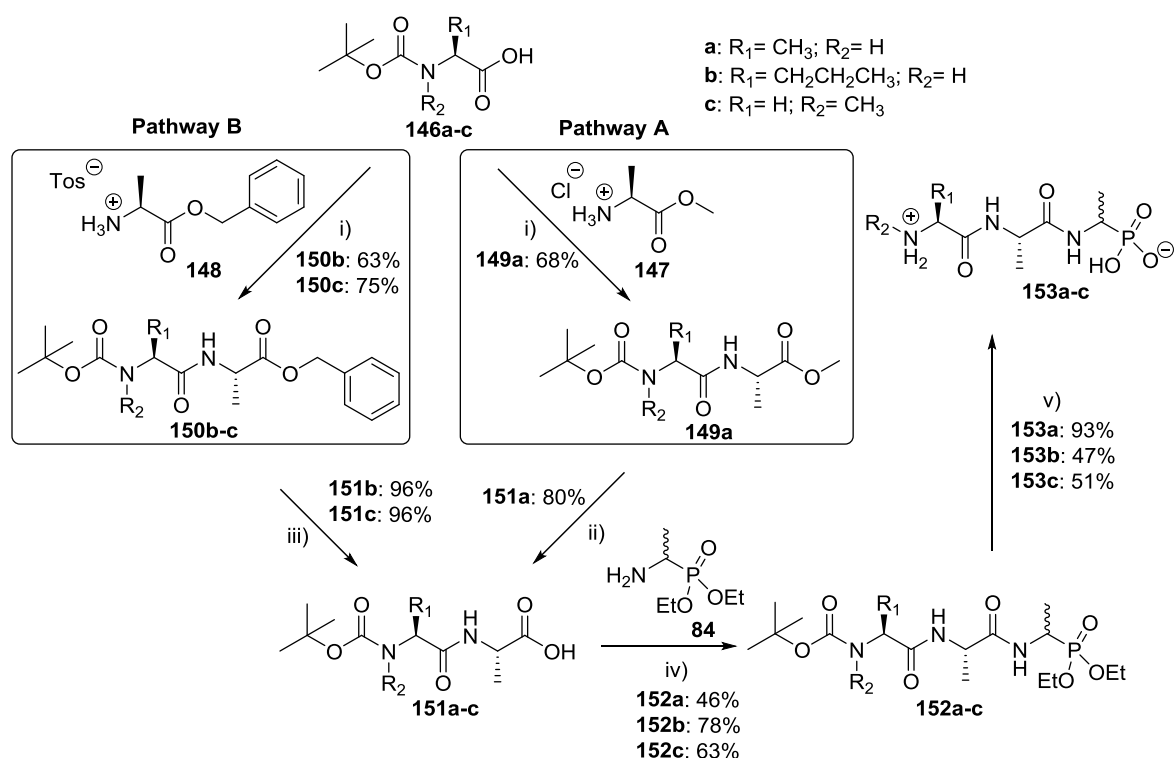
Table 2.4: Assignment of NMR signals of diastereoisomers, L-Pyroglu-L-Fos and L-Pyroglu-D-Fos (**141-LL** and **141-LD**), at 300 MHz ($^1\text{H-NMR}$) and 75 MHz ($^{13}\text{C-NMR}$)



	δ_{H} , (D_2O)	δ_{C} (D_2O)
$\text{CH}_3\text{-2}'$	1.05-1.29 (3H, m)	14.8, 15.1
$\text{CH}_2\text{-3}$	2.00-2.04 (1H, m) 2.11-2.15 (1H, m)	25.1, 25.6
$\text{CH}_2\text{-4}$	2.33-2.39 (1H, m) 2.45-2.64 (1H, m)	29.1, 29.3
CH-2	3.50-3.65 (1H, m)	65.3
$\text{CH-1}'$	3.79-4.15 (1H, m)	52.5
NH	Exchanged	-
C=O-1	-	165.4
C=O-5	-	173.7

2.4.2: Preparation of phosphonotripeptide derivatives containing the L-Ala-D/L-fosfalin moiety

Three phosphonotripeptide derivatives were synthesised with varying side chains (denoted by the R-group) as shown in Scheme 2.11. Two different pathways were evaluated; one used L-Ala-OMe hydrochloride salt (**147**) (Pathway A) and the other used L-Ala-OBzl tosylate salt (**148**) (Pathway B) for reaction with the *N*-protected amino acid (**146a-c**). The benzyl ester protecting group was found to be preferable over the methyl ester group throughout the peptide coupling reaction in this work, due to its ease of removal under hydrogenation and the high yields obtained, in conjunction with relatively clean products. The resulting dipeptide derivatives (**149a**, **150b-c**) were *O*-deprotected and then coupled to D/L-fosfalin diethyl ester (**84**). Both of the protecting groups of the phosphonotripeptide derivatives were later removed and the products treated with propylene oxide to afford the zwitterionic products (**153a-c**).



Scheme 2.11: General preparation of phosphonotripeptide derivatives containing D/L-fosfalin

Reagents and conditions: i) DIPEA, IBCF, NMM, THF/DCM, -5 °C to r.t., 24hrs; ii) 1M NaOH, MeOH, H₂O, 24hrs; iii) H₂, Pd/C, MeOH; iv) IBCF, NMM, THF, -5 °C to r.t., 24hrs; v) HBr, AcOH, 16-18hrs then propylene oxide

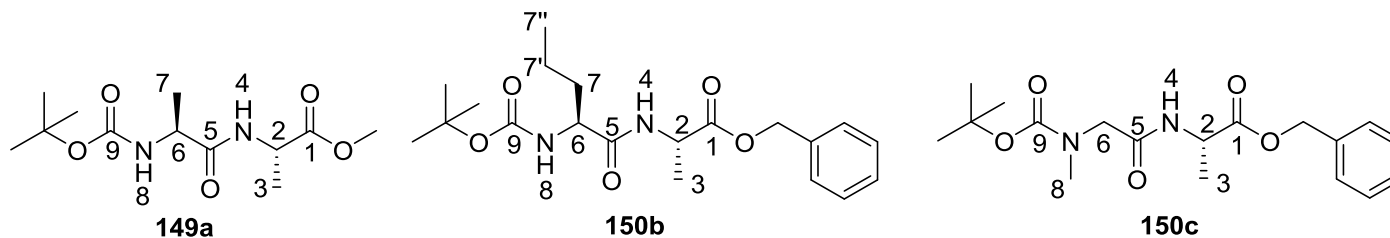
2.4.2.1: Synthesis of *N*-protected dipeptide derivatives (151a-c)

Each *N*-protected amino acid with its different R-group (**146a-c**) was coupled, to either the L-alanine methyl ester hydrochloride salt (**147**) or L-alanine benzyl ester tosylate salt (**148**), using the IBCF/NMM method (Scheme 2.11). The successful coupling between the different protected amino acids was confirmed by NMR spectroscopy; the assignments are summarised in Tables 2.6 and 2.7 using the structural numbering system in Table 2.5. In these tables, signals for both the *tert*-butyl group and methyl ester group were clearly visible on the NMR spectra of ¹Hoc-L-Ala-L-Ala-OMe (**149a**), while the presence of *tert*-butyl and benzyl ester signals were observed on the spectra of ¹Hoc-L-Nva-L-Ala-OBzl (**150b**) and ¹Hoc-Sar-L-Ala-OBzl (**150c**). Additional evidence, such as mass spectrometry and melting point, further supported the structure of ¹Hoc-L-Ala-L-Ala-OMe (**149a**); while high-resolution mass spectrometry supported the structures of ¹Hoc-L-Nva-L-Ala-OBzl (**150b**) and ¹Hoc-Sar-L-Ala-OBzl (**150c**).

Table 2.5: Structure of ¹Hoc-L-Ala-L-Ala-OMe (**149a**), ¹Hoc-L-Nva-L-Ala-OBzl (**150b**) and ¹Hoc-Sar-L-Ala-OBzl (**150c**), with corresponding numbering system used for NMR assignment

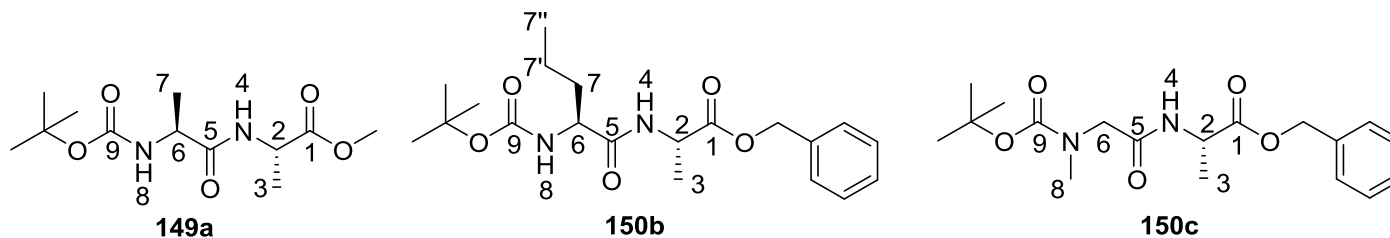
Compound name	Structure
¹ Hoc-L-Ala-L-Ala-OMe (149a)	
¹ Hoc-L-Nva-L-Ala-OBzl (150b)	
¹ Hoc-Sar-L-Ala-OBzl (150c)	

Table 2.6: Assignment of ¹H-NMR signals of ^tBoc-L-Ala-L-Ala-OMe (**149a**), ^tBoc-L-Nva-L-Ala-OBzl (**150b**) and ^tBoc-Sar-L-Ala-OBzl (**150c**) at 300 MHz



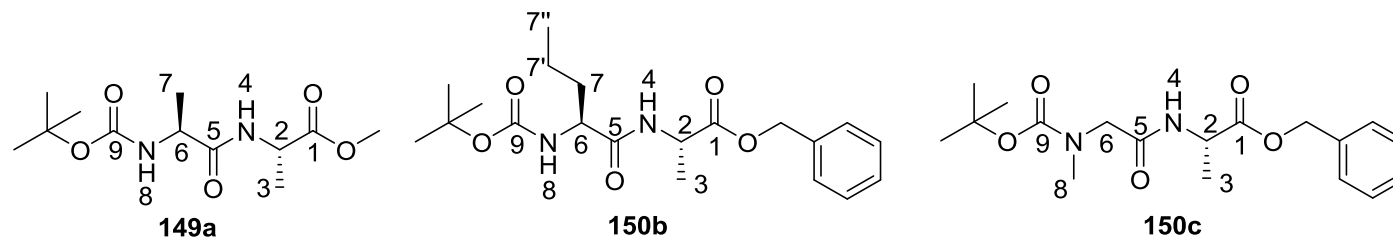
	δ_{H} (CDCl ₃)		
	^t Boc-L-Ala-L-Ala-OMe (149a)	^t Boc-L-Nva-L-Ala-OBzl (150b)	^t Boc-Sar-L-Ala-OBzl (150c)
CH ₃ -7''	-	0.83 (3H, d, ³ J _{H-H} =9.0 Hz)	-
CH ₂ -7'	-	1.25-1.31 (2H, m)	-
CH ₃ -7	1.33 (3H, d, ³ J _{H-H} =6.9 Hz)	-	-
CH ₂ -7	-	1.42-1.51 (1H, m) 1.64-1.73 (1H, m)	-
CH ₃ -3	1.37 (3H, d, ³ J _{H-H} =7.2 Hz)	1.34 (3H, d, ³ J _{H-H} =6.0 Hz)	1.35 (3H, d, ³ J _{H-H} =6.0 Hz)
C(CH ₃) ₃	1.42 (9H, s)	1.36 (9H, s)	1.39 (9H, s)
OCH ₃	3.72 (3H, s)	-	-
CH-2	4.54 (1H, pentet, ³ J _{H-H} =7.2 Hz)	4.54 (1H, pentet, ³ J _{H-H} =6.0 Hz)	4.58 (1H, pentet, ³ J _{H-H} =6.0 Hz)
CH ₂ -6	-	-	3.72 (1H, d, ² J _{H-H} =15.0 Hz) 3.88 (1H, d, ² J _{H-H} =15.0 Hz)

Table 2.6 (cont.d): Assignment of ¹H-NMR signals of ^tBoc-L-Ala-L-Ala-OMe (**149a**), ^tBoc-L-Nva-L-Ala-OBzl (**150b**) and ^tBoc-Sar-L-Ala-OBzl (**150c**) at 300 MHz



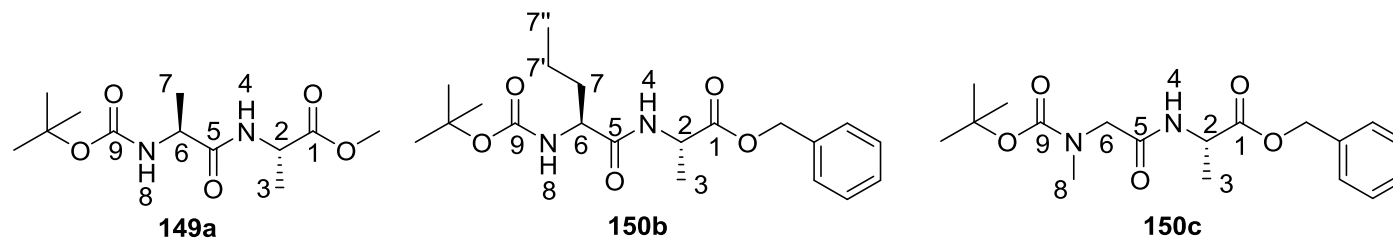
	δ_{H} (CDCl ₃)		
	^t Boc-L-Ala-L-Ala-OMe (149a)	^t Boc-L-Nva-L-Ala-OBzl (150b)	^t Boc-Sar-L-Ala-OBzl (150c)
CH-6	4.14 (1H, pentet, ³ J _{H-H} =6.9 Hz)	4.02 (1H, m)	-
NH-4	6.63 (1H, d, ³ J _{H-H} =6.3 Hz)	6.56 (1H, d, ³ J _{H-H} =6.0 Hz)	6.51 (1H, br)
NH-8	5.00 (H, d, ³ J _{H-H} =6.0 Hz)	4.96 (1H, d, ³ J _{H-H} =9.0 Hz)	-
NCH ₃ -8	-	-	2.85 (3H, s)
OCH ₂	-	5.07 (1H, d, ² J _{H-H} =12.0 Hz) 5.12 (1H, d, ² J _{H-H} =12.0 Hz)	5.08 (1H, d, ² J _{H-H} =12.0 Hz) 5.13 (1H, d, ² J _{H-H} =12.0 Hz)
C ₆ H ₅	-	7.27 (5H, m)	7.25-7.29 (5H, m)

Table 2.7: Assignment of ^{13}C -NMR signals of $^t\text{Boc-L-Ala-L-Ala-OMe}$ (**149a**), $^t\text{Boc-L-Nva-L-Ala-OBzl}$ (**150b**) and $^t\text{Boc-Sar-L-Ala-OBzl}$ (**150c**) at 75 MHz



	δ_c (CDCl_3)		
	$^t\text{Boc-L-Ala-L-Ala-OMe}$ (149a)	$^t\text{Boc-L-Nva-L-Ala-OBzl}$ (150b)	$^t\text{Boc-Sar-L-Ala-OBzl}$ (150c)
$\text{CH}_3\text{-}7''$	-	12.7	-
$\text{CH}_2\text{-}7'$	-	17.8	-
$\text{CH}_3\text{-}7$	18.6	-	-
$\text{CH}_2\text{-}7$	-	33.7	-
$\text{CH}_3\text{-}3$	18.6	17.3	17.5
$\text{C}(\text{CH}_3)_3$	28.5 $\text{C}(\text{CH}_3)_3$ 80.4 $\text{C}(\text{CH}_3)_3$	27.3 $\text{C}(\text{CH}_3)_3$ 79.0 $\text{C}(\text{CH}_3)_3$	27.3 $\text{C}(\text{CH}_3)_3$ 79.8 $\text{C}(\text{CH}_3)_3$
OCH_3	52.6	-	-
$\text{NCH}_3\text{-}8$	-	-	34.7
$\text{CH}\text{-}2$	48.2	47.1	47.0
$\text{CH}_2\text{-}6$	-	-	52.1

Table 2.7 (cont.d): Assignment of ^{13}C -NMR signals of $^t\text{Boc-L-Ala-L-Ala-OMe}$ (**149a**), $^t\text{Boc-L-Nva-L-Ala-OBzl}$ (**150b**) and $^t\text{Boc-Sar-L-Ala-OBzl}$ (**150c**) at 75 MHz



	δ_c (CDCl_3)		
	$^t\text{Boc-L-Ala-L-Ala-OMe}$ (149a)	$^t\text{Boc-L-Nva-L-Ala-OBzl}$ (150b)	$^t\text{Boc-Sar-L-Ala-OBzl}$ (150c)
CH-6	50.3	53.4	-
OCH ₂	-	66.1	66.2
C ₆ H ₅	-	127.1-127.6 (CH_{Ar}) 134.3 (C_{quat.})	127.1-127.6 (CH_{Ar}) 134.3 (C_{quat.})
C=O-9	155.4	154.6	155.0
C=O-1	173.4	171.5	171.5
C=O-5	172.4	170.8	167.9

The methyl ester protecting group of **149a** was later removed under basic conditions, while the benzyl ester protecting groups of **150b** and **150c** was removed by catalytic hydrogenation (Scheme 2.11) to give the corresponding carboxylic acid products (**151a-c**). The successful removal of these protecting groups was confirmed by the IR spectra, where a broad absorbance peak between 3500-2900 cm^{-1} , indicating the presence of an acidic hydroxyl functional group, was observed for all three compounds (**151a-c**). The disappearance of the protecting group, either methyl ester or benzyl ester, was confirmed by NMR spectroscopy, as the signals corresponding to these groups had vanished. ^1H -Boc-L-Ala-L-Ala-OH (**151a**) was further confirmed by comparison with its literature melting point (2011TL1260) and molecular weight, while the molecular weights corresponding to the structures of ^1H -Boc-L-Nva-L-Ala-OH (**151b**) and ^1H -Boc-Sar-L-Ala-OH (**151c**) were also confirmed by high-resolution mass spectrometry.

2.4.2.2: Synthesis of phosphotripeptide derivatives (**153a-c**)

Each *N*-protected dipeptide (**151a-c**) was coupled with D/L-fosfalin diethyl ester (**84**). The protecting groups, *tert*-butoxycarbonyl and phosphonate diethyl ester groups, were later removed under acidic conditions to afford the phosphotripeptide derivatives, as summarised in Scheme 2.11.

The essential structural changes in proceeding from **151a-c** to products (**152a-c**) were confirmed by IR spectroscopy: the broad absorbance peak between 3500-3000 cm^{-1} as observed in compounds (**151a-c**), indicating the presence of an acidic hydroxyl functional group, was missing, indicating successful amide bond formation with D/L-fosfalin diethyl ester (**84**). The structures of products (**152a-c**) were also confirmed by NMR spectroscopy; each peak assignment is summarised in Tables 2.9 and 2.10 using the structural numbering system in Table 2.8.

The presence of diastereoisomers, as well as phosphorus coupling, was observed on the NMR spectra of **152a-c**, resulting in overlapping signals and extra splitting. Due to these features, the side chain methyl groups of each product gave rise to overlapping signals that were not separable. Assignments of the overlapping signals, particularly at 1.21-1.33 ppm, 1.18-1.34 ppm and 1.19-1.34 ppm,

corresponding to the signals of **152a**, **152b** and **152c**, respectively, were attempted with the aid of 2D HMQC spectra; however, separate assignments were still not possible.

In the ^1H -NMR spectra, two signals were observed for CH_2 -9 at δ 3.72-3.87 ppm, corresponding to the two diastereoisomers of **152c**; another two signals corresponding to the two diastereoisomers of **152b** were also observed at δ 5.19-5.23 ppm (NH-11), δ 6.78-6.87 ppm (NH-7) and δ 7.15-7.23 ppm (NH-3). Each of these signals corresponding to 0.5H for the diastereoisomers of each product. Similar separate peaks were seen for NH-3 of the diastereoisomers of **152c**. However, the NH-3, NH-7 and NH-11 signals of the diastereoisomers of **152a** coincided. The presence of phosphorus coupling contributed to the complicated multiplets obtained and made the ^1H -NMR spectra (Table 2.9) difficult to interpret; however, this coupling effect was observed in the ^{13}C -NMR spectra.

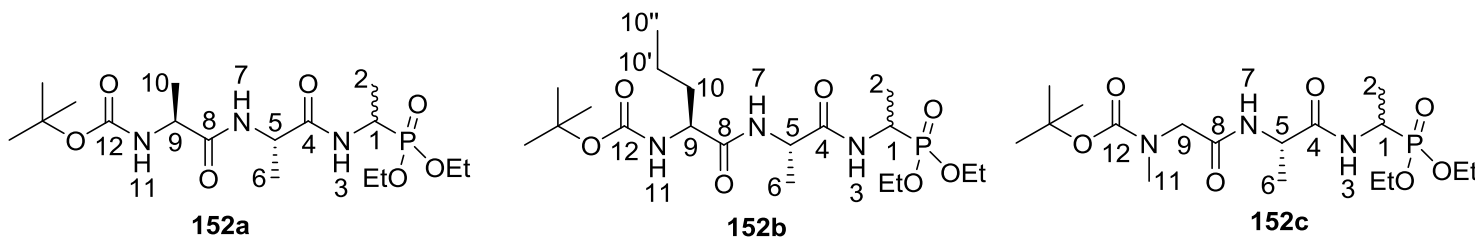
In the ^{13}C -NMR spectra (Table 2.10), the diastereotopic ethyl groups of both diastereoisomers resulted in two signals for each methyl and methylene carbon of the phosphonate diethyl ester groups of **152a-c** being observed. Each of these methylene carbon signals appeared as a doublet due to phosphorus coupling, displaying a $^2J_{\text{C-P}}$ coupling constant of 6.8-7.5 Hz, while the methyl carbon of the phosphonate diethyl ester groups of **152c** displayed a $^3J_{\text{C-P}}$ coupling constant of 3.0 Hz. Another phosphorus coupling was also observed at δ 39.9-41.2 ppm, corresponding to the CH-1 carbon of **152a-c**, displaying a $^1J_{\text{C-P}}$ coupling constant of 156.8-157.5 Hz. The successful synthesis of these compounds (**152a-c**) was further supported by high-resolution mass spectrometry, while the purity of **152a-b** was confirmed by CHN analysis.

Table 2.8: Structures of diastereoisomeric products, ¹Hoc-L-Ala-L-Ala-D/L-Fos diethyl ester (**152a**), ¹Hoc-L-Nva-L-Ala-D/L-Fos diethyl ester (**152b**) and ¹Hoc-Sar-L-Ala-D/L-Fos diethyl ester (**152c**), with corresponding numbering systems used for NMR assignment

Compound name	Structure
¹ Hoc-L-Ala-L-Ala-D/L-Fos diethyl ester (152a)	
¹ Hoc-L-Nva-L-Ala-D/L-Fos diethyl ester (152b)	
¹ Hoc-Sar-L-Ala-D/L-Fos diethyl ester (152c)	

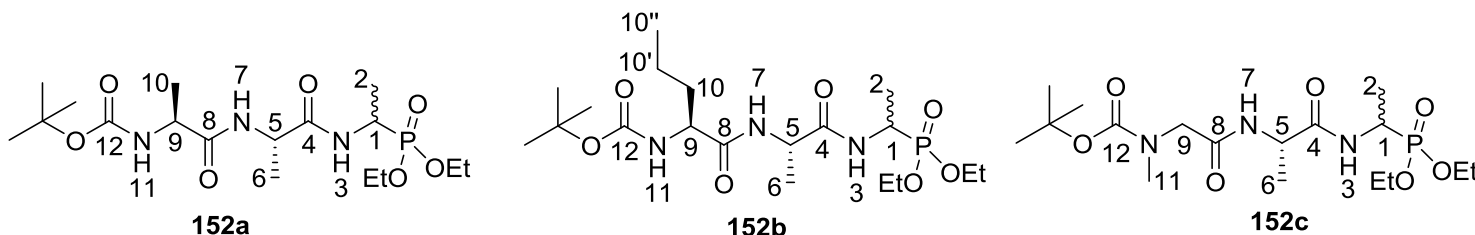
The resulting compounds (**152a-c**) were deprotected under acidic conditions, removing the *tert*-butoxycarbonyl and diethyl ester groups simultaneously. Subsequent treatment with propylene oxide afforded **153a-c** in zwitterionic form. The sharp peak at 3248-3289 cm⁻¹ and the broad peak at 3500-2900 cm⁻¹ in the IR spectra indicated the presence of the NH₃⁺ and OH functional groups of **153a-c**. The disappearance of signals corresponding to the *tert*-butoxycarbonyl and diethyl phosphonate ester protecting groups from the NMR spectra provided further evidence for their removal. The summary of the assigned NMR signals of **153a-c** is presented in Tables 2.11 and 2.12. The identity of these compounds (**153a-c**) was further supported by high-resolution mass spectrometry, while the purity of **153a-b** was confirmed by CHN analysis.

Table 2.9: Assignment of ¹H-NMR signals of diastereoisomeric ^tBoc-L-Ala-L-Ala-D/L-Fos diethyl ester (**152a**) at 500 MHz, ^tBoc-L-Nva-L-Ala-D/L-Fos diethyl ester (**152b**) and ^tBoc-Sar-L-Ala-D/L-Fos diethyl ester (**152c**) at 300MHz.



	δ_H (CDCl ₃)		
	^t Boc-L-Ala-L-Ala-D/L-Fos diethyl ester (152a)	^t Boc-L-Nva-L-Ala-D/L-Fos diethyl ester (152b)	^t Boc-Sar-L-Ala-D/L-Fos diethyl ester (152c)
CH ₃ -10''	-	0.85 (3H, t, ³ J _{H-H} =9.0 Hz)	-
CH ₂ -10'	-	1.18-1.34 (2H, m)	-
CH ₃ -2	1.21-1.33 (3H, m)	1.18-1.34 (3H, m)	1.19-1.34 (3H, m)
CH ₃ -6	1.21-1.33 (3H, m)	1.18-1.34 (3H, m)	1.19-1.34 (3H, m)
CH ₃ -10	1.21-1.33 (3H, m)	-	-
CH ₂ -10	-	1.47-1.54 (1H, m) 1.65-1.73 (1H, m)	-
NCH ₃ -11	-	-	2.87 (3H, s)

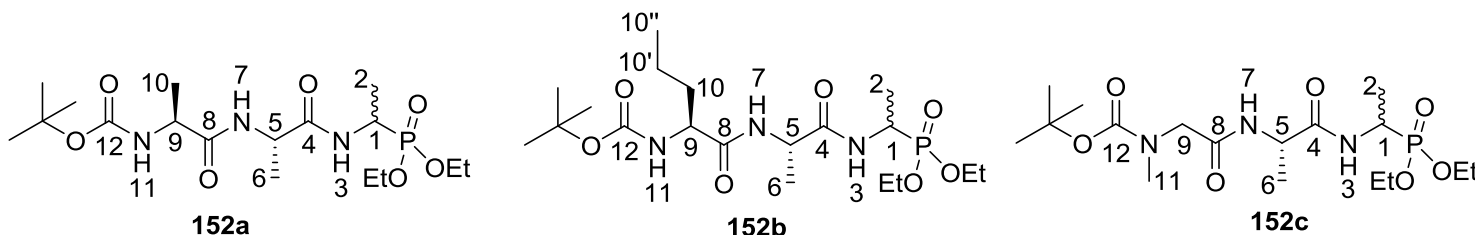
Table 2.9 (cont.d): Assignment of ¹H-NMR signals of diastereoisomeric ¹Boc-L-Ala-L-Ala-D/L-Fos diethyl ester (**152a**) at 500 MHz, ¹Boc-L-Nva-L-Ala-D/L-Fos diethyl ester (**152b**) and ¹Boc-Sar-L-Ala-D/L-Fos diethyl ester (**152c**) at 300MHz



	δ_H (CDCl ₃)		
	¹ Boc-L-Ala-L-Ala-D/L-Fos diethyl ester (152a)	¹ Boc-L-Nva-L-Ala-D/L-Fos diethyl ester (152b)	¹ Boc-Sar-L-Ala-D/L-Fos diethyl ester (152c)
OCH ₂ CH ₃	1.21-1.33 (6H, m, 2 x CH ₃) 3.98-4.12 (4H, m, 2 x CH ₂)	1.18-1.34 (6H, m, 2 x CH ₃) 3.98-4.12 (4H, m, 2 x CH ₂)	1.19-1.34 (6H, m, 2 x CH ₃) 4.00-4.11 (4H, m, 2 x CH ₂)
C(CH ₃) ₃	1.37 (9H, s)	1.37 (9H, s)	1.40 (9H, s)
CH-5	4.47-4.53 (1H, m)	4.48-4.54 (1H, m)	4.47-4.52 (1H, m)
CH ₂ -9	-	-	3.72, 3.78 [†] (1H, d, ² J _{H-H} =15.0 Hz) 3.81, 3.87 [†] (1H, d, ² J _{H-H} =15.0 Hz)

[†]Two signals were observed due to diastereoisomers

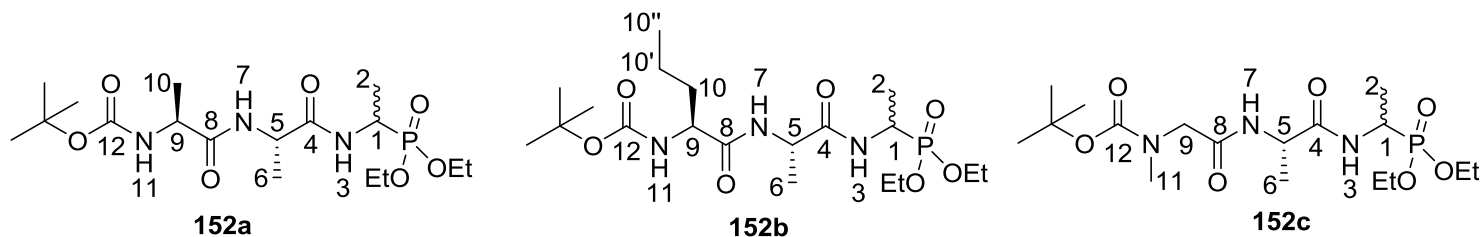
Table 2.9 (cont.d): Assignment of ¹H-NMR signals of diastereoisomeric ^tBoc-L-Ala-L-Ala-D/L-Fos diethyl ester (**152a**) at 500 MHz, ^tBoc-L-Nva-L-Ala-D/L-Fos diethyl ester (**152b**) and ^tBoc-Sar-L-Ala-D/L-Fos diethyl ester (**152c**) at 300MHz



	δ_H (CDCl ₃)		
	^t Boc-L-Ala-L-Ala-D/L-Fos diethyl ester (152a)	^t Boc-L-Nva-L-Ala-D/L-Fos diethyl ester (152b)	^t Boc-Sar-L-Ala-D/L-Fos diethyl ester (152c)
CH-9	3.98-4.12 (1H, m)	3.98-4.12 (1H, m)	-
CH-1	4.34-4.43 (1H, m)	4.33-4.34 (1H, m)	4.35-4.43 (1H, m)
NH-7	6.83-6.94 (1H, m)	6.78 (1H*, d, ³ J _{H-H} =6.0 Hz) 6.87 (1H*, d, ³ J _{H-H} =6.0 Hz)	6.67 (1H, d, ³ J _{H-H} =9.0 Hz)
NH-11	5.26-5.37 (1H, m)	5.19 (1H*, d, ³ J _{H-H} =6.0 Hz) 5.23 (1H*, d, ³ J _{H-H} =6.0 Hz)	-
NH-3	7.10-7.20 (1H, m)	7.15 (1H*, d, ³ J _{H-H} =9.0 Hz) 7.23 (1H*, d, ³ J _{H-H} =9.0 Hz)	6.98 (1H*, d, ³ J _{H-H} =9.0 Hz) 7.15 (1H*, d, ³ J _{H-H} =9.0 Hz)

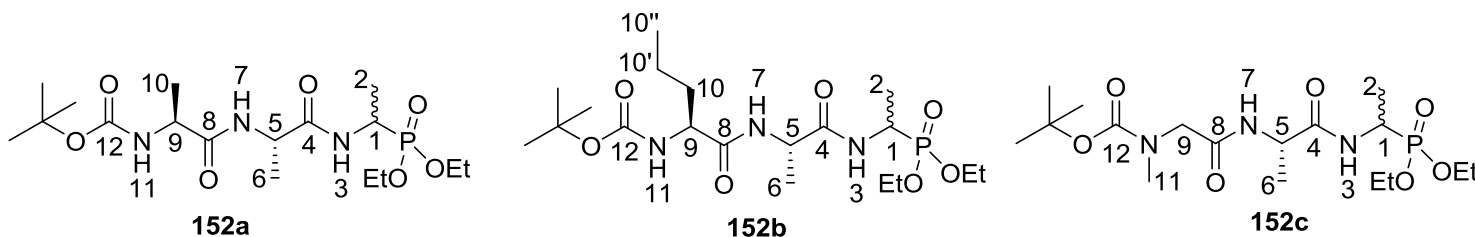
* Actual proton integration was 0.5

Table 2.10: Assignment of ^{13}C -NMR signals of diastereoisomeric $^t\text{Boc-L-Ala-L-Ala-D/L-Fos}$ diethyl ester (**152a**) at 125 MHz, $^t\text{Boc-L-Nva-L-Ala-D/L-Fos}$ diethyl ester (**152b**) and $^t\text{Boc-Sar-L-Ala-D/L-Fos}$ diethyl ester (**152c**) at 75 MHz



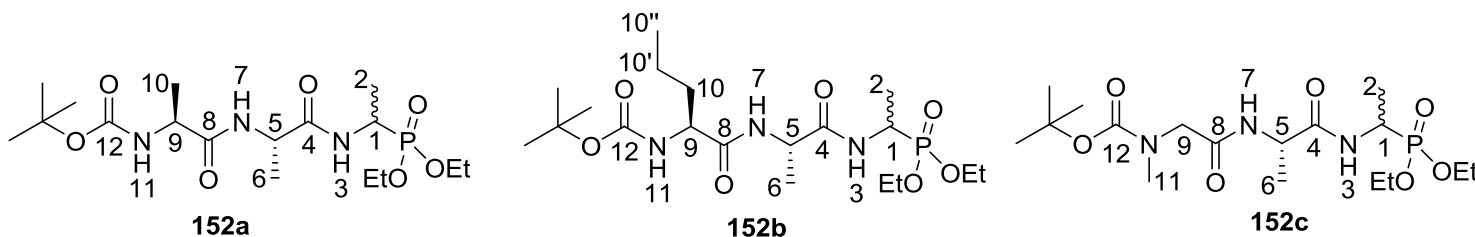
	δ_{C} (CDCl_3)		
	$^t\text{Boc-L-Ala-L-Ala-D/L-Fos}$ diethyl ester (152a)	$^t\text{Boc-L-Nva-L-Ala-D/L-Fos}$ diethyl ester (152b)	$^t\text{Boc-Sar-L-Ala-D/L-Fos}$ diethyl ester (152c)
$\text{CH}_3\text{-10''}$	-	12.7	-
$\text{CH}_2\text{-10'}$	-	17.8, 17.9	-
$\text{CH}_3\text{-2}$	15.4, 15.5	14.4, 14.5	15.5, 15.5
$\text{CH}_3\text{-6}$	16.7 or 18.7	17.6, 17.7	18.7
$\text{CH}_3\text{-10}$	16.7 or 18.7	-	-
$\text{CH}_2\text{-10}$	-	33.8, 33.9	-
$\text{NCH}_3\text{-11}$	-	-	35.8

Table 2.10 (cont.d): Assignment of ^{13}C -NMR signals of diastereoisomeric $^t\text{Boc-L-Ala-L-Ala-D/L-Fos}$ diethyl ester (**152a**) at 125 MHz, $^t\text{Boc-L-Nva-L-Ala-D/L-Fos}$ diethyl ester (**152b**) and $^t\text{Boc-Sar-L-Ala-D/L-Fos}$ diethyl ester (**152c**) at 75 MHz



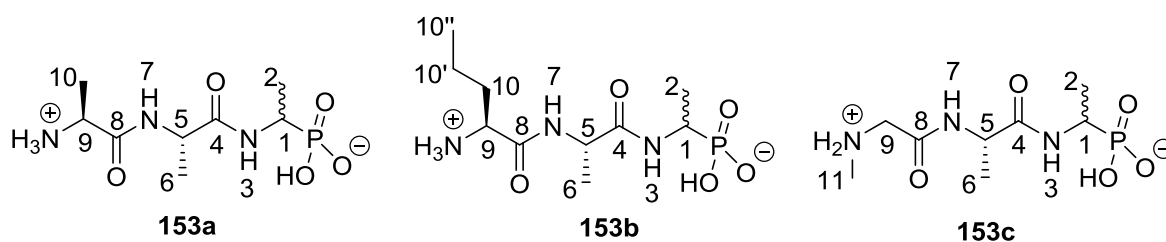
	δ_{C} (CDCl_3)		
	$^t\text{Boc-L-Ala-L-Ala-D/L-Fos}$ diethyl ester (152a)	$^t\text{Boc-L-Nva-L-Ala-D/L-Fos}$ diethyl ester (152b)	$^t\text{Boc-Sar-L-Ala-D/L-Fos}$ diethyl ester (152c)
OCH_2CH_3	16.6, 16.6, 16.6, 16.6 (CH_3)	15.3, 15.4, 15.5, 15.6 (CH_3)	16.3, 16.4
	62.7, 62.8, 62.9, 63.1 4 x (d, $^2J_{\text{C-P}}=6.9$ Hz, CH_2)	61.5, 61.6, 61.7, 61.9 4 x (d, $^2J_{\text{C-P}}=7.5$ Hz, CH_2)	62.5, 62.6, 62.7, 62.9 4 x (d, $^2J_{\text{C-P}}=6.8$ Hz, CH_2)
$\text{C}(\text{CH}_3)_3$	28.5 $\text{C}(\text{CH}_3)_3$ 80.2 $\text{C}(\text{CH}_3)_3$	27.3 $\text{C}(\text{CH}_3)_3$ 78.9 $\text{C}(\text{CH}_3)_3$	28.3 $\text{C}(\text{CH}_3)_3$ 80.7 $\text{C}(\text{CH}_3)_3$
CH-5	49.0 or 49.1	47.7, 47.9	48.5
CH_2 -9	-	-	53.0
CH-9	49.0 or 49.1	53.5, 53.5	-

Table 2.10 (cont.d): Assignment of ^{13}C -NMR signals of diastereoisomeric $^t\text{Boc-L-Ala-L-Ala-D/L-Fos}$ diethyl ester (**152a**) at 125 MHz, $^t\text{Boc-L-Nva-L-Ala-D/L-Fos}$ diethyl ester (**152b**) and $^t\text{Boc-Sar-L-Ala-D/L-Fos}$ diethyl ester (**152c**) at 75 MHz



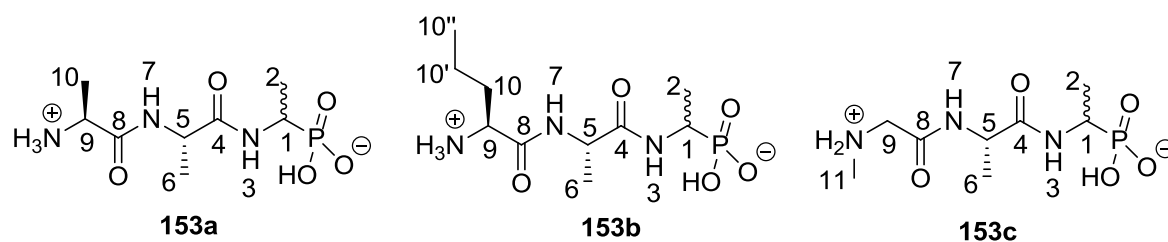
	δ_{C} (CDCl_3)		
	$^t\text{Boc-L-Ala-L-Ala-D/L-Fos}$ diethyl ester (152a)	$^t\text{Boc-L-Nva-L-Ala-D/L-Fos}$ diethyl ester (152b)	$^t\text{Boc-Sar-L-Ala-D/L-Fos}$ diethyl ester (152c)
CH-1	41.2 (d, $^1J_{\text{C-P}}=157.2$ Hz)	39.9 (d, $^1J_{\text{C-P}}=157.5$ Hz) 40.0 (d, $^1J_{\text{C-P}}=156.8$ Hz)	41.0 (d, $^1J_{\text{C-P}}=157.5$ Hz)
C=O-12	150.0	154.7	156.0
C=O-4	171.9 or 172.7	170.6, 170.7 or 171.0, 171.1	171.5 or 171.6
C=O-8	171.9 or 172.7	170.6, 170.7 or 171.0, 171.1	171.5 or 171.6

Table 2.11: Summary of $^1\text{H-NMR}$ spectra of diastereoisomeric L-Ala-L-Ala-D/L-Fos (**153a**), L-Nva-L-Ala-D/L-Fos (**153b**) and Sar-L-Ala-D/L-Fos (**153c**) at 300 MHz



	δ_{H}		
	153a (D ₂ O)	153b (D ₂ O)	153c (D ₂ O)
CH ₃ -10''	-	0.96 (3H, t, $^3J_{\text{H-H}}=7.1$ Hz)	-
CH ₂ -10'	-	1.40-1.42 (2H, m)	-
CH ₂ -10	-	1.88-1.86 (2H, m)	-
CH ₃ -10	1.35 (3H, d, $^3J_{\text{H-H}}=5.8$ Hz) or 1.51 (3H, d, $^3J_{\text{H-H}}=5.3$ Hz)	-	-
CH ₃ -2	1.24 (3H, m)	1.27-1.32 (3H, m)	1.14-1.57 (3H, m)
CH ₃ -6	1.35 (3H, d, $^3J_{\text{H-H}}=5.8$ Hz) or 1.51 (3H, d, $^3J_{\text{H-H}}=5.3$ Hz)	1.40-1.42 (3H, m)	1.14-1.57 (3H, m)
CH ₂ -9	-	-	3.84-4.07 (2H, m)
CH-9	4.29 or 4.31 (1H, m)	4.00-4.02 (1H, m)	-
CH-5	4.29 or 4.31 (1H, m)	4.34-4.39 (1H, m)	4.32-4.58 (1H, m)
CH-1	4.04 (1H, m) 4.31 (1H*, m)	4.00-4.02 (1H, m)	3.84-4.07 (1H, m)
NH-7	Exchanged	Exchanged	Exchanged
NH-3	Exchanged	Exchanged	Exchanged
NCH ₃ -11	-	-	2.74 (3H, s)

Table 2.12: Summary of ^{13}C -NMR spectra of diastereoisomeric L-Ala-L-Ala-D/L-Fos (**153a**), L-Nva-L-Ala-D/L-Fos (**153b**) and Sar-L-Ala-D/L-Fos (**153c**) at 75 MHz



	δ_{C}		
	153a (D ₂ O)	153b (D ₂ O)	153c (D ₂ O)
CH ₃ -10''	-	13.4	-
CH ₂ -10'	-	18.1, 18.2	-
CH ₂ -10	-	33.5, 33.6	-
CH ₃ -10	16.5, 16.6 or 16.7, 16.8	-	-
CH ₃ -2	15.3, 15.4	16.0	15.4
CH ₃ -6	16.5, 16.6 or 16.7, 16.8	17.1, 17.2	16.8
CH ₂ -9	-	-	49.4
CH-9	50.0	53.5	-
CH-5	50.0	50.5, 50.8	50.0
CH-1	48.9	53.5	43.9 (d, $^1J_{\text{P-C}}=148.5$ Hz)
C=O-4	170.5 or 173.7	174.7	173.7
C=O-8	170.5 or 173.7	170.4, 170.6	166.0
NCH ₃ -11	-	-	32.9

Liquid chromatography-mass spectrometry (LC-MS) of products (**153a-c**) indicated a purity of more than 95 %. The diastereoisomers of phosphonotripeptides L,L,L- and L,L,D-**153a-c** were visible as individual peaks with approximately 1:1 ratio (Figure 2.5). However, the assignment of these two peaks to the respective diastereoisomers was not possible in the absence of standards.

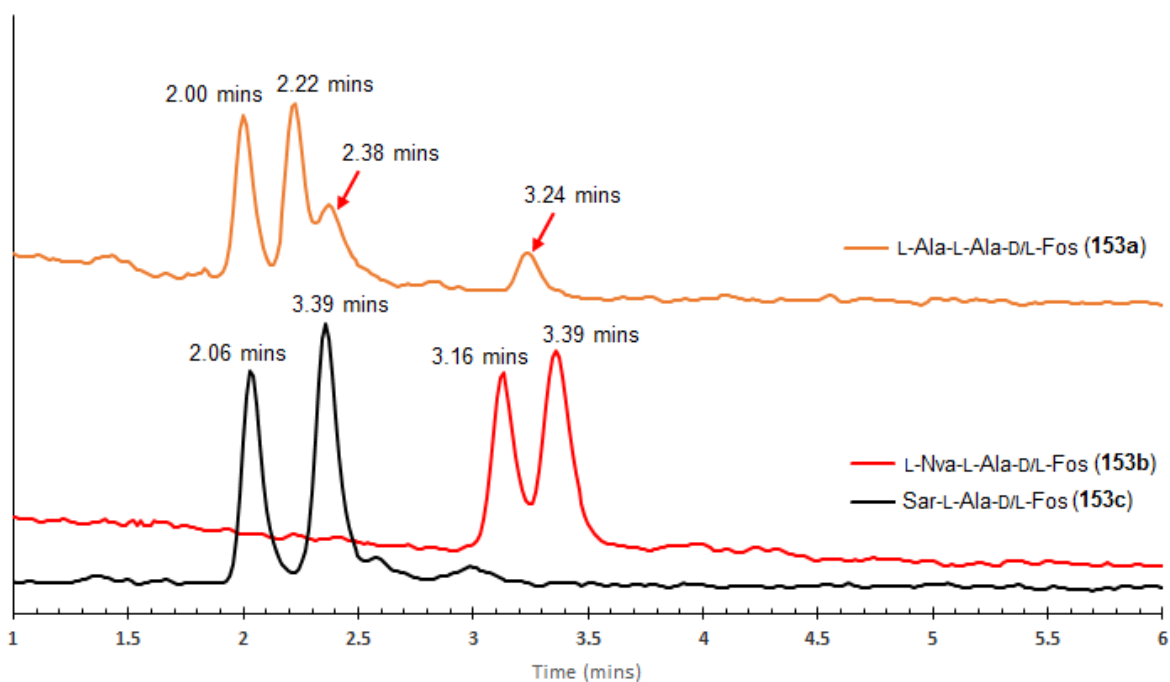
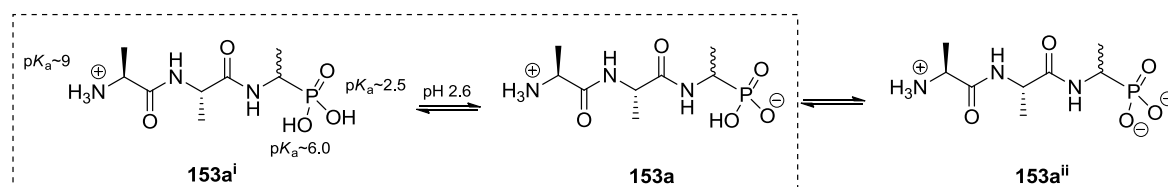


Figure 2.5: Reversed phase LC-MS chromatograms of L-Ala-L-Ala-D/L-Fos (**153a**), L-Nva-L-Ala-D/L-Fos (**153b**) and Sar-L-Ala-D/L-Fos (**153c**) with specific ions extracted at MH^+ m/z 268, m/z 296 and m/z 268, respectively. LC-MS condition (6.2.1) was used. For clarity, the chromatograms are displayed between the range 1.0 - 6.0 mins

The chromatogram (Figure 2.5) also gave an indication of the hydrophobicity of the phosphonotripeptides (**153a-c**): **153b** displayed greater hydrophobicity with a higher retention time compared to **153a** and **153c**. This may be ascribed to the different amino acids with hydrophobic side chains attached at the *N*-terminal amino acid: the propyl group of L-norvaline, the methyl group of L-alanine and the *N*-methyl group of sarcosine.

Two additional peaks were observed at 2.38 and 3.24 mins on the chromatogram of phosphonotripeptide **153a** (Figure 2.5), which may be assigned to the fully protonated L,L,L- and L,L,D-diastereoisomers **153a** due to the pH used being close to the first pK_a of the phosphonic acid. At the pH used for LC-MS (pH 2.6), an equilibrium between **153a** and **153aⁱ** could have resulted (Scheme 2.12). Similar, though smaller, additional peaks were visible on the chromatogram of Sar-L-Ala-D/L-Fos (**153c**) and barely visible on that of L-Nva-L-Ala-D/L-Fos (**153b**), suggesting slight variation in the pK_a values of these compounds or the coincidence of these peaks.



Scheme 2.12: Equilibrium between **153a**, **153aⁱ** and **153aⁱⁱ** at pH 2.6

Although the presence of these additional peaks could have also suggested racemisation of **153a**, this was ruled out when only two sets of diastereoisomeric signals were observed on the NMR spectra of the precursor, ¹Boc-L-Ala-L-Ala-D/L-Fos diethyl ester (**152a**) (Tables 2.10). The presence of two diastereoisomers, L,L,L- and L,L,D-**152a**, was confirmed by LC-MS analysis, in which only two peaks were observed, at 2.81 mins and 3.22 mins (Figure 2.6). The phosphonate ester groups prevent the acid-base equilibrium of **153a** (Scheme 2.12); the lack of additional peaks on the chromatogram of **152a** (Figure 2.6) further supported the explanation above of acid-base equilibrium forms of **153a**.

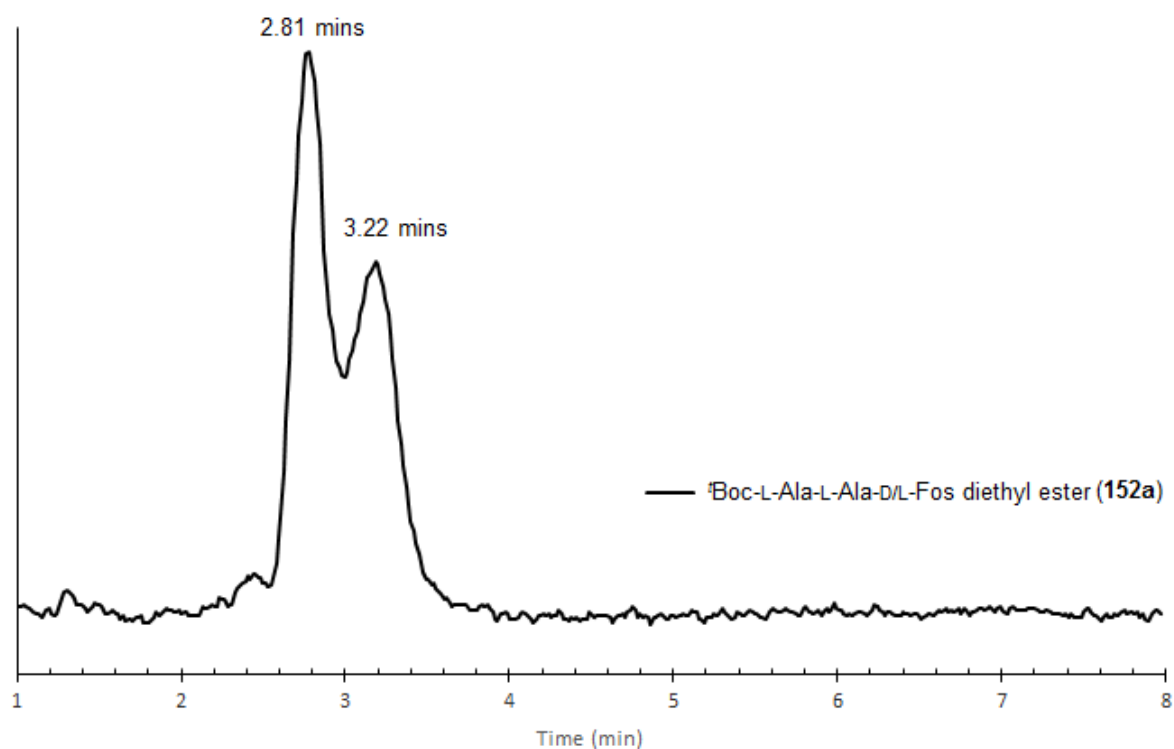
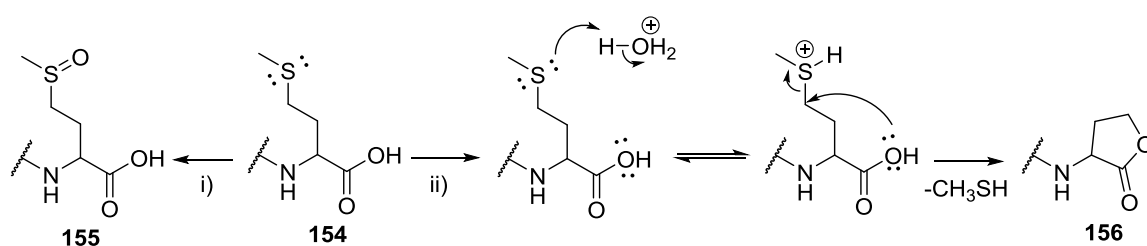


Figure 2.6: Reversed phase LC-MS chromatogram of ¹Boc-L-Ala-L-Ala-D/L-Fos diethyl ester (**152a**) with specific ions extracted at MH⁺ *m/z* 424. LC-MS condition (6.2.2) was used. For clarity, the chromatogram is displayed between 1.0 - 8.0 mins

2.4.3: Preparation of phosphonotripeptide, L-Met-L-Ala-D/L-Fos (160)

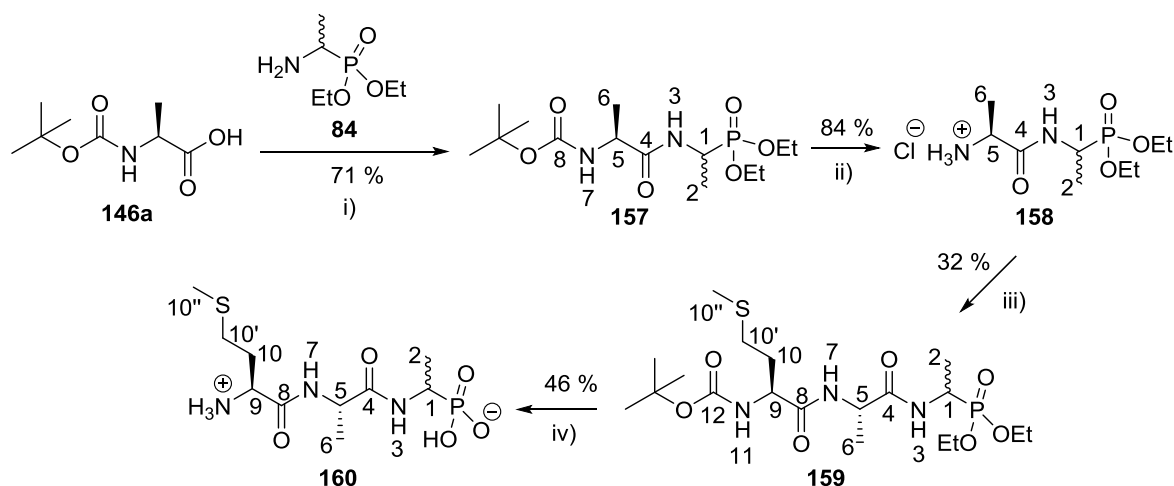
The synthetic routes discussed so far were suitable for the synthesis of phosphonotripeptide derivatives, L-Ala-L-Ala-D/L-Fos (**153a**), L-Nva-L-Ala-D/L-Fos (**153b**) and Sar-L-Ala-D/L-Fos (**153c**). However, the involvement of a labile amino acid with a sensitive side chain, such as the thioether side chain of L-methionine in **154**, required reconsideration of the synthetic route to prevent any unwanted side reactions during the coupling reaction. The thioether functionality of methionine is susceptible to two main side reactions: oxidation to the sulfoxide (**155**) and cyclisation to the lactone (**156**) under acidic conditions (2009CRW2455) (Scheme 2.13).



Scheme 2.13: Possible side reactions occurring at the thioether side chain of methionine

Reactions: i) Oxidation; ii) Protonation/cyclisation

For the preparation of L-Met-L-Ala-D/L-Fos (**160**), a different synthetic route was devised (Scheme 2.14), in which the L-methionine moiety was introduced at the last step of the synthesis, in order to prevent prolonged exposure of the sulfur group to any unwanted side reactions.



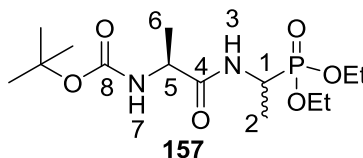
Scheme 2.14: Preparation of phosphonotripeptide, L-Met-L-Ala-D/L-Fos (**160**)

Reagents and conditions: i) IBCF, NMM, THF, -5 °C to r.t., 24hrs; ii) 2M HCl in diethyl ether, r.t., 48hrs; iii) DIPEA, IBCF, NMM, ^tBoc-L-Met-OH, THF/DCM, -5 °C to r.t., 24hrs; iv) HBr, AcOH, 16-18hrs then propylene oxide

2.4.3.1: Synthesis of *tert*-butyl ((2*S*)-1-((-1-(diethoxyphosphoryl)ethyl) amino)-1-oxopropan-2-yl)carbamate or ¹Boc-L-Ala-D/L-Fos diethyl ester (**157**)

The coupling between ¹Boc-L-Ala-OH (**146a**) and D/L-Fos diethyl ester (**84**), using the method as shown in Scheme 2.14, resulted in ¹Boc-L-Ala-D/L-Fos diethyl ester (**157**). The presence of two carboxyl and a phosphonate P=O functional groups, observed in the IR spectrum at 1710, 1652 and 1229 cm⁻¹, confirmed successful coupling between the two different amino acid moieties. The structure of **157** was further confirmed by NMR spectroscopy; the individual peak assignments are summarised in Table 2.13.

Table 2.13: Assignment of NMR signals of the diastereoisomers, ¹Boc-L-Ala-L-Fos diethyl ester and ¹Boc-L-Ala-D-Fos diethyl ester (**157**), at 300 MHz (¹H-NMR) and 75 MHz (¹³C-NMR)



	δ_{H} (CDCl ₃)	δ_{C} (CDCl ₃)
OCH ₂ CH ₃	1.23-1.34 (6H, m, 2 x CH ₃) 4.06-4.23 (4H, m, 2 x CH ₂)	16.3, 16.4, 16.5, 16.6 4 x (d, ³ J _{C-P} =2.3 Hz, CH ₃) 62.4, 62.5, 62.6, 62.8 4 x (d, ² J _{C-P} =6.8 Hz, CH ₂)
CH ₃ -6	1.23-1.34 (3H, m)	18.4
CH ₃ -2	1.23-1.34 (3H, m)	15.6
C(CH ₃) ₃	1.44 (9H, s)	28.3 C(CH ₃) ₃ 80.0 C(CH ₃) ₃
CH-5	4.06-4.23 (1H, m)	50.0
CH-1	4.40-4.52 (1H, m)	40.8 (d, ¹ J _{C-P} =156.8 Hz) 41.0 (d, ¹ J _{C-P} =156.8 Hz)
NH-7	5.12 (1H*, d, ³ J _{H-H} =1.5 Hz) 5.14 (1H*, d, ³ J _{H-H} =1.5 Hz)	-
NH-3	6.72 (1H*, d, ³ J _{H-H} =2.3 Hz) 6.74 (1H*, d, ³ J _{H-H} =2.3 Hz)	-
C=O-8	-	155.2
C=O-4	-	172.1

* Actual proton integration was 0.5

The presence of signals corresponding to the *tert*-butoxycarbonyl and phosphonate diethyl ester groups showed the successful coupling between these two species, **146a** and **84**. As usual with these compounds containing racemic fosfalin, the diastereoisomers were observed by NMR with overlapping signals, compounded by the diastereotopic ethyl ester groups and phosphorus coupling to both protons and carbons. As a result, some of the signals were observed as unresolved multiplets in the ^1H -NMR spectrum. Despite this, two sets of doublets were found at δ 5.12-5.14 ppm and δ 6.72-6.74 ppm, corresponding to the NH-7 and NH-3 protons of the diastereoisomers. In the ^{13}C -NMR spectrum, the presence of diastereotopic ethyl groups and phosphorus coupling resulted in four doublets corresponding to the methyl and methylene carbon atoms of the phosphonate diethyl ester at δ 16.3-16.6 ppm and at δ 62.4-62.8 ppm, displaying $^3J_{\text{C-P}}=2.3$ Hz and $^2J_{\text{C-P}}=6.8$ Hz, respectively. The effects were also observed at δ 40.8 ppm and δ 41.0 ppm, where two doublets displaying a $^1J_{\text{C-P}}$ coupling constant of 156.8 Hz were assigned to the CH-1 carbon. High-resolution mass spectrometry and CHN analysis further supported the identity and purity of this compound (**157**).

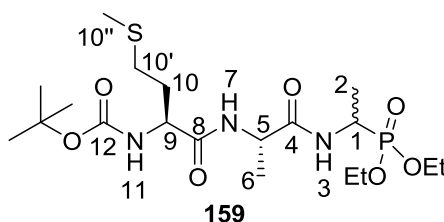
2.4.3.2: Synthesis of (2S)-1-((1-(diethoxyphosphoryl)ethyl)amino)-1-oxopropan-2-aminium chloride or L-Ala-D/L-Fos diethyl ester hydrochloride (158)

The *tert*-butoxycarbonyl at the *N*-terminus of ^tBoc -L-Ala-D/L-Fos diethyl ester (**157**) was removed under acidic conditions, resulting in L-Ala-D/L-Fos diethyl ester hydrochloride (**158**). The successful removal of this group was supported by IR spectroscopy, where a sharp absorbance peak at 2986 cm^{-1} was observed, indicating the presence of an NH_3^+ functional group. The signals corresponding to the ^tBoc group were missing from the NMR spectra and a molecular weight corresponding to that of **158** was observed by high-resolution mass spectrometry.

2.4.3.3: Synthesis of *tert*-butyl ((2*S*)-1-(((2*S*)-1-((1-(diethoxyphosphoryl) ethyl)amino)-1-oxopropan-2-yl)amino)-4-(methylthio)-1-oxobutan-2-yl) carbamate or ¹Boc-L-Met-L-Ala-D/L-Fos diethyl ester (**159**)

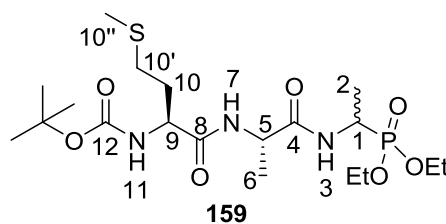
The *N*-protected L-methionine amino acid was coupled with L-Ala-D/L-Fos diethyl ester hydrochloride (**158**). As anticipated, the opportunity for side reactions involving the reactive thioether group led to a low yield of the product (**159**). The successful coupling showed the presence of *tert*-butoxycarbonyl and phosphonate diethyl ester signals on the NMR spectra, as well as thioether signals corresponding to the L-methionine. The assignment of each ¹Boc-L-Met-L-Ala-D/L-Fos diethyl ester (**159**) signal is summarised in Table 2.14. Other evidence of this successful synthesis was provided by high-resolution mass spectrometry.

Table 2.14: Assignment of NMR signals of the diastereoisomers, ¹Boc-L-Met-L-Ala-L-Fos diethyl ester and ¹Boc-L-Met-L-Ala-D-Fos diethyl ester (**159-LLL** and **159-LLD**), at 300 MHz (¹H-NMR) and 75 MHz (¹³C-NMR)



	δ_{H} (CDCl ₃)	δ_{C} (CDCl ₃)
OCH ₂ CH ₃	1.16-1.36 (6H, m, 2 x CH ₃) 4.00-4.12 (4H, m, 2 x CH ₂)	15.4, 15.5 2 x (d, ³ J _{C-P} =3.0 Hz, CH ₃) 15.4, 15.5 2 x (d, ³ J _{C-P} =2.3 Hz, CH ₃) 61.5, 61.6, 61.7, 61.9 4 x (d, ² J _{C-P} =6.8 Hz, CH ₂)
CH ₃ -2	1.16-1.36 (3H, m)	14.2, 14.3
CH ₃ -6	1.16-1.36 (3H, m)	17.7
C(CH ₃) ₃	1.36 (9H, s)	27.3 C(CH ₃) ₃ 79.1 C(CH ₃) ₃
CH ₂ -10	1.82-2.01 (2H, m)	30.8, 30.9
CH ₃ -10''	2.04 (3H, s)	14.5, 14.6
CH ₂ -10'	2.49 (2H, dd, ³ J _{H-H} =9.0 Hz, 3.0 Hz)	29.2, 29.3

Table 2.14 (cont.d): Assignment of NMR signals of the diastereoisomers, ^tBoc-L-Met-L-Ala-L-Fos diethyl ester and ^tBoc-L-Met-L-Ala-D-Fos diethyl ester (**159-LLL** and **159-LLD**), at 300 MHz (¹H-NMR) and 75 MHz (¹³C-NMR)



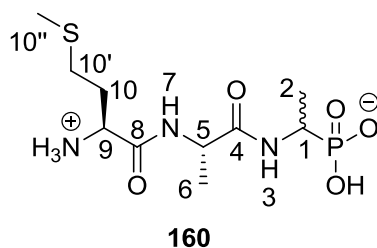
	δ_{H} (CDCl ₃)	δ_{C} (CDCl ₃)
CH-9	4.16-4.26 (1H, m)	52.6
CH-1	4.33-4.43 (1H, m)	39.9 (d, ¹ J _{C-P} =156.8 Hz) 40.0 (d, ¹ J _{C-P} =156.8 Hz)
CH-5	4.45-4.53 (1H, m)	47.9, 48.0
NH-11	5.40 (1H*, d, ³ J _{H-H} =9.0 Hz) 5.44 (1H*, d, ³ J _{H-H} =6.0 Hz)	-
NH-7	6.85 (1H*, d, ³ J _{H-H} =6.0 Hz) 6.92 (1H*, d, ³ J _{H-H} =6.0 Hz)	-
NH-3	7.07 (1H*, d, ³ J _{H-H} =9.0 Hz) 7.16 (1H*, d, ³ J _{H-H} =9.0 Hz)	-
C=O-12	-	154.6
C=O-4	-	170.3, 170.4 or 170.5, 170.6
C=O-8	-	170.3, 170.4 or 170.5, 170.6

* Actual proton integration was 0.5

2.4.3.4: Synthesis of (1-((S)-2-((S)-2-amino-4-(methylthio)butanamido)propanamido)ethyl)phosphonic acid or L-Met-L-Ala-D/L-Fos (**160**)

The *tert*-butoxycarbonyl and phosphonate diethyl ester protecting groups of ^tBoc-L-Met-L-Ala-D/L-Fos diethyl ester (**159**) were removed under acidic conditions. The successful removal of these protecting groups resulted in a sharp NH₃⁺ peak and a broad OH peak at 3263 cm⁻¹ and 2834 cm⁻¹, respectively, on the IR spectrum. The signals corresponding to these protecting groups had vanished from the NMR spectra, as compared to the precursor (**159**). The NMR signals of **160** were assigned accordingly and are summarised in Table 2.15. The successful synthesis of this compound (**160**) was also supported by high-resolution mass spectrometry.

Table 2.15: Assignment of NMR signals of diastereoisomers, L-Met-L-Ala-L-Fos and L-Met-L-Ala-D-Fos (**160-LLL** and **160-LLD**), at 300 MHz ($^1\text{H-NMR}$) and 75 MHz ($^{13}\text{C-NMR}$)



	δ_{H} , (D_2O)	δ_{C} (D_2O)
$\text{CH}_3\text{-10''}$	2.15 (3H, s)	16.9
$\text{CH}_2\text{-10'}$	2.62 (2H, m)	32.8, 33.0
$\text{CH}_2\text{-10}$	2.20 (2H, m)	30.7, 31.0
$\text{CH}_3\text{-2}$	1.29-1.33 (3H, m)	18.4
$\text{CH}_3\text{-6}$	1.42 (3H, d, $^3J_{\text{H-H}}=6.0$ Hz)	19.5, 19.6
CH-9	4.14 (1H, m)	55.0
CH-5	4.39-4.41 (1H, m)	52.9, 53.0
CH-1	4.05 (1H, m)	44.4
NH-7	Exchanged	-
NH-3	Exchanged	-
C=O-4	-	176.1
C=O-8	-	176.1

LC-MS analysis of L-Met-L-Ala-D/L-Fos (**160**) indicated a purity of about 98 %. The presence of two diastereoisomers of **160** was also supported by the LC-MS analysis, where two peaks with approximately 1:2 ratio were observed from the spectrum, Figure 2.7. It is unclear why the peak ratio was 1:2 instead of 1:1. The retention time of **160**, however, was higher compared to the retention time of **153a-c** (Figure 2.5), probably due to the hydrophobic methionine side chain. Although the observation of two peaks by LC-MS (Figure 2.7) confirmed the presence of two diastereoisomers, L,L,L-**160** and L,L,D-**160**, the assignment of these two diastereoisomers to their corresponding peaks was not possible without standards.

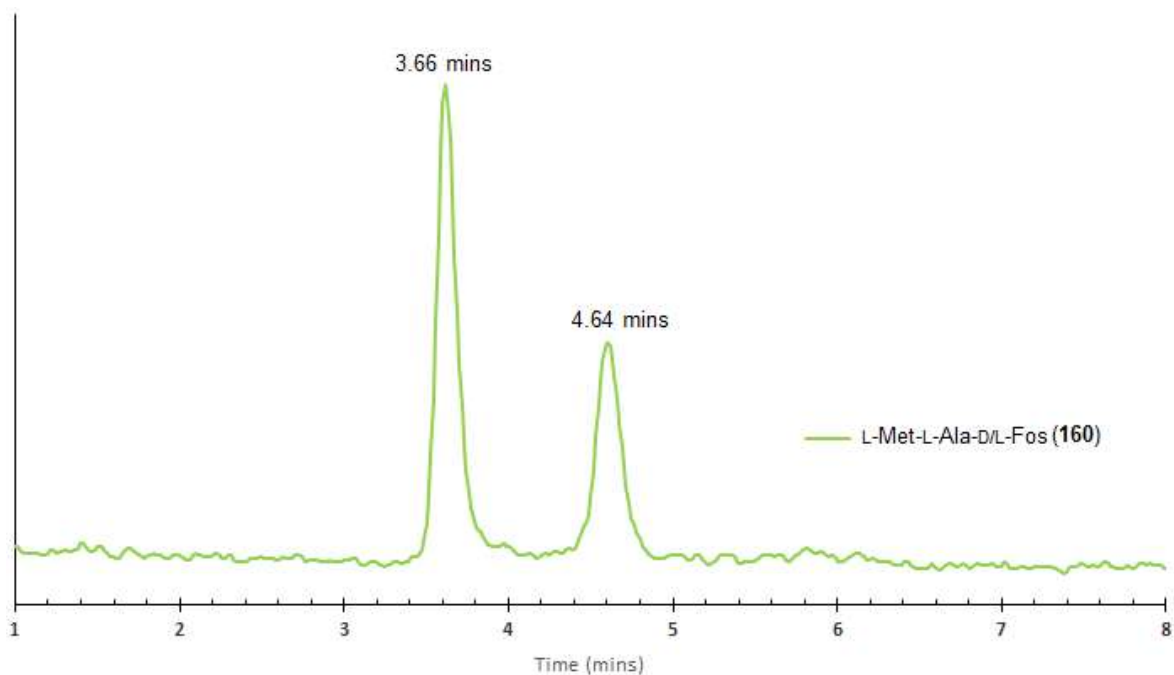


Figure 2.7: Reversed phase LC-MS chromatogram of L-Met-L-Ala-D/L-Fos (**160**) with specific ion extracted at MH^+ m/z 328. LC-MS condition (6.2.1) was used. For clarity, the chromatogram is displayed between 1.0 - 8.0 mins

2.5: Conclusion

D/L-Fosfalin (**13-DL**) was synthesised by improving an established method, as discussed in Section 2.2.1. The subsequent protecting groups were introduced and removed orthogonally to afford D/L-Fos diethyl ester (**84**). A series of coupling reactions between D/L-Fos diethyl ester (**84**) and different peptides or amino acids resulted in five diastereoisomeric phosphonodipeptides and phosphonotripeptides, L-Pyroglu-D/L-Fos (**141**), L-Ala-L-Ala-D/L-Fos (**153a**), L-Nva-L-Ala-D/L-Fos (**153b**), Sar-L-Ala-D/L-Fos (**153c**) and L-Met-L-Ala-D/L-Fos (**160**). The purity and diastereoisomeric composition of **153a-c** and **160** were supported by LC-MS analysis. As a result of the solubility issue encountered for L-pyroglutamic acid, additional steps were required, in which a ^tBoc group was introduced prior to peptide coupling. A different synthetic route was used for the synthesis of L-Met-L-Ala-D/L-Fos (**160**) due to the thioether side chain on L-methionine being prone to unwanted side reactions. All of the synthesised compounds (**141**, **153a**, **153b**, **153c**, **160**) were subjected to microbiology testing, which will be discussed in Chapter 4.

CHAPTER 3

SYNTHESIS OF SUICIDE SUBSTRATES BASED ON β -CHLORO-L-ALANINE AND STABILITY STUDY OF β -CHLORO-L-ALANYL-D/L-FOSFALIN ACROSS THE pH RANGE 6.1 - 9.1

3.1: Synthesis of peptides derivatives containing β -chloro-L-alanine-D/L-fosfalin

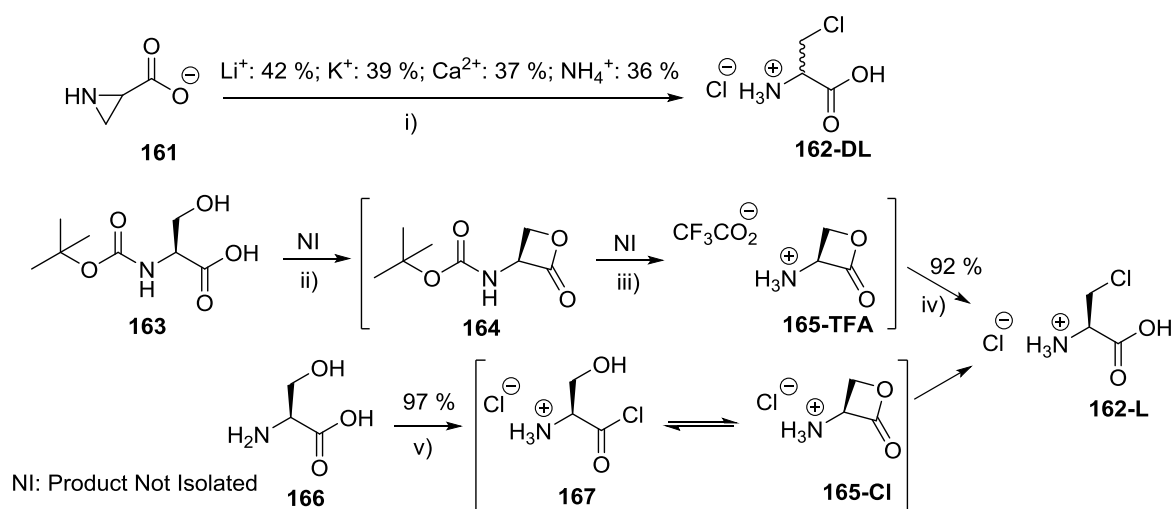
As already observed with fosfalin, an alanine analogue can serve as a good suicide substrate for alanine racemase, as reported by Atherton and co-workers (1979AAC677, 1986JMC29). Another alanine analogue, β -chloroalanine (**38**) also exhibits good antibacterial activities, both on its own and upon coupling with other peptides or amino acids, as reported by Cheung and co-workers (1983JMC1733, 1986 JMC2060). The detailed evaluation of antibacterial activities of β -chloroalanine and its dipeptide derivatives have been discussed previously (see Section 1.5.2).

Although many studies have been performed in the past based on these two different inhibitors, peptide derivatives based on fosfalin or based on β -chloroalanine, limited studies have been carried out to evaluate the inhibitory effects upon simultaneous incorporation of these two different inhibitors into a peptide derivative. Since a good antibacterial effect was reported in the peptide derivatives containing either a fosfalin or β -chloroalanine residue, an enhancement or broad inhibitory spectrum was anticipated from an inhibitor that combines these units. Initial work, carried out by Bedernjak (P-2015MI27) and Váradi (T-2013MI192) on β -chloro-L-alanyl-L-fosfalin showed a promising enhancement on the bacterial inhibitory effects. This finding was a trigger to further investigation on novel peptide derivatives based on these two moieties.

In the following section, the synthesis of β -chloro-L-alanine and peptide derivatives based on β -chloro-L-Ala-D/L-fosfalin will be discussed. In addition, the synthesis of other potential growth inhibitors will also be covered. As a result of the presence of a chlorine atom at the β -position of alanine, β -chloro-L-alanine is prone to degradation, especially under basic conditions; hence, the stability study of β -chloro-L-Ala-D/L-fosfalin at pH range 6.1 – 9.1 will be investigated.

3.1.1: Published methods for the preparation of β -chloro-L-alanine derivatives

Although β -chloro-L-alanine (**38-L**) is commercially available as the hydrochloride salt (**162-L**) and is readily used for peptide synthesis, it would be very expensive for this work, due to the large quantity required. Fortunately, there are a few published methods reported for this synthesis (Scheme 3.1), which facilitated in-house synthesis and made feasible the use of β -chloro-L-alanine (**38-L**) in this work.



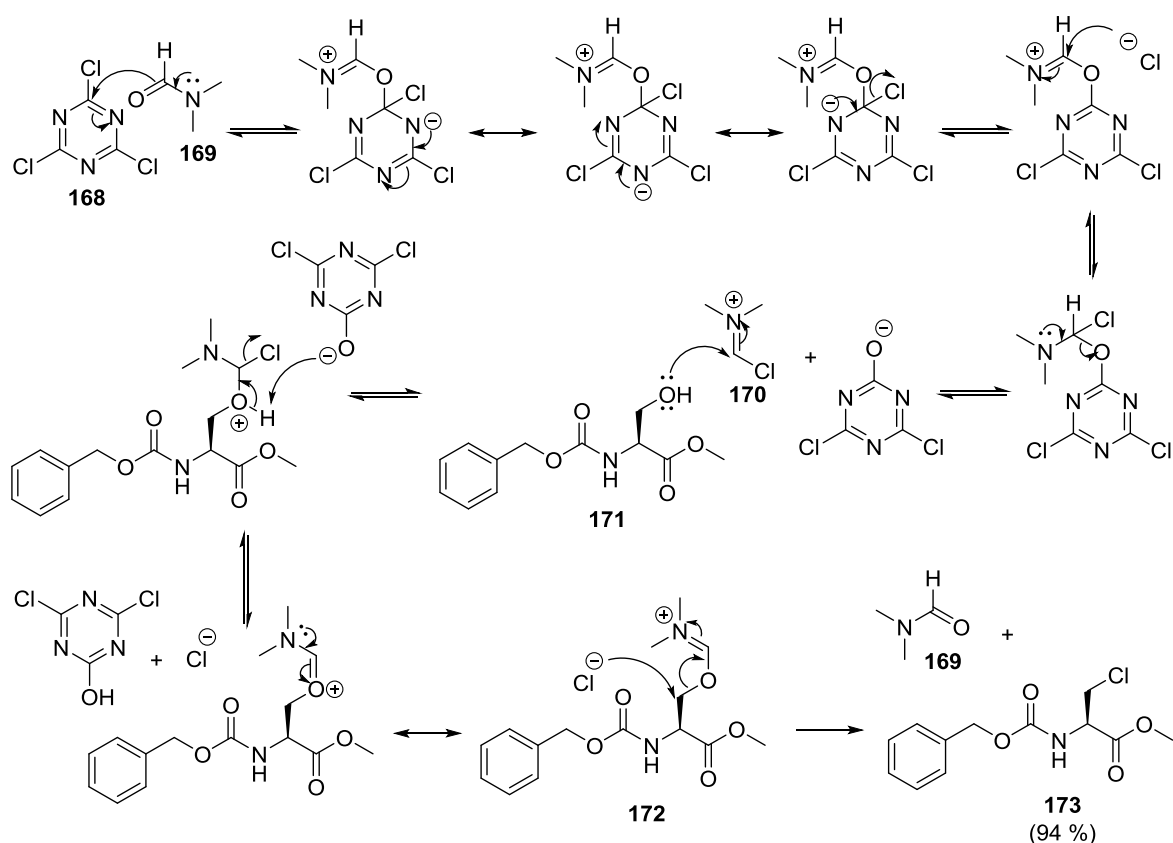
Scheme 3.1: Synthesis of racemic β -chloroalanine hydrochloride salt (**162-DL**) and optically pure β -chloro-L-alanine hydrochloride salt (**162-L**)

Reagents and conditions: i) 35 % HCl, H_2O , 10 hrs, r.t. then 4hrs 0 °C; ii) diethyl azodicarboxylate (DEAD, **88**), Ph_3P (**89**), -78 °C, dry THF; iii) TFA, 0-5 °C, 10 min; iv) Conc HCl, H_2O , Recryst MeOH/Et₂O; v) 1,2-dimethoxyethane, HCl gas, r.t., then SOCl_2 , 50 °C, 10 hrs

The synthesis of racemic β -chloroalanine (**38**) was first reported in a patent, published by Mitsui Toatsu Chemicals in 1984 (P-1984MI6). It was prepared by reacting aziridine-2-carboxylate with concentrated hydrochloric acid in an aqueous medium. As a result of the undefined stereochemistry of the aziridine-2-carboxylate used in this synthesis, a racemic salt product (**162-DL**) was obtained. When different counter-ions of aziridine-2-carboxylate were used, such as lithium, potassium, calcium and ammonium, different yields were reported. The synthesis of optically pure β -chloro-L-alanine hydrochloride (**162-L**) is possible from the optically pure starting material, L-aziridine-2-carboxylate (**161-L**); however, it is very expensive commercially.

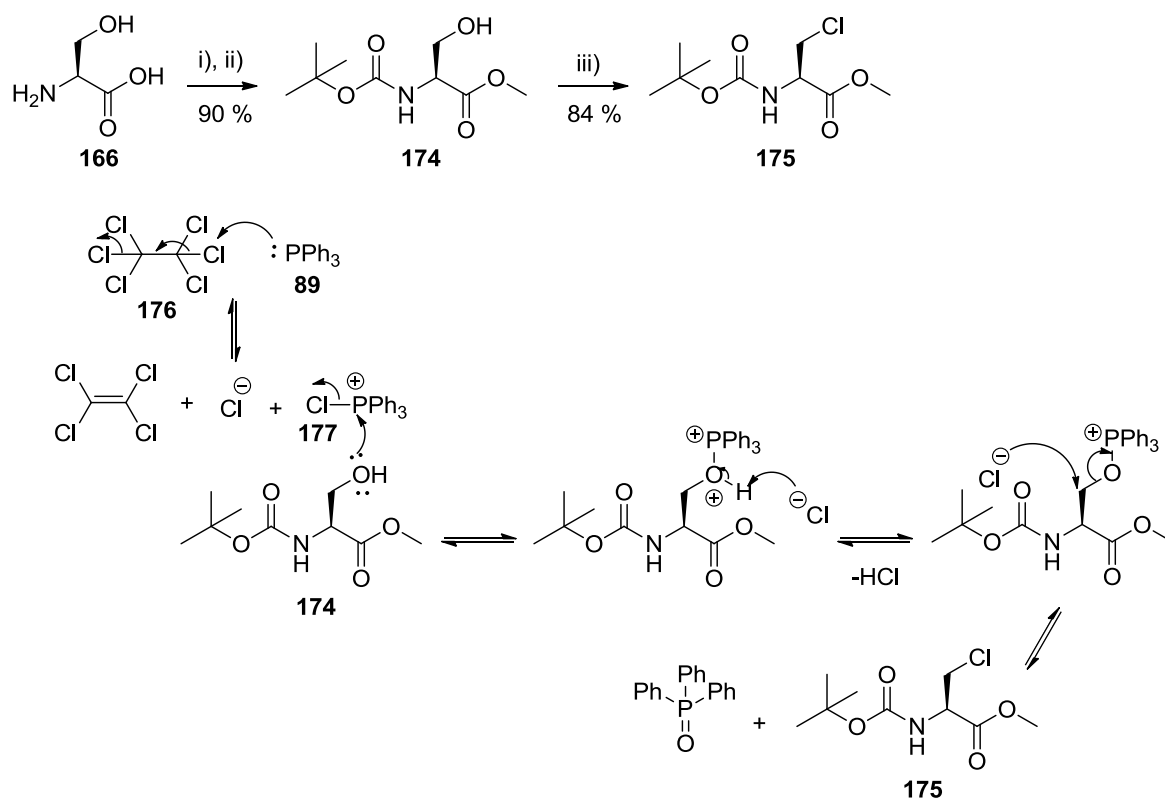
Optically pure β -chloro-L-alanine (**38-L**) was later synthesised from L-serine by Arnold in 1987 (1988JACS2237). In this synthesis, ^tBoc-L-serine (**163**) was cyclised using the Mitsunobu reaction, forming ^tBoc-L-serine β -lactone (**164**). The *tert*-butoxycarbonyl group was removed with trifluoroacetic acid and subsequent chlorination of L-serine β -lactone trifluoroacetate salt (**165-TFA**) by concentrated hydrochloric acid, formed optically pure β -chloro-L-alanine hydrochloride (**162-L**). This synthesis was later adapted by Kaneka Corporation in 2002 (P-2002MI15), using L-serine (**166**) as a starting material. The cyclisation reaction was facilitated by formation of the acid chloride intermediate (**167**), instead of a Mitsunobu reaction. The L-serine β -lactone hydrochloride salt (**165-Cl**) was later chlorinated by hydrogen chloride gas, resulting in formation of β -chloro-L-alanine hydrochloride (**162-L**). Although this is a one-pot reaction, it involved the use of hydrogen chloride gas, which makes this reaction less easy to handle compared to the synthesis reported by Arnold.

The use of hydrogen chloride as a chlorinating agent in these classical methods was later improved by using less corrosive and easier approaches. According to Lucas (2002OL553), the chlorination of the β -amino alcohol was performed under mild conditions, using 2,4,6-trichloro[1,3,5]triazine (TCT) (**168**) and *N,N*-dimethyl formamide (DMF) (**169**) in DCM at room temperature. In this synthesis (Scheme 3.2), the chlorinating agent, *N,N*-dimethyl chloroiminium ions (Vilsmeier reagent) (**170**), reacted with the β -amino alcohol group of Cbz-L-Ser-OMe (**171**), forming a reactive species (**172**), which facilitated an S_N2 reaction to form Cbz- β -chloro-L-Ala-OMe (**173**) and re-generated DMF (**169**) as a by-product.



Scheme 3.2: Conversion of β -amino alcohol (171) into corresponding alkyl chloride (173)

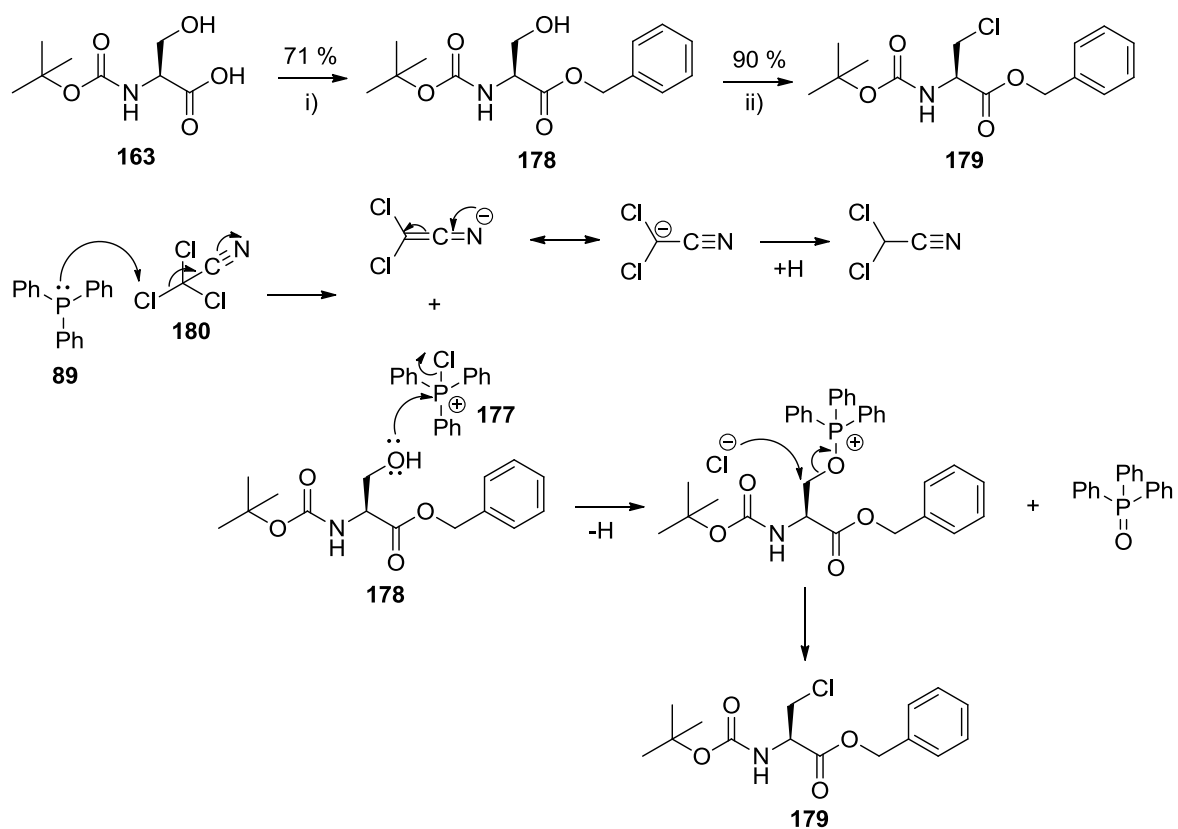
Another chlorination of the β -amino alcohol of L-serine was reported by Barfoot in 2005 (2005T3403), using hexachloroethane (176) and triphenylphosphine (89) to generate the chlorinating agent (177). In this synthesis, *tert*-butoxycarbonyl and methyl ester protecting groups were first introduced at the respective *N*-terminus and *C*-terminus of L-serine (166) (1994S31), followed by the conversion of the β -amino alcohol of ^tBoc-L-Ser-OMe (174) to form ^tBoc- β -chloro-L-Ala-OMe (175), with the mechanism as shown in Scheme 3.3.



Scheme 3.3: Synthesis of ^tBoc-β-chloro-L-Ala-OMe (**175**) via the conversion of β-amino alcohol (**174**) into the corresponding alkyl chloride (**175**)

Reagents and conditions: i) MeOH, HCl; ii) (Boc)₂O, Et₃N, THF; iii) C₂Cl₆, Ph₃P, DCM, r.t., 2hrs

The β-serine alcohol group can be converted into the chlorinated analogue with good efficiency in the presence of a range of chlorinating agents. For example, the hexachloroethane (**176**) can be replaced by trichloroacetonitrile (**180**), which acts as a source of chlorine in the presence of triphenylphosphine (**89**) and also efficiently replaces the β-serine alcohol group with a chlorine atom. The mechanism of this conversion was reported by Váradi in 2013 (T-2013MI257), Scheme 3.4. In this synthesis, the benzyl ester group was introduced at the C-terminus of ^tBoc-L-serine (**163**), followed by the conversion of the protected β-serine alcohol (**178**) to the corresponding alkyl chloride (**179**). The use of the benzyl ester instead of the methyl ester protecting group is favourable, as the benzyl ester can be readily removed by hydrogenation.

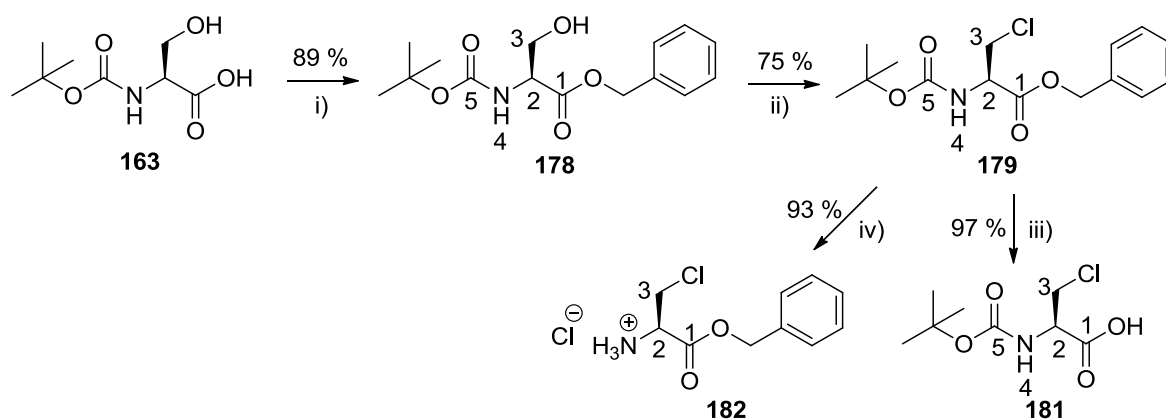


Scheme 3.4: Synthesis of 'Boc-β-chloro-L-Ala-OBzl (**179**) via the conversion of β-amino alcohol (**178**) into the corresponding alkyl chloride (**179**)

Reagents and conditions: i) DBU, benzyl bromide, dry benzene, r.t., 24hrs; ii) trichloroacetonitrile (**180**), PPh₃ (**89**), dry DCM, r.t., 24hrs

3.1.2: Synthesis of β -chloro-L-alanine derivatives

The synthetic approach reported by Váradi (T-2013MI257) was adopted in the preparation of t Boc- β -chloro-L-Ala-OBzl (**179**), due to ease of synthesis and high yield reported, followed by chemoselective deprotection, resulting in the formation of N_α or carboxyl protected β -chloro-L-alanine derivatives (**181**) and (**182**), Scheme 3.5.



Scheme 3.5: Synthesis of β -chloro-L-alanine derivatives, t Boc- β -chloro-L-alanine (**181**) and β -chloro-L-alanine benzyl ester hydrochloride salt (**182**)

Reagents and conditions: i) DBU, benzyl bromide, dry benzene, r.t., 24hrs; ii) trichloroacetonitrile (**180**), PPh_3 (**89**), dry DCM, r.t., 24hrs; iii) MeOH, 10 % Pd/C, 3.5 bar H_2 , r.t., 24hrs; iv) 2M HCl in diethyl ether, r.t., 48hrs

3.1.2.1: Synthesis of (S)-benzyl 2-((tert-butoxycarbonyl)amino)-3-hydroxypropanoate or t Boc-L-Ser-OBzl (**178**)

Base-catalysed esterification of t Boc-L-serine (**163**) was achieved in good yield, using 1,8-diazabicyclo[5.4.0]undec-7-ene (DBU) and benzyl bromide (1981CR229), Scheme 3.5. NMR spectroscopic analysis confirmed the synthesis of t Boc-L-Ser-OBzl (**178**), showing the additional benzyl signals at δ 5.11 ppm and δ 5.16 ppm (two doublets for the diastereotopic benzylic protons) and δ 7.27 ppm (aromatic protons' multiplet). The serine β -protons (CH_2 -3) also displayed diastereotopicity, giving rise to two doublet of doublets at δ 3.82 ppm and δ 3.90 ppm, Figure 3.1. The successful synthesis of this compound was further confirmed by its melting point (consistent with the literature value) and low resolution mass spectrometry.

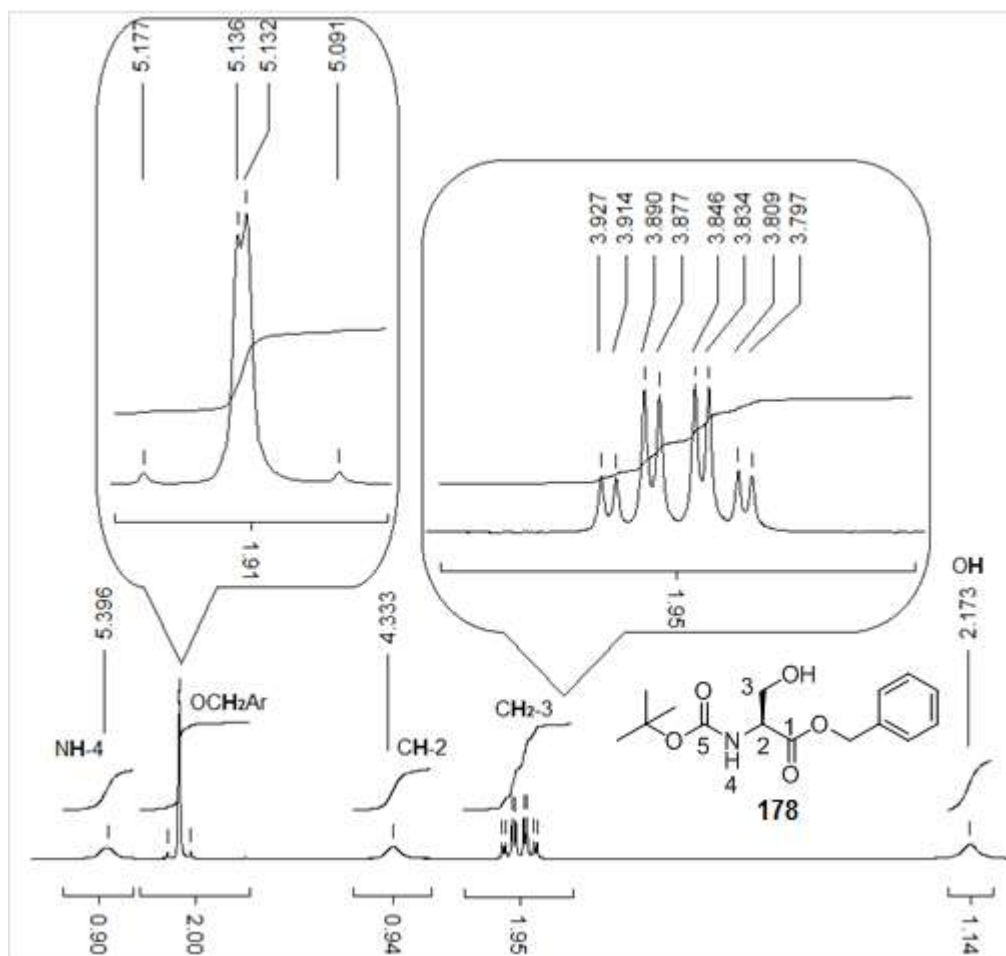


Figure 3.1: $^1\text{H-NMR}$ spectrum of $^t\text{Boc-L-Ser-OBzl}$ (**178**) in CDCl_3 at 300 MHz, range δ 2.10 - 5.40 ppm

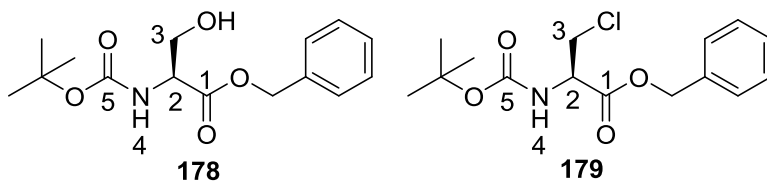
3.1.2.2: Synthesis of (*R*)-benzyl 2-((*tert*-butoxycarbonyl)amino)-3-chloropropanoate or $^t\text{Boc-}\beta\text{-Cl-L-Ala-OBzl}$ (**179**)

Chlorination of $^t\text{Boc-L-Ser-OBzl}$ (**178**) was carried out using trichloroacetonitrile (**180**) and triphenylphosphine (**89**) (T-2013MI257), according to the mechanism shown in Scheme 3.4. Evidence for the successful replacement of the β -alcohol group by chlorine was provided by the absence of the OH signal from both the IR and NMR spectra of the product (**179**). Apart from this, substitution of the OH group with the less electronegative chlorine atom resulted in a relatively shielded signal corresponding to C-3 being observed, at 45.5 ppm (**179**) rather than 62.3 ppm (**178**). The NMR spectra of both precursor (**178**) and the product (**179**) are summarised in Table 3.1.

Table 3.1: NMR spectra comparison between ^tBoc-L-Ser-OBzl (**179**) and ^tBoc-β-chloro-L-Ala-OBzl (**178**) at 300 MHz (¹H-NMR) and 75 MHz (¹³C-NMR)

	^t Boc-L-Ser-OBzl (178)		^t Boc-β-chloro-L-Ala-OBzl (179)	
	δ _H (CDCl ₃)	δ _C (CDCl ₃)	δ _H (CDCl ₃)	δ _C (CDCl ₃)
C(CH ₃) ₃	1.36 (9H, s)	27.1 C(CH ₃) ₃ 79.1 C(CH ₃) ₃	1.38 (9H, s)	28.3 C(CH ₃) ₃ 80.5 C(CH ₃) ₃
OH	2.17 (1H, br)	-	-	-
CH ₂ -3	3.82 (1H, dd, ² J _{H-H} =11.1 Hz, ³ J _{H-H} =3.6 Hz) 3.90 (1H, dd, ² J _{H-H} =11.1 Hz, ³ J _{H-H} =3.9 Hz)	62.3	3.78 (1H, dd, ² J _{H-H} =11.2 Hz, ³ J _{H-H} =3.2 Hz) 3.92 (1H, dd, ² J _{H-H} =11.3 Hz, ³ J _{H-H} =3.0 Hz)	45.5
CH-2	4.33 (1H, m)	54.7	4.67 (1H, m)	54.2
OCH ₂	5.11 (1H, d, ² J _{H-H} =12.3 Hz) 5.16 (1H, d, ² J _{H-H} =12.3 Hz)	66.2	5.13 (1H, d, ² J _{H-H} =12.2 Hz) 5.18 (1H, d, ² J _{H-H} =12.2 Hz)	67.8
NH-4	5.40 (1H, br)	-	5.37 (1H, d, ³ J _{H-H} =7.5 Hz)	-
C ₆ H ₅	7.27 (5H, m)	127.0-127.4 (CH _{Ar}) 134.1 (CH _{Ar} quat.)	7.29 (5H, m)	128.4-128.7 (CH _{Ar}) 134.9 (CH _{Ar} quat.)
C=O-5	-	153.0	-	155.0
C=O-1	-	170.7	-	169.0

Literature ¹H-NMR spectrum of ^tBoc-L-Ser-OBzl, acquired at 100 MHz (CDCl₃) was reported (1981CR229). Similar NMR result without multiplicity was reported in literature



Apart from the less deshielded CH₂-3 signal on the NMR spectra when OH was replaced by Cl, most of the NMR signals of the product (**179**) were similar to those of the precursor (**178**); for example, the same protons displayed diastereotopic effects in both compounds. The purity of product (**179**) was supported by CHN analysis and its identity was further supported by low resolution mass spectrometry. The presence of chlorine was confirmed by the MS: a 3:1 ratio of ³⁵Cl:³⁷Cl was observed on the MS spectrum, Figure 3.2.

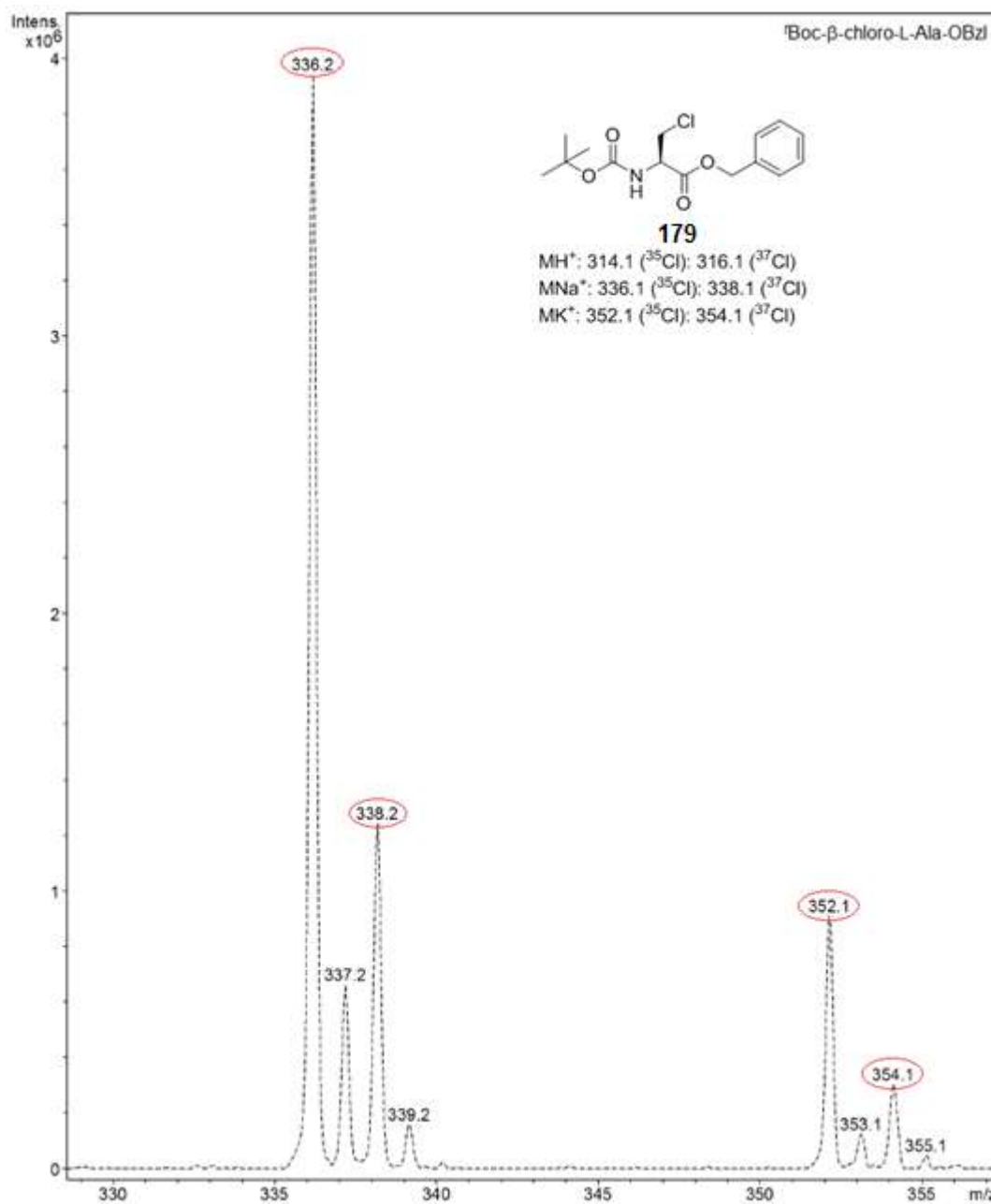


Figure 3.2: Low resolution MS spectrum of ¹³C-Boc-β-chloro-L-Ala-OBzl (**179**), showing the 3:1 ratio of ³⁵Cl:³⁷Cl

3.1.2.3: Synthesis of (*R*)-2-((*tert*-butoxycarbonyl)amino)-3-chloropropanoic acid or ¹Boc-β-Cl-L-Ala-OH (**181**)

The benzyl ester protecting group at the C-terminus of ¹Boc-β-chloro-L-Ala-OBzl (**179**) was removed *via* hydrogenation (Scheme 3.5). The successful removal of this protecting group was confirmed by the IR spectrum, in which a broad absorbance peak at 2973 cm⁻¹ indicated the presence of a carboxylic hydroxyl functional group. The disappearance of signals corresponding to the benzyl ester was also confirmed by NMR spectroscopy, where the signals corresponding to the aromatic protons and carbons had vanished. The melting point obtained fell within the range of the literature melting point (1983JMC1733), which further supported the identity of this compound (**181**). Low resolution mass spectrometry confirmed the presence of chlorine with a 3:1 ratio of ³⁵Cl:³⁷Cl observed for the molecular ion peak.

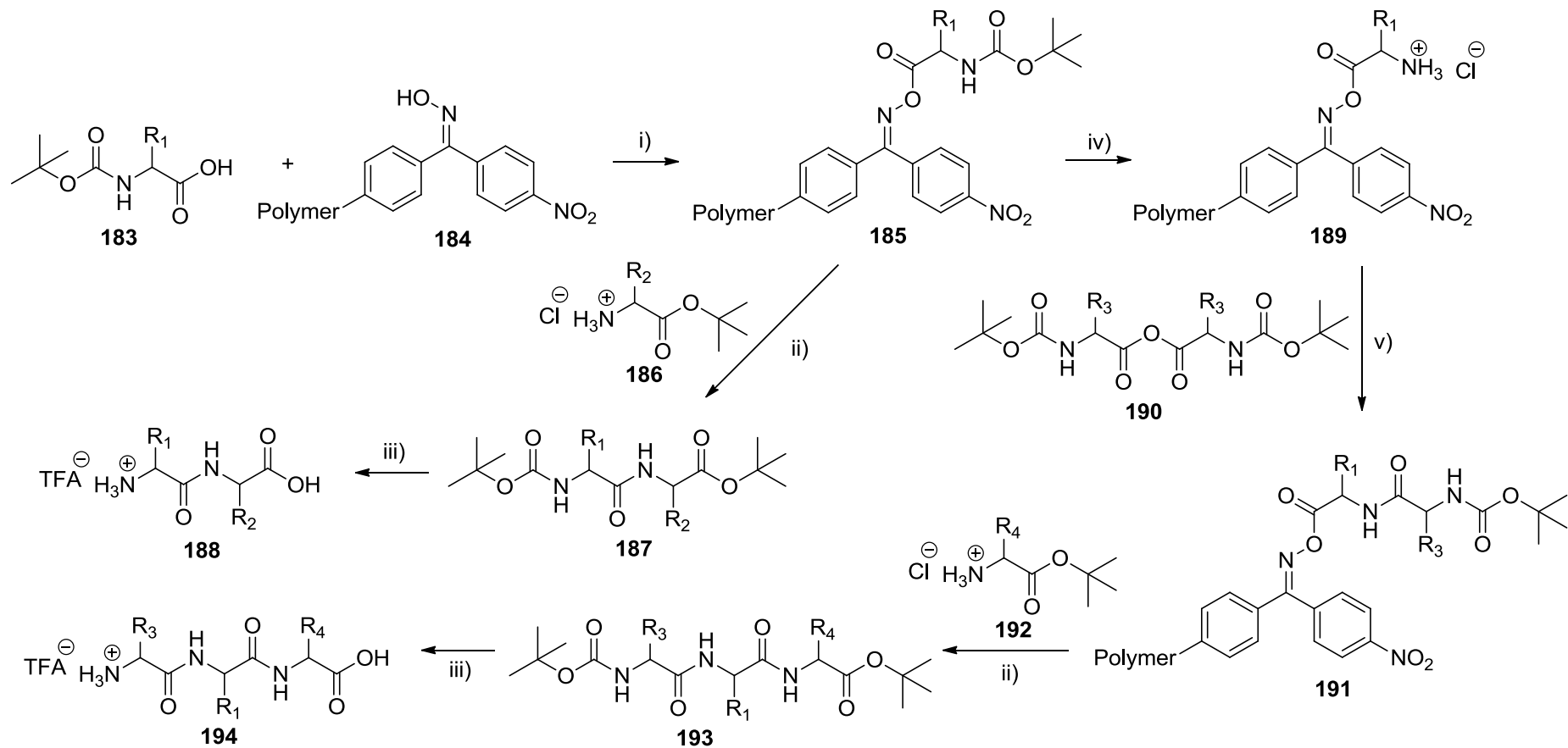
3.1.2.4: Synthesis of (*R*)-1-(benzyloxy)-3-chloro-1oxopropan-2-aminium chloride or β-Cl-L-Ala-OBzl hydrochloride (**182**)

The *tert*-butoxycarbonyl protecting group at the N-terminus of ¹Boc-β-chloro-L-Ala-OBzl (**179**) was removed under acidic conditions (Scheme 3.5). The successful removal of the protecting group was confirmed by the IR spectrum, where the absorbance peak at 2841 cm⁻¹ indicated the presence of NH₃⁺ functional group. ¹Boc hydrolysis was also confirmed by NMR spectroscopy, where the signals corresponding to the *tert*-butyl protons and carbons had vanished. The purity of this compound (**182**) was confirmed by CHN analysis, while its identity and the presence of chlorine were supported by low resolution mass spectrometry.

3.2: Published methods for the preparation of peptides containing the β -chloro-L-alanine moiety

The synthesis of different peptide derivatives incorporating the β -chloroalanine moiety using a solid phase method (1980JOC1295) was reported by Cheung and his co-worker in 1983 (1983JMC1733) and 1986 (1986JMC2060). For dipeptide synthesis (Scheme 3.6), the t Boc protected *N*-terminal amino acid (**183**) was first coupled to a *p*-nitro-benzophenone-oxime bound polymer (**184**), with the aid of DCC, forming a t Boc amino acid-oxime complex (**185**). The oxime residue was later removed with simultaneous formation of a new peptide bond, by adding t butyl ester protected *C*-terminal amino acid (**186**) and acetic acid. After this aminolysis, the protecting groups at the *C*- and *N*-termini of (**187**) were removed simultaneously, using anisole and trifluoroacetic acid, resulting in the formation of dipeptides (**188**) in variable overall yield (Table 3.2). For tripeptide synthesis (Scheme 3.6), additional steps were required after formation of the t Boc amino acid-oxime complex (**185**). The t Boc protecting group of (**185**) was removed by HCl in dioxane to afford (**189**), which was then coupled with the symmetrical anhydride of the *N*-protected amino acid (**190**). The oxime residue of (**191**) was removed upon coupling with *C*-protected amino acid (**192**), under the aminolysis conditions, to form the protected tripeptide (**193**). The subsequent acidic deprotection afforded the tripeptide (**194**) in low to moderate yield (Table 3.2).

The solid phase technique is widely used for the synthesis of peptides. Different resins and polymers are available commercially, depending upon the type of amino acids involved in the synthesis and the desired functionality at the carboxyl terminus. Although the solid phase technique can generate different oligopeptides in a short time by using an automated peptide synthesiser, the overall yields obtained are variable (see Table 3.2), due to the requirement for extensive purification of the final products (1980JOC1295). The classical solution phase peptide technique, in contrast, produces more homogeneous products, as purification and characterisation are performed on each intermediate, providing confidence in the final structure. Despite the merits of purification, however, it increases significantly the time required for peptide synthesis, especially when dealing with oligopeptides. Fortunately, the current work focuses on the synthesis of di- and tripeptides, for which the use of solution phase methods is favourable.



Scheme 3.6: Solid phase synthesis of dipeptide derivatives containing the β -chloroalanine moiety (the exact stereochemistry and identity are reported in Table 3.2)

Reagents and conditions: i) DCC, DCM, r.t., 48hrs; ii) DIPEA, acetic acid, DCM, r.t., 48hrs; iii) anisole, TFA, 0 °C then r.t., 3.5hrs; iv) HCl, dioxane, r.t., 1hr; v) DIPEA, DCM, r.t., 1hr

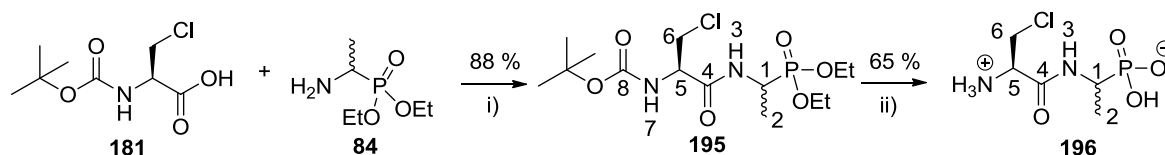
Table 3.2: Overall yields of dipeptide derivatives containing the β -chloroalanine moiety using solid phase synthesis, Scheme 3.6 (1983JMC1733) (1986JMC2060)

Di- (188) and Tripeptide (194)	R ₁	R ₂	R ₃	R ₄	Overall yield (%)
β -Cl-L-Ala-L-Ala	CH ₂ Cl	CH ₃	-	-	91
β -Cl-D-Ala-D-Ala	CH ₂ Cl	CH ₃	-	-	55
L-Ala- β -Cl-L-Ala	CH ₃	CH ₂ Cl	-	-	32
D-Ala- β -Cl-D-Ala	CH ₃	CH ₂ Cl	-	-	13
L-Ala- β -Cl-D-Ala	CH ₃	CH ₂ Cl	-	-	60
β -Cl-L-Ala- β -Cl-L-Ala	CH ₂ Cl	CH ₂ Cl	-	-	43
L-Met- β -Cl-L-Ala	(CH ₂) ₂ SCH ₃	CH ₂ Cl	-	-	60
L-Nva- β -Cl-L-Ala	(CH ₂) ₂ CH ₃	CH ₂ Cl	-	-	67
L-Met-L-Ala- β -Cl-L-Ala	CH ₃	-	(CH ₂) ₂ SCH ₃	CH ₂ Cl	9
L-Met- β -Cl-L-Ala- β -Cl-L-Ala	CH ₂ Cl	-	(CH ₂) ₂ SCH ₃	CH ₂ Cl	13
L-Ala-L-Ala- β -Cl-L-Ala	CH ₃	-	CH ₃	CH ₂ Cl	35
β -Cl-L-Ala- β -Cl-L-Ala- β -Cl-L-Ala	CH ₂ Cl	-	CH ₂ Cl	CH ₂ Cl	45

3.2.1: Preparation of phosphonodipeptide containing β -chloro-L-alanine and D/L-fosfalin

The synthesis and good *in vitro* antibacterial activity of β -chloro-L-Ala-L-fosfalin were reported by Váradi (T-2013MI192). However, the cost of this L,L-dipeptide synthesis is not feasible on a commercial scale due to the large quantity of expensive L-fosfalin required. Fortunately, a cheap and simple synthetic approach to racemic fosfalin, D/L-fosfalin was optimised previously (section 2.2.1), which allows the synthesis of β -chloro-L-Ala-D/L-fosfalin instead of β -chloro-L-Ala-L-fosfalin to take place feasibly. Since the antibacterial activity of the racemic fosfalin-containing diastereoisomeric β -chloro-L-Ala-D/L-fosfalin has not been studied, this became part of the current study.

The dipeptide derivative containing both D/L-fosfalin and β -chloro-L-alanine, β -chloro-L-Ala-D/L-fosfalin (**196**), was synthesised *via* the synthetic route shown in Scheme 3.7. In this synthesis, the ^tBoc- β -chloro-L-alanine (**181**) was coupled with the D/L-Fos diethyl ester (**84**), again using the IBCF/NMM coupling approach. The protecting groups, *tert*-butoxycarbonyl at the *N*-terminus and diethyl phosphonate ester groups at the *O*-termini of **195** were removed simultaneously under acidic conditions, giving rise to β -chloro-L-Ala-D/L-fosfalin (**196**).



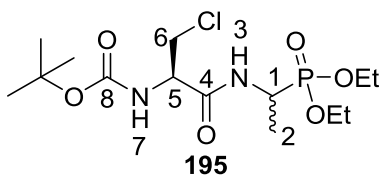
Scheme 3.7: Synthesis of β -chloro-L-Ala-D/L-fosfalin (**196**)

Reagents and conditions: i) NMM, IBCF, THF, -5 °C to r.t., 24hrs; ii) HBr, AcOH, 16-18hrs then propylene oxide

3.2.1.1: Synthesis of *tert*-butyl ((2*R*)-3-chloro-1-((1-(diethoxyphosphoryl)ethyl)amino)-1-oxopropan-2-yl)carbamate or ¹Boc-β-chloro-L-Ala-D/L-Fos diethyl ester (**195**)

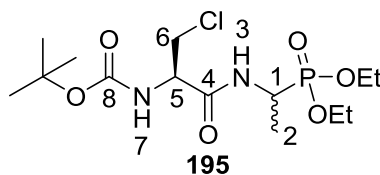
¹Boc-β-Chloro-L-Ala-D/L-Fos diethyl ester (**195**) was synthesised *via* the synthetic route as shown in Scheme 3.7. Evidence for coupling was seen in the NMR spectra (Table 3.3), in which phosphorus coupling, diastereoisomer signals and diastereotopic protons and groups were observed.

Table 3.3: NMR assignment of distereoisomers, ¹Boc-β-chloro-L-Ala-L-Fos diethyl ester and ¹Boc-β-chloro-L-Ala-D-Fos diethyl ester (**195**), at 300 MHz (¹H-NMR) and 75 MHz (¹³C-NMR)



	δ_{H} (CDCl ₃)	δ_{C} (CDCl ₃)
OCH ₂ CH ₃	1.15-1.46 (6H, m, 2 x CH ₃) 4.06-4.22 (4H, m, 2 x CH ₂)	16.3, 16.4 2 x (d, ³ J _{C-P} =1.5 Hz, CH ₃) 16.4, 16.4 2 x (d, ³ J _{C-P} =2.3 Hz, CH ₃) 62.6, 62.6, 63.0, 63.0 4 x (d, ² J _{C-P} =6.8 Hz, CH ₂)
CH ₃ -2	1.15-1.46 (3H, m)	15.6, 15.7
C(CH ₃) ₃	1.47 (9H, s)	28.2 C(CH ₃) ₃ 80.8 C(CH ₃) ₃
CH ₂ -6	3.74 (1H, dd, ² J _{H-H} =12.0 Hz, ³ J _{H-H} =6.0 Hz) 4.00 (1H, dd, ² J _{H-H} =12.0 Hz, ³ J _{H-H} =6.0 Hz)	55.2
CH-1	4.40-4.56 (1H, m)	41.2, 41.3 2 x (d, ¹ J _{C-P} =157.5 Hz)
CH-5	4.40-4.56 (1H, m)	55.3

Table 3.3 (cont.d): NMR assignment of distereoisomers, ¹Boc-β-chloro-L-Ala-L-Fos diethyl ester and ¹Boc-β-chloro-L-Ala-D-Fos diethyl ester (**195**), at 300 MHz (¹H-NMR) and 75 MHz (¹³C-NMR)



	δ_{H} (CDCl ₃)	δ_{C} (CDCl ₃)
NH-3	5.46 (1H*, d, ³ J _{H-H} =6.0 Hz) 5.48 (1H*, d, ³ J _{H-H} =9.0 Hz), or 7.01 (1H*, m) 7.09 (1H*, m)	-
NH-7	5.46 (1H*, d, ³ J _{H-H} =6.0 Hz) 5.48 (1H*, d, ³ J _{H-H} =9.0 Hz), or 7.01 (1H*, m) 7.09 (1H*, m)	-
C=O-8	-	155.0
C=O-4	-	168.3

* Actual proton integration was 0.5

Phosphorus coupling was observed on the ¹³C-NMR spectrum: doublets instead of singlets were observed for the phosphonate ester methylene carbon atoms at δ 62.6-63.0 ppm and the directly attached methine CH-1 at δ 41.2-41.3 ppm (Table 3.3). The spectra were further complicated by diastereoisomeric effects, giving rise to signals corresponding to more than one proton assignment on the ¹H-NMR spectrum. For instance, a 9 proton signal at δ 1.15-1.39 ppm corresponded to the methyl protons of OCH₂CH₃ and CH₃-2, such that the splitting pattern appeared as a multiplet and was unable to be assigned to individual protons/groups. However, two clear doublet of doublets corresponding to the diastereotopic CH₂-6 protons, were observed at δ 3.74 ppm and δ 4.00 ppm. The carbamate and amide protons at δ 5.46-5.48 ppm and δ 7.01-7.09 ppm were unable to be assigned ambiguously, due to limited supporting evidence in the 2D NMR data.

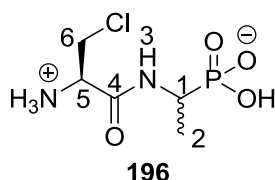
The successful synthesis of ¹Boc-β-chloro-L-Ala-D/L-Fos diethyl ester (**195**) was supported by the co-existent NMR signals corresponding to the ¹Boc and diethyl phosphonate ester protecting groups and its identity was confirmed by high

resolution mass spectrometry. The presence of chlorine was supported by the 3:1 signal ratio for MH⁺ on the MS spectrum.

3.2.1.2: Synthesis of (1-((R)-2-amino-3-chloropropanamido)ethyl) phosphonic acid or β-chloro-L-Ala-D/L-fos (196)

Both of the protecting groups, *tert*-butoxycarbonyl and diethyl phosphonate ester groups at the *N*-terminus and *O*-termini of *t*Boc-β-chloro-L-Ala-D/L-Fos diethyl ester (**195**) were removed simultaneously under acidic conditions. Subsequently treatment with propylene oxide formed the zwitterionic product (**196**). Evidence of the successful removal of these protecting groups was the presence of a sharp absorbance peak at 3300 cm⁻¹ and a broad peak at 2928 cm⁻¹ on the IR spectrum, indicating the presence of NH₃⁺ and OH functional groups. The removal of these protecting groups was further supported by the disappearance of signals corresponding to the *tert*-butyl group and diethyl phosphonate ester groups from the NMR spectra, while the remaining NMR signals of **196** were assigned and presented in Table 3.4. The purity of zwitterion (**196**) was confirmed by CHN analysis, while the presence of the chlorine atom was confirmed by low resolution mass spectrometry.

Table 3.4: Assignment of NMR signals of diastereoisomers, β-chloro-L-Ala-L-Fos and β-chloro-L-Ala-D-Fos (**196-LL** and **196-LD**), at 300 MHz (¹H-NMR) and 75 MHz (¹³C-NMR)



	δ_H (D ₂ O)	δ_C (D ₂ O)
CH ₃ -2	1.29 (3H, d, ³ J _{H-H} =6.9 Hz)	15.2
CH ₂ -6	4.02 (2H, m)	42.3, 42.6
CH-5	4.38 (1H, m)	54.0, 54.1
CH-1	4.02 (1H, m)	44.3 (d, ¹ J _{P-C} =147.0 Hz)
NH-3	Exchanged	-
C=O-4	-	165.7

The purity of β -chloro-L-Ala-D/L-Fos (**196**) was also supported by LC-MS analysis, in which more than 95 % purity was observed. The specific ion with MH^+ m/z 231 of **196** was extracted to confirm the presence of diastereoisomers, L,L-**196** and L,D-**196** and their ratio, Figure 3.3. The main peaks appeared at 1.93 mins and 2.64 mins and showed an approximate 1:1 ratio; again, the assignment of these main peaks to their corresponding L,L-**196** and L,D-**196** diastereoisomers was not possible without standards.

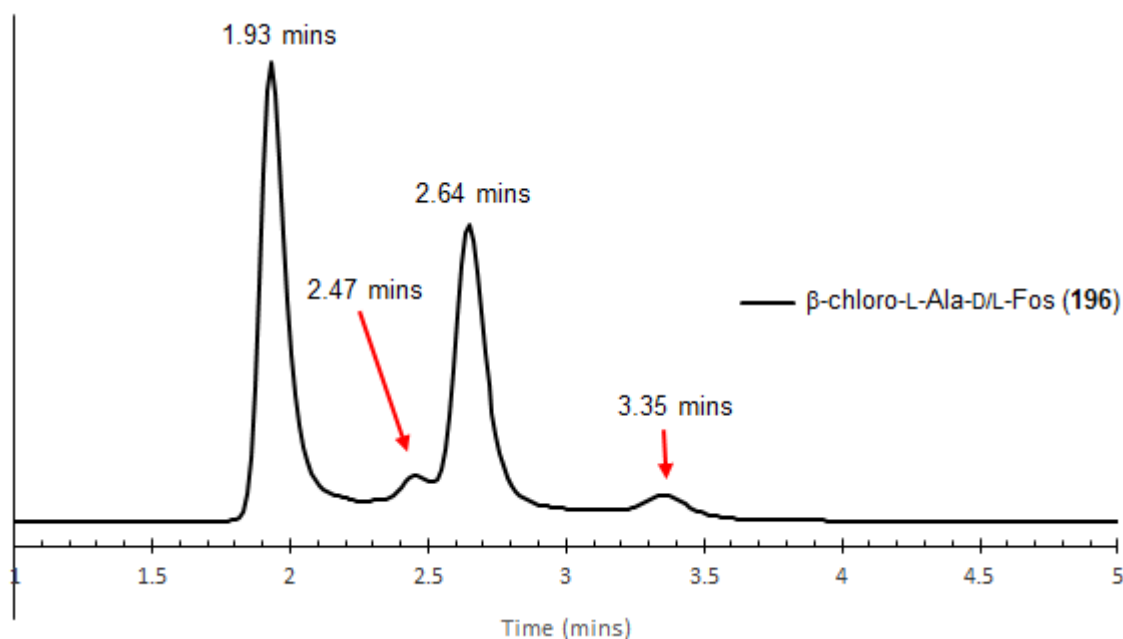
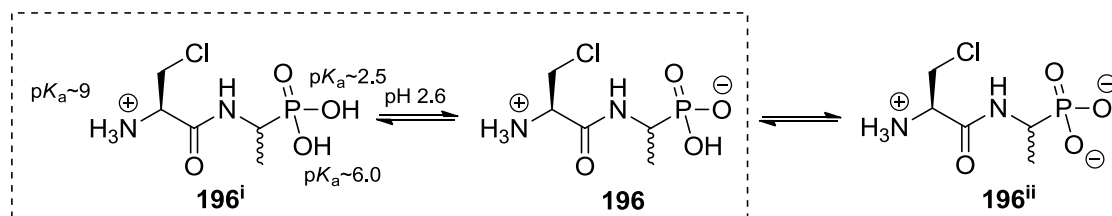


Figure 3.3: Reversed phase LC-MS chromatogram of β -chloro-L-Ala-D/L-Fos (**196**) with specific ion extracted at MH^+ 231. LC-MS condition (6.2.1) was used. For clarity, the chromatogram is displayed at 1.0 - 5.0 mins

There are an additional two peaks observed at 2.47 mins and 3.35 mins, Figure 3.3. This suggested the existence of equilibrium between the different phosphonic acid ionised states (**196**, **196ⁱ**, **196ⁱⁱ**), due to their different pK_a values ($pK_{a1} \sim 2.5$, 6.0), Scheme 3.8. Analyte **196** was dissolved in a solution containing 0.1 % formic acid (pH 2.6), in which a mixture of **196** and **196ⁱ** with less than 1 % of **196ⁱⁱ** would be expected. The different ionised states of the phosphonic group could interact differently with the stationary phase of the LC column and therefore two small peaks appearing at different retention times, 2.47 mins and 3.35 mins, are likely to be due to the diastereoisomers L,L-**196ⁱ** and L,D-**196ⁱ**.



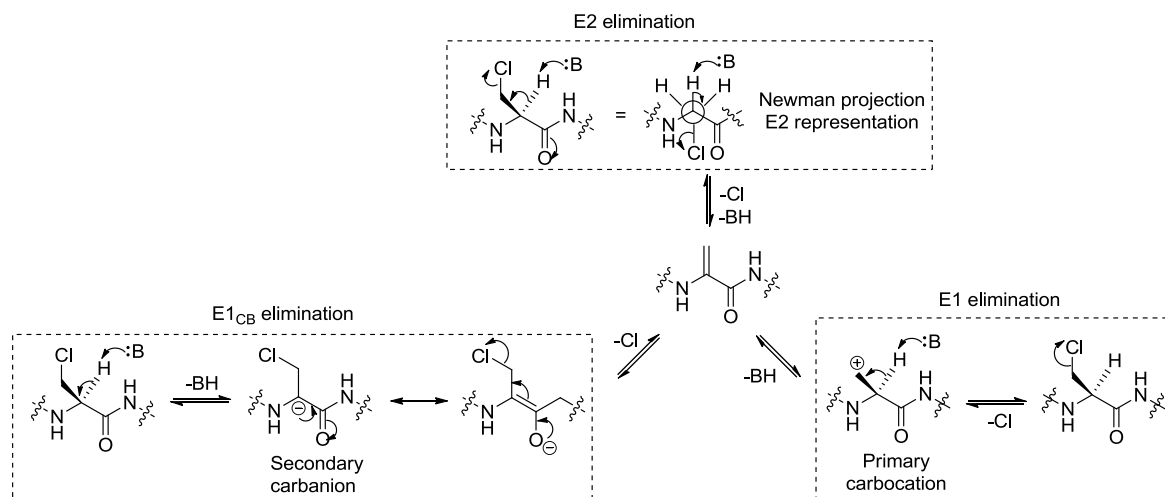
Scheme 3.8: Equilibrium between **196**, **196ⁱ** and **196ⁱⁱ** at pH 2.6

3.2.2: Stability study of β -chloro-L-Ala-D/L-Fos (**196**) under different pH conditions

In order for a selective inhibitor to be used in commercial agar plates, its stability must be evaluated to understand any possible degradation at the different pH conditions to which it could be exposed during storage or bacterial cell culture. In this section, studies on the stability of β -chloro-L-Ala-D/L-Fos (**196**) at four different pH values (6.1, 7.1, 8.1 and 9.1) at set time intervals are described, for which NMR spectroscopy operated at 26 °C was used. Samples were stored at the same temperature throughout the analysis period.

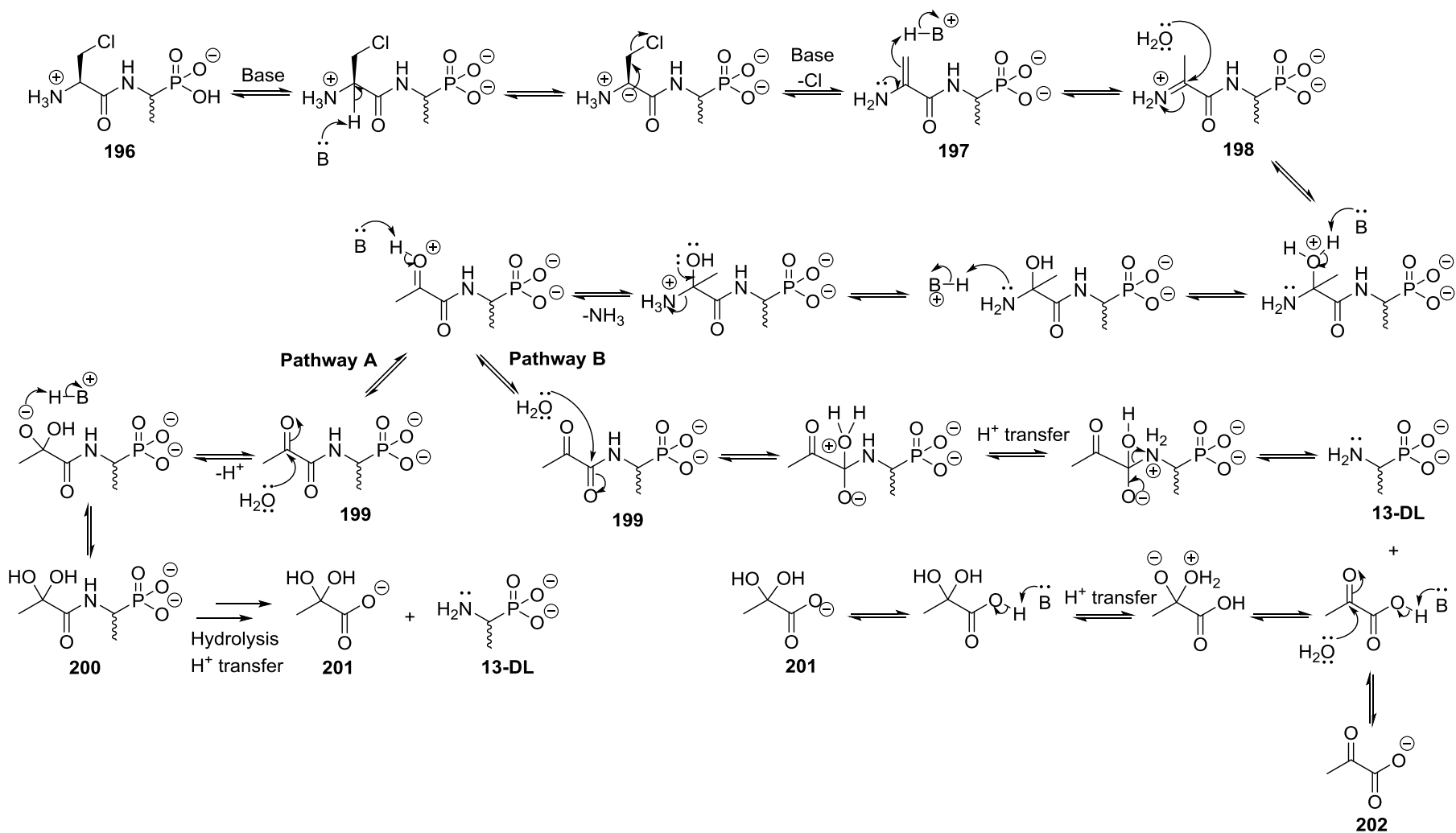
The β -chloro-L-alanine residue is labile and prone to degradation, especially under basic conditions, due to the presence of a good leaving group: the chlorine atom at the β -position of the alanine. The presence of the chlorine atom increases the acidity of the α -proton of the β -chloro-L-alanine, which is subject to ready abstraction by base, followed by elimination of chloride (β -elimination).

There are three possible β -elimination mechanisms, E1, E2 and E1_{CB}, Scheme 3.9. The E1 elimination is less likely to occur in this case due to the relatively unstable primary carbocation that would be formed. The E2 elimination is unfavourable, as the concerted elimination occurs when the α -proton is at the anti-periplanar position to the chlorine atom, requiring positioning of the chlorine atom between the two sterically large groups as represented in a Newman projection, Scheme 3.9. Although this staggered conformation with anti-periplanar position can be adopted, this conformation is likely to be less stable. The E1_{CB} elimination is more likely to occur in this case, as the carbanion formed after the α -proton abstraction can be stabilised by resonance with the carbonyl, and negative inductive effects (-I) with of the carbonyl and nitrogen.



Scheme 3.9: Racemisation of β -chloroalanine due to different types of β -elimination under basic conditions

Upon β -elimination, the resulting dehydroala-D/L-fosfalin intermediate (**197**) can tautomerise to the corresponding imine (**198**), Scheme 3.10, which follows a series of acid-base proton transfer equilibria, eventually liberating pyruvate-D/L-fosfalin (**199**) and ammonia. This intermediate (**199**) can undergo further degradation by two different pathways, depending on which carboxyl groups of **199** are targeted, generating different products. The hydrated pyruvate-D/L-fosfalin (**200**) product is generated, followed by further degradation to hydrated pyruvate (**201**) and D/L-fosfalin (**13-DL**), *via* Pathway A. The same products, D/L-fosfalin (**13-DL**) and hydrated pyruvate (**201**), are also liberated *via* Pathway B with additional pyruvate (**202**). These products (**199**, **200**, **13-DL**, **201** and **202**) can be identified with the aid of NMR spectroscopy. The formation of these products will be discussed in the following section with the support of NMR and literature data.



Scheme 3.10: Possible by-products generated from β-chloro-L-Ala-D/L-Fos (**196**) under basic conditions

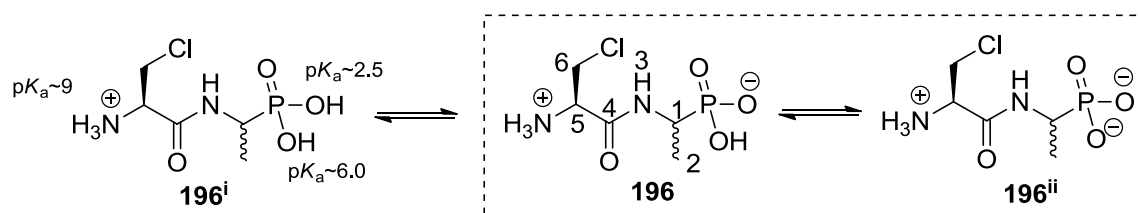
3.2.2.1: NMR study of base-catalysed hydrolysis of β -chloro-L-Ala-D/L-Fos (**196**)

In this $^1\text{H-NMR}$ study, β -chloro-L-Ala-D/L-Fos (**196**) was dissolved in deuterium oxide (D_2O) and adjusted to four different pH values (6.1, 7.1, 8.1 and 9.1) using deuterated sodium hydroxide (NaOD). The $^1\text{H-NMR}$ spectrum of each pH adjusted sample was run at 500 MHz at set time intervals: 3 mins, 5 mins, 13 mins, 33 mins, 63 mins, 123 mins, 243 mins, 363 mins, 723 mins, 1 week, 2 weeks, 3 weeks, 4 weeks, 8 weeks and 16 weeks. Although **196** is a zwitterionic compound, its aqueous solution is slightly acidic (pH 3.8 in D_2O), due to the presence of the phosphonic acid group. As a result of the instantaneous reaction upon addition of base (NaOD) and the approx. 3 mins lag-time before acquisition of the NMR spectrum, the sample (before addition of NaOD) served as a reference sample at $t=0$ min for the pH adjusted samples.

*Analysis of β -chloro-L-Ala-D/L-Fos (**196**) at pH 6.1*

In the $^1\text{H-NMR}$ spectra, the chemical shift of all peaks, apart from the solvent (D_2O), was shielded slightly (moved to the right) as the pH of the sample increased (from pH 3.8 to pH 6.1), Figure 3.4. It is unclear why the peaks appeared at this chemical shift, particularly the signal corresponding to the CH-5, as the ionised state of the amine group was unaffected at pH 6.1.

As shown in Figure 3.4, the multiplets at δ 4.38 ppm corresponding to CH-5 separated into two multiplets upon addition of base and remained unchanged throughout the 723 mins analysis time. The two peaks observed throughout the 723 mins could be due to the presence of two predominant equilibrium products, **196** and **196ⁱⁱ** at pH 6.1, Scheme 3.11.



Scheme 3.11: Equilibrium between **196**, **196ⁱ** and **196ⁱⁱ** at pH 6.1, pH 7.1 and pH 8.1

However, after 12 weeks of prolonged exposure to base, these two multiplets coalesced back into one signal, Figure 3.5. This could be due to the loss of some HCl after prolonged basic exposure, which would increase the acidity of the solution and thus the chemical equilibrium might shift predominantly to **196** for the remaining material. There were no massive changes of the peak area (proton integration) of each signal and no emergence of new peaks as compared to the reference sample at pH 3.8. However, the steady decrease of the peak area of **CH-5** observed over 1 week's analysis suggests the loss of HCl was taking place at a slow rate.

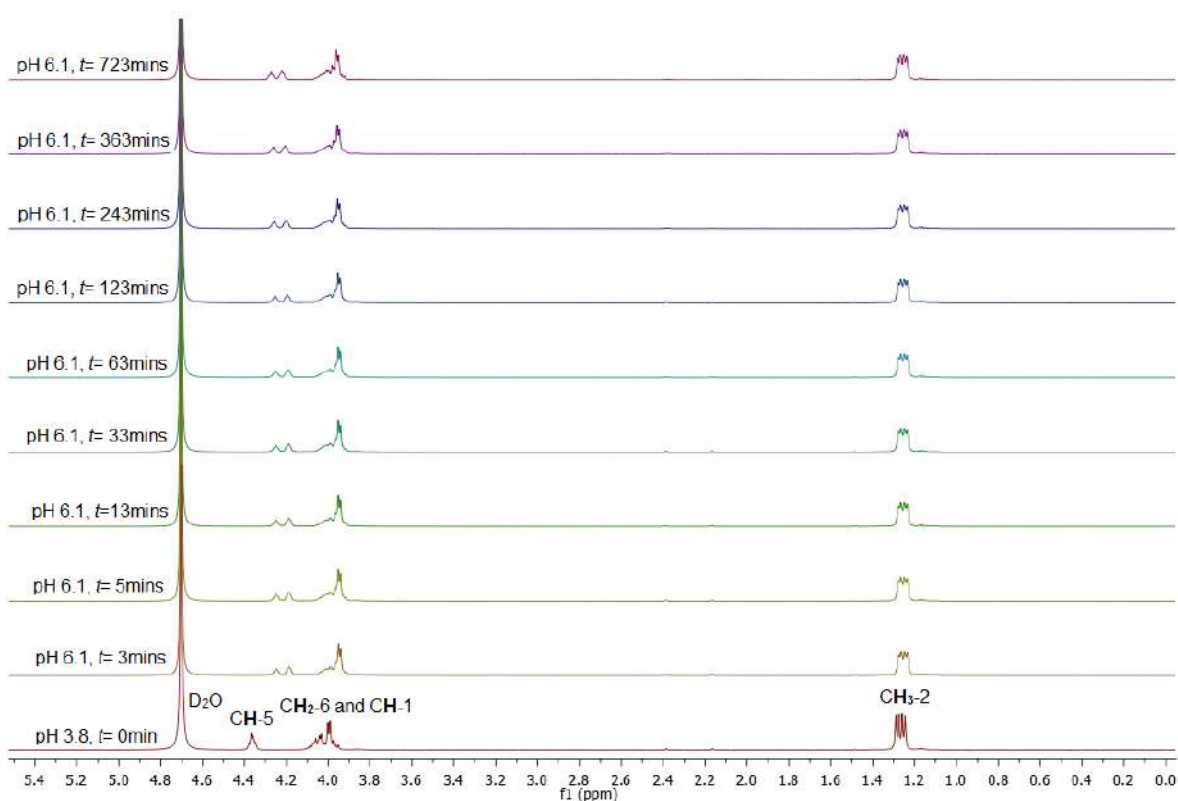


Figure 3.4: $^1\text{H-NMR}$ spectra of β -chloro-L-Ala-D/L-Fos (**196**) at pH 6.1, up to 723 mins analysis. Reference sample (pH 3.8) was prepared in a different tube for sample (pH 6.1) comparison.

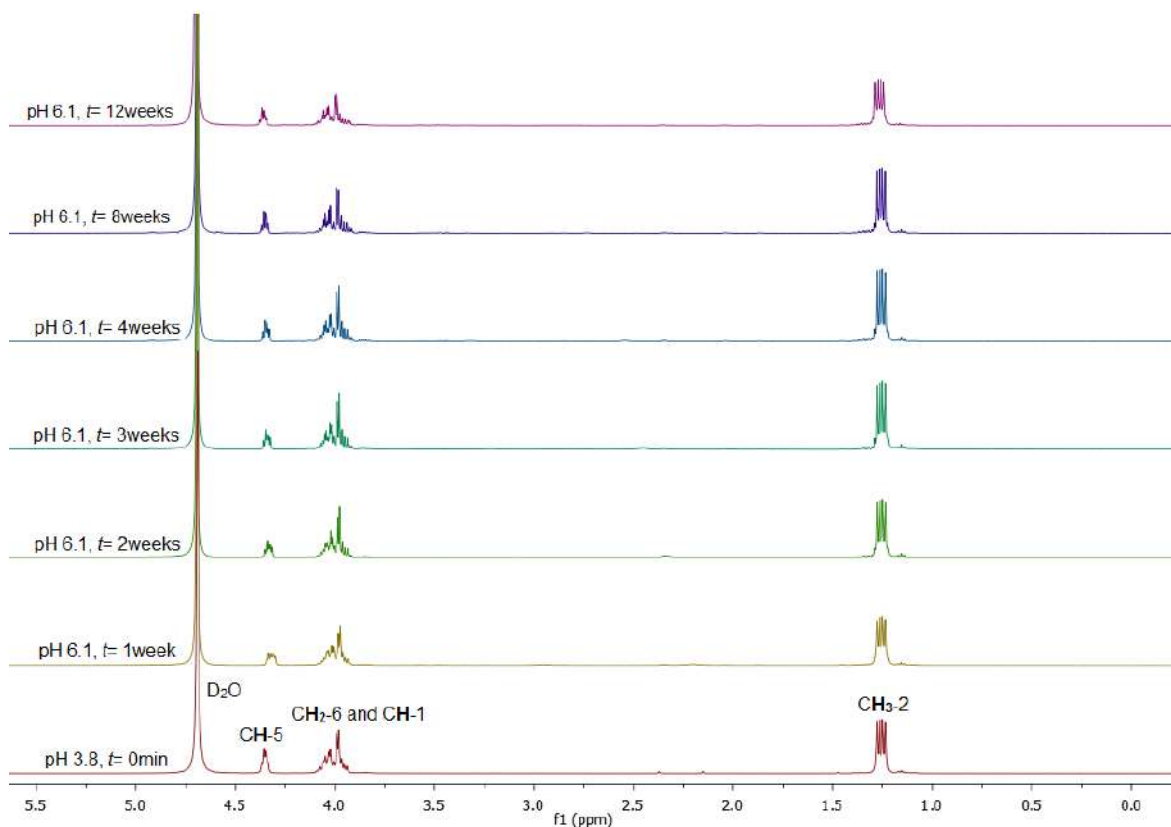


Figure 3.5: $^1\text{H-NMR}$ spectra of β -chloro-L-Ala-D/L-Fos (**196**) at pH 6.1, up to 12 weeks analysis. Reference sample (pH 3.8) was prepared in a different tube for sample (pH 6.1) comparison.

*Analysis of β -chloro-L-Ala-D/L-Fos (**196**) at pH 7.1*

At pH 7.1, a similar shielding of the signals was observed, but the multiplet corresponding to CH-5 did not appear to separate into two multiplets and was shifted closer to the multiplets of CH₂-6 and CH-1, Figure 3.6, compared to the signals seen in the spectra at pH 6.1. It can be expected that the chemical equilibrium would have shifted predominantly towards **196ⁱⁱ**, Scheme 3.11, as the pH of the solution increases and thus only a multiplet corresponding to CH-5 was observed. Two new signals appeared at δ 2.17 ppm and δ 2.39 ppm, with increasing peak area (integration) over time (up to 723mins). However, these peaks disappeared after 1 week with the occurrence of four new signals at δ 1.33, δ 1.90-2.05, δ 2.63-2.79, and δ 3.47-3.58 ppm, Figure 3.7. The generation/degeneration of these signals indicated that compound (**196**) degraded slowly under the reaction conditions at pH 7.1. The signals observed were assigned to the speculative products (**199**, **200**, **201**, **202** and **13-DL**, Scheme 3.10), Table 3.5.

Table 3.5: Assignment of signals observed on the NMR spectra, Figures 3.6 and 3.7, to the structures of **199**, **200**, **201**, **202** and **13-DL**

δ_H	Comment
1.33	Methyl protons, CH_3 of D/L-fosfalin (13-DL)
1.90-2.05	Methyl protons, CH_3 of hydrated pyruvate (201)
2.17	Methyl protons, CH_3 of hydrated pyruvate-D/L-fosfalin (200)
2.39	Methyl protons, CH_3 of pyruvate-D/L-fosfalin (199)
2.63-2.79	Methyl protons, CH_3 of pyruvate (202)
3.47-3.58	Methine proton, CH of D/L-fosfalin (13-DL)

The signals of D/L-fosfalin were assigned based on the NMR signal of this compound discussed earlier (section 2.2.1), while the assignment of pyruvate (**202**) and hydrated pyruvate (**201**) was supported by literature - the NMR study of hydration of pyruvic acid (1967TFS673). The methyl protons of pyruvate (**202**) were deshielded compared to the corresponding methyl protons of hydrated pyruvate (**201**), due to the second carbonyl group in pyruvate (**202**).

As shown in Figure 3.6, the signals corresponding to **201** and **202** were not visible throughout 723 mins analysis time, suggesting that prolonged exposure of **196** to base might be required for formation of these products. However, new signals appeared at δ 2.17 ppm and δ 2.39 ppm suggesting degradation of **196** was taking place. These two additional signals could potentially be due to the presence of **199** and **200**, as these two products are generated under basic conditions, Scheme 3.10. There was no literature evidence to support the NMR assignments of **199** and **200** (Table 3.4); however, these assignments are plausible as the signals started to disappear with the emergence of new signals corresponding to **13-DL**, **201** and **202** after 1 week of exposure of **196** to base, Figure 3.7. The further degradation of **199** and **200** as observed in the NMR spectra (Figures 3.6 and 3.7) suggested the amide bond might not be stable in prolonged exposure under these conditions (pH 7.1). Given that the signals of **13-DL**, **199**, **200**, **201** and **202** were observed from the NMR spectra (Figure 3.6 and 3.7), both degradation pathways as discussed earlier (Scheme 3.10) may take place simultaneously.

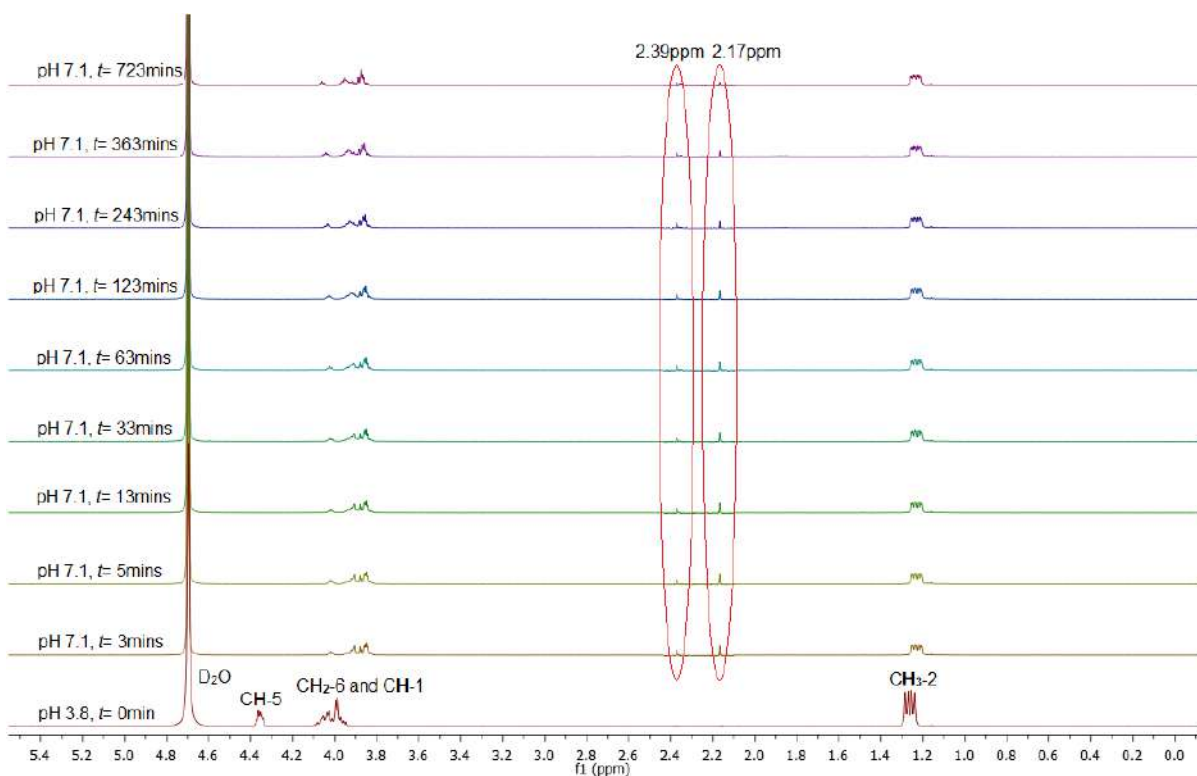


Figure 3.6: $^1\text{H-NMR}$ spectra of β -chloro-L-Ala-D/L-Fos (**196**) at pH 7.1, up to 723mins
Reference sample (pH 3.8) was prepared in a different tube for sample (pH 7.1) comparison

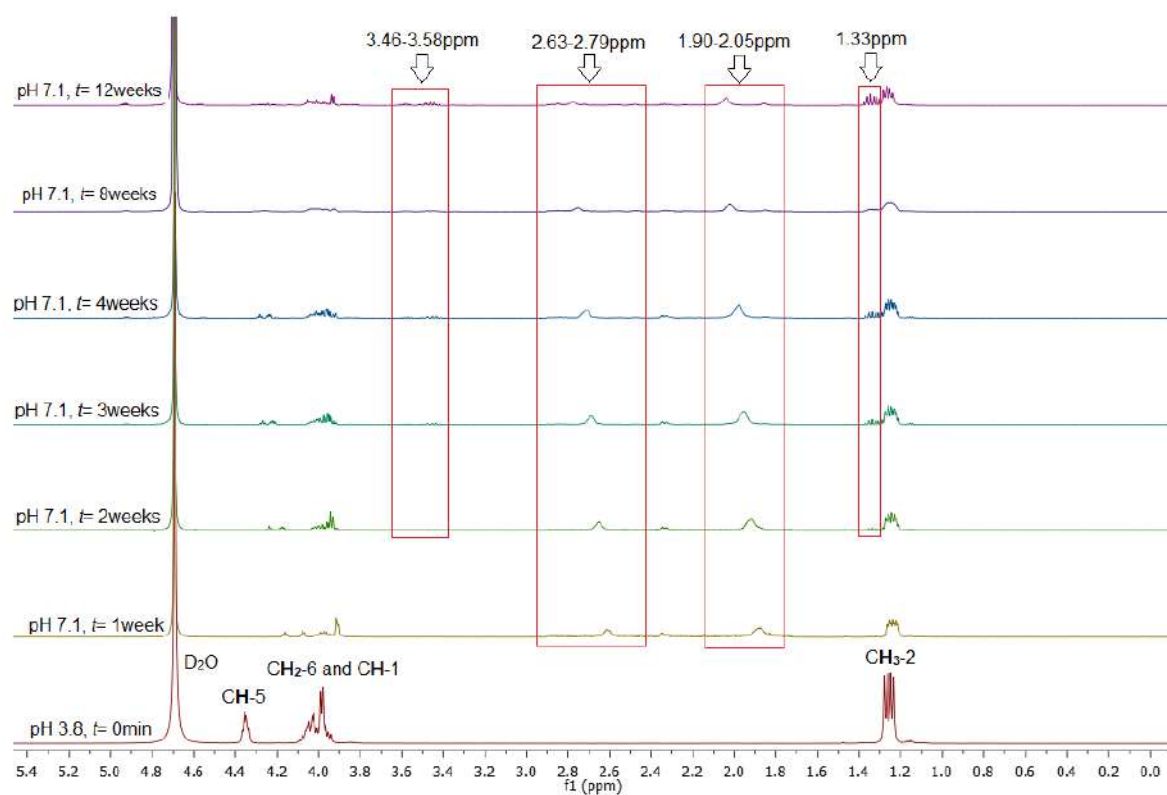


Figure 3.7: $^1\text{H-NMR}$ spectra of β -chloro-L-Ala-D/L-Fos (**196**) at pH 7.1, up to 12 weeks analysis
Reference sample (pH 3.8) was prepared in a different tube for sample (pH 7.1) comparison

Analysis of β -chloro-L-Ala-D/L-Fos (**196**) at pH 8.1

The rationalisation as discussed earlier facilitates assignments of the NMR signals observed in Figure 3.8 and 3.9. Considering the ^1H -NMR spectra (Figures 3.8 and 3.9), signals of **196** were shielded at pH 8.1 compared to pH 3.8. In addition, the degradation of β -chloro-L-Ala-D/L-Fos (**196**) was more rapid. It started upon addition of base, shown by visible peaks at δ 2.17 ppm and δ 2.39 ppm, corresponding to the methyl protons of hydrated pyruvate-D/L-fosfalin (**200**) and pyruvate-D/L-fosfalin (**199**), respectively. The generation of signals corresponding to the methyl protons of hydrated pyruvate (**201**) at δ 1.87 ppm and pyruvate (**202**) at δ 2.58 ppm started to appear at 363 mins and were clearer at 723 mins. The methyl protons of D/L-fosfalin (**13-DL**) at δ 1.33 ppm, pyruvate (**202**) at δ 2.58 ppm, hydrated pyruvate (**201**) at δ 1.87 ppm, and methine proton of D/L-fosfalin (**13-DL**) at δ 3.40-3.60 ppm were clearly observed after 1 week at pH 8.1, Figure 3.9.

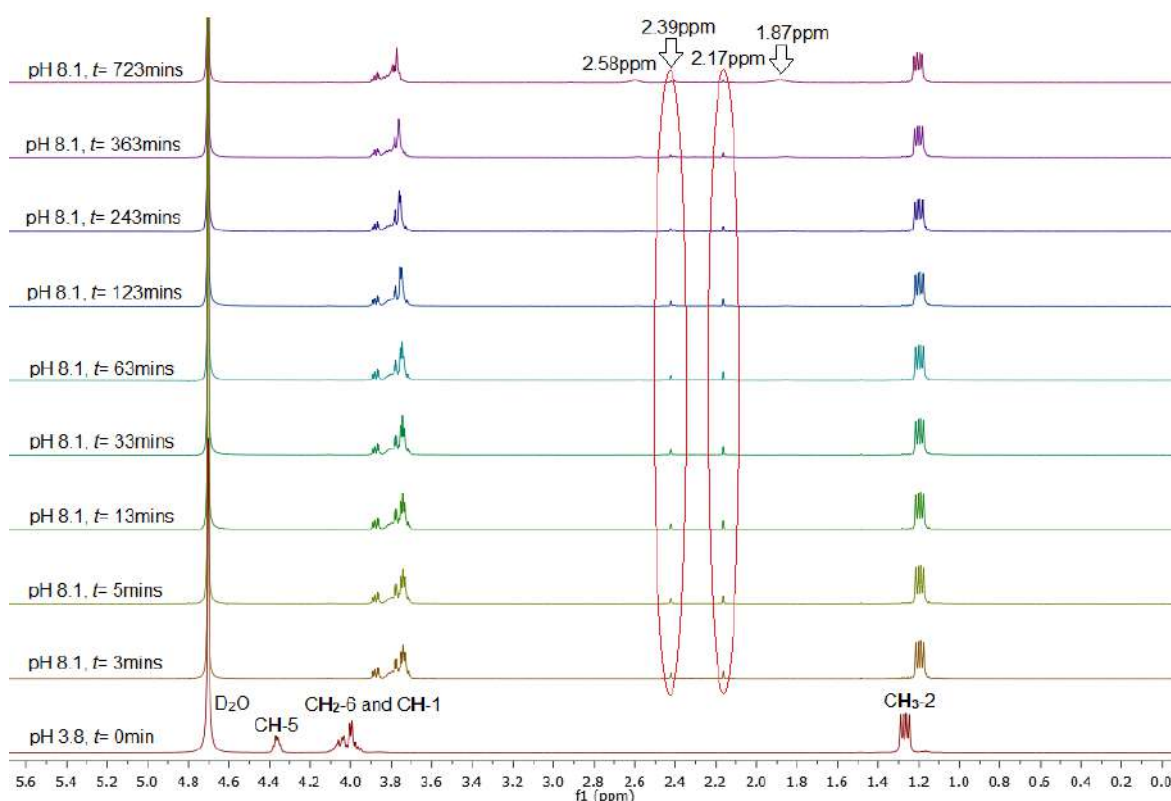


Figure 3.8: ^1H -NMR spectra of β -chloro-L-Ala-D/L-Fos (**196**) at pH 8.1, up to 723 mins

Reference sample (pH 3.8) was prepared in a different tube for sample (pH 8.1) comparison

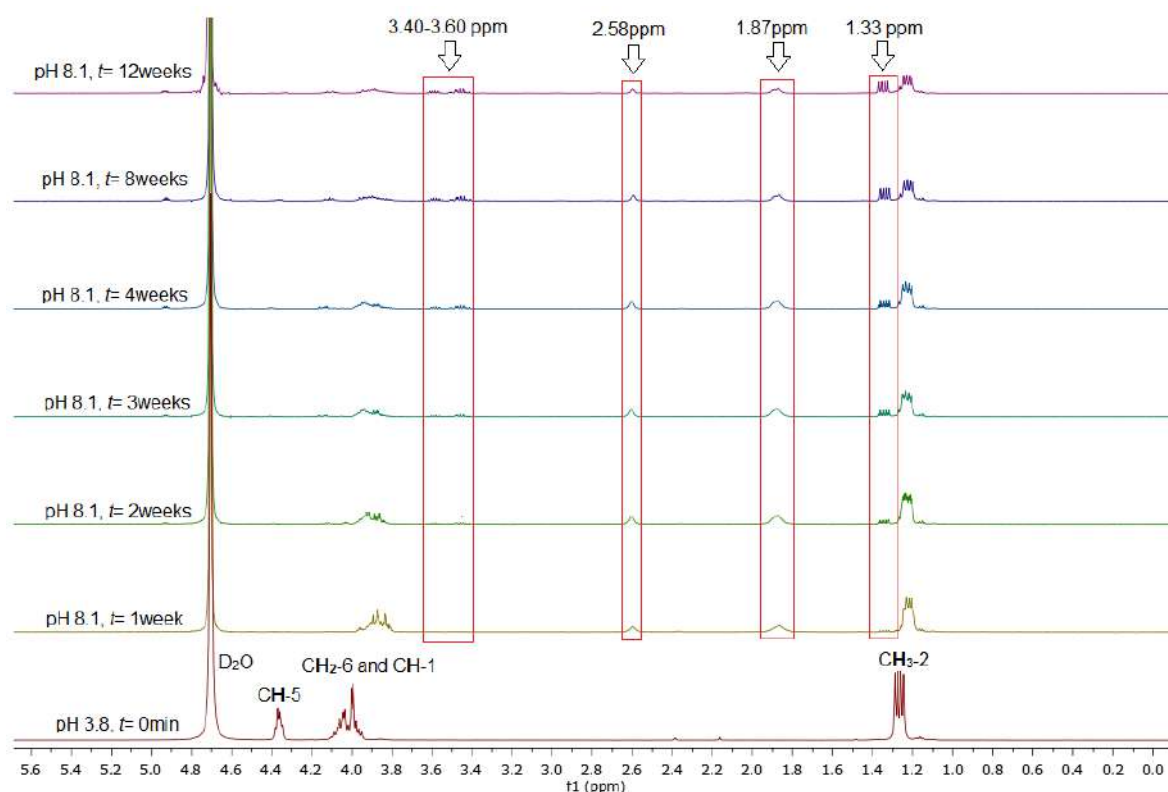


Figure 3.9: ^1H -NMR spectra of β -chloro-L-Ala-D/L-Fos (**196**) at pH 8.1, up to 12 weeks
Reference sample (pH 3.8) was prepared in a different tube for sample (pH 8.1) comparison

*Analysis of β -chloro-L-Ala-D/L-Fos (**196**) at pH 9.1*

As a result of the higher pH used in this experiment, the degradation products of β -chloro-L-Ala-D/L-Fos (**196**) appeared much earlier in the NMR spectra (Figure 3.10). Not only were the signals at δ 2.17 ppm and δ 2.39 ppm, corresponding to the methyl protons of hydrated pyruvate-D/L-fosfalin (**200**) and pyruvate-D/L-fosfalin (**199**), already visible on the 3 mins spectrum, the methyl protons of hydrated pyruvate (δ 1.87 ppm) and pyruvate (δ 2.58 ppm) were visible on the spectrum recorded at 243 mins. The integrals of these peaks varied over the 12 weeks of analysis; the signals at δ 2.17 ppm and δ 2.39 ppm appeared and then reduced over the course of the experiment, while the signals at δ 1.87 ppm and δ 2.58 ppm started to appear later, but increased over time, supporting the cleavage of the amide bond to liberate D/L-fosfalin (**13-DL**), pyruvate (**202**) and hydrated pyruvate (**201**) as products, Figure 3.11.

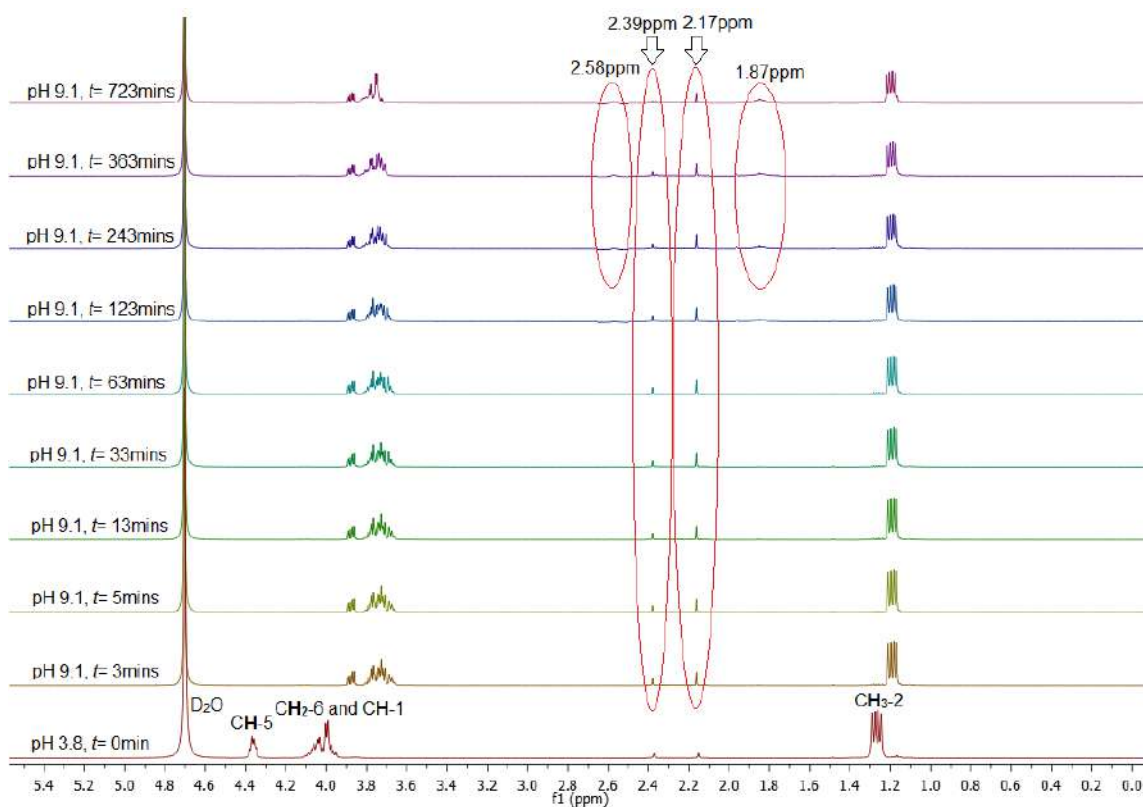


Figure 3.10: $^1\text{H-NMR}$ spectra of β -chloro-L-Ala-D/L-Fos (**196**) at pH 9.1, up to 723 mins
Reference sample (pH 3.8) was prepared in a different tube for sample (pH 9.1) comparison

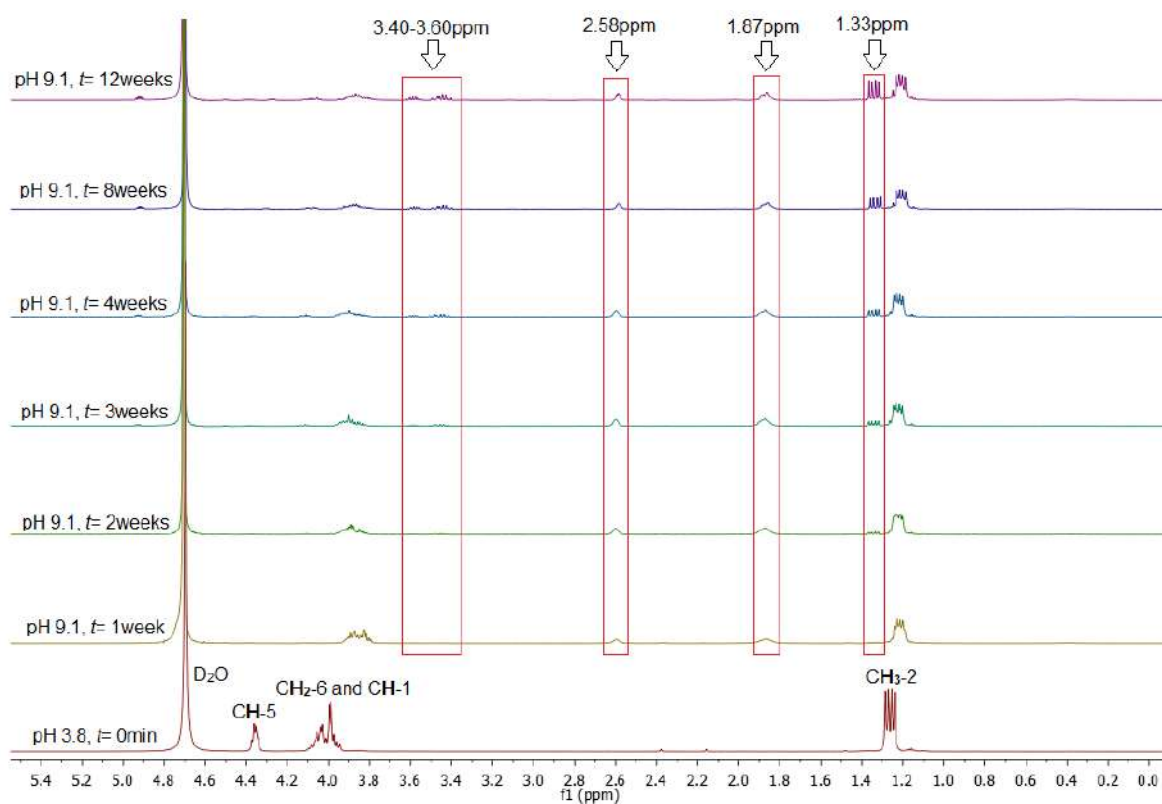


Figure 3.11: $^1\text{H-NMR}$ spectra of β -chloro-L-Ala-D/L-Fos (**196**) at pH 9.1, up to 12 weeks
Reference sample (pH 3.8) was prepared in a different tube for sample (pH 9.1) comparison

Conclusions drawn from the stability study under different pH conditions

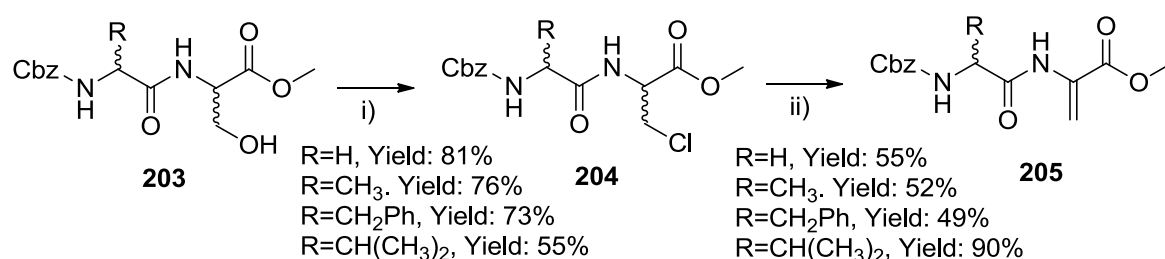
The β -chloro-L-Ala-D/L-Fos (**196**) was shown to be prone to degradation at pH values of 6.1 and above, as evidenced by the observation of CH-5 integral reduction and new peaks assignable to **13-DL**, **199**, **200**, **201** and **202**. As degradation was slow and incomplete at pH 6.1, the degradation may be minimised by keeping the pH conditions below 6.1. Although dehydroala-D/L-fosfalin (**197**) was expected upon β -elimination of HCl from β -chloro-L-Ala-D/L-Fos (**196**), Scheme 3.10, it was not detected in the NMR spectra, probably due to its instability; it is likely that it was rapidly degraded further to the pyruvate-D/L-fosfalin (**199**) and hydrated pyruvate-D/L-fosfalin (**200**). These intermediates (**199** and **200**) were identified by their distinctive methyl signals at δ 2.39 ppm and δ 2.17 ppm, but they reduced upon prolonged exposure to pH 7.1, with new signals formed at δ 1.33, δ 1.87, δ 2.58 and δ 3.40-3.60 ppm, corresponding to the methyl protons of D/L-fosfalin (**13-DL**), hydrated pyruvate (**201**), pyruvate (**202**), and methine proton of D/L-fosfalin (**13-DL**), respectively. Based on the evidence that shows the presence of **13-DL**, **199**, **200**, **201** and **202**, it is suggested that both degradation pathways can take place simultaneously, as discussed earlier (Scheme 3.10).

3.2.3: Attempted preparation of a phosphonodipeptide containing dehydroalanine and D/L-fosfalin

As a result of the good antibacterial activity of β -chloro-L-alanyl based peptide derivatives reported by Cheung (1983JMC1733) (1986JMC2060) and Váradi (T-2013MI192), the inhibitory mechanism of β -chloro-L-alanine on alanine racemase was investigated. During alanine racemase inhibition, Scheme 1.6, formation of dehydroalanine from β -chloro-L-alanine is plausible upon the removal of β -chlorine is mediated by the Lys₃₉. The subsequent complex formation between dehydroalanine and the alanine racemase causes the inactivation of the normal enzymatic activity of alanine racemase, thus the inhibitory effects. As a result of the significant role of dehydroalanine in the inhibitory mechanism, the synthesis of dehydroalanine derivatives and their microbiological evaluation became of interest to the current work. Comparison between the microbiological activities of β -chloro-L-alanine and dehydroalanine-D/L-fosfalin will be made in order to investigate if the

dehydroalanine moiety is actually an intermediate, as suggested by earlier literatures.

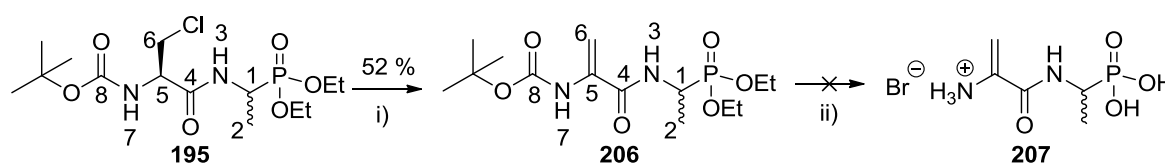
The synthesis of dehydroalanine derivatives under basic conditions was reported by Srinivasan (1977JOC2253). According to his work, the chlorination of a serine-containing peptide was first achieved using phosphorus pentachloride, prior to treatment with triethylamine to facilitate the α,β -elimination of chlorine and hydrogen, Scheme 3.12. Apart from these dipeptide derivatives, tripeptides containing dehydroalanine were also synthesised *via* this approach, in which the β -chlorine was removed successfully from the tripeptide containing β -chloroalanine.



Scheme 3.12: Preparation of dehydroalanine derivatives (**205**) from serine containing peptides (**203**)

Reagents and conditions: i) PCl_5 , CHCl_3 , r.t., 12-16hrs; ii) TEA, EtOAc, r.t., 8-12hrs

The well-established methods available to remove the chlorine atom from the β -chloroalanine derivatives facilitated the synthesis of ¹⁴C-Boc-dehydroala-D/L-fosfalin diethyl ester (**206**) from its precursor, ¹⁴C-Boc- β -chloro-L-Ala-D/L-Fos diethyl ester (**195**). Subsequent acidic deprotection was expected to result in the product of interest (**207**), Scheme 3.13. In this synthetic approach, however, potassium *tert*-butoxide, $(\text{CH}_3)_3\text{COK}$ was used instead of triethylamine, which gave a similar reasonable amount of product to that claimed by Srinivasan (1977JOC2253).



Scheme 3.13: Preparation of dehydroala-D/L-fosfalin hydrobromide (**207**)

Reagents and conditions: i) $(\text{CH}_3)_3\text{COK}$, $(\text{CH}_3)_3\text{COH}$, 30 °C, 16-18hrs; ii) 33% HBr in AcOH, r.t.

3.2.3.1: Synthesis of *tert*-butyl (3-((1-(diethoxyphosphoryl)ethyl)amino)-3-oxoprop-1-en-2-yl)carbamate or ¹³C-Boc-dehydroala-D/L-Fos diethyl ester (**206**)

The elimination of HCl from ¹³C-Boc- β -chloro-L-Ala-D/L-Fos diethyl ester (**195**) resulted in the protected dehydroala-D/L-fosfalin derivative (**206**), Scheme 3.13. The successful removal of the β -chlorine was supported by mass spectrometry, due to the missing peaks of 3:1 ratio (³⁵Cl:³⁷Cl) from the MS spectrum. In the ¹H-NMR spectrum, the β -methylene signals at δ 3.74 ppm and δ 4.00 ppm were replaced by two signals at δ 5.24 ppm and δ 6.02 ppm, corresponding to the alkenic β -methylene protons. In the ¹³C-NMR spectrum, the sp³ methylene carbon signal of CH₂-6 at δ 55.2 ppm (**195**) was replaced by a sp² carbon signal at δ 98.6 ppm (**206**) and an additional sp² quaternary carbon signal of C-5 at δ 134.6 ppm (**206**). The assignment of the C-5 carbon signal was supported by the absent methine signal from the DEPT spectrum. The presence of phosphorus coupling was seen in the ¹H-NMR spectrum, where this additional coupling resulted in a doublet of doublets, instead of a doublet, being observed at δ 1.42 ppm, which corresponded to the CH₃-2 protons. In the ¹³C-NMR spectrum, on the other hand, this effect was seen at δ 41.7 ppm (CH-1) with a ¹J_{C-P} coupling constant of 157.5 Hz, and at δ 62.3 ppm and δ 62.5 ppm (methylenes of OCH₂CH₃) with a ²J_{C-P} coupling constant of 6.8 Hz. The purity and identity of this compound (**206**) was confirmed by CHN analysis and low resolution mass spectrometry.

3.2.3.2: Attempted synthesis of 3-oxo-3-((1-phosphonoethyl)amino) prop-1-ene-2-aminium bromide or dehydroala-D/L-Fos hydrobromide (207)

Acidic conditions, hydrogen bromide in acetic acid, commonly used to remove both *tert*-butoxycarbonyl and diethyl phosphonate ester protecting groups simultaneously from the protected peptide derivatives, was also anticipated to be effective for ^tBoc-dehydroala-D/L-Fos diethyl ester (**206**), Scheme 3.13. However, under these conditions, the dehydroala-D/L-Fos hydrobromide (**207**) was not synthesised. The NMR signals corresponding to CH₂-6 of **206** disappeared with the emergence of other unidentified signals on the NMR spectrum of **207**. This suggested that the disappearance of the enamine group resulted in the formation of other products, which was further supported when **207** was analysed by MS after 3.5 hrs and 20 hrs of acidic hydrolysis, Figure 3.12.

In the MS spectra (Figure 3.12), there were no signals corresponding to **207** or its intermediates (**208** and **209**); instead, other products were formed after 3.5 hours and 20 hours of acidic hydrolysis. To investigate the possible products that might have formed, the *m/z* values noted on both MS spectra were used to correlate to the molecular weight of potential products formed (Scheme 3.14). The peaks of 1:1 ratio of ⁷⁹Br and ⁸¹Br isotopes found on the MS spectra indicated that some of the products formed contained a bromine atom, possibly brominated products (**210**, **211** and **215**). However, there is no evidence to indicate whether these products were formed during the acidic hydrolysis or *in-situ* in the MS. Each brominated product could exist as two different isomers, depending on whether the addition of HBr was based on Markonikov's rule (most likely during acidic hydrolysis, **210a**, **211a** and **215a**) or by radical formation (during *in-situ* MS, **210b**, **211b** and **215b**). The presence of these brominated products suggested that the enamine group is sensitive towards the use of concentrated HBr in acetic acid and it favours rapid bromination of the enamine group. Apart from bromination, further degradation led to the formation of suspected pyruvate based derivatives, as the reported *m/z* values matched the molecular weight of the pyruvate based derivatives (**199**, **200**, **212-214**).

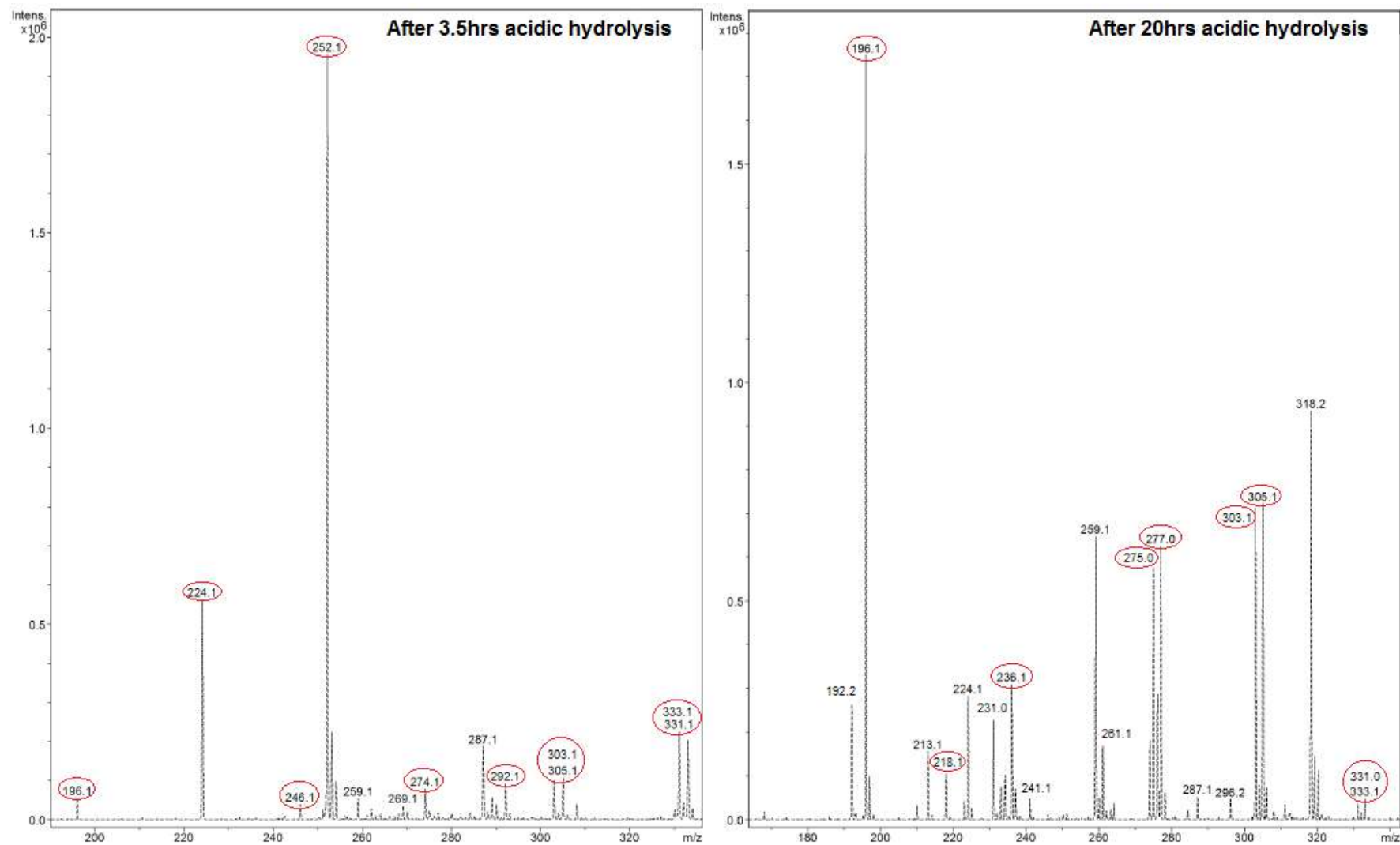
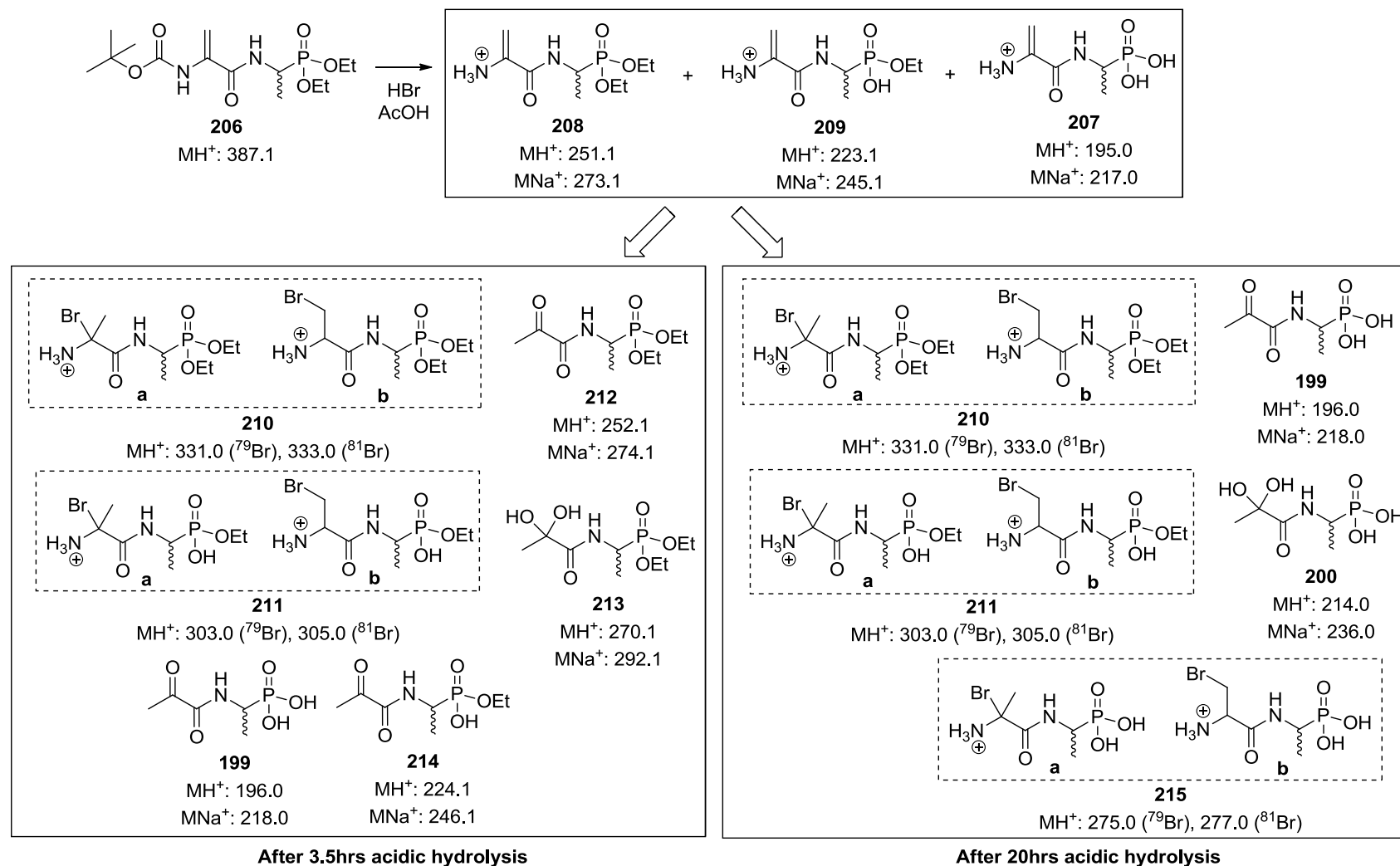


Figure 3.12: MS spectra of 'Boc-dehydroala-D/L-Fos diethyl ester (206) when subjected to 3.5hrs and 20hrs acidic hydrolysis (HBr/AcOH)

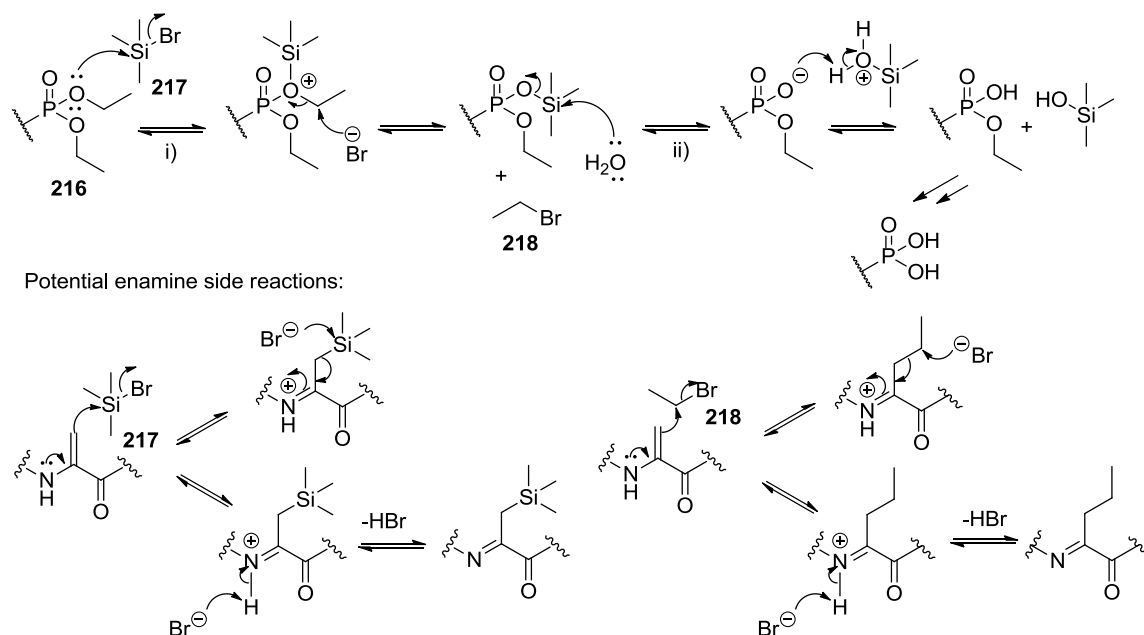


Scheme 3.14: Potential products formed from ¹³C-Boc-dehydroala-D/L-Fos diethyl ester (**206**) when subjected to 3.5hrs and 20hrs acidic hydrolysis (HBr/AcOH)

According to the MS spectra (Figure 3.12), there were no signals corresponding to **207**, **208** or **209**. However, other products that were identified in Scheme 3.14 suggested that **208**, **209** and maybe some **207** were formed then subjected to further reaction to **199**, **200**, **210-215**. For instance, the identified **210** and **212** were more likely to have originated from **208**, while **211**, **214** and **199** are believed to be formed from **209** and **207**, after 3.5 hrs acidic hydrolysis. However, some of these identified products, **212**, **213** and **214** disappeared or diminished, while the content of **199** was increased, after 20 hrs acidic hydrolysis. These differences in intermediate formation between 3.5 hrs and 20 hrs would suggest the degradation pathway of **206** under the acidic conditions, in which **208** formed first in the reaction, followed by **210** or **212** and **213**. The loss of one ethyl phosphonate ester, **211** and **214**, which could be resulted from **210** and **212** or **209**, was also noted. New intermediate (**215**) and more **199** formed over time (20 hrs), suggesting that the removal of the diethyl phosphonate ester groups requires prolonged exposure to acid.

In a nutshell, the *N*-terminus of ¹³C-Boc-dehydroala-D/L-Fos diethyl ester (**206**) was deprotected rapidly as the ¹³C-Boc group was fully removed after 3.5 hrs, while the phosphonate ester groups were more resistant and extended exposure to acid was required. Although the presence of brominated products (**210**, **211** and **215**) and pyruvate derivatives (**199**, **200**, **212-214**) (Scheme 3.14) was able to be predicted according to their respective *m/z* values from the MS results, other MS signals were not identified, especially those signals generated after prolonged acidic exposure (20 hrs). This suggested that other degradation was taking place during acidic hydrolysis, although it is also possible that some degradation took place during ESI-MS (electrospray ionisation-MS) fragmentation. Although the usual neutralisation step by treatment with propylene oxide was omitted in order to avoid the formation of degradation products, pyruvate derivatives (**199**, **200**, **212-214**) were still generated, as well as three brominated species (**210**, **211** and **215**), in this synthesis. This could be due to the high reactivity of the enamine functional group, particularly after the ¹³C-Boc group is removed.

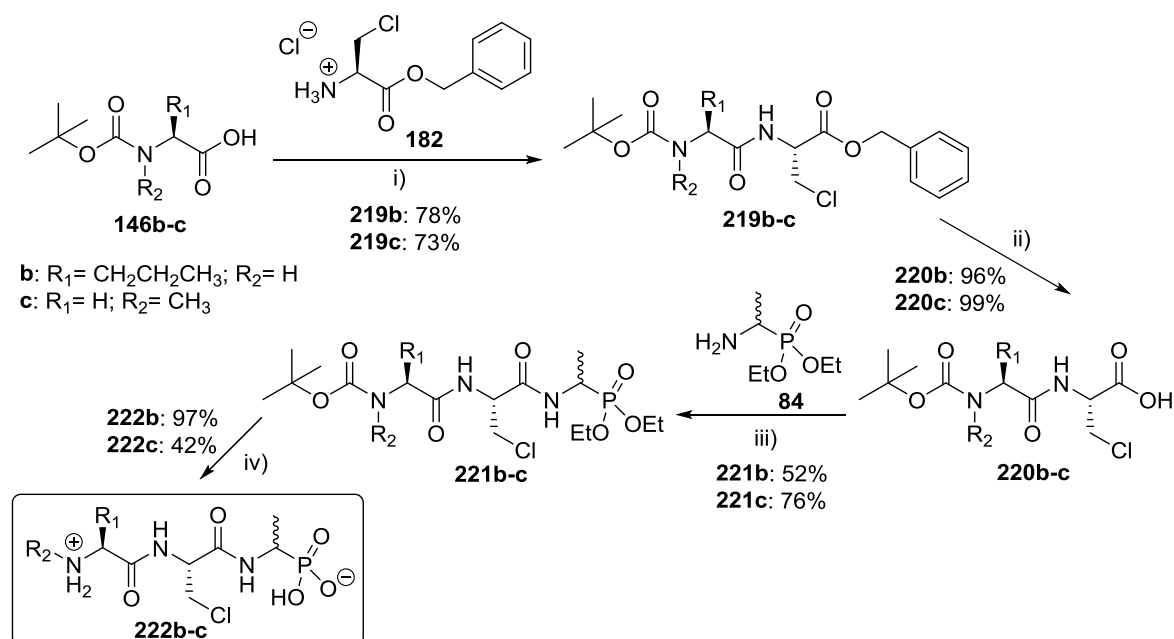
The synthesis of dehydroala-D/L-Fos hydrobromide (**207**) was unsuccessful; therefore, a different synthetic strategy was sought, in which orthogonal deprotection of the diethyl phosphonate ester and *tert*-butoxycarbonyl groups would not affect the enamine. However, the feasibility of this strategy was limited due to the need to remove carbamate and phosphonate ester groups, while avoiding strongly acidic conditions. Most reported methods involved the deprotection of one ethyl phosphonate ester instead of both ester groups (B-1998MI671); however, bromotrimethylsilane (TMSBr, **217**) in acetonitrile was reported to give mild deprotection of two ethyl phosphonate ester groups (**216**), Scheme 3.15 (1995JOC2563). There is a lack of supportive data showing that this deprotection approach, TMSBr in acetonitrile, would not result in degradation of the enamine group present in the compound. One concern is that the enamine group is labile and could be potentially silylated by the TMSBr (**217**) or even react with the liberated ethyl bromide (**218**) (generated upon removal of ethyl ester), Scheme 3.15. Consequently, and due to lack of time, this synthesis was not further developed.



Scheme 3.15: Deprotection of phosphonate diethyl ester (**216**) using bromotrimethylsilane (**217**)
 Reagents and conditions: i) TMSBr (**217**), MeCN, 65 °C, 1hr; ii) aqueous MeOH

3.2.4: Preparation of phosphonotripeptides containing both β -chloro-L-alanine and D/L-fosfalin

The synthetic route already discussed in 2.4.2 was used to synthesise two new phosphonotripeptides containing β -chloro-L-alanine and D/L-fosfalin, one with L-norvaline at the *N*-terminus and the other with sarcosine, Scheme 3.16. In this synthesis, β -chloro-L-alanine benzyl ester hydrochloride salt (**182**), synthesised from t Boc-L-serine, was coupled to *N*- t Boc protected L-norvaline or sarcosine (**146b-c**). As a result of the ready β -elimination of the hydrogen chloride from β -chloroalanine and its derivatives under basic conditions (Scheme 3.10), care was taken to use exactly 1.0 mole equivalent of base (NMM) during the coupling reactions. The resulting dipeptide derivatives (**219b-c**) were debenzylated by catalytic reduction and coupled with D/L-Fos diethyl ester (**84**). All protecting groups on the phosphonotripeptide derivatives (**221b-c**) were removed by treatment with HBr in acetic acid and the products neutralised with propylene oxide to afford the products of interest (**222b-c**).



Scheme 3.16: General preparation of phosphonotripeptide derivatives (**222b-c**) containing β -chloro-L-alanine and D/L-fosfalin

Reagents and conditions: i) IBCF, NMM, THF/DCM, -5°C to r.t., 24hrs; ii) H_2 , Pd/C, MeOH, 24hrs; iii) IBCF, NMM, THF, -5°C to r.t., 24hrs; iv) HBr, AcOH, 16-18hrs, then propylene oxide

3.2.4.1: Synthesis of *N*-protected dipeptide derivatives containing the β -chloro-L-alanine moiety (**220b-c**)

N-^tBoc-norvaline and *N*-^tBoc-sarcosine (**146b-c**) were coupled with β -chloro-L-alanine benzyl ester hydrochloride (**182**), using IBCF and NMM coupling reagents, Scheme 3.16. Successful coupling was confirmed by NMR spectroscopy, due to the presence of signals corresponding to the *tert*-butoxycarbonyl and benzyl ester groups, Tables 3.7 and 3.8. Each NMR signal was assigned according to the structural numbering system in Table 3.6.

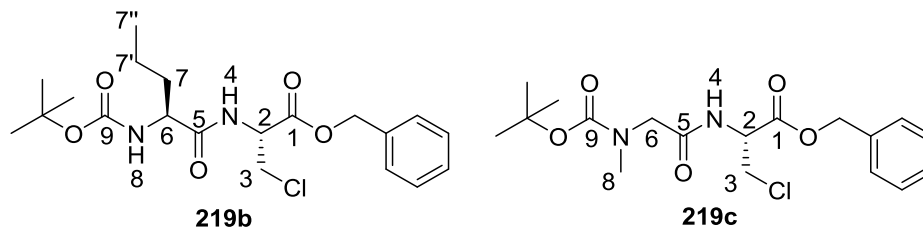
Table 3.6: Structures of ^tBoc-L-Nva- β -chloro-L-Ala-OBzl (**219b**) and ^tBoc-Sar- β -chloro-L-Ala-OBzl (**219c**) with the corresponded numbering systems used for NMR assignment

Compound name	Structure
^t Boc-L-Nva- β -chloro-L-Ala-OBzl (219b)	
^t Boc-Sar- β -chloro-L-Ala-OBzl (219c)	

In the ¹H-NMR spectra, diastereotopic geminal proton-proton coupling was observed over both products (**219b-c**), due to the presence of chiral centres. For example, a doublet of doublets instead of a doublet, was seen at δ 3.89-3.99 (**219b**) and δ 3.83-3.94 ppm (**219c**), corresponding to the β -chloroalanyl methylene group in each compound. Likewise the methylene protons of the benzyl ester groups were also observed as two doublets at δ 5.20-5.25 (**219b**) and δ 5.13-5.18 ppm (**219c**). In the spectrum of **219b**, a complicated splitting pattern, which appeared as a multiplet, was observed at δ 1.52-1.65 and δ 1.75-1.82 ppm, corresponding to each CH₂-7 proton. However, CH₂-6 of **219c** appeared as two clear doublets at δ 3.80 ppm and δ 3.82 ppm, due to the absence of ³J proton-proton coupling in **219c** as compared to **219b**. The identities of these protected dipeptides (**219b-c**) were further supported by high resolution mass spectrometry

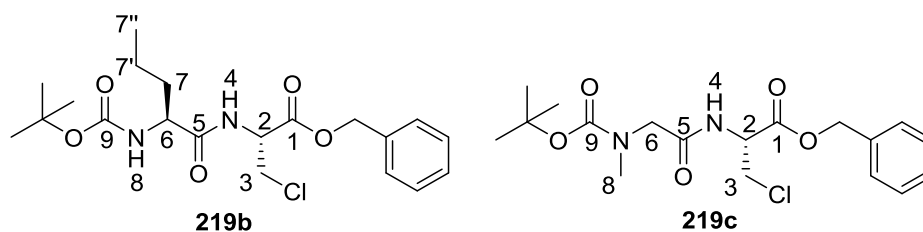
and the presence of a chlorine atom was observed on the MS spectrum with a 3:1 ratio of $^{35}\text{Cl}:$ ^{37}Cl signals. The CHN analysis confirmed the purity of **219b**.

Table 3.7: Assignment of $^1\text{H-NMR}$ signals of diastereoisomeric $^t\text{Boc-L-Nva-}\beta\text{-chloro-L-Ala-OBzl}$ (**219b**) and $^t\text{Boc-Sar-}\beta\text{-chloro-L-Ala-OBzl}$ (**219c**) at 300 MHz



	δ_{H} (CDCl_3)	
	$^t\text{Boc-L-Nva-}\beta\text{-chloro-L-Ala-OBzl}$ (219b)	$^t\text{Boc-Sar-}\beta\text{-chloro-L-Ala-OBzl}$ (219c)
$\text{CH}_3\text{-7''}$	0.92 (3H, t, $^3J_{\text{H-H}}=9.0$ Hz)	-
$\text{CH}_2\text{-7'}$	1.32-1.43 (2H, m)	-
$\text{CH}_2\text{-7}$	1.52-1.65 (1H, m) 1.75-1.82 (1H, m)	-
$\text{C}(\text{CH}_3)_3$	1.45 (9H, s)	1.40 (9H, s)
$\text{NCH}_3\text{-8}$	-	2.87 (3H, s)
$\text{CH}_2\text{-3}$	3.89 (1H, dd, $^2J_{\text{H-H}}=12.0$ Hz, $^3J_{\text{H-H}}=3.0$ Hz) 3.99 (1H, dd, $^2J_{\text{H-H}}=12.0$ Hz, $^3J_{\text{H-H}}=3.0$ Hz)	3.83 (1H, dd, $^2J_{\text{H-H}}=12.0$ Hz, $^3J_{\text{H-H}}=3.0$ Hz) 3.94 (1H, dd, $^2J_{\text{H-H}}=12.0$ Hz, $^3J_{\text{H-H}}=3.0$ Hz)
$\text{CH}_2\text{-6}$	-	3.80 (1H, d, $^2J_{\text{H-H}}=15.0$ Hz) 3.82 (1H, d, $^2J_{\text{H-H}}=15.0$ Hz)
CH-6	4.11-4.15 (1H, m)	-
CH-2	4.96-5.00 (1H, m)	4.91-4.96 (1H, m)
NH-8	4.96-5.00 (1H, m)	-
OCH_2	5.20 (1H, d, $^2J_{\text{H-H}}=12.0$ Hz) 5.25 (1H, d, $^2J_{\text{H-H}}=12.0$ Hz)	5.13 (1H, d, $^2J_{\text{H-H}}=12.0$ Hz) 5.18 (1H, d, $^2J_{\text{H-H}}=12.0$ Hz)
NH-4	6.97 (1H, d, $^3J_{\text{H-H}}=6.0$ Hz)	6.97 (1H, d, $^3J_{\text{H-H}}=6.0$ Hz)
C_6H_5	7.33-7.37 (5H, m)	7.26-7.30 (5H, m)

Table 3.8: Assignment of ^{13}C -NMR signals of diastereoisomeric $^t\text{Boc-L-Nva-}\beta\text{-chloro-L-Ala-OBzl}$ (**219b**) and $^t\text{Boc-Sar-}\beta\text{-chloro-L-Ala-OBzl}$ (**219c**) at 75 MHz



	δ_{C} (CDCl_3)	
	$^t\text{Boc-L-Nva-}\beta\text{-chloro-L-Ala-OBzl}$ (219b)	$^t\text{Boc-Sar-}\beta\text{-chloro-L-Ala-OBzl}$ (219c)
$\text{CH}_3\text{-7''}$	12.7	-
$\text{CH}_2\text{-7'}$	17.8	-
$\text{CH}_2\text{-7}$	33.4	-
$\text{C}(\text{CH}_3)_3$	27.3 $\text{C}(\text{CH}_3)_3$ 79.3 $\text{C}(\text{CH}_3)_3$	28.2 $\text{C}(\text{CH}_3)_3$ 81.0 $\text{C}(\text{CH}_3)_3$
$\text{NCH}_3\text{-8}$	-	35.6
$\text{CH}_2\text{-3}$	43.8	44.9
$\text{CH}_2\text{-6}$	-	53.0
CH-6	53.4	-
CH-2	52.2	53.0
OCH_2	67.2	68.0
C_6H_5	127.4-127.7 (CH_{Ar}) 133.8 ($\text{C}_{\text{quat.}}$)	128.4-128.7 (CH_{Ar}) 134.8 ($\text{C}_{\text{quat.}}$)
C=O-9	154.5	154.5
C=O-1	167.5	168.4
C=O-5	171.2	169.4

The benzyl ester protecting group of the protected dipeptides, $^t\text{Boc-L-Nva-}\beta\text{-chloro-L-Ala-OBzl}$ (**219b**) and $^t\text{Boc-Sar-}\beta\text{-chloro-L-Ala-OBzl}$ (**219c**), was removed by catalytic hydrogenation, resulting in $^t\text{Boc-L-Nva-}\beta\text{-chloro-L-Ala-OH}$ (**220b**) and $^t\text{Boc-Sar-}\beta\text{-chloro-L-Ala-OH}$ (**220c**). Evidence of the successful removal of this protecting group was the appearance of a broad absorbance peak at 3342 - 3312 cm^{-1} in the IR spectrum, indicating the presence of the carboxylic hydroxyl

functional group. The removal of this protecting group was also supported by NMR spectroscopy, as the signals corresponding to the benzyl ester group had vanished. The identity of these products, **220b** and **220c** was further supported by mass spectrometry, while the appearance of 3:1 intensity ratio of $^{35}\text{Cl}:$ ^{37}Cl on the MS spectra confirmed the presence of chlorine. The purity of these compounds was also confirmed by CHN analysis.

3.2.4.2: Synthesis of protected phosphotripeptides (**221b-c**) containing the β -chloro-L-Ala-D/L-fosfalin moiety

The *N*-protected dipeptides (**220b-c**) were coupled with D/L-Fos diethyl ester (**84**), using the NMM and IBCF coupling method as shown in Scheme 3.16. Successful coupling was supported by IR spectroscopy, where the broad absorbance peak indicating the presence of the carboxylic hydroxyl group had disappeared, while strong absorbance peaks at 1224 cm^{-1} and 1229 cm^{-1} indicated the presence of the P=O group of the phosphonate ester in both compounds (**221b-c**), respectively. The structure of these compounds was also confirmed by NMR spectroscopy, with individual signals assigned accordingly (Table 3.10) using the structural numbering system shown (Table 3.9).

Table 3.9: Structure of the diastereoisomeric $^t\text{Boc-L-Nva-}\beta\text{-chloro-L-Ala-D/L-Fos}$ diethyl ester (**221b**) and $^t\text{Boc-Sar-}\beta\text{-chloro-L-Ala-D/L-Fos}$ diethyl ester (**221c**) with corresponding numbering systems used for NMR assignment

Compound name	Structure
$^t\text{Boc-L-Nva-}\beta\text{-chloro-L-Ala-D/L-Fos}$ diethyl ester (221b)	
$^t\text{Boc-Sar-}\beta\text{-chloro-L-Ala-D/L-Fos}$ diethyl ester (221c)	

Table 3.10: Assignment of NMR signals of the diastereoisomers of ^tBoc-L-Nva-β-Cl-L-Ala-D/L-Fos diethyl ester (**221b**) and ^tBoc-Sar-β-Cl-L-Ala-D/L-Fos diethyl ester (**221c**), at 300 MHz (¹H-NMR) and 75 MHz (¹³C-NMR)

	^t Boc-L-Nva-β-Cl-L-Ala-D/L-Fos diethyl ester (221b)		^t Boc-Sar-β-Cl-L-Ala-D/L-Fos diethyl ester (221c)	
	δ _H (CDCl ₃)	δ _C (CDCl ₃)	δ _H (CDCl ₃)	δ _C (CDCl ₃)
CH ₃ -10''	0.86 (3H*, t, ³ J _{H-H} =9.0 Hz), 0.88 (3H*, t, ³ J _{H-H} =9.0 Hz)	12.7	-	-
CH ₂ -10'	1.22-1.34 (2H, m)	17.9, 18.0	-	-
CH ₂ -10	1.53-1.59 (1H, m) 1.70-1.77 (1H, m)	33.2	-	-
OCH ₂ CH ₃	1.22-1.34 (6H, m, 2 x CH ₃) 3.97-4.13 (4H, m, 2 x CH ₂)	15.3, 15.4, 15.5, 15.6 (CH ₃) 61.4, 61.6, 61.7, 61.9 (d, ² J _{C-P} =6.8 Hz, CH ₂)	1.11-1.35 (6H, m, 2 x CH ₃) 4.02-4.13 (4H, m, 2 x CH ₂)	16.3, 16.4 (CH ₃) 62.7 (d, ² J _{C-P} =6.0 Hz, CH ₂) 63.0 (d, ² J _{C-P} =6.5 Hz, CH ₂)
CH ₃ -2	1.22-1.34 (3H, m)	14.5	1.11-1.35 (3H, m)	15.2, 15.6
C(CH ₃) ₃	1.38 (9H, s)	27.0, 27.3 C(CH ₃) ₃ 79.4 C(CH ₃) ₃	1.41 (9H, s)	28.3 C(CH ₃) ₃ 81.0 C(CH ₃) ₃
CH ₂ -9	-	-	3.70-3.88 (2H, m)	53.1
CH-9	3.88-3.93 (1H, m)	70.5	-	-

*Actual proton integration was 1.5

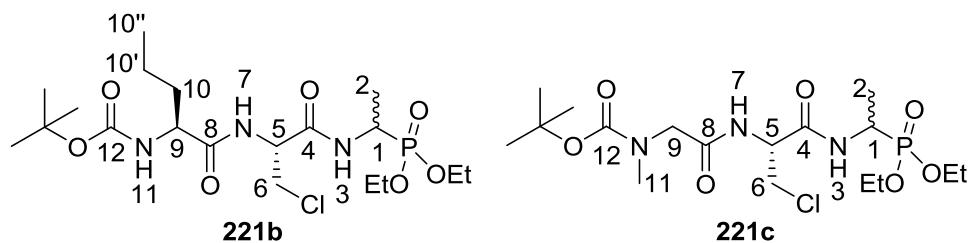
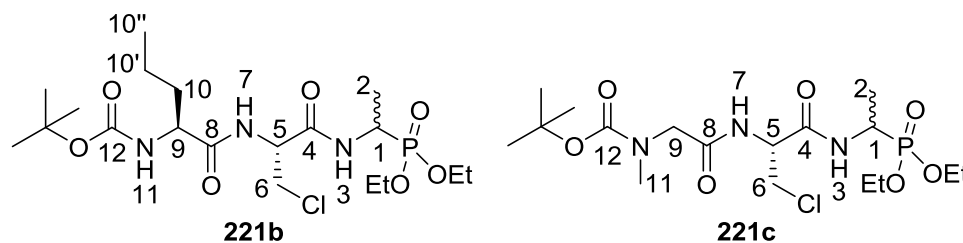


Table 3.10 (cont.d): Assignment of NMR signals of the diastereoisomers of ¹Boc-L-Nva-β-Cl-L-Ala-D/L-Fos diethyl ester (**221b**) and ¹Boc-Sar-β-Cl-L-Ala-D/L-Fos diethyl ester (**221c**), at 300 MHz (¹H-NMR) and 75 MHz (¹³C-NMR)

	¹ Boc-L-Nva-β-Cl-L-Ala-D/L-Fos diethyl ester (221b)		¹ Boc-Sar-β-Cl-L-Ala-D/L-Fos diethyl ester (221c)	
	δ _H (CDCl ₃)	δ _C (CDCl ₃)	δ _H (CDCl ₃)	δ _C (CDCl ₃)
CH ₂ -6	3.69 (1H, dd, ² J _{H-H} =12.0 Hz, ³ J _{H-H} =6.0 Hz) 3.91 (1H, dd, ² J _{H-H} =12.0 Hz, ³ J _{H-H} =6.0 Hz)	43.4	3.70-3.88 (2H, m)	44.7
CH-1	4.35-4.46 (1H, m)	40.4 (d, ¹ J _{C-P} =157.5 Hz)	4.36-4.47 (1H, m)	41.2 (d, ¹ J _{C-P} =156.8 Hz)
CH-5	4.73-4.79 (1H, m)	52.6, 52.8	4.78-4.82 (1H, m)	53.4
NCH ₃ -11	-	-	2.90 (3H, s)	35.9
NH-11	4.97-5.03 (1H, m)	-	-	-
NH-7	7.01 (1H*, d, ³ J _{H-H} =9.0 Hz) 7.09 (1H*, d, ³ J _{H-H} =9.0 Hz)	-	6.94 (1H, m)	-
NH-3	7.25 (1H*, d, ³ J _{H-H} =9.0 Hz) 7.33 (1H*, d, ³ J _{H-H} =9.0 Hz)	-	7.36 (1H, m)	-
C=O-12	-	154.7	-	152.3
C=O-4	-	166.8	-	167.7 or 169.4
C=O-8	-	171.4	-	167.7 or 169.4

*Actual proton integration was 0.5

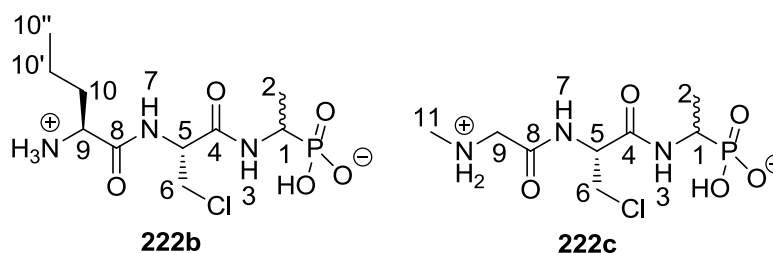


The use of racemic fosfalin diethyl ester (**84**) gave rise to diastereoisomeric products, the L,L,L and L,L,D forms of *t*Boc-Nva- β -chloro-Ala-Fos diethyl ester (**221b**) and L,L and L,D forms of Sar- β -chloro-Ala-Fos diethyl ester (**221c**). Therefore, two sets of signals were observed in the NMR spectra of each product **221b-c** (Table 3.9). For instance, in the $^1\text{H-NMR}$ spectrum of **221b**, an additional set of signals was found at δ 0.86, δ 7.01 and δ 7.25 ppm, corresponding to the methyl protons of CH₃-10'', the NH-7 proton and the NH-3 proton, respectively. This effect was also observed in the $^{13}\text{C-NMR}$ spectrum of **221b**, where two signals corresponding to the methylene carbon of CH₂-10' at δ 17.9 and δ 18.0 ppm were observed. Besides the diastereoisomeric signals, diastereotopic effects were also seen at δ 3.69 and δ 3.91 ppm, where the geminal proton-proton coupling resulted in a doublet of doublets instead of a doublet, corresponding to each CH₂-6 proton of the two diastereoisomers of **221b**. The presence of phosphorus coupling also resulted in additional coupling on the ^1H and $^{13}\text{C-NMR}$ spectra, resulting in complicated splitting patterns on the $^1\text{H-NMR}$; thus multiplets were mainly reported for **221b** and **221c**. However, distinct signals due to phosphorus coupling were observed in the $^{13}\text{C-NMR}$ spectra. For instance, a doublet was observed at δ 40.4 and δ 41.2 ppm, with $^1J_{\text{C-P}}$ coupling constant of 157.5 Hz and 156.8 Hz, corresponding to the CH-1 carbons of **221b** and **221c**, respectively, while $^2J_{\text{C-P}}$ coupled signals corresponding to the methylene carbons of the OCH₂CH₃ groups were also observed. The presence of phosphorus in these compounds (**221b-c**) was supported by the phosphorus-proton decoupled NMR spectra, while the continued presence of chlorine was evidenced by the 3:1 ratio of the ^{35}Cl : ^{37}Cl signals found on the MS spectra. High resolution mass spectrometry further supported the identity of these compounds (**221b-c**) and the purity of **221b** was confirmed by the CHN analysis.

These protected phosphonotripeptides (**221b-c**) were each subjected to acidic hydrolysis to remove both protecting groups, *tert*-butoxycarbonyl and phosphonate diethyl ester groups simultaneously. After acidic hydrolysis, the resulting phosphonotripeptides (**222b-c**) were isolated and supported by the IR spectroscopy, where a sharp peak at about 3290 cm⁻¹ and a broad peak at about 3000 cm⁻¹ were observed on the IR spectra, indicating the presence of NH₃⁺ and

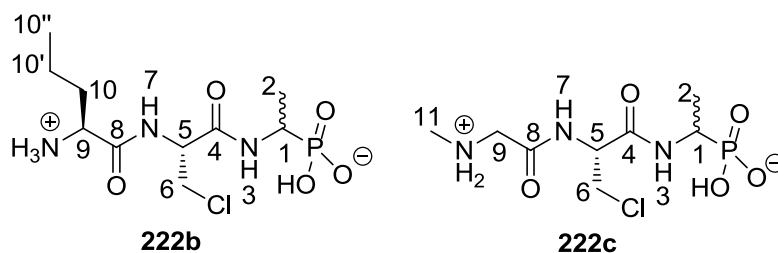
hydroxyl functional groups. The successful removal of these protecting groups was also confirmed by the NMR spectroscopy, where the signals corresponding to *tert*-butoxycarbonyl and phosphonate diethyl ester had vanished. The NMR spectra of **222b** and **222c** are summarised in Tables 3.11 and 3.12. High resolution mass spectrometry further confirmed the identity of L-Nva- β -chloro-L-Ala-D/L-Fos (**222b**) and Sar- β -chloro-L-Ala-D/L-Fos (**222c**), as well as the presence of chlorine with a 3:1 ratio of ^{35}Cl : ^{37}Cl signals observed on the MS spectra.

Table 3.11: Assignment of ^1H -NMR signals of diastereoisomeric L-Nva- β -chloro-L-Ala-D/L-Fos (**222b**) and Sar- β -chloro-L-Ala-D/L-Fos (**222c**) at 300 MHz (^1H -NMR)



	δ_{H}	
	222b (D_2O)	222c (CD_3OD)
$\text{CH}_3\text{-}10''$	1.01 (3H, t, $^3J_{\text{H-H}}=9.0$ Hz)	-
$\text{CH}_2\text{-}10'$	1.44-1.54 (2H, br m)	-
$\text{CH}_2\text{-}10$	1.90-1.98 (2H, br m)	-
$\text{CH}_3\text{-}2$	1.30-1.37 (3H, br m)	1.24 (3H, dd, $^3J_{\text{H-P}}=15.0$ Hz, $^3J_{\text{H-H}}=6.0$ Hz)
$\text{CH}_2\text{-}6$	3.91-4.15 (2H, br m)	3.81-3.87 (2H, m)
$\text{CH}_2\text{-}9$	-	3.93-3.94 (2H, m)
$\text{CH}\text{-}9$	3.91-4.15 (1H, br m)	-
$\text{CH}\text{-}5$	4.79 (1H, br m)	4.79 (1H, m)
$\text{CH}\text{-}1$	3.91-4.15 (1H, br m)	3.97-4.10 (1H, m)
$\text{NH}\text{-}7$	Exchanged	Exchanged
$\text{NH}\text{-}3$	Exchanged	Exchanged
$\text{NCH}_3\text{-}11$		2.74 (3H, s)

Table 3.12: Assignment of ^{13}C -NMR signals of diastereoisomeric L-Nva- β -chloro-L-Ala-D/L-Fos (**222b**) and Sar- β -chloro-L-Ala-D/L-Fos (**222c**) at 75 MHz (^{13}C -NMR)



	δ_{C}	
	222b (D_2O)	222c (CD_3OD)
CH_3 -10''	12.9	-
CH_2 -10'	17.6	-
CH_2 -10	33.0	-
CH_3 -2	15.7	15.4
CH_2 -6	43.3	43.6
CH_2 -9	-	49.5
CH -9	53.1	-
CH -5	55.0	54.6
CH -1	53.1	44.1 (d, $^1J_{\text{C-P}}=148.5$ Hz)
$\text{C}=\text{O}$ -4	170.4	166.4 or 166.9
$\text{C}=\text{O}$ -8	170.4	166.4 or 166.9
NCH_3 -11	-	32.9

The diastereoisomeric compositions of **222b-c** were confirmed by LC-MS analysis, where two peaks with approximately 1:1 ratio were observed from the chromatogram, Figure 3.13. These two peaks also evidenced the presence of two diastereoisomers: L,L,L and L,L,D of Nva- β -chloro-Ala-Fos (**222b**) and L,L and L,D of Sar- β -chloro-Ala-Fos (**222c**). However, the assignment of the two peaks to their corresponding diastereoisomers was impossible without standards.

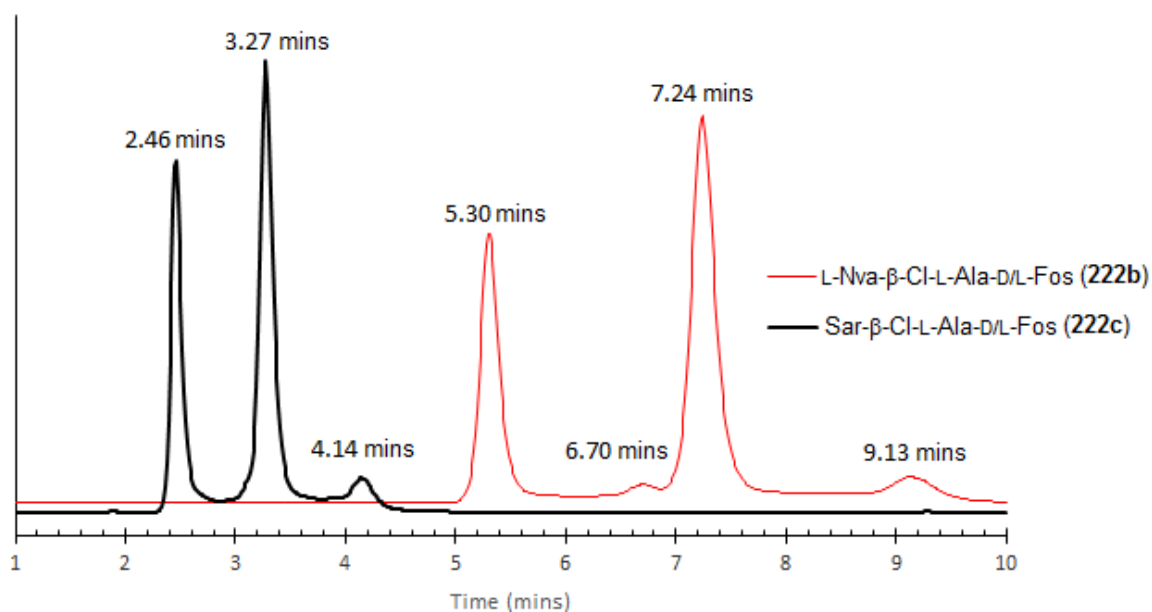
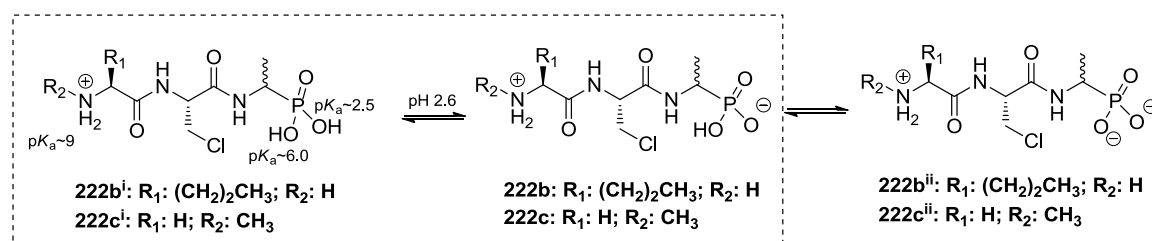


Figure 3.13: Reversed phase LC-MS chromatogram of L-Nva-β-Cl-L-Ala-D/L-Fos (**222b**) and Sar-β-Cl-L-Ala-D/L-Fos (**222c**) with specific ions extracted at MH^+ m/z 330 and m/z 302, respectively. LC-MS condition (6.2.1) was used. For clarity, the chromatogram is displayed at 1.0 - 10.0 mins

The retention time between L-Nva-β-chloro-L-Ala-D/L-Fos (**222b**) and Sar-β-chloro-L-Ala-D/L-Fos (**222c**) was different. This could be due to the hydrophobicity difference between **222b** and **222c**, as a result of presence of propyl aliphatic side chain at the α -carbon of L-Nva of **222b** and no α -carbon side chain on Sar (**222c**), although it gains some hydrophobicity from the *N*-methyl group. It is likely that, the presence of an α -hydrocarbon side chain would have great influence on the hydrophobicity of the compounds and their retention time. Although the retention times of **222b-c** (Figure 3.13) were similar to **153b-c** (Figure 2.5), the hydrophobicity of **222b-c** was relatively higher with longer retention time compared to **153b-c**, due to the additional chlorine atom on **222b-c**.

Aside from the different retention times, there are additional peaks observed at 4.14 mins (**222c**), 6.70 mins and 9.13 mins (**222b**), Figure 3.13. These extra peaks could be due to the different ionised states of the phosphonic group of **222b** and **222c** being detected by the LC-MS. As a result of the use of an acidic (pH 2.6) solvent for LC-MS analysis of these compounds (**222b-c**), the phosphonic acid with two pK_a values might be ionised differently during analysis (Scheme 3.17). For instance, the chemical equilibrium between **222b-c** and **222b-cⁱ** might have been favourable at pH 2.6 with less than 1 % formation of **222b-cⁱⁱ**. This

favourable equilibrium could result in potential detection of **222b-c** and **222b-cⁱ** and thus additional peaks observed from the chromatogram (Figure 3.13).

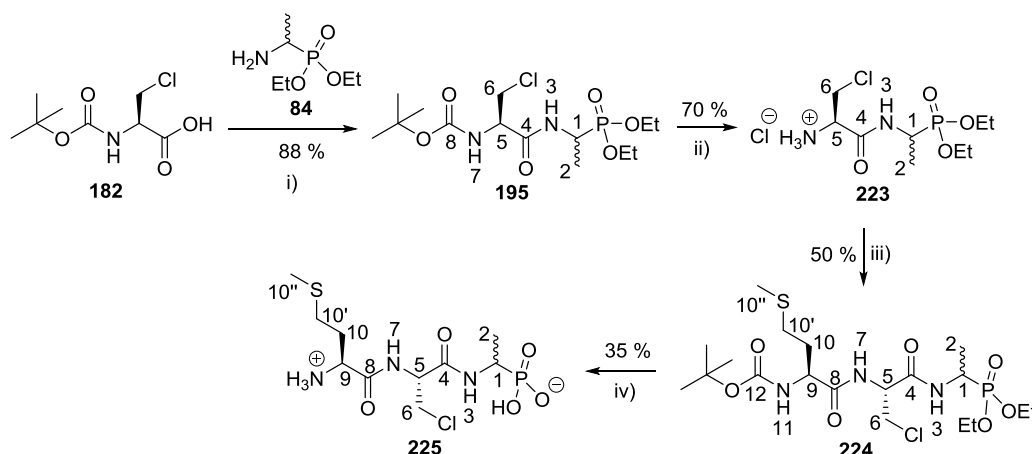


Scheme 3.17: Equilibrium between **222b-c**, **222b-cⁱ** and **222b-cⁱⁱ** at pH 2.6

Although the additional peaks observed could also suggested potential racemisation with formation of extra diastereoisomers, this was less likely to be the case, because only two sets of diastereoisomeric signals were observed from the NMR spectra of **222b-c** (Tables 3.11 and 3.12) and their precursors, **221b-c** (Table 3.10).

3.2.5: Preparation of phosphonotripeptide, L-Met- β -chloro-L-Ala-D/L-Fos (**225**)

The thioether side chain of L-methionine is prone to unwanted side reactions (Scheme 2.13), so a different synthetic route was required when coupling this amino acid. A similar approach to that used in the preparation of L-Met-L-Ala-D/L-Fos (**160**), where the L-methionine was introduced as late as possible, was employed in the synthesis of L-Met- β -chloro-L-Ala-D/L-Fos (**225**), Scheme 3.18.



Scheme 3.18: Preparation of phosphonotripeptide, L-Met- β -chloro-L-Ala-D/L-Fos (**225**)

Reagents and conditions: i) IBCF, NMM, **86**, THF, -5 °C to r.t., 24hrs; ii) 2M HCl in diethyl ether, r.t., 48hrs; iii) IBCF, NMM, *t*Boc-L-Met-OH, THF/DCM, -5 °C to r.t., 24hrs; iv) HBr, AcOH, 16-18hrs then propylene oxide

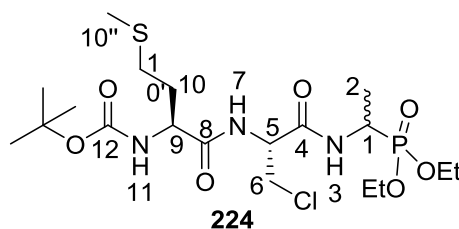
3.2.5.1: Synthesis of (2*R*)-3-chloro-1-((1-(diethoxyphosphoryl)ethyl)amino)-1-oxopropan-2-aminium chloride or β -Cl-L-Ala-D/L-Fos diethyl ester hydrochloride (**223**)

The *tert*-butoxycarbonyl protecting group of the previously synthesised ¹Hoc- β -chloro-L-Ala-D/L-Fos diethyl ester (**195**) was removed under acidic conditions, Scheme 3.18, to afford β -chloro-L-Ala-D/L-Fos diethyl phosphonate ester hydrochloride (**223**). The successful removal of this group was supported by IR spectroscopy, where a sharp absorbance peak at 3204 cm⁻¹ indicated the presence of the NH₃⁺ functional group. The absence of signals corresponding to the ¹Hoc protecting group from the NMR spectra further confirmed successful deprotection. The identity of the resulting compound (**223**) was supported by high resolution mass spectrometry; the presence of chlorine was confirmed with a 3:1 ratio of ³⁵Cl:³⁷Cl found on the MS spectrum.

3.2.5.2: Synthesis of *tert*-butyl ((2*S*)-1-(((2*R*)-3-chloro-1-((1-(diethoxyphosphoryl)ethyl)amino)-1-oxopropan-2-yl)amino)-4-(methylthio)-1-oxobutan-2-yl)carbamate or ¹Hoc-L-Met- β -Cl-L-Ala-D/L-Fos diethyl phosphonate ester (**224**)

The reaction between ¹Hoc-L-methionine and β -chloro-L-Ala-D/L-Fos diethyl phosphonate ester hydrochloride (**223**) used the general coupling method, Scheme 3.18. The presence of both *tert*-butoxycarbonyl and diethyl phosphonate ester signals were observed on the NMR spectra of the product (**224**). In addition, the presence of a distinct singlet corresponding to the thiomethyl group on the NMR spectra further supported the successful synthesis of ¹Hoc-L-Met- β -Cl-L-Ala-D/L-Fos diethyl ester (**224**). The NMR signals of this compound (**224**) are summarised in Table 3.13.

Table 3.13: Assignment of NMR signals of diastereoisomers, ¹Boc-L-Met-β-Cl-L-Ala-L-Fos diethyl ester and ¹Boc-L-Met-β-Cl-L-Ala-D-Fos diethyl ester (**224**), at 300 MHz (¹H-NMR) and 75 MHz (¹³C-NMR)



	δ_{H} (CDCl ₃)	δ_{C} (CDCl ₃)
OCH ₂ CH ₃	1.17-1.36 (6H, m, 2 x CH ₃) 3.99-4.12 (4H, m, 2 x CH ₂)	15.3, 15.4, 15.5, 15.6 (CH ₃) 61.6 (d, ² J _{P-C} =6.8 Hz, CH ₂) 61.7 (d, ² J _{P-C} =6.0 Hz, CH ₂) 62.0 (d, ² J _{P-C} =6.8 Hz, CH ₂) 62.1 (d, ² J _{P-C} =7.5 Hz, CH ₂)
CH ₃ -2	1.17-1.36 (3H, m)	14.3, 14.4
C(CH ₃) ₃	1.38 (9H, s)	27.3 C(CH ₃) ₃ 79.6 C(CH ₃) ₃
CH ₂ -10	1.87-2.03 (2H, m)	30.2, 30.4
CH ₃ -10''	2.04 (3H, s)	14.5
CH ₂ -10'	2.48-2.54 (2H, m)	29.2, 29.3
CH ₂ -6	3.71 (1H, dd, ² J _{H-H} =12.0 Hz, ³ J _{H-H} =6.0 Hz) 3.88 (1H, dd, ² J _{H-H} =12.0 Hz, ³ J _{H-H} =6.0 Hz)	43.5, 43.7
CH-9	4.20 (1H, m)	53.1
CH-1	4.37-4.47 (1H, m)	40.3 (d, ¹ J _{P-C} =159.0 Hz)
CH-5	4.78-4.84 (1H, m)	52.7
NH-11	5.39 (1H*, d, ³ J _{H-H} =6.0 Hz) 5.41 (1H*, d, ³ J _{H-H} =6.0 Hz)	-
NH-7	7.15 (1H*, d, ³ J _{H-H} =6.0 Hz) 7.24 (1H*, d, ³ J _{H-H} =6.0 Hz)	-
NH-3	7.52 (1H, m)	-
C=O-12	-	154.8
C=O-4	-	166.7, 166.8
C=O-8	-	170.7, 170.8

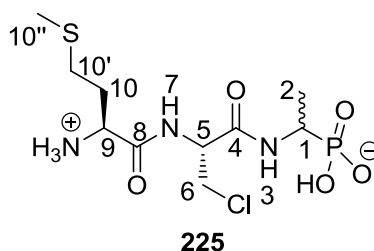
*Actual proton integration was 0.5

In the $^1\text{H-NMR}$ spectrum, the diastereotopic protons on $\text{CH}_2\text{-6}$ were seen as a doublet of doublets at δ 3.71 ppm and δ 3.78 ppm, due to geminal coupling. The presence of diastereoisomers was indicated by more than one signal for some protons. For instance, two sets of doublets integrating for 0.5H each were assigned to each of NH-11 and NH-7 , with $^3J_{\text{H-H}}$ coupling constant of 6.0 Hz, at δ 5.39-5.41 ppm and δ 7.15-7.24 ppm, respectively. This effect was also seen in the $^{13}\text{C-NMR}$ spectrum, where two sets of signals were assigned to the carbons of $\text{CH}_3\text{-2}$, $\text{CH}_2\text{-10}$, $\text{CH}_2\text{-10'}$, $\text{CH}_2\text{-6}$ and the amide carboxyl groups. For the methylene carbon of OCH_2CH_3 , there were four sets of doublets found, where two of the four sets were assigned to each methylene carbon, due to 2J phosphorus-carbon coupling in diastereoisomers. Other phosphorus coupling in the $^{13}\text{C-NMR}$ spectrum was seen at 40.3 ppm, corresponding to the methine carbon of CH-1 , with $^1J_{\text{P-C}}$ coupling constant of 159.0 Hz. As a result, complicated splitting patterns and overlapping signals were obtained for most of the $^1\text{H-NMR}$ signals reported in Table 3.10. The assignment of the NMR signals was aided by their proton integration and the 2D-NMR spectra. The identity of *t*Boc-L-Met- β -Cl-L-Ala-D/L-Fos diethyl phosphonate ester (**224**) and the presence of chlorine were also supported by high resolution mass spectrometry, while its purity was confirmed by CHN analysis.

3.2.5.3: Synthesis of (1-((*R*)-2-((*S*)-2-ammonio-4-(methylthio)butanamido)-3-chloropropanamido)ethyl)phosphonic acid or L-Met- β -Cl-L-Ala-D/L-Fos (**225**)

The *tert*-butoxycarbonyl and diethyl phosphonate ester protecting groups of the protected phosphonotriptide (**224**) were removed simultaneously under acidic hydrolysis (Scheme 3.17). The removal of these groups resulted in a sharp NH_3^+ peak at 3264 cm^{-1} and a broad OH peak at 2829 cm^{-1} of the IR spectrum. In addition, the disappearance of NMR signals corresponding to these protecting groups supported their removal and the signals that remained were consistent with the target compounds (**225**). The NMR signals of **225** are presented in Table 3.14. The identity of L-Met- β -Cl-L-Ala-D/L-Fos (**225**) was confirmed by high resolution mass spectrometry and the presence of chlorine by a peak of 3:1 ratio (^{35}Cl : ^{37}Cl) in the MS spectrum.

Table 3.14: Assignment of NMR signals of diastereoisomers, L-Met- β -chloro-L-Ala-L-Fos and L-Met- β -chloro-L-Ala-D-Fos (**225-LLL** and **225-LLD**), at 300 MHz ($^1\text{H-NMR}$) and 75 MHz ($^{13}\text{C-NMR}$)



	δ_{H} , (D_2O)	δ_{C} (D_2O)
CH ₃ -10''	2.13 (3H, s)	16.9, 17.0
CH ₂ -10'	2.63-2.69 (2H, m)	31.1
CH ₂ -10	2.18-2.29 (2H, m)	32.9
CH ₃ -2	1.31 (3H, dd, $^3J_{\text{H-P}}=15.0$ Hz, $^3J_{\text{H-H}}=6.0$ Hz)	18.4
CH ₂ -6	3.89 (1H, dd, $^2J_{\text{H-H}}=12.0$ Hz, $^3J_{\text{H-H}}=6.0$ Hz) 3.97 (1H, dd, $^2J_{\text{H-H}}=12.0$ Hz, $^3J_{\text{H-H}}=6.0$ Hz)	46.2
CH-9	4.22 (1H, m)	52.2, 52.3
CH-5	4.75-4.79 (1H, m)	57.8, 58.0
CH-1	4.01-4.13 (1H, m)	47.0 (d, $^1J_{\text{C-P}}=147.0$ Hz)
NH-7	Exchanged	-
NH-3	Exchanged	-
C=O-4	-	171.7, 171.8
C=O-8	-	172.3

The presence of diastereoisomers, L,L,L and L,L,D of Met- β -Cl-Ala-Fos (**225**) was confirmed by LC-MS analysis, where two main peaks with approximate 1:1 ratio at 6.83 mins and 10.98 mins were observed, Figure 3.14. The assignment of these two main peaks to their corresponding diastereoisomer was not possible without standards. The retention time of L-Met- β -Cl-L-Ala-D/L-Fos (**225**) (Figure 3.14) was higher compared to L-Met-L-Ala-D/L-Fos (**160**) (Figure 2.7), in agreement with the assumption that the presence of a chlorine atom would increase the hydrophobicity of a compound.

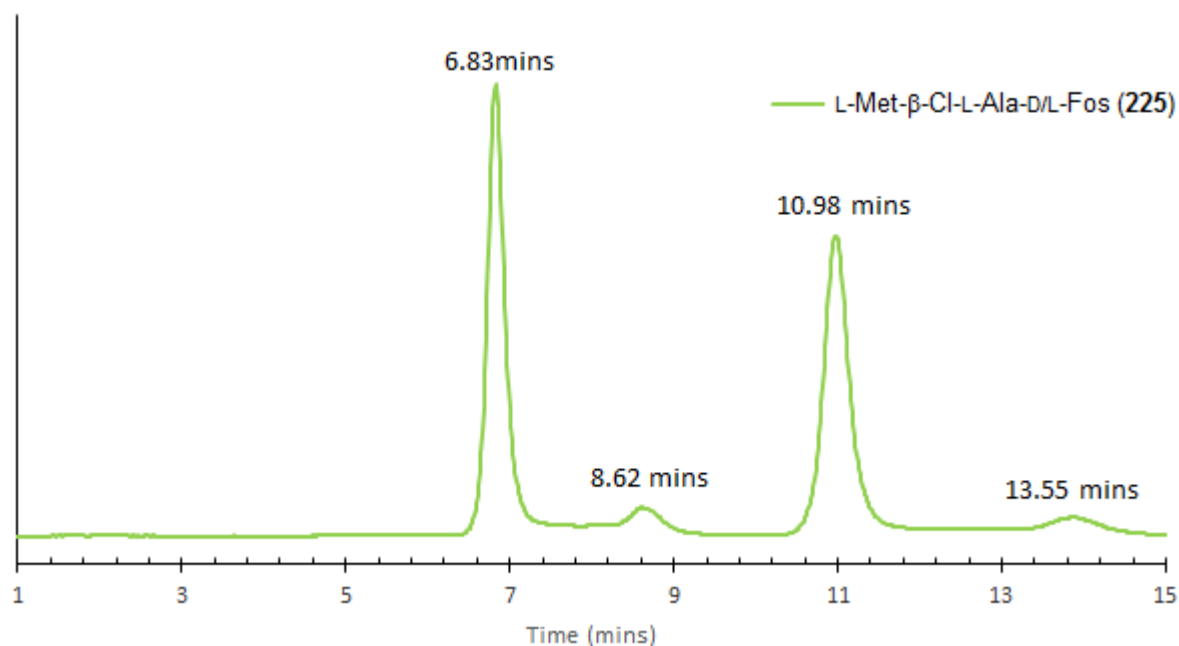
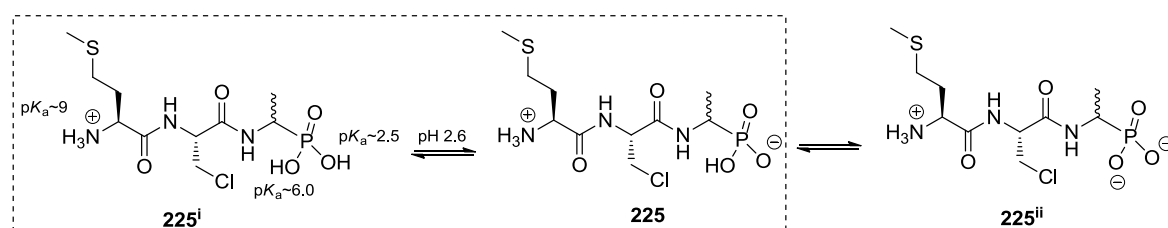


Figure 3.14: Reversed phase LC-MS chromatogram of L-Met- β -Cl-L-Ala-D/L-Fos (**225**) with specific ions extracted at MH^+ m/z 362. LC-MS condition (6.2.1) was used. For clarity, the chromatogram is displayed at 1.0 - 15.0 mins

Additional peaks appeared at 8.62 mins and 13.55 mins (Figure 3.14) which could reflect the presence of other diastereoisomers due to racemisation. However, only two sets of diastereoisomeric signals were observed on NMR spectra of 'Boc-L-Met- β -Cl-L-Ala-D/L-Fos diethyl phosphonate ester (**224**) (Table 3.13) and L-Met- β -Cl-L-Ala-D/L-Fos (**225**) (Table 3.14). These additional peaks (8.62 mins and 13.55 mins) could again be due to the detection of different ionisation states of the phosphonic acid, formed in an acidic solution (pH 2.6), Scheme 3.19. At pH 2.6, two equilibrium products (**225**, **225ⁱ**) would be most likely to be detected and therefore the additional peaks at 8.62 mins and 13.55 mins seem likely to be due to the diastereoisomers of **225ⁱ**.



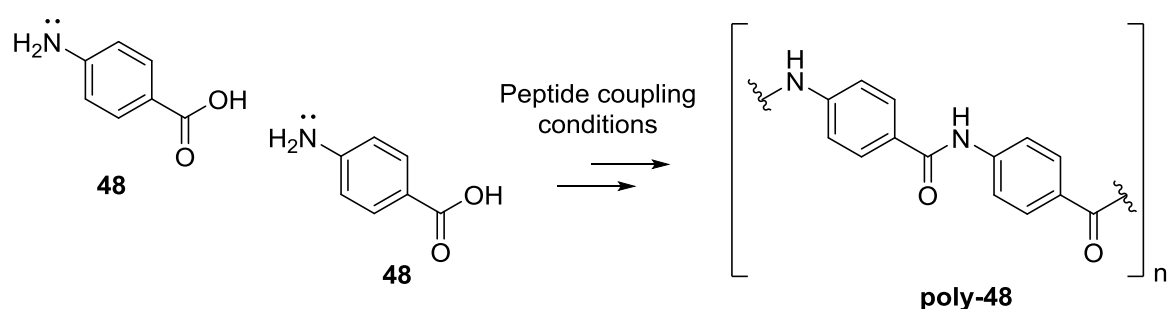
Scheme 3.19: Equilibrium between **225**, **225ⁱ** and **225ⁱⁱ** at pH 2.6

3.3: Synthesis of dipeptide derivatives containing (PABA)

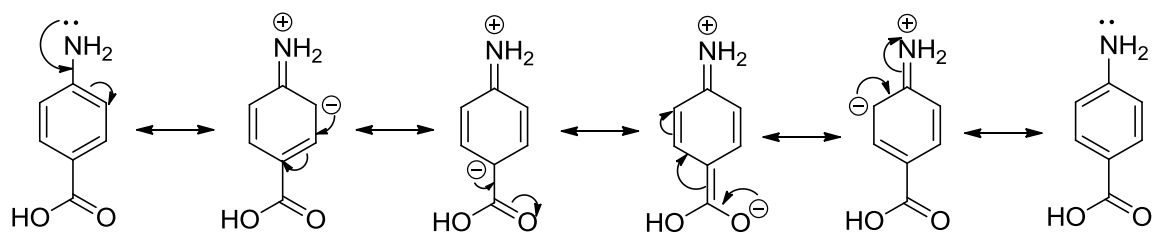
As discussed in the introduction (section 1.4.4), a slight growth inhibitory effect of PABA (**48**) was reported in some studies. This was investigated further in the current work by the synthesis and evaluation of peptide-PABA derivatives for any potential inhibitory effects. The anticipated enhanced antibacterial effects observed with derivatives containing β -chloro-L-alanine resulted in its further application here. In the following section, the synthesis of two different PABA derivatives, β -chloro-L-alanine-PABA (**235**) and L-alanine-PABA (**234**), are discussed, while their antibacterial evaluation will be covered in the next chapter.

3.3.1: Synthesis of C-protected *para*-aminobenzoic acid, *tert*-butyl 4-aminobenzoate (**229**)

Like other amino acids, PABA (**48**) can polymerise under peptide coupling conditions, due to the presence of the primary amino group and carboxylic acid group in the same molecule, to form a PABA polymer (**poly-48**), Scheme 3.20. Although the lone pair of the amino group is not freely available for this reaction, due to the resonance with the carboxylic acid at the 4th position of PABA, Scheme 3.21, the polymerisation can still take place. As a result, introduction of an appropriate protecting group on either side of PABA is necessary prior to any coupling reactions.

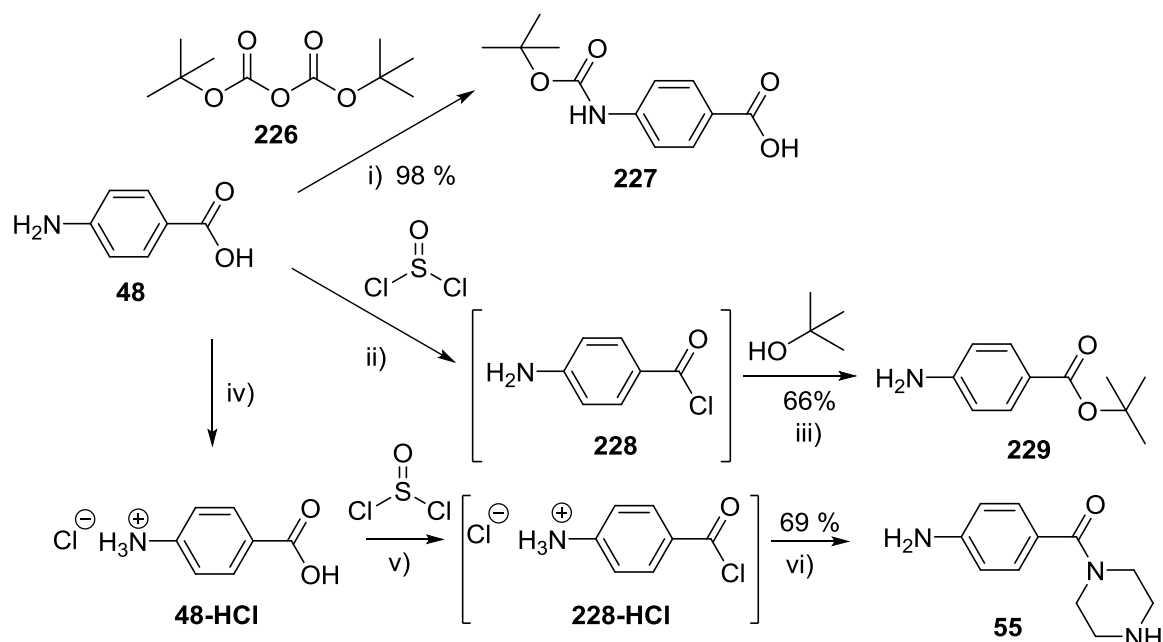


Scheme 3.20: Polymerisation of *para*-aminobenzoic acid (PABA)



Scheme 3.21: Resonance delocalisation of lone pair electrons in PABA (**48**)

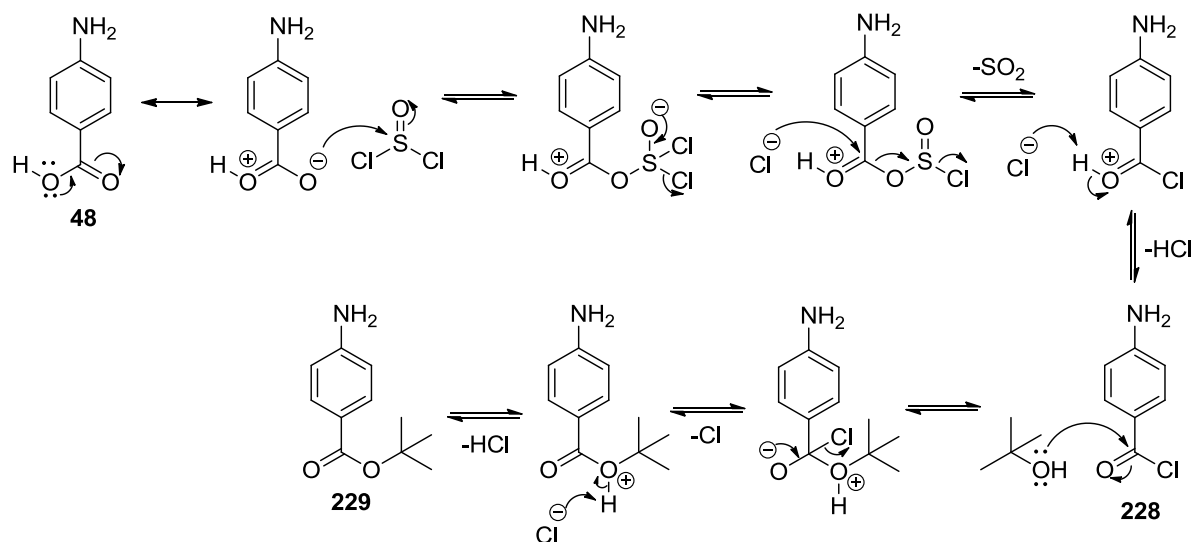
Different protecting groups can be introduced to the *N*-terminus or the *C*-terminus of the PABA, depending on which terminus will be involved in the subsequent coupling reaction. For protection of the *N*-terminus, introduction of *tert*-butoxycarbonyl group was reported by Guo and his co-workers in 2005, using di-*tert*-butyl dicarbonate (**226**) and triethylamine (2005S1061), Scheme 3.22. Protection at the *N*-terminus can also be achieved by converting to its hydrochloride salt (**48-HCl**) with concentrated hydrochloric acid (2009AJRC300). The subsequent coupling reaction between **48-HCl** and piperazine was achieved by conversion of **48-HCl** to the corresponding acyl chloride salt (**228-HCl**), Scheme 3.22. Protection of the *C*-terminus, as its *tert*-butyl ester, can be achieved using thionyl chloride and *tert*-butanol (P-1991MI8), Scheme 3.22.



Scheme 3.22: Synthesis of *N*-protected or *C*-protected PABA

Reagents and conditions: i) Boc_2O (**226**), TEA, 24hrs, r.t.; ii) SOCl_2 , reflux; iii) DCM, *tert*-butanol, 0 °C then r.t., 24hrs; iv) Conc. HCl; v) SOCl_2 , pyridine, 0-5 °C, 30mins; vi) piperazine, 30mins, r.t.

For the current work, a free amino group is required for the subsequent peptide coupling reaction with ^tBoc-L-alanine (**146a**) or ^tBoc-β-chloro-L-alanine (**181**); hence, the C-terminus of PABA (**48**) was protected as its *tert*-butyl ester, as shown in Scheme 3.23. In this synthetic mechanism, acyl chloride (**228**) reacted with *tert*-butanol, resulting in the formation of *tert*-butyl 4-aminobenzoate (**229**), with generation of gaseous by-products, hydrogen chloride and sulphur dioxide. As a result of the sensitivity of the *tert*-butyl ester group to acid, a moderate yield (approx. 60 %) was achieved, perhaps due to the acidic by-products that could hydrolyse some of the *tert*-butyl ester protecting group of **229**.

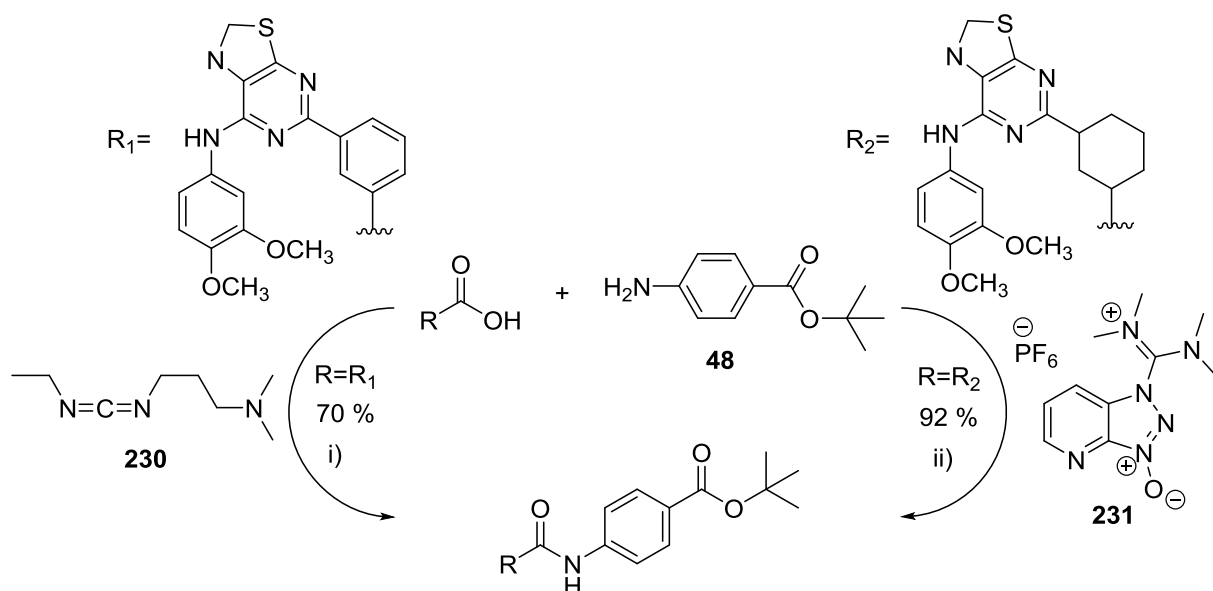


Scheme 3.23: Mechanism of *tert*-butyl 4-aminobenzoate (**229**) formation via the acyl chloride pathway

The successful introduction of the *tert*-butyl ester group at the C-terminus of PABA (**48**) was confirmed by IR spectroscopy, due to the missing carboxylic acid OH absorbance. The presence of the *tert*-butyl ester group was also supported by the NMR spectra: the signals corresponding to this protecting group were observed at δ 1.57 (¹H-NMR), δ 28.3 (¹³C-NMR) and δ 80.0 ppm (¹³C-NMR). The identity of this compound (**229**) was further confirmed by low resolution mass spectrometry and its melting point, which was close to that reported in the literature.

3.3.2: Published methods for the synthesis of amino acid-PABA derivatives

The subsequent coupling between C-protected PABA (**229**) and either ^tBoc-L-alanine (**146a**) or ^tBoc- β -chloro-L-alanine (**181**) can be achieved using the general peptide coupling approach as discussed previously in Chapters 2 and 3. Alternative approaches have been reported for similar peptide coupling reactions; however, different coupling reagents were used, such as 1-ethyl-3-(3-dimethylaminopropyl)carbodiimide, (EDCI, **230**) or 2-(7-aza-1H-benzotriazole-1-yl)-1,1,3,3-tetramethyluronium hexafluorophosphate (HATU, **231**), Scheme 3.24 (2012JMC10414). Despite this, the IBCF/NMM coupling method was favoured due to ready solubility of the reactants and the low cost of these coupling reagents compared to EDCI (**230**) and HATU (**231**).

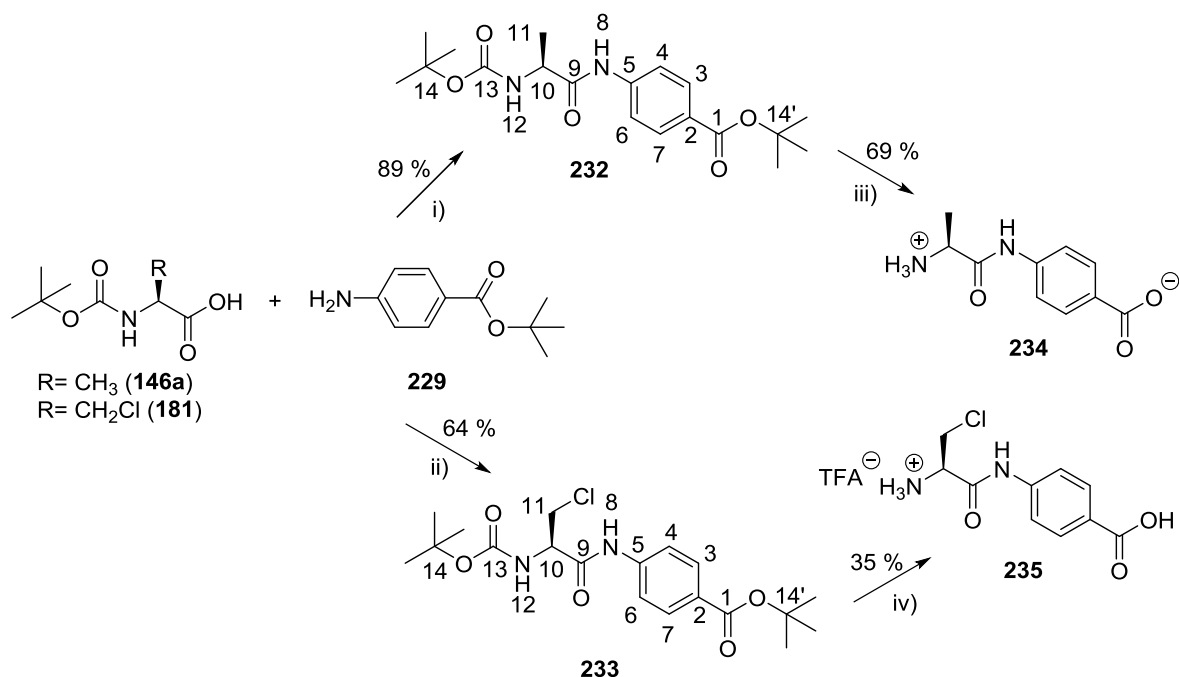


Scheme 3.24: Published coupling approaches between C-protected PABA (**50**) and other carboxylic acids (2012JMC10414)

Reagents and conditions: i) EDCI (**230**), DMAP, DMF, 2hrs, r.t.; ii) HATU (**231**), DIPEA, DMF, 72hrs, r.t.

3.3.2.1: Synthesis of ^tBoc-L-Ala-PABA-O^tbutyl (**232**) and ^tBoc-β-chloro-L-Ala-PABA-O^tbutyl (**233**)

The synthesis of L-Ala-PABA (**234**) and β-chloro-L-Ala-PABA·TFA (**235**) is summarised in Scheme 3.25, using the IBCF/NMM approach for amide coupling, followed by acidic hydrolysis to remove both *tert*-butyl and ^tBoc protecting groups simultaneously. As β-chlorine is prone to elimination under harsh acidic conditions, hydrogen bromide in acetic acid, as discussed previously (section 3.2.3.2), trifluoroacetic acid was used instead.

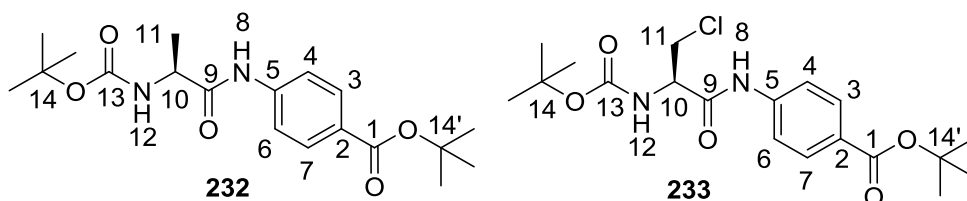


Scheme 3.25: Synthetic route of L-Ala-PABA (**234**) and β-chloro-L-Ala-PABA·TFA (**235**)

Reagents and conditions: i) DIPEA, IBCF, NMM, THF, -5 °C to r.t., 24hrs; ii) IBCF, NMM, THF, -5 °C to r.t., 24hrs; iii) 33 % HBr in acetic acid, r.t., 16-18hrs then propylene oxide; iv) 100 % CF₃COOH, r.t., 16-18hrs

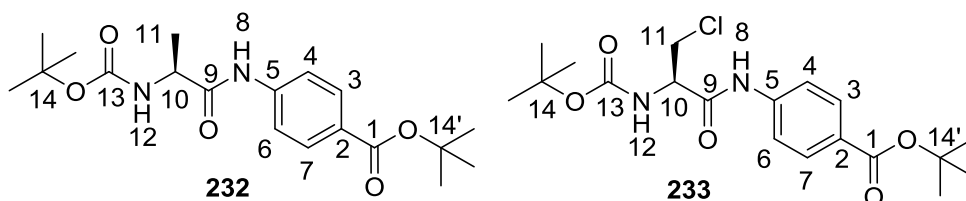
The amide bond formed between **146a** or **181** and **229** was confirmed by NMR spectroscopy (Tables 3.15 and 3.16), where there were two distinct signals corresponding to the *tert*-butoxycarbonyl and *tert*-butyl ester at the respective *N*-terminus and *C*-terminus of **232** and **233**, observed on the NMR spectra. In the ¹H-NMR spectrum of **233**, the diastereotopic methylene protons of CH₂-11 were observed as two sets of doublets of doublets at δ 3.85 and δ 4.10 ppm.

Table 3.15: Assignment of ¹H-NMR signals ^tBoc-L-Ala-PABA-O^tbutyl (**232**) at 300 MHz and ^tBoc-β-chloro-L-Ala-PABA-O^tbutyl (**233**) at 500 MHz



	δ_{H} (CDCl ₃)	
	^t Boc-L-Ala-PABA-O ^t butyl (232)	^t Boc-β-chloro-L-Ala-PABA-O ^t butyl (233)
C(CH ₃) ₃ -14	1.39 (9H, s)	1.51 (9H, s)
C(CH ₃) ₃ -14'	1.50 (9H, s)	1.60 (9H, s)
CH ₃ -11	1.37 (3H, d, ³ J _{H-H} =9.0 Hz)	-
CH ₂ -11	-	3.85 (1H, dd, ² J _{H-H} =12.0 Hz, ³ J _{H-H} =6.0 Hz) 4.10 (1H, dd, ² J _{H-H} =12.0 Hz, ³ J _{H-H} =6.0 Hz)
CH-10	4.28 (1H, m)	4.64 (1H, m)
NH-12	5.09 (1H, d, ³ J _{H-H} =9.0 Hz)	5.45 (1H, d, ³ J _{H-H} =6.0 Hz)
CH _{Ar} -4/6	7.47 (2H, d, ³ J _{H-H} =6.0 Hz)	7.60 (2H, d, ³ J _{H-H} =6.0 Hz)
CH _{Ar} -3/7	7.83 (2H, d, ³ J _{H-H} =6.0 Hz)	7.97 (2H, d, ³ J _{H-H} =6.0 Hz)
NH-8	8.76 (1H, br)	8.50 (1H, br)

Table 3.16: Assignment of ^{13}C -NMR signals of $^t\text{Boc-L-Ala-PABA-O}^t\text{butyl}$ (**232**) at 75 MHz and $^t\text{Boc-}\beta\text{-chloro-L-Ala-PABA-O}^t\text{butyl}$ (**233**) at 125 MHz



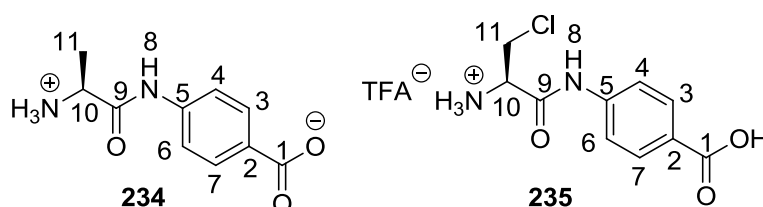
	δ_{C} (CDCl_3)	
	$^t\text{Boc-L-Ala-PABA-O}^t\text{butyl}$ (232)	$^t\text{Boc-}\beta\text{-chloro-L-Ala-PABA-O}^t\text{butyl}$ (233)
$\text{C}(\text{CH}_3)_3\text{-14}$	28.2	28.2
$\text{C}(\text{CH}_3)_3\text{-14}'$	28.3	28.3
$\text{CH}_3\text{-11}$	17.3	-
$\text{CH}_2\text{-11}$	-	44.1
CH-10	51.0	56.0
$\text{C}(\text{CH}_3)_3\text{-14}$	79.9	82.2
$\text{C}(\text{CH}_3)_3\text{-14}'$	79.8	81.3
$\text{CH}_{\text{Ar}}\text{-4/6}$	118.7	119.1
$\text{CH}_{\text{Ar}}\text{-2}$	127.5	128.2
$\text{CH}_{\text{Ar}}\text{-3/7}$	130.5	130.6
$\text{CH}_{\text{Ar}}\text{-5}$	141.6	140.7
C=O-13	156.2	155.7
C=O-1	165.3	165.2
C=O-9	171.1	167.3

The loss of the broad OH absorbance peak of carboxylic acid of **146a** and **181** from its corresponding IR region further supported successful amide bond formation. The identity of these synthesised compounds (**232**, **233**) was consistent with the low resolution mass spectrometry results, while the presence of the chlorine atom in **233** was confirmed by the 3:1 ratio of ^{35}Cl : ^{37}Cl signals on the MS spectrum. The purity of these compounds was also confirmed by CHN analysis.

3.3.2.2: Synthesis of L-Ala-PABA (**234**) and β -chloro-L-Ala-PABA·TFA (**235**)

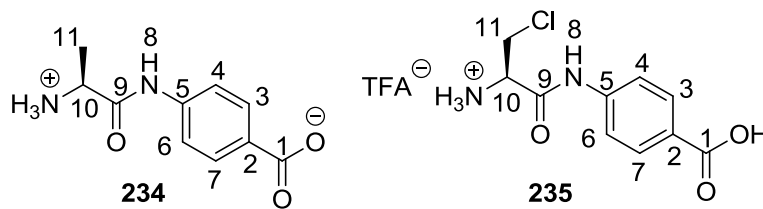
The *tert*-butoxycarbonyl and *tert*-butyl ester protecting groups of *t*-Boc-L-Ala-PABA-O^tbutyl (**232**) and *t*-Boc- β -chloro-L-Ala-PABA-O^tbutyl (**233**) were removed under acidic conditions. Treatment of **232** with HBr in acetic acid yielded L-Ala-PABA (**234**), while TFA effected deprotection of **233** to give β -chloro-L-Ala-PABA·TFA (**235**). The successful removal of these protecting groups was confirmed by the IR spectra, where broad absorbance peaks at 3500-2500 cm⁻¹ (**234**) and 3386-2650 cm⁻¹ (**235**), indicating the presence of hydroxyl functional groups, and sharp absorbance NH₃⁺ peaks at 2991 cm⁻¹ (**234**) and 2978 cm⁻¹ (**235**) were observed. Due to its isolation as the zwitterion obtained after propylene oxide treatment, a broad OH peak was observed at 3500-2500 cm⁻¹ in the IR spectrum of **234**, which could be due to the presence of a trace amount of water, as evidenced by CHN analysis. The removal of these protecting groups was also supported by loss of the *t*-Boc and *t*-Butyl signals in the NMR spectra. The NMR results of **234** and **235** are presented in Tables 3.17 and 3.18. The continued presence of chlorine in **235** was confirmed by high resolution mass spectrometry.

Table 3.17: Assignment of ¹H-NMR signals L-Ala-PABA (**234**) at 300 MHz (D₂O) and β -chloro-L-Ala-PABA·TFA (**235**) at 500 MHz (CD₃OD)



	δ_{H}	
	L-Ala-PABA (234)	β -chloro-L-Ala-PABA·TFA (235)
CH ₃ -11	1.58 (3H, d, ³ J _{H-H} =9.0 Hz)	-
CH ₂ -11	-	4.12 (2H, m)
CH-10	4.17 (1H, q, ³ J _{H-H} =9.0 Hz)	4.43 (1H, m)
CH _{Ar} -4/6	7.40 (2H, d, ³ J _{H-H} =9.0 Hz)	7.73 (2H, d, ³ J _{H-H} =5.0 Hz)
CH _{Ar} -3/7	7.87 (2H, d, ³ J _{H-H} =9.0 Hz)	8.01 (2H, d, ³ J _{H-H} =5.0 Hz)
NH-8	Exchanged	Exchanged

Table 3.18: Assignment of ^{13}C -NMR signals L-Ala-PABA (**234**) at 75 MHz (D_2O) and β -chloro-L-Ala-PABA·TFA (**235**) at 125 MHz (CD_3OD)



	δ_{C}	
	L-Ala-PABA (234)	β -chloro-L-Ala-PABA·TFA (235)
CH_3 -11	16.5	-
CH_2 -11	-	49.3
CH-10	49.8	56.3
CH_{Ar} -4/6	120.4	120.4
CH_{Ar} -2	138.9	143.1
CH_{Ar} -3/7	129.2	131.9
CH_{Ar} -5	133.0	128.1
C=O-1	174.7	169.3
C=O-9	169.1	165.9

3.4: Conclusion

The protected β -chloro-L-alanine derivatives (**181**, **182**) were synthesised from the precursor, ^tBoc-L-serine (**163**), using the synthetic approach discussed in 3.1.2. The synthesised β -chloro-L-alanine derivatives (**181**, **182**) were then coupled with fosfalin or fosfalin and amino acid, resulting in β -chloro-L-Ala-D/L-Fos (**196**) and selected phosphonotripeptides containing the β -chloro-L-Ala moiety: L-Nva- β -chloro-L-Ala-D/L-Fos (**222b**), Sar- β -chloro-L-Ala-D/L-Fos (**222c**) and L-Met- β -chloro-L-Ala-D/L-Fos (**225**). A different synthetic route was required for the synthesis of L-Met- β -chloro-L-Ala-D/L-Fos (**225**) in order to prevent unwanted side reactions involving the thioether side chain. These successfully synthesised compounds (**196**, **222b**, **222c**, **225**) were subjected to microbiological evaluation; their inhibitory results will be discussed in Chapter 4. The synthesis of dehydroala-D/L-fosfalin hydrobromide (**207**) was attempted to investigate the role of dehydroalanine as a potential inhibitor for alanine racemase. However, the synthesis of **207** was unsuccessful and requires further consideration of the synthetic strategy.

The stability of β -chloro-L-Ala-D/L-Fos (**196**) at different pH conditions was investigated by ¹H-NMR, to understand its pH resistance and by-product formation throughout the analysis time, providing useful information on the appropriate pH conditions for the preparation of culture media containing **196** or any phosphonotripeptides containing the **196** moiety. The stability results showed that degradation of **196** occurred at a high pH and slow degradation was observed after prolonged exposure at pH 6.1. The lack of stability suggests it is unsuitable for commercial culture media development.

The synthesis of peptide-PABA derivatives involved the introduction of a suitable protecting group, *tert*-butyl ester, at the C-terminus of PABA (**48**), prior to coupling with other *N*-protected amino acids, either ^tBoc-L-alanine (**146a**) or ^tBoc- β -chloro-L-alanine (**181**). Subsequent acidic hydrolysis removed both protecting groups simultaneously, resulting in the formation of L-Ala-PABA (**234**) and β -chloro-L-Ala-PABA·TFA salt (**235**). The antibacterial activity of these two compounds was compared and will be discussed in Chapter 4.

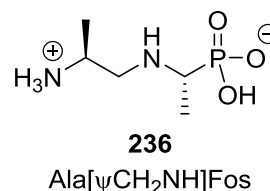
CHAPTER 4

MICROBIOLOGY TESTING

4.1: Introduction

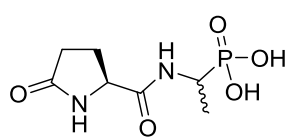
The syntheses of phosphonopeptide derivatives and PABA based derivatives were discussed in Chapters 2 and 3. In this chapter, the antimicrobial activity of each synthesised compound as the diastereoisomeric mixture (Figure 4.1) will be presented: L-Pyroglu-D/L-Fos (**141**), L-Ala-L-Ala-D/L-Fos (**153a**), L-Nva-L-Ala-D/L-Fos (**153b**), Sar-L-Ala-D/L-Fos (**153c**), L-Met-L-Ala-D/L-Fos (**160**), β -chloro-L-Ala-D/L-Fos (**196**), L-Nva- β -chloro-L-Ala-D/L-Fos (**222b**), Sar- β -chloro-L-Ala-D/L-Fos (**222c**), L-Met- β -chloro-L-Ala-D/L-Fos (**225**), and the single enantiomers L-Ala-PABA (**234**) and β -chloro-L-Ala-PABA·TFA salt (**235**). The inhibitory action of these compounds can be realised upon successful uptake of these molecules across the bacterial cell membrane, hydrolysis of specific peptide bonds by aminopeptidases, release of the inhibitor(s) and PABA, and expression of inhibitory effects upon binding of inhibitors or PABA on the target(s). A detailed explanation of these factors was presented in section 1.5.1.

As a result of the incorporation of different moieties or amino acids into the di- and tripeptide derivatives, different intracellular aminopeptidases will be required for the liberation of D/L-fosfalin, β -chloro-L-alanine, and PABA, in order to act on the target enzyme(s). The liberated or free fosfalin is essential for inhibitory action; evidence was obtained for this requirement through the synthesis and evaluation of reduced L-alanyl-L-fosfalin (Ala[ψ CH₂NH]Fos, **236**), which had no antibacterial activity (T-2004MI72).

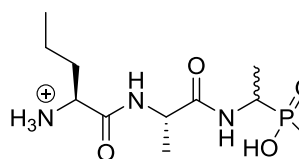


The occurrence of intracellular aminopeptidases varies across the different bacterial species; however, only a few specific aminopeptidases are relevant to this project. L-Alanyl, L-methionyl, L-pyroglutamyl and glycyL aminopeptidases are mainly found in the bacterial cytosol (1996FMR319, 2004AB345) and sometimes in the plasma membrane (e.g. L-alanyl aminopeptidase was found in the plasma membrane of *P. aeruginosa*, 2003AMP217). The presence of these specific aminopeptidases at various locations across different bacterial species also serves as a source of selective inhibition, as inhibitor(s) and PABA will only be liberated in bacteria expressing these enzymes at the specific location.

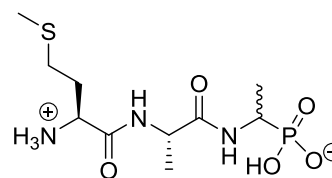
Di- and tripeptide-D/L-Fos derivatives



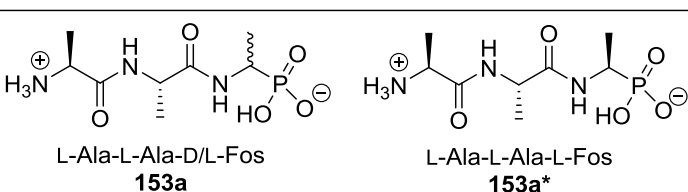
L-Pyroglu-D/L-Fos
141
cLogP: -1.99
TPSA: 115.72



L-Nva-L-Ala-D/L-Fos
153b
cLogP: -4.14
TPSA: 146.19



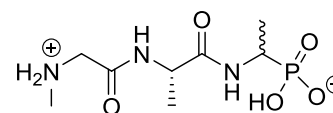
L-Met-L-Ala-D/L-Fos
160
cLogP: -4.58
TPSA: 146.19



L-Ala-L-Ala-D/L-Fos
153a

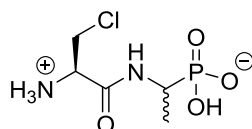
L-Ala-L-Ala-L-Fos
153a*

cLogP: -4.79
TPSA: 146.19

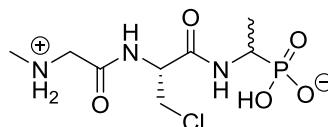


Sar-L-Ala-D/L-Fos
153c
cLogP: -4.91
TPSA: 135.16

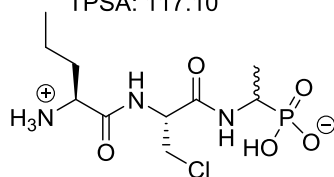
Di- and tripeptide-β-Cl-L-Ala-D/L-Fos derivatives



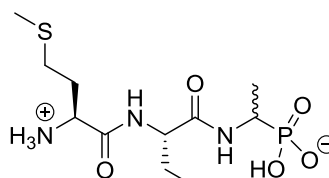
β-Cl-L-Ala-D/L-Fos
196
cLogP: -4.35
TPSA: 117.10



Sar-β-Cl-L-Ala-D/L-Fos
222c
cLogP: -4.79
TPSA: 135.16

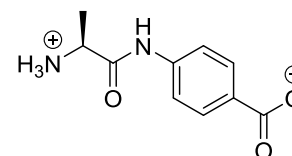


L-Nva-β-Cl-L-Ala-D/L-Fos
222b
cLogP: -3.88
TPSA: 146.19

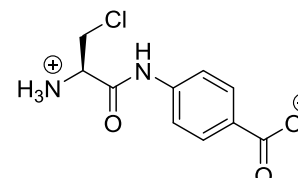


L-Met-β-Cl-L-Ala-D/L-Fos
225
cLogP: -4.42
TPSA: 146.19

Dipeptide-PABA derivatives



L-Ala-PABA
234
cLogP: -2.48
TPSA: 96.87



β-Cl-L-Ala-PABA
235
cLogP: -2.25
TPSA: 96.87

Figure 4.1: Di- and triphosphonopeptide derivatives and dipeptide-PABA derivatives subjected to microbiological evaluation. cLogP and TPSA values were obtained using online molinspiration chemoinformatics (WS-8). β-Chloro-L-Ala-PABA·TFA (**235**) is displayed in its zwitterionic form to reflect the (pH 7.0) of the medium

The liberation of inhibitor(s) from the phosphonopeptide derivatives (**141**, **153a**, **153a*** and **196**) or PABA from dipeptide derivatives (**234** and **235**) is relatively simple, as only one aminopeptidase, L-pyroglutamyl or L-alanyl aminopeptidase, is involved in each case. However, more than one different aminopeptidase are required when dealing with the phosphonotripeptides (**153b**, **153c**, **160**, **222b**, **222c** and **225**), reflecting a narrow inhibitory activity might be anticipated. Removal of the amino acid (L-Nva, L-Met and Sar) at the *N*-terminus of the phosphonotripeptides most likely requires different aminopeptidases prior to the action of L-alanyl aminopeptidase for the liberation of inhibitors D/L-fosfalin and β -chloro-L-alanine. Although the aminopeptidase activity is generally believed to be specific, amino acid analogues that resemble the natural amino acids found in bacteria could also utilise the same aminopeptidases. For instance, sarcosine is an analogue of glycine, L-norvaline is an analogue of L-methionine and β -chloro-L-alanine is an analogue of L-alanine, such that each analogue could be susceptible to glycylyl, L-methionyl and L-alanyl aminopeptidase activities, respectively.

The presence of different moieties coupled to the *N*-terminus of the inhibitors or PABA is not only able to improve selective inhibition, but also affects the lipophilicity of the molecules and therefore their membrane permeability across the bacterial cells. Membrane permeability of a molecule is associated with common molecular descriptors, such as logP (partition coefficient), molecular weight and hydrogen bonding acceptors and donors in a molecule, as well as topological polar surface area (TPSA) (2012M5095). LogP is a measure of the partition coefficient of a molecule equilibrating between octanol and water layers, as a model for the partition of a molecule between the lipophilic plasma membrane and the aqueous external or internal media. The TPSA originated from polar surface area (PSA), a surface sum of all the polar fragments of a molecule, which is an important molecular descriptor that correlates well with passive diffusion of a molecule across the plasma membranes of mammalian cells (2000JMC3714). These two descriptors can be easily obtained by calculation and can be usefully associated with the membrane permeability of the tested compounds. The logP and TPSA values of the tested molecules (Figure 4.1) were calculated using online software Molinspiration (WS-8).

LogP and TPSA are useful molecular descriptors that are frequently used for prediction of oral bioavailability of a drug and relates to mammalian cells, such as intestinal cells (1999PR1520) and the blood-brain barrier (1999PR1514). Although it is recognised that bacterial cells have extra barriers, the cell wall and outer membrane, these molecular descriptors were recently used to rationalise the results of bacterial-targeted drugs (2015BMC5218, 2011IJAA70). By comparing the physicochemical properties of the human and bacterial targeted drugs, it was observed that antibacterial action through targeting the riboproteins did not comply with Lipinski's rules (1997ADDR3); instead higher molecular weight (>500 Da), lower clogP (<-8.4) and higher PSA (>130 Å²) were preferable for better activity. For instance, a very low lipophilicity of the three aminoglycosides, neomycin (clogP -8.96), amikacin (clogP -8.43) and paromomycin (clogP -8.67) was reported by Mugumbate (2015BMC5218). For the non-riboprotein-targeted bacterial inhibitors or bacterial protein-targeted ligands, small and moderately lipophilic compounds with low molecular weight (<500 Da), low PSA (<130 Å²) and less lipophilicity (lower clogP) than ligands targeting human proteins were reported (2015BMC5218).

The usefulness of clogP and TPSA values enables the prediction of molecular ability to cross biological membranes *via* passive diffusion and may correlate with any antibacterial activity observed from the tested compounds. The permeability of these compounds (Figure 4.1) is likely to be affected by these descriptors; however, their uptake across the bacterial cells is likely to exploit active transport, *via* the di- and tripeptide permeases. Although these di- and tri-peptide analogues are likely to exploit the di- and tri-peptide permeases for entry into bacterial cells, the mode of entry has not been investigated as part of the current work and passive transport across the bacterial cell wall, as well as access *via* porins, cannot be excluded. A brief explanation of both passive and active transports have been presented in section 1.5.1, when it was noted that lipophilicity is equally important for both passive and active transport across the bacterial cell wall.

In this chapter, the inhibitory potency, selectivity and feasibility of incorporating these compounds into a growth medium for commercial development of selective culture media will be discussed based upon the microbiological testing of these compounds (Figure 4.1). The testing was performed in collaboration with Professor John Perry, Clinical Microbiologist at the Freeman Hospital, Newcastle upon Tyne. The inhibitory profile of these compounds was generated upon testing against a set of commensal, pathogenic and β -lactam resistant bacteria, which are commonly encountered in human clinical samples. The methodology that was reported by Atherton (1979AAC677) was adapted, with slight modifications for culture medium preparation, while the different bacterial strains were mainly acquired from the National Collection of Type Cultures (NCTC) and American Type Culture Collection (ATCC). The details of the preparations are described in Chapter 6 (section 6.4).

4.2: Antibacterial activity of L-Ala-L-Ala-L-Fos (153a*) and L-Ala-L-Ala-D/L-Fos (153a)

Initial microbiology evaluation of L-Ala-L-Ala-L-Fos (**153a***) was performed by Váradi (T-2013MI192) against a set of clinical bacteria: commensal and pathogenic bacteria and β -lactam resistant bacteria (Classes A-D, Table 6.2). Good inhibitory activity was observed (Table 4.1), providing evidence for the successful cleavage of the amide bond and the release of L-fosfalin to impose inhibitory action on the selected bacterial strains. A comparison between the optically pure **153a*** and diastereoisomeric mixture **153a** was made in order to determine the potency or effects of phosphonopeptide derivatives containing a racemic fosfalin moiety (D/L-fosfalin).

In this parallel comparison (Table 4.1), it can be seen that L-Ala-L-Ala-L-Fos (**153a***) had twice the potency of L-Ala-L-Ala-D/L-Fos (**153a**), suggesting that only the L,L,L-diastereoisomer possesses potent growth inhibitory activity. This finding is supported by Atherton's work, which claimed that L-stereochemistry was essential for phosphonopeptides to exhibit *in vitro* antibacterial activity (1986JMC29). It may be expected that the intracellular peptidase is stereospecific,

restricting hydrolysis to the peptide bond of the peptide derivatives in a L-stereochemical form (1983JMC1733).

Table 4.1: Minimum inhibitory concentration of L-Ala-L-Ala-L-fosfalin (**153a***) and diastereoisomeric L-Ala-L-Ala-D/L-fosfalin (**153a**) against selected pathogenic bacteria

Species		MIC (mg/L) after 22hrs	
		153a*	153a
Gram negative bacteria			
<i>P. rettgeri</i>	NCTC7475	>32	>32
<i>P. aeruginosa</i>	NCTC10662	16	32
<i>S. enteritidis</i>	NCTC6676	>32	>32
<i>S. typhimurium</i>	NCTC74	16	32
<i>S. marcescens</i>	NCTC10211	0.125	0.25
<i>C. freundii</i> **	NDM	32	>32
<i>E. cloacae</i> **	CTX-M9	4	16
<i>E. cloacae</i> **	NDM	32	>32
<i>E. coli</i> **	NDM	0.25	0.5
<i>E. coli</i> **	OXA-48	0.125	0.5
<i>E. coli</i> **	LAT-4	<0.063	0.125
<i>E. coli</i> **	TEM52	4	8
<i>K. pneumoniae</i> **	OXA-48	4	16
<i>K. pneumoniae</i> **	NDM	0.5	1
<i>K. pneumoniae</i> **	KPC-4	16	32
Gram positive bacteria			
<i>E. faecalis</i>	NCTC775	<0.063	<0.063
<i>E. faecium</i>	NCTC7171	0.5	1
<i>S. aureus</i>	NCTC6571	0.5	2
<i>S. aureus</i> (MRSA)	NCTC11939	8	16
<i>S. pyogenes</i>	NCTC8306	>32	32

**β-Lactam resistant bacteria with classification and acquisition stated in Table 6.2

Note: Negative and positive controls, two plates: one containing suicide substrates only and one containing bacteria only were performed. As the bacterial strains used were obtained from NCTC, they have established antibacterial susceptibility and these were not repeated in these experiments. The susceptibility testing of NCTC bacteria were established by standardised methods (2001JAC5). For the β-lactam resistant bacteria**, on the other hand, their antibacterial susceptibility have not been performed

As previously discussed (section 1.5.1), significant antibacterial activity requires the uptake of target compounds across the bacterial cell membrane, release of inhibitor(s) and interaction between inhibitor(s) and target enzyme(s). L-Alanine aminopeptidase is found more readily in Gram negative bacteria over Gram positive bacteria (2007BMCL1418) and liberation of fosfalin upon hydrolysis of the L-alanyl peptide bond of **153a*** and **153a** and exhibition of antibacterial activity would be anticipated in Gram negative bacteria alone. However, only negligible antibacterial activity was seen against *S. typhimurium* and *P. aeruginosa*, with almost no inhibition of *P. rettgeri* and *S. enteritidis*. These poor inhibitory activities were consistent with Perry's findings, that no detectable alafosfalin inhibitory activity against *Acinetobacter*, *Pseudomonas*, *Proteus*, *Providencia* and *Morganella* was observed (2002JCM3913).

The different inhibitory activities could be also due to different rates of transportation of inhibitors across the cell membrane of different bacterial strains. Some bacteria secrete extracellular peptidases and periplasmic peptidases that could potentially inactivate **153a*** and **153a** before they enter the bacteria. For instance, different extracellular endopeptidases, periplasmic aminopeptidases and plasma membrane L-alanyl aminopeptidase were found in *P. aeruginosa* (2001JBC43645, 2003AMP217), which may be able to hydrolyse the L-alanyl peptide bonds of **153a*** and **153a** extracellularly, releasing the fosfalin inhibitor prior to entering the cell. This extracellularly liberated fosfalin is unable to penetrate the cell membrane itself due to its multiply ionised structure (1995AEM226), thus reducing inhibitory action. The presence of efflux pumps and biofilm formation in *P. aeruginosa* also potentially reduces the likelihood of **153a*** and **153a** crossing the cell membrane and having inhibitory activity (2013V223).

Phosphonotripeptides **153a*** and **153a** were also found to be active against most of the Gram negative β -lactam resistant strains. However, some of the bacteria, *C. freundii* (NDM), *E. cloacae* (NDM) and *K. pneumoniae* (KPC-4) were less susceptible to **153a*** and **153a** inhibition. Moderate antibacterial activity of alafosfalin against the growth of the non- β -lactam resistant bacteria, *Citrobacter spp.* (mean MIC: 2.8 mg/L), *Enterobacter spp.* (mean MIC: 6.4 mg/L) and *Klebsiella spp.* (mean MIC: 3.2 mg/L), reported by Perry (2002JCM3913),

suggesting that the negligible inhibitory action of **153a*** and **153a** against these β -lactam resistant bacteria is likely to be due to the presence of other resistance mechanisms, as discussed previously (Section 1.1), such as efflux pumps, hydrolysing enzymes and different cell wall morphology, which could also diminish the likelihood of these compounds entering the bacterial cell.

Although L-alanine aminopeptidase is believed to be found mainly in Gram negative bacteria, the inhibitory effects of **153a*** and **153a** also extended to some Gram positive bacteria, such as *E. faecalis*, *E. faecium*, *S. aureus* and *S. aureus* (MRSA), suggesting the likely presence of L-alanine aminopeptidase in these selected Gram positive bacteria. This finding was consistent with the evidence reported by Cellier (2014BMC5249), who claimed the detection of a chromogenic response upon hydrolysis of the L-alanyl aminopeptidase substrates by *E. faecalis* and *E. faecium*. The presence of this enzymatic activity in *Staphylococcus spp.*, *Streptococcus spp.* and *E. faecalis* was also reported by Hoosain (2009LAM675).

4.3: Antibacterial activity of L-Pyroglu-D/L-Fos (141), L-Nva-L-Ala-D/L-Fos (153b), Sar-L-Ala-D/L-Fos (153c) and L-Met-L-Ala-D/L-Fos (160)

According to the results (Table 4.1), the antibacterial potency of the phosphonopeptide derivative containing racemic fosfalin, L-Ala-L-Ala-D/L-Fos (**153a**), was generally half that of the phosphonopeptide derivative containing optically pure L-fosfalin, L-Ala-L-Ala-L-Fos (**153a***). This constructive finding allows further development of other phosphonopeptide derivatives containing the economically favourable racemic fosfalin rather than the expensive enantiomerically pure L-fosfalin. To investigate other phosphonopeptide derivatives containing racemic fosfalin, four examples (**141**, **153b**, **153c** and **160**) were synthesised for microbiology evaluation; their MIC results are summarised in Table 4.2. These compounds were of interest for microbiology evaluation due to the reasons discussed in section 1.5.4.

Table 4.2: Minimum inhibitory concentration of diastereoisomeric L-Pyroglu-D/L-fosfalin (**141**), L-Nva-L-Ala-D/L-fosfalin (**153b**), Sar-L-Ala-D/L-fosfalin (**153c**) and L-Met-L-Ala-L-fosfalin (**160**) against selected pathogenic bacteria

Species		MIC (mg/L) after 22hrs			
		141	153b	153c	160
Gram negative bacteria					
<i>A. baumannii</i>	ATCC 19606	>128	>8	>8	>8
<i>B. cepacia</i>	ATCC 25416	>128	>8	>8	>8
<i>E. cloacae</i>	NCTC 11936	>128	>8	>8	>8
<i>E. coli</i>	NCTC 10418	8	2	>8	1
<i>E. coli</i>	NCTC 12241	16	2	8	2
<i>K. pneumoniae</i>	NCTC 9528	2	0.5	2	0.25
<i>P. rettgeri</i>	NCTC 7475	>128	>8	>8	>8
<i>P. aeruginosa</i>	NCTC 10662	>128	>8	>8	>8
<i>S. typhimurium</i>	NCTC 74	128	>8	>8	>8
<i>S. enteritidis</i>	NCTC 6676	>128	>8	>8	>8
<i>S. marcescens</i>	NCTC 10211	16	0.25	1	0.25
<i>Y. enterocolitica</i>	NCTC 11176	32	0.25	0.25	0.25
Gram positive bacteria					
<i>B. subtilis</i>	NCTC9372	<0.125	NT	NT	NT
<i>E. faecalis</i>	NCTC 775	16	0.063	4	0.063
<i>E. faecium</i>	NCTC 7171	64	2	>8	2
<i>L. monocytogenes</i>	NCTC 11994	>128	>8	>8	>8
<i>S. epidermidis</i>	NCTC 11047	<0.125	1	>8	2
<i>S. aureus</i>	NCTC 6571	4	2	>8	0.5
<i>S. aureus</i> (MRSA)	NCTC 11939	32	>8	>8	4
<i>S. pyogenes</i>	NCTC 8306	2	NT	>8	>8

NT: Not tested because they were tested on different day and no growth on positive control

Note: Negative and positive controls, two plates: one containing suicide substrates only and one containing bacteria only were performed. As the bacterial strains used were obtained from NCTC and ATCC, they have established antibacterial susceptibility and these were not repeated in these experiments. The susceptibility testing of NCTC and ATCC bacteria was established by standardised methods (2001JAC5)

In this parallel comparison (Table 4.2), similar inhibitory profiles were observed, as these phosphonopeptide derivatives (**141**, **153b**, **153c** and **160**) inhibited almost the same bacterial strains, presumably due to the release of fosfalin. However, different levels of antibacterial activity were observed. L-Pyroglu-D/L-Fos (**141**) had generally high MIC values compared to phosphonotripeptides **153b** and **160**. Although the MIC values of **141** were high, some inhibitory activity was observed on both Gram positive and Gram negative bacteria. This is likely due to the presence of the L-pyroglutamyl peptide bond of **141**, which is specifically hydrolysed by bacteria expressing L-pyroglutamyl aminopeptidase. Unlike L-alanine aminopeptidase, which is mainly expressed by Gram negative bacteria, the presence of L-pyroglutamyl aminopeptidase reflects the inhibited Gram negative and Gram positive bacteria. For instance, expression of L-pyroglutamyl aminopeptidase in the genera *Bacillus*, *Streptococcus*, *Staphylococcus*, *Micrococcus*, *Sarcina*, *Neisseria* and *Pseudomonas* was reported by Mulczyk (1970JGM9). More bacterial genera were later discovered with this enzymatic expression, such as Group A *Streptococci* and *Enterococci* (1987DMID283), *Citrobacter*, *Yersinia* and *Serratia spp.* (1996JCM1811).

High MIC values that reflect low inhibitory activity of L-Pyroglu-D/L-Fos (**141**) against *K. pneumonia*, *S. marcescens*, *Y. enterocolitica*, *E. faecalis*, *E. faecium*, *S. aureus*, *S. aureus* (MRSA) and *S. pyogenes* were observed, though L-pyroglutamyl aminopeptidase is reported to be present in these genera. This suggests that the expression of this enzyme, or the rate of **141** transportation, can vary between the different bacteria. For instance, the growth of *S. epidermidis*, *S. aureus* and *S. aureus* (MRSA) was inhibited differently, even though these bacteria are from the same genera. There was no inhibitory activity of *E. cloacae* observed, although L-pyroglutamyl aminopeptidase was reported in this bacterium (1994P34). This could be due to the ability of this bacterium to form a biofilm (2012FM887) and expression of efflux pumps (2007AAC3247, 2011AM759), both of which can potentially restrict cell permeability and the uptake of **141**. Although there is no current literature supporting the presence of L-pyroglutamyl aminopeptidase in *E. coli*, the MIC results observed suggest that this enzyme could be present with low expression.

Although the inhibitory activity of L-Nva-L-Ala-D/L-Fos (**153b**), Sar-L-Ala-D/L-Fos (**153c**) and L-Met-L-Ala-D/L-Fos (**160**) was not tested against the growth of *B. subtilis*, the low MIC value of L-Pyroglu-D/L-Fos (**141**) showed selective inhibition with good potency. The low MIC value observed on this bacterium not only suggests the presence of L-pyroglutamyl aminopeptidase, but also the expression of alanine racemase, which is the inhibition target of fosfalin. *B. subtilis* is prone to spore formation in response to nutrient limitations or harsh conditions (2011JB4075); an outermost layer, known as exosporium, is commonly found surrounding the *B. subtilis* spores for extra protection. The expression of alanine racemase found in the exosporium of *B. subtilis* (2000AA375) may explain the good potency against this bacterium in comparison to bacteria expressing cytosolic alanine racemase.

Although the MIC value of L-Pyroglu-D/L-Fos (**141**) was generally high, its high potency against the growth of *B. subtilis* and *S. epidermidis* also offers selective inhibition of these bacteria. The selective inhibition by **141** against the growth of *B. subtilis* offers a great finding as it can be used to improve the reliability of identification and detection of *L. monocytogenes*. The growth of *L. monocytogenes* in culture can be greatly influenced by the presence of *B. subtilis* (2013MR125), which has the ability to produce surfactin, an antibacterial agent that dissolves the bacterial phospholipid bilayer cell membrane, leading to cell death (1999AMB553) and under-estimation of *L. monocytogenes* numbers. The application of **141** can prevent potential false results obtained due to the presence of *B. subtilis* in a sample containing *L. monocytogenes*.

As discussed previously (section 4.1), unlike L-Ala-L-Ala-L-Fos (**153a***) and L-Ala-L-Ala-D/L-Fos (**153a**), L-Nva-L-Ala-D/L-Fos (**153b**), Sar-L-Ala-D/L-Fos (**153c**) and L-Met-L-Ala-D/L-Fos (**160**) would rely on other aminopeptidases to liberate the L-Ala-D/L-Fos moiety prior to the L-alanyl aminopeptidase hydrolysis. Depending on the nature of the *N*-terminal amino acids of the phosphonotripeptides (**153b**, **153c** and **160**), the rates of hydrolysis and antibacterial activities would be expected to be different, which was the case (Table 4.2). For instance, weak inhibitory activity of **153c** was observed on most species compared to **153b** and **160**. This finding was consistent with Atherton's work, in which similar low inhibitory activity of Sar-L-Ala-

L-fosfalin was reported (1980ACC897). However, good antibacterial activity of Sar-L-Nva-L-fosfalin, Sar-L-Ala-L-Ala-L-fosfalin and Sar-L-Nva-L-Nva-L-fosfalin was noted and, of these sarcosyl phosphono-peptides, Sar-L-Ala-L-Ala-L-fosfalin and Sar-L-Nva-L-Nva-L-fosfalin showed good potency against the respiratory tract pathogens, *H. influenzae*, *S. pneumoniae* and *S. pyogenes* (1980ACC897). There is limited explanation on these findings; however, it is believed that these sarcosyl phosphono-peptides could be subjected to different rates of transport and intracellular hydrolysis in the bacterial cell.

Aside from different rates of intracellular hydrolysis of L-Nva-L-Ala-D/L-Fos (**153b**), Sar-L-Ala-D/L-Fos (**153c**) and L-Met-L-Ala-D/L-Fos (**160**), poor transportation of **153c** across the bacterial cell membrane due to low lipophilicity compared to **153b** and **160** could also potentially result in poor inhibitory effects. The low lipophilicity of **153c** was evident in the previous LC-MS analysis (Figure 2.5), where a short retention time resulting from the weak interaction between the **153c** analyte and the C-18 (non-polar) stationary phase was observed. This finding is also consistent with the calculated logP values (Figure 4.1), in which a low clogP value of **153c** (-4.91) was noted compared to the clogP values of **153b** (-4.14) and **160** (-4.58).

As a result of the absence of a long hydrophobic side chain from the α -carbon and the presence of the *N*-methyl group of the sarcosine amino acid (**153c**), it is not a surprise to see weak antibacterial effects, probably due to poor transportation. Poor uptake was also noted in the literature, which claims that the protein permeases favour the transportation of peptides with large and/or hydrophobic side chains (2012EMBO3411, 2013PNAS11343). Although the polarity of L-Ala-L-Ala-D/L-Fos (**153a**) and **153c** was similar according to LC-MS analysis (Figure 2.5), their transportation could vary due to their different clogP and TPSA values, as well as the absence of α -carbon side chain. With a higher calculated lipophilicity, the uptake of **153a** (clogP -4.79) could be expected to be better than that of **153c** (clogP -4.91) if relying heavily in passive transportation.

As discussed previously, L-alanine aminopeptidase is found mainly in Gram negative and some selected Gram positive bacteria. Comparing between L-Ala-L-

Ala-D/L-Fos (**153a**), L-Nva-L-Ala-D/L-Fos (**153b**) and L-Met-L-Ala-D/L-Fos (**160**), consistent inhibition of Gram positive bacteria, *E. faecalis*, *E. faecium*, *S. aureus* and *S. aureus* (MRSA) was noted, further supporting the previous conclusion that expression of L-alanine aminopeptidase is consistently found in these bacteria. The growth inhibition of *S. epidermidis* was also observed and this could be also due to the presence of L-alanine aminopeptidase, as this enzyme is found in *Staphylococcus spp.* (2009LAM675).

Although the expression of L-alanine aminopeptidase is found in Gram negative bacteria, the inhibitory effects of these phosphonopeptides varied among different Gram negative bacteria. For instance, no antibacterial activities of L-Nva-L-Ala-D/L-Fos (**153b**) and L-Met-L-Ala-D/L-Fos (**160**) were observed on *A. baumannii*, *B. cepacia*, *E. cloacae*, *P. rettgeri*, *P. aeruginosa*, *S. typhimurium* and *S. enteritidis*. The absence of antibacterial activity could be due to poor transportation of **153b** and **160**, as the uptake could be greatly affected by the presence of extracellular and periplasmic aminopeptidases, efflux pumps and biofilm formation in some of these species (2001JBC43645, 2011AM759, 2012FM887). Inability to hydrolyse *N*-L-Nva and *N*-L-Met derivatives, due to the lack of appropriate enzymes could also account for no inhibitory activity.

The inhibitory potency of L-Met-L-Ala-D/L-Fos (**160**) on some bacteria was higher than that of L-Nva-L-Ala-D/L-Fos (**153b**), as relatively low MIC values were noted with *K. pneumoniae*, *S. aureus* and *S. aureus* (MRSA). This suggests that the presence of the thioether group or sulphur atom could improve the uptake of **160** across the cell membrane due to peptides with large and/or hydrophobic side chains being favoured (2012EMBO3411, 2013PNAS11343), followed by the subsequent intracellular hydrolysis. Although the inhibitory effect of Sar-L-Ala-D/L-Fos (**153c**) was weak, its good potency against the growth of *Y. enterocolitica* (MIC: 0.25 mg/L) over other bacterial strains offers selective inhibition of this bacterium.

4.4: Antibacterial activity of β -Cl-L-Ala-D/L-Fos (196), L-Nva- β -Cl-L-Ala-D/L-Fos (222b), Sar- β -Cl-L-Ala-D/L-Fos (222c) and L-Met- β -Cl-L-Ala-D/L-Fos (225)

So far, the antibacterial evaluation of L-Pyroglu-D/L-Fos (141), L-Ala-L-Ala-L-Fos (153a*), L-Ala-L-Ala-D/L-Fos (153a), L-Nva-L-Ala-D/L-Fos (153b), Sar-L-Ala-D/L-Fos (153c) and L-Met-L-Ala-D/L-Fos (160) involves the presence of a single inhibitor, fosfalin. The good antibacterial activities of some phosphonotripeptides (Table 4.2) justified further investigation with another known alanine racemase inhibitor, β -chloroalanine (2000PAC373). Detailed microbiological evaluation of β -chloroalanine has been well reported by Cheung (1983JMC1733) (1986JMC1733), who also claimed that the β -Cl-L-Ala- β -Cl-L-Ala, incorporating two identical inhibitors, showing a high inhibitory potency against both Gram positive and negative bacteria. However, there was no microbiological evaluation of inhibitors containing two different alanine racemase inhibitors. Therefore, the antibacterial effects of phosphonopeptides containing two different known inhibitors, fosfalin (1998B10438) and β -chloroalanine (2000PAC373), are presented in this section.

The interesting microbiological activities obtained from the previous phosphonopeptide derivatives containing a single inhibitor with different *N*-terminal amino acids, L-Nva, L-Met and Sar (section 4.3), serves as a good starting point for the following syntheses and microbiological comparison. The rationale of using these *N*-terminal amino acids has also been discussed in section 1.5.4. To investigate phosphonopeptide derivatives containing β -chloro-L-alanine and racemic fosfalin, a known example, β -chloro-L-Ala-D/L-Fos (196) (P-2015MI27), and three new examples, L-Nva- β -chloro-L-Ala-D/L-Fos (222b), Sar- β -chloro-L-Ala-D/L-Fos (222c) and L-Met- β -chloro-L-Ala-D/L-Fos (225) (P-2015MI27), were synthesised for microbiological evaluation; their MIC results are summarised in Table 4.3.

Table 4.3: Minimum inhibitory concentration of diastereoisomeric β -chloro-L-Ala-D/L-fosfalin (**196**), L-Nva- β -chloro-L-Ala-D/L-fosfalin (**222b**), Sar- β -chloro-L-Ala-D/L-fosfalin (**222c**) and L-Met- β -chloro-L-Ala-L-fosfalin (**225**) against selected pathogenic bacteria

Species		MIC (mg/L) after 22hrs			
		196	222b	222c	225
Gram negative bacteria					
<i>A. baumannii</i>	ATCC 19606	>128	>8	>8	>8
<i>B. cepacia</i>	ATCC 25416	>128	>8	>8	>8
<i>E. cloacae</i>	NCTC 11936	1	4	>8	4
<i>E. coli</i>	NCTC 10418	0.25	0.5	4	0.5
<i>E. coli</i>	NCTC 12241	<0.125	0.5	4	0.5
<i>K. pneumoniae</i>	NCTC 9528	<0.125	0.25	2	0.5
<i>P. rettgeri</i>	NCTC 7475	16	>8	>8	>8
<i>P. aeruginosa</i>	NCTC 10662	>128	>8	>8	>8
<i>S. typhimurium</i>	NCTC 74	32	>8	>8	>8
<i>S. enteritidis</i>	NCTC 6676	16	>8	>8	>8
<i>S. marcescens</i>	NCTC 10211	4	0.25	2	0.25
<i>Y. enterocolitica</i>	NCTC 11176	0.5	0.25	0.5	0.25
Gram positive bacteria					
<i>B. subtilis</i>	NCTC9372	<0.125	NT	NT	NT
<i>E. faecalis</i>	NCTC 775	16	0.063	4	0.032
<i>E. faecium</i>	NCTC 7171	128	1	>8	1
<i>L. monocytogenes</i>	NCTC 11994	>128	>8	>8	>8
<i>S. epidermidis</i>	NCTC 11047	<0.125	2	>8	1
<i>S. aureus</i>	NCTC 6571	0.5	4	>8	2
<i>S. aureus</i> (MRSA)	NCTC 11939	1	>8	>8	>8
<i>S. pyogenes</i>	NCTC 8306	<0.125	>8	NT	NT

NT: Not tested because they were tested on different day and no growth on positive control

Note: Negative and positive controls, two plates: one containing suicide substrates only and one containing bacteria only were performed. As the bacterial strains used were obtained from NCTC and ATCC, they have established antibacterial susceptibility and these were not repeated in these experiments. The susceptibility testing of NCTC and ATCC bacteria was established by standardised methods (2001JAC5)

In this parallel comparison (Table 4.3), a similar inhibitory profile of β -chloro-L-Ala-D/L-Fos (**196**), L-Nva- β -chloro-L-Ala-D/L-Fos (**222b**) and L-Met- β -chloro-L-Ala-D/L-Fos (**225**) was observed. However, the inhibitory potency of **196** was generally greater than **222b** and **225**. In addition, the inhibitory spectrum of **196** was extended to additional Gram positive bacteria, *S. aureus* (MRSA) and *S. pyogenes*. One source of these varied inhibitory effects could be different rates of intracellular hydrolysis between phosphonodipeptide (**196**) and phosphonotripeptides (**222b**, **222c** and **225**), as additional intracellular aminopeptidases would be required to remove the different *N*-terminal amino acids (L-Nva, Sar and L-Met), for the liberation of the β -chloro-L-Ala-D/L-Fos moiety prior to the hydrolysis by L-alanyl aminopeptidase.

Interestingly, β -chloro-L-Ala-D/L-Fos (**196**) shows high MIC values compared to L-Nva- β -chloro-L-Ala-D/L-Fos (**222b**) and L-Met- β -chloro-L-Ala-D/L-Fos (**225**) against the growth of *S. marcescens*, *E. faecalis* and *E. faecium* (Table 4.3). The different *N*-terminal amino acids with varying side chains and different length (dipeptide/tripeptide) of these phosphonopeptides (**196**, **222b** and **225**) could result in different rates of uptake across the bacterial cell membrane, due to their different lipophilic properties (Figure 4.1). Although these phosphonopeptides may be transported by *via* passive diffusion, their uptake might still depend upon active di- and tripeptide permeases, which prefer peptides with large and/or hydrophobic side chains (2012EMBO3411, 2013PNAS11343). The long side chain of **222b** and **225** could therefore be transported more readily across these bacterial membranes.

If there is improved uptake of peptides with large and/or hydrophobic side chains, it is not surprising to observe different antibacterial activities within the three different phosphonotripeptides, **222b**, **222c** and **225** (Table 4.3). For instance, high MIC values, indicating low potency, of Sar- β -chloro-L-Ala-D/L-Fos (**222c**) were observed and it also showed a different inhibitory profile compared to **222b** and **225**, in which the growth of *E. cloacae*, *E. faecium*, *S. epidermidis* and *S. aureus* was not susceptible to inhibition by **222c**.

Similar inhibitory profiles of L-Nva- β -chloro-L-Ala-D/L-Fos (**222b**) and L-Met- β -chloro-L-Ala-D/L-Fos (**225**) were noted (Table 4.3), although the potency of **225** was slightly higher than that of **222b**, in terms of targeting the Gram positive bacteria. This finding was consistent with the results obtained with the analogous L-Nva-L-Ala-D/L-Fos (**153b**) and L-Met-L-Ala-D/L-Fos (**160**) (Table 4.2), further supporting the idea that both *N*-L-norvalyl and *N*-L-methionyl containing phosphonotripeptide derivatives could be subjected to different rates of transportation across the bacterial cell membranes due to their different length and size of the side chains. For instance, a long side chain with a sulphur atom could influence the uptake of the *N*-L-methionyl phosphonotripeptides and thus their uptake by the tripeptide permeases would be different compared to the *N*-L-norvalyl phosphonotripeptides. The potential of different rates of intracellular hydrolysis of *N*-L-norvalyl and *N*-L-methionyl phosphonotripeptides for the liberation of inhibitor(s) might also account for the different inhibitory effects, due to the absence of bacterial L-norvalyl aminopeptidase. The hydrolysis of *N*-L-norvalyl phosphonotripeptides would probably depend on L-methionyl aminopeptidase, due to the structural similarity of L-norvaline and L-methionine, although it is likely to be a less favourable substrate.

As anticipated, lower MIC values, showing a greater inhibitory potency of phosphonotripeptides containing two inhibitors (Table 4.3) compared to phosphonotripeptides containing the single inhibitor, fosfalin (Table 4.2) were observed. For instance, the MIC values of L-Nva- β -chloro-L-Ala-D/L-Fos (**222b**), Sar- β -chloro-L-Ala-D/L-Fos (**222c**) and L-Met- β -chloro-L-Ala-D/L-Fos (**225**) were almost half those of the corresponding phosphonopeptides containing a single inhibitor, L-Nva-L-Ala-D/L-Fos (**153b**), Sar-L-Ala-D/L-Fos (**153c**) and L-Met-L-Ala-D/L-Fos (**160**), against the growth of *E. coli* (n=2). The observation of inhibitory activity by β -chloroalanyl peptides on both alanine racemase and transaminase B of *E. coli* JSR-O, reported by Cheung (1986JMC2060), provides a possible explanation for the increased inhibition by phosphonopeptides incorporating both β -chloro-L-alanine and fosfalin. Another possible explanation could be the potential inhibition of β -chloro-L-alanine and fosfalin on another target, alanine racemase (dadB), due to their analogous structures to L-alanine. The alanine racemase

(dadB) is different from the constitutive alanine racemase (alr), though both are the source of D-alanine production. A detailed explanation of these two alanine racemases was made in section 1.4.1.

It is therefore not surprising to see the extended inhibitory spectrum of L-Nva- β -chloro-L-Ala-D/L-Fos (**222b**) and L-Met- β -chloro-L-Ala-D/L-Fos (**225**) against the growth of *E. cloacae*, compared to L-Nva-L-Ala-D/L-Fos (**153b**) and L-Met-L-Ala-D/L-Fos (**160**). However, this bacterium was not susceptible to Sar- β -chloro-L-Ala-D/L-Fos (**222c**) inhibition, which could be again due to the poor uptake of **222c** by the tripeptide permeases as mentioned previously.

The similar inhibitory and activity profiles of the various phosphonopeptides reported in Tables 4.1, 4.2 and 4.3 provide evidence that these analogous inhibitors act by a similar mechanism involving the release of phosphonodipeptides, L-Ala-D/L-Fos and β -chloro-L-Ala-D/L-Fos, followed by the L-alanyl aminopeptidase activity to release D/L-fosfalin and either L-alanine or β -chloro-L-alanine. Their activity against several Gram positive bacteria, as well as the expected Gram negative bacteria, further supports the observation of L-alanyl aminopeptidase activity in some Gram positive species. Although the potency of phosphonopeptides containing two inhibitors (**196**, **222b**, **222c** and **225**) was generally greater than the phosphonopeptides containing a single inhibitor (**141**, **153b**, **153c** and **160**), there was still little or no inhibitory action observed on some Gram negative bacteria (Table 4.3). This suggested that besides the different rates of uptake facilitated by active peptide transport, other elements including lack of porins, presence of efflux pumps and biofilm formation could also account for the negligible inhibitory effects. Similarly, the lack of inhibitory activity noted on *A. baumannii*, *B. cepacia* and *P. aeruginosa* may be due to their ability for biofilm formation and their lack of porins (2010IJAA219, 2010FM1087, 2013V223).

The enhancement of inhibitory potency against the growth of certain Gram negative bacteria and potent inhibition of *E. cloacae* were noted upon incorporation of two different inhibitors into phosphonopeptides (except **222c**), suggesting a potential application for these β -chloro-L-alanyl phosphonopeptides

(except **222c**) in the selective inhibition of specific Gram negative bacteria, particularly *E. cloacae*, *E. coli* (n=2), *K. pneumoniae*, *S. marcescens* and *Y. enterocolitica* in bacterial culture of clinical samples. These findings are useful for the enhancement of the detection and identification of bacterial infections in cystic fibrosis, as these bacteria, *E. cloacae* (2010JCF130), *E. coli* (2014IJMM415), *K. pneumoniae* (1998CID158), *S. marcescens* (1998CID158) are commonly found in cystic fibrosis samples, can be selectively inhibited, and thus prevent overgrowth of *B. cepacia* and *P. aeruginosa* which cause severe lung infections in these patients. Besides that, it can also be useful for detection of *Salmonella spp.* by inhibiting the growth of *E. coli*, which may overgrow *Salmonella spp.* when isolated from stool samples (2002JCM3913), as inhibition of *E. coli* can be selectively achieved at a low concentration (MIC: < 4 mg/L).

4.5: Antibacterial activity of L-Ala-PABA (234) and β -Cl-L-Ala-PABA TFA salt (235)

Aside from the evaluation of alanine racemase inhibitors, fosfalin and β -chloro-L-alanine, another molecule, *para*-aminobenzoic acid (PABA), was also of interest in this work. PABA is an important intermediate for the survival of bacteria. However, the inhibitory action of PABA at high concentration was reported in some literature (section 1.4.3). For instance, the growth of Rickettsiae, *P. aeruginosa* and *E. cloacae* was inhibited at 500-1000 $\mu\text{g/mL}$ (1952Sci710), 1500 $\mu\text{g/mL}$ (1992IJP195) and 1200 $\mu\text{g/mL}$ (1992IJP195), respectively. Further investigation of this effect was made by combining either L-alanine or β -chloro-L-alanine with the PABA moiety.

Due to the enhanced inhibitory effect of phosphonopeptides incorporating β -chloro-L-alanine (Table 4.3), β -chloro-L-alanine was incorporated with the PABA moiety. L-Alanine was also coupled to the PABA moiety for comparison of antibacterial activity. To investigate these PABA based dipeptide derivatives, L-Ala-PABA (**234**) and β -chloro-L-Ala-PABA-TFA (**235**) were synthesised for microbiology evaluation; their MIC results are summarised in Table 4.4.

Table 4.4: Minimum inhibitory concentration (MIC) of L-Ala-PABA (**234**), β -chloro-L-Ala-PABA-TFA (**235**) against selected pathogenic bacteria

Species		MIC (mg/L) after 22hrs	
		234	235
Gram negative bacteria			
<i>A. baumannii</i>	ATCC19606	>128	>128
<i>B. cepacia</i>	ATCC25416	>128	>128
<i>E. cloacae</i>	NCTC11936	>128	>128
<i>E. coli</i>	NCTC10418	>128	>128
<i>E. coli</i>	NCTC12241	>128	>128
<i>K. pneumoniae</i>	NCTC9528	>128	>128
<i>P. rettgeri</i>	NCTC7475	>128	>128
<i>P. aeruginosa</i>	NCTC10662	>128	>128
<i>S. typhimurium</i>	NCTC74	>128	>128
<i>S. enteritidis</i>	NCTC6676	>128	>128
<i>S. marcescens</i>	NCTC10211	>128	>128
<i>Y. enterocolitica</i>	NCTC11176	>128	>128
Gram positive bacteria			
<i>B. subtilis</i>	NCTC9372	4	<1
<i>E. faecalis</i>	NCTC775	>128	16
<i>E. faecium</i>	NCTC7171	>128	>128
<i>L. monocytogenes</i>	NCTC11994	>128	>128
<i>S. epidermidis</i>	NCTC11047	>128	>128
<i>S. aureus</i>	NCTC6571	32	>128
<i>S. aureus</i> (MRSA)	NCTC11939	32	>128
<i>S. pyogenes</i>	NCTC8306	>128	32

Note: Negative and positive controls, two plates: one containing suicide substrates only and one containing bacteria only were performed. As the bacterial strains used were obtained from NCTC and ATCC, they have established antibacterial susceptibility and these were not repeated in these experiments. The susceptibility testing of NCTC and ATCC bacteria was established by standardised methods (2001JAC5)

According to the microbiology results (Table 4.4), both L-Ala-PABA (**234**) and β -chloro-L-Ala-PABA-TFA (**235**) were not active and there was no inhibition against all tested strains of Gram negative bacteria, although β -chloro-L-alanine is known to have some antibacterial effects against certain Gram negative bacteria as seen previously (Table 4.3). It is not surprising to observe no inhibitory activity on *A. baumannii*, *B. cepacia* and *P. aeruginosa*, due to their ability for biofilm formation (2010IJAA219, 2010FM1087, 2013V223), which can reduce the permeability of **234** and **235** across the cell membrane. However, the total absence of antibacterial activity on all the tested Gram negative bacteria suggested that the presence of the PABA moiety could have potentially restricted the uptake of these molecules (**234** and **235**) across these bacterial cell membranes, due to the presence of an outer membrane. Aside from the poor transportation, inefficient liberation of β -chloro-L-alanine and PABA moieties within the bacterial cell could also account for the total absence of antibacterial effects on Gram negative bacteria.

Although the growth of Gram negative bacteria was not inhibited by the L-Ala-PABA (**234**) and β -chloro-L-Ala-PABA-TFA (**235**), the limited antibacterial activities noted on Gram positive bacteria, such as *B. subtilis*, *E. faecalis*, *S. aureus*, *S. aureus* (MRSA) and *S. pyogenes* further supported the previous assumption made, that is the presence of the outer membrane on the Gram negative bacteria could impose an extra barrier for the uptake of these dipeptide derivatives (**234** and **235**). The uptake of these molecules was less affected in the absence of this barrier in the Gram positive bacteria.

Depending on the tested molecule (**234** or **235**), a different inhibitory profile was observed against the growth of these tested Gram positive bacteria (Table 4.4). For instance, inhibition of the growth of *B. subtilis*, *S. aureus* and *S. aureus* (MRSA) by **234** was noted, while **235** inhibited the growth of *B. subtilis*, *E. faecalis* and *S. pyogenes* more strongly. The different inhibitory profiles observed could be due to the different side chains of *N*-terminal amino acids coupled to the PABA moiety, as the presence of a chlorine atom can change the lipophilic properties of the molecules and therefore the uptake of **234** (clogP -2.48) and **235** (clogP -2.25)

across the bacterial cells was observed differently. The different inhibitory activity observed by these molecules suggested that *B. subtilis*, *E. faecalis* and *S. pyogenes* could have favoured the uptake of a good lipophilic molecule (**235**), while *S. aureus* and *S. aureus* (MRSA) could have preferred the uptake of the less lipophilic molecule (**234**).

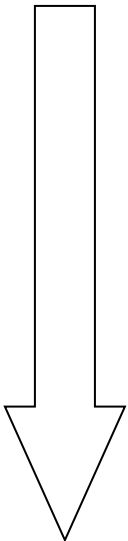
In general, the high MIC values (except against *B. subtilis*) and low inhibitory effect observed (Table 4.4) were consistent with Davis's findings, who claimed that inhibition by PABA took place only at a very high concentration. The role of PABA as an essential precursor in the biosynthesis of tetrahydrofolate at a low concentration (1951JEM243) is likely to be an important reason for its low inhibition of most bacteria. The introduction of a known inhibitor, β -chloro-L-alanine, with PABA showed no inhibitory enhancement against the growth of Gram negative bacteria; however, the growth of *B. subtilis*, *E. faecalis* and *S. pyogenes* was affected. It is surprising to observe a good inhibitory activity against the growth of *B. subtilis* by L-Ala-PABA (**234**) and β -chloro-L-Ala-PABA-TFA (**235**), suggesting the PABA concentration required by this bacterium for the biosynthesis of tetrahydrofolate could be much lower than that of other tested Gram positive bacteria. In other words, the threshold or maximum PABA concentration required by *B. subtilis* for biosynthesis might be low; therefore, it could be easily inhibited by a concentration above the threshold. Although the growth of *B. subtilis* can be inhibited by **234** and **235** at a moderate concentration (MIC: <4 mg/L), the generally high MIC against the growth of all the tested pathogenic bacteria suggest unsuitable use of the PABA based peptide derivatives for most pathogenic and commensal bacteria inhibition.

4.6: Relationship between the physicochemical properties (logP and TPSA) and antibacterial activity of the tested compounds

The antibacterial action of the tested compounds (**141**, **153a-c**, **160**, **196**, **222b-c**, **225**, **234** and **235**) depends upon their inhibitory pharmacophore and ability to cross bacterial cell membranes and act on the target enzyme(s). As discussed previously, the permeability of molecules across the biological membrane depends on their physicochemical properties. Depending on the types of target proteins, human- or bacterial-targeted proteins, different physicochemical properties of a molecule will be expected, due to the different intrinsic properties of human and bacterial cells. For instance, Lipinski's rule of five is usually followed by molecules that target human proteins, while this rule is less important for molecules targeting bacterial proteins. There is limited study showing a favourable range of physicochemical properties is required for good *in vitro* antibacterial activity on bacterial-targeted proteins. Therefore, the physicochemical properties of the tested compounds will be analysed in this section, in order to determine their potential relationship with the antibacterial activity discussed previously (Tables 4.2, 4.3 and 4.4).

The clogP and TPSA values of the tested compounds: L-Pyroglu-D/L-Fos (**141**), L-Ala-L-Ala-D/L-Fos (**153a**), L-Nva-L-Ala-D/L-Fos (**153b**), Sar-L-Ala-D/L-Fos (**153c**), L-Met-L-Ala-D/L-Fos (**160**), β -chloro-L-Ala-D/L-Fos (**196**), L-Nva- β -chloro-L-Ala-D/L-Fos (**222b**), Sar- β -chloro-L-Ala-D/L-Fos (**222c**), L-Met- β -chloro-L-Ala-D/L-Fos (**225**), L-Ala-PABA (**234**) and β -Cl-L-Ala-PABA·TFA (**235**), which were calculated using the online Molinspiration software, are summarised in Table 4.5. Despite the differences in likely targets and mechanisms, a general trend was observed. The compounds are sorted into descending order based on their respective clogP values.

Table 4.5: Summary of physicochemical properties of the tested compounds. Those with low antibacterial activity and generally high MIC are highlighted in yellow

cLog P	Lipophilicity	TPSA	Compounds
-1.99	 Decrease	115.72	L-Pyroglu-D/L-Fos (141)
-2.25		96.87	β -Cl-L-Ala-PABA·TFA (235)
-2.48		96.87	L-Ala-PABA (234)
-3.88		146.19	L-Nva- β -chloro-L-Ala-D/L-Fos (222b)
-4.14		146.19	L-Nva-L-Ala-D/L-Fos (153b)
-4.35		117.10	β -chloro-L-Ala-D/L-Fos (196)
-4.42		146.19	L-Met- β -chloro-L-Ala-D/L-Fos (225)
-4.58		146.19	L-Met-L-Ala-D/L-Fos (160)
-4.79		146.19	L-Ala-L-Ala-D/L-Fos (153a)
-4.79		135.16	Sar- β -chloro-L-Ala-D/L-Fos (222c)
-4.91		135.16	Sar-L-Ala-D/L-Fos (153c)

As discussed previously, the inhibitory potency of the β -chloroalanyl phosphonotripeptides was higher compared to the corresponding phosphonotripeptides. One of the reasons for the inhibitory differences could be due to the presence of a heteroatom, a chlorine atom changes the lipophilicity of the molecules, which was the case (Table 4.5). However, good antibacterial activity is not necessarily linked to high lipophilic properties of a molecule: the high MIC of L-Pyroglu-D/L-Fos (**141**) and the negligible antibacterial activity of L-Ala-PABA (**234**) and β -Cl-L-Ala-PABA·TFA (**235**) were reported, regardless of their high lipophilicity. This suggests that molecules with clogP below -3.88 are required to achieve some antibacterial activities, a finding consistent with the recent study performed by Mugumbate (2015BMC5218), who claimed that bacterial-protein and bacterial-riboprotein inhibitors were generally less lipophilic than the human-protein inhibitors.

Although low clogP was initially thought to improve antibacterial activity, a limitation was noted at clogP below -4.79, seen as weak antibacterial activity of sarcosyl phosphonotripeptides (**153c** and **222c**) with respect to the L-norvalyl and L-methionyl phosphonotripeptides. This suggested that, providing they incorporate

the required pharmacophore, molecules with a clogP value between -3.88 and -4.79 are favoured. No physicochemical comparison can be made between the L-alanyl phosphonotriptide (**153a**) and other phosphonotriptides, due to different bacterial species being tested against **153a**. Therefore, it is difficult to draw a conclusion on whether similar antibacterial activity will be observed between **153a** and Sar- β -chloro-L-Ala-D/L-Fos (**222c**), although both share an identical clogP value. However, different antibacterial activity of **153a** could be anticipated due to its high polar surface area or TPSA value.

Polarity of a molecule surface is also an important element that can also influence the permeability of a molecule, thereby its antibacterial activity. The negligible antibacterial activity of **234** and **235** associated with low polar surface area (TPSA: 96.87 Å²), while some antibacterial activities of **141** (TPSA: 115.72 Å²) were noted, suggesting TPSA above 115 Å² is significant for antibacterial activity, providing the tested compounds retain the required pharmacophore, ability of uptake and release of the inhibitor(s) in the bacterial cell. However, there is a limit of polar surface area when targeting bacterial proteins or non-ribosome proteins. Since fosfalin and β -chloro-L-alanine are inhibitors of alanine racemase, non-riboprotein inhibitors, PSA below 130 Å² is preferable, as reported by Mugumbate (2015BMC5218), who claimed that some bacterial-protein ligands displayed a PSA value below 130 Å². The polar surface area difference between the phosphonotriptides (TPSA >130 Å²) and the phosphonodipeptides (TPSA <130 Å²) is likely to be one of the reasons for the high inhibitory potency of β -chloro-L-Ala-D/L-Fos (**196**) reported previously, compared to other tested phosphonotriptides (**153a**, **153b**, **153c**, **160**, **222b**, **222c** and **225**).

Interestingly, although the TPSA value of L-Pyroglu-D/L-Fos (**141**) was similar to that of β -chloro-L-Ala-D/L-Fos (**196**), the inhibitory potency of **141** was low, suggesting both lipophilic and polar surface area properties are equally significant for permeability of a molecule and antibacterial activity. Although the polar surface area of the tested phosphonotriptides (**153a-c**, **196**, **222b-c**, **225**) was generally above 130 Å² and above the limit reported by Mugumbate (2015BMC5218), antibacterial activity of these phosphonotriptides noted previously (sections 4.2,

4.3 and 4.4), suggests that the antibacterial activity of the tested compounds was not entirely depending on the physicochemical factors only, but other factors, such as inhibitory pharmacophore of the molecules, ability of uptake by the active transport proteins, release of the inhibitor(s) at the appropriate location(s) and acting on the target enzyme(s).

In a nutshell, clogP and TPSA are important physicochemical properties to predict the permeability of a molecule across the bacterial cells and associate with the antibacterial activity as discussed above; however, the antibacterial activity of the tested compounds also relies on the active transport, the ease of liberation of the inhibitors, fosfalin and β -chloro-L-alanine, and PABA at the appropriate location(s), as well as their important pharmacophore.

4.7: Conclusion

The release of D/L-fosfalin and β -chloro-L-alanine inhibitors and PABA from dipeptide derivatives L-Ala-D/L-Fos, β -chloro-L-Ala-D/L-Fos, L-Ala-PABA and β -chloro-L-Ala-PABA, is dependent on the presence of L-alanyl aminopeptidase. This enzymatic activity is significant as it determines whether or not the inhibitory action of the tested molecules will be possible. The expression of this enzyme is mainly reported in Gram negative bacteria; however, the inhibitory activity observed from Tables 4.1, 4.2, 4.3 and 4.4, shows the expression of L-alanyl aminopeptidase in some Gram positive bacteria.

The phosphonotripeptide containing racemic fosfalin, L-Ala-L-Ala-D/L-Fos (**153a**) showed a similar inhibitory profile to that of the phosphonotripeptide containing optically pure fosfalin, L-Ala-L-Ala-L-Fos (**153a***). Although the potency of **153a*** was almost twice that of **153a**, it indicates the significance of L-stereochemistry of the fosfalin moiety. The similar inhibitory profiles support the use of D/L-fosfalin, which is cheaper and easy to synthesise.

A similar inhibitory profile against the growth of Gram negative bacteria was noted on phosphonotripeptides containing D/L-fosfalin (**153b**, **153c** and **160**) and phosphono-peptides containing D/L-fosfalin and β -chloro-L-alanine (**196**, **222b**,

222c and **225**). However, low inhibitory potency observed with sarcosyl based phosphonotripeptides (**153c** and **222c**), shows that the presence of a free amino group (-NH₂) rather than methylamino (-NHMe) group at *N*-terminus of phosphonotripeptides may facilitate uptake across the bacterial cells, while the enhancement of inhibitory potency noted with L-norvalyl and L-methionyl based phosphonotripeptides (**153b**, **160**, **222b** and **225**) is likely due to the presence of a long α -carbon side chain at the *N*-terminal amino acid of phosphonopeptides and their relatively high clogP values compared to **153c** and **222c**.

The inhibitory potency of L-Pyroglu-D/L-fosfalin (**141**) was low compared to the phosphonotripeptides containing D/L-fosfalin (**153b**, **153c** and **160**). However, selective inhibition was noted on bacteria which express L-pyroglutamyl aminopeptidase, such as *E. coli*, *K. pneumoniae*, *S. marcescens*, *Y. enterocolitica*, *B. subtilis*, *E. faecalis*, *E. faecium*, *S. epidermidis*, *S. aureus*, *S. aureus* (MRSA) and *S. pyogenes*. This finding is important for the selective inhibition of some *Enterobacteriaceae* (e.g. *Escherichia*, *Klebsiella* and *Serratia*) and other bacteria that express L-pyroglutamyl aminopeptidase, covering both Gram positive and Gram negative bacteria.

The incorporation of an extra inhibitor, a β -chloro-L-alanyl moiety, into the phosphonopeptides enhanced the inhibitory potency (**196**, **222b**, **222c** and **225**) against the growth of Gram negative bacteria, particularly *E. coli* (n=2), *K. pneumoniae* (**222b**) and *E. cloacae* (except **222c**). The inhibitory potency against the growth of these bacteria was greatest by β -chloro-L-alanyl phosphonodipeptide (**196**). The good potency and selective inhibition of these bacteria are beneficial towards the detection and identification of *P. aeruginosa* present in cystic fibrosis samples, as well as *Salmonella spp.* present in food-poisoning faecal samples. The enhancement of inhibitory potency was also noted on some Gram positive bacteria, *E. faecalis* (**225**), *E. faecium* (except **222c**), *S. epidermidis* (**225**), *S. aureus* (**225**) and *S. aureus* (MRSA) (**225**).

Negligible antibacterial activities of PABA based dipeptide derivatives (**234** and **235**) against the growth of Gram negative and Gram positive bacteria (except *B. subtilis*) were noted, suggesting the presence of the PABA moiety could affect the uptake of these molecules across the bacterial cell, particularly bacteria with outer membrane, as no inhibitory action against the growth of all tested Gram negative bacteria. Aside from the poor uptake factor, the weak inhibitory effects could be also due to inefficient release of the inhibitor, β -chloro-L-alanine and/or PABA at the target site(s). As a result, it is not surprising to notice a weak antibacterial activity on bacteria without the outer membrane, Gram positive bacteria. The generally high MIC values of these molecules (**234** and **235**) against the tested bacteria (except *B. subtilis*) further support the important role of PABA as a precursor for the biosynthesis of tetrahydrofolate at a low concentration. A negative feedback inhibition by PABA may have led to the differences in the growth of certain Gram positive bacteria, particularly *B. subtilis* which was inhibited at a much lower concentration (MIC: <4 mg/L).

The different inhibitory profile noted on these molecules (**234** and **235**) indicated that the presence of a chlorine atom at the *N*-terminus of α -carbon amino acid side chain (**235**) was unable to enhance the inhibitory effect, instead the uptake of the molecules or the release of the inhibitor, β -chloro-L-alanine in the bacterial cell could be affected, and thus different antibacterial activity was observed. Although modest antibacterial activity of **234** and **235** noted on *B. subtilis*, the generally weak antibacterial action against the growth of almost all the tested bacteria, suggesting their unfeasible use for most pathogenic and commensal bacteria inhibition.

The growth of *B. subtilis* is sensitive not only towards the PABA based dipeptides (**234** and **235**) but also the phosphonodipeptides (**141** and **196**), therefore low MIC were frequently observed in this work (Tables 4.2, 4.3 and 4.4). The good inhibitory effects of these compounds against the growth of *B. subtilis* enable their application for enhancement of *L. monocytogenes* detection and identification, as the presence of *B. subtilis* could affect the numbers of *L. monocytogenes* growing on the culture medium.

A relationship between the physicochemical properties and antibacterial activities of the tested compounds can be drawn, due to the physicochemical properties associated with the permeability of a molecule across the bacterial cell. High lipophilicity is not necessarily associated with good cell membrane permeation that leads to good antibacterial activity; instead, lipophilicity with a clogP between -3.88 and -4.79 is favourable, while the polar surface area of a molecule with TPSA above 115 is preferable. Though the physicochemical factors are important for antibacterial activity, the inhibitory pharmacophore of a molecule and an effective release of an inhibitor at the target site are most significant.

CHAPTER 5

CONCLUSION AND FUTURE WORK

5.1: Conclusion

The continued emergence of resistant bacteria has increased the need for new, rapid, economical and user-friendly bacterial detection and identification methods. Their development is significant for clinical applications to enable selection of the most effective antibiotic to control specific pathogenic bacteria. Apart from its clinical use, bacterial detection is also widely used in food quality control and environmental areas, in order to ensure that food and water can be maintained free from possible disease-causing bacteria. There are many bacterial detection methods available, as discussed previously, involving both conventional and sophisticated instrumental methods, such as microscopic techniques, immunological techniques, genetic techniques and mass spectrometry. However, most of these techniques are time-consuming, costly and can be operated only by fully trained or experienced personnel.

Biochemical techniques that rely on enzymatic substrate reactions have led to further development of a variety of chromogenic and fluorogenic media for bacterial detection and identification. In this method, bacteria are detected *via* the secretion of specific bacterial enzymes that target specific substrates, resulting in chromogenic or fluorogenic responses. This method is not only able to overcome the mentioned problems, being potentially rapid, economical, and user-friendly (no extensive training required), but is also suitable for routine analysis. However, the secretion of similar enzymes by different strains of bacteria that act upon the same substrate, as well as the presence of unwanted bacteria, camouflage the bacteria of interest and may result in false results. Consequently, the introduction of an appropriate selective suicide substrate into the chromogenic or fluorogenic medium is essential to overcome these problems, while improving the reliability, accuracy and selectivity of the media.

A range of different peptide derivatives containing suicide inhibitors, D/L-fosfalin and β -chloro-L-alanine, or *para*-aminobenzoic acid (PABA), was synthesised for microbiology evaluation and tested against twenty different commensal and pathogenic bacterial strains. The antibacterial activities observed were different depending on the stereochemistry of the peptide derivatives, the number of suicide

inhibitors incorporated into the peptide derivatives, and the presence of α -carbon side chain or *N*-methyl group at the *N*-terminal amino acid of the peptide derivatives. L-Stereochemistry of fosfalin was most effective and twice the potency compared to racemic fosfalin against the twenty different bacterial strains, as evidenced by the minimum inhibitory concentration (MIC) of the L-Ala-L-Ala-D/L-fosfalin being double the MIC of L-Ala-L-Ala-L-fosfalin. The inhibitory potency of the phosphonopeptides containing two inhibitors, D/L-fosfalin and β -chloro-L-alanine, was higher compared to the phosphonopeptides containing a single inhibitor. Meanwhile, the presence of a long and/or large α -carbon side chain at the *N*-terminus of phosphonopeptides mediates the uptake of a molecule for the subsequent antibacterial action, as evidenced by the good antibacterial activities of L-norvalyl and L-methionyl phosphonotripeptides (**153b**, **160**, **222b** and **225**) in comparison to sarcosyl phosphonotripeptides (**153c** and **222c**).

Selective inhibition by phosphonotripeptides containing the inhibitor D/L-fosfalin (**153b**, **153c** and **160**) was observed, particularly on Gram negative bacteria, *E. coli* (n=2) (except **153c**), *K. pneumoniae*, *S. marcescens* and *Y. enterocolitica*. Comparison with the corresponding phosphonotripeptides containing two inhibitors (**222b**, **222c** and **225**) showed higher potency of the latter with similar inhibitory profiles and broad inhibitory spectrum that inhibited the growth of *E. cloacae* (except **222c**). Similar findings were also observed with phosphonodipeptide, β -chloro-L-Ala-D/L-Fos (**196**); however, much higher potency against the growth of *E. coli* (n=2), *K. pneumoniae* and *Y. enterocolitica* was noted. These bacteria are commonly present in patients with respiratory tract, urinary tract and food-borne diseases. As a result of these bacteria being susceptible to inhibition at a low concentration, these compounds are feasible for use in the enhancement of bacterial detection media by targeting the growth of these bacteria.

Aside from the Gram negative bacteria, some Gram positive bacteria were also selectively inhibited, such as *E. faecalis*, *E. faecium*, *S. epidermidis* and *S. aureus*. Of these bacteria, *E. faecalis* and *E. faecium* are commensal bacteria that are commonly found in the human gastrointestinal tract. The selective inhibition of these bacteria at a low concentration (low MIC) by the phosphonotripeptides **153a**,

153b, **160**, **222b** and **225**, except inhibition of *E. faecium* by **153c** and **222c**, makes these compounds good candidates for media designed for the identification of infectious gastrointestinal bacteria. The inhibitory activities seen on these selected strains of Gram positive bacteria suggest that L-alanyl aminopeptidase is not found exclusively in Gram negative bacteria. A different inhibitory profile of L-Pyroglu-D/L-Fos (**141**) was noted, most likely due to the release of the inhibitor, fosfalin, being specific to the bacteria expressing L-pyroglutamyl aminopeptidase, instead of L-alanyl aminopeptidase.

Although good inhibitory potency of β -chloroalanyl phosphonopeptides was found, the presence of a β -chlorine atom makes them prone to degradation and pH sensitive. A stability study of β -chloro-L-Ala-D/L-Fos (**196**) was performed at different pH values, 6.1, 7.1, 8.1 and 9.1. Degradation of **196** was noted after 1 week of exposure at pH 6.1, due to slow decrease of NMR signals corresponding to the proton signals of **196**. This finding suggested the potential reduction of inhibitory effects of phosphonopeptides containing the β -chloroalanyl moiety upon prolonged exposure at pH 6.1 and above. Although the inhibitory potency of phosphonopeptides containing a single inhibitor was not as good as β -chloroalanyl phosphonopeptides, similar inhibitory profiles, the absence of β -chlorine, and their ease of synthesis make them more feasible for further development for application in bacterial culture media, particularly pH sensitive culture media.

Poor antibacterial activity of PABA based dipeptides was observed, particularly with Gram negative bacteria. Although the inhibitory effects of phosphonopeptides containing β -chloro-L-alanine (**196**, **222b**, **222c** and **225**) were seen in this work, incorporation of this inhibitor into the PABA derivative (**235**) was unable to confer any inhibitory action on the Gram negative bacteria or enhance any antibacterial activity in comparison to L-Ala-PABA (**234**). The presence of the PABA moiety is likely to restrict the uptake of PABA based dipeptides across the bacterial outer membrane and could reduce activity of L-alanyl aminopeptidase, therefore minimizing the amount of β -chloro-L-alanine released for antibacterial activity. However, the selective inhibition of some Gram positive bacteria, particularly *B. subtilis* could be advantageous to bacterial cell culture.

Bacillus subtilis is a sensitive bacterium that can be inhibited not only by the PABA based dipeptides (**234** and **235**), but also fosfalin and β -chloro-L-alanyl based phosphonodipeptides (**141** and **196**). Greater potency was observed with **141** and **196**, due to their low MIC values, compared to **234** and **235**. This finding makes these compounds (**141**, **196**, **234** and **235**) good candidates for enhancement of current *L. monocytogenes* detection and identification in culture media, because the growth of *L. monocytogenes* can be adversely affected by surfactin, a bacteriocin that is secreted by *B. subtilis*.

The relationship between selected physicochemical properties and antibacterial activities was studied, as the physicochemical properties of a molecule are frequently associated with its permeability across the bacterial cell membrane for subsequent antibacterial action. The polar surface area (TPSA) and lipophilicity (logP) of the tested compounds (**141**, **153a**, **153b**, **153c**, **160**, **196**, **222b**, **222c**, **225**, **234** and **235**) were calculated using online Molinspiration software. As these compounds are not for human consumption, but for *in vitro* antibacterial testing, it is not surprising that some of the physicochemical properties of these compounds did not conform to Lipinski's rules for good oral bioavailability. Although there has been limited physicochemical study of antibacterial compounds that target bacterial proteins reported in the literature, lipophilicity, clogP between -3.88 and -4.79 and polar surface area above 115 (TPSA) were preferred in this study.

According to the literature, dehydroalanine, generated from β -chloroalanine, is believed to be an essential contributor to alanine racemase inhibition. Therefore, the inhibitory role of dehydroalanine was investigated by comparing the antibacterial activity between β -chloro-L-Ala-D/L-Fos (**196**) and dehydroalanine-D/L-Fos (**207**). The synthesis of dehydroalanine-D/L-fosfalin was attempted but unsuccessful, due to the enamine group, which was prone to degradation under the acidic conditions used. Possible degradation products were identified with the aid of mass spectrometry.

Although the inhibitory profile of both fosfalin and β -chloroalanine derivatives are well established over many years, their application in the enhancement of bacterial

detection media has yet to be fully exploited. The inhibitory potency and/or selectivity enhancement observed from the peptides containing a single or two different inhibitors, fosfalin or fosfalin and β -chloro-L-alanine offer a novel application for bacterial detection and identification. However, the generally poor antibacterial activity of *para*-aminobenzoic acid (PABA) based peptide derivatives suggested their unfeasible use for this application.

5.2: Future work

The good antibacterial activities observed from the phosphonotripeptides with a long and/or large side chain attached at the α -carbon of the *N*-terminal amino acids, suggest that other non-polar aliphatic side chains at the α -carbon, such as butyl, pentyl, hexyl and heptyl, are worth further investigation. Good antibacterial activities of phosphonodipeptides containing hydrophobic and aliphatic side chains at the α -carbon have been reported (1980AAC897). High potency will be anticipated in phosphonotripeptides containing the β -chloroalanyl moiety along with these long aliphatic side chains. Aside from the non-natural hydrophobic amino acids, other non-polar amino acids, valine, isoleucine, isoleucine, phenylalanine, and possibly tyrosine and tryptophan can be considered for incorporation.

Although good inhibitory potency of β -chloroalanyl phosphonopeptides has been shown, the stability study at different pH values showed the β -chloroalanine was susceptible to easy degradation. However, an additional stability study of β -chloro-L-Ala-D/L-Fos (**196**) should be performed in order to confirm the findings. In particular, a stability study that incorporates **196** into the culture medium at different pH values is yet to be performed. Different stability results could be anticipated by introducing **196** into culture media that are fixed at a set pH range. The results obtained from this study could be also used to predict the shelf-life of the β -chloroalanyl phosphonopeptides in culture media. Therefore, these compounds are worth further investigation. Providing that β -chloro-L-Ala-D/L-Fos (**196**) is stable, confirmed by the stability study, different substituents or leaving groups at the β -position of L-alanine, such as methanesulfonate, cyano, and

pentafluorophenyl ether can be considered as future work to evaluate their inhibitory effects.

Aside from D/L-fosfalin, β -chloro-L-alanine and *para*-aminobenzoic acid (PABA), other known alanine racemase inhibitors could be worth investigation, such as *O*-acetylserine and *O*-carbamoylserine (1978B1313), (1-aminoethyl)boronic acid (1989B3541), β -fluorovinylglycine and β -chlorovinylglycine (1991JBC21657), and D-cycloserine (2004JBC46143). Of these inhibitors, D-cycloserine and (1-aminoethyl)boronic acid are of huge interest due to their ability to target not only alanine racemase, but to exert other antibacterial activities, such as D-alanyl-D-alanine ligase inhibition (2004JBC46143), β -lactamase inhibition (2003JACS685), penicillin binding proteins inhibition (2003EJB23) and quorum sensing inhibition (2008BBRC590).

The synthesis of dehydroalanine-fosfalin (**207**) was unsuccessful. A different synthetic approach or dehydroalanine-prodrug development, which releases the dehydroalanine inside the bacterial cells, is worth consideration for future work. This mechanistic study will be useful for selection of different leaving groups at the β -position of L-alanine.

CHAPTER 6
EXPERIMENTAL

6.1: Chemistry

6.1.1: Reagents and instruments

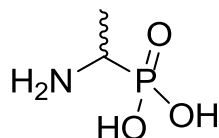
All commercially available reagents and solvents were acquired from Sigma-Aldrich, Fluka, Alfa-aesar, Fluorochem, Fischer Scientific and Bachem. All deuterated solvents were purchased from Goss Scientific and Apollo Scientific. Solvents were dried using the solvent purification system, PureSolv 400-5-MD, which was purchased from Innovative Technology (currently known as Inert). Hydrogenation was performed using series 4560 mini reactors, which was acquired from Parr Instrument. Radleys Carousel Standard Stirring Hotplate was used for synthesis involves stirring and heating. Column chromatography was performed using Silica 60A (35-70 or 70-200 micron) Davisil[®] chromatography grade. The LC column, ACE Excel 5 Super C18 (150 x 4.6 mm i.d.) was acquired from HICHROM.

6.1.2: Analytical instruments

Melting points were recorded using a Reichart-Kofler hot stage microscope apparatus. Infrared spectra were recorded in the range 4000 – 550 cm⁻¹ using a Perkin Elmer Spectrum BX FT-IR spectrophotometer. NMR spectra were acquired using a Bruker Ultrashield 300 sepctrometer at 300 MHz for ¹H spectra, 75 MHz for ¹³C spectra, 121 MHz for ³¹P-¹H decoupled spectra and 282 MHz for ¹⁹F-¹H decoupled spectra, or using a Bruker Avance III Ultrashield spectrometer at 500 MHz for ¹H spectra, 125 MHz for ¹³C spectra and 282 MHz for ³¹P-¹H decoupled spectra. NMR data was analysed by MestReNova. Low-resolution mass spectra were obtained from a Bruker Esquire 3000plus analyser using an electrospray source in either positive or negative ion mode. High-resolution mass spectra were acquired from Thermo Scientific LTQ Orbitrap XL using an electrospray source in either positive or negative ion mode. Elemental analyses were performed using an Exeter Analytical CE-440 Elemental Analyzer. Thin layer chromatography was performed on Merck TLC Silica Gel 60 F₂₅₄ or Fluka Silca on TLC Alu foils.

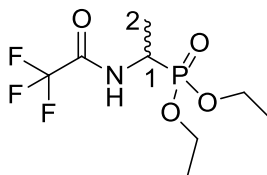
6.1.3: Synthesis of D/L-fosfalin derivatives

6.1.3.1: 1-aminoethylphosphonic acid or D/L-fosfalin (13-DL) (1978S469)



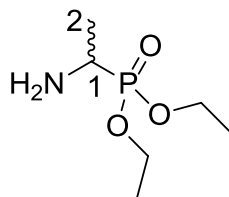
To suspension of *N*-phenylthiourea (100.0 mmol, 15.2 g) in glacial acetic acid (50 mL), acetaldehyde (130.0 mmol, 7.40 mL) was added dropwise, followed by triphenyl phosphite (100.0 mmol, 27.0 mL). The mixture was stirred at room temperature for 5 mins, then refluxed at 80 °C for 1 hr until a clear solution was obtained. A mixture of glacial acetic acid (5 mL) and hydrochloric acid (37 %, 50 mL) was added and the reaction was refluxed overnight. The solution was cooled to room temperature and concentrated *in vacuo* to afford a brown slurry. Ethanol (150 mL) was added while stirring and the resulting off-white solid was collected by filtration and dried in a desiccator containing phosphorus(V) oxide. The crude solid was recrystallised from hot water/ethanol to afford **13-DL** as white crystals, as a mixture of enantiomers (12.2 g, 98 mmol, 98 %); m.p. 271 – 274 °C (sublim) (lit. m.p. 271 – 275 °C (2002PJC1105)); $[\alpha]^{20}_{\text{D}} 0^\circ$ (c 1.0, H₂O); $\bar{\nu}_{\text{max}}/\text{cm}^{-1}$ 2910 (br OH), 1532 (NH bend), 1143 (P=O), 1035 (P-O-C), 930 (P-OH); ¹H NMR (300 MHz, D₂O) δ_{H} 1.40 (3H, dd, ³J_{H-P}=14.7 Hz, ³J_{H-H}=7.2 Hz, CH₃), 3.33 (1H, m, CH); ¹³C NMR (75 MHz, D₂O) δ_{C} 13.5 (d, ²J_{C-P}=2.6 Hz, CH₃), 44.7 (d, ¹J_{C-P}=144.2 Hz, CH); ³¹P-¹H_{decoupl} NMR (121 MHz, D₂O) δ_{P} 14.2; CHN [Found: C, 19.45; H, 6.48; N, 11.18. C₂H₈NO₃P requires C, 19.21; H, 6.45; N, 11.20 %]; *m/z* (ESI) calcd for (C₂H₉NO₃P)⁺, MH⁺: 126.0, found 126.1.

6.1.3.2: Diethyl (1-(2,2,2-trifluoroacetamido)ethyl)phosphonate or trifluoroacetyl-D/L-Fos diethyl ester (**116**) (1995S509)



1-Aminoethylphosphonic acid (**13-DL**) (51.7 mmol, 6.5 g) was added to a mixture of trifluoroacetic acid (65.3 mmol, 5 mL) and trifluoroacetic anhydride (177.4 mmol, 25 mL). The solution was stirred and refluxed at 60 °C for 1 hour, then cooled to room temperature and triethyl orthoformate (901.8 mmol, 150 mL) was added dropwise. The solution was refluxed at 110 °C for 2 hours, then cooled to room temperature. The solution was concentrated *in vacuo* to afford a brown solid, which was re-dissolved in DCM and purified by column chromatography using a gradient elution [DCM (100) to DCM/MeOH (95:5)] to give **116** as an off-white solid, a mixture of enantiomers (11.4 g, 41.0 mmol, 80%); m.p. 101 – 103 °C (sublim) (lit. m.p. 101 – 102 °C (1995S509)); $[\alpha]^{20}_{\text{D}} 0^\circ$ (c 1.0, CH₃OH); $\bar{\nu}_{\text{max}}/\text{cm}^{-1}$ 3202 (NH), 1715 (C=O), 1565 (NH bend), 1210 (P=O), 1011 (P-O-C), 968 (P-O-C); ¹H NMR (300 MHz, CDCl₃) δ_{H} 1.24 (3H, t, ³J_{H-H}=7.2 Hz, OCH₂CH₃), 1.27 (3H, t, ³J_{H-H}=7.2 Hz, OCH₂CH₃), 1.38 (3H, dd, ³J_{H-P}=16.5 Hz, ³J_{H-H}=7.2 Hz, CH₃-2), 4.06 (4H, m, 2 x OCH₂CH₃), 4.39 (1H, m, CH-1), 8.00 (1H, d, ³J_{H-H}=6.0 Hz, NH); ¹³C NMR (75 MHz, CDCl₃) δ_{C} 14.8 (CH₃-2), 16.2 (d, ³J_{C-P}=2.3 Hz, OCH₂CH₃), 16.3 (d, ³J_{C-P}=2.3 Hz, OCH₂CH₃), 41.8 (d, ¹J_{C-P}=159.1 Hz, CH-1), 62.8 (d, ²J_{C-P}=7.0 Hz, OCH₂CH₃), 63.2 (d, ²J_{C-P}=7.1 Hz, OCH₂CH₃), 115.9 (q, ¹J_{C-F}=285.8 Hz, CF₃), 156.9 (q, ²J_{C-F}=5.8 Hz, C=O); ³¹P-¹H_{decoupl} NMR (121 MHz, CDCl₃) δ_{P} 23.0; ¹⁹F-¹H_{decoupl} NMR (282 MHz, CDCl₃) δ_{F} -75.5; *m/z* (ESI) calcd for (C₈H₁₆F₃NO₄P)⁺, MH⁺: 278.1, found 278.1.

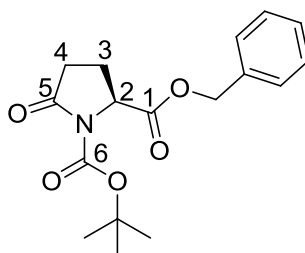
6.1.3.3: Diethyl 1-aminoethylphosphonate or D/L-Fos diethyl ester (**84**) (2003T6095)



Diethyl (1-(2,2,2-trifluoroacetamido)ethyl)phosphonate (**116**) (20.0 mmol, 5.6 g) was dissolved in ethanol (200 ml) and excess sodium borohydride (200.0 mmol, 7.7 g) was added slowly with stirring. The resulting mixture was stirred at room temperature for 1 hour, then heated at reflux for 4 hours. The mixture was cooled to room temperature and the solvent was removed *in vacuo* to afford a white solid, which was dissolved in saturated NaHCO₃ (96 g/L) (60 mL) with the addition of 10 % aqueous K₂CO₃ (20 mL). The product was extracted into DCM (6 x 30 mL) and dried over MgSO₄. The filtrate was concentrated *in vacuo* to afford a pale yellow liquid and purified by column chromatography using a gradient elution [DCM (100) to DCM/MeOH (90:10)] to afford **84** as a yellow liquid, a mixture of enantiomers (3.5 g, 19.3 mmol, 97 %); $[\alpha]^{20}_{\text{D}} 0^\circ$ (c 1.0, CH₃OH); $\bar{\nu}_{\text{max}}/\text{cm}^{-1}$ 3431 (NH), 1215 (P=O), 1020 (P-O-C), 967 (P-O-C); ¹H NMR (300 MHz, CDCl₃) δ_{H} 1.26 (6H, t, ³J_{H-H}=7.2 Hz, 2 x OCH₂CH₃), 1.34 (3H, dd, ³J_{H-P}=17.7 Hz, ³J_{H-H}=7.2 Hz, CH₃-2), 1.68 (2H, br, NH₂), 3.02-3.12 (1H, m, CH-1), 4.06-4.17 (4H, m, 2 x OCH₂CH₃); ¹³C NMR (75 MHz, CDCl₃) δ_{C} 16.4 (OCH₂CH₃), 16.5 (OCH₂CH₃), 17.2 (CH₃-2), 44.2 (d, ¹J_{C-P}=148.5 Hz, CH-1), 62.1 (d, ²J_{C-P}=7.5 Hz, OCH₂CH₃), 62.1 (d, ²J_{C-P}=7.5 Hz, OCH₂CH₃); ³¹P-¹H_{decoupl} NMR (121 MHz, CDCl₃) δ_{P} 29.6; HRMS (NSI) calcd for (C₆H₁₇NO₃P)⁺, MH⁺: 204.0760, found 204.0762.

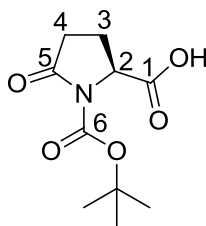
6.1.4: Synthesis of L-pyrroglutamic acid derivatives

6.1.4.1: (S)-2-Benzyl 1-*tert*-butyl 5-oxopyrrolidine-1,2-dicarboxylate or **Boc-L-Pyroglu-OBzl (143)** (2007BMC3474)



L-Pyroglutamic acid (20.0 mmol, 2.6 g) was suspended in THF (100 mL). To this was added triethylamine (22.0 mmol, 3.0 mL) and benzyl bromide (22.0 mmol, 2.6 mL). The resulting mixture was stirred at reflux for 5 days; the volume of solvent was maintained with the addition of THF if necessary. The mixture was cooled to room temperature and water (100 mL) was added to result in a clear yellow solution. The organic solvent was removed under reduced pressure and the aqueous layer was extracted with DCM (5 x 40 mL). The solution was cooled to 0 °C, then triethylamine (22.0 mmol, 3.0 mL), di-*tert*-butyl dicarbonate (40.0 mmol, 8.7 g), and 4-dimethylaminopyridine (22.0 mmol, 2.7 g) were added. The resulting solution was stirred at 0 °C for 60 mins and then room temperature overnight. The solution was concentrated *in vacuo* to afford a yellow liquid residue that was washed with 10 % citric acid (2 x 50 mL), 10 % potassium carbonate (50 mL), water (50 mL) and brine (50 mL). The organic layer was dried over magnesium sulfate and concentrated *in vacuo* to afford a dark red liquid, which was recrystallised from hot ethyl acetate/heptanes to afford **143** as a pale orange crystalline solid (4.8 g, 15.1 mmol, 76 %); m.p. 61 – 63 °C (lit. m.p. 62 – 65 °C (2007BMC3474)); $\bar{\nu}_{\max}/\text{cm}^{-1}$ 1780 (C=O), 1738 (C=O), 1702 (C=O), 1154 (C-O); ^1H NMR (300 MHz, CDCl_3) δ_{H} 1.39 (9H, s, $\text{C}(\text{CH}_3)_3$), 1.89-1.99 (1H, m, $\text{CH}_{\text{a/b-3}}$), 2.16-2.30 (1H, m, $\text{CH}_{\text{a/b-3}}$), 2.34-2.60 (2H, m, $\text{CH}_2\text{-4}$), 4.57 (1H, dd, $^3J_{\text{H-H}}=9.6$ Hz, 2.8 Hz, CH-2), 5.11 (1H, d, $^2J_{\text{H-H}}=12.0$ Hz, $\text{OCH}_{\text{a/b}}$), 5.16 (1H, d, $^2J_{\text{H-H}}=12.2$ Hz, $\text{OCH}_{\text{a/b}}$), 7.28 (5H, m, 5 x CH_{Ar}); ^{13}C NMR (75 MHz, CDCl_3) δ_{C} 20.6 ($\text{CH}_2\text{-3}$), 26.8 ($\text{C}(\text{CH}_3)_3$), 30.1 ($\text{CH}_2\text{-4}$), 58.0 (CH-2), 66.4 (OCH_2), 82.6 ($\text{C}(\text{CH}_3)_3$), 127.5 (CH_{Ar}), 127.6 (CH_{Ar}), 134.1 ($\text{CH}_{\text{Ar quat.}}$), 148.3 (C=O-6), 170.2 (C=O-1), 172.1 (C=O-5); m/z (ESI) calcd for $(\text{C}_{17}\text{H}_{21}\text{NNaO}_5)^+$, MNa^+ : 342.1, found 342.2.

6.1.4.2: (S)-1-(Tert-butoxycarbonyl)-5-oxopyrrolidine-2-carboxylic acid or 'Boc-L-Pyroglu-OH (144) (2002AEJ2516)



(S)-2-Benzyl 1-*tert*-butyl 5-oxopyrrolidine-1,2-dicarboxylate (**143**) (15 mmol, 4.8 g) was dissolved in methanol (100 mL), then transferred, and washed with methanol, into a stainless steel container. 5 % Palladium on charcoal (0.5 g) was added and the reaction was stirred at 3.5 *bar* pressure of H₂ at room temperature overnight. The resulting mixture was filtered using Celite and the filtrate was concentrated *in vacuo* to afford a crude material that was re-crystallised from hot ethyl acetate/petrol to afford **144** as a white solid (3.4 g, 14.6 mmol, 97 %); m.p. 76 - 79 °C (lit. m.p. 77 – 80 °C (2002AEJ2516)); $\bar{\nu}_{\max}/\text{cm}^{-1}$ 3134 (br OH), 1781 (C=O), 1740 (C=O), 1687 (C=O), 1210 (C-O), 1152 (C-O); ¹H NMR (300 MHz, CDCl₃) δ_{H} 1.43 (9H, s, C(CH₃)₃), 2.03-2.11 (1H, m, CH_{a/b}-3), 2.27-2.34 (1H, m, CH_{a/b}-3), 2.38-2.62 (2H, m, CH₂-4), 4.59 (1H, dd, ³J_{H-H}=9.6 Hz, 3.0 Hz, CH-2), 9.20 (1H, br, OH); ¹³C NMR (75 MHz, CDCl₃) δ_{C} 20.4 (CH₂-3), 26.9 (C(CH₃)₃), 30.2 (CH₂-4), 57.7 (CH-2), 83.1 (C(CH₃)₃), 148.4 (C=O-6), 172.5 (C=O-5), 175.3 (C=O-1); *m/z* (ESI) calcd for (C₁₀H₁₅NNaO₅)⁺, MNa⁺: 252.1, found 252.1.

6.1.5: General synthesis methods

6.1.5.1: Peptide coupling Method (T-2004MI164)

In a flask A, $C\alpha$ -protected amine salt (1.0 equiv) or phosphonate ester protected amine salt (when L-Met was used) was dissolved in dry DCM or dry THF and cooled to $-5\text{ }^{\circ}\text{C}$ in an ice/brine bath. To this was added N,N -diisopropylethylamine, DIPEA (1.5 equiv) or N -methyl morpholine, NMM (1.0 equiv) (when β -Cl-L-Ala was used). In a flask B, $N\alpha$ -protected amino acid (1.0 equiv) was dissolved in dry THF and to this was added N -methyl morpholine, NMM (1.5 equiv or 1.0 equiv when β -Cl-L-Ala moiety was involved) and isobutyl chloroformate (1.0 equiv) while stirring at $-5\text{ }^{\circ}\text{C}$. The Flask B solution was stirred for 2-3hrs at $-5\text{ }^{\circ}\text{C}$, after which time the neutralised $C\alpha$ -protected or phosphonate ester protected amine solution in Flask A was then added. The resulting mixture was stirred at $-5\text{ }^{\circ}\text{C}$ for 10mins and then room temperature overnight (16-18hrs). Work-up procedure: the mixture was filtered and filtrate was concentrated *in vacuo* to afford a crude product, which was dissolved in DCM and washed with 10 %w/v citric acid (2 x 30 mL), 10 %w/v potassium carbonate (30 mL) and water (30 mL). The organic layer was dried over magnesium sulfate, filtered, concentrated *in vacuo*, and purified by column chromatography using an appropriate solvent system to afford the product of interest.

6.1.5.2: Removal of benzyl ester protecting group under hydrogenation

$C\alpha$ -Benzyl ester amino acid or peptide was dissolved in methanol and to this was added 5-10% palladium on carbon (10 gram%). The mixture was stirred at 3.5 bar pressure of hydrogen at room temperature overnight (16-18hrs). The catalyst was filtered using Celite and the filtrate was concentrated *in vacuo* to afford the product of interest.

6.1.5.3: Removal of *N*-*tert*-butoxycarbonyl protecting group under acidic conditions

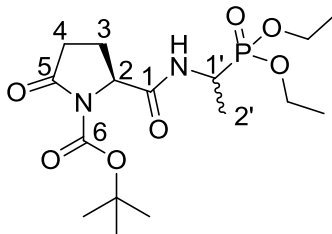
N-*t*Boc amino acid or peptide was dissolved in excess of a solution of dry 2M HCl in diethyl ether. The resulting solution was stirred at room temperature for 2 days to afford a crude solid, which was collected by filtration and washed with excess dry diethyl ether to afford the product of interest.

6.1.5.4: Simultaneous removal of *tert*-butoxycarbonyl and diethyl phosphonate ester protecting groups from phosphonopeptides

Phosphonopeptide containing *N*-*tert*-butoxycarbonyl and *O,O*-diethyl phosphonate ester was dissolved in 35 %wt HBr in acetic acid (10 equiv) and stirred at room temperature overnight (16-18hrs). Dry diethyl ether was added to afford a precipitation. The resulting mixture was stored in the freezer overnight (16-18hrs) to result in more precipitation. The solvent was decanted and remaining crude solid was triturated (x 3) with dry diethyl ether. The resulting solid was dissolved in dry methanol and propylene oxide was added in excess to afford a crude precipitation, which was recrystallised from the appropriate solvent system to afford the product of interest.

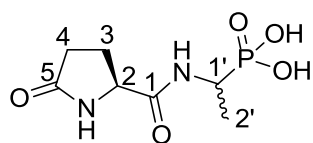
6.1.6: Synthesis of L-Pyroglu-D/L-fosfalin (141)

6.1.6.1: (2S)-Tert-butyl 2-((1-(diethoxyphosphoryl)ethyl)carbamoyl)-5-oxopyrrolidine-1-carboxylate or ^tBoc-L-Pyroglu-D/L-Fos diethyl ester (145)



The general peptide coupling method (6.1.5.1) was followed, using (S)-1-(*tert*-butoxycarbonyl)-5-oxopyrrolidine-2-carboxylic acid (**144**) (11 mmol, 2.53 g) and diethyl 1-aminophosphonate (**84**) (10 mmol, 1.85 g) in dry THF. The pale yellow crude liquid was purified by column chromatography [ethyl acetate/methanol (90:10)], to afford **145** as a white solid composed of 2 diastereoisomers, ^tBoc-L-Pyroglu-L-Fos diethyl ester and ^tBoc-L-Pyroglu-D-Fos diethyl ester (3.15 g, 8.0 mmol, 80 %); m.p. 190 – 193 °C; $\bar{\nu}_{\max}/\text{cm}^{-1}$ 3225 (NH), 1785 (C=O), 1755 (C=O), 1686 (C=O), 1547 (NH bend), 1220 (P=O), 1153 (C-O), 1017 (P-O-C), 965 (P-O-C); ¹H NMR (300 MHz, CDCl₃) δ_{H} 1.19-1.37 (9H, m, 2 x OCH₂CH₃, CH₃-2'), 1.44 (9H, s, C(CH₃)₃), 1.95-2.07 (1H, m, CH_{a/b}-3), 2.09-2.26 (1H, m, CH_{a/b}-3), 2.32-2.43 (1H, m, CH_{a/b}-4), 2.58-2.71 (1H, m, CH_{a/b}-4), 3.99-4.13 (4H, m, 2 x OCH₂CH₃), 4.36-4.53 (2H, m, CH-1', CH-2), 6.89 (0.5H, d, ³J_{H-H}=9.0 Hz, NH), 6.95 (0.5H, d, ³J_{H-H}=9.0 Hz, NH); ¹³C NMR (75 MHz, CDCl₃) δ_{C} 14.5 (CH₃-2'), 14.6 (CH₃-2'), 15.4 (d, ³J_{C-P}=2.3 Hz, OCH₂CH₃), 15.4 (d, ³J_{C-P}=2.3 Hz, OCH₂CH₃), 15.5 (d, ³J_{C-P}=2.3 Hz, OCH₂CH₃), 15.5 (d, ³J_{C-P}=2.3 Hz, OCH₂CH₃), 21.3 (CH₂-3), 21.4 (CH₂-3), 26.9 (C(CH₃)₃), 27.0 (C(CH₃)₃), 30.5 (CH₂-4), 30.6 (CH₂-4), 39.9 (d, ¹J_{C-P}= 156.0 Hz, CH-1'), 58.7 (CH-2), 59.0 (CH-2), 61.5 (d, ²J_{C-P}=6.8 Hz, OCH₂CH₃), 61.6 (d, ²J_{C-P}=6.8 Hz, OCH₂CH₃), 61.8 (d, ²J_{C-P}=6.8 Hz, OCH₂CH₃), 61.9 (d, ²J_{C-P}=6.8 Hz, OCH₂CH₃), 82.5 (C(CH₃)₃), 82.7 (C(CH₃)₃), 148.9 (C=O-6), 149.0 (C=O-6), 169.4 (C=O-1), 169.5 (C=O-1), 172.5 (C=O-5), 172.6 (C=O-5); ³¹P-¹H_{decoupl} NMR (121 MHz, CDCl₃) δ_{P} 24.9; CHN [Found: C, 46.66; H, 7.46; N, 6.71. C₁₆H₂₉N₂O₇·H₂O requires C, 46.83; H, 7.61; N, 6.83 %]; *m/z* (ESI) calcd for (C₁₆H₂₉N₂NaO₇P)⁺, MNa⁺: 415.2, found 415.2.

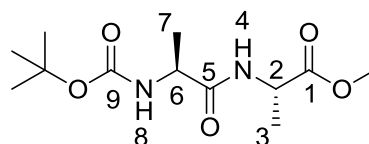
6.1.6.2: (1-((S)-5-oxopyrrolidine-2-carboxamido)ethyl)phosphonic acid or L-Pyroglu-D/L-fosfalin (**141**)



The acidic deprotection method (6.1.5.4) was followed, using (2S)-*tert*-butyl 2-((1-(diethoxyphosphoryl)ethyl)carbamoyl)-5-oxopyrrolidine-1-carboxylate (**145**) (7.9 mmol, 3.09 g). The pale green crude solid was recrystallised from ethanol/acetone to give **141** as green solid composed of 2 diastereoisomers, L-Pyroglu-L-fosfalin and L-Pyroglu-D-fosfalin (0.74 g, 3.12 mmol, 40 %); m.p. 61 – 64 °C; $\bar{\nu}_{\max}/\text{cm}^{-1}$ 3255 (NH), 2934 (br OH), 1665 (C=O), 1650 (C=O), 1542 (NH bend), 1266 (P=O), 1139 (C-O), 1043 (P-O-C), 931 (P-OH); ^1H NMR (300 MHz, D₂O) δ_{H} 1.05-1.29 (3H, m, CH₃-2'), 2.00-2.04 (1H, m, CH_{a/b}-3), 2.11-2.15 (1H, m, CH_{a/b}-3), 2.33-2.39 (1H, m, CH_{a/b}-4), 2.45-2.64 (1H, m, CH_{a/b}-4), 3.50-3.65 (1H, m, CH-2), 3.79-4.15 (1H, m, CH-1'); ^{13}C NMR (75 MHz, D₂O) δ_{C} 14.8 (CH₃-2'), 15.1 (CH₃-2'), 25.1 (CH₂-3), 25.6 (CH₂-3), 29.1 (CH₂-4), 29.3 (CH₂-4), 52.5 (CH-1'), 65.3 (CH-2), 165.4 (C=O-1), 173.7 (C=O-5); ^{31}P - ^1H _{decoupl} NMR (121 MHz, D₂O) δ_{P} 19.9; HRMS (NSI) calcd for (C₇H₁₂N₂O₅P)⁻, MH⁻: 235.0489, found 235.0488.

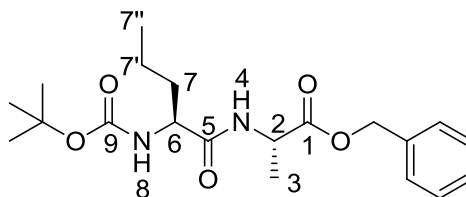
6.1.7: Synthesis of phosphonotripeptide derivatives containing L-Ala-D/L-Fos

6.1.7.1: (S)-Methyl 2-((S)-((tert-butoxycarbonyl)amino)propanamido)propanoate or ¹³C-Boc-L-Ala-L-Ala-OMe (149a)



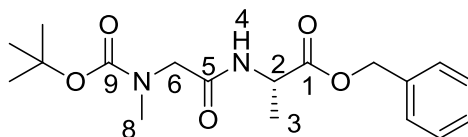
The general peptide coupling method (6.1.5.1) was followed, using ¹³C-Boc-L-Ala-OH (20 mmol, 3.78 g) in dry THF and L-alanine methyl ester hydrochloride (20 mmol, 2.79 g) in dry DCM. The white crude solid was purified by column chromatography [petrol/ethyl acetate (4:6)] to give **149a** as a white solid (3.75 g, 14 mmol, 68 %); m.p. 107 – 109 °C (lit. m.p. 108 – 109 °C [1983BCSJ568]); $\bar{\nu}_{\text{max}}/\text{cm}^{-1}$ 3308 (NH), 1738 (C=O), 1679 (C=O); 1652 (C=O), 1240 (C-O), 1160 (C-O); ¹H NMR (300 MHz, CDCl₃) δ_{H} 1.33 (3H, d, ³J_{H-H}=6.9 Hz, CH₃-7), 1.37 (3H, d, ³J_{H-H}=7.2 Hz, CH₃-3), 1.42 (9H, s, C(CH₃)₃), 3.72 (3H, s, OCH₃), 4.14 (1H, pentet, ³J_{H-H}=6.9 Hz, CH-6), 4.54 (1H, pentet, ³J_{H-H}=7.2 Hz, CH-2), 5.00 (1H, d, ³J_{H-H}=6.0 Hz, NH-8), 6.63 (1H, d, ³J_{H-H}=6.3 Hz, NH-4); ¹³C NMR (75 MHz, CDCl₃) δ_{C} 18.6 (CH₃-3/7), 28.5 (C(CH₃)₃), 48.2 (CH-2), 50.3 (CH-6), 52.6 (OCH₃), 80.4 (C(CH₃)₃), 155.4 (C=O-9), 172.4 (C=O-5), 173.4 (C=O-1); *m/z* (ESI) calcd for (C₁₂H₂₂N₂NaO₅)⁺, MNa⁺: 297.1, found 297.2.

6.1.7.2: (S)-Benzyl 2-((S)-2-((tert-butoxycarbonyl)amino)pentanamido)propanoate or ⁴Boc-L-Nva-L-Ala-OBzl (150b)



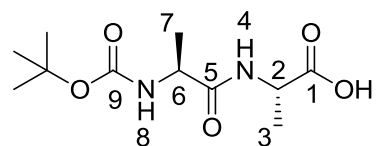
The general peptide coupling method (6.1.5.1) was followed, using ⁴Boc-L-Nva-OH (10.0 mmol, 2.17 g) in dry THF and L-alanine benzyl ester *p*-tosylic acid (10.0 mmol, 3.52 g) in dry DCM. The yellow crude liquid was purified by column chromatography [40-60 petrol/ethyl acetate (7:3)] to give **150b** as an off-white solid (2.40 g, 6.3 mmol, 63 %); m.p. 60 – 63 °C; $\bar{\nu}_{\max}/\text{cm}^{-1}$ 3332 (NH), 1743 (C=O), 1655 (br C=O), 1527 (NH bend), 1245 (C-O), 1162 (C-O); ¹H NMR (300 MHz, CDCl₃) δ_{H} 0.83 (3H, t, ³J_{H-H}=9.0 Hz, CH₃-7''), 1.25-1.31 (2H, m, CH₂-7'), 1.34 (3H, d, ³J_{H-H}=6.0 Hz, CH₃-3), 1.36 (9H, s, C(CH₃)₃), 1.42-1.54 (1H, m, CH_{a/b}-7), 1.64-1.73 (1H, m, CH_{a/b}-7), 4.02 (1H, m, CH-6), 4.54 (1H, pentet, ³J_{H-H}=6.0 Hz, CH-2), 4.96 (1H, d, ³J_{H-H}=9.0 Hz, NH-8), 5.07 (1H, d, ²J_{H-H}=12.0 Hz, OCH_{a/b}Ar), 5.12 (1H, d, ²J_{H-H}=12.0 Hz, OCH_{a/b}Ar), 6.56 (1H, d, ³J_{H-H}=6.0 Hz, NH-4), 7.27 (5H, m, 5 x CH_{Ar}); ¹³C NMR (75 MHz, CDCl₃) δ_{C} 12.7 (CH₃-7''), 17.3 (CH₃-3), 17.8 (CH₂-7'), 27.3 (C(CH₃)₃), 33.7 (CH₂-7), 47.1 (CH-2), 53.4 (CH-6), 66.1(OCH₂Ar), 79.0 (C(CH₃)₃), 127.1-127.6 (CH_{Ar}), 134.3 (CH_{Ar} quat.), 154.6 (C=O-9), 170.8 (C=O-5), 171.5 (C=O-1); CHN [Found: C, 63.75; H, 8.37; N, 7.86. C₂₀H₃₀N₂O₅ requires C, 63.47; H, 7.99; N, 7.40 %]; HRMS (NSI) calcd for (C₂₀H₃₁N₂O₅)⁺, MH⁺: 379.2227, found 379.2222.

6.1.7.3: (S)-Benzyl 2-(2-((tert-butoxycarbonyl)(methyl)amino)acetamido)propanoate or ^tBoc-Sar-L-Ala-OBzl (150c)



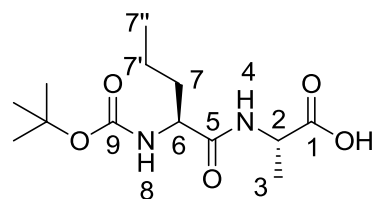
The general peptide coupling method (6.1.5.1) was followed, using ^tBoc-Sar-OH (15.0 mmol, 2.84 g) in dry THF and L-alanine benzyl ester *p*-tosylic acid (15.0 mmol, 5.27 g) in dry DCM. The yellow crude liquid was purified by column chromatography [40-60petrol/ethyl acetate (1:1)] to give **150c** as a colourless liquid (3.93 g, 11 mmol, 75 %); $\bar{\nu}_{\max}/\text{cm}^{-1}$ 3311 (NH), 1742 (C=O), 1670 (C=O), 1666 (C=O), 1536 (NH bend), 1242 (C-O), 1145 (C-O); ¹H NMR (300 MHz, CDCl₃) δ_{H} 1.35 (3H, t, ³J_{H-H}=6.0 Hz, CH₃-3), 1.39 (9H, s, C(CH₃)₃), 2.85 (3H, s, CH₃-8), 3.72 (1H, d, ²J_{H-H}=15.0 Hz, CH_{a/b}-6), 3.88 (1H, d, ²J_{H-H}=15.0 Hz, CH_{a/b}-6), 4.58 (1H, pentet, ³J_{H-H}=6.0 Hz, CH-2), 5.08 (1H, d, ²J_{H-H}=12.0 Hz, OCH_{a/b}Ar), 5.13 (1H, d, ²J_{H-H}=12.0 Hz, OCH_{a/b}Ar), 6.51 (1H, br, NH-4), 7.25-7.29 (5H, m, 5 x CH_{Ar}); ¹³C NMR (75 MHz, CDCl₃) δ_{C} 17.5 (CH₃-3), 27.3 (C(CH₃)₃), 34.7 (CH₃-8), 47.0 (CH-2), 52.1 (CH₂-6), 66.2 (OCH₂Ar), 79.8 (C(CH₃)₃), 127.1-127.6 (CH_{Ar}), 134.3 (CH_{Ar} quat.), 155.0 (C=O-9), 167.9 (C=O-5), 171.5 (C=O-1); HRMS (NSI) calcd for (C₁₈H₂₇N₂O₅)⁺, MH⁺: 351.1914, found 351.1916.

6.1.7.4: (S)-Methyl 2-((S)-2-((tert-butoxycarbonyl)amino)propanamido)propanoic acid or 'Boc-L-Ala-L-Ala-OH (151a) (1970JMB47)



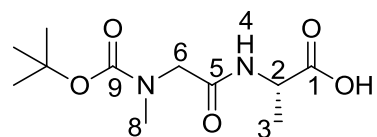
(S)-Methyl 2-((S)-2-((tert-butoxycarbonyl)amino)propanamido)propanoate (**149a**) (8 mmol, 2.20 g) was dissolved in methanol (20 mL). 1M Sodium hydroxide (35 mL) was added and the solution was stirred overnight at room temperature. Once the reaction completed, the solvent was removed under reduced pressure to afford a liquid residue. The residue was transferred and washed with water into a separating funnel, followed by extraction with DCM (5 x 10 mL). The water layer was retained and acidified by 37 %w/w concentrated HCl to pH0.5-1. The solution was diluted by addition of water (100 mL) and stored in fridge overnight to afford **151a** as a white solid (1.67 g, 6.4 mmol, 80 %); m.p. 105 – 108 °C (lit. m.p. 106 – 109 °C (2011TL1260)); $\bar{\nu}_{\max}/\text{cm}^{-1}$ 3500 (br OH), 3347 (NH), 1664 (br C=O), 1535 (NH bend); $^1\text{H NMR}$ (500 MHz, DMSO_4) δ_{H} 1.17 (3H, d, $^3J_{\text{H-H}} = 7.1$ Hz, CH_3 -3), 1.27 (3H, d, $^3J_{\text{H-H}} = 7.3$ Hz, CH_3 -7), 1.37 (9H, s, $\text{C}(\text{CH}_3)_3$), 3.37 (1H, br, OH), 4.00 (1H, m, CH -6), 4.20 (1H, m, CH -2), 6.85 (1H, d, $^3J_{\text{H-H}} = 7.7$ Hz, NH -8), 7.98 (1H, d, $^3J_{\text{H-H}} = 7.4$ Hz, NH -4); $^{13}\text{C NMR}$ (125 MHz, DMSO_4) δ_{C} 17.7 (CH_3 -7), 18.6 (CH_3 -3), 28.7 ($\text{C}(\text{CH}_3)_3$), 47.8 (CH -6), 49.8 (CH -2), 78.5 ($\text{C}(\text{CH}_3)_3$), 155.4 (C=O-9), 173.0 (C=O-5), 174.5 (C=O-1); m/z (ESI) calcd for $(\text{C}_{11}\text{H}_{20}\text{N}_2\text{NaO}_5)^+$, MNa^+ : 283.1, found 283.2.

6.1.7.5: (S)-2-((S)-2-((Tert-butoxycarbonyl)amino)pentanamido)propanoic acid or 'Boc-L-Nva-L-Ala-OH (151b)



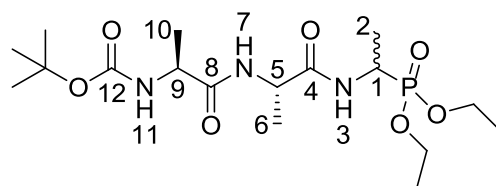
The hydrogenation deprotection method (6.1.5.2) was followed, using (S)-benzyl 2-((S)-2-((*tert*-butoxycarbonyl)amino)pentanamido)propanoate (**150b**) (6.0 mmol, 2.27 g) to afford **151b** as a white solid (1.66 g, 5.7 mmol, 96.0 %); m.p. 55 - 58 °C (decomp.); $\bar{\nu}_{\max}/\text{cm}^{-1}$ 3500-3000 (br, OH), 3300 (NH), 1688 (br C=O), 1655 (C=O), 1522 (NH bend), 1245 (C-O), 1164 (C-O); $^1\text{H NMR}$ (300 MHz, CDCl_3) δ_{H} 0.85 (3H, t, $^3J_{\text{H-H}}=9.0$ Hz, $\text{CH}_3\text{-7''}$), 1.27-1.31 (5H, m, $\text{CH}_3\text{-3}$, $\text{CH}_2\text{-7'}$), 1.39 (9H, s, $\text{C}(\text{CH}_3)_3$), 1.48-1.53 (1H, m, $\text{CH}_{a/b}\text{-7}$), 1.67-1.71 (1H, m, $\text{CH}_{a/b}\text{-7}$), 4.10 (1H, m, CH-6), 4.50 (1H, m, CH-2), 5.27 (1H, m, NH-8), 6.93 (1H, m, NH-4), 8.87 (1H, br, OH); $^{13}\text{C NMR}$ (75 MHz, CDCl_3) δ_{C} 13.7 ($\text{CH}_3\text{-7''}$), 18.0 ($\text{CH}_3\text{-3}$), 18.8 ($\text{CH}_2\text{-7'}$), 28.3 ($\text{C}(\text{CH}_3)_3$), 34.5 ($\text{CH}_2\text{-7}$), 48.1 (CH-2), 54.3 (CH-6), 80.4 ($\text{C}(\text{CH}_3)_3$), 156.0 (C=O-9), 172.5 (C=O-5), 175.5 (C=O-1); CHN [Found: C, 54.18; H, 8.78; N, 9.62. $\text{C}_{13}\text{H}_{24}\text{N}_2\text{O}_5$ requires C, 54.15; H, 8.39; N, 9.72 %]; HRMS (NSI) calcd for $(\text{C}_{13}\text{H}_{25}\text{N}_2\text{O}_5)^+$, MH^+ : 289.1758, found 289.1758.

6.1.7.6: (S)-Benzyl 2-(2-((tert-butoxycarbonyl)(methyl)amino)acetamido) propanoic acid or ^tBoc-Sar-L-Ala-OH (151c)



The hydrogenation deprotection method (6.1.5.2) was followed, using (S)-benzyl 2-(2-((tert-butoxycarbonyl)(methyl)amino)acetamido) propanoate (**150c**) (10.0 mmol, 3.51 g) to afford **151c** as a colorless syrup (2.50 g, 9.6 mmol, 96 %); $\bar{\nu}_{\max}/\text{cm}^{-1}$ 3301 (NH), 2961 (broad OH), 1736 (C=O), 1664 (br C=O), 1542 (NH bend), 1241 (C-O), 1147 (C-O); $^1\text{H NMR}$ (300 MHz, CDCl_3) δ_{H} 1.36 (3H, t, $^3J_{\text{H-H}}=6.0$ Hz, CH_3 -3), 1.39 (9H, s, $\text{C}(\text{CH}_3)_3$), 2.89 (3H, s, CH_3 -8), 3.72 (1H, d, $^2J_{\text{H-H}}=18.0$ Hz, $\text{CH}_{\text{a/b}}$ -6), 3.98 (1H, d, $^2J_{\text{H-H}}=18.0$ Hz, $\text{CH}_{\text{a/b}}$ -6), 4.57 (1H, m, CH -2), 6.96 (1H, m, NH -4), 7.26 (1H, br, OH); $^{13}\text{C NMR}$ (75 MHz, CDCl_3) δ_{C} 17.2 (CH_3 -3), 27.3 ($\text{C}(\text{CH}_3)_3$), 46.8 (CH -2), 49.6 (CH_3 -8), 52.1 (CH_2 -6), 80.6 ($\text{C}(\text{CH}_3)_3$), 155.5 ($\text{C}=\text{O}$ -9), 168.3 ($\text{C}=\text{O}$ -5), 174.1 ($\text{C}=\text{O}$ -1); HRMS (NSI) calcd for $(\text{C}_{11}\text{H}_{19}\text{N}_2\text{O}_5)^-$, MH^- : 259.1299, found 259.1295.

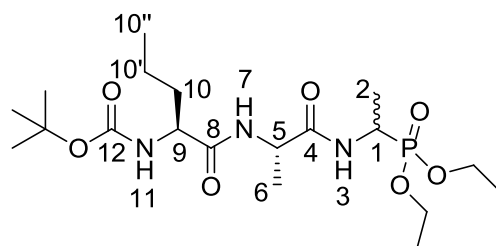
6.1.7.7: Tert-butyl ((2S)-1-(((2S)-1-((1-(diethoxyphosphoryl)ethyl) amino)-1-oxopropan-2-yl)carbamate or ^tBoc-L-Ala-L-Ala-D/L-Fos diethyl ester (152a)



The general peptide coupling method (6.1.5.1) was followed, using (S)-methyl 2-((S)-2-((tert-butoxycarbonyl)amino)propanamido)propanoic acid (**151a**) (3.1 mmol, 0.81 g) in dry THF and diethyl 1-aminoethylphosphonate (**84**) (3.1 mmol, 0.56 g) in dry THF. The white crude solid was purified by column chromatography [ethyl acetate/MeOH (98:2)] to afford **152a** as a white solid composed of 2 diastereoisomers, ^tBoc-L-Ala-L-Ala-L-Fos diethyl ester and ^tBoc-L-Ala-L-Ala-D-Fos diethyl ester (0.61 g, 1.44 mmol, 46 %); m.p. 144 – 148 °C; $\bar{\nu}_{\max}/\text{cm}^{-1}$ 3310 (NH), 1708 (C=O), 1672 (C=O), 1636 (C=O), 1518 (NH bend), 1236 (P=O), 1165 (C-O), 1016 (P-O-C), 960 (P-O-C); $^1\text{H NMR}$ (500 MHz, CDCl_3) δ_{H} 1.21-1.33 (15H, m,

CH₃-2, CH₃-6, CH₃-10, 2 x OCH₂CH₃), 1.37 (9H, s, C(CH₃)₃), 3.98-4.12 (5H, m, CH-9, 2 x OCH₂CH₃), 4.34-4.43 (1H, m, CH-1), 4.47-4.53 (1H, m, CH-5), 5.26-5.37 (1H, m, NH-11), 6.83-6.94 (1H, m, NH-7); 7.10-7.20 (1H, m, NH-3); ¹³C NMR (125 MHz, CDCl₃) δ_C 15.4 (CH₃-2), 15.5 (CH₃-2), 16.6 (OCH₂CH₃), 16.6 (OCH₂CH₃), 16.6 (OCH₂CH₃), 16.6 (OCH₂CH₃), 16.7 (CH₃-6 or CH₃-10), 18.7 (CH₃-6 or CH₃-10), 28.5 (C(CH₃)₃), 41.2 (d, ¹J_{C-P}=157.2 Hz, CH-1), 49.0 (CH-5 or CH-9), 49.1 (CH-5 or CH-9), 62.7 (d, ²J_{C-P}=6.9 Hz, OCH₂CH₃), 62.8 (d, ²J_{C-P}=6.9 Hz, OCH₂CH₃), 62.9 (d, ²J_{C-P}=6.9 Hz, OCH₂CH₃), 63.1 (d, ²J_{C-P}=6.9 Hz, OCH₂CH₃), 80.2 (C(CH₃)₃), 150.0 (C=O-12), 171.9 (C=O-4 or C=O-8), 172.7 (C=O-4 or C=O-8); ³¹P-¹H_{decoupled} NMR (202 MHz, CDCl₃) δ_P 25.1, 25.2; CHN [Found: C, 48.22; H, 8.09; N, 9.92. C₁₇H₃₄N₃O₇P requires C, 48.22; H, 8.32; N, 9.96 %]; HRMS (NSI) calcd for (C₁₇H₃₅N₃O₇P)⁺, MH⁺: 424.2207, found 424.2200.

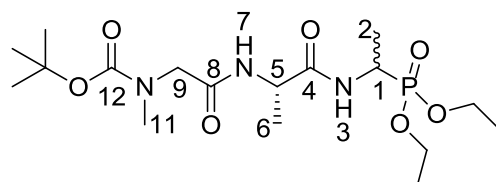
6.1.7.8: *Tert*-butyl ((2*S*)-1-(((2*S*)-1-((1-(diethoxyphosphoryl)ethyl)amino)-1-oxopropan-2-yl)amino)-1-oxopentan-2-yl)carbamate or 'Boc-L-Nva-L-Ala-D/L-Fos diethyl ester (152b)



The general peptide coupling method (6.1.5.1) was followed, using (*S*)-2-((*S*)-2-((*tert*-butoxycarbonyl)amino)pentanamido)propanoic acid (**151b**) (5.0 mmol, 1.45 g) in dry THF and diethyl 1-aminoethylphosphonate (**84**) (4.8 mmol, 0.87 g) in dry THF. The white crude solid was purified by column chromatography using 100 % DCM, increasing to 90:10 DCM/methanol, to afford **152b** as a white solid composed of 2 diastereoisomers, 'Boc-L-Nva-L-Ala-L-Fos diethyl ester and 'Boc-L-Nva-L-Ala-D-Fos diethyl ester (1.70 g, 3.8 mmol, 78 %); m.p. 165 - 168 °C; $\bar{\nu}_{\text{max}}/\text{cm}^{-1}$ 3267 (NH), 1708 (C=O), 1638 (br C=O), 1537 (NH bend), 1227 (P=O), 1165 (C-O), 1019 (P-O-C), 966 (P-O-C); ¹H NMR (300 MHz, CDCl₃) δ_H 0.85 (3H, t, ³J_{H-H}=9.0 Hz, CH₃-10''), 1.18-1.34 (14H, m, 2 x OCH₂CH₃, CH₃-2, CH₃-6, CH₂-10'), 1.37 (9H, s, C(CH₃)₃), 1.47-1.54 (1H, m, CH_{a/b}-10), 1.65-1.73 (1H, m, CH_{a/b}-10), 3.98-4.12 (5H, m, 2 x OCH₂CH₃, CH-9), 4.33-4.44 (1H, m, CH-1), 4.48-4.54 (1H,

m, **CH-5**), 5.19 (0.5H, d, $^3J_{H-H}=6.0$ Hz, **NH-11**), 5.23 (0.5H, d, $^3J_{H-H}=6.0$ Hz, **NH-11**), 6.78 (0.5H, d, $^3J_{H-H}=6.0$ Hz, **NH-7**), 6.87 (0.5H, d, $^3J_{H-H}=6.0$ Hz, **NH-7**), 7.15 (0.5H, d, $^3J_{H-H}=9.0$ Hz, **NH-3**), 7.23 (0.5H, d, $^3J_{H-H}=9.0$ Hz, **NH-3**); ^{13}C NMR (75 MHz, CDCl_3) δ_{C} 12.7 (**CH₃-10''**), 14.4 (**CH₃-2**), 14.5 (**CH₃-2**), 15.3 (**OCH₂CH₃**), 15.4 (**OCH₂CH₃**), 15.5 (**OCH₂CH₃**), 15.6 (**OCH₂CH₃**), 17.6 (**CH₃-6**), 17.7 (**CH₃-6**), 17.8 (**CH₂-10'**), 17.9 (**CH₂-10'**), 27.3 (**C(CH₃)₃**), 33.8 (**CH₂-10**), 33.9 (**CH₂-10**), 39.9 (d, $^1J_{P-C}=157.5$ Hz, **CH-1**), 40.0 (d, $^1J_{P-C}=156.8$ Hz, **CH-1**), 47.7 (**CH-5**), 47.9 (**CH-5**), 53.5 (**CH-9**), 53.5 (**CH-9**), 61.5 (d, $^2J_{C-P}=7.5$ Hz, **OCH₂CH₃**), 61.6 (d, $^2J_{C-P}=7.5$ Hz, **OCH₂CH₃**), 61.7 (d, $^2J_{C-P}=7.5$ Hz, **OCH₂CH₃**), 61.9 (d, $^2J_{C-P}=7.5$ Hz, **OCH₂CH₃**), 78.9 (**C(CH₃)₃**), 154.7 (**C=O-12**), 170.6 (**C=O-4** or **C=O-8**), 170.7 (**C=O-4** or **C=O-8**), 171.0 (**C=O-4** or **C=O-8**), 171.1 (**C=O-4** or **C=O-8**); ^{31}P - ^1H decoupled NMR (121 MHz, CDCl_3) δ_{P} 25.0, 25.1; CHN [Found: C, 50.74; H, 8.55; N, 9.51. $\text{C}_{19}\text{H}_{38}\text{N}_3\text{O}_7\text{P}$ requires C, 50.54; H, 8.48; N, 9.31 %]; HRMS (NSI) calcd for $(\text{C}_{19}\text{H}_{39}\text{N}_3\text{O}_7\text{P})^+$, MH^+ : 452.2520, found 452.2518.

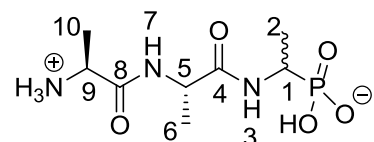
6.1.7.9: *Tert*-butyl (2-(((2*S*)-1-((1-(diethoxyphosphoryl)ethyl)amino)-1-oxopropan-2-yl)amino)-2-oxoethyl)(methyl)carbamate or ⁴Boc-Sar-L-Ala-D/L-Fos (152c)



The general peptide coupling method (6.1.5.1) was followed, using (*S*)-benzyl 2-(2-((*tert*-butoxycarbonyl)(methyl)amino)acetamido)propanoic acid (**151c**) (6.0 mmol, 1.57 g) in dry THF and diethyl 1-aminoethylphosphonate (**84**) (6.0 mmol, 1.10 g) in dry THF. The yellow crude liquid was purified by column chromatography, using 100 % DCM and increasing to 90:10 DCM/methanol, to afford **152c** as a colorless liquid composed of 2 diastereoisomers, ⁴Boc-Sar-L-Ala-L-Fos diethyl ester and ⁴Boc-Sar-L-Ala-D-Fos diethyl ester (1.60 g, 3.8 mmol, 63 %); $\bar{\nu}_{\text{max}}/\text{cm}^{-1}$ 3270 (NH), 1700 (br C=O), 1655 (C=O), 1545 (NH bend), 1225 (P=O), 1149 (C-O), 1018 (P-O-C), 966 (P-O-C); ^1H NMR (300 MHz, CDCl_3) δ_{H} 1.19-1.34 (12H, m, **CH₃-2**, **CH₃-6**, 2 x **OCH₂CH₃**), 1.40 (9H, s, **C(CH₃)₃**), 2.87 (3H, s, **CH₃-11**), 3.72 (0.5H, d, $^2J_{H-H}=15.0$ Hz, **CH_{a/b}-9**), 3.78 (0.5H, d, $^2J_{H-H}=15.0$ Hz,

CH_{a/b}-9), 3.81 (0.5H, d, ²J_{H-H}=15.0 Hz, CH_{a/b}-9), 3.87 (0.5H, d, ²J_{H-H}=15.0 Hz, CH_{a/b}-9), 4.00-4.11 (4H, m, 2 x OCH₂CH₃), 4.35-4.43 (1H, m, CH-1), 4.47-4.52 (1H, m, CH-5), 6.67 (1H, d, ³J_{H-H}=9.0 Hz, NH-7), 6.98 (0.5H, d, ³J_{H-H}=9.0 Hz, NH-3), 7.15 (0.5H, d, ³J_{H-H}=9.0 Hz, NH-3); ¹³C NMR (75 MHz, CDCl₃) δ_C 15.5 (CH₃-2), 15.5 (CH₃-2), 16.3 (d, ³J_{P-C}=3.0 Hz, OCH₂CH₃), 16.4 (d, ³J_{P-C}=3.0 Hz, OCH₂CH₃), 18.7 (CH₃-6), 28.3 (C(CH₃)₃), 35.8 (CH₃-11), 41.0 (d, ¹J_{P-C}=157.5 Hz, CH-1), 48.5 (CH-5), 53.0 (CH₂-9), 62.5 (d, ²J_{P-C}=6.8 Hz, OCH₂CH₃), 62.6 (d, ²J_{P-C}=6.8 Hz, OCH₂CH₃), 62.7 (d, ²J_{P-C}=6.8 Hz, OCH₂CH₃), 62.9 (d, ²J_{P-C}=6.8 Hz, OCH₂CH₃), 80.7 (C(CH₃)₃), 156.0 (C=O-12), 171.5 (C=O-4 or C=O-8), 171.6 (C=O-4 or C=O-8); ³¹P-¹H_{decoupl} NMR (121 MHz, CDCl₃) δ_P 25.0, 25.1; HRMS (NSI) calcd for (C₁₇H₃₅N₃O₇P)⁺, MH⁺: 424.2207, found 424.2203.

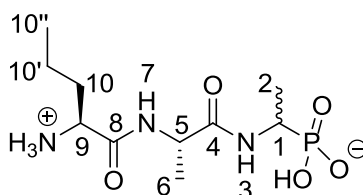
6.1.7.10: (1-((S)-2-((S)-2-Aminopropanamido)propanamido)ethyl) phosphonic acid or L-Ala-L-Ala-D/L-Fos (153a)



The *tert*-butoxycarbonyl and diethyl ester protecting groups of *tert*-butyl ((2*S*)-1-(((2*S*)-1-((1-(diethoxyphosphoryl)ethyl)amino)-1-oxopropan-2-yl)carbamate (**152a**) (1.2 mmol, 0.51 g) were removed under acidic deprotection method (6.1.5.4). The pale green crude solid was recrystallised from hot water/acetone to give **153a** as a pale green solid composed of 2 diastereoisomers, L-Ala-L-Ala-L-fosfalin and L-Ala-L-Ala-D-fosfalin (0.30 g, 1.12 mmol, 93 %); m.p. 235 – 238 °C (decomp.); $\bar{\nu}_{\max}$ /cm⁻¹ 3248 (NH⁺), 3500-2900 (br OH), 1641 (br C=O), 1548 (NH bend), 1119 (P=O), 1048 (P-O-C), 916 (P-OH); ¹H NMR (300 MHz, D₂O) δ_H 1.24 (3H, m, CH₃-2), 1.35 (3H, d, ³J_{H-H}=5.8 Hz, CH₃-6 or CH₃-10), 1.51 (3H, d, ³J_{H-H}=5.3 Hz, CH₃-6 or CH₃-10), 4.04 (1H, m, CH-1), 4.29 (1H, m, CH-5 or CH-9), 4.31 (1H, m, CH-5 or CH-9); ¹³C NMR (75 MHz, CDCl₃) δ_C 15.3 (CH₃-2), 15.4 (CH₃-2), 16.5 (CH₃-6 or CH₃-10), 16.6 (CH₃-6 or CH₃-10), 16.7 (CH₃-6 or CH₃-10), 16.8 (CH₃-6 or CH₃-10), 48.9 (CH-1), 50.0 (CH-5, CH-9), 170.5 (C=O-4 or C=O-8), 173.7 (C=O-4 or C=O-8); ³¹P-¹H_{decoupl} NMR (121 MHz, CDCl₃) δ_P 19.3; CHN [Found: C, 32.78; H, 6.67; N, 14.20. C₈H₁₈N₃O₅P·1.3H₂O requires C, 33.06; H, 7.14; N, 14.46 %]; HRMS (NSI)

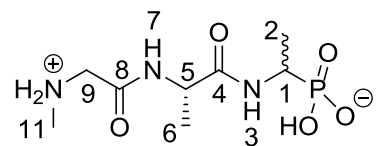
calcd for (C₈H₁₉N₃O₅P)⁺, MH⁺: 268.1057, found 268.1060; LCMS purity >95 % (C-18 reversed phase, MeOH-H₂O).

6.1.7.11: (1-((S)-2-((S)-2-Aminopentanamido)propanamido)ethyl) phosphonic acid or L-Nva-L-Ala-D/L-Fos (153b)



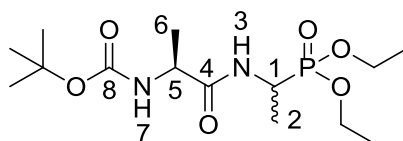
The *tert*-butoxycarbonyl and diethyl ester protecting groups of *tert*-butyl ((2*S*)-1-(((2*S*)-1-((1-(diethoxyphosphoryl)ethyl)amino)-1-oxopropan-2-yl)amino)-1-oxopentan-2-yl)carbamate (**152b**) (1.6 mmol, 0.72 g) were removed under acidic deprotection method (6.1.5.4). The pale green crude solid was recrystallised from hot water/acetone to give **153b** as a pale green solid composed of 2 diastereoisomers, L-Nva-L-Ala-L-Fos and L-Nva-L-Ala-D-Fos (0.22 g, 0.75 mmol, 47 %); m.p. 207 – 210 °C (decomp.); $\bar{\nu}_{\max}/\text{cm}^{-1}$ 3280 (NH⁺), 3500-2900 (br OH), 1643 (br C=O), 1552 (NH bend), 1149 (P=O), 1037 (P-O-C), 922 (P-OH); ¹H NMR (300 MHz, D₂O) δ_{H} 0.96 (3H, t, ³J_{H-H}=7.1 Hz, CH₃-10''), 1.27-1.32 (3H, d, ³J_{H-H}=6.8 Hz, CH₃-2), 1.40-1.42 (3H, m, CH₃-6), 1.40-1.42 (2H, m, CH₂-10'), 1.88-1.86 (2H, m, CH₂-10), 4.00-4.02 (2H, m, CH-1, CH-9), 4.34-4.39 (1H, m, CH-5); ¹³C NMR (75 MHz, D₂O) δ_{C} 13.4 (CH₃-10''), 16.0 (CH₃-2), 17.1 (CH₃-6), 17.2 (CH₃-6), 18.1 (CH₂-10'), 18.2 (CH₂-10'), 33.5 (CH₂-10), 33.6 (CH₂-10), 50.5 (CH-5), 50.8 (CH-5), 53.5 (CH-1, CH-9), 170.4 (C=O-8), 170.6 (C=O-8), 174.7 (C=O-4); ³¹P-¹H_{decoupled} NMR (121 MHz, CDCl₃) δ_{P} 18.5; CHN [Found: C, 37.61; H, 7.51; N, 12.91. C₁₀H₂₂N₃O₅P·1.4H₂O requires C, 37.48; H, 7.80; N, 13.11 %]; HRMS (NSI) calcd for (C₁₀H₂₃N₃O₅P)⁺, MH⁺: 296.1370, found 296.1373; LCMS purity >95 % (C-18 reversed phase, MeOH-H₂O).

6.1.7.12: (1-((S)-2-(2-(Methylamino)acetamido)propanamido)ethyl)phosphonic acid or Sar-L-Ala-D/L-Fos (153c)



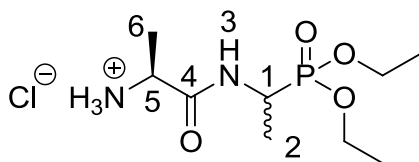
The *tert*-butoxycarbonyl and diethyl ester protecting groups of (1-((S)-2-((S)-2-aminopropanamido)propanamido)ethyl)phosphonic acid (**152c**) (3.3 mmol, 1.40 g) were removed under acidic deprotection method (6.1.5.4). The pale green crude solid was recrystallised from hot water/ethanol to give **153c** as a pale green solid composed of 2 diastereoisomers, Sar-L-Ala-L-Fos and Sar-L-Ala-D-Fos (0.45 g, 1.7 mmol, 51 %); m.p. 241 – 245 °C (decomp.); $\bar{\nu}_{\max}/\text{cm}^{-1}$ 3289 (NH⁺), 3500-2900 (br OH), 1632 (br C=O), 1556 (NH bend), 1174 (P=O), 1059 (P-O-C), 919 (P-OH); ¹H NMR (300 MHz, D₂O) δ_{H} 1.14-1.57 (6H, m, CH₃-2, CH₃-6), 2.74 (3H, s, CH₃-11), 3.84-4.07 (3H, m, CH₂-9, CH-1), 4.32-4.58 (1H, m, CH-5); ¹³C NMR (75 MHz, D₂O) δ_{C} 15.4 (CH₃-2), 16.8 (CH₃-6), 32.9 (CH₃-11), 43.9 (d, ¹J_{P-C}=148.5 Hz, CH-1), 49.4 (CH₂-9), 50.0 (CH-5), 166.0 (C=O-8), 173.7 (C=O-4); ³¹P-¹H_{decoupl} NMR (121 MHz, CDCl₃) δ_{P} 19.2; HRMS (NSI) calcd for (C₈H₁₉N₃O₅P)⁺, MH⁺: 268.1057, found 268.1016; LCMS purity >95 % (C-18 reversed phase, MeOH-H₂O).

6.1.7.13: Tert-butyl ((2S)-1-((-1-(diethoxyphosphoryl)ethyl)amino)-1-oxopropan-2-yl)carbamate or ^tBoc-L-Ala-D/L-Fos diethyl ester (157**)**



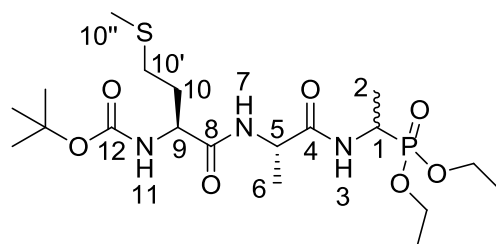
The general peptide coupling method (6.1.5.1) was followed, using ^tBoc-L-Ala-OH (**146a**) (10.0 mmol, 1.90 g) in dry THF and diethyl 1-aminoethylphosphonate (**84**) (10.0 mmol, 1.84 g) in dry THF. The pale yellow crude syrup was purified by column chromatography, using 100 % DCM and increasing to 95:5 DCM/methanol, to afford **157** as an off-white solid composed of 2 diastereoisomers, ^tBoc-L-Ala-L-Fos diethyl ester and ^tBoc-L-Ala-D-Fos diethyl ester (2.49 g, 7.1 mmol, 71 %); m.p. 102 – 105 °C; $\bar{\nu}_{\max}/\text{cm}^{-1}$ 3280 (NH), 1710 (C=O), 1652 (C=O), 1556 (NH bend), 1229 (P=O), 1173 (C-O), 1013 (P-O-C), 973 (P-O-C); ¹H NMR (300 MHz, CDCl₃) δ_{H} 1.23-1.43 (12H, m, CH₃-2, CH₃-6, 2 x OCH₂CH₃), 1.44 (9H, s, C(CH₃)₃), 4.06-4.23 (5H, m, 2 x OCH₂CH₃, CH-5), 4.40-4.52 (1H, m, CH-1), 5.12 (0.5H, d, ³J_{H-H}=1.5 Hz, NH-7), 5.14 (0.5H, d, ³J_{H-H}=1.5 Hz, NH-7), 6.72 (0.5H, d, ³J_{H-H}=2.3 Hz, NH-3), 6.74 (0.5H, d, ³J_{H-H}=2.3 Hz, NH-3); ¹³C NMR (75 MHz, CDCl₃) δ_{C} 15.6 (CH₃-2), 16.3 (d, ³J_{C-P}=3.0 Hz, OCH₂CH₃), 16.4 (d, ³J_{C-P}=2.3 Hz, OCH₂CH₃), 16.5 (d, ³J_{C-P}=3.0 Hz, OCH₂CH₃), 16.6 (d, ³J_{C-P}=2.3 Hz, OCH₂CH₃), 18.4 (CH₃-6), 28.3 (C(CH₃)₃), 40.8 (d, ¹J_{C-P}=156.8 Hz, CH-1), 41.0 (d, ¹J_{C-P}=156.8 Hz, CH-1), 50.0 (CH-5), 62.4 (d, ²J_{C-P}=6.8 Hz, OCH₂CH₃), 62.5 (d, ²J_{C-P}=6.8 Hz, OCH₂CH₃), 62.6 (d, ²J_{C-P}=6.8 Hz, OCH₂CH₃), 62.8 (d, ²J_{C-P}=6.8 Hz, OCH₂CH₃), 80.0 (C(CH₃)₃), 155.2 (C=O-8), 172.1 (C=O-4); ³¹P-¹H_{decoupled} NMR (121 MHz, CDCl₃) δ_{P} 25.2; CHN [Found: C, 48.22; H, 8.58; N, 7.87. C₁₄H₂₉N₂O₆P requires C, 47.92; H, 8.30; N, 7.95 %]; HRMS (NSI) calcd for (C₁₇H₃₅N₃O₇P)⁺, MH⁺: 424.2207, found 424.2200.

6.1.7.14: (2S)-1-((1-(Diethoxyphosphoryl)ethyl)amino)-1-oxopropan-2-aminium chloride or L-Ala-D/L-Fos diethyl ester hydrochloride (158)



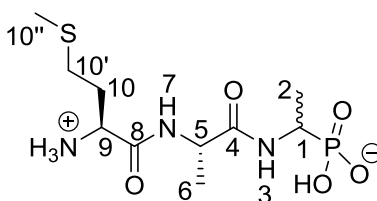
The *tert*-butoxycarbonyl at the *N*-terminus of *tert*-butyl ((2S)-1-((-1-(diethoxyphosphoryl)ethyl)amino)-1-oxopropan-2-yl)carbamate (**157**) (6.0 mmol, 2.13 g) was removed under acidic deprotection method (6.1.5.3). The off-white hygroscopic crude solid was washed with petrol to afford **158** as a pale green solid composed of 2 diastereoisomers, L-Ala-L-Fos diethyl ester hydrochloride and L-Ala-D-Fos diethyl ester hydrochloride (1.46 g, 5.1 mmol, 84 %); m.p. 60 – 63 °C; $\bar{\nu}_{\text{max}}/\text{cm}^{-1}$ 2986 (NH⁺), 1673 (C=O), 1555 (NH bend), 1212(P=O), 1017 (P-O-C), 970 (P-O-C); ¹H NMR (300 MHz, CD₃OD) δ_{H} 1.29-1.44 (9H, m, 2 x OCH₂CH₃, CH₃-2), 1.51 (3H, d, ³J_{H-H}=6.0 Hz, CH₃-6), 3.90-3.98 (1H, m, CH-5), 4.08-4.22 (4H, m, 2 x OCH₂CH₃), 4.28-4.47 (1H, m, CH-1); ¹³C NMR (75 MHz, CD₃OD) δ_{C} 13.7 (CH₃-2), 14.0 (CH₃-2), 15.4 (2 x OCH₂CH₃), 16.3 (CH₃-6), 41.1 (d, ¹J_{C-P}=158.3 Hz, CH-1), 41.4 (d, ¹J_{C-P}=158.3 Hz, CH-1), 48.8 (CH-5), 48.9 (CH-5), 62.7-63.0 (2 x OCH₂CH₃), 169.0 (C=O-4); ³¹P-¹H_{decoupl} NMR (121 MHz, CDCl₃) δ_{P} 29.0, 29.1; HRMS (NSI) calcd for (C₉H₂₂N₂O₄P)⁺, M⁺: 253.1312, found 253.1316.

6.1.7.15: Tert-butyl ((2S)-1-(((2S)-1-((1-(diethoxyphosphoryl)ethyl)amino)-1-oxopropan-2-yl)amino)-4-(methylthio)-1-oxobutan-2-yl)carbamate or ^tBoc-L-Met-L-Ala-D/L-Fos diethyl ester (159**)**



The general peptide coupling method (6.1.5.1) was followed, using ^tBoc-L-Met-OH (3.4 mmol, 0.88 g) in dry THF and (2S)-1-(((2S)-1-((1-(diethoxyphosphoryl)ethyl)amino)-1-oxopropan-2-aminium chloride (**158**) (3.4 mmol, 0.97 g) in dry DCM. The yellow crude solid was purified by column chromatography [DCM/MeOH (95:5)] to give **159** as an off-white solid composed of 2 diastereoisomers, ^tBoc-L-Met-L-Ala-L-Fos diethyl ester and ^tBoc-L-Met-L-Ala-D-Fos diethyl ester (0.53 g, 1.1 mmol, 32 %); m.p. 172 – 176 °C; $\bar{\nu}_{\text{max}}/\text{cm}^{-1}$ 3272 (NH), 1708 (C=O), 1673 (C=O), 1637 (C=O), 1530 (NH bend), 1226 (P=O), 1165 (C-O), 1020 (P-O-C), 976 (P-O-C); ¹H NMR (300 MHz, CDCl₃) δ_{H} 1.16-1.36 (12H, m, CH₃-2, CH₃-6, 2 x OCH₂CH₃), 1.36 (9H, s, C(CH₃)₃), 1.82-2.01 (2H, m, CH₂-10), 2.04 (3H, s, CH₃-10''), 2.49 (2H, dd, ³J_{H-H}=9.0 Hz, 3.0 Hz, CH₂-10'), 4.00-4.12 (4H, m, 2 x OCH₂CH₃), 4.16-4.26 (1H, m, CH-9), 4.33-4.43 (1H, m, CH-1), 4.45-4.53 (1H, m, CH-5), 5.40 (0.5H, d, ³J_{H-H}=9.0 Hz, NH-11), 5.44 (0.5H, d, ³J_{H-H}=6.0 Hz, NH-11), 6.85 (0.5H, d, ³J_{H-H}=6.0 Hz, NH-7), 6.92 (0.5H, d, ³J_{H-H}=6.0 Hz, NH-7), 7.07 (0.5H, d, ³J_{H-H}=9.0 Hz, NH-3), 7.16 (0.5H, d, ³J_{H-H}=9.0 Hz, NH-3); ¹³C NMR (75 MHz, CDCl₃) δ_{C} 14.2 (CH₃-2), 14.3 (CH₃-2), 14.5 (CH₃-10''), 14.6 (CH₃-10''), 15.4 (d, ³J_{C-P}=3.0 Hz, OCH₂CH₃), 15.4 (d, ³J_{C-P}=2.3 Hz, OCH₂CH₃), 15.5 (d, ³J_{C-P}=3.0 Hz, OCH₂CH₃), 15.5 (d, ³J_{C-P}=2.3 Hz, OCH₂CH₃), 17.7 (CH₃-6), 27.3 (C(CH₃)₃), 29.2 (CH₂-10'), 29.3 (CH₂-10'), 30.8 (CH₂-10), 30.9 (CH₂-10), 39.9 (d, ¹J_{C-P}=156.8 Hz, CH-1), 40.0 (d, ¹J_{C-P}=156.8 Hz, CH-1), 47.9 (CH-5), 48.0 (CH-5), 52.6 (CH-9), 61.5 (d, ²J_{C-P}=6.8 Hz, OCH₂CH₃), 61.6 (d, ²J_{C-P}=6.8 Hz, OCH₂CH₃), 61.7 (d, ²J_{C-P}=6.8 Hz, OCH₂CH₃), 61.9 (d, ²J_{C-P}=6.8 Hz, OCH₂CH₃), 79.1 (C(CH₃)₃), 154.6 (C=O-12), 170.3 (C=O-4 or C=O-8), 170.4 (C=O-4 or C=O-8), 170.5 (C=O-4 or C=O-8), 170.6 (C=O-4 or C=O-8); ³¹P-¹H_{decoupled} NMR (121 MHz, CDCl₃) δ_{P} 25.0, 25.1; HRMS (NSI) calcd for (C₁₉H₃₉N₃O₇PS)⁺, MH⁺: 484.2241, found 484.2228.

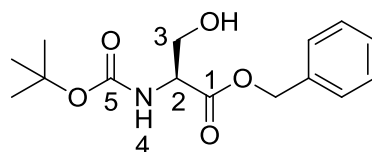
6.1.7.16: (1-((S)-2-((S)-2-Amino-4-(methylthio)butanamido)propanamido)ethyl)phosphonic acid or L-Met-L-Ala-D/L-Fos (160)



The *tert*-butoxycarbonyl and diethyl ester protecting groups of *tert*-butyl ((2S)-1-(((2S)-1-((1-(diethoxyphosphoryl)ethyl)amino)-1-oxopropan-2-yl)amino-4-(methylthio)-1-oxobutan-2-yl)carbamate (**159**) (0.9 mmol, 0.43 g) were removed under acidic deprotection method (6.1.5.4). The green crude solid was recrystallised from hot water/ethanol to give **160** as a pale green solid composed of 2 diastereoisomers, L-Met-L-Ala-L-Fos and L-Met-L-Ala-D-Fos (0.13 g, 0.41 mmol, 46 %); m.p. 214 – 217 °C (decomp.); $\bar{\nu}_{\max}/\text{cm}^{-1}$ 3263 (NH⁺), 2834 (broad OH), 1641 (br C=O), 1552 (NH bend), 1150 (P=O), 1041 (P-O-C), 919 (P-OH); ¹H NMR (300 MHz, D₂O) δ_{H} 1.29-1.33 (3H, m, CH₃-2), 1.42 (3H, d, ³J_{H-H}=6.0 Hz, CH₃-6), 2.15 (3H, s, CH₃-10''), 2.20 (2H, m, CH₂-10), 2.62 (2H, m, CH₂-10'), 4.05 (1H, m, CH-1), 4.14 (1H, m, CH-9), 4.39-4.41 (1H, m, CH-5); ¹³C NMR (75 MHz, D₂O) δ_{C} 16.9 (CH₃-10''), 18.4 (CH₃-2), 19.5 (CH₃-6), 19.6 (CH₃-6), 32.8 (CH₂-10'), 33.0 (CH₂-10'), 30.7 (CH₂-10), 31.0 (CH₂-10), 44.4 (CH-1), 52.9 (CH-5), 53.0 (CH-5), 55.0 (CH-9), 176.1 (C=O-4, C=O-8); ³¹P-¹H_{decoupl} NMR (121 MHz, CDCl₃) δ_{P} 20.7; HRMS (NSI) calcd for (C₁₀H₂₃N₃O₅PS)⁺, MH⁺: 328.1091, found 328.1094; LCMS purity >95 % (C-18 reversed phase, MeOH-H₂O).

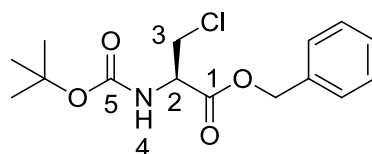
6.1.8: Synthesis of β -chloro-L-alanine derivatives

6.1.8.1: (S)-Benzyl 2-((tert-butoxycarbonyl)amino)-3-hydroxypropanoate or **Boc-L-Ser-OBzl (178)** (1981CR229)



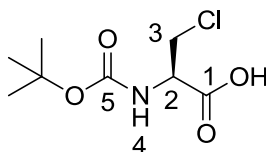
Boc-L-Serine (20 mmol, 4.10 g) and 1,8-diazabicyclo[5.4.0]undec-7-ene (DBU) (30 mmol, 4.5 mL) were dissolved in a round-bottom flask containing dry benzene (80 mL), followed by the addition of benzyl bromide (30 mmol, 3.60 mL). The solution was stirred overnight at room temperature under nitrogen and later the solvent was removed under reduced pressure to afford an off-white residue. Ethyl acetate (100 mL) was added, the flask contents were sonicated and then washed with 1M HCl (50 mL) and brine (2 x 50 mL). The organic layer was dried over MgSO_4 , filtered, concentrated *in vacuo* and purified by column chromatography [petrol/ethyl acetate (1:1)] to give **178** as a white solid (5.24 g, 17.7 mmol, 89 %); m.p. 61 – 63 °C (lit. m.p. 59 – 60 °C (1981CR229)); $\bar{\nu}_{\text{max}}/\text{cm}^{-1}$ 3416 (NH, OH), 1756 (C=O), 1666 (C=O), 1522 (NH bend), 1200 (C-O), 1154 (C-O); $^1\text{H NMR}$ (300 MHz, CDCl_3) δ_{H} 1.36 (9H, s, C(CH_3)₃), 2.17 (1H, br, OH), 3.82 (1H, dd, $^2J_{\text{H-H}}=11.1$ Hz, $^3J_{\text{H-H}}=3.6$ Hz, $\text{CH}_{\text{a/b-3}}$), 3.90 (1H, dd, $^2J_{\text{H-H}}=11.1$ Hz, $^3J_{\text{H-H}}=3.9$ Hz, $\text{CH}_{\text{a/b-3}}$), 4.33 (1H, m, CH-2), 5.11 (1H, d, $^2J_{\text{H-H}}=12.3$ Hz, $\text{OCH}_{\text{a/bAr}}$), 5.16 (1H, d, $^2J_{\text{H-H}}=12.3$ Hz, $\text{OCH}_{\text{a/bAr}}$), 5.40 (1H, br, NH-4), 7.27 (5H, m, 5 x CH_{Ar}); $^{13}\text{C NMR}$ (75 MHz, CDCl_3) δ_{C} 27.1 (C(CH_3)₃), 54.7 (CH-2), 62.3 ($\text{CH}_2\text{-3}$), 66.2 (OCH_2Ar), 79.1 (C(CH_3)₃), 127.0 (2 x CH_{Ar}), 127.3 (CH_{Ar}), 127.4 (2 x CH_{Ar}), 134.1 (CH_{Ar} quat.), 153.0 (C=O-5), 170.7 (C=O-1); m/z (ESI) calcd for $(\text{C}_{15}\text{H}_{21}\text{NNaO}_5)^+$, MNa^+ : 318.3, found 318.2.

6.1.8.2: (R)-Benzyl 2-((tert-butoxycarbonyl)amino)-3-chloropropanoate or 'Boc-β-Cl-L-Ala-OBzl (179) (T-2013MI257)



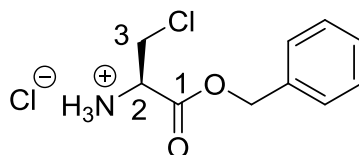
(S)-Benzyl 2-((tert-butoxycarbonyl)amino)-3-hydroxypropanoate (**178**) (15 mmol, 4.43 g) was dissolved in dry DCM (40 mL), followed by the addition of trichloroacetonitrile (30 mmol, 3 ml). The solution was stirred at room temperature for 2 hours. To this solution, triphenylphosphine (30 mmol, 7.87 g) in dry DCM (50 mL) was added slowly. The resulting solution was stirred overnight at room temperature under nitrogen; brine (100 mL) was added to quench the reaction. The organic layer was washed with brine (3 x 100 mL), dried over MgSO₄, filtered and concentrated *in vacuo* to afford an orange residue. The residue was purified by column chromatography [petrol/ethyl acetate (7:3)] to give **179** as a white solid (3.53 g, 11.2 mmol, 75 %); m.p. 55 – 58 °C; $\bar{\nu}_{\max}/\text{cm}^{-1}$ 3364 (NH), 1725 (C=O), 1680 (C=O), 1519 (NH bend), 1208 (C-O), 1158 (C-O); ¹H NMR (300 MHz, CDCl₃) δ_{H} 1.38 (9H, s, C(CH₃)₃), 3.78 (1H, dd, ²J_{H-H}=11.2 Hz, ³J_{H-H}=3.2 Hz, CH_{a/b}-3), 3.92 (1H, dd, ²J_{H-H}=11.3 Hz, ³J_{H-H}=3.0 Hz, CH_{a/b}-3), 4.67 (1H, m, CH-2), 5.13 (1H, d, ²J_{H-H}=12.2 Hz, OCH_{a/b}Ar), 5.18 (1H, d, ²J_{H-H}=12.2 Hz, OCH_{a/b}Ar), 5.37 (1H, d, ³J_{H-H}=7.5 Hz, NH-4), 7.29 (5H, m, 5 x CH_{Ar}); ¹³C NMR (75 MHz, CDCl₃) δ_{C} 28.3 (C(CH₃)₃), 45.5 (CH₂-3), 54.5 (CH-2), 67.8 (OCH₂Ar), 80.5 (C(CH₃)₃), 128.4 (CH_{Ar}), 128.6 (CH_{Ar}), 128.7 (CH_{Ar}), 134.9 (CH_{Ar} quat.), 155.0 (C=O-5), 169.0 (C=O-1); CHN [Found: C, 57.71; H, 6.46; N, 4.38. C₁₅H₂₀ClNO₄ requires C, 57.42; H, 6.42; N, 4.46 %]; *m/z* (ESI) calcd for (C₁₅H₂₀ClNNaO₄)⁺, MNa⁺: 336.1 (³⁵Cl), 338.1 (³⁷Cl), found 336.2 (³⁵Cl), 338.2 (³⁷Cl).

6.1.8.3: (*R*)-2-((*Tert*-butoxycarbonyl)amino)-3-chloropropanoic acid or **Boc-β-Cl-L-Ala-OH (181)**



The hydrogenation deprotection method (6.1.5.2) was followed, using (*R*)-benzyl 2-((*tert*-butoxycarbonyl)amino)-3-chloropropanoate (**179**) (7.0 mmol, 2.20 g) to afford **181** as an off-white solid (1.52 g, 6.78 mmol, 97 %); m.p. 125 – 128 °C (lit. m.p. 127 – 129 °C (1983JMC1733)); $\bar{\nu}_{\max}/\text{cm}^{-1}$ 3434 (NH), 2973 (br OH), 1752 (C=O), 1735 (C=O), 1519 (NH bend), 1159 (C-O), 1148 (C-O); $^1\text{H NMR}$ (300 MHz, CDCl_3) δ_{H} 1.40 (9H, s, $\text{C}(\text{CH}_3)_3$), 3.80 (1H, dd, $^2J_{\text{H-H}}=12.0$ Hz, $^3J_{\text{H-H}}=3.0$ Hz, $\text{CH}_{\text{a/b-3}}$), 3.95 (1H, dd, $^2J_{\text{H-H}}=12.0$ Hz, $^3J_{\text{H-H}}=3.0$ Hz, $\text{CH}_{\text{a/b-3}}$), 4.70 (1H, m, CH-2), 5.42 (1H, d, $^3J_{\text{H-H}}=7.2$ Hz, NH-4), 9.03 (1H, br, OH); $^{13}\text{C NMR}$ (75 MHz, CDCl_3) δ_{C} 27.1 ($\text{C}(\text{CH}_3)_3$), 44.0 ($\text{CH}_2\text{-3}$), 53.1 (CH-2), 79.8 ($\text{C}(\text{CH}_3)_3$), 154.2 (C=O-5), 172.1 (C=O-1); m/z (ESI) calcd for $(\text{C}_8\text{H}_{14}\text{ClNNaO}_4)^+$, MNa^+ : 246.1 (^{35}Cl), 248.1 (^{37}Cl), found 246.1 (^{35}Cl), 248.1 (^{37}Cl).

6.1.8.4: (*R*)-1-(Benzyloxy)-3-chloro-1oxopropan-2-aminium chloride or **β-Cl-L-Ala-OBzl hydrochloride (182)**

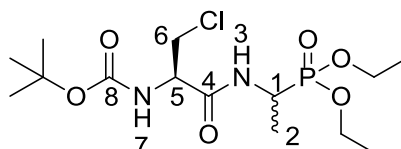


The *tert*-butoxycarbonyl at the *N*-terminus of (*R*)-benzyl 2-((*tert*-butoxycarbonyl)amino)-3-chloropropanoate (**179**) (15 mmol, 4.71 g) was removed under acidic deprotection method (6.1.5.3). The white crude solid was filtered and washed by diethyl ether to give **182** as a white solid (3.47 g, 13.4 mmol, 93%); m.p. 145 °C (sub); $\bar{\nu}_{\max}/\text{cm}^{-1}$ 2841 (NH^+), 1750 (C=O), 1231 (C-O); $^1\text{H NMR}$ (300 MHz, D_2O) δ_{H} 4.06 (1H, dd, $^2J_{\text{H-H}}=15.0$ Hz, $^3J_{\text{H-H}}=6.0$ Hz, $\text{CH}_{\text{a/b-3}}$), 4.20 (1H, dd, $^2J_{\text{H-H}}=15.0$ Hz, $^3J_{\text{H-H}}=6.0$ Hz, $\text{CH}_{\text{a/b-3}}$), 4.70 (1H, t, $^3J_{\text{H-H}}=6.0$ Hz, CH-2), 5.29 (1H, d, $^2J_{\text{H-H}}=12.0$ Hz, $\text{OCH}_{\text{a/bAr}}$), 5.37 (1H, d, $^2J_{\text{H-H}}=12.0$ Hz, $\text{OCH}_{\text{a/bAr}}$), 7.42-7.47 (5H, m, 5 x CH_{Ar}); $^{13}\text{C NMR}$ (75 MHz, D_2O) δ_{C} 41.8 ($\text{CH}_2\text{-3}$), 54.0 (CH-2), 69.1 (OCH_2Ar), 128.6-129.1 (CH_{Ar}), 134.5 (CH_{Ar} quart.), 167.0 (C=O-1); CHN [Found:

C, 47.16; H, 5.43; N, 5.43. C₁₀H₁₃Cl₂NO₂·0.2H₂O requires C, 47.34; H, 5.32; N, 5.52 %]; *m/z* (ESI) calcd for (C₁₀H₁₃ClNO₂), M⁺: 214.1 (³⁵Cl), 216.1 (³⁷Cl), found 214.1 (³⁵Cl), 216.1 (³⁷Cl).

6.1.9: Synthesis of β-chloro-L-Ala-D/L-fosfalin

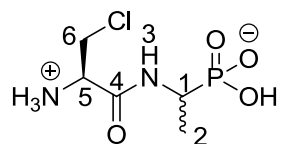
6.1.9.1: *Tert*-butyl ((2*R*)-3-chloro-1-((1-(diethoxyphosphoryl)ethyl)amino)-1-oxopropan-2-yl)carbamate or ¹³C-Boc-β-chloro-L-Ala-D/L-Fos diethyl ester (**195**)



The general peptide coupling method (6.1.5.1) was followed, using (*R*)-2-((*tert*-butoxycarbonyl)amino)-3-chloropropanoic acid (**181**) (6.0 mmol, 1.34 g) in dry THF and diethyl 1-aminoethylphosphonate (**84**) (6.0 mmol, 1.09 g) in dry THF. The light yellow crude liquid was purified by column chromatography, using 100 % petrol and increasing to 100 % ethyl acetate, to afford **195** as colorless syrup composed of 2 diastereoisomers, ¹³C-Boc-β-Cl-L-Ala-L-Fos diethyl ester and ¹³C-Boc-β-Cl-L-Ala-D-Fos diethyl ester (2.03 g, 5.2 mmol, 88 %); $\bar{\nu}_{\max}/\text{cm}^{-1}$ 3261 (NH), 1713 (C=O), 1670 (C=O), 1517 (NH bend), 1225 (P=O), 1164 (C-O), 1020 (P-O-C), 970 (P-O-C); ¹H NMR (300 MHz, CDCl₃) δ_{H} 1.15-1.46 (9H, m, CH₃-2, 2 x OCH₂CH₃), 1.47 (9H, s, C(CH₃)₃), 3.74 (1H, dd, ²J_{H-H}=12.0 Hz, ³J_{H-H}=6.0 Hz, CH_{a/b}-6), 4.00 (1H, dd, ²J_{H-H}=12.0 Hz, ³J_{H-H}=6.0 Hz, CH_{a/b}-6), 4.06-4.22 (4H, m, 2 x OCH₂CH₃), 4.40-4.56 (2H, m, CH-1, CH-5), 5.46 (0.5H, d, ³J_{H-H}=6.0 Hz, NH-3 or NH-7), 5.48 (0.5H, d, ³J_{H-H}=9.0 Hz, NH-3 or NH-7), 7.01 (0.5H, m, NH-3 or NH-7), 7.09 (0.5H, m, NH-3 or NH-7); ¹³C NMR (75 MHz, CDCl₃) δ_{C} 15.6 (CH₃-2), 15.7 (CH₃-2), 16.3 (d, ³J_{C-P}=1.5 Hz, OCH₂CH₃), 16.4 (d, ³J_{C-P}=2.3 Hz, OCH₂CH₃), 16.4 (d, ³J_{C-P}=1.5 Hz, OCH₂CH₃), 16.4 (d, ³J_{C-P}=2.3 Hz, OCH₂CH₃), 28.2 (C(CH₃)₃), 41.2 (d, ¹J_{C-P}=157.5 Hz, CH-1), 41.3 (d, ¹J_{C-P}=157.5 Hz, CH-1), 55.2 (CH₂-6), 55.3 (CH-5), 62.6 (d, ²J_{C-P}=6.8 Hz, OCH₂CH₃), 62.6 (d, ²J_{C-P}=6.8 Hz, OCH₂CH₃), 63.0 (d, ²J_{C-P}=6.8 Hz, OCH₂CH₃), 63.0 (d, ²J_{C-P}=6.8 Hz, OCH₂CH₃), 80.8 (C(CH₃)₃), 155.0 (C=O-8), 168.3 (C=O-4); ³¹P-¹H_{decoupl} NMR (121 MHz, CDCl₃) δ_{P} 24.7, 24.8; HRMS (NSI)

calcd for (C₁₄H₂₈ClN₂O₆P), MH⁺: 409.1266 (³⁵Cl), 411.1237 (³⁷Cl), found 409.1258 (³⁵Cl), 411.1231 (³⁷Cl).

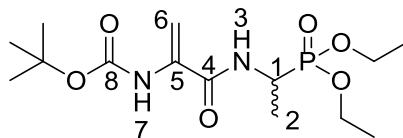
6.1.9.2: (1-((*R*)-2-Amino-3-chloropropanamido)ethyl)phosphonic acid, or β-chloro-L-Ala-D/L-Fos (196)



The *tert*-butoxycarbonyl and diethyl ester protecting groups of *tert*-butyl ((2*R*)-3-chloro-1-((1-(diethoxyphosphoryl)ethyl)amino)-1-oxopropan-2-yl)carbamate (**195**) (5.7 mmol, 2.21 g) were removed under acidic deprotection method (6.1.5.4). The pale green crude solid was recrystallised from hot water/acetone to give **196** as a pale green solid composed of 2 diastereoisomers composed of 2 diastereoisomers, β-Cl-L-Ala-L-Fos and β-Cl-L-Ala-D-Fos (0.85 g, 3.7 mmol, 65 %); m.p. 210 – 213 °C (decomp.); $\bar{\nu}_{\max}/\text{cm}^{-1}$ 3300 (NH⁺), 2928 (br OH), 1665 (C=O), 1565 (NH bend), 1150 (P=O), 1039 (P-O-C), 926 (P-OH); ¹H NMR (300 MHz, D₂O) δ_{H} 1.29 (3H, d, ³J_{H-H}=6.9 Hz, CH₃-2), 4.02 (3H, m, CH-1, CH₂-6), 4.38 (1H, m, CH-5); ¹³C NMR (75 MHz, D₂O) δ_{C} 15.2 (CH₃-2), 42.3 (CH₂-6), 42.6 (CH₂-6), 44.3 (d, ¹J_{P-C}=147.0 Hz, CH-1), 54.0 (CH-5), 54.1 (CH-5), 165.7 (C=O-4); ³¹P-¹H_{decoupl} NMR (121 MHz, CDCl₃) δ_{P} 18.7; CHN [Found: C, 25.90; H, 5.37; N, 11.80. C₅H₁₂ClN₂O₄P requires C, 26.04; H, 5.25; N, 12.15 %]; *m/z* (ESI) calcd for (C₅H₁₂ClN₂O₄P), MH⁺: 231.0 (³⁵Cl), 233.0 (³⁷Cl), found 231.1 (³⁵Cl), 233.1 (³⁷Cl); LCMS purity >95 % (C-18 reversed phase, MeOH-H₂O).

6.1.10: Synthesis of dehydroala-D/L-Fos hydrobromide

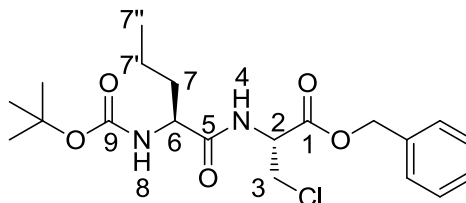
6.1.10.1: *Tert*-butyl (3-((1-(diethoxyphosphoryl)ethyl)amino)-3-oxoprop-1-en-2-yl)carbamate or 'Boc-dehydroala-D/L-Fos diethyl ester (206)



To the solution of *tert*-butyl ((2*R*)-3-chloro-1-((1-(diethoxyphosphoryl)ethyl)amino)-1-oxopropan-2-yl)carbamate (**195**) (0.75 mmol, 0.29 g) in distilled *tert*-butanol (15 mL), potassium *tert*-butoxide (0.75 mmol, 0.08 g) was added. The resulting solution was stirred at 30 °C under nitrogen for 20 hours, and then the solvent was removed *in vacuo* to afford a creamy white liquid. DCM (40 mL) was added and washed with 10 %w/v citric acid (2 x 10 mL), 10 % w/v potassium carbonate (10 mL) and water (2 x 10 mL). The organic layer was dried over magnesium sulphate, filtered and concentrated *in vacuo* to afford a white solid, then re-crystallised from hot heptanes to give **206** as white solid (0.14 g, 0.39 mmol, 52 %); m.p. 111 – 114 °C; $\bar{\nu}_{\max}/\text{cm}^{-1}$ 1726 (C=O), 1661 (C=O), 1632 (C=O), 1554 (NH bend), 1228 (P=O), 1160 (C-O), 1025 (P-O-C), 978 (P-O-C); $^1\text{H NMR}$ (300 MHz, CDCl_3) δ_{H} 1.31 (3H, t, $^3J_{\text{H-H}}=7.2$ Hz, OCH_2CH_3), 1.34 (3H, t, $^3J_{\text{H-H}}=7.2$ Hz, OCH_2CH_3), 1.42 (3H, dd, $^3J_{\text{P-H}}=16.8$ Hz, $^3J_{\text{H-H}}=7.2$ Hz, CH_3 -2), 1.48 (9H, s, $\text{C}(\text{CH}_3)_3$), 4.06-4.19 (4H, m, 2 x OCH_2CH_3), 4.48-4.59 (1H, m, CH -1), 5.24 (1H, s, $\text{CH}_{a/b}$ -6), 6.02 (1H, s, $\text{CH}_{a/b}$ -6), 6.90 (1H, d, $^3J_{\text{H-H}}=9.3$ Hz, NH -3), 7.29 (1H, br, NH -7); $^{13}\text{C NMR}$ (75 MHz, CDCl_3) δ_{C} 15.4 (CH_3 -2), 16.4 (2 x OCH_2CH_3), 28.2 ($\text{C}(\text{CH}_3)_3$), 41.7 (d, $^1J_{\text{C-P}}=157.5$ Hz, CH -1), 62.3 (d, $^2J_{\text{P-C}}=6.8$ Hz, OCH_2CH_3), 62.5 (d, $^2J_{\text{P-C}}=6.8$ Hz, OCH_2CH_3), 80.5 ($\text{C}(\text{CH}_3)_3$), 98.3 (CH_2 -6), 152.7 ($\text{C}=\text{O}$ -8), 134.6 (C -5), 163.5 ($\text{C}=\text{O}$ -4); ^{31}P - $^1\text{H}_{\text{decoupl}}$ NMR (121 MHz, CDCl_3) δ_{P} 24.9; CHN [Found: C, 48.00; H, 7.77; N, 8.00. $\text{C}_{14}\text{H}_{27}\text{N}_2\text{O}_6\text{P}$ requires C, 48.16; H, 8.01; N, 8.01 %]; m/z (ESI) calcd for $(\text{C}_{14}\text{H}_{27}\text{N}_2\text{NaO}_6\text{P})^+$, MNa^+ : 373.1, found 373.2.

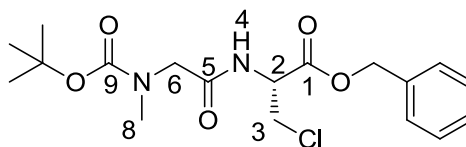
6.1.11: Synthesis of phosphonotripeptide derivatives containing the β -chloro-L-Ala-D/L-Fos moiety

6.1.11.1: (*R*)-Benzyl 2-((*S*)-2-((tert-butoxycarbonyl)amino)pentanamido)-3-chloropropanoate or 'Boc-L-Nva- β -chloro-L-Ala-OBzl (219b)



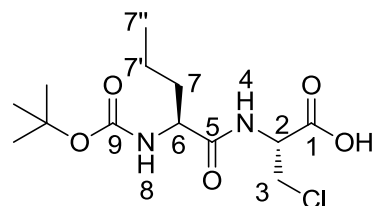
The general peptide coupling method (6.1.5.1) was followed, using 'Boc-L-Nva-OH (6.0 mmol, 1.31 g) in dry THF and (*R*)-1-(benzyloxy)-3-chloro-1oxopropan-2-aminium chloride (**182**) (5.4 mmol, 1.36 g) in dry DCM. The yellow crude liquid was purified by column chromatography [40-60 petrol/ethyl acetate (7:3)] to give **219b** as a white solid (1.74 g, 4.2 mmol, 78 %); m.p. 95 – 98 °C; $\bar{\nu}_{\max}/\text{cm}^{-1}$ 3327 (NH), 1743 (C=O), 1688 (C=O), 1653 (C=O), 1518 (NH bend), 1206 (C-O), 1169 (C-O); ^1H NMR (300 MHz, CDCl_3) δ_{H} 0.92 (3H, t, $^3J_{\text{H-H}}=9.0$ Hz, $\text{CH}_3\text{-7''}$), 1.32-1.43 (2H, m, $\text{CH}_2\text{-7'}$), 1.45 (9H, s, $\text{C}(\text{CH}_3)_3$), 1.52-1.65 (1H, m, $\text{CH}_{\text{a/b}}\text{-7}$), 1.75-1.82 (1H, m, $\text{CH}_{\text{a/b}}\text{-7}$), 3.89 (1H, dd, $^2J_{\text{H-H}}=12.0$ Hz, $^3J_{\text{H-H}}=3.0$ Hz, $\text{CH}_{\text{a/b}}\text{-3}$), 3.99 (1H, dd, $^2J_{\text{H-H}}=12.0$ Hz, $^3J_{\text{H-H}}=3.0$ Hz, $\text{CH}_{\text{a/b}}\text{-3}$), 4.11-4.15 (1H, m, CH-6), 4.96-5.00 (2H, m, CH-2 , NH-8), 5.20 (1H, d, $^2J_{\text{H-H}}=12.0$ Hz, $\text{OCH}_{\text{a/b}}\text{Ar}$), 5.25 (1H, d, $^2J_{\text{H-H}}=12.0$ Hz, $\text{OCH}_{\text{a/b}}\text{Ar}$), 6.97 (1H, d, $^3J_{\text{H-H}}=6.0$ Hz, NH-4), 7.33-7.37 (5H, m, 5 x CH_{Ar}); ^{13}C NMR (75 MHz, CDCl_3) δ_{C} 12.7 ($\text{CH}_3\text{-7''}$), 17.8 ($\text{CH}_2\text{-7'}$), 27.3 ($\text{C}(\text{CH}_3)_3$), 33.4 ($\text{CH}_2\text{-7}$), 43.8 ($\text{CH}_2\text{-3}$), 52.2 (CH-2), 53.4 (CH-6), 67.0 (OCH_2Ar), 79.3 ($\text{C}(\text{CH}_3)_3$), 127.4 (CH_{Ar}), 127.6 (CH_{Ar}), 127.7 (CH_{Ar}), 133.8 (CH_{Ar} quat.), 154.5 (C=O-9), 167.5 (C=O-1), 171.2 (C=O-5); CHN [Found: C, 58.49; H, 7.22; N, 6.81. $\text{C}_{20}\text{H}_{29}\text{ClN}_2\text{O}_5$ requires C, 58.18; H, 7.08; N, 6.78 %]; HRMS (NSI) calcd for $(\text{C}_{20}\text{H}_{30}\text{ClN}_2\text{O}_5)^+$, MH^+ : 413.1838 (^{35}Cl), 415.1809 (^{37}Cl), found 413.1837 (^{35}Cl), 415.1807 (^{37}Cl).

6.1.11.2: (R)-Benzyl 2-(2-((tert-butoxycarbonyl)(methyl)amino)acetamido)-3-chloropropanoate or ⁴Boc-Sar-β-chloro-L-Ala-OBzl (219c)



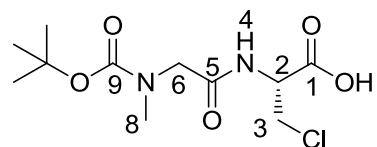
The general peptide coupling method (6.1.5.1) was followed, using ⁴Boc-Sar-OH (13.0 mmol, 2.46 g) in dry THF and (*R*)-1-(benzyloxy)-3-chloro-1oxopropan-2-aminium chloride (**182**) (13.3 mmol, 3.34 g) in dry DCM. The yellow crude liquid was purified by column chromatography [40-60 petrol/ethyl acetate (7:3)] to give **219c** as a light yellow syrup (3.63 g, 9.4 mmol, 73 %); $\bar{\nu}_{\max}/\text{cm}^{-1}$ 3302 (NH), 1747 (C=O), 1686 (br C=O), 1522 (NH bend), 1175 (C-O), 1148 (C-O); ¹H NMR (300 MHz, CDCl₃) δ_{H} 1.40 (9H, s, C(CH₃)₃), 2.87 (3H, s, NCH₃-8), 3.80 (1H, d, ²J_{H-H}=15.0 Hz, CH_{a/b}-6), 3.82 (1H, d, ²J_{H-H}=15.0 Hz, CH_{a/b}-6), 3.83 (1H, dd, ²J_{H-H}=12.0 Hz, ³J_{H-H}=3.0 Hz, CH_{a/b}-3), 3.94 (1H, dd, ²J_{H-H}=12.0 Hz, ³J_{H-H}=3.0 Hz, CH_{a/b}-3), 4.91-4.96 (1H, m, CH-2), 5.13 (1H, d, ²J_{H-H}=12.0 Hz, OCH_{a/b}Ar), 5.18 (1H, d, ²J_{H-H}=12.0 Hz, OCH_{a/b}Ar), 6.97 (1H, d, ³J_{H-H}=6.0 Hz, NH-4), 7.26-7.30 (5H, m, 5 x CH_{Ar}); ¹³C NMR (75 MHz, CDCl₃) δ_{C} 28.2 (C(CH₃)₃), 35.6 (NCH₃-8), 44.9 (CH₂-3), 53.0 (CH₂-6), 53.0 (CH-2), 68.0 (OCH₂Ar), 81.0 (C(CH₃)₃), 128.4 (CH_{Ar}), 128.6 (CH_{Ar}), 128.7 (CH_{Ar}), 134.8 (CH_{Ar} quat.), 154.5 (C=O-9), 168.4 (C=O-1), 169.4 (C=O-5); HRMS (NSI) calcd for (C₁₈H₂₆ClN₂O₅)⁺, MH⁺: 385.1525 (³⁵Cl), 387.1496 (³⁷Cl), found 385.1527 (³⁵Cl), 387.1498 (³⁷Cl).

6.1.11.3: (R)-2-((S)-2-((tert-Butoxycarbonyl)amino)pentanamido)-3-chloropropanoic acid or 'Boc-L-Nva-β-chloro-L-Ala-OH (220b)



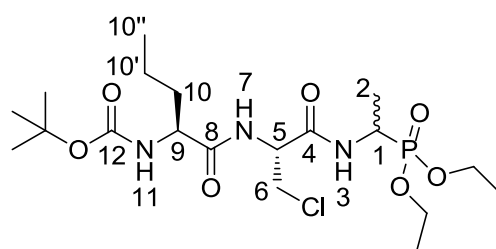
The hydrogenation deprotection method (6.1.5.2) was followed, using (*R*)-benzyl 2-((*S*)-2-((*tert*-butoxycarbonyl)amino)pentanamido)-3-chloropropanoate (**219b**) (5.8 mmol, 2.41 g) to afford **220b** as a light yellow solid (1.81 g, 5.61 mmol, 96 %); m.p. 60 - 63 °C; $\bar{\nu}_{\text{max}}/\text{cm}^{-1}$ 3312 (br OH), 2963 (NH), 1655 (br C=O), 1509 (NH bend), 1161 (C-O); $^1\text{H NMR}$ (300 MHz, DMSO) δ_{H} 0.85 (3H, t, $^3J_{\text{H-H}}=9.0$ Hz, CH_3 -7''), 1.24-1.34 (2H, m, CH_2 -7'), 1.38 (9H, s, $\text{C}(\text{CH}_3)_3$), 1.42-1.52 (1H, m, $\text{CH}_{\text{a/b}}$ -7), 1.54-1.59 (1H, m, $\text{CH}_{\text{a/b}}$ -7), 3.34 (1H, br, OH), 3.84 (1H, dd, $^2J_{\text{H-H}}=12.0$ Hz, $^3J_{\text{H-H}}=6.0$ Hz, $\text{CH}_{\text{a/b}}$ -3), 3.91 (1H, dd, $^2J_{\text{H-H}}=12.0$ Hz, $^3J_{\text{H-H}}=6.0$ Hz, $\text{CH}_{\text{a/b}}$ -3), 3.95-4.02 (1H, m, CH-6), 4.62-4.67 (1H, m, CH-2), 6.92 (1H, d, $^3J_{\text{H-H}}=9.0$ Hz, NH-8), 8.07 (1H, d, $^3J_{\text{H-H}}=9.0$ Hz, NH-4); $^{13}\text{C NMR}$ (75 MHz, CDCl_3) δ_{C} 14.1 (CH_3 -7''), 19.1 (CH_2 -7'), 28.6 ($\text{C}(\text{CH}_3)_3$), 34.4 (CH_2 -7), 45.1 (CH_2 -3), 53.6 (CH-2), 54.5 (CH-6), 78.5 ($\text{C}(\text{CH}_3)_3$), 155.8 (C=O-9), 170.6 (C=O-5), 173.0 (C=O-1); CHN [Found: C, 48.67; H, 7.51; N, 8.42. $\text{C}_{13}\text{H}_{23}\text{ClN}_2\text{O}_5$ requires C, 48.37; H, 7.18; N, 8.68 %]; m/z (ESI) calcd for $(\text{C}_{13}\text{H}_{23}\text{ClN}_2\text{NaO}_5)^+$, MNa^+ : 345.1 (^{35}Cl), 347.1 (^{37}Cl), found 345.2 (^{35}Cl), 347.2 (^{37}Cl).

6.1.11.4: (R)-2-(2-((tert-butoxycarbonyl)(methyl)amino)acetamido)-3-chloropropanoic acid or 'Boc-Sar-β-chloro-L-Ala-OH (220c)



The hydrogenation deprotection method (6.1.5.2) was followed, using (*R*)-benzyl 2-(2-((*tert*-butoxycarbonyl)(methyl)amino)acetamido)-3-chloropropanoate (**219c**) (6.2 mmol, 2.40 g) to afford **220c** as an off-white solid (1.81 g, 6.1 mmol, 99 %); m.p. 89 - 91 °C; $\bar{\nu}_{\max}/\text{cm}^{-1}$ 3342 (NH), 2982 (br OH), 1734 (C=O), 1672 (C=O), 1644 (C=O), 1524 (NH bend), 1152 (C-O); $^1\text{H NMR}$ (300 MHz, CDCl_3) δ_{H} 1.47 (9H, s, $\text{C}(\text{CH}_3)_3$), 2.99 (3H, s, NCH_3 -8), 3.81-4.17 (4H, m, CH_2 -6, CH_2 -3), 5.01 (1H, m, CH -2), 7.07 (1H, br, NH -4), 7.45 (1H, br, OH); $^{13}\text{C NMR}$ (75 MHz, CDCl_3) δ_{C} 28.3 ($\text{C}(\text{CH}_3)_3$), 36.1 (NCH_3 -8), 44.5 (CH_2 -3), 53.0 (CH_2 -6 and CH -2), 81.8 ($\text{C}(\text{CH}_3)_3$), 156.8 ($\text{C}=\text{O}$ -9), 169.5 ($\text{C}=\text{O}$ -1 and $\text{C}=\text{O}$ -5); CHN [Found: C, 43.98; H, 6.69; N, 9.53. $\text{C}_{11}\text{H}_{19}\text{ClN}_2\text{O}_5 \cdot 0.3\text{H}_2\text{O}$ requires C, 44.02; H, 6.58; N, 9.33 %]; m/z (ESI) calcd for $(\text{C}_{11}\text{H}_{19}\text{ClN}_2\text{NaO}_5)^+$, MNa^+ : 317.1 (^{35}Cl), 319.1 (^{37}Cl), found 317.1 (^{35}Cl), 319.1 (^{37}Cl).

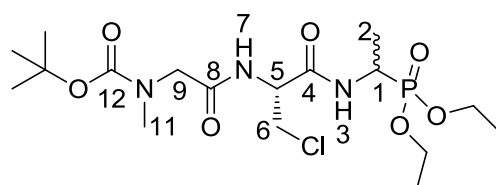
6.1.11.5: *Tert*-butyl ((2*S*)-1-(((2*R*)-3-chloro-1-((1-(diethoxyphosphoryl)ethyl)amino)-1-oxopropan-2-yl)amino)-1-oxopentan-2-yl)carbamate or ¹Boc-L-Nva-β-chloro-L-Ala-D/L-Fos diethyl ester (221b**)**



The general peptide coupling method (6.1.5.1) was followed, using (*R*)-2-((*S*)-2-((*tert*-butoxycarbonyl)amino)pentanamido)-3-chloropropanoic acid (**220b**) (1.8 mmol, 0.58 g) in dry THF and diethyl 1-aminoethylphosphonate (**84**) (1.8 mmol, 0.33 g) in dry THF. The light yellow crude liquid was purified by column chromatography, using ethyl acetate/methanol (96:4), to afford **221b** as a white solid composed of 2 diastereoisomers, ¹Boc-L-Nva-β-Cl-L-Ala-L-Fos diethyl ester and ¹Boc-L-Nva-β-Cl-L-Ala-D-Fos diethyl ester (0.45 g, 0.93 mmol, 52 %); m.p. 196 °C (decomp); $\bar{\nu}_{\max}/\text{cm}^{-1}$ 3272 (NH), 1709 (C=O), 1680 (C=O), 1644 (C=O), 1530 (NH bend), 1229 (P=O), 1165 (C-O), 1019 (P-O-C), 972 (P-O-C); ¹H NMR (300 MHz, CDCl₃) δ_{H} 0.86 (1.5H, t, ³*J*_{H-H}=9.0 Hz, CH₃-10''), 0.88 (1.5H, t, ³*J*_{H-H}=9.0 Hz, CH₃-10''), 1.22-1.34 (11H, m, 2 x OCH₂CH₃, CH₃-2, CH₂-10'), 1.38 (9H, s, C(CH₃)₃), 1.53-1.59 (1H, m, CH_{a/b}-10), 1.70-1.77 (1H, m, CH_{a/b}-10), 3.69 (1H, dd, ²*J*_{H-H}=12.0 Hz, ³*J*_{H-H}=6.0 Hz, CH_{a/b}-6), 3.78-3.81 (1H, m, CH-9), 3.91 (1H, dd, ²*J*_{H-H}=12.0 Hz, ³*J*_{H-H}=6.0 Hz, CH_{a/b}-6), 3.97-4.13 (4H, m, 2 x OCH₂CH₃), 4.35-4.46 (1H, m, CH-1), 4.73-4.79 (1H, m, CH-5), 4.97-5.03 (1H, m, NH-11), 7.01 (0.5H, d, ³*J*_{H-H}=9.0 Hz, NH-7), 7.09 (0.5H, d, ³*J*_{H-H}=9.0 Hz, NH-7), 7.25 (0.5H, d, ³*J*_{H-H}=9.0 Hz, NH-3), 7.33 (0.5H, d, ³*J*_{H-H}=9.0 Hz, NH-3); ¹³C NMR (75 MHz, CDCl₃) δ_{C} 12.7 (CH₃-10''), 14.5 (CH₃-2), 15.3 (OCH₂CH₃), 15.4 (OCH₂CH₃), 15.5 (OCH₂CH₃), 15.6 (OCH₂CH₃), 17.9 (CH₂-10'), 18.0 (CH₂-10'), 27.0 (C(CH₃)₃), 27.3 (C(CH₃)₃), 33.2 (CH₂-10), 40.4 (d, ¹*J*_{C-P}=157.5 Hz, CH-1), 43.4 (CH₂-6), 52.6 (CH-5), 52.8 (CH-5), 61.4 (d, ²*J*_{C-P}=6.8 Hz, OCH₂CH₃), 61.6 (d, ²*J*_{C-P}=6.8 Hz, OCH₂CH₃), 61.7 (d, ²*J*_{C-P}=6.8 Hz, OCH₂CH₃), 61.9 (d, ²*J*_{C-P}=6.8 Hz, OCH₂CH₃), 70.5 (CH-9), 79.4 (C(CH₃)₃), 154.7 (C=O-12), 166.8 (C=O-4), 171.4 (C=O-8); ³¹P-¹H_{decoupled} NMR (121 MHz, CDCl₃) δ_{P} 24.9, 25.0; HRMS (NSI) calcd for (C₁₉H₃₈ClN₃O₇P)⁺ 486.2130, found 486.2124; CHN [Found: C, 46.61; H, 7.76; N, 8.31. C₁₉H₃₇ClN₃O₇P requires

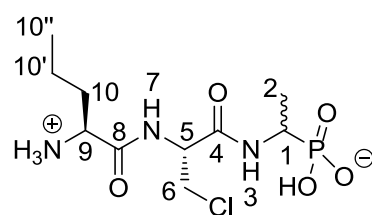
C, 46.96; H, 7.67; N, 8.65 %]; HRMS (NSI) calcd for (C₁₉H₃₈ClN₃O₇P)⁺, MH⁺: 486.2130 (³⁵Cl), 488.2102 (³⁷Cl), found 486.2124 (³⁵Cl), 488.2098 (³⁷Cl).

6.1.11.6: *Tert*-butyl (2-(((2*R*)-3-chloro-1-((1-(diethoxyphosphoryl)ethyl)amino)-1-oxopropan-2-yl)amino)-2-oxoethyl)(methyl)carbamate or ^tBoc-Sar-β-chloro-L-Ala-D/L-Fos diethyl ester (221c**)**



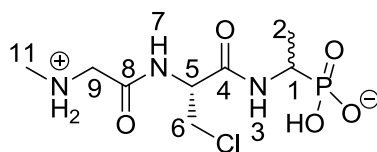
The general peptide coupling method (6.1.5.1) was followed, using (*R*)-2-(2-((*tert*-butoxycarbonyl)(methyl)amino)acetamido)-3-chloropropanoic acid (**220c**) (5.5 mmol, 1.61 g) in dry THF and diethyl 1-aminoethylphosphonate (**84**) (6.0 mmol, 1.09 g) in dry THF. The light yellow crude liquid was purified by column chromatography, using DCM/methanol (95:5), to afford **221c** as a light yellow syrup composed of 2 diastereoisomers, ^tBoc-Sar-β-Cl-L-Ala-L-Fos diethyl ester and ^tBoc-Sar-β-Cl-L-Ala-D-Fos diethyl ester (1.93 g, 4.21 mmol, 76 %); $\bar{\nu}_{\max}/\text{cm}^{-1}$ 3218 (NH), 1690 (C=O), 1665 (br C=O), 1518 (NH bend), 1224 (P=O), 1148 (C-O), 1018 (P-O-C), 967 (P-O-C); ¹H NMR (300 MHz, CDCl₃) δ_{H} 1.11-1.35 (9H, m, 2 x OCH₂CH₃, CH₃-2), 1.41 (9H, s, C(CH₃)₃), 2.90 (3H, s, CH₃-11), 3.70-3.88 (4H, m, CH₂-6, CH₂-9), 4.02-4.13 (4H, m, 2 x OCH₂CH₃), 4.36-4.47 (1H, m, CH-1), 4.78-4.82 (1H, m, CH-5), 6.94 (1H, m, NH-7), 7.36 (1H, m, NH-3); ¹³C NMR (75 MHz, CDCl₃) δ_{C} 15.2 (CH₃-2), 15.6 (CH₃-2), 16.3 (OCH₂CH₃), 16.4 (OCH₂CH₃), 28.3 (C(CH₃)₃), 35.9 (CH₃-11), 41.2 (d, ¹J_{C-P}=156.8 Hz, CH-1), 44.7 (CH₂-6), 53.1 (CH₂-9), 53.4 (CH-5), 62.7 (d, ²J_{C-P}=6.0 Hz, OCH₂CH₃), 63.0 (d, ²J_{C-P}=7.5 Hz, OCH₂CH₃), 81.0 (C(CH₃)₃), 152.3 (C=O-12), 167.7 (C=O-4 or C=O-8), 169.4 (C=O-4 or C=O-8); ³¹P-¹H_{decoupled} NMR (121 MHz, CDCl₃) δ_{P} 24.7, 24.8; HRMS (NSI) calcd for (C₁₆H₃₄ClN₃O₇P)⁺, MH⁺: 480.1637 (³⁵Cl), 482.1608 (³⁷Cl), found 480.1642 (³⁵Cl), 482.1612 (³⁷Cl).

6.1.11.7: (1-((*R*)-2-((*S*)-2-Ammoniopentanamido)-3-chloropropanamido) ethyl)phosphonic acid or L-Nva-β-chloro-L-Ala-D/L-Fos (**222b**)



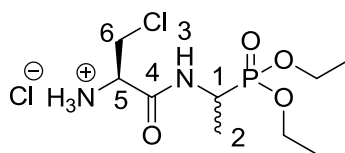
The *tert*-butoxycarbonyl and diethyl ester protecting groups of *tert*-butyl ((2*S*)-1-(((2*R*)-3-chloro-1-((1-(diethoxyphosphoryl)-ethyl)amino)-1-oxopropan-2-yl)amino)-1-oxopentan-2-yl)carbamate (**221b**) (2.0 mmol, 0.99 g) were removed under acidic deprotection method (6.1.5.4). The pale green crude solid was washed with diethyl ether to give **222b** as a pale green solid composed of 2 diastereoisomers, L-Nva-β-Cl-L-Ala-L-Fos and L-Nva-β-Cl-L-Ala-D-Fos (0.64 g, 1.94 mmol, 97 %); m.p. 175 °C (sub); $\bar{\nu}_{\max}/\text{cm}^{-1}$ 3294 (NH⁺), 3000 (br OH), 1668 (C=O), 1645 (C=O), 1538 (NH bend), 1132 (P=O), 1039 (P-O-C), 921 (P-OH); ¹H NMR (300 MHz, D₂O) δ_{H} 1.01 (3H, t, ³J_{H-H}=9.0 Hz, CH₃-10''), 1.30-1.37 (3H, br m, CH₃-2), 1.44-1.54 (2H, br m CH₂-10'), 1.90-1.98 (2H, br m, CH₂-10), 3.91-4.15 (4H, br m, CH₂-6, CH-9, CH-1), 4.79 (1H, br m, CH-5); ¹³C NMR (75 MHz, D₂O) δ_{C} 12.9 (CH₃-10''), 15.7 (CH₃-2), 17.6 (CH₂-10'), 33.0 (CH₂-10), 43.3 (CH₂-6), 53.1 (CH-1 and CH-9), 55.0 (CH-5), 170.4 (C=O-4 and C=O-8); ³¹P-¹H_{decoupled} NMR (121 MHz, CDCl₃) δ_{P} 18.5; HRMS (NSI) calcd for (C₁₀H₂₀ClN₃O₅P)⁻ MH⁻: 328.0835 (³⁵Cl), 330.0805 (³⁷Cl), found 328.0833 (³⁵Cl), 330.0800 (³⁷Cl); LCMS purity >90 % (C-18 reversed phase, MeOH-H₂O).

6.1.11.8: 1-((*R*)-3-Chloro-2-(2-(methylammonio)acetamido)propanamido)ethyl)phosphonic acid or Sar- β -chloro-L-Ala-D/L-Fos (222c)



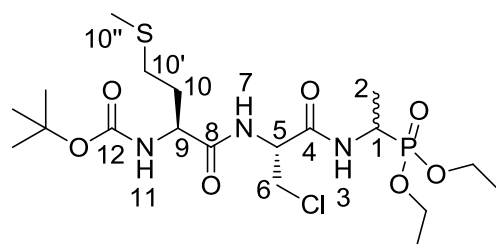
The *tert*-butoxycarbonyl and diethyl ester protecting groups of *tert*-butyl (2-(((2*R*)-3-chloro-1-((1-(diethoxyphosphoryl)ethyl)amino)-1-oxopropan-2-yl)amino)-2-oxoethyl)(methyl)carbamate (**221c**) (3.8 mmol, 1.74 g) were removed under acidic deprotection method (6.1.5.4). The pale green crude solid was recrystallised from hot water/ethanol to give **222c** as an off-white solid composed of 2 diastereoisomers, Sar- β -Cl-L-Ala-L-Fos and Sar- β -Cl-L-Ala-D-Fos (0.49 g, 1.61 mmol, 42 %); m.p. 185-188 °C (decomp.); $\bar{\nu}_{\max}/\text{cm}^{-1}$ 3287 (NH⁺), 3000 (br OH), 1657 (C=O), 1634 (C=O), 1552 (NH bend), 1172 (P=O), 1054 (P-O-C), 919 (P-OH); ¹H NMR (300 MHz, CD₃OD) δ_{H} 1.24 (3H, dd, ³J_{H-P}=15.0 Hz, ³J_{H-H}=6.0 Hz, CH₃-2), 2.74 (3H, s, NCH₃-11), 3.81-3.87 (2H, m, CH₂-6), 3.93-3.94 (2H, m, CH₂-9), 3.97-4.10 (1H, m, CH-1), 4.79 (1H, m, CH-5); ¹³C NMR (75 MHz, CD₃OD) δ_{C} 15.4 (CH₃-2), 32.9 (NCH₃-11), 43.6 (CH₂-6), 44.1 (d, ¹J_{C-P}=148.5 Hz, CH-1), 49.5 (CH₂-9), 54.6 (CH-5), 166.4 (C=O-4 or C=O-9), 166.9 (C=O-4 or C=O-9); ³¹P-¹H_{decoupl} NMR (121 MHz, CDCl₃) δ_{P} 18.8; HRMS (NSI) calcd for (C₈H₁₈ClN₃O₅P)⁺·MH⁺: 302.0667 (³⁵Cl), 304.0638 (³⁷Cl), found 302.0670 (³⁵Cl), 304.0640 (³⁷Cl); LCMS purity >90 % (C-18 reversed phase, MeOH-H₂O).

6.1.11.9: (2R)-3-Chloro-1-((1-(diethoxyphosphoryl)ethyl)amino)-1-oxopropan-2-aminium chloride or β -Cl-L-Ala-D/L-Fos diethyl ester hydrochloride (223)



The *tert*-butoxycarbonyl at the *N*-terminus of *tert*-butyl ((2*R*)-3-chloro-1-((1-(diethoxyphosphoryl)ethyl)amino)-1-oxopropan-2-yl)carbamate (**195**) (6.7 mmol, 2.59 g) was removed under acidic deprotection method (6.1.5.3). The off-white hygroscopic crude solid was washed with petrol to afford **223** as a pale green solid composed of 2 diastereoisomers, β -Cl-L-Ala-L-Fos diethyl ester hydrochloride and β -Cl-L-Ala-D-Fos diethyl ester hydrochloride (1.51 g, 4.7 mmol, 70 %); m.p. 129 – 133 °C (decomp.); $\bar{\nu}_{\text{max}}/\text{cm}^{-1}$ 3204 (NH⁺), 1687 (C=O), 1562 (NH bend), 1204 (P=O), 1010 (P-O-C), 961 (P-O-C); ¹H NMR (300 MHz, D₂O) δ_{H} 1.28 (3H, t, ³J_{H-H}=6.0 Hz, OCH₂CH₃), 1.29 (3H, t, ³J_{H-H}=6.0 Hz, OCH₂CH₃), 1.37 (3H, dd, ³J_{P-H}=18.0 Hz, ³J_{H-H}=6.0 Hz, CH₃-2), 3.92-4.04 (2H, m, CH₂-6), 4.07-4.21 (4H, m, 2 x OCH₂CH₃), 4.38-4.48 (2H, m, CH-1, CH-5); ¹³C NMR (75 MHz, D₂O) δ_{C} 13.7 (CH₃-2), 14.0 (CH₃-2), 15.7 (OCH₂CH₃), 15.7 (OCH₂CH₃), 41.7 (d, ¹J_{P-C}=158.3 Hz, CH-1), 42.0 (d, ¹J_{P-C}=157.5 Hz, CH-1), 42.4 (CH₂-6), 53.7 (CH-5), 53.8 (CH-5), 64.3 (d, ²J_{P-C}=6.8 Hz, OCH₂CH₃), 64.5 (d, ²J_{P-C}=6.8 Hz, OCH₂CH₃), 165.7 (C=O-4), 165.8 (C=O-4); ³¹P-¹H_{decoupl} NMR (121 MHz, CDCl₃) δ_{P} 26.1, 26.2; HRMS (NSI) calcd for (C₉H₂₁ClN₂O₄P)⁺. M⁺: 287.0922 (³⁵Cl), 289.0892 (³⁷Cl), found 287.0922 (³⁵Cl), 289.0890 (³⁷Cl).

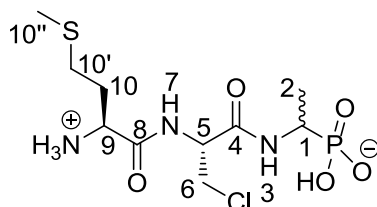
6.1.11.10: *Tert*-butyl ((2*S*)-1-(((2*R*)-3-chloro-1-((1-(diethoxyphosphoryl)ethyl)amino)-1-oxopropan-2-yl)amino)-4-(methylthio)-1-oxobutan-2-yl) carbamate or ¹Boc-L-Met-β-Cl-L-Ala-D/L-Fos diethyl ester (224**)**



The general peptide coupling method (6.1.5.1) was followed, using ¹Boc-L-Met-OH (3.4 mmol, 0.85 g) in dry THF and (2*R*)-3-chloro-1-((1-(diethoxyphosphoryl)ethyl)amino)-1-oxopropan-2-aminium chloride (**223**) (3.4 mmol, 1.10 g) in dry DCM. The yellow crude liquid was purified by column chromatography [DCM/MeOH (95:5)] and recrystallized from diethyl ether/ petrol to give **224** as a white solid composed of 2 diastereoisomers, ¹Boc-L-Met-β-Cl-L-Ala-L-Fos diethyl ester and ¹Boc-L-Met-β-Cl-L-Ala-D-Fos diethyl ester (0.88 g, 1.7 mmol, 50 %); m.p. 96 – 99 °C; $\bar{\nu}_{\text{max}}/\text{cm}^{-1}$ 3278 (NH), 1709 (C=O), 1687 (C=O), 1639 (C=O), 1523 (NH bend), 1228 (P=O), 1165 (C-O), 1018 (P-O-C), 970 (P-O-C); ¹H NMR (300 MHz, CDCl₃) δ_{H} 1.17-1.36 (9H, m, CH₃-2, 2 x OCH₂CH₃), 1.38 (9H, s, C(CH₃)₃), 1.87-2.03 (2H, m, CH₂-10), 2.04 (3H, s, CH₃-10''), 2.48-2.54 (2H, m, CH₂-10'), 3.71 (1H, dd, ²J_{H-H}=12.0 Hz, ³J_{H-H}=6.0 Hz, CH_{a/b}-6), 3.88 (1H, dd, ²J_{H-H}=12.0 Hz, ³J_{H-H}=6.0 Hz, CH_{a/b}-6), 3.99-4.13 (4H, m, 2 x OCH₂CH₃), 4.20 (1H, m, CH-9), 4.37-4.47 (1H, m, CH-1), 4.78-4.84 (1H, m, CH-5), 5.39 (0.5H, d, ³J_{H-H}=6.0 Hz, NH-11), 5.41 (0.5H, d, ³J_{H-H}=6.0 Hz, NH-11), 7.15 (0.5H, d, ³J_{H-H}=6.0 Hz, NH-7), 7.24 (0.5H, d, ³J_{H-H}=6.0 Hz, NH-7), 7.52 (1H, m, NH-3); ¹³C NMR (75 MHz, CDCl₃) δ_{C} 14.3 (CH₃-2), 14.4 (CH₃-2), 14.5 (CH₂-10''), 15.3 (OCH₂CH₃), 15.4 (OCH₂CH₃), 15.5 (OCH₂CH₃), 15.6 (OCH₂CH₃), 27.3 (C(CH₃)₃), 29.2 (CH₂-10'), 29.3 (CH₂-10'), 30.2 (CH₂-10), 30.4 (CH₂-10), 40.3 (d, ¹J_{P-C}=159.0 Hz, CH-1), 43.5 (CH₂-6), 43.7 (CH₂-6), 52.7 (CH-5), 53.1 (CH-9), 61.6 (d, ²J_{P-C}=6.8 Hz, OCH₂CH₃), 61.7 (d, ²J_{P-C}=6.0 Hz, OCH₂CH₃), 62.0 (d, ²J_{P-C}=6.8 Hz, OCH₂CH₃), 62.1 (d, ²J_{P-C}=7.5 Hz, OCH₂CH₃), 79.6 (C(CH₃)₃), 154.8 (C=O-12), 166.7 (C=O-4), 166.8 (C=O-4), 170.7 (C=O-8), 170.8 (C=O-8); ³¹P-¹H_{decoupled} NMR (121 MHz, CDCl₃) δ_{P} 24.5, 24.8; CHN [Found: C, 44.08; H, 7.47; N, 8.18. C₁₉H₃₇ClN₃O₇PS requires C,

44.06; H, 7.20; N, 8.11 %]; HRMS (NSI) calcd for (C₁₉H₃₁ClN₃O₇PS)⁺ MH⁺: 518.1851 (³⁵Cl), 520.1821 (³⁷Cl), found 518.1842 (³⁵Cl), 520.1814 (³⁷Cl).

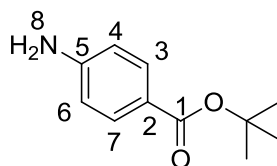
6.1.11.11: (1-((*R*)-2-((*S*)-2-Ammonio-4-(methylthio)butanamido)-3-chloro propanamido)ethyl)phosphonic acid or L-Met-β-Cl-L-Ala-D/L-Fos (**225**)



The *tert*-butoxycarbonyl and diethyl ester protecting groups of *tert*-butyl ((2*S*)-1-(((2*R*)-3-chloro-1-((1-(diethoxyphosphoryl) ethyl)amino)-1-oxopropan-2-yl)amino)-4-(methylthio)-1-oxobutan-2-yl)carbamate (**224**) (1.4 mmol, 0.71 g) were removed under acidic deprotection method (6.1.5.4). The green crude solid was recrystallised from hot water/ethanol to give **225** as a pale green solid composed of 2 diastereoisomers, L-Met-β-Cl-L-Ala-L-Fos and L-Met-β-Cl-L-Ala-D-Fos (0.17 g, 0.48 mmol, 35 %); m.p. 175 – 179 °C (decomp.); $\bar{\nu}_{\text{max}}/\text{cm}^{-1}$ 3264 (NH⁺), 2829 (broad OH), 1666(C=O), 1641 (C=O), 1546 (NH bend), 1149 (P=O), 1041 (P-O-C), 921 (P-OH); ¹H NMR (300 MHz, D₂O) δ_{H} 1.31 (3H, dd, ³J_{H-P}=15.0 Hz, ³J_{H-H}=6.0 Hz, CH₃-2), 2.13 (3H, s, CH₃-10''), 2.18-2.29 (2H, m, CH₂-10), 2.63-2.69 (2H, m, CH₂-10'), 3.89 (1H, dd, ²J_{H-H}=12.0 Hz, ³J_{H-H}=6.0 Hz, CH_{a/b}-6), 3.97 (1H, dd, ²J_{H-H}=12.0 Hz, ³J_{H-H}=6.0 Hz, CH_{a/b}-6), 4.01-4.13 (1H, m, CH-1), 4.22 (1H, br m, CH-9), 4.75-4.79 (1H, m, CH-5); ¹³C NMR (75 MHz, D₂O) δ_{C} 16.9 (CH₃-10''), 17.0 (CH₃-10''), 18.4 (CH₃-2), 31.1 (CH₂-10'), 32.9 (CH₂-10), 46.2 (CH₂-6), 47.0 (d, ¹J_{C-P}=147.0 Hz, CH-1), 52.2 (CH-9), 52.3 (CH-9), 57.8 (CH-5), 58.0 (CH-5), 171.7 (C=O-4), 171.8 (C=O-4), 172.3 (C=O-8); ³¹P-¹H_{decoupled} NMR (121 MHz, CDCl₃) δ_{P} 18.7; HRMS (NSI) calcd for (C₁₀H₂₁ClN₃O₅PS), MNa⁺: 384.0520 (³⁵Cl), 386.0489 (³⁷Cl), found 384.0523 (³⁵Cl), 386.0491 (³⁷Cl); LCMS purity >90 % (C-18 reversed phase, MeOH-H₂O).

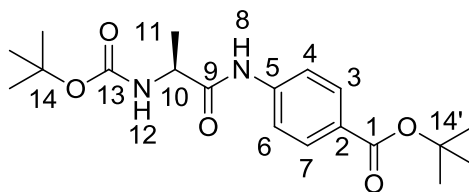
6.1.12: Synthesis of dipeptides containing *para*-aminobenzoic acid (PABA) derivatives

6.1.12.1: *Tert*-butyl 4-aminobenzoate or PABA-O^tButyl (**229**) (P-1991MI8)



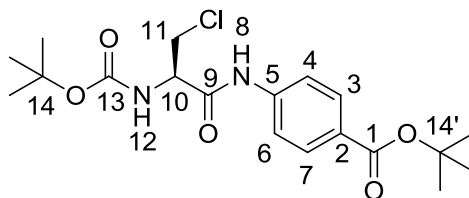
4-Aminobenzoic acid (20 mmol, 2.75 g) was added into a round-bottom flask containing distilled thionyl chloride (30 mL). The solution was heated to a gentle reflux at 80 °C until the solution went completely clear yellow for approx. 3 hours. The solution was cooled to room temperature and the solvent was removed under reduced pressure. The last trace was azeotrope with dry DCM (3 x 25 mL). The resulting yellow syrup was dissolved in dry DCM (30 mL) and cooled to 0 °C, followed by addition of *t*-butanol (25 mL). The resulting solution was continuously stirred for 10 minutes under nitrogen at 0 °C then overnight at room temperature. The solution was concentrated *in vacuo* to afford yellow syrup. The syrup was re-dissolved in DCM (100 mL) and later washed with 10 %w/v NaHCO₃ (2 x 30 mL) and water (40 mL). The organic layer was dried over MgSO₄, filtered and concentrated *in vacuo* to afford yellowish brown solid. The solid was purified by column chromatography [petrol/ethyl acetate (8:2)] to give **229** as an off-white solid (2.18 g, 11.3 mmol, 57 %); m.p. 105 – 108 °C (lit. m.p. 106 – 108 °C (2004SC1489)); $\bar{\nu}_{\max}/\text{cm}^{-1}$ 3416 (NH), 1683 (C=O), 1513 (NH bend), 1289 (C-O); ¹H NMR (300 MHz, CDCl₃) δ_{H} 1.57 (9H, s, C(CH₃)₃), 4.01 (2H, br, NH₂-8), 6.62 (2H, d, ³J_{H-H}=6.0 Hz, 2 x CH_{Ar}-4/6), 7.80 (2H, d, ³J_{H-H}=6.0 Hz, 2 x CH_{Ar}-3/7); ¹³C NMR (75 MHz, CDCl₃) δ_{C} 28.3 (C(CH₃)₃), 80.0 (C(CH₃)₃), 113.7 (2 x CH_{Ar}-4/6), 121.8 (CH_{Ar}-2), 131.4 (2 x CH_{Ar}-3/7), 150.4 (CH_{Ar}-5), 166.0 (C=O-1); *m/z* (ESI) calcd for (C₁₁H₁₅NaNO₂)⁺, MNa⁺: 216.1, found 216.1.

6.1.12.2: (S)-Tert-butyl 4-(2-((tert-butoxycarbonyl)amino)propanamido)benzoate or ^tBoc-L-Ala-PABA-O^tButyl (**232**)



The general peptide coupling method (6.1.5.1) was followed, using ^tBoc-L-Ala-OH (**146a**) (13.0 mmol, 2.46 g) in dry THF and *tert*-butyl 4-aminobenzoate (**229**) (12.0 mmol, 2.32 g) in dry THF. The yellowish orange crude syrup was purified by column chromatography [40-60 petrol/ethyl acetate (7:3)] to give **232** as an off-white solid (3.89 g, 10.7 mmol, 89 %); m.p. 57 – 60 °C; $\bar{\nu}_{\max}/\text{cm}^{-1}$ 3310 (NH), 1708 (C=O), 1672 (C=O), 1601 (C=O), 1534 (NH bend), 1291 (C-O), 1251 (C-O), 1159 (C-O); ¹H NMR (300 MHz, CDCl₃) δ_{H} 1.37 (3H, d, ³J_{H-H}=9.0 Hz, CH₃-11), 1.39 (9H, s, C(CH₃)₃-14), 1.50 (9H, s, C(CH₃)₃-14'), 4.28 (1H, m, CH-10), 5.09 (1H, d, ³J_{H-H}=9.0 Hz, NH-12), 7.47 (2H, d, ³J_{H-H}=6.0 Hz, 2 x CH_{Ar}-4/6), 7.83 (2H, d, ³J_{H-H}=6.0 Hz, 2 x CH_{Ar}-3/7), 8.76 (1H, br, NH-8); ¹³C NMR (75 MHz, CDCl₃) δ_{C} 17.3 (CH₃-11), 28.2 (C(CH₃)₃-14), 28.3 (C(CH₃)₃-14'), 51.0 (CH-10), 79.9 (C(CH₃)₃-14), 79.8 (C(CH₃)₃-14'), 118.7 (2 x CH_{Ar}-4/6), 127.5 (CH_{Ar}-2), 130.5 (2 x CH_{Ar}-3/7), 141.6 (CH_{Ar}-5), 156.2 (C=O-13), 165.3 (C=O-1), 171.1 (C=O-9); CHN [Found: C, 62.62; H, 7.74; N, 7.69. C₁₉H₂₈N₂O₅ requires C, 62.44; H, 7.88; N, 7.49 %]; HRMS (NSI) calcd for (C₁₉H₂₉N₂O₅)⁺, MH⁺: 365.2071, found 365.2070.

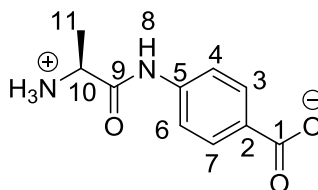
6.1.12.3: (R)-Tert-butyl 4-(2-((tert-butoxycarbonyl)amino)-3-chloropropanamido)benzoate or ^tBoc- β -chloro-L-Ala-PABA-O^tButyl (**233**)



The general peptide coupling method (6.1.5.1) was followed, using ^tBoc- β -chloro-L-Ala-OH (**181**) (6.0 mmol, 1.35 g) in dry THF and *tert*-butyl 4-aminobenzoate (**229**) (5.9 mmol, 1.14 g) in dry THF. The yellowish orange crude syrup was purified by column chromatography [40-60 petrol/ethyl acetate (8:3)] and azeotroped by diethyl ether to give **233** as an off-white solid (1.52 g, 3.81 mmol, 64

%); m.p. 55 – 58 °C; $\bar{\nu}_{\max}/\text{cm}^{-1}$ 3303 (NH), 1704 (C=O), 1677 (C=O), 1602 (C=O), 1530 (NH bend), 1511 (NH bend), 1292 (C-O), 1250 (C-O), 1160 (C-O); ^1H NMR (500 MHz, CDCl_3) δ_{H} 1.51 (9H, s, $\text{C}(\text{CH}_3)_3$ -14), 1.60 (9H, s, $\text{C}(\text{CH}_3)_3$ -14'), 3.85 (1H, dd, $^2J_{\text{H-H}}=12.0$ Hz, $^3J_{\text{H-H}}=6.0$ Hz, $\text{CH}_{\text{a/b}}$ -11), 4.10 (1H, dd, $^2J_{\text{H-H}}=12.0$ Hz, $^3J_{\text{H-H}}=6.0$ Hz, $\text{CH}_{\text{a/b}}$ -11), 4.64 (1H, m, CH -10), 5.45 (1H, d, $^3J_{\text{H-H}}=6.0$ Hz, NH -12), 7.60 (2H, d, $^3J_{\text{H-H}}=6.0$ Hz, 2 x CH_{Ar} -4/6), 7.97 (2H, d, $^3J_{\text{H-H}}=6.0$ Hz, 2 x CH_{Ar} -3/7), 8.50 (1H, br, NH -8); ^{13}C NMR (125 MHz, CDCl_3) δ_{C} 28.2 ($\text{C}(\text{CH}_3)_3$ -14), 28.3 ($\text{C}(\text{CH}_3)_3$ -14'), 44.1 (CH_2 -11), 56.0 (CH -10), 81.3 ($\text{C}(\text{CH}_3)_3$ -14'), 82.2 ($\text{C}(\text{CH}_3)_3$ -14), 119.1 (2 x CH_{Ar} -4/6), 128.2 (CH_{Ar} -2), 130.6 (2 x CH_{Ar} -3/7), 140.7 (CH_{Ar} -5), 155.7 ($\text{C}=\text{O}$ -13), 165.2 ($\text{C}=\text{O}$ -1), 167.3 ($\text{C}=\text{O}$ -9); CHN [Found: C, 57.22; H, 6.95; N, 6.65. $\text{C}_{19}\text{H}_{27}\text{ClN}_2\text{O}_5$ requires C, 57.21; H, 6.82; N, 7.02 %]; m/z (ESI) calcd for $(\text{C}_{19}\text{H}_{27}\text{ClN}_2\text{O}_5)^+$, MNa^+ : 421.2 (^{35}Cl), 423.2 (^{37}Cl), found 421.2 (^{35}Cl), 423.2 (^{37}Cl).

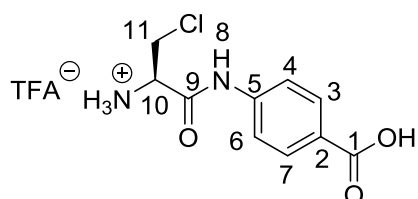
6.1.12.4: (S)-4-(2-Ammoniopropanamido)benzoic acid or L-Ala-PABA (234)



A solution of (S)-*tert*-butyl 4-(2-((*tert*-butoxycarbonyl)amino)propanamido)-benzoate (**232**) (10 mmol, 3.66 g) in glacial hydrogen bromide/acetic acid (33 %) (10.0 mL) was stirred overnight at room temperature. Dry diethyl ether (150 mL) was added and the mixture was placed in a freezer overnight. The solvent was decanted and the crude product was triturated with dry diethyl ether (5 x 50 mL). The brownish-orange crude product was dissolved in methanol (5 mL) and excess propylene oxide was added. The mixture was filtered and washed with dry diethyl ether to afford a white crude, which was dried in desiccator containing phosphorus (V) oxide and recrystallised from mixture hot acetonitrile/water to give **234** as a white solid (1.44 g, 6.9 mmol, 69 %); m.p. 225 °C (sub); $\bar{\nu}_{\max}/\text{cm}^{-1}$ 3500-2500 (broad OH), 2991 (NH^+), 1688 (C=O), 1603 (C=O), 1530 (NH bend), 1175 (C-O); ^1H NMR (300 MHz, D_2O) δ_{H} 1.58 (3H, d, $^3J_{\text{H-H}}=9.0$ Hz, CH_3 -11), 4.17 (1H, q, $^3J_{\text{H-H}}=9.0$ Hz, CH -10), 7.40 (2H, d, $^3J_{\text{H-H}}=9.0$ Hz, 2 x CH_{Ar} -4/6), 7.87 (2H, d, $^3J_{\text{H-H}}=9.0$

Hz, 2 x $\text{CH}_{\text{Ar-3/7}}$); ^{13}C NMR (75 MHz, D_2O) δ_{C} 16.5 (CH_3 -11), 49.8 (CH -10), 120.4 (2 x $\text{CH}_{\text{Ar-4/6}}$), 129.2 (2 x $\text{CH}_{\text{Ar-3/7}}$), 133.0 ($\text{CH}_{\text{Ar-5}}$), 138.9 ($\text{CH}_{\text{Ar-2}}$), 169.1 ($\text{C}=\text{O}$ -9), 174.7 ($\text{C}=\text{O}$ -1); CHN [Found: C, 52.81; H, 6.10; N, 12.37. $\text{C}_{10}\text{H}_{12}\text{N}_2\text{O}_3 \cdot 1.1\text{H}_2\text{O}$ requires C, 52.67; H, 6.28; N, 12.29 %]; HRMS (NSI) calcd for $(\text{C}_{10}\text{H}_{13}\text{N}_2\text{O}_3)^+$, MH^+ : 209.0921, found 209.0920.

6.1.12.5: (R)-1-((4-Carboxyphenyl)amino)-3-chloro-1-oxopropan-2-aminium 2,2,2-trifluoroacetate or β -chloro-L-Ala-PABA·TFA (235**)**



A solution of (*R*)-*tert*-butyl 4-(2-((*tert*-butoxycarbonyl)amino)-3-chloropropanamido) benzoate (**233**) (1.5 mmol, 0.62 g) in trifluoroacetic acid (15.0 mmol, 2.0 mL) was stirred overnight at room temperature. Dry diethyl ether (50 mL) was added and the mixture was placed in a freezer overnight. The solvent was decanted and the crude product was triturated while sonicated with dry diethyl ether (4 x 50 mL) and the last trace solvent was removed under reduced pressure to give **235** as an off-white solid (0.19 g, 0.5 mmol, 35 %); m.p. 107 – 110 °C (sub); $\bar{\nu}_{\text{max}}/\text{cm}^{-1}$ 3386-2650 (broad OH), 2978 (NH^+), 1672 ($\text{C}=\text{O}$), 1603 ($\text{C}=\text{O}$), 1546 (NH bend), 1176 (C-O); ^1H NMR (500 MHz, CD_3OD) δ_{H} 4.12 (2H, m, CH_2 -11), 4.43 (1H, m, CH -10), 7.73 (2H, d, $^3J_{\text{H-H}}=5.0$ Hz, 2 x $\text{CH}_{\text{Ar-4/6}}$), 8.01 (2H, d, $^3J_{\text{H-H}}=5.0$ Hz, 2 x $\text{CH}_{\text{Ar-3/7}}$); ^{13}C NMR (125 MHz, CD_3OD) δ_{C} 49.3 (CH_2 -11), 56.3 (CH -10), 120.4 (2 x $\text{CH}_{\text{Ar-4/6}}$), 128.1 ($\text{CH}_{\text{Ar-5}}$), 131.9 (2 x $\text{CH}_{\text{Ar-3/7}}$), 143.1 ($\text{CH}_{\text{Ar-2}}$), 165.9 ($\text{C}=\text{O}$ -9), 169.3 ($\text{C}=\text{O}$ -1); HRMS (NSI) calcd for $(\text{C}_{10}\text{H}_{11}\text{ClN}_2\text{O}_3)$, MNa^+ : 265.0350 (^{35}Cl), 265.0321 (^{37}Cl), found 265.0350 (^{35}Cl), 265.0318 (^{37}Cl).

6.2: LC-MS analysis

LC-MS analysis was performed using an Agilent 1290 Infinity Series HPLC system and an Agilent 6120 Quadrupole LC-MS detector. ACE Excel 5 Super C18 (150 x 4.6 mm i.d.) LC column was used. LC-MS data was analysed by Agilent ChemStation.

6.2.1: LC-MS conditions for diastereoisomeric phosphonopeptides analysis (153a, 153b, 153c, 160, 196, 222b, 222c and 225)

Mobile phase: water and methanol (95:5) + 0.1 % formic acid

Flow time: 0.75 mL/min

Injection volume: 10 μ L

Column temperature: 35 $^{\circ}$ C

Vial temperature: 25 $^{\circ}$ C

Sample concentration: 0.1 mg/mL in mobile phase

6.2.2: LC-MS conditions for diastereoisomeric ¹³C-Boc-L-Ala-L-Ala-D/L-Fos diethyl ester (152a) and PABA based dipeptides analysis (234 and 235) analyses

Conditions as above (section 6.2.1) were followed, except

Mobile phase: water and methanol (20:80) + 0.1 % formic acid

Sample concentration: 0.1 mg/mL in water and methanol (95:5) + 0.1 % formic acid

6.3: Stability study

6.3.1: Reagents and instruments

Deuterated oxide (D₂O) and sodium deuterioxide (30 %, NaOD) were acquired from Sigma-Aldrich. β -Chloro-L-Ala-D/L-fosfalin was prepared from 6.1.9.2. NMR spectra were obtained using a Bruker Avance III Ultrashield spectrometer at 500 MHz for ¹H spectra.

6.3.2: Sample preparation

β -Chloro-L-Ala-D/L-fosfalin (10 mg) was dissolved in D₂O (1.0 mL) and analysed as a blank sample by NMR. This sample was subsequently adjusted to pH 6.1, pH 7.1, pH 8.1 and pH 9.1 using sodium deuterioxide (0.05M, NaOD).

6.3.3: Sample analysis

Each pH sample was analysed using the NMR spectrometry at the time stated in Table 6.1. The peaks observed throughout the analysis were recorded and rationalised accordingly, in order to determine the stability pH range of β -chloro-L-Ala-D/L-fosfalin.

Table 6.1: Analysis time for β -chloro-L-Ala-D/L-fosfalin after adjusted to the corresponded pH

0 mins	3 mins	5 mins	13 mins
33 mins	63 mins	123 mins	243 mins
363 mins	723 mins	1 week	2 weeks
3 weeks	4 weeks	8 weeks	12 weeks

6.4: Microbiological testing

6.4.1: Media constituents

L-Arginine, L-aspartic acid, L-cysteine, glycine, L-histidine, L-isoleucine, L-lysine, L-methionine, L-phenylalanine, L-proline, L-serine, L-threonine, L-tryptophan, L-valine, magnesium sulphate, haem and D-(+)-glucose were purchased from Sigma Chemical Co. (Poole, UK). L-Tyrosine, uracil, guanine, cytosine, adenine, ammonium sulphate, potassium dihydrogen phosphate, saponin and dipotassium hydrogen phosphate were acquired from BDH Merck Ltd. (Poole, England). Yeast extract was supplied by bioMérieux (Craponne, France) and bacteriological agar from Oxoid (Basingstoke, UK). Nicotinamide adenine dinucleotide (NAD) was obtained from Merck (Darmstadt, Germany) and heparinised horse blood from TCS Biosciences (Buckingham, UK).

6.4.2: Microbial strains

Microbial reference strains were obtained from National Collection of Type Cultures (NCTC) (Colindale, UK) and the American Type Culture Collection (ATCC) (Manassas, US). These included twelve Gram negative bacteria: *A. baumannii*, *B. cepacia*, *E. cloacae*, *E. coli* (n=2), *K. pneumonia*, *P. rettgeri*, *P. aeruginosa*, *S. typhimurium*, *S. enteritidis*, *S. marcescens* and *Y. enterocolitica*; as well as eight Gram positive bacteria: *B. subtilis*, *E. faecalis*, *E. faecium*, *L. monocytogenes*, *S. epidermidis*, *S. aureus*, *S. aureus* (MRSA) and *S. pyogenes*. These 20 bacterial strains were maintained on Columbia agar.

Different β -lactamase classes of microbial resistant strains, such as Class A: Carbapenem-Resistant-Klebsiella pneumonia (KPC), Temoneira- β -lactamase (TEM) and Cefotaximas-Munich- β -lactamase (CTXM); Class B: New Delhi Metallo- β -lactamase (NDM); Class C Cefoxitin-Hydrolysing- β -lactamase (LAT); Class D Oxacillin-Hydrolysing- β -lactamase (OXA) were acquired from sources stated in Table 6.2.

Table 6.2: Sources of β -Lactam resistant strains

Class	Gene	Strain	Source
A	KPC-4	<i>K. pneumonia</i>	BioMérieux, La Balme-les-Grottes, France
	TEM52	<i>E. coli</i>	Universitätsklinikum Hamburg-Eppendorf, Germany
	CTX-M9	<i>E. cloacae</i>	Universitätsklinikum Hamburg-Eppendorf, Germany
B	NDM	<i>E.coli</i>	Rawalpindi Military hospital, Parkistan (2011JMC2288)
		<i>C. freundii</i>	
		<i>E. cloacae</i>	
		<i>K. pneumonia</i>	
C	LAT-4	<i>E. coli</i>	BioMérieux, La Balme-les-Grottes, France
D	OXA-48	<i>E. coli</i>	BioMérieux, La Balme-les-Grottes, France
		<i>K. pneumonia</i>	

6.4.3: Preparation of antagonist-free (AF) medium

The methodology, which was reported by Atherton (1979AAC677), was adapted with slight modification. In this method, 1.5% (15 g/L) bacteriological agar and 0.5 % (5 g/L) glucose were added to 880 mL deionised water. The resulting mixture was autoclaved at 121 °C for 15 minutes, followed by addition of 2 %v/v (20 mL/L) saponin-lysed blood, 25 mg/L haemin, 25 mg/L NAD and AF-supplement as outlined in Table 6.3. The saponin-lysed blood was prepared by incubating 100 mL sterile horse blood at 37 ± 0.5 °C for 15 minutes, adding 5 mL 10 % saponin and re-incubating for 15 minutes or longer to ensure completely blood lysis. The saponin-lysed blood was stored at 4 °C until used. The pH of media was 7.0.

Table 6.3: Contents of antagonist-free supplement per litre of deionised water

Component	Quantity	Component	Quantity
L-Arginine	1 g	L-Tryptophan	1 g
L-Aspartic acid	1 g	L-Tyrosine	1 g
L-Cysteine	1 g	L-Valine	1 g
Glycine	1 g	Adenine	0.1 g
L-Histidine	1 g	Cytosine	0.1 g
L-Isoleucine	1 g	Guanine	0.1 g
L-Leucine	1 g	Uracil	0.1 g
L-Methionine	1 g	Ammonium sulphate	5 g
L-Phenylalanine	1 g	Dipotassium hydrogen phosphate	70 g
L-Proline	1 g	Magnesium sulphate	1 g
L-Serine	1 g	Potassium hydrogen phosphate	20 g
L-Threonine	1 g	Yeast extract	1 g

6.4.4: Preparation of media containing suicide substrates

Each substrate was dissolved in sterile deionised water (SDW) and incorporated with AF-agar at a concentration range of 0.125 – 128 mg/L. A series of dilution was performed to achieve the required concentration and then poured into the sterile Petri dishes. Solidified agar plates were placed in a warm cabinet (37 ± 0.5 °C) for 5 minutes or until used.

6.4.5: Multipoint inoculation of agar

Each microbial strain was isolated from the respective Columbia agar and suspended in SDW, with a density equivalent to 0.5 McFarland standard under a densitometer. 100 µL of each suspension was transferred into the corresponded wells of a multipoint inoculation device. 1 µL of the bacterial suspension, equivalent to 1.5×10^5 organisms was applied as a spot by this instrument on the incubated plates, which were prepared in section 6.3.4. Twenty different bacterial strains were applied on a plate and incubated for 22hrs at 37 ± 0.5 °C.

6.4.6: Determination of minimum inhibitory concentration (MIC)

The inhibitory activity of each plate containing respective suicide substrates was determined by visual inspection. Bacterial growth with more than ten colonies indicated positive results or poor inhibition, while less than ten colonies indicated negative results, where the microbial viability was suppressed. The lowest concentration of suicide substrate that exhibited these negative results was recorded as the MIC.

CHAPTER 7

REFERENCES

7.1: Journals/Articles

- 1905JH333 MacConkey, A. *Journal of Hygiene*. 1905, **5**(3), 333
- 1951JEM243 Davis, B. D. *Journal of Experimental Medicine*. 1951, **94**(3), 243
- 1952Sci710 Takemori, N.; Kitaoka, M. *Science*. 1952, **116**(3026), 710
- 1959JBC904 Reed, L. J.; Schram, A. C.; Loveless, L. E. *Journal of Biological Chemistry*. 1959, **234**(4), 904
- 1960JACS998 Strominger, J. L.; Ito, E.; Threnn, R. H. *Journal of the American Chemical Society*. 1960, **82**, 998
- 1962JB381 Mossel, D. A. A.; Mengerink, W. H. J.; Scholts, H. H. *Journal of Bacteriology*. 1962, **84**(2), 381
- 1970JGM9 Mulczyk, M.; Szewczuk, A. *Journal of General Microbiology*. 1970. **61**, 9
- 1970JMB47 Doyle, B. B.; Traub, W.; Lorenzi, G. P.; Brown, F. R.; Blout, E. R. *Journal of Molecular Biology*. 1970, **51**(1), 47
- 1970JOA567 Dulaney, E. L. *The Journal of Antibiotics*. 1970, **23**(11), 567
- 1975ARM485 Miller, C. G. *Annual Review of Microbiology*. 1975, **28**, 485
- 1975JB1208 Naider, F.; Becker, J. M. *Journal of Bacteriology*. 1975, **122**(3), 1208
- 1975JB353 Desmond, E. P.; Starnes, W. L.; Behal, F. J. *Journal of Bacteriology*. 1975, **124**(1), 353
- 1975JMC106 Huber III, J. W.; Gilmore, W. F.; Robertson, L. W. *Journal of Medicinal Chemistry*. 1975, **18**(1), 106
- 1976BBRC793 Henderson, L. L.; Johnston, R. B. *Biochemical and Biophysical Research Communications*. 1976, **68**(3), 793
- 1977AAC638 Neuhaus, F. C.; Goyer, S.; Neuhaus, D. W. *Antimicrobial Agents and Chemotherapy*. 1977, **11**, 638
- 1977JOC2253 Srinivasan, A.; Stephenson, R. W.; Olsen, R. K. *Journal of Organic Chemistry*. 1977, **42**, 2253
- 1978B1313 Wang, E.; Walsh, C. *Biochemistry*. 1978, **17**(7), 1313
- 1978S469 Kudzin, Z. H.; Stec, W. J. *Synthesis*. 1978. **1978**(6), 469
- 1978S479 Oleksyszyn, J.; Tyka, R.; Mastalerz, P. *Synthesis*. 1978. **1978**(6), 479

- 1979AAC677 Atherton, F. R.; Hall, M. J.; Hassall, C. H.; Lambert, R. W.; Ringrose, P. S. *Antimicrobial Agents and Chemotherapy*. 1979, **15**(5), 677
- 1979AAC696 Atherton, F. R.; Hall, M. J.; Hassall, C. H.; Lambert, R. W.; Lloyd, W. J.; Ringrose, P. S. *Antimicrobial Agents and Chemotherapy*. 1979, **15**(5), 696
- 1979CJM1298 Schiemann, D. A. *Canadian Journal of Microbiology*. 1979, **25**(11), 1298
- 1979JCM214 George, W. L.; Sutter, V. L.; Citron, D.; Finegold, S. M. *Journal of Clinical Microbiology*. 1979, **9**(2), 214
- 1980AAC897 Atherton, F. R.; Hall, M. J.; Hassall, C. H.; Holmes, S. W.; Lambert, R. W.; Lloyd, W. J.; Ringrose, P. S. *Antimicrobial Agents and Chemotherapy*. 1980, **18**(6), 897
- 1980JBC3977 Yocum, R. R.; Rasmussen, J. R.; Strominger, J. L. *Journal of Biological Chemistry*. 1980, **255**(9), 3977
- 1980JOC1295 DeGrado, W. F.; Kaier, E. T. *Journal of Organic Chemistry*. 1980, **45**(7), 1295
- 1980S1028 Kudzin, Z. H.; Kotynski, A. *Synthesis*. 1980, **1980**(12), 1028
- 1981B7539 Wang, E. A.; Walsh, C. *Biochemistry*. 1981, **20**(26), 7539
- 1981CR229 Lavielle, S.; Ling, N. C.; Saltman, R.; Guillemin, R. C. *Carbohydrate Research*. 1981, **89**(2), 229
- 1982JCM697 Edelstein, P. H. *Journal of Clinical Microbiology*. 1982, **16**(4), 697
- 1982JCP462 Bolton, F. J.; Robertson, L. *Journal of Pathology*. 1982, **35**(4), 462
- 1982S653 Baraldi, P. G.; Guarneri, M.; Moroder, F.; Pollini, G. P.; Simoni, D. *Synthesis*. 1982, **1982**(8), 653
- 1982T871 Walsh, C. *Tetrahedron*. 1982, **38**(7), 871
- 1983BCSJ568 Ueda, T.; Saito, M.; Kato, T.; Izumiya, N. *Bulletin of the Chemical Society of Japan*. 1983, **56**(2), 568
- 1983JB1439 Wasserman, S. A.; Walsh, C. T.; Botstein, D. *Journal of Bacteriology*. 1983, **153**(3), 1439
- 1983JMC1733 Cheung, K.S.; Wasserman, S. A.; Dudek, E.; Lerner, S. A.; Johnston, M. *Journal of Medicinal Chemistry*. 1983, **26**(12), 1733

- 1985FML333 Alves, R. A.; Gleaves, J. T.; Payne, J. W. *FEMS Microbiology Letters*. 1985, **27**(3), 333
- 1985JB722 Benz, R.; Schmid, A.; Hancock, R. E. W. *Journal of Bacteriology*. 1985, **162**(2), 722
- 1986B3261 Esaki, N.; Walsh, C. T. *Biochemistry*. 1986, **25**(11), 3261
- 1986B3275 Badet, B.; Inagaki, K.; Soda, K.; Walsh, C. T. *Biochemistry*. 1986, **25**(11), 3275
- 1986JMC29 Atherton, F. R.; Hassall, C. H.; Lambert, R. W. *Journal of Medicinal Chemistry*. 1986, **29**(1), 29
- 1986JMC2060 Cheung, K. S.; Boisvert, W.; Lerner, S. A.; Johnston, M. *Journal of Medicinal Chemistry*. 1986, **29**(10), 2060
- 1987BBRC194 Heller, D.; Fenselau, C.; Cotter, R.; Demirev, P.; Olthoff, J.; Honovich, J. *Biochemical and Biophysical Research Communications*. 1987, **142**, 194
- 1987DMID283 Mitchell, M. J.; Conville, P. S.; Gill, V. J. *Diagnostic Microbiology and Infectious Disease*. 1987, **6**(4), 283
- 1987JCM1730 Welch, D. F.; Muszynski, M. J.; Pai, C. H.; Marcon, M. J.; Hribar, M. M.; Gilligan, P. H.; Matsen, J. M.; Ahlin, P. A.; Hilman, B. C.; Chartrand, S. A. *Journal of Clinical Microbiology*. 1987, **25**(9), 1730
- 1988AAC319 Patchett, A. A.; Taub, D.; Weissberger, B.; Valiant, M. E.; Gadebusch, H.; Thornberry, N. A.; Bull, H. G. *Antimicrobial Agents and Chemotherapy*. 1988, **32**(3), 319
- 1988JACS2237 Arnold, L. D.; May, R. G.; Vederas, J. C. *Journal of American Chemical Society*. 1988, **110**, 2237
- 1989B3541 Duncan, K.; Faraci, W. S.; Matteson, D. S.; Walsh, C. T. *Biochemistry*. 1989, **28**(8), 3541
- 1989BCSJ3177 Oshikawa, T.; Yamashita, M. *Bulletin Chemical Society Japan*. 1989, **62**, 3177
- 1990SGO S19 Rittenbury, M. S. *Surgery, Gynecology and Obstetrics*. 1990, **171**, S 19
- 1991JBC770 Nikaido, H.; Nikaido, K.; Harayama, S. *Journal of Biological Chemistry*. 1991, **266**(2), 770

- 1991JBC21657 Thornberry, N. A.; Bull, H. G.; Taub, D.; Wilson, K. E.; Gimenez-Gallego, G.; Rosegay, A.; Soderman, D. D.; Patchett, A. A. *Journal of Biological Chemistry*. 1991, 266(32), 21657
- 1991JCM1645 Wolff, L. F.; Anderson, L.; Sandberg, G. P.; Aepple, D. M.; Shelburne, C. E. *Journal of Clinical Microbiology*. 1991, 29(8), 1645
- 1991NEJM601 Jacoby, G. A.; Archer, G. L. *The New England Journal of Medicine*. 1991, 324(9), 601
- 1992IJP107 Richards, R. M.; Xing, D. K. L. *International Journal of Pharmaceutics*. 1992, 82, 107
- 1992IJP195 Richards, R. M.; Xing, D. K. L. *International Journal of Pharmaceutics*. 1992, 87, 195
- 1992JB471 Hancock, R. E. W.; Egli, C.; Benz, R.; Siehnel, R. J. *Journal of Bacteriology*. 1992, 174(2), 471
- 1992JB4913 Whitfield, C.; Perry, M. B.; MacLean, L. L.; Yu, S. H. *Journal of Bacteriology*. 1992, 174(15), 4913
- 1992JB5196 Bellido, F.; Martin, N. L.; Siehnel, R. J.; Hancock, R. E. W. *Journal of Bacteriology*. 1992, 174(16), 5196
- 1992JCP812 Aspinall, S. T.; Hutchinson, D. N. *Journal of Clinical Pathology*. 1992, 45(9), 812
- 1992JP1093 Wolff, L. F.; Anderson, L.; Sandberg, G. P.; Reither, L.; Binsfeld, C. A.; Corinaldesi, G.; Shelburne, C. E. *Journal of Periodontology*. 1992, 63(12), 1093
- 1994JB260 Handwerger, S.; Pucci, M. J.; Liu, J.; Lee, M. S. *Journal of Bacteriology*. 1994, 176(1), 260
- 1994JB1500 Lobočka, M.; Hennig, J.; Wild, J.; Kłopotowski, T. *Journal of Bacteriology*. 1994, 176(5), 1500
- 1994NAR3866 Kirpekar, F.; Nordhoff, E.; Kristiansen, K.; Roepstorff, P.; Lezius, A.; Hahner, S.; Karas, M.; Hillenkamp, F. *Nucleic Acids Research*. 1994, 22(19), 3866
- 1994P34 Awadé, A. C.; Cleuziat, F.; Gonzalès, T.; Robert-Baudouy, J. *Proteins: Structure, Function, and Bioinformatics*. 1994, 20(1), 34

- 1994RCMS1026 Cain, T.; Lubman, D.; Weber, W. *Rapid Communications in Mass Spectrometry*, 1994, **8**, 1026
- 1994S31 McKillop, A.; Taylor, R. J. K.; Watson, R. J.; Lewis, N. *Synthesis*. 1994, **1994**(1), 34
- 1995AEM226 Verheul, A.; Hagting, A.; Amezaga, M. R.; Booth, I. R.; Rombouts, F. M.; Abee, T. *Applied and Environmental Microbiology*. 1995, **61**(1), 226
- 1995JAB209 Richards, R. M. E.; Xing, D. K. L.; King, T. P. *Journal of Applied Bacteriology*. 1995, **78**(3), 209
- 1995JOC2563 Matulic-Adamic, J.; Haeberli, P.; Usman, N. *Journal of Organic Chemistry*. 1995, **60**, 2563
- 1995S509 Kudzin, Z. H.; Luczak, J. *Synthesis*. 1995, **1995**(5), 509
- 1996FMR319 Gonzales, T.; Baudouy, J. R. *FEMS Microbiology Reviews*. 1996, **18**, 319
- 1996IJFM45 Manafi, M. *International Journal of Food Microbiology*. 1996, **31**, 45
- 1996IJFM103 Meng, J. H.; Zhao, S. H.; Doyle, M. P.; Kresovich, S. *International Journal of Food Microbiology*. 1996, **32**, 103
- 1996JCM1811 Inoue, K.; Miki, K.; Tamura, K.; Sakazaki, R. *Journal of Clinical Microbiology*. 1996, **34**, 1811
- 1996RCMS377 Hurst, G.; Doktycz, M.; Vass, A.; Buchanan, M. *Rapid Communications in Mass Spectrometry*, 1996, **10**, 377
- 1997ADDR3 Lipinski, C. A.; Lombardo, F.; Dominy, B. W.; Feeney, P. J. *Advanced Drug Delivery Reviews*. 1997, **23**, 3
- 1997B1329 Shaw, J. P.; Petsko, G. P.; Ringe, D. *Biochemistry*. 1997, **36**, 1329
- 1998AC2693 Hurst, G.; Weaver, K.; Doktycz, M.; Buchanan, M.; Costello, A.; Lidstrom. *Analytical Chemistry*. 1998, **70**, 2693
- 1998B10438 Stamper, C. G. F.; Morollo, A. A.; Ringe, D. *Biochemistry*. 1998, **37**, 10438
- 1998CID158 Burns, J. L.; Emerson, J.; Stapp, J. R.; Yim, D. L.; Krzewinski, J.; Loudon, L.; Ramsey, B. W.; Clausen, C. R. *Clinical Infectious Diseases*. 1998, **27**, 158

- 1998CMR318 Bascomb, S.; Manafi, M. *Clinical Microbiology Reviews*. 1998, **11**(2), 318
- 1998JACS2268 Peisach, D.; Chipman, D. M.; Van Ophem, P. W.; Manning, J. M.; Ringe, D. *Journal of American Chemical Society*. 1998, **120**(10), 2268
- 1999AC2334 Kirpekar, F.; Berkenkamp, S.; Hillenkamp, F. *Analytical Chemistry*. 1999, **71**, 2334
- 1999AMB553 Peypoux, F.; Bonmatin, J. M.; Wallach, J. *Applied Microbiology and Biotechnology*. 1999, **51**(5), 553
- 1999JIC61 Nakajima, Y. *Journal of Infection and Chemotherapy*. 1999, **5**(2), 61
- 1999JMM25 Kloeke, F. V. O.; Baty, A. M.; Eastburn, C. C.; Diwu, Z.; Geesey, G. G. *Journal of Microbiological Methods*. 1999, **38**, 25
- 1999PR1514 Kelder, J.; Grootenhuis, P. D. J.; Bayada, D. M.; Delbressine, L. P. C.; Ploemen, J. P. *Pharmaceutical Research*. 1999, **16**(10), 1514
- 1999PR1520 Stenberg, P.; Luthman, K.; Ellens, H.; Lee, C. P.; Smith, P. L.; Lago, A.; Elliot, J. D.; Artursson, P. *Pharmaceutical Research*. 1999, **16**(10), 1520
- 2000AA375 Kanda-Nambu, K.; Yasuda, Y.; Tochikubo, K. *Amino Acids*. 2000, **18**(4), 375
- 2000PAC373 Adams, B.; Axelsson, B. S.; Beresford, K. J. M.; Church, N. J.; Spencer, P. A.; Whyte, S. M.; Young, D. W. *Pure and Applied Chemistry*. 2000, **72**(3), 373
- 2000PNAS12487 Detmers, F. J. M.; Lanfermeijer, F. C.; Abele, R.; Jack, R. W.; Tempé, R.; Konings, W. N.; Poolman, B. *Proceedings of the National Academy of Sciences of the United States of America*. 2000, **97**(23), 12487
- 2001AC746 Ryzhov, V.; Fenselau, C. *Analytical Chemistry*. 2001, **73**, 746
- 2001JAC5 Andrews, J. M. *Journal of Antimicrobial Chemotherapy*. 2001, **48**(suppl. 1), 5
- 2001JBC43645 Cahan, R.; Axelrad, I.; Safrin, M.; Ohman, D. E.; Kessier, E. *Journal of Biological Chemistry*. 2001, **276**(47), 43645
- 2001MSR172 Lay, J. O. *Mass Spectrometry Reviews*. 2001, **20**, 172

- 2002AEJ2516 Bernardi, F.; Garavelli, M.; Scatizzi, M.; Tomasini, C.; Trigari, V.; Crisma, M.; Formaggio, F.; Peggion, C.; Toniolo, C. *A European Journal*. 2002, **8**(11), 2516
- 2002JB4321 Strych, U.; Benedik, M. J. *Journal of Bacteriology*. 2002, **184**(15), 4321
- 2002JBC19166 Watanabe, A. Yoshimura, T. Mikami, B. Hayashi, H. Kagamiyama, H. Esaki, N. *Journal of Biological Chemistry*. 2002, **227**(21), 19166
- 2002JCB73 Sauer, S.; Gut, I. *Journal of Chromatography B*. 2002, **782**, 73
- 2002JCM3913 Perry, J. D.; Riley, G.; Gould, F. K.; Perez, J. M.; Boissier, E.; Ouedraogo, R. T. Freydiere, A. M. *Journal of Clinical Microbiology*. 2002, **40**(11), 3913
- 2002OL553 Luca, L. D.; Giacomelli, G.; Porcheddu, A. *Organic Letters*. 2002, **4**(4), 553
- 2002PJC1105 Boduszek, B.; Soroka, M. *Polish Journal of Chemistry*. 2002, **76**(8), 1105
- 2002WR2802 Kong, R. Y. C.; Lee, S. K. Y.; Law, T. W. F.; Law, S. H. W.; Wu, R. S. S. *Water Research*. 2002, **36**, 2802
- 2003AMP217 Jankiewicz, U.; Bielawski, W. *Acta Microbiologica Polonica*. 2003, **52**(3), 217
- 2003B5775 Fenn, T. D.; Stamper, G. F.; Morollo, A. A.; Ringe, D. *Biochemistry*. 2003, **42**, 5775
- 2003CC1041 Annesley, T. M. *Clinical Chemistry*. 2003, **49**(7), 1041
- 2003EJB23 Stefanova, M. E.; Tomberg, J.; Davies, C.; Nicholas, R. A.; Gutheil, W. G. *European Journal Biochemistry*. 2003, **271**, 23
- 2003JACS685 Morandi, F.; Caselli, E.; Morandi, S.; Focia, P. J.; Blasquez, J.; Shoichet, B. K. *Journal of The America Chemical Society*. 2003, **125**, 685
- 2003JACS15730 Fillgrove, K. L.; Pakhomova, S.; Newcomer, M. E.; Armstrong, R. N. *Journal of The America Chemical Society*. 2003, **125**, 15730
- 2003T6095 Yuan, C.; Xu, C.; Zhang, Y. *Tetrahedron*. 2003, **59**(32), 6095
- 2004AB345 Li, L. F.; Hsieh, C. H.; Liu, P. F.; Tsai, S. P.; Tam, M. F. *Analytical Biochemistry*. 2004, **329**(2), 345

- 2004CMLS2200 Poole, K. *Cellular and Molecular Life Sciences*. 2004, **2004**(61), 2200
- 2004IP359 Kapoor, S.; Gathwala, G. *Indian Pediatrics*. 2004, **41**(4), 359
- 2004JBC46143 Noda, M.; Kawahara, Y.; Ichikawa, A.; Matoba, U.; Matsuo, H.; Lee, D. G.; Kumagai, T.; Sugiyama, M. *Journal of Biological Chemistry*. 2004, **279**(44), 46143
- 2004JBC46153 Noda, M.; Matoba, Y.; Kumagai, T.; Sugiyama, M. *Journal of Biological Chemistry*. 2004, **279**, 46153
- 2004SC1489 Venkatachalam, T. K.; Huang, H.; Yu, G.; Uckun, F. M. *Synthetic Communication*. 2004, **34**(8), 1489
- 2005ABB279 Toney, M. D. *Archives of Biochemistry and Biophysics*. 2005, **433**, 279
- 2005ADDR1451 Wright, G. D. *Advanced Drug Delivery Review*. 2005, **57**(10), 1451
- 2005ADDR1486 Kumar, A.; Schweizer, H. P. *Advanced Drug Delivery Reviews*. 2005, **57**(10), 1486
- 2005CMR521 Fournier, B.; Philpott, D. J. *Clinical Microbiology Reviews*. 2005, **18**(3), 521
- 2005JCM5536 Flayhart, D.; Hindler, J. F.; Bruckner, D. A.; Hall, G.; Shrestha, R. K.; Vogel, S. A.; Richter, S. S.; Howard, W.; Walther, R.; Carroll, K. C. *Journal of Clinical Microbiology*. 2005, **43**(11), 5536
- 2005S1061 Guo, H.; Wang, Z.; Ding, K. *Synthesis*. 2005, **2005**(7), 1061
- 2005T3403 Barfoot, C. W.; Harvey, J. E.; Kenworthy, M. N.; Kilburn, J. P.; Ahmed, M.; Taylor, R. J. K. *Tetrahedron*. 2005, **2005**(61), 3403
- 2006AJM20 Paterson, D. L. *American Journal of Medicine*. 2006, **119**(6), S20
- 2006PNAS4404 Meroueh, S. O.; Bencze, K. Z.; Heseck, D.; Lee, M.; Fisher, J. F.; Stemmler, T. L.; Mobashery, S. *Proceedings of the National Academy of Sciences of the United States of America*. 2006, **103**(12), 4404
- 2007AAC3247 Pérez, A.; Canle, D.; Latasa, C.; Poza, M.; Beceiro, A.; Tomás, M. M.; Fernández, A.; Mallo, S.; Pérez, S.; Molina, F.; Villanueva, R.; Lasa, I.; Bou, G. *Antimicrobial Agents and Chemotherapy*. 2007, **51**(9), 3247

- 2007AEM1467 Kanki, M.; Yoda, T.; Tsukamoto, T.; Baba, E. *Applied and Environmental Microbiology*. 2007, **73**(5), 1467
- 2007AEM2673 Wegkamp, A.; van Oorschot, W.; de Vos, W. M.; Smid, E. J. *Applied and Environmental Microbiology*. 2007, **73**(8), 2673
- 2007BMC3474 Suaifan, G. A. R. Y.; Arafat, T.; Threadgill, M. D. *Bioorganic and Medicinal Chemistry*. 2007, **15**(10), 3474
- 2007BMCL1418 James, A. L.; Perry, J. D.; Rigby, A.; Stanforth, S. P. *Bioorganic and Medicinal Chemistry Letters*. 2007. **17**, 1418
- 2007JAM2046 Perry, J. D.; Freydière, A. M. *Journal of Applied Microbiology*. 2007, **103**, 2046
- 2007JAMA1763 Klevens, R. M.; Morrison, M. A.; Nadle, J.; Petit, S.; Gershman, K.; Ray, S.; Harrison, L. H.; Lynfield, R.; Dumyati, G.; Townes, J. M.; Craig, A. S.; Zell, E. R.; Fosheim, G. E.; McDougal, L. K.; Carey, R. B.; Fridkin, S. K. *Journal of the American Medical Association*. 2007, **298**(15), 1763
- 2008BBRC590 Ni, N.; Chou, H. T.; Wang, J.; Li, M.; Lu, C. D.; Tai, P. C.; Wang, B. *Biochemical and Biophysical Research Communications*. 2008, **369**, 590
- 2008BML832 Anderson, R. J.; Groundwater, P. W.; Huang, Y.; James, A. L.; Orenga, S.; Rigby, A.; Roger-Dalbert, C.; Perry, J. D. *Bioorganic and Medicinal Chemistry Letters*. 2008, **18**, 832
- 2008PS1066 Wu, D.; Hu, T.; Zhang, L.; Chen, J.; Du, J.; Ding, J.; Jiang, H.; Shen, X. *Protein Science*. 2008, **17**(6), 1066
- 2009AJRC300 Kulkarni, S, S.; Mehere, A.; Shenoy, P. A. *Asian Journal of Research in Chemistry*. 2009, **2**(3), 300
- 2009BBA1030 Priyadarshi, A.; Lee, E. H.; Sung, M. W.; Nam, K. H.; Lee, W. H.; Kim, E. E. K.; Hwang, K. Y. *Biochimica et Biophysica Acta-Proteins and Proteomics*. 2009, **1794**(7), 1030
- 2009CRW2455 Isidro-Llobet, A., Alvarez, M., Albericio, F. *Chemical Reviews*. 2002. **109**. 2455
- 2009JAA105 Masterton, R. G. *International Journal of Antimicrobial Agent*. 2009, **33**, 105

- 2009JMM139 Orenga, S.; James, A. L.; Manafi, M.; Perry, J. D.; Pincus, D. H. *Journal of Microbiological Methods*. 2009, **79**, 139
- 2009LAM675 Hossain, N.; Lastovica, A. J. *Letters in Applied Microbiology*. 2009. **48**, 675
- 2009LID228 Nordmann, P.; Cuzon, G.; Nass, T. *The Lancet Infectious Diseases*. 2009, **9**, 228
- 2010EID674 Flgtree, M.; Lee, R.; Baln, L.; Kennedy, T.; Mackertlch, S.; Urban, M.; Cheng, Q.; Hudson, B. J. *Emerging Infectious Diseases*. 2010, **16**(4), 674
- 2010FM1087 Coenye, T. *Future Microbiology*. 2010, **5**(7), 1087
- 2010IJAA219 Gordon, N. C.; Wareham, D. W. *International Journal of Antimicrobial Agents*. 2010, **35**(3), 219
- 2010JCF130 Bonestroo, H. J. C.; de Winter-de Groot, K. M.; van der Ent, C. K.; Arets, H. G. M. *Journal of Cystic Fibrosis*. 2010, **9**(2), 130
- 2010NRM890 Dworkin, J.; Shah, I. M. *Nature Reviews Microbiology*. 2010, **8**, 890
- 2011AM759 He. G. X.; Thorpe, C.; Walsh, D.; Crow. R.; Chen. H.; Kumar, S.; Varela, M. F. *Achieves of Microbiology*. 2011, **193**(10), 759
- 2011CC215 Bassetti, M.; Ginocchio, F.; Mikulska, M. *Critical Care*. 2011, **15**(2), 215
- 2011FIM1 Van Hoek, A. H. A. M.; Meviux, D.; Guerra, B.; Mullany, P.; Roberts, A. P.; Aarts, H. J. M. *Frontiers in Microbiology*. 2011, **2**(203), 1
- 2011IJAA70 Ramalhete, C.; Spengler, G.; Martins, A.; Martins, M.; Viveiros, M.; Mulhovo, S.; Ferreira, M. J. U.; Amaral, L. *International Journal of Antimicrobial Agents*. 2011, **37**(1), 70
- 2011JACS15496 Oliveira, E. F.; Cerqueira, N. M. S. A.; Fernandes, P. A.; Ramos, M. J. *Journal of the American Chemical Society*. 2011, **133**, 15496
- 2011JB4075 Imamura, D.; Kuwana, R.; Takamatsu, H.; Watabe, K. *Journal of Bacteriology*. 2011. **193**(16), 4075
- 2011JCM2868 Alatoon, A.; Cunningham, S.; Ihde, S.; Mandrekar, J.; Patel, R. *Journal of Clinical Microbiology*. 2011, **8**, 2868

- 2011JMC2288 Perry, J. D.; Naqvi, S. H.; Mirza, I. A.; Alizai, S. H.; Hussain, A.; Ghirardi, S.; Orenca, S.; Wilkinson, K.; Woodford, N.; Zhang, J.; Livermore, D. M.; Abbasi, S. A.; Raza, M. W. *Journal of Antimicrobial Chemotherapy*. 2011, **66**(10), 2288
- 2011PLoS20374 Anthony, K.G.; Strych, U.; Yeung, K. R.; Shoen, C. S.; Perez, O.; Krause, K. L.; Cynamon, M. H.; Aristoff, P. A.; Koski, R. A. *PLoS ONE*. 2011, **6**(5), e20374
- 2011PR750 Huttunen, K. M.; Raunio, H.; Routio, J. Koulu, M. *Pharmacology Reviews*. 2011, **63**(3), 750
- 2011TL1260 Jahani, F.; Tajbakhsh, M.; Golchoubian, H.; Khaksar, S. *Tetrahedron Letters*. 2011, **52**(12), 1260
- 2012AR2337 Shimada, M.; Kadowaki, T.; Taniguchi, Y.; Inagawa, H.; Okazaki, K.; Soma, G. *Anticancer Research*. 2012, **32**(6), 2337
- 2012CPPS843 Galdiero, S.; Falanga, A.; Cantisani, M.; Tarallo, R.; Pepa, M. E. D.; D'Oriano, V.; Galdiero, M. *Current Protein and Peptide Science*. 2012, **13**, 843
- 2012CW48 Sansom, C. *Chemistry World*. 2012, **9**(9), 48
- 2012EBO3411 Solcan, N.; Kwok, J.; Fowler, P. W.; Cameron, A. D.; Drew, D.; Iwata, S.; Newstead, S. *The EMBO Journal*. 2012, **31**(16), 3411
- 2012FC369 Taskila, S.; Tuomola, M.; Ojamo, H. *Food Control*. 2012, **26**(2), 369
- 2012FM887 Mezzatesta, M. L.; Gona, F.; Stefani, S. *Future Microbiology*. 2012, **7**(7), 887
- 2012JACS18275 Fonseca, F.; Chudyk, E. I.; Kamp, M. W.; Correia, A.; Mulholland, A. J.; Spencer, J. *Journal of The America Chemical Society*. 2012, **134**, 18275
- 2012JMC10414 Lucas, M. C.; Goldstein, D. M.; Hermann, J. C.; Kuglstatler, A.; Liu, W.; Luk, K. C.; Padilla, F.; Slade, M.; Villasenor, A. G.; Wanner, J.; Xie, W.; Zhang, X.; Liao, C. *Journal of Medicinal Chemistry*. 2012, **55**(23), 10414
- 2012M5095 Oliveira, C. S.; Lira, B. F.; Falcão-Silva, V. S.; Siqueira-Junior, J. P.; Barbosa-Filho, J. M.; Athayde-Filho, P. F. *Molecules*. 2012, **17**, 5095

- 2012MMWR262 Chittick, P.; Russo, V.; Sims, M.; Oleszkowicz, S.; Sawarynski, K.; Powell, K.; Makin, J.; Darnell, E.; Robinson-Dunn, B.; Boyanton, B. L.; Band, J. *Morbidity and Mortality Weekly Report*. 2012, **61**(15), 262
- 2012V421 Hollenbeck, B. L.; Rice, L. B. *Virulence*. 2012, **3**(5), 421
- 2013ARM313 Brown, S.; Maria Jr, J. P. S.; Walker, S. *Annual Review of Microbiology*. 2013, **67**, 313
- 2013IJMS67 Krasny, L.; Hynek, R.; Hochel, I. *International Journal of Mass Spectrometry*. 2013, **353**, 67
- 2013JID1 Gan, S. D.; Patel, K. R. *Journal of Investigative Dermatology*. 2013, **133**(9), 1
- 2013LAM303 Ehrmann, E.; Jolivet-Gougeon, A.; Bonnaure-Mallet, M.; Fosse, T. *Letters in Applied Microbiology*. 2013, **57**(4), 303
- 2013MR125 Daniela, C.; Sabaté, M.; Audisio, C. *Microbiological Research*. 2013, **168**(3), 125
- 2013NC1 Ito, K.; Hikida, A.; Kawai, S.; Lan, V. T. T.; Motoyama, T.; Kitagawa, S.; Yoshikawa, Y.; Kato, R.; Kawarasaki, Y. *Nature Communications*. 2013, **4**(2502), 1
- 2013NI676 Brestoff, J. R.; Artis, D. *Natural Immunology*. 2013, **14**, 676
- 2013PNAS11343 Doki, S.; Kato, H. E.; Solcan, N.; Iwaki, M.; Koyama, M.; Hattori, M.; Iwase, N.; Tsukazaki, T.; Sugita, Y.; Kandori, H.; Newstead, S.; Ishitani, R.; Nureki, O. *Proceedings of the National Academy of Sciences of the United States of America*. 2013. **110**(28), 11343
- 2013V223 Soto, S. M. *Virulence*. 2013, **4**(3), 223
- 2014BMC5249 Cellier, M.; James, A. L.; Orenge, S.; Perry, J. D.; Rasul, A. K.; Robinson, S. N.; Stanforth, S. P. *Bioorganic and Medicinal Chemistry*. 2014. **22**, 5249
- 2014IJMM415 Barillova, P.; Tchesnokova, V.; Dübbers, A.; Küster, P.; Peters, G.; Dobrindt, U.; Sokurenko, E. V.; Kahl, B. C. *International Journal of Medical Microbiology*. 2014, **304**, 415
- 2014RAR1 O'Neill, J. *Review on Antimicrobial Resistances: Antimicrobial Resistance*. 2014, **2014**, 1
- 2015BBA488 Newstead, S. *Biochimica et Biophysica Acta*. 2015, **1850**(3), 488

2015BMC5218 Mugumbate, G.; Overington, J. P. *Bioorganic and Medicinal Chemistry*. 2015, **23**(16), 5218

7.2: Books

- B-1990MI105 Salzman, G.; Singham, S. B.; Johnston, R. G.; Bohren, C. F., 1990. Light scattering and cytometry: *Flow cytometry and sorting*. Melamed, M. R.; Lindmo, T.; Mendelsohn, M. L. eds. John Wiley. pg 105-153
- B-1993MI27 Allman, R.; Manchee, R.; Lloyd, D. 1993. Flow cytometric analysis of heterogeneous bacterial populations: *Flow Cytometry in Microbiology*, Lloyd, D. ed. Springer-Verlag London Limited. pp 27-47
- B-1998MI671 Greene, T. W.; Wuts, P. G. M. 1998. Protection For The Phosphate Group: *Protective Groups in Organic Synthesis*. 3rd edn. John Wiley & Sons. pg 671
- B-2006MI56 Brock, T. D. 2006. Cell Structure or Function: *Brock Biology of Microorganisms*. 11th edn. Pearson Prentice Hall. pg 56-63
- B-2007MI182 Forbes, B. A.; Sahm, D. F.; Weissfeld, A. S. Bailey and Scott's Diagnostic Microbiology: *General Principles in Clinical Microbiology*. 12th edn. Mosby Elsevier. pg. 182
- B-2007MI285 Frey, P. A.; Hegeman, A. D. 2007. Alanine Racemase: *Enzymatic Reaction Mechanisms*. Oxford University Press. pg 285-289
- B-2008MI31 Yousef, A. E. 2008. Detection of Bacterial Pathogens in Different Matrices: Current Practices and Challenges: *Principles of Bacterial Detection*. Zourob, M.; Elwary, S.; Turner, A. eds. Springer Science. pg 31-48
- B-2011MI80 Sun, Y.; Li, Y.; Song, H.; Zhu, Y. 2011. Microbial Fermentation for Food Preservation: *Natural Antimicrobial in Food Safety and Quality*. Rai, M.; Chikinda, M. eds. CAB International. pg 80
- B-2013MI3 Giguere, S. 2013. Antimicrobial Drug Action and Interaction: *An Introduction. Antimicrobial Therapy in Veterinary Medicine*. 4th edn. Giguere, S.; Prescott.; Dowling, P. M. eds. Wiley Blackwell. pg. 3

7.3: Theses

- T-2004MI72 Huang, Y. PhD Thesis. *Synthesis and evaluation of suicide substrates for the enhanced detection of bacterial pathogens*. University of Sunderland. 2004. Pg. 72
- T-2004MI164 Huang, Y. PhD Thesis. *Synthesis and evaluation of suicide substrates for the enhanced detection of bacterial pathogens*. University of Sunderland. 2004. Pg. 164
- T-2013MI192 Varadi, L. PhD Thesis. *Synthesis and evaluation of fluorogenic and suicide substrates for the detection and identification of bacteria*. University of Sunderland. 2013. Pg. 192
- T-2013MI257 Varadi, L. PhD Thesis. *Synthesis and evaluation of fluorogenic and suicide substrates for the detection and identification of bacteria*. University of Sunderland. 2013. Pg. 257

7.4: Patent

- P-1984MI6 Patent. *Preparation process of β -chloroalanine*. 4484003, 1984
- P-1991MI8 Patent. *Novel derivatives*. EP0283563A2, 1991
- P-2002MI15 Patent. *Process for producing β -halogeno- α -amino-carboxylic acids and phenylcysteine derivatives and intermediates thereof*. US6372941B1, 2002
- P-2015MI27 Patent. *Antimicrobial compounds*. WO2015/140481A1, 2015

7.5: Webpages

- WS-1 <http://www.generalmicroscience.com/bacteriology/microbiology-morphology-of-bacterial-cell/> (Last assessed: 21June2015)
- WS-2 <http://classes.midlandstech.edu/carterp/courses/bio225/chap04/lecture2.htm> (Last accessed: 21June2015)
- WS-3 <http://www.shmoop.com/biology-cells/prokaryotic-cells.html> (Last accessed: 09February2014)
- WS-4 <http://gmgmesjwk.pbworks.com/f/gram-stain.jpg>. (Last accessed: 22June2015)
- WS-5 <http://www.studyblue.com/notes/n/bacteria-structure-and->

- function/deck/3870396. (Last accessed:03March2014)
- WS-6 <http://www.biomerieux-culturemedia.com/product/14-chromid-salmonella> .
(Last accessed: 28June2015)
- WS-7 http://www.biomerieux-usa.com/servlet/srt/bio/usa/dynPage?open=USA_NWS_CNN_2011_May&doc=USA_NWS_CNN_2011_May_G_FCK_1&pubparams.sform=0&lang=en
. (Last accessed:10December 2012)
- WS-8 Cheminformatics. [http:// www.molinspiration.com](http://www.molinspiration.com) (Last accessed: 30
June2016)

CHAPTER 8

APPENDICES

Appendices containing summary of proton (^1H), carbon (^{13}C) and proton decoupled phosphorus (^{31}P - ^1H) NMR of synthesised compounds, as well as a published patent paper were stored in a CD-ROM.

Appendices

Appendix 8.1: Summary of ^1H -NMR of synthesised compounds.....	2
Appendix 8.2: Summary of ^{13}C -NMR of synthesised compounds.....	22
Appendix 8.3: Summary of ^{31}P - ^1H decoupled NMR of synthesised compounds.....	37
Appendix 8.4: Publication	41

Appendix 8.1: Summary of $^1\text{H-NMR}$ of synthesised compounds

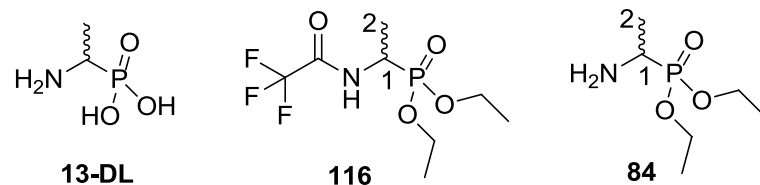


Table 8.1: Summary of $^1\text{H-NMR}$ spectra of D/L-fosfalin (**13-DL**), trifluoroacetyl-D/L-Fos diethyl ester (**116**) and D/L-Fos diethyl ester (**84**) at 300 MHz

	δ_{H}		
	13-DL (D_2O)	116 (CDCl_3)	84 (CDCl_3)
$\text{CH}_3\text{-2}$	1.40 (3H, dd, $^3J_{\text{H-P}}=14.7$ Hz, $^3J_{\text{H-H}}=7.2$ Hz)	1.38 (3H, dd, $^3J_{\text{H-P}}=16.5$ Hz, $^3J_{\text{H-H}}=7.2$ Hz)	1.34 (3H, dd, $^3J_{\text{H-P}}=17.7$ Hz, $^3J_{\text{H-H}}=7.2$ Hz)
CH-1	3.33 (1H, m)	4.39 (1H, m)	3.02-3.12 (1H, m)
OCH_2CH_3	-	1.24 (3H, t, $^3J_{\text{H-H}}=7.2$ Hz, CH_3) 1.27 (3H, t, $^3J_{\text{H-H}}=7.2$ Hz, CH_3) 4.06 (4H, m, 2 x CH_2)	1.26 (6H, t, $^3J_{\text{H-H}}=7.2$ Hz, 2 x CH_3) 4.06-4.17 (4H, m, 2 x CH_2)
NH	-	8.00 (1H, d, $^3J_{\text{H-H}}=6.0$ Hz)	-
NH_2	Exchanged	-	1.68 (2H, br)

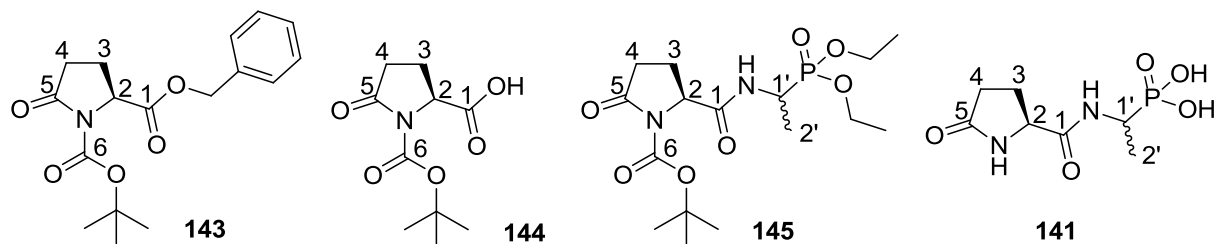


Table 8.2: Summary of $^1\text{H-NMR}$ of $^t\text{Boc-L-Pyroglu-OBzl}$ (**143**), $^t\text{Boc-L-Pyroglu-OH}$ (**144**), $^t\text{Boc-L-Pyroglu-D/L-Fos}$ diethyl ester (**145**) and L-Pyroglu-D/L-Fos (**141**) at 300 MHz

	δ_{H}			
	143 (CDCl_3)	144 (CDCl_3)	145 (CDCl_3)	141 (D_2O)
$\text{C}(\text{CH}_3)_3$	1.39 (9H, s)	1.43 (9H, s)	1.44 (9H, s)	-
OCH_2CH_3	-	-	1.19-1.37 (6H, m, 2 x CH_3) 3.99-4.13 (4H, m, 2 x CH_2)	-
$\text{CH}_3\text{-2}'$	-	-	1.19-1.37 (3H, m)	1.05-1.29 (3H, m)
$\text{CH}_2\text{-3}$	1.89-1.99 (1H, m) 2.16-2.30 (1H, m)	2.03-2.11 (1H, m) 2.27-2.34 (1H, m)	1.95-2.07 (1H, m) 2.09-2.26 (1H, m)	2.00-2.04 (1H, m) 2.11-2.15 (1H, m)
$\text{CH}_2\text{-4}$	2.34-2.60 (2H, m)	2.38-2.62 (2H, m)	2.32-2.43 (1H, m) 2.58-2.71 (1H, m)	2.33-2.39 (1H, m) 2.45-2.64 (1H, m)
CH-2	4.57 (1H, dd, $^3J_{\text{H-H}}=9.6, 2.8$ Hz)	4.59 (1H, dd, $^3J_{\text{H-H}}=9.6, 3.0$ Hz)	4.36-4.53 (1H, m)	3.50-3.65 (1H, m)
$\text{CH-1}'$	-	-	4.36-4.53 (1H, m)	3.79-4.15 (1H, m)

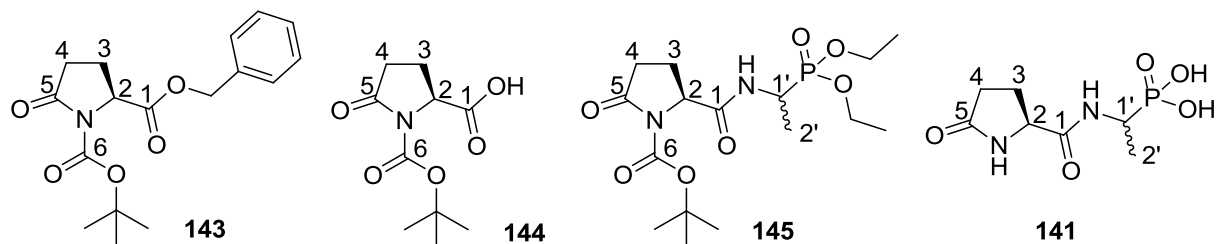


Table 8.2 (cont'd): Summary of $^1\text{H-NMR}$ of $^t\text{Boc-L-Pyroglu-OBzl}$ (**143**), $^t\text{Boc-L-Pyroglu-OH}$ (**144**), $^t\text{Boc-L-Pyroglu-D/L-Fos}$ diethyl ester (**145**) and L-Pyroglu-D/L-Fos (**141**) at 300 MHz

	δ_{H}			
	143 (CDCl_3)	144 (CDCl_3)	145 (CDCl_3)	141 (D_2O)
OCH ₂	5.11 (1H, d, $^2J_{\text{H-H}}=12.0$ Hz) 5.16 (1H, d, $^2J_{\text{H-H}}=12.2$ Hz)	-	-	-
C ₆ H ₅	7.28 (5H, m)	-	-	-
OH	-	9.20 (1H, br)	-	-
NH	-	-	6.89 (1H*, d, $^3J_{\text{H-H}}=9.0$ Hz) 6.95 (1H*, d, $^3J_{\text{H-H}}=9.0$ Hz)	Exchanged

*Actual proton integration was 0.5

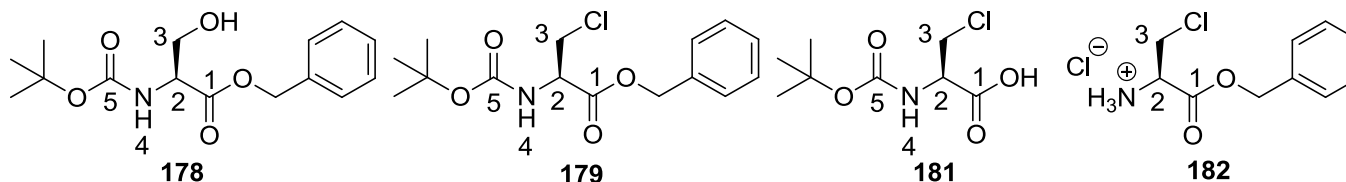


Table 8.3: Summary of $^1\text{H-NMR}$ spectra of $^t\text{Boc-L-Ser-OBzl}$ (**178**), $^t\text{Boc-}\beta\text{-chloro-L-Ala-OBzl}$ (**179**), $^t\text{Boc-}\beta\text{-chloro-L-Ala-OH}$ (**181**) and $\beta\text{-chloro-L-Ala-OBzl}$ hydrochloride (**182**) at 300 MHz

	δ_{H}			
	178 (CDCl_3)	179 (CDCl_3)	181 (CDCl_3)	182 (D_2O)
$\text{C}(\text{CH}_3)_3$	1.36 (9H, s)	1.38 (9H, s)	1.40 (9H, s)	-
$\text{CH}_2\text{-3}$	3.82 (1H, dd, $^2J_{\text{H-H}}=11.1$ Hz, $^3J_{\text{H-H}}=3.6$ Hz) 3.90 (1H, dd, $^2J_{\text{H-H}}=11.1$ Hz, $^3J_{\text{H-H}}=3.9$ Hz)	3.78 (1H, dd, $^2J_{\text{H-H}}=11.2$ Hz, $^3J_{\text{H-H}}=3.2$ Hz) 3.92 (1H, dd, $^2J_{\text{H-H}}=11.3$ Hz, $^3J_{\text{H-H}}=3.0$ Hz)	3.80 (1H, dd, $^2J_{\text{H-H}}=12.0$ Hz, $^3J_{\text{H-H}}=3.0$ Hz) 3.95 (1H, dd, $^2J_{\text{H-H}}=12.0$ Hz, $^3J_{\text{H-H}}=3.0$ Hz)	4.06 (1H, dd, $^2J_{\text{H-H}}=15.0$ Hz, $^3J_{\text{H-H}}=6.0$ Hz) 4.20 (1H, dd, $^2J_{\text{H-H}}=15.0$ Hz, $^3J_{\text{H-H}}=6.0$ Hz)
OCH_2	5.11 (1H, d, $^2J_{\text{H-H}}=12.3$ Hz) 5.16 (1H, d, $^2J_{\text{H-H}}=12.3$ Hz)	5.13 (1H, d, $^2J_{\text{H-H}}=12.2$ Hz) 5.18 (1H, d, $^2J_{\text{H-H}}=12.2$ Hz)	-	5.29 (1H, d, $^2J_{\text{H-H}}=12.0$ Hz) 5.37 (1H, d, $^2J_{\text{H-H}}=12.0$ Hz)
CH-2	4.33 (1H, m)	4.67 (1H, m)	4.70 (1H, m)	4.70 (1H, t, $^3J_{\text{H-H}}=6.0$ Hz)
C_6H_5	7.27 (5H, m)	7.29 (5H, m)	-	7.42-7.47 (5H, m)
NH-4	5.40 (1H, br)	5.37 (1H, d, $^3J_{\text{H-H}}=7.5$ Hz)	5.42 (1H, d, $^3J_{\text{H-H}}=7.2$ Hz)	Exchanged
OH	2.17 (1H, br)	-	9.03 (1H, br)	-

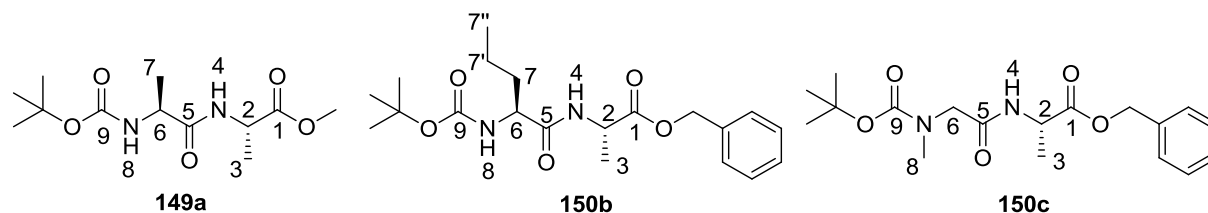


Table 8.4: Summary of $^1\text{H-NMR}$ spectra of $^t\text{Boc-L-Ala-L-Ala-OMe}$ (**149a**), $^t\text{Boc-L-Nva-L-Ala-OBzl}$ (**150b**) and $^t\text{Boc-Sar-L-Ala-OBzl}$ (**150c**) at 300 MHz

	δ_{H}		
	149a (CDCl_3)	150b (CDCl_3)	150c (CDCl_3)
$\text{CH}_3\text{-}7''$	-	0.83 (3H, t, $^3J_{\text{H-H}}=9.0$ Hz)	-
$\text{CH}_2\text{-}7'$	-	1.25-1.31 (2H, m)	-
$\text{CH}_2\text{-}7$	-	1.42-1.54 (1H, m) 1.64-1.73 (1H, m)	-
$\text{CH}_3\text{-}7$	1.33 (3H, d, $^3J_{\text{H-H}}=6.9$ Hz)	-	-
$\text{CH}_3\text{-}3$	1.37 (3H, d, $^3J_{\text{H-H}}=7.2$ Hz)	1.34 (3H, d, $^3J_{\text{H-H}}=6.0$ Hz)	1.35 (3H, t, $^3J_{\text{H-H}}=6.0$ Hz)
$\text{C}(\text{CH}_3)_3$	1.42 (9H, s)	1.36 (9H, s)	1.39 (9H, s)
OCH_3	3.72 (3H, s)	-	-
OCH_2	-	5.07 (1H, d, $^2J_{\text{H-H}}=12.0$ Hz) 5.12 (1H, d, $^2J_{\text{H-H}}=12.0$ Hz)	5.08 (1H, d, $^2J_{\text{H-H}}=12.0$ Hz) 5.13 (1H, d, $^2J_{\text{H-H}}=12.0$ Hz)
$\text{CH}_2\text{-}6$	-	-	3.72 (1H, d, $^2J_{\text{H-H}}=15.0$ Hz) 3.88 (1H, d, $^2J_{\text{H-H}}=15.0$ Hz)
$\text{CH-}6$	4.14 (1H, pentet, $^3J_{\text{H-H}}=6.9$ Hz)	4.02 (1H, m)	-
$\text{CH-}2$	4.54 (1H, pentet, $^3J_{\text{H-H}}=7.2$ Hz)	4.54 (1H, pentet, $^3J_{\text{H-H}}=6.0$ Hz)	4.58 (1H, pentet, $^3J_{\text{H-H}}=6.0$ Hz)

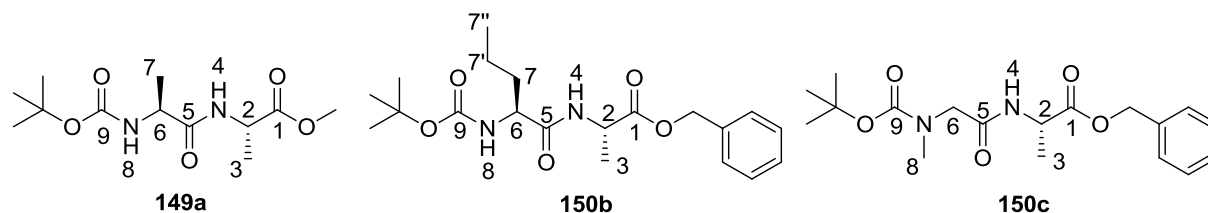


Table 8.4 (cont'd): Summary of $^1\text{H-NMR}$ spectra of $^t\text{Boc-L-Ala-L-Ala-OMe}$ (**149a**), $^t\text{Boc-L-Nva-L-Ala-OBzl}$ (**150b**) and $^t\text{Boc-Sar-L-Ala-OBzl}$ (**150c**) at 300 MHz

	δ_{H}		
	149a (CDCl_3)	150b (CDCl_3)	150c (CDCl_3)
NH-8	5.00 (1H, d, $^3J_{\text{H-H}}=6.0$ Hz)	4.96 (1H, d, $^3J_{\text{H-H}}=9.0$ Hz)	-
NH-4	6.63 (1H, d, $^3J_{\text{H-H}}=6.3$ Hz)	6.56 (1H, d, $^3J_{\text{H-H}}=6.0$ Hz)	6.51 (1H, br)
NCH ₃ -8	-	-	2.85 (3H, s)
C ₆ H ₅	-	7.27 (5H, m)	7.25-7.29 (5H, m)

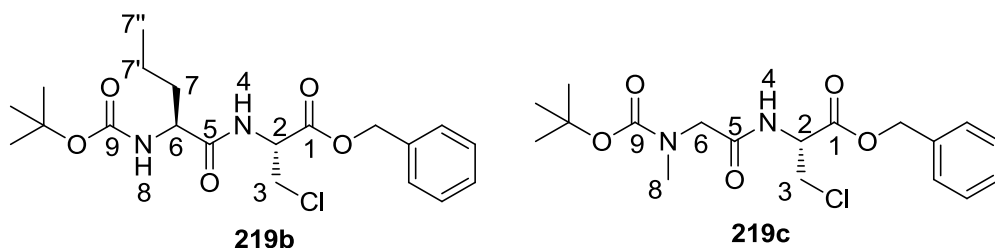


Table 8.5: Summary of $^1\text{H-NMR}$ spectra of $^t\text{Boc-L-Nva-}\beta\text{-chloro-L-Ala-OBzl}$ (**219b**) and $^t\text{Boc-Sar-}\beta\text{-chloro-L-Ala-OBzl}$ (**219c**) at 300 MHz

	δ_{H}	
	219b (CDCl_3)	219c (CDCl_3)
$\text{CH}_3\text{-7''}$	0.92 (3H, t, $^3J_{\text{H-H}}=9.0$ Hz)	-
$\text{CH}_2\text{-7'}$	1.32-1.43 (2H, m)	-
$\text{CH}_2\text{-7}$	1.52-1.65 (1H, m) 1.75-1.82 (1H, m)	-
$\text{C}(\text{CH}_3)_3$	1.45 (9H, s)	1.40 (9H, s)
OCH_2	5.20 (1H, d, $^2J_{\text{H-H}}=12.0$ Hz) 5.25 (1H, d, $^2J_{\text{H-H}}=12.0$ Hz)	5.13 (1H, d, $^2J_{\text{H-H}}=12.0$ Hz) 5.18 (1H, d, $^2J_{\text{H-H}}=12.0$ Hz)
$\text{CH}_2\text{-3}$	3.89 (1H, dd, $^2J_{\text{H-H}}=12.0$ Hz, $^3J_{\text{H-H}}=3.0$ Hz) 3.99 (1H, dd, $^2J_{\text{H-H}}=12.0$ Hz, $^3J_{\text{H-H}}=3.0$ Hz)	3.83 (1H, dd, $^2J_{\text{H-H}}=12.0$ Hz, $^3J_{\text{H-H}}=3.0$ Hz) 3.94 (1H, dd, $^2J_{\text{H-H}}=12.0$ Hz, $^3J_{\text{H-H}}=3.0$ Hz)
$\text{CH}_2\text{-6}$	-	3.80 (1H, d, $^2J_{\text{H-H}}=15.0$ Hz) 3.82 (1H, d, $^2J_{\text{H-H}}=15.0$ Hz)
CH-6	4.11-4.15 (1H, m)	-
CH-2	4.96-5.00 (1H, m)	4.91-4.96 (1H, m)
NH-4	6.97 (1H, d, $^3J_{\text{H-H}}=6.0$ Hz)	6.97 (1H, d, $^3J_{\text{H-H}}=6.0$ Hz)
NH-8	4.96-5.00 (1H, m)	-
$\text{NCH}_3\text{-8}$	-	2.87 (3H, s)
C_6H_5	7.33-7.37 (5H, m)	7.26-7.30 (5H, m)

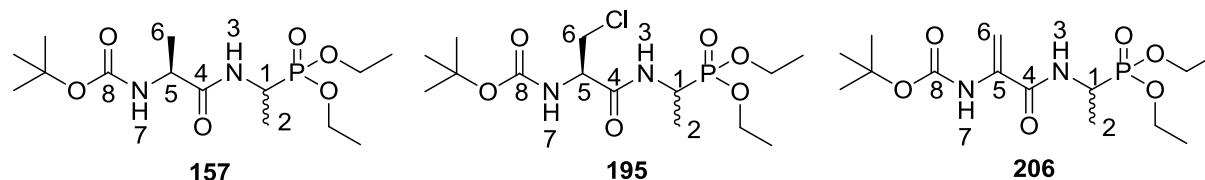


Table 8.6: Summary of $^1\text{H-NMR}$ spectra of diastereoisomeric $^t\text{Boc-L-Ala-D/L-Fos}$ diethyl ester (**157**), $^t\text{Boc-}\beta\text{-chloro-D/L-Fos}$ diethyl ester (**195**) and enantiomeric $^t\text{Boc-dehydroala-D/L-Fos}$ diethyl ester (**206**) at 300 MHz

	δ_{H}		
	157 (CDCl_3)	195 (CDCl_3)	206 (CDCl_3)
$\text{C}(\text{CH}_3)_3$	1.44 (9H, s)	1.47 (9H, s)	1.48 (9H, s)
OCH_2CH_3	1.23-1.43 (6H, m, 2 x CH_3) 4.06-4.23 (4H, m, 2 x CH_2)	1.15-1.46 (6H, m, 2 x CH_3) 4.06-4.22 (4H, m, 2 x CH_2)	1.31 (3H, t, $^3J_{\text{H-H}}=7.2$ Hz, CH_3) 1.34 (3H, t, $^3J_{\text{H-H}}=7.2$ Hz, CH_3) 4.06-4.19 (4H, m, 2 x CH_2)
$\text{CH}_3\text{-2}$	1.23-1.43 (3H, m)	1.15-1.46 (3H, m)	1.42 (3H, dd, $^3J_{\text{P-H}}=16.8$ Hz, $^3J_{\text{H-H}}=7.2$ Hz)
$\text{CH}_3\text{-6}$	1.23-1.43 (3H, m)	-	-
$\text{CH}_2\text{-6}$	-	3.74 (1H, dd, $^2J_{\text{H-H}}=12.0$ Hz, $^3J_{\text{H-H}}=6.0$ Hz) 4.00 (1H, dd, $^2J_{\text{H-H}}=12.0$ Hz, $^3J_{\text{H-H}}=6.0$ Hz)	5.24 (1H, s) 6.02 (1H, s)
CH-5	4.06-4.23 (1H, m)	4.40-4.56 (1H, m)	-
CH-1	4.40-4.52 (1H, m)	4.40-4.56 (1H, m)	4.48-4.59 (1H, m)

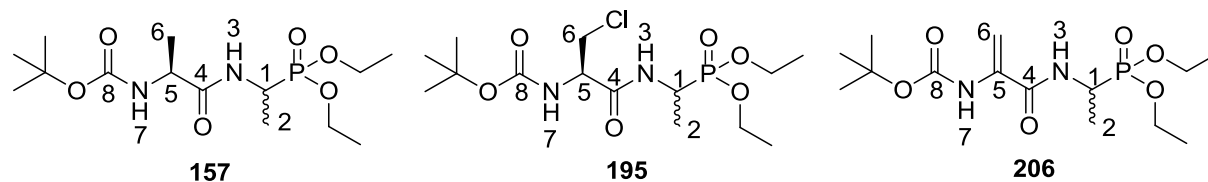


Table 8.6 (cont'd): Summary of $^1\text{H-NMR}$ spectra of diastereomeric $^t\text{Boc-L-Ala-D/L-Fos}$ diethyl ester (**157**), $^t\text{Boc-}\beta\text{-chloro-D/L-Fos}$ diethyl ester (**195**) and $^t\text{Boc-dehydroala-D/L-Fos}$ diethyl ester (**206**) at 300 MHz

	δ_{H}		
	157 (CDCl_3)	195 (CDCl_3)	206 (CDCl_3)
NH-7	5.12 (1H*, d, $^3J_{\text{H-H}}=1.5$ Hz) 5.14 (1H*, d, $^3J_{\text{H-H}}=1.5$ Hz)	5.46 (1H*, d, $^3J_{\text{H-H}}=6.0$ Hz) 5.48 (1H*, d, $^3J_{\text{H-H}}=9.0$ Hz) or 7.01 (1H*, m) 7.09 (1H*, m)	7.29 (1H, br)
NH-3	6.72 (1H*, d, $^3J_{\text{H-H}}=2.3$ Hz) 6.74 (1H*, d, $^3J_{\text{H-H}}=2.3$ Hz)	5.46 (1H*, d, $^3J_{\text{H-H}}=6.0$ Hz) 5.48 (1H*, d, $^3J_{\text{H-H}}=9.0$ Hz) or 7.01 (1H*, m) 7.09 (1H*, m)	6.90 (1H, d, $^3J_{\text{H-H}}=9.3$ Hz)

*Actual proton integration was 0.5

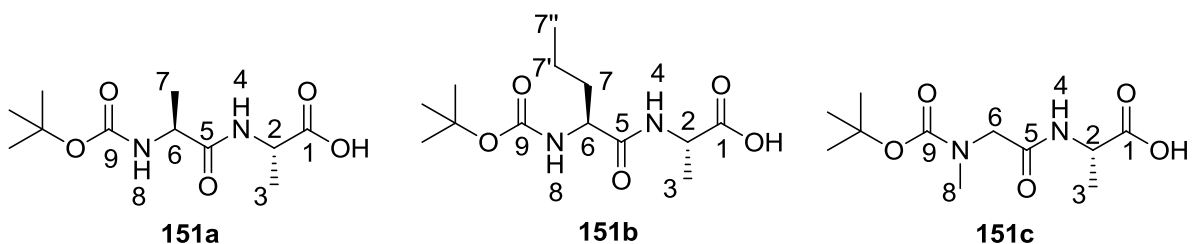


Table 8.7: Summary of $^1\text{H-NMR}$ spectra of 'Boc-L-Ala-L-Ala-OH (**151a**) at 500 MHz, 'Boc-L-Nva-L-Ala-OH (**151b**) and 'Boc-Sar-L-Ala-OH (**151c**) at 300 MHz

	δ_{H}		
	151a (DMSO ₄)	151b (CDCl ₃)	151c (CDCl ₃)
C(CH ₃) ₃	1.37 (9H, s)	1.39 (9H, s)	1.39 (9H, s)
CH ₃ -3	1.17 (3H, d, $^3J_{\text{H-H}}=7.1$ Hz)	1.27-1.31 (3H, m)	1.36 (3H, t, $^3J_{\text{H-H}}=6.0$ Hz)
CH ₃ -7	1.27 (3H, d, $^3J_{\text{H-H}}=7.3$ Hz)	-	-
CH ₃ -7''	-	0.85 (3H, t, $^3J_{\text{H-H}}=9.0$ Hz)	-
CH ₂ -7'	-	1.27-1.31 (2H, m)	-
CH ₂ -7	-	1.48-1.53 (1H, m) 1.67-1.71 (1H, m)	-
CH ₂ -6	-	-	3.72 (1H, d, $^2J_{\text{H-H}}=18.0$ Hz) 3.98 (1H, d, $^2J_{\text{H-H}}=18.0$ Hz)
CH-6	4.00 (1H, m)	4.10 (1H, m)	
CH-2	4.20 (1H, m)	4.50 (1H, m)	4.57 (1H, m)
NH-4	7.98 (1H, d, $^3J_{\text{H-H}}=7.4$ Hz)	6.93 (1H, m)	6.96 (1H, m)
NH-8	6.85 (1H, d, $^3J_{\text{H-H}}=7.7$ Hz)	5.27 (1H, m)	-
NCH ₃ -8	-	-	2.89 (3H, s)
OH	3.37 (1H, br)	8.87 (1H, br)	7.26 (1H, br)

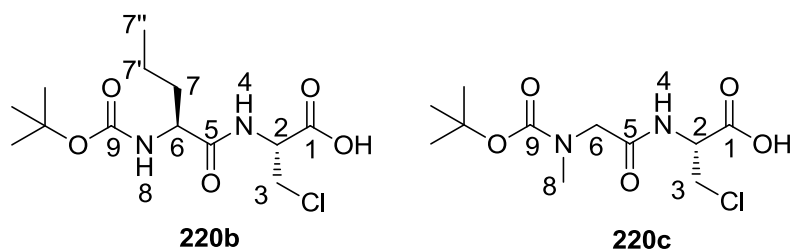


Table 8.8: Summary of $^1\text{H-NMR}$ spectra of $^t\text{Boc-L-Nva-}\beta\text{-chloro-L-Ala-OH}$ (**220b**) and $^t\text{Boc-Sar-}\beta\text{-chloro-L-Ala-OH}$ (**220c**) at 300 MHz

	δ_{H}	
	220b (DMSO)	220c (CDCl ₃)
C(CH ₃) ₃	1.38 (9H, s)	1.47 (9H, s)
CH ₃ -7''	0.85 (3H, t, $^3J_{\text{H-H}}=9.0$ Hz)	-
CH ₂ -7'	1.24-1.34 (2H, m)	-
CH ₂ -7	1.42-1.52 (1H, m) 1.54-1.59 (1H, m)	-
CH ₂ -3	3.84 (1H, dd, $^2J_{\text{H-H}}=12.0$ Hz, $^3J_{\text{H-H}}=6.0$ Hz) 3.91 (1H, dd, $^2J_{\text{H-H}}=12.0$ Hz, $^3J_{\text{H-H}}=6.0$ Hz)	3.81-4.17 (2H, m)
CH ₂ -6	-	3.81-4.17 (2H, m)
CH-6	3.95-4.02 (1H, m)	-
CH-2	4.62-4.67 (1H, m)	5.01 (1H, m)
NH-4	8.07 (1H, d, $^3J_{\text{H-H}}=9.0$ Hz)	7.07 (1H, br)
NH-8	6.92 (1H, d, $^3J_{\text{H-H}}=9.0$ Hz)	-
NCH ₃ -8	-	2.99 (3H, s)
OH	3.34 (1H, br)	7.45 (1H, br)

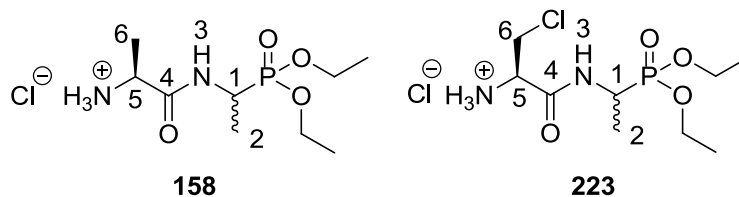


Table 8.9: Summary of $^1\text{H-NMR}$ spectra of diastereoisomeric L-Ala-D/L-Fos diethyl ester hydrochloride (**158**) and β -chloro-D/L-Fos diethyl ester hydrochloride (**223**) at 300 MHz

	δ_{H}	
	158 (CD_3OD)	223 (D_2O)
OCH_2CH_3	1.29-1.44 (6H, m, 2 x CH_3) 4.08-4.22 (4H, m, 2 x CH_2)	1.28 (3H, t, $^3J_{\text{H-H}}=6.0$ Hz, CH_3) 1.29 (3H, t, $^3J_{\text{H-H}}=6.0$ Hz, CH_3) 4.07-4.21 (4H, m, 2 x CH_2)
$\text{CH}_3\text{-2}$	1.29-1.44 (3H, m)	1.37 (3H, dd, $^3J_{\text{P-H}}=18.0$ Hz, $^3J_{\text{H-H}}=6.0$ Hz)
$\text{CH}_3\text{-6}$	1.51 (3H, d, $^3J_{\text{H-H}}=6.0$ Hz)	-
$\text{CH}_2\text{-6}$	-	3.92-4.04 (2H, m)
CH-1	4.28-4.47 (1H, m)	4.38-4.48 (1H, m)
CH-5	3.90-3.98 (1H, m)	4.38-4.48 (1H, m)
NH-3	Exchanged	Exchanged

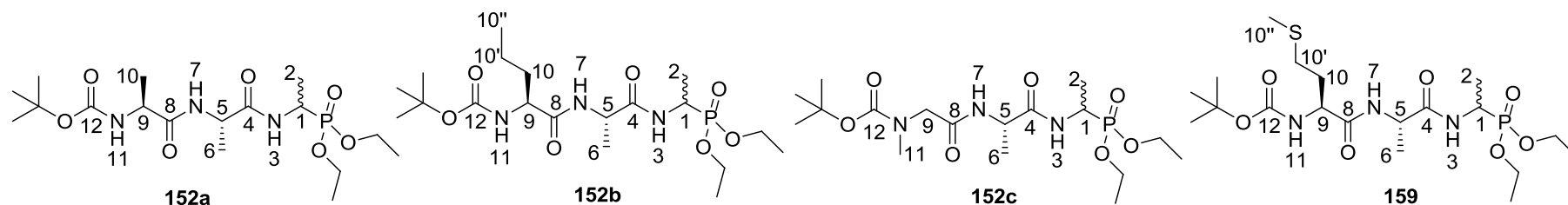


Table 8.10: Summary of $^1\text{H-NMR}$ spectra of diastereoisomeric $^t\text{Boc-L-Ala-L-Ala-D/L-Fos}$ diethyl ester (**152a**) at 500 MHz, $^t\text{Boc-L-Nva-L-Ala-D/L-Fos}$ diethyl ester (**152b**), $^t\text{Boc-Sar-L-Ala-D/L-Fos}$ diethyl ester (**152c**) and $^t\text{Boc-L-Met-L-Ala-D/L-Fos}$ diethyl ester (**159**) at 300 MHz

	δ_{H}			
	152a (CDCl_3)	152b (CDCl_3)	152c (CDCl_3)	159 (CDCl_3)
$\text{C}(\text{CH}_3)_3$	1.37 (9H, s)	1.37 (9H, s)	1.40 (9H, s)	1.36 (9H, s)
OCH_2CH_3	1.21-1.33 (6H, m, 2 x CH_3) 3.98-4.12 (4H, m, 2 x CH_2)	1.18-1.34 (6H, m, 2 x CH_3) 3.98-4.12 (4H, m, 2 x CH_2)	1.19-1.34 (6H, m, 2 x CH_3) 4.00-4.11 (4H, m, 2 x CH_2)	1.16-1.36 (6H, m, 2 x CH_3) 4.00-4.12 (4H, m, 2 x CH_2)
$\text{CH}_3\text{-10}''$	-	0.85 (3H, t, $^3J_{\text{H-H}}=9.0$ Hz)	-	2.04 (3H, s)
$\text{CH}_2\text{-10}'$	-	1.18-1.34 (2H, m)	-	2.49 (2H, dd, $^3J_{\text{H-H}}=9.0$ Hz, 3.0 Hz)
$\text{CH}_2\text{-10}$	-	1.47-1.54 (1H, m) 1.65-1.73 (1H, m)	-	1.82-2.01 (2H, m)
$\text{CH}_3\text{-10}$	1.21-1.33 (3H, m)	-	-	-
$\text{CH}_3\text{-2}$	1.21-1.33 (3H, m)	1.18-1.34 (3H, m)	1.19-1.34 (3H, m)	1.16-1.36 (3H, m)
$\text{CH}_3\text{-6}$	1.21-1.33 (3H, m)	1.18-1.34 (3H, m)	1.19-1.34 (3H, m)	1.16-1.36 (3H, m)
$\text{CH}_2\text{-9}$	-	-	3.72, 3.78 ^t (1H, d, $^2J_{\text{H-H}}=15.0$ Hz) 3.81, 3.87 ^t (1H, d, $^2J_{\text{H-H}}=15.0$ Hz)	-

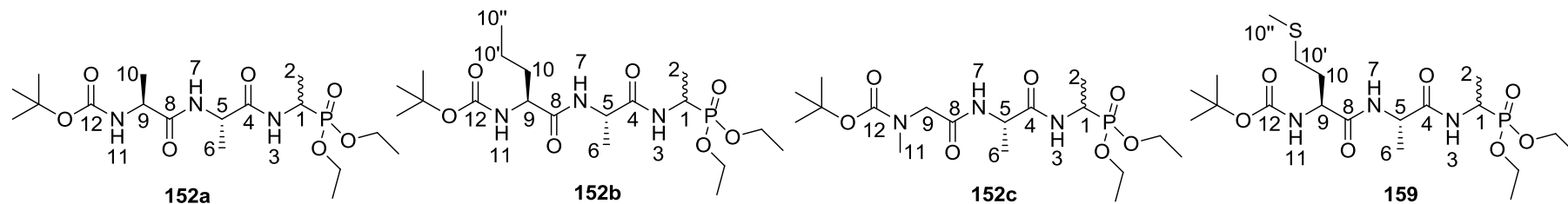


Table 8.10 (cont'd): Summary of $^1\text{H-NMR}$ spectra of diastereoisomeric $^t\text{Boc-L-Ala-L-Ala-D/L-Fos}$ diethyl ester (**152a**) at 500 MHz, $^t\text{Boc-L-Nva-L-Ala-D/L-Fos}$ diethyl ester (**152b**), $^t\text{Boc-Sar-L-Ala-D/L-Fos}$ diethyl ester (**152c**) and $^t\text{Boc-L-Met-L-Ala-D/L-Fos}$ diethyl ester (**159**) at 300 MHz

	δ_{H}			
	152a (CDCl_3)	152b (CDCl_3)	152c (CDCl_3)	159 (CDCl_3)
CH-9	3.98-4.12 (1H, m)	3.98-4.12 (1H, m)	-	4.16-4.26 (1H, m)
CH-5	4.47-4.53 (1H, m)	4.48-4.54 (1H, m)	4.47-4.52 (1H, m)	4.45-4.53 (1H, m)
CH-1	4.34-4.43 (1H, m)	4.33-4.44 (1H, m)	4.35-4.43 (1H, m)	4.33-4.43 (1H, m)
NH-7	6.83-6.94 (1H, m)	6.78 (1H*, d, $^3J_{\text{H-H}}=6.0$ Hz) 6.87 (1H*, d, $^3J_{\text{H-H}}=6.0$ Hz)	6.67 (1H, d, $^3J_{\text{H-H}}=9.0$ Hz)	6.85 (1H*, d, $^3J_{\text{H-H}}=6.0$ Hz) 6.92 (1H*, d, $^3J_{\text{H-H}}=6.0$ Hz)
NH-3	7.10-7.20 (1H, m)	7.15 (1H*, d, $^3J_{\text{H-H}}=9.0$ Hz) 7.23 (1H*, d, $^3J_{\text{H-H}}=9.0$ Hz)	6.98 (1H*, d, $^3J_{\text{H-H}}=9.0$ Hz) 7.15 (1H*, d, $^3J_{\text{H-H}}=9.0$ Hz)	7.07 (1H*, d, $^3J_{\text{H-H}}=9.0$ Hz) 7.16 (1H*, d, $^3J_{\text{H-H}}=9.0$ Hz)
NH-11	5.26-5.37 (1H, m)	5.19 (1H*, d, $^3J_{\text{H-H}}=6.0$ Hz) 5.23 (1H*, d, $^3J_{\text{H-H}}=6.0$ Hz)	-	5.40 (1H*, d, $^3J_{\text{H-H}}=9.0$ Hz) 5.44 (1H*, d, $^3J_{\text{H-H}}=6.0$ Hz)
NCH ₃ -11	-	-	2.87 (3H, s)	-

^tTwo signals were observed due to diastereoisomers; *Actual proton integration was 0.5

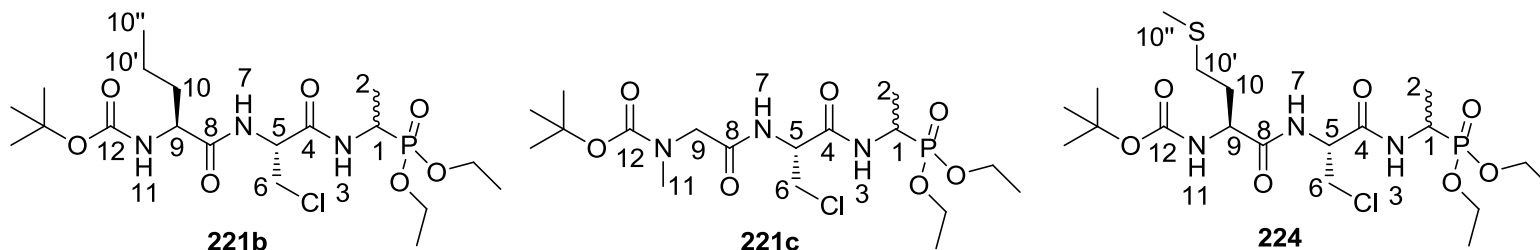


Table 8.11: Summary of $^1\text{H-NMR}$ spectra of diastereoisomeric $^t\text{Boc-L-Nva-}\beta\text{-chloro-L-Ala-D/L-Fos}$ diethyl ester (**221b**), $^t\text{Boc-Sar-}\beta\text{-chloro-L-Ala-D/L-Fos}$ diethyl ester (**221c**), $^t\text{Boc-L-Met-}\beta\text{-chloro-L-Ala-D/L-Fos}$ diethyl ester (**224**) at 300 MHz

	δ_{H}		
	221b (CDCl_3)	221c (CDCl_3)	224 (CDCl_3)
$\text{C}(\text{CH}_3)_3$	1.38 (9H, s)	1.41 (9H, s)	1.38 (9H, s)
OCH_2CH_3	1.22-1.34 (6H, m, 2 x CH_3) 3.97-4.13 (4H, m, 2 x CH_2)	1.11-1.35 (6H, m, 2 x CH_3) 4.02-4.13 (4H, m, 2 x CH_2)	1.17-1.36 (6H, m, 2 x CH_3) 3.99-4.13 (4H, m, 2 x CH_2)
$\text{CH}_3\text{-10}''$	0.86 (3H*, t, $^3J_{\text{H-H}}=9.0$ Hz) 0.88 (3H*, t, $^3J_{\text{H-H}}=9.0$ Hz)	-	2.04 (3H, s)
$\text{CH}_2\text{-10}'$	1.22-1.34 (3H, m)	-	2.48-2.54 (2H, m)
$\text{CH}_2\text{-10}$	1.53-1.59 (1H, m) 1.70-1.77 (1H, m)	-	1.87-2.03 (2H, m)
$\text{CH}_3\text{-2}$	1.22-1.34 (3H, m)	1.11-1.35 (3H, m)	1.17-1.36 (3H, m)
$\text{CH}_2\text{-6}$	3.69 (1H, dd, $^2J_{\text{H-H}}=12.0$ Hz, $^3J_{\text{H-H}}=6.0$ Hz) 3.91 (1H, dd, $^2J_{\text{H-H}}=12.0$ Hz, $^3J_{\text{H-H}}=6.0$ Hz)	3.70-3.88 (2H, m)	3.71 (1H, dd, $^2J_{\text{H-H}}=12.0$ Hz, $^3J_{\text{H-H}}=6.0$ Hz) 3.88 (1H, dd, $^2J_{\text{H-H}}=12.0$ Hz, $^3J_{\text{H-H}}=6.0$ Hz)

* Actual proton integration was 1.5

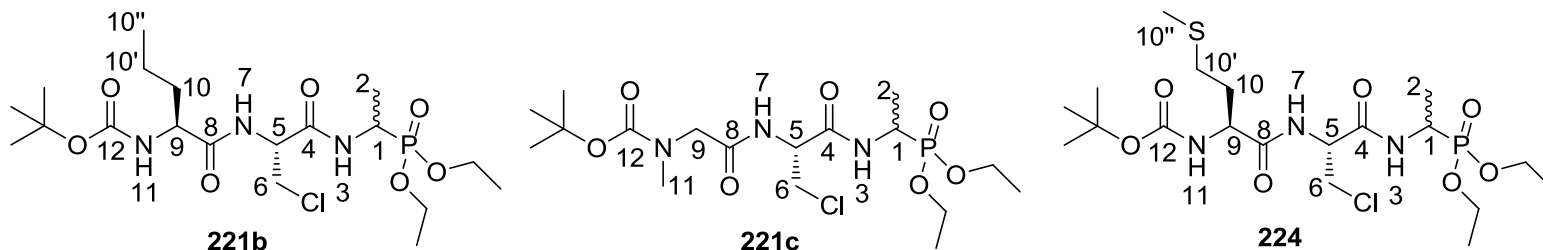


Table 8.11 (cont'd): Summary of $^1\text{H-NMR}$ spectra of diastereoisomeric 'Boc-L-Nva- β -chloro-L-Ala-D/L-Fos diethyl ester (**221b**), 'Boc-Sar- β -chloro-L-Ala-D/L-Fos diethyl ester (**221c**), 'Boc-L-Met- β -chloro-L-Ala-D/L-Fos diethyl ester (**224**) at 300 MHz

	δ_{H}		
	221b (CDCl_3)	221c (CDCl_3)	224 (CDCl_3)
CH_2 -9	-	3.70-3.88 (2H, m)	-
CH-9	3.78-3.81 (1H, m)	-	4.20 (1H, m)
CH-5	4.73-4.79 (1H, m)	4.78-4.82 (1H, m)	4.78-4.84 (1H, m)
CH-1	4.35-4.46 (1H, m)	4.36-4.47 (1H, m)	4.37-4.47 (1H, m)
NH-7	7.01 (1H*, d, $^3J_{\text{H-H}}=9.0$ Hz) 7.09 (1H*, d, $^3J_{\text{H-H}}=9.0$ Hz)	6.94 (1H, m)	7.15 (1H*, d, $^3J_{\text{H-H}}=6.0$ Hz) 7.24 (1H*, d, $^3J_{\text{H-H}}=6.0$ Hz)
NH-3	7.25 (1H*, d, $^3J_{\text{H-H}}=9.0$ Hz) 7.33 (1H*, d, $^3J_{\text{H-H}}=9.0$ Hz)	7.36 (1H, m)	7.52 (1H, m)
NH-11	4.97-5.03 (1H, m)	-	5.39 (1H*, d, $^3J_{\text{H-H}}=6.0$ Hz) 5.41 (1H*, d, $^3J_{\text{H-H}}=6.0$ Hz)
NCH_3 -11	-	2.90 (3H, s)	-

* Actual proton integration was 0.5

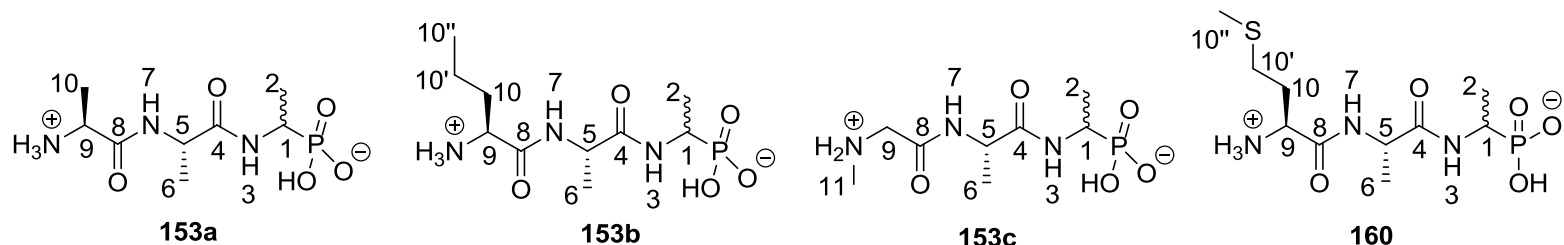


Table 8.12: Summary of $^1\text{H-NMR}$ spectra of diastereoisomeric L-Ala-L-Ala-D/L-Fos (**153a**), L-Nva-L-Ala-D/L-Fos (**153b**), Sar-L-Ala-D/L-Fos (**153c**), L-Met-L-Ala-D/L-Fos (**160**) at 300 MHz

	δ_{H}			
	153a (D_2O)	153b (D_2O)	153c (D_2O)	160 (D_2O)
CH ₃ -10''	-	0.96 (3H, t, $^3J_{\text{H-H}}=7.1$ Hz)	-	2.15 (3H, s)
CH ₂ -10'	-	1.40-1.42 (2H, m)	-	2.62 (2H, m)
CH ₂ -10	-	1.88-1.86 (2H, m)	-	2.20 (2H, m)
CH ₃ -10	1.35 (3H, d, $^3J_{\text{H-H}}=5.8$ Hz) or 1.51 (3H, d, $^3J_{\text{H-H}}=5.3$ Hz)	-	-	-
CH ₃ -2	1.24 (3H, m)	1.27-1.32 (3H, d, $^3J_{\text{H-H}}=6.8$ Hz)	1.14-1.57 (3H, m)	1.29-1.33 (3H, m)
CH ₃ -6	1.35 (3H, d, $^3J_{\text{H-H}}=5.8$ Hz) or 1.51 (3H, d, $^3J_{\text{H-H}}=5.3$ Hz)	1.40-1.42 (3H, m)	1.14-1.57 (3H, m)	1.42 (3H, d, $^3J_{\text{H-H}}=6.0$ Hz)
CH ₂ -9	-	-	3.84-4.07 (2H, m)	-

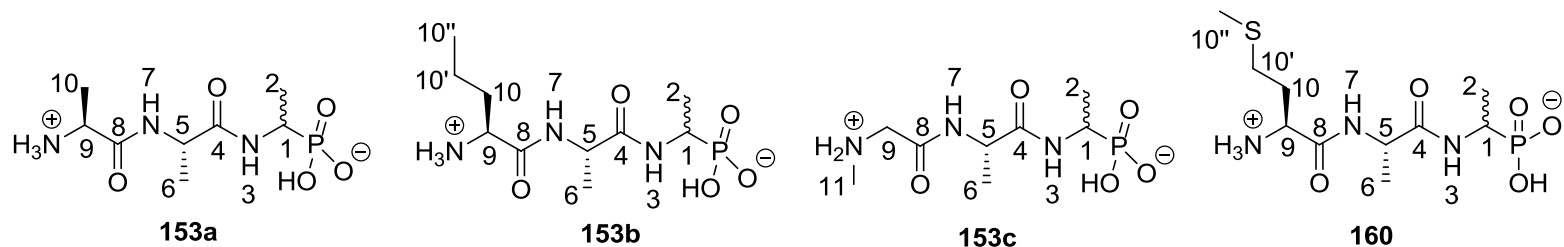


Table 8.12 (cont'd): Summary of $^1\text{H-NMR}$ spectra of diastereoisomeric L-Ala-L-Ala-D/L-Fos (**153a**), L-Nva-L-Ala-D/L-Fos (**153b**), Sar-L-Ala-D/L-Fos (**153c**), L-Met-L-Ala-D/L-Fos (**160**) at 300 MHz

	δ_{H}			
	153a (D_2O)	153b (D_2O)	153c (D_2O)	160 (D_2O)
CH-9	4.29 or 4.31 (1H, m)	4.00-4.02 (1H, m)	-	4.14 (1H, m)
CH-5	4.29 or 4.31 (1H, m)	4.34-4.39 (1H, m)	4.32-4.58 (1H, m)	4.39-4.41 (1H, m)
CH-1	4.04 (1H, m)	4.00-4.02 (1H, m)	3.84-4.07 (1H, m)	4.05 (1H, m)
NH-7	Exchanged	Exchanged	Exchanged	Exchanged
NH-3	Exchanged	Exchanged	Exchanged	Exchanged
NCH ₃ -11	-	-	2.74 (3H, s)	-

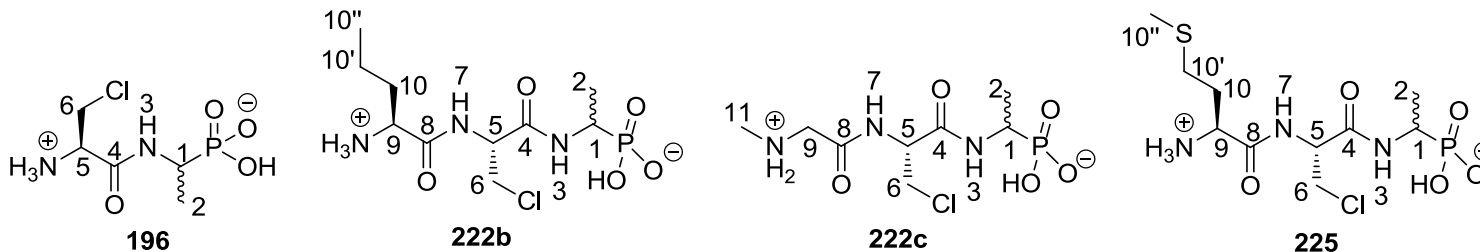


Table 8.13: Summary of $^1\text{H-NMR}$ spectra of diastereoisomeric β -chloro-L-Ala-D/L-Fos (**196**), L-Nva- β -chloro-L-Ala-D/L-Fos (**222b**), Sar- β -chloro-L-Ala-D/L-Fos (**222c**), L-Met- β -chloro-L-Ala-D/L-Fos (**225**) at 300 MHz

	δ_{H}			
	196 (D_2O)	222b (D_2O)	222c (CD_3OD)	225 (D_2O)
$\text{CH}_3\text{-}10''$	-	1.01 (3H, t, $^3J_{\text{H-H}}=9.0$ Hz)	-	2.13 (3H, s)
$\text{CH}_2\text{-}10'$	-	1.44-1.54 (2H, br m)	-	2.63-2.69 (2H, m)
$\text{CH}_2\text{-}10$	-	1.90-1.98 (2H, br m)	-	2.18-2.29 (2H, m)
$\text{CH}_3\text{-}2$	1.29 (3H, d, $^3J_{\text{H-H}}=6.9$ Hz)	1.30-1.37 (3H, br m)	1.24 (3H, dd, $^3J_{\text{H-P}}=15.0$ Hz, $^3J_{\text{H-H}}=6.0$ Hz)	1.31 (3H, dd, $^3J_{\text{H-P}}=15.0$ Hz, $^3J_{\text{H-H}}=6.0$ Hz)
$\text{CH}_2\text{-}6$	4.02 (2H, m)	3.91-4.15 (2H, br m)	3.81-3.87 (2H, m)	3.89 (1H, dd, $^2J_{\text{H-H}}=12.0$ Hz, $^3J_{\text{H-H}}=6.0$ Hz) 3.97 (1H, dd, $^2J_{\text{H-H}}=12.0$ Hz, $^3J_{\text{H-H}}=6.0$ Hz)
$\text{CH}_2\text{-}9$	-	-	3.93-3.94 (2H, m)	-
$\text{CH-}9$	-	3.91-4.15 (1H, br m)	-	4.22 (1H, m)
$\text{CH-}5$	4.38 (1H, m)	4.79 (1H, br m)	4.79 (1H, m)	4.75-4.79 (1H, m)
$\text{CH-}1$	4.02 (1H, m)	3.91-4.15 (1H, br m)	3.97-4.10 (1H, m)	4.01-4.13 (1H, m)
$\text{NH-}7$	-	Exchanged	Exchanged	Exchanged
$\text{NH-}3$	Exchanged	Exchanged	Exchanged	Exchanged
$\text{NCH}_3\text{-}11$	-	-	2.74 (3H, s)	-

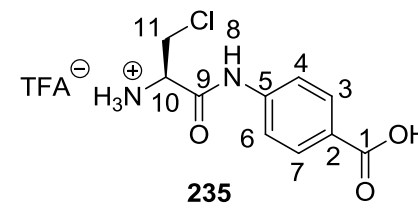
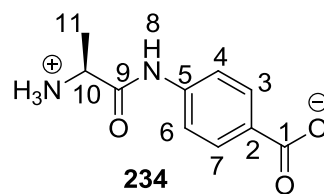
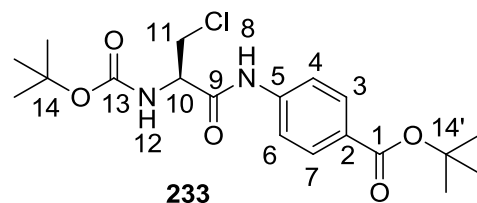
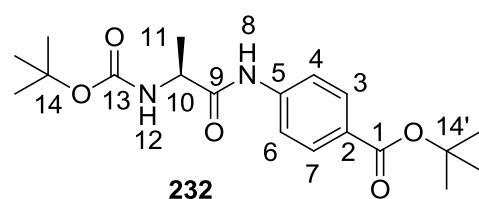


Table 8.14: Summary of $^1\text{H-NMR}$ spectra of $^t\text{Boc-L-Ala-PABA-O}^t\text{Butyl}$ (**232**) and L-Ala-PABA (**234**) at 300 MHz, and $^t\text{Boc-}\beta\text{-chloro-L-Ala-PABA-O}^t\text{Butyl}$ (**233**), $\beta\text{-chloro-L-Ala-PABA}\cdot\text{trifluoroacetate}$ (**235**) at 500 MHz

	δ_{H}			
	232 (CDCl_3)	233 (CDCl_3)	234 (D_2O)	235 (CD_3OD)
$\text{C}(\text{CH}_3)_3\text{-14}$	1.39 (9H, s)	1.51 (9H, s)	-	-
$\text{C}(\text{CH}_3)_3\text{-14}'$	1.50 (9H, s)	1.60 (9H, s)	-	-
$\text{CH}_3\text{-11}$	1.37 (3H, d, $^3J_{\text{H-H}}=9.0$ Hz)	-	1.58 (3H, d, $^3J_{\text{H-H}}=9.0$ Hz)	-
$\text{CH}_2\text{-11}$	-	3.85 (1H, dd, $^2J_{\text{H-H}}=12.0$ Hz, $^3J_{\text{H-H}}=6.0$ Hz) 4.10 (1H, dd, $^2J_{\text{H-H}}=12.0$ Hz, $^3J_{\text{H-H}}=6.0$ Hz)	-	4.12 (2H, m)
CH-10	4.28 (1H, m)	4.64 (1H, m)	4.17 (1H, q, $^3J_{\text{H-H}}=9.0$ Hz)	4.43 (1H, m)
$\text{CH}_{\text{Ar}}\text{-4/6}$	7.47 (2H, d, $^3J_{\text{H-H}}=6.0$ Hz)	7.60 (2H, d, $^3J_{\text{H-H}}=6.0$ Hz)	7.40 (2H, d, $^3J_{\text{H-H}}=9.0$ Hz)	7.73 (2H, d, $^3J_{\text{H-H}}=5.0$ Hz)
$\text{CH}_{\text{Ar}}\text{-3/7}$	7.83 (2H, d, $^3J_{\text{H-H}}=6.0$ Hz)	7.97 (2H, d, $^3J_{\text{H-H}}=6.0$ Hz)	7.87 (2H, d, $^3J_{\text{H-H}}=9.0$ Hz)	8.01 (2H, d, $^3J_{\text{H-H}}=5.0$ Hz)
NH-12	5.09 (1H, d, $^3J_{\text{H-H}}=9.0$ Hz)	5.45 (1H, d, $^3J_{\text{H-H}}=6.0$ Hz)	-	-
NH-8	8.76 (1H, br)	8.50 (1H, br)	Exchanged	Exchanged

Appendix 8.2: Summary of ^{13}C -NMR of synthesised compounds

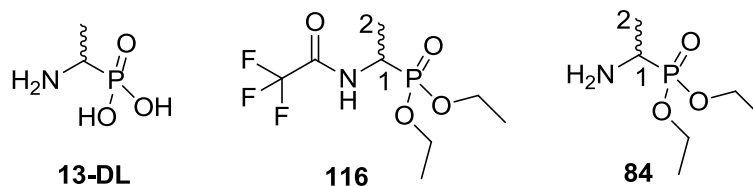


Table 8.15: Summary of ^{13}C -NMR spectra of D/L-fosfalin (**13-DL**), trifluoroacetyl-D/L-Fos diethyl ester (**116**) and D/L-Fos diethyl ester (**84**) at 75 MHz

	δ_{C}		
	13-DL (D_2O)	116 (CDCl_3)	84 (CDCl_3)
CH ₃ -2	13.5 (d, $^2J_{\text{C-P}}=2.6$ Hz)	14.8	17.2
CH-1	44.7 (d, $^1J_{\text{C-P}}=144.2$ Hz)	41.8 (d, $^1J_{\text{C-P}}=159.1$ Hz)	44.2 (d, $^1J_{\text{C-P}}=148.5$ Hz)
OCH ₂ CH ₃	-	16.2 (d, $^3J_{\text{C-P}}=2.3$ Hz, CH ₃) 16.3 (d, $^3J_{\text{C-P}}=2.3$ Hz, CH ₃) 62.8 (d, $^2J_{\text{C-P}}=7.0$ Hz, CH ₂) 63.2 (d, $^2J_{\text{C-P}}=7.1$ Hz, CH ₂)	16.4 (CH ₃) 16.5 (CH ₃) 62.1 (d, $^2J_{\text{C-P}}=7.5$ Hz, CH ₂) 62.1 (d, $^2J_{\text{C-P}}=7.5$ Hz, CH ₂)
CF ₃	-	115.9 (q, $^1J_{\text{C-F}}=285.8$ Hz)	-
C=O	-	156.9 (q, $^2J_{\text{C-F}}=5.8$ Hz)	-

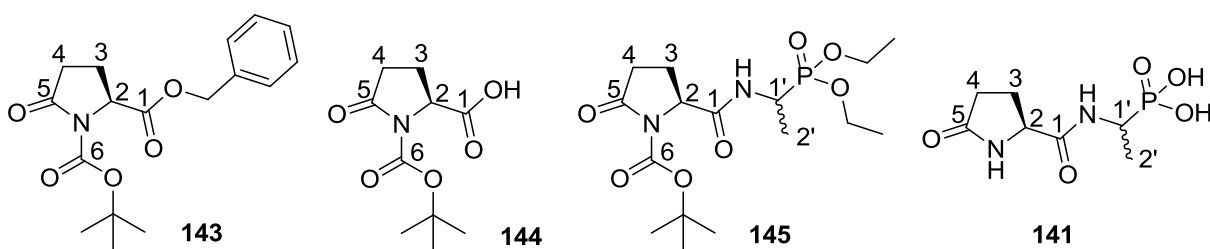


Table 8.16: Summary of ^{13}C -NMR of $^t\text{Boc-L-Pyroglu-OBzl}$ (**143**), $^t\text{Boc-L-Pyroglu-OH}$ (**144**), $^t\text{Boc-L-Pyroglu-D/L-Fos}$ diethyl ester (**145**) and L-Pyroglu-D/L-Fos (**141**) at 75 MHz

	δ_{C}			
	143 (CDCl_3)	144 (CDCl_3)	145 (CDCl_3)	141 (D_2O)
$\text{C}(\text{CH}_3)_3$	26.8 ($\text{C}(\text{CH}_3)_3$) 82.6 ($\text{C}(\text{CH}_3)_3$)	26.9 ($\text{C}(\text{CH}_3)_3$) 83.1 ($\text{C}(\text{CH}_3)_3$)	26.9, 27.0 ($\text{C}(\text{CH}_3)_3$) 82.5, 82.7 ($\text{C}(\text{CH}_3)_3$)	-
OCH_2CH_3	-	-	15.4, 15.4, 15.5, 15.5 4 x (d, $^3J_{\text{C-P}}=2.3$ Hz, CH_3) 61.5, 61.6, 61.8, 61.9 4 x (d, $^2J_{\text{C-P}}=6.8$ Hz, CH_2)	-
$\text{CH}_3\text{-}2'$	-	-	14.5, 14.6	14.8, 15.1
$\text{CH}_2\text{-}3$	20.6	20.4	21.3, 21.4	25.1, 25.6
$\text{CH}_2\text{-}4$	30.1	30.2	30.5, 30.6	29.1, 29.3
$\text{CH-}2$	58.0	57.7	58.7, 59.0	65.3
$\text{CH-}1'$	-	-	39.9 (d, $^1J_{\text{C-P}}=156.0$ Hz)	52.5
OCH_2	66.4	-	-	-
C_6H_5	127.5, 127.6 (CH_{Ar}) 134.1 ($\text{C}_{\text{quat.}}$)	-	-	-
$\text{C=O-}6$	148.3	148.4	148.9, 149.0	-
$\text{C=O-}1$	170.2	175.3	169.4, 169.5	165.4
$\text{C=O-}5$	172.1	172.5	172.5, 172.6	173.7

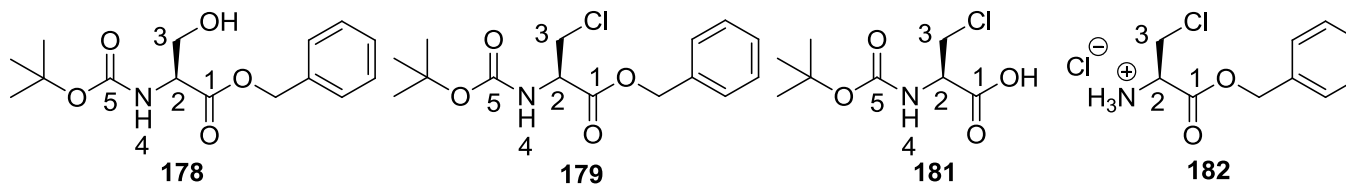


Table 8.17: Summary of ^{13}C -NMR spectra of $^t\text{Boc-L-Ser-OBzl}$ (**178**), $^t\text{Boc-}\beta\text{-chloro-L-Ala-OBzl}$ (**179**), $^t\text{Boc-}\beta\text{-chloro-L-Ala-OH}$ (**181**) and $\beta\text{-chloro-L-Ala-OBzl}$ hydrochloride (**182**) at 75 MHz

	δ_{C}			
	178 (CDCl_3)	179 (CDCl_3)	181 (CDCl_3)	182 (D_2O)
$\text{C}(\text{CH}_3)_3$	27.1 ($\text{C}(\text{CH}_3)_3$) 79.1 ($\text{C}(\text{CH}_3)_3$)	28.3 ($\text{C}(\text{CH}_3)_3$) 80.5 ($\text{C}(\text{CH}_3)_3$)	27.1 ($\text{C}(\text{CH}_3)_3$) 79.8 ($\text{C}(\text{CH}_3)_3$)	-
$\text{CH}_2\text{-3}$	62.3	45.5	44.0	41.8
OCH_2	66.2	67.8	-	69.1
CH-2	54.7	54.5	53.1	54.0
C_6H_5	127.0-127.4 (CH_{Ar}) 134.1 ($\text{C}_{\text{quat.}}$)	128.4-128.7 (CH_{Ar}) 134.9 ($\text{C}_{\text{quat.}}$)	-	128.6-129.1 (CH_{Ar}) 134.5 ($\text{C}_{\text{quat.}}$)
C=O-5	153.0	155.0	154.2	-
C=O-1	170.7	169.0	172.1	167.0

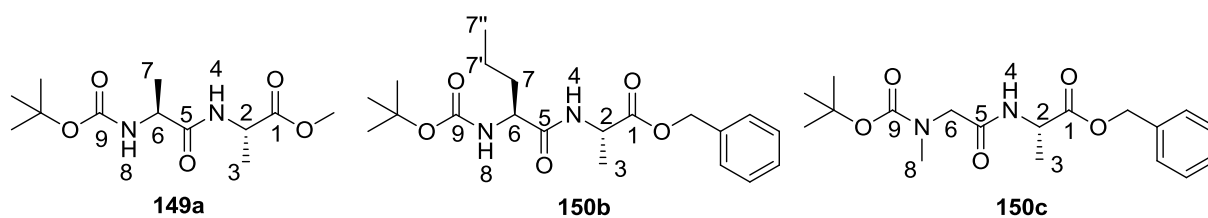


Table 8.18: Summary of ^{13}C -NMR spectra of $^t\text{Boc-L-Ala-L-Ala-OMe}$ (**149a**), $^t\text{Boc-L-Nva-L-Ala-OBzl}$ (**150b**) and $^t\text{Boc-Sar-L-Ala-OBzl}$ (**150c**) at 75 MHz

	δ_{C}		
	149a (CDCl_3)	150b (CDCl_3)	150c (CDCl_3)
$\text{CH}_3\text{-}7''$	-	12.7	-
$\text{CH}_2\text{-}7'$	-	17.8	-
$\text{CH}_2\text{-}7$	-	33.7	-
$\text{CH}_3\text{-}7$	18.6	-	-
$\text{CH}_3\text{-}3$	18.6	17.3	17.5
$\text{C}(\text{CH}_3)_3$	28.5 ($\text{C}(\text{CH}_3)_3$) 80.4 ($\text{C}(\text{CH}_3)_3$)	27.3 ($\text{C}(\text{CH}_3)_3$) 79.0 ($\text{C}(\text{CH}_3)_3$)	27.3 ($\text{C}(\text{CH}_3)_3$) 79.8 ($\text{C}(\text{CH}_3)_3$)
OCH_3	52.6	-	-
OCH_2	-	66.1	66.2
$\text{CH}_2\text{-}6$	-	-	52.1
$\text{CH-}6$	50.3	53.4	-
$\text{CH-}2$	48.2	47.1	47.0
$\text{C=O-}9$	155.4	154.6	155.0
$\text{C=O-}5$	172.4	170.8	167.9
$\text{C=O-}1$	173.4	171.5	171.5
$\text{NCH}_3\text{-}8$	-	-	34.7
C_6H_5	-	127.1-127.6 (CH_{Ar}) 134.3 ($\text{C}_{\text{quat.}}$)	127.1-127.6 (CH_{Ar}) 134.3 ($\text{C}_{\text{quat.}}$)

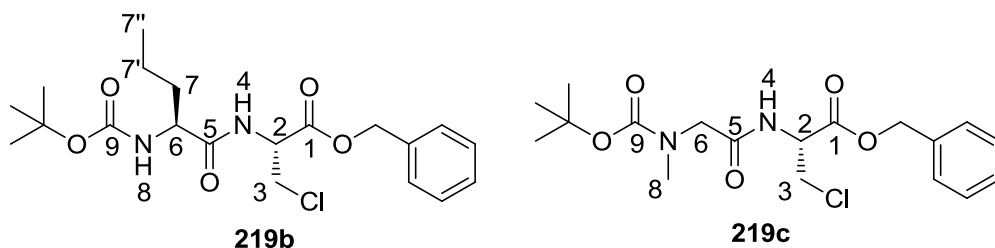


Table 8.19: Summary of ^{13}C -NMR spectra of t -Boc-L-Nva- β -chloro-L-Ala-OBzl (**219b**) and t -Boc-Sar- β -chloro-L-Ala-OBzl (**219c**) at 75 MHz

	δ_{C}	
	219b (CDCl_3)	219c (CDCl_3)
$\text{CH}_3\text{-}7''$	12.7	-
$\text{CH}_2\text{-}7'$	17.8	-
$\text{CH}_2\text{-}7$	33.4	-
$\text{C}(\text{CH}_3)_3$	27.3 ($\text{C}(\text{CH}_3)_3$) 79.3 ($\text{C}(\text{CH}_3)_3$)	28.2 ($\text{C}(\text{CH}_3)_3$) 81.0 ($\text{C}(\text{CH}_3)_3$)
OCH_2	67.0	68.0
$\text{CH}_2\text{-}3$	43.8	44.9
$\text{CH}_2\text{-}6$	-	53.0
$\text{CH-}6$	53.4	-
$\text{CH-}2$	52.2	53.0
C_6H_5	127.4-127.7 (CH_{Ar}) 133.8 ($\text{C}_{\text{quat.}}$)	128.4-128.7 (CH_{Ar}) 134.8 ($\text{C}_{\text{quat.}}$)
$\text{C=O-}9$	154.5	154.5
$\text{C=O-}1$	167.5	168.4
$\text{C=O-}5$	171.2	169.4
$\text{NCH}_3\text{-}8$	-	35.6

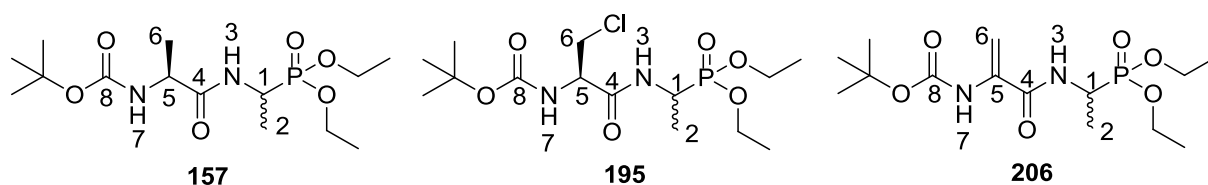


Table 8.20: Summary of ^{13}C -NMR spectra of diastereoisomeric $^t\text{Boc-L-Ala-D/L-Fos}$ diethyl ester (**157**), $^t\text{Boc-}\beta\text{-chloro-D/L-Fos}$ diethyl ester (**195**) and $^t\text{Boc-dehydroala-D/L-Fos}$ diethyl ester (**206**) at 75 MHz

	δ_{C}		
	157 (CDCl_3)	195 (CDCl_3)	206 (CDCl_3)
$\text{C}(\text{CH}_3)_3$	28.3 ($\text{C}(\text{CH}_3)_3$) 80.0 ($\text{C}(\text{CH}_3)_3$)	28.2 ($\text{C}(\text{CH}_3)_3$) 80.8 ($\text{C}(\text{CH}_3)_3$)	28,2 ($\text{C}(\text{CH}_3)_3$) 80.5 ($\text{C}(\text{CH}_3)_3$)
OCH_2CH_3	16.3, 16.5, 16.4, 16.6 4 x (d, $^3J_{\text{C-P}}=3.0$ Hz, CH_3) 62.4, 62.5, 62.6, 62.8 4 x (d, $^2J_{\text{C-P}}=6.8$ Hz, CH_2)	16.3, 16.4 2 x (d, $^3J_{\text{C-P}}=1.5$ Hz, CH_3) 16.4, 16.4 2 x (d, $^3J_{\text{C-P}}=2.3$ Hz, CH_3) 62.6, 62.6, 63.0, 63.0 4 x (d, $^2J_{\text{C-P}}=6.8$ Hz, CH_2)	16.4 (2 x CH_3) 62.3, 62.5 2 x (d, $^2J_{\text{P-C}}=6.8$ Hz, CH_2)
$\text{CH}_3\text{-2}$	15.6	15.6, 15.7	15.4
$\text{CH}_3\text{-6}$	18.4	-	-
$\text{CH}_2\text{-6}$	-	55.2	98.3
CH-5	50.0	55.3	-
C-5	-	-	134.6
CH-1	40.8, 41.0 2 x (d, $^1J_{\text{C-P}}=156.8$ Hz)	41.2, 41.3 2 x (d, $^1J_{\text{C-P}}=157.5$ Hz)	41.7 (d, $^1J_{\text{C-P}}=157.5$ Hz)
C=O-8	155.2	155.0	152.7
C=O-4	172.1	168.3	163.5

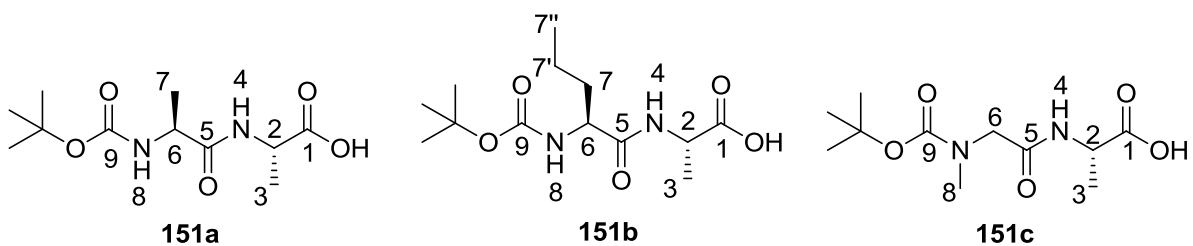


Table 8.21: Summary of ^{13}C -NMR spectra of $^t\text{Boc-L-Ala-L-Ala-OH}$ (**151a**) at 125 MHz, $^t\text{Boc-L-Nva-L-Ala-OH}$ (**151b**) and $^t\text{Boc-Sar-L-Ala-OH}$ (**151c**) at 75 MHz

	δ_{C}		
	151a (DMSO ₄)	151b (CDCl ₃)	151c (CDCl ₃)
C(CH ₃) ₃	28.7 (C(CH ₃))	28.3 (C(CH ₃) ₃)	27.3 (C(CH ₃) ₃)
	78.5 (C(CH ₃) ₃)	80.4 (C(CH ₃) ₃)	80.6 (C(CH ₃) ₃)
CH ₃ -3	18.6	18.0	17.2
CH ₃ -7	17.7	-	-
CH ₃ -7''	-	13.7	-
CH ₂ -7'	-	18.8	-
CH ₂ -7	-	34.5	-
CH ₂ -6	-	-	52.1
CH-6	47.8	54.3	
CH-2	49.8	48.1	46.8
C=O-9	155.4	156.0	155.5
C=O-5	173.0	172.5	168.3
C=O-1	174.5	175.5	174.1
NCH ₃ -8	-	-	49.6

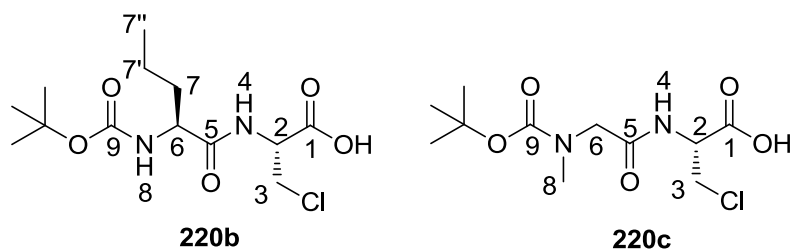


Table 8.21: Summary of ^{13}C -NMR spectra of $^t\text{Boc-L-Nva-}\beta\text{-chloro-L-Ala-OH}$ (**220b**) and $^t\text{Boc-Sar-}\beta\text{-chloro-L-Ala-OH}$ (**220c**) at 75 MHz

	δ_{C}	
	220b (DMSO)	220c (CDCl ₃)
C(CH ₃) ₃	28.6 (C(CH ₃) ₃) 78.5 (C(CH ₃) ₃)	28.3 (C(CH ₃) ₃) 81.8 (C(CH ₃) ₃)
CH ₃ -7''	14.1	-
CH ₂ -7'	19.1	-
CH ₂ -7	34.4	-
CH ₂ -3	45.1	44.5
CH ₂ -6	-	53.0
CH-6	54.5	-
CH-2	53.6	53.0
C=O-9	155.8	156.8
C=O-5	170.6	169.5
C=O-1	173.0	169.5
NCH ₃ -8	-	36.1

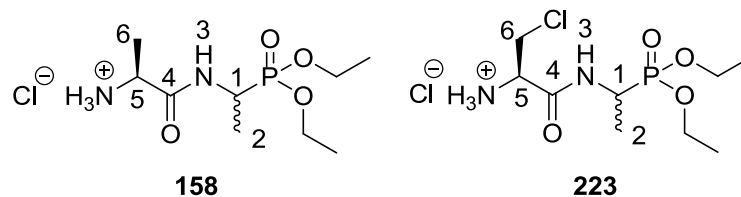


Table 8.22: Summary of ^{13}C -NMR spectra of diastereoisomeric L-Ala-D/L-Fos diethyl ester hydrochloride (**158**) and β -chloro-D/L-Fos diethyl ester hydrochloride (**223**) at 75 MHz

	δ_{C}	
	158 (CD_3OD)	223 (D_2O)
OCH ₂ CH ₃	15.4 (2 x CH ₃) 62.7-63.0 (2 x CH ₂)	15.7 (CH ₃) 15.7 (CH ₃) 64.3 (d, $^2J_{\text{P-C}}=6.8$ Hz, CH ₂) 64.5 (d, $^2J_{\text{P-C}}=6.8$ Hz, CH ₂)
CH ₃ -2	13.7, 14.0	13.7, 14.0
CH ₃ -6	16.3	-
CH ₂ -6	-	42.4
CH-1	41.1, 41.4 (d, $^1J_{\text{C-P}}=158.3$ Hz)	41.7 (d, $^1J_{\text{P-C}}=158.3$ Hz) 42.0 (d, $^1J_{\text{P-C}}=157.5$ Hz)
CH-5	48.8, 48.9	53.7, 53.8
C=O-4	169.0	165.8

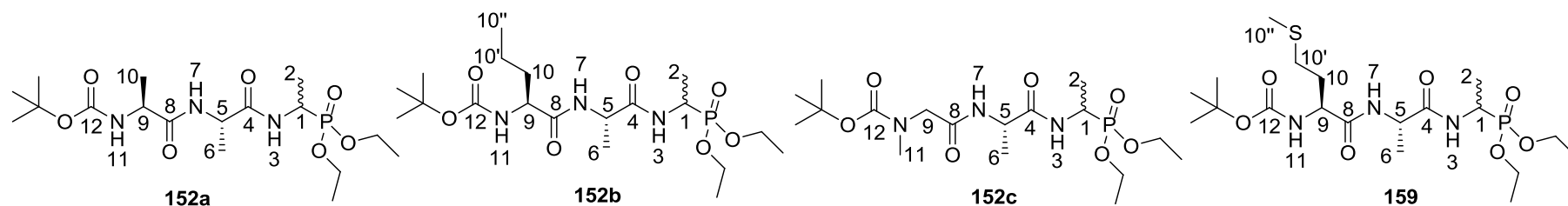


Table 8.23: Summary of ^{13}C -NMR spectra of diastereoisomeric $^t\text{Boc-L-Ala-L-Ala-D/L-Fos}$ diethyl ester (**152a**) at 125 MHz, $^t\text{Boc-L-Nva-L-Ala-D/L-Fos}$ diethyl ester (**152b**), $^t\text{Boc-Sar-L-Ala-D/L-Fos}$ diethyl ester (**152c**) and $^t\text{Boc-L-Met-L-Ala-D/L-Fos}$ diethyl ester (**159**) at 75 MHz

	δC			
	152a (CDCl_3)	152b (CDCl_3)	152c (CDCl_3)	159 (CDCl_3)
$\text{C}(\text{CH}_3)_3$	28.5 ($\text{C}(\text{CH}_3)_3$) 80.2 ($\text{C}(\text{CH}_3)_3$)	27.3 ($\text{C}(\text{CH}_3)_3$) 78.9 ($\text{C}(\text{CH}_3)_3$)	28.3 ($\text{C}(\text{CH}_3)_3$) 80.7 ($\text{C}(\text{CH}_3)_3$)	27.3 ($\text{C}(\text{CH}_3)_3$) 79.1 ($\text{C}(\text{CH}_3)_3$)
OCH_2CH_3	16.6, 16.6, 16.6, 16.6 (CH_3) 62.7, 62.8, 62.9, 63.1 4 x (d, $^2J_{\text{C-P}}=6.9$ Hz, CH_2)	15.3, 15.4, 15.5, 15.6 (CH_3) 61.5, 61.6, 61.7, 61.9 4 x (d, $^2J_{\text{C-P}}=7.5$ Hz, CH_2)	16.3, 16.4 2 x (d, $^3J_{\text{P-C}}=3.0$ Hz, CH_3) 62.5, 62.6, 62.7, 62.9 4 x (d, $^2J_{\text{C-P}}=6.8$ Hz, CH_2)	15.4, 15.5 2 x (d, $^3J_{\text{P-C}}=3.0$ Hz, CH_3) 15.4, 15.5 2 x (d, $^3J_{\text{P-C}}=2.3$ Hz, CH_3) 61.5, 61.6, 61.7, 61.9 4 x (d, $^2J_{\text{C-P}}=6.8$ Hz, CH_2)
$\text{CH}_3\text{-}10''$	-	12.7	-	14.5, 14.6
$\text{CH}_2\text{-}10'$	-	17.8, 17.9	-	29.2, 29.3
$\text{CH}_2\text{-}10$	-	33.8, 33.9	-	30.8, 30.9
$\text{CH}_3\text{-}10$	16.7 or 18.7	-	-	-
$\text{CH}_3\text{-}2$	15.4, 15.5	14.4, 14.5	15.5, 15.5	14.2, 14.3

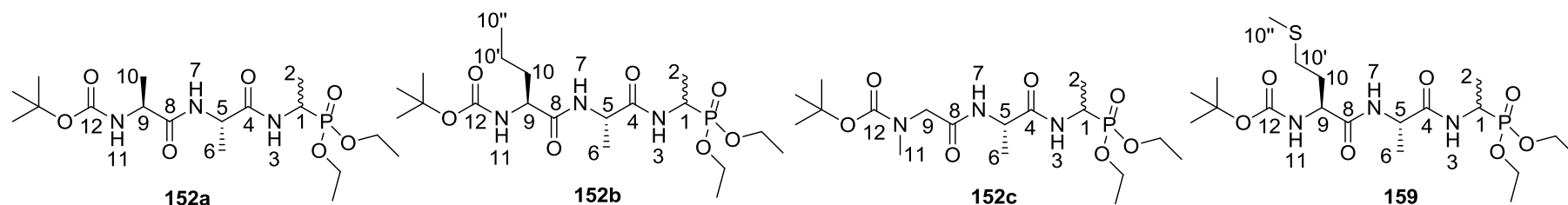


Table 8.23 (cont'd): Summary of ^{13}C -NMR spectra of diastereomeric $^t\text{Boc-L-Ala-L-Ala-D/L-Fos}$ diethyl ester (**152a**) at 125 MHz, $^t\text{Boc-L-Nva-L-Ala-D/L-Fos}$ diethyl ester (**152b**), $^t\text{Boc-Sar-L-Ala-D/L-Fos}$ diethyl ester (**152c**) and $^t\text{Boc-L-Met-L-Ala-D/L-Fos}$ diethyl ester (**159**) at 75 MHz

	δ_{C}			
	152a (CDCl_3)	152b (CDCl_3)	152c (CDCl_3)	159 (CDCl_3)
CH_3 -6	16.7 or 18.7	17.6, 17.7	18.7	17.7
CH_2 -9	-	-	53.0	-
CH -9	49.0 or 49.1	53.5, 53.5	-	52.6
CH -5	49.0 or 49.1	47.7, 47.9	48.5	47.9, 48.0
CH -1	41.2 (d, $^1J_{\text{C-P}}=157.2$ Hz)	39.9 (d, $^1J_{\text{P-C}}=157.5$ Hz) 40.0 (d, $^1J_{\text{P-C}}=156.8$ Hz)	41.0 (d, $^1J_{\text{P-C}}=157.5$ Hz)	39.9, 40.0 (d, $^1J_{\text{C-P}}=156.8$ Hz)
$\text{C}=\text{O}$ -12	150.0	154.7	156.0	154.6
$\text{C}=\text{O}$ -4	171.9 or 172.7	170.6, 170.7 or 171.0, 171.1	171.5 or 171.6	170.3, 170.4 or 170.5, 170.6
$\text{C}=\text{O}$ -8	171.9 or 172.7	170.6, 170.7 or 171.0, 171.1	171.5 or 171.6	170.3, 170.4 or 170.5, 170.6
NCH_3 -11	-	-	35.8	-

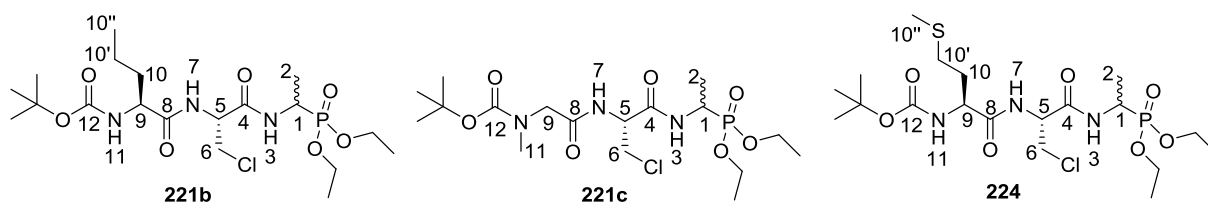


Table 8.24: Summary of ^{13}C -NMR spectra of diastereoisomeric $^t\text{Boc-L-Nva-}\beta\text{-chloro-L-Ala-D/L-Fos}$ diethyl ester (**221b**), $^t\text{Boc-Sar-}\beta\text{-chloro-L-Ala-D/L-Fos}$ diethyl ester (**221c**), $^t\text{Boc-L-Met-}\beta\text{-chloro-L-Ala-D/L-Fos}$ diethyl ester (**224**) at 75 MHz

	δ_{C}		
	221b (CDCl_3)	221c (CDCl_3)	224 (CDCl_3)
$\text{C}(\text{CH}_3)_3$	27.0, 27.3 ($\text{C}(\text{CH}_3)_3$) 79.4 ($\text{C}(\text{CH}_3)_3$)	28.3 ($\text{C}(\text{CH}_3)_3$) 81.0 ($\text{C}(\text{CH}_3)_3$)	27.3 ($\text{C}(\text{CH}_3)_3$) 79.6 ($\text{C}(\text{CH}_3)_3$)
OCH_2CH_3	15.3, 15.4, 15.5, 15.6 (CH_3) 61.4, 61.6, 61.7, 61.9 4 x (d, $^2J_{\text{C-P}}=6.8$ Hz, CH_2)	16.3, 16.4 (CH_3) 62.7 (d, $^2J_{\text{C-P}}=6.0$ Hz, CH_2) 63.0 (d, $^2J_{\text{C-P}}=7.5$ Hz, CH_2)	15.3, 15.4, 15.5, 15.6 (CH_3) 61.6, 62.0 2 x (d, $^2J_{\text{P-C}}=6.8$ Hz, CH_2) 61.7 (d, $^2J_{\text{P-C}}=6.0$ Hz, CH_2) 62.1 (d, $^2J_{\text{P-C}}=7.5$ Hz, CH_2)
$\text{CH}_3\text{-}10''$	12.7	-	14.5
$\text{CH}_2\text{-}10'$	17.9, 18.0	-	29.2, 29.3
$\text{CH}_2\text{-}10$	33.2	-	30.2, 30.4
$\text{CH}_3\text{-}2$	14.5	15.2, 15.6	14.3, 14.4
$\text{CH}_2\text{-}6$	43.4	44.7	43.5, 43.7
$\text{CH}_2\text{-}9$	-	53.1	-
$\text{CH-}9$	70.5	-	53.1
$\text{CH-}5$	52.6, 52.8	53.4	52.7
$\text{CH-}1$	40.4 (d, $^1J_{\text{C-P}}=157.5$ Hz)	41.2 (d, $^1J_{\text{C-P}}=156.8$ Hz)	40.3 (d, $^1J_{\text{P-C}}=159.0$ Hz)
$\text{C=O-}12$	154.7	152.3	154.8
$\text{C=O-}4$	166.8	167.7 or 169.4	166.7, 166.8
$\text{C=O-}8$	171.4	167.7 or 169.4	170.7, 170.8
$\text{NCH}_3\text{-}11$	-	35.9	-

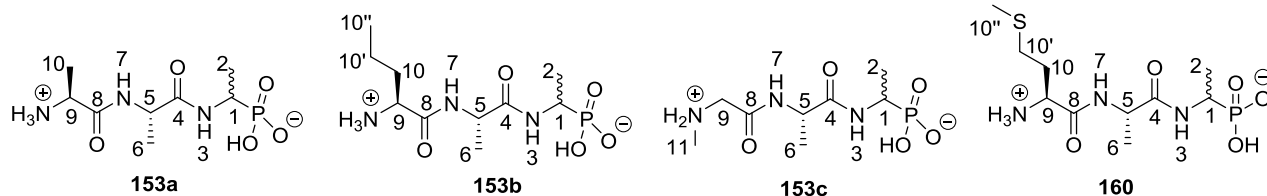


Table 8.25: Summary of ^{13}C -NMR spectra of diastereoisomeric L-Ala-L-Ala-D/L-Fos (**153a**), L-Nva-L-Ala-D/L-Fos (**153b**), Sar-L-Ala-D/L-Fos (**153c**), L-Met-L-Ala-D/L-Fos (**160**) at 75 MHz

	δ_{C}			
	153a (D ₂ O)	153b (D ₂ O)	153c (D ₂ O)	160 (D ₂ O)
CH ₃ -10''	-	13.4	-	16.9
CH ₂ -10'	-	18.1, 18.2	-	32.8, 33.0
CH ₂ -10	-	33.5, 33.6	-	30.7, 31.0
CH ₃ -10	16.5, 16.6 or 16.7, 16.8	-	-	-
CH ₃ -2	15.3, 15.4	16.0	15.4	18.4
CH ₃ -6	16.5, 16.6 or 16.7, 16.8	17.1, 17.2	16.8	19.5, 19.6
CH ₂ -9	-	-	49.4	-
CH-9	50.0	53.5		55.0
CH-5	50.0	50.5, 50.8	50.0	52.9, 53.0
CH-1	48.9	53.5	43.9 (d, $^1J_{\text{P-C}}=148.5$ Hz)	44.4
C=O-4	170.5 or 173.7	174.7	173.7	176.1
C=O-8	170.5 or 173.7	170.4, 170.6	166.0	176.1
NCH ₃ -11	-	-	32.9	-

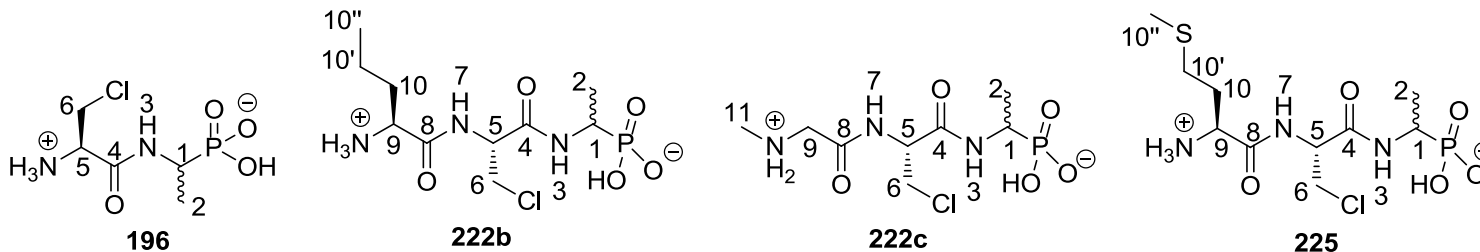


Table 8.26: Summary of ^{13}C -NMR spectra of diastereoisomeric β -chloro-L-Ala-D/L-Fos (**196**), L-Nva- β -chloro-L-Ala-D/L-Fos (**222b**), Sar- β -chloro-L-Ala-D/L-Fos (**222c**), L-Met- β -chloro-L-Ala-D/L-Fos (**225**) at 75 MHz

	δ_{C}			
	196 (D_2O)	222b (D_2O)	222c (CD_3OD)	225 (D_2O)
CH_3 -10''	-	12.9	-	16.9, 17.0
CH_2 -10'	-	17.6	-	31.1
CH_2 -10	-	33.0	-	32.9
CH_3 -2	15.2	15.7	15.4	18.4
CH_2 -6	42.3, 42.6	43.3	43.6	46.2
CH_2 -9	-	-	49.5	-
CH -9	-	53.1	-	55.2, 55.3
CH -5	54.0, 54.1	55.0	54.6	57.8, 58.0
CH -1	44.3 (d, $^1J_{\text{P-C}}=147.0$ Hz)	53.1	44.1 (d, $^1J_{\text{C-P}}=148.5$ Hz)	47.0 (d, $^1J_{\text{C-P}}=147.0$ Hz)
$\text{C}=\text{O}$ -4	165.7	170.4	166.4 or 166.9	171.7, 171.8
$\text{C}=\text{O}$ -8	-	170.4	166.4 or 166.9	172.3
NCH_3 -11	-	-	32.9	-

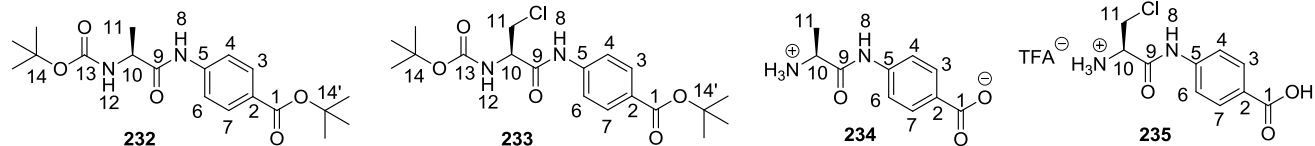


Table 8.27: Summary of ^{13}C -NMR spectra of $^t\text{Boc-L-Ala-PABA-O}^t\text{Butyl}$ (**232**) and L-Ala-PABA (**234**) at 75 MHz, and $^t\text{Boc-}\beta\text{-chloro-L-Ala-PABA-O}^t\text{Butyl}$ (**233**), $\beta\text{-chloro-L-Ala-PABA}$ · trifluoroacetate (**235**) at 125 MHz

	δ_{C}			
	232 (CDCl_3)	233 (CDCl_3)	234 (D_2O)	235 (CD_3OD)
$\text{C}(\text{CH}_3)_3\text{-14}$	28.2 ($\text{C}(\text{CH}_3)_3$) 79.9 ($\text{C}(\text{CH}_3)_3$)	28.2 ($\text{C}(\text{CH}_3)_3$) 82.2 ($\text{C}(\text{CH}_3)_3$)	-	
$\text{C}(\text{CH}_3)_3\text{-14}'$	28.3 ($\text{C}(\text{CH}_3)_3$) 79.9 ($\text{C}(\text{CH}_3)_3$)	28.3 ($\text{C}(\text{CH}_3)_3$) 81.3 ($\text{C}(\text{CH}_3)_3$)	-	
$\text{CH}_3\text{-11}$	17.3	-	16.5	-
$\text{CH}_2\text{-11}$	-	44.1	-	49.3
CH-10	51.0	56.0	49.8	56.3
$\text{CH}_{\text{Ar}}\text{-4/6}$	118.7	119.1	120.4	120.4
$\text{CH}_{\text{Ar}}\text{-2}$	127.5	128.2	138.9	143.1
$\text{CH}_{\text{Ar}}\text{-3/7}$	130.5	130.6	129.2	131.9
$\text{CH}_{\text{Ar}}\text{-5}$	141.6	140.7	133.0	128.1
C=O-13	156.2	155.7	-	-
C=O-1	165.3	165.2	174.7	169.3
C=O-9	171.1	167.3	169.1	165.9

Appendix 8.3: Summary of ^{31}P - ^1H decoupled NMR of synthesised compounds

Table 8.28: Chemical shift of ^{31}P - ^1H decoupled of phosphonate ester

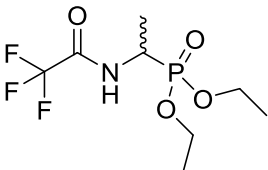
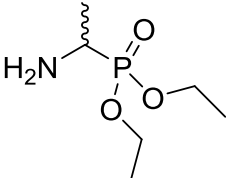
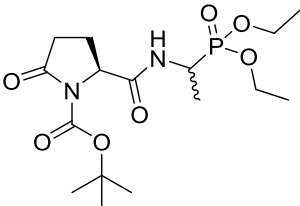
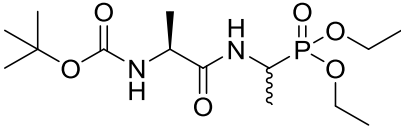
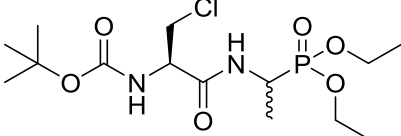
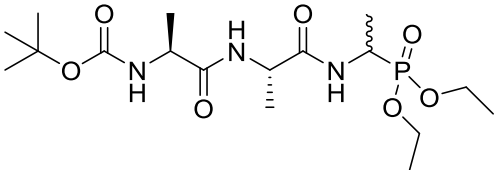
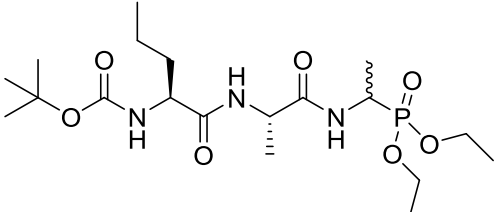
Structure	Name	$\delta_{\text{P-H}}$
	Trifluoroacetyl-D/L-Fos diethyl ester (116)	23.0
	D/L-Fos diethyl ester (84)	29.6
	$^t\text{Boc-L-Pyroglu-D/L-Fos}$ diethyl ester (145)	24.9
	$^t\text{Boc-L-Ala-D/L-Fos}$ diethyl ester (157)	25.2
	$^t\text{Boc-}\beta\text{-Cl-L-Ala-D/L-Fos}$ diethyl ester (195)	24.7, 24.8
	$^t\text{Boc-L-Ala-L-Ala-D/L-Fos}$ diethyl ester (152a)	25.1, 25.2
	$^t\text{Boc-L-Nva-L-Ala-D/L-Fos}$ diethyl ester (152b)	25.0, 25.1

Table 8.28 (cont.d): Chemical shift of ^{31}P - ^1H decoupled of phosphonate ester

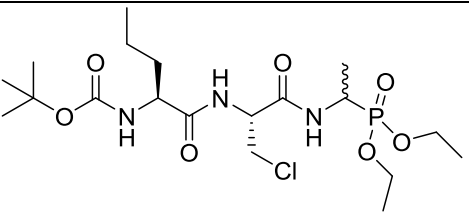
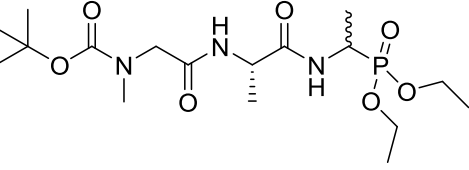
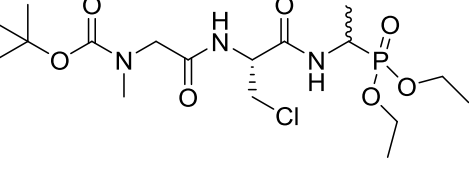
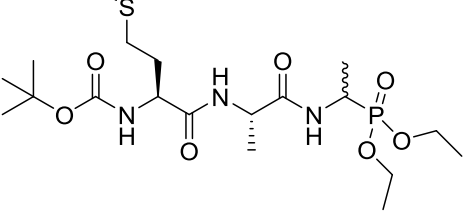
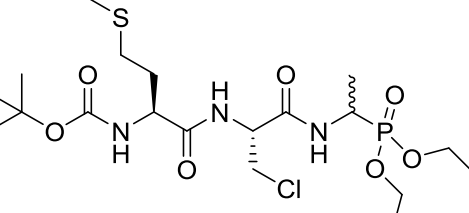
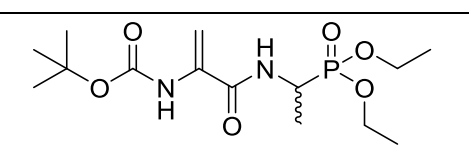
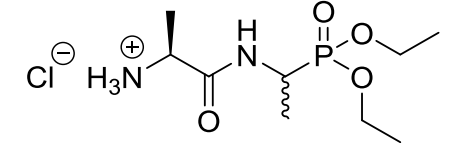
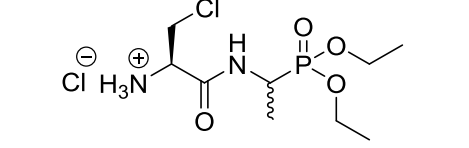
Structure	Name	$\delta_{\text{P-H}}$
	$^1\text{Boc-L-Nva-}\beta\text{-chloro-L-Ala-D/L-Fos diethyl ester (221b)}$	24.9, 25.0
	$^1\text{Boc-Sar-L-Ala-D/L-Fos diethyl ester (152c)}$	25.0, 25.1
	$^1\text{Boc-Sar-}\beta\text{-chloro-L-Ala-D/L-Fos diethyl ester (221c)}$	24.7, 24.8
	$^1\text{Boc-L-Met-L-Ala-D/L-Fos diethyl ester (159)}$	25.0, 25.1
	$^1\text{Boc-L-Met-}\beta\text{-Cl-L-Ala-D/L-Fos diethyl ester (224)}$	24.5, 24.8
	$^1\text{Boc-dehydroala-D/L-Fos diethyl ester (206)}$	24.9
	L-Ala-D/L-Fos diethyl ester hydrochloride (158)	29.0, 29.1
	$\beta\text{-Cl-L-Ala-D/L-Fos diethyl ester hydrochloride (223)}$	26.1, 26.2

Table 8.29: Chemical shift of ^{31}P - ^1H decoupled of phosphonic acid

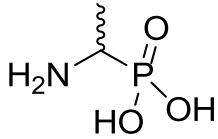
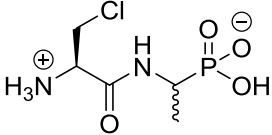
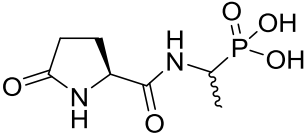
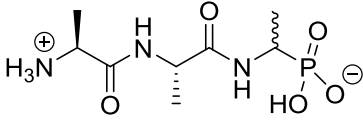
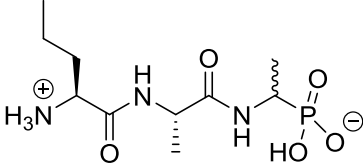
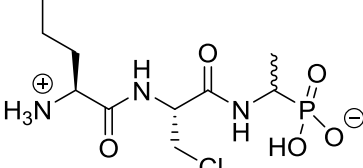
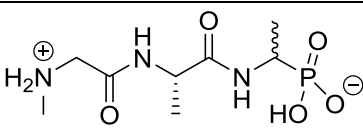
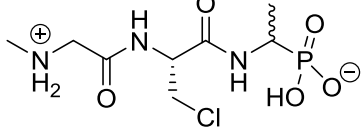
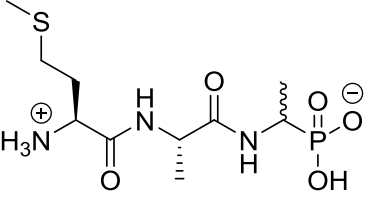
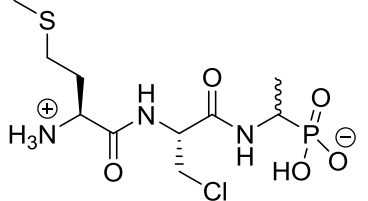
Structure	Name	$\delta_{\text{P-H}}$
	D/L-Fosfalin (13-DL)	14.2
	β -Cl-L-Ala-D/L-Fos (196)	18.7
	L-Pyroglu-D/L-Fos (141)	19.9
	L-Ala-L-Ala-D/L-Fos (153a)	19.3
	L-Nva-L-Ala-D/L-Fos (153b)	18.5
	L-Nva- β -chloro-L-Ala-D/L-Fos (222b)	18.5
	Sar-L-Ala-D/L-Fos (153c)	19.2
	Sar- β -chloro-L-Ala-D/L-Fos (222c)	18.8

Table 8.29 (cont.d): Chemical shift of ^{31}P - ^1H decoupled of phosphonic acid

Structure	Name	$\delta_{\text{P-H}}$
	L-Met-L-Ala-D/L-Fos (160)	20.7
	L-Met- β -Cl-L-Ala-D/L-Fos (225)	18.7

Appendix 8.4: Publication

(12) DEMANDE INTERNATIONALE PUBLIÉE EN VERTU DU TRAITÉ DE COOPÉRATION EN MATIÈRE DE BREVETS (PCT)

(19) Organisation Mondiale de la
Propriété Intellectuelle
Bureau international



(10) Numéro de publication internationale
WO 2015/140481 A1

(43) Date de la publication internationale
24 septembre 2015 (24.09.2015) **WIPO | PCT**

(51) Classification internationale des brevets :
C07K 5/06 (2006.01) C07K 5/10 (2006.01)
C07K 5/08 (2006.01) A61K 38/00 (2006.01)

(21) Numéro de la demande internationale :
PCT/FR2015/050727

(22) Date de dépôt international :
23 mars 2015 (23.03.2015)

(25) Langue de dépôt : français

(26) Langue de publication : français

(30) Données relatives à la priorité :
1452424 21 mars 2014 (21.03.2014) FR

(71) Déposant : BIOMÉRIEUX [FR/FR]; F-69280 Marcy-L'Etoile (FR).

(72) Inventeurs : ANDERSON, Rosaleen Joy; 6 Park Parade, Roker, Sunderland Tyne and Wear SR6 9LU (GB). BERNERJAK, Alexandre F.; 3 Rue des Varennes, F-18570 Morthomiers (FR). CELLIER, Marie; 5 rte Champagne, F-38390 Montaliou Vereieu (FR). NG, Keng Tiong; 60 Jalan 5/62B, Bandar Menjalara, Kepong, Kuala Lumpur, 52200 (MY). ORENGA, Sylvain; 164 route du Suran, Saint André-le-Bas, F-01160 Neuville-sur-Ain (FR). PERRY, John D.; Newlands, Benton Bank, High Heaton, Newcastle upon Tyne Tyne and Wear NE7 7BH (GB). VÁRADI, Linda; Váci M. u. l., H-3712 Sajovamos (HU).

(74) Mandataire : RICHAUD, Richaud; Cabinet Murgitroyd, 55 Allée Pierre Ziller, Immeuble Atlantis CS50105, F-06902 Valbonne Sophia Antipolis (FR).

(81) États désignés (sauf indication contraire, pour tout titre de protection nationale disponible) : AE, AG, AL, AM, AO, AT, AU, AZ, BA, BB, BG, BH, BN, BR, BW, BY, BZ, CA, CH, CL, CN, CO, CR, CU, CZ, DE, DK, DM, DO, DZ, EC, EE, EG, ES, FI, GB, GD, GE, GH, GM, GT, HN, HR, HU, ID, IL, IN, IR, IS, JP, KE, KG, KN, KP, KR, KZ, LA, LC, LK, LR, LS, LU, LY, MA, MD, ME, MG, MK, MN, MW, MX, MY, MZ, NA, NG, NI, NO, NZ, OM, PA, PE, PG, PH, PL, PT, QA, RO, RS, RU, RW, SA, SC, SD, SE, SG, SK, SL, SM, ST, SV, SY, TH, TJ, TM, TN, TR, TT, TZ, UA, UG, US, UZ, VC, VN, ZA, ZM, ZW.

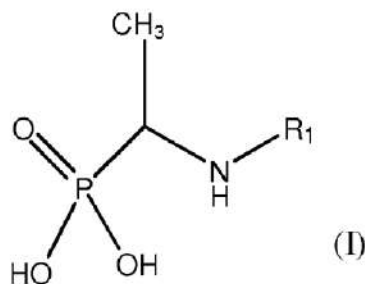
(84) États désignés (sauf indication contraire, pour tout titre de protection régionale disponible) : ARIPO (BW, GH, GM, KE, LR, LS, MW, MZ, NA, RW, SD, SL, ST, SZ, TZ, UG, ZM, ZW), eurasien (AM, AZ, BY, KG, KZ, RU, TJ, TM), européen (AL, AT, BE, BG, CH, CY, CZ, DE, DK, EE, ES, FI, FR, GB, GR, HR, HU, IE, IS, IT, LT, LU, LV, MC, MK, MT, NL, NO, PL, PT, RO, RS, SE, SI, SK, SM, TR), OAPI (BF, BJ, CF, CG, CI, CM, GA, GN, GQ, GW, KM, ML, MR, NE, SN, TD, TG).

Publiée :

- avec rapport de recherche internationale (Art. 21(3))
- avant l'expiration du délai prévu pour la modification des revendications, sera republiée si des modifications sont reçues (règle 48.2.h))

(54) Title : ANTIMICROBIAL COMPOUNDS

(54) Titre : COMPOSÉS ANTIMICROBIENS



(57) Abstract : Antimicrobial compound, as well as the salts, derivatives and analogues thereof, said compound being represented by the general formula (I): where R₁ is a peptide part P1 or a peptide part P2.

(57) Abrégé : Composé antimicrobien, ainsi que ses sels, dérivés et analogues, ledit composé étant représenté par la formule générale (I) : dans laquelle R₁ représente une partie peptidique P1 ou une partie peptidique P2.

WO 2015/140481 A1